Structural Behaviour and Optimization of Moment-Shaped Reinforced Concrete Beams

by

Fariborz Khaleghi Hashemian

A Thesis submitted to the Faculty of Graduate Studies of

The University of Manitoba

in partial fulfilment of the requirements for the degree of

DOCTOR OF PHILOSOPHY

Department of Civil Engineering

Faculty of Engineering

University of Manitoba

Winnipeg

Abstract

This research includes a preliminary study prior to the commencement of the Ph.D. work and three phases of design, construction and testing of three generations of moment-shaped beams. Each phase of the research brought a better understanding of curved beams which follow the shape of the moment diagram. The moment diagram in this study was for simply supported beams supporting a uniformly distributed load as would be the case in the majority of building designs.

The original theory for this research can be described as follows: Moment-shaped beams are the natural outcome of a fundamental understanding of stress paths in a horizontal load bearing member. By following these stress paths we may provide materials where required to most efficiently carry the compression and tension stresses to the supports. Allowing stresses to follow their naturally desired paths reduces regions where stresses cross paths called disturbed regions.

The outcome of the final phase of this research was the development of the third generation of curved beams with a camber. These beams, designated as Cambered Curve beams (CCBs), exhibited the same behaviour as the rectangular control beam design using CSA-A23.3 up to the serviceability failure of L/360 (12mm).

The CCB moment-shaped beams require 20% less concrete and 40% less reinforcing steel (no shear stirrups) to carry the ultimate load which is only 12% less than that carried by the CSA-designed control beam.

Due to a closed system of internal forces, the moment-shaped beams remain intact and are able to sustain self weight, even after total failure.

A significant part of this research was to modify and verify a FORTRAN-based finite element analysis program: FINIT-Y. This program was reconstructed to analyse a full size beam, and enabled the researcher to model and correctly predict the maximum load, crack pattern and failure mode.

This study found that moment-shaped beams with no shear reinforcement have the same stiffness and load carrying capacity as the CSA-designed rectangular control beam with shear reinforcement up to serviceability failure (L/360). The study also found that moment-shaped beams have significantly lower ductility at the ultimate load.

Acknowledgments

I am grateful to my advisors, Professor Aftab Mufti and Professor Mark West, for showing me a world with no boundaries. Without their continual support and guidance, this work would not have been possible.

I would also like to thank the following laboratory staff and ISIS office staff for their support and contributions: Dr. Darshan Sidhu, Dr. Hugues Vogel, Mr. Murray McVey, Mr. Chad Klowak, Dr. Liting Han, Mrs. Evangeline Morrison, Miss Charleen Choboter and Miss Nancy Fehr.

Finally, I gratefully acknowledge the work of my examination committee: Professor Ron Britton, Professor Doug Thompson, and my external examiner, Professor Remo Pedreschi.

Thank you all for your time and your invaluable contributions to this research.

I would like to extend a special thanks to my amazing wife Aynslee, my son Victor and my dear friend Ramona Junio who have supported me throughout the years.

Table of Contents

List of Tables

List of Figures

CHAPTER 5

CHAPTER 6

CHAPTER 9

1   *Introduction*

Fabric formwork is the original inspiration for this study. This construction method has the potential for the practical creation of structurally efficient forms which can reduce the amount of materials consumed in constructing reinforced concrete members (and ultimately structures) and it is a construction method that can be developed for building economies where wood and steel formwork is not readily available.   This study is focused on the potential material and structural efficiencies made possible by the formation of beams shaped, along their span, to follow their own bending moment curve.   This corresponds with the international movement towards sustainability and environmental responsibility for designers.

Preliminary testing of beams constructed during the studies of fabric formwork unveiled various opportunities for complex studies on structural design, shear stress distribution and form. These studies have to be completed before fabric-formed beams can be widely accepted and mass constructed as a viable structural option.

This research is an experimental and analytical study of stress distribution in moment-shaped reinforced concrete (RC) beams, focused on understanding their behaviour and most importantly the failure mode since the curved beams have no shear stirrups or reinforcement. Several RC beams were designed, fabricated, and tested, and the results were compared with a Finite Element Model (FEM) Analysis program. The research is. The research was persistent in

seeking to fully understand the behaviour of the moment-shaped beam instead of simply fixing problems as they arose.

Prior to the commencement of a discussion on curved beams it is essential to review the idealized and actual modes of structural behaviour of conventional, rectangular, prismatic reinforced concrete beams based on current design and construction practice. Section 1.2 will present a review and interpretation of the structural behaviour of conventional, rectangular, reinforced concrete beams.

1.1   *Behaviour of Uniform Section Rectangular Reinforced Concrete Beams*

The behaviour of rectangular concrete beams before and after cracking is a well-established subject with numerous papers, reports and books available on this topic. Herein, a simplified explanation of conventional reinforced concrete beam behaviour is presented for general information and for future comparison of the behaviour of bending moment shaped RC beams.

Before cracking – A reinforced concrete beam that is subjected to combined flexure and shear, behaves like a homogeneous elastic beam prior to cracking. The behaviour of homogeneous beams under flexure and shear is well established. Once load levels increase and cracking starts, the mechanism of internal stress transfer and distribution in a reinforced concrete beam becomes substantially different. Although for design practices only the behaviour of cracked beams is relevant, the behaviour of uncracked rectangular beams

2

provide a fundamental understanding of after cracking behaviour of uniform-section beams and will shed light on the behaviour of form-active or curved beams.

Consider a simply supported uncracked RC beam with a rectangular cross-section subjected to a uniformly distributed load (w). As the result of the applied forces, internal bending moments and shear forces develop in the beam. The maximum bending moment (M_{max}) occurs at the midspan where the vertical shear force is equal to zero, while the maximum vertical shear forces (V_{max}) develop at the support. A reinforced concrete beam under uniformly distributed load (UDL) and the corresponding bending moment and shear force diagrams have been illustrated in Figure 1.1.
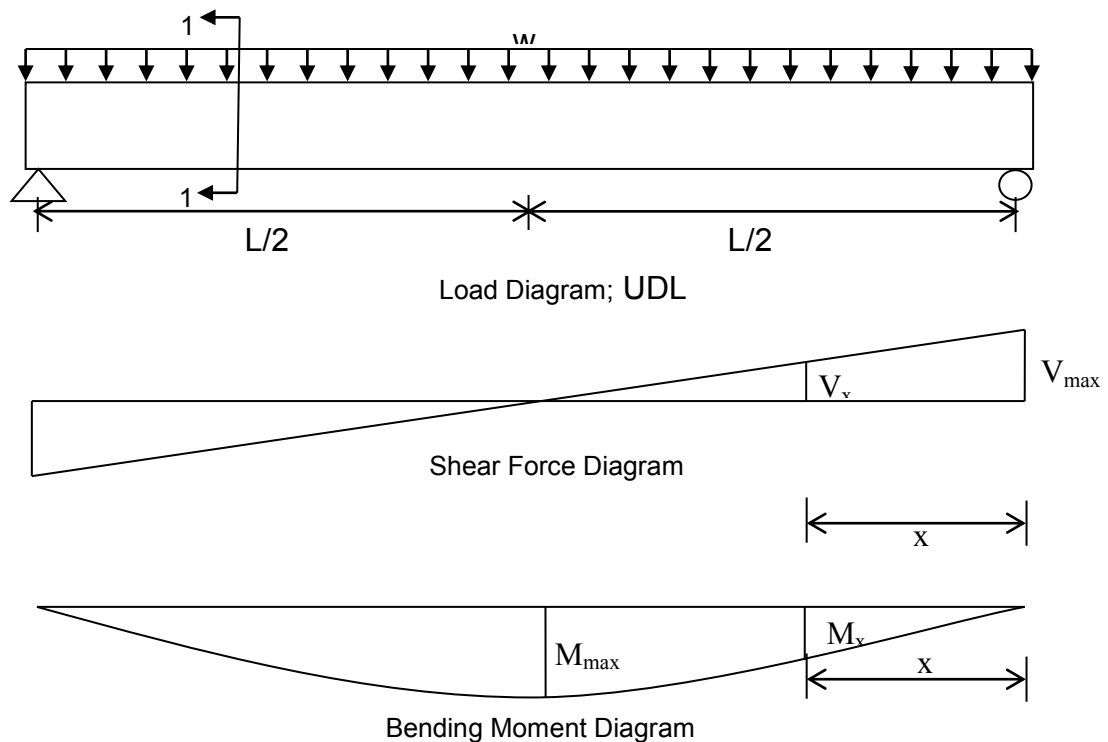
Figure 1.1 – Reinforce concrete beam under uniform load and corresponding bending moment and shear force diagrams.

Flexural stress distribution can be reviewed at section 1-1 of the beam shown in Figure 1.2. Longitudinal section 1-1 is located at a distance from the support equal to the effective depth of the beam.

Flexural Stress (σ)   Shear Stress (v)
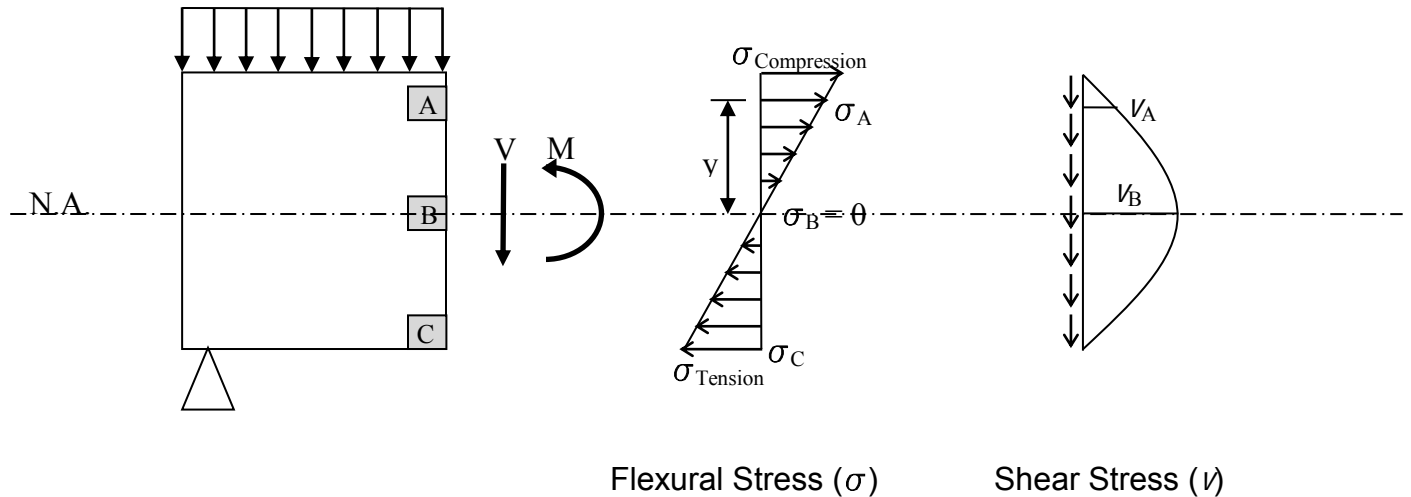
Figure 1.2 – Longitudinal section 1-1

To show the stress distribution in the beam, three stress-representative blocks of concrete can be selected across the beam's cross section as shown in Figure 1.2. Block A is located in the compression zone, block B is located on the natural axis where the flexural stress is equal to zero, and block C is located at the extreme bottom fibre which is subjected to tensile flexural stress. The maximum and minimum normal stresses (or extreme stresses) acting on these blocks are called principal stresses. The principal stresses acting on each block can be shown as follows in Figure 1.3. Stress distribution across a reinforced concrete flexural member has been discussed thoroughly in the Canadian Concrete Design Handbook, Chapters 2 and 5.

4

Block A at the compression zone:
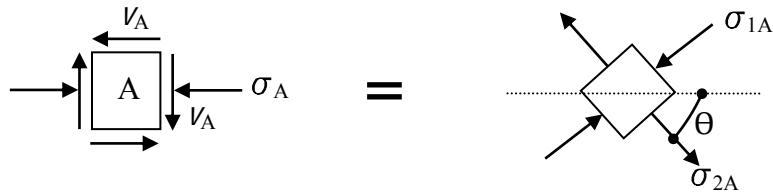
Block B at the neutral axis:
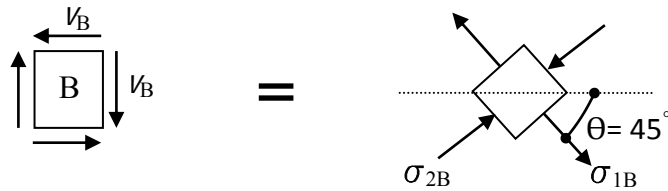
Block C at the extreme tension fibre:
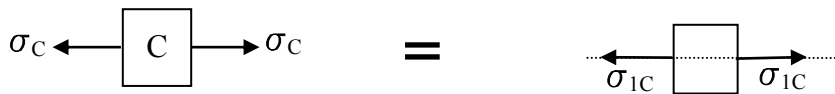
Figure 1.3 – Stress blocks

Where σ_1 and σ_2 are the maximum and minimum principal stresses, respectively, these principal stresses can be calculated using stress transformation equations based on stress equilibrium for a small element. Principal stresses for block B, for example, can be calculated from: circle

$$\sigma_1 = \sigma/2 + [(\sigma/2)^2 + V^2]^{1/2}$$

$$\sigma_2 = \sigma/2 - [(\sigma/2)^2 + V^2]^{1/2}$$

If several blocks or elements are taken at various locations along the beam and if the values and direction of principal stresses are known at these locations, it is

possible to draw curves or stress trajectories, tangential to the principal stress

directions within these elements. The stress trajectories for the above beam can

be drawn as shown in Figure 1.4. Prior to cracking the behaviour of the beam is

linear. Figure 1.4 shows idealized stress trajectories for a homogeneous

uniform-section beam.

Tension ———
Compression - - - - - - - -
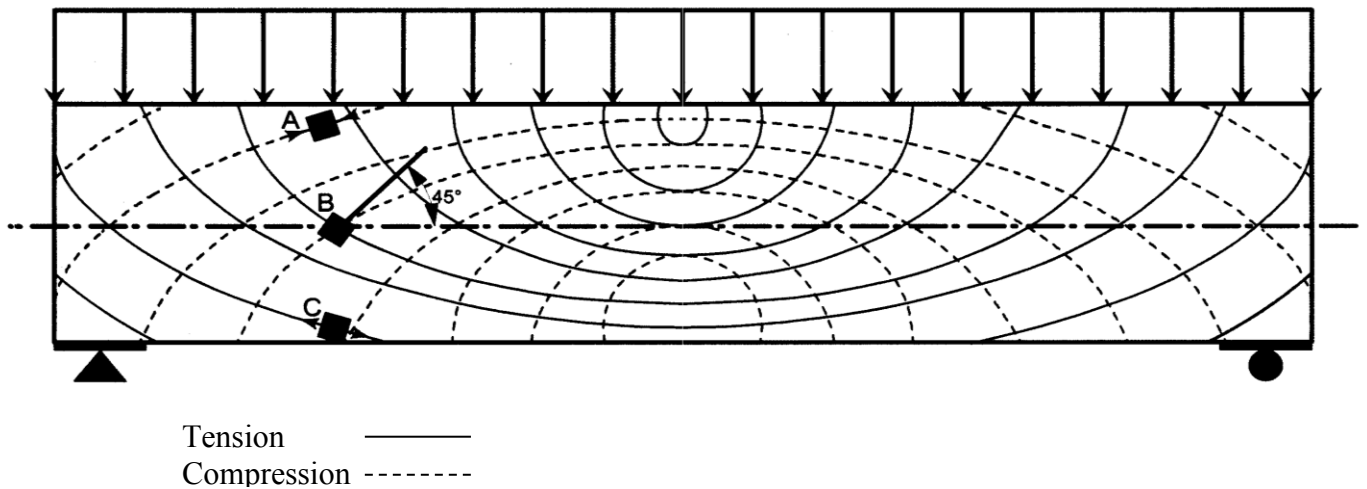
Figure 1.4 – Tensile and compressive stress trajectory
in a homogeneous (ideal) beam

RC beams are not homogeneous because they are designed and fabricated

using both concrete and steel and they are assumed to be cracked when

designed. Figure 1.5 shows the actual stress distribution in a RC beam. The

stress distribution in uniform-section RC beams is not uniform along the beam;

distribution of strain along the reinforcement is more highly concentrated at the

mid-span (at the area of maximum moment). Compression and tension stresses

are concentrated at the top and at the bottom at the mid-span of the beam and

"fan out" or "spread open" as they get closer to the supports where they cross

paths creating a "disturbed" region that will be explained further in this section.

Tension ———
Compression --------

Disturbed zone or region
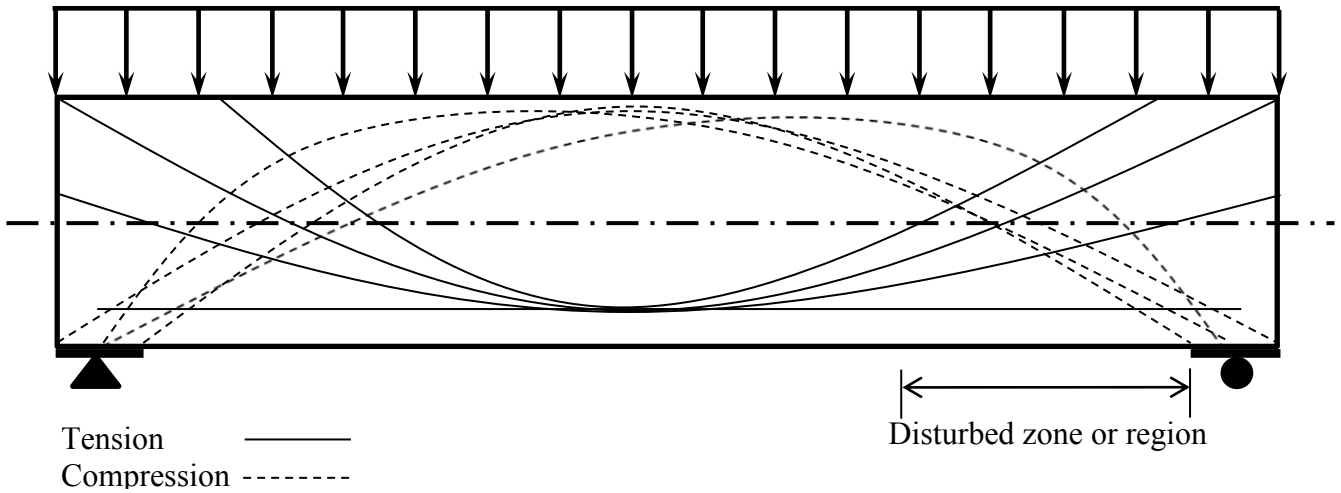
Figure 1.5 – Actual stress distribution in a RC beam (nonhomogeneous)

After cracking – Once the stresses increase and exceed the tension capacity of

the concrete alone, flexural cracks will appear and the beam no longer behaves

linearly. Figure 1.6 illustrates the typical crack pattern developing due to tension

stresses in the beam's tension zone, and the diagonal tension cracks due to the

tension and compression stresses crossing paths (Block B in Figure 1.4).

Diagonal
tension or
"shear"
cracks

Flexural cracks
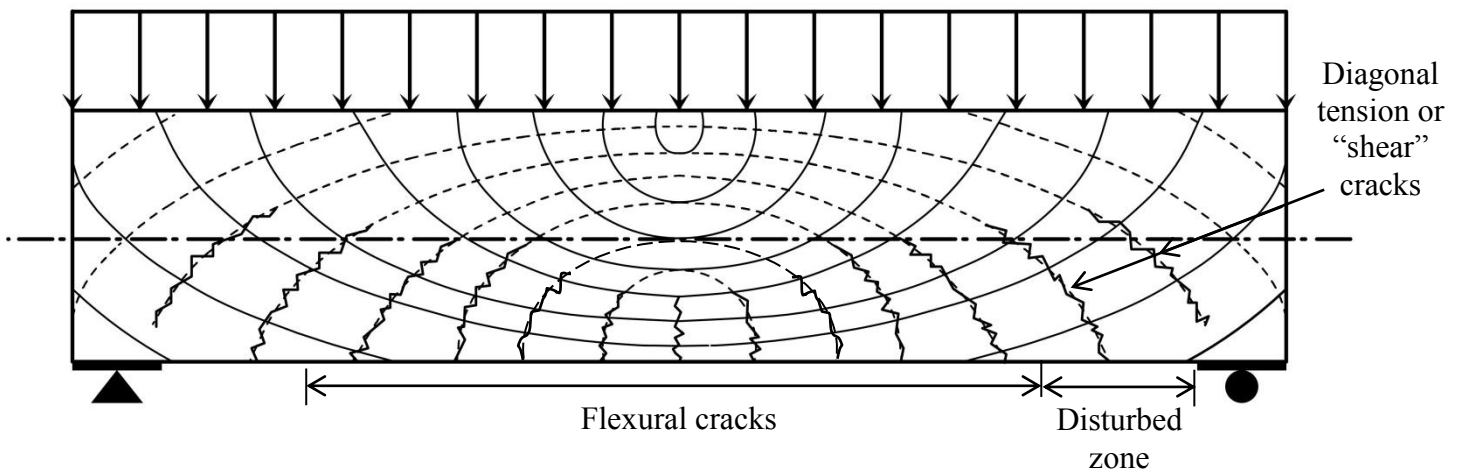
Disturbed
zone

Figure 1.6 – Cracks developed in the beam tension zone

The portion of the beam where diagonal tension could occur is called the disturbed zone or region (shown in both Figures 1.5 and 1.6). Diagonal tension cracks due to diagonal tension stresses shown in Figure 1.6 are due to compression and tension stress applied on the same block (or cross paths as illustrated in Figure 1.3). This phenomenon of diagonal tension near the support of a beam is conventionally named "shear". Conventional "shear" will be shown in quotations in this document when the author is comparing or referring to this phenomenon of diagonal tension, and to distinguish this diagonal tension from the true shear stress.

Once flexural cracks appear (the section becomes cracked section) the beam's load carrying capacity can be determined by equilibrium principals and by balancing the compression and tension forces in the concrete and steel respectively. Currently, the solution for preventing diagonal tension or "shear" failure in rectangular beams is to place vertical reinforcement along the length of the beam, in particular near the supports, to resist the diagonal tension and maintain the integrity of the beam. In principal, the vertical reinforcement or "shear" stirrups are placed to cross the "shear" cracks to stop crack propagation.

After cracking, the "shear" analysis or modeling may be determined by several mechanics-based models that are also the basis for vertical "shear" design procedures prescribed by design codes. One relatively simple model for vertical "shear" behaviour of reinforced concrete beams with "shear" reinforcement is Truss Analogy which forms the basis for the simplified method of "shear" design in accordance with CSA 23.3. The truss model of a reinforced concrete beam

under one concentrated load is presented in Figure 1.7. "Shear" behaviour of reinforced concrete beams, though perhaps still not well understood, is one of the most studied research subjects, and therefore, numerous papers and books are available on the subject.

In Figure 1.7, d_v is equal to the moment arm of the internal forces T (tension) and C (compression) resisting the bending moment. The internal forces C and T develop in a reinforced concrete beam to resist the flexure due to external forces.
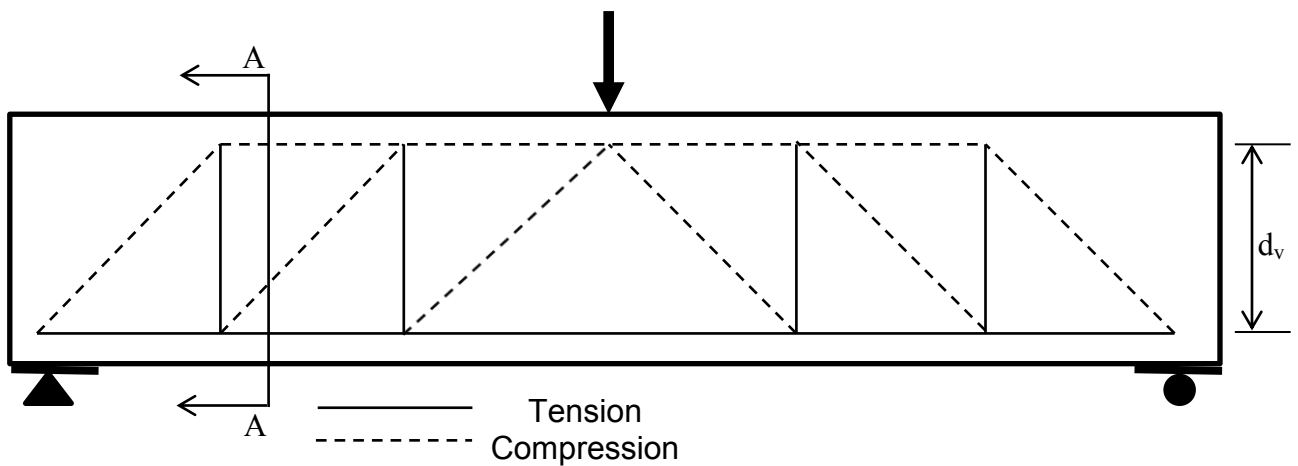
Figure 1.7 – Truss model for reinforced concrete beam

The free-body-diagram (FBD) at cross section A-A for the above beam showing applied forces and the reaction is illustrated in Figure 1.8.
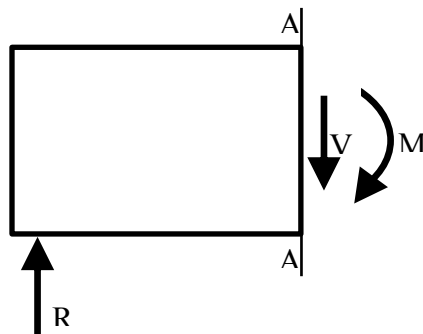
Figure 1.8 – FBD of a reinforced concrete beam subjected to flexure; section A-A

In Figure 1.8, M is the moment and V is the vertical shear force due to the external force. R is the reaction at the support. Force V is the vertical transference of the load to the support and shown in FBD's as a pure shear. In response to the applied moment M the RC beam develops an internal couple (equal and opposite forces) to resist the applied moment. This couple is generated by the compression force in the concrete and tension force in the steel reinforcement separated by the beam's effective depth, which is the moment arm for the couple.

The internal forces after cracking are shown in Figure 1.9.
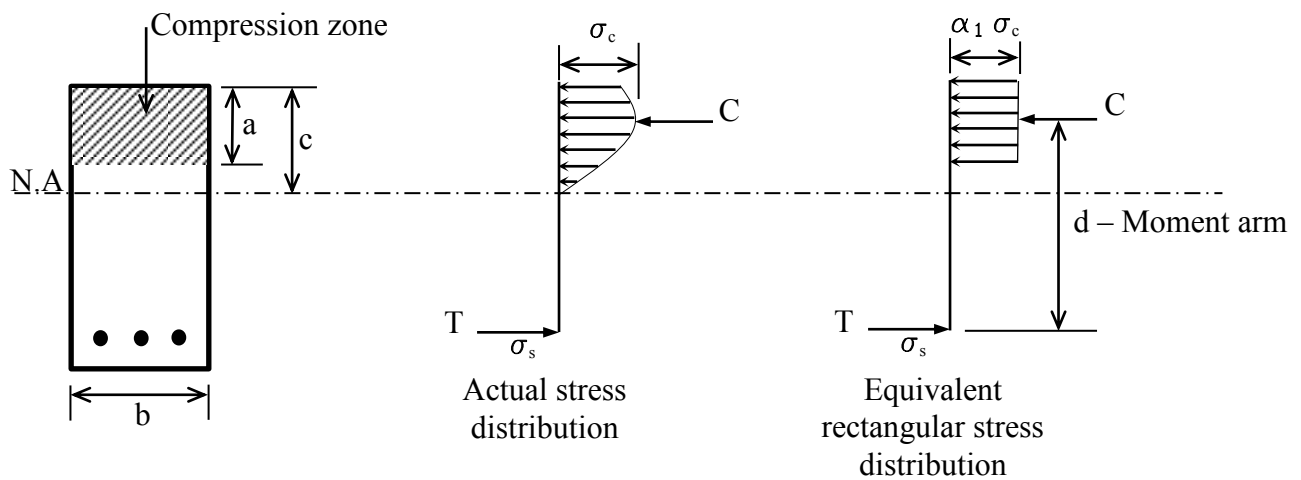
Figure 1.9 – Stress distribution in a RC beam subjected to flexure

σ_c and σ_s are the stresses in concrete and steel respectively. Multiplying stresses to the respective areas of the working material yields the force couple separated by the moment arm d generating the resisting moment M_r.

1.2   Original Hypothesis/Theory for Developing Moment-shaped Curve Beams

It is the author's opinion that the current rectangular shapes of RC beams are predominant due to the material used for formwork to construct RC beams; i.e. plywood, sawn lumber and timber. Uniform section prismatic geometries of RC beams are based on economy and ease of fabrication of formwork construction using panelized materials. The rectangular shape of RC beams, driven by formwork construction economies, creates the disturbed region where diagonal tension occurs, requiring the need for "shear" stirrups. The need for "shear" stirrups increases the material and labour requirements of constructing RC beams.

Fundamental structural theory suggests that a variable-section beam that follows the shape of the bending moment of its applied load could transfer the internal stresses to its supports without creating the disturbed region, offering an effective strategy for reducing the volume of material required in the structure.

Curved truss shapes, such as Lenticular Trusses, prove that compression and tension forces can be fully confined to the upper and lower cords of the truss respectively. This suggests that fabricating a RC beam which follows its bending moment diagram shape would largely confine the compression and tension stresses in the upper and lower surfaces of the beam simply by virtue of the beam's shape, thus eliminating, or significantly reducing tension and compression forces in the "web" portion of the beam and therefore eliminating or reducing the need for "shear" stirrups in such RC beams.

Following this reasoning it was anticipated that such a moment-shaped RC beam could be designed so that the compression and tension stresses would follow their natural paths to meet at the support, thus creating a "structural node" over the support, eliminating diagonal tension or "shear" stresses in the web portion of the beam. The term "structural node" in this work denotes a point at which all internal and external forces are resolved creating equilibrium (such as occurs at the support of the truss, for example). Figure 1.10 shows the proposed structural node at the support of a beam. Figure 1.10a shows the intended ideal situation where both internal forces meet over the support. Figure 1.10b shows the horizontal and vertical components of the internal forces. The horizontal components cancel each other out and the vertical components are resisted by the external reaction at the support, hence equilibrium.

a – End-beam and internal
forces over the support

b – Components of internal forces
and support reaction at equilibrium
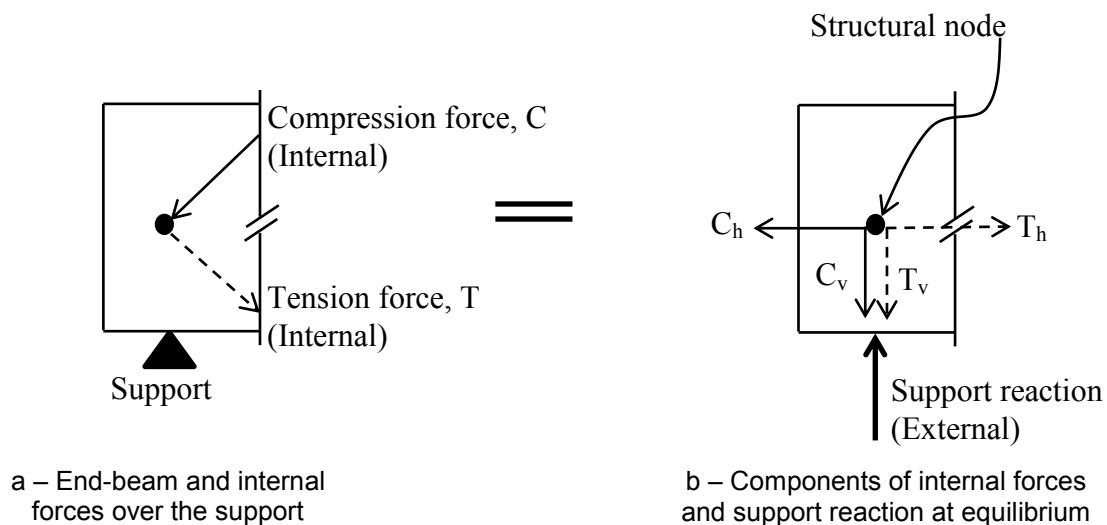
Figure 1.10 – Structural node over the support

Flexible formwork technology presents an economical method for the production of variable section beams, effectively removing the economic constraint of uniform section formwork construction in RC beam design.

Based on the argument, the following hypothesis was formed:

"A reinforced concrete beam design with a longitudinally variable section to follow the same curve as its bending moment diagram, due to a specific load condition, will work more efficiently[1] than a rectangular reinforced concrete beam for the same span and load condition. Specifically, as variable section moment-shaped beams provide a path for the natural flow of stresses, the diagonal tension (or "shear" stresses) will not develop in the web portion of the beam, thus reducing or eliminating "shear" reinforcing requirements, consequently reducing material and labour requirements to produce such a beam."

---

[1] In this thesis "Efficiency" is defined as both a lower ratio of self-weight to load capacity, and a more uniform distribution of internal stresses within the materials of the beam.

1.3 Finite Element Analysis of Reinforced Concrete Structures

During the design and planning of the research programme it was decided to develop and use a finite element analysis (FEA) program for analysing moment-shape RC beams instead of using a readily available finite element analysis program packages such as ANSYS or ADINA. This decision was based on facilitating full control over both the modeling and the method of analysis. The analysis method in a FEA ready package is closed and cannot be changed to fit a specific problem, and users only have control over the modeling of the specimen. For example, the FEA program developed for this research, FEM-NRC (or FINIT –Y), enables the users to use data for the bond characteristics of steel or FRP reinforcement and concrete from actual testing instead of a predetermined quantity in a readily available package that cannot be altered. Previous studies show that significant tuning of modelling parameters are required to produce a good correlation between the experimental results and the results achieved by ADINA. One such study (Wegner and Mufti, 1994) compares the experimental investigation of a fibre-reinforced concrete slab under point load to finite element analysis conducted by ADINA which concludes that the three-dimensional isoparametric element used to model the deck slab produces overly stiff responses. This paper further concluded that despite the advances in nonlinear finite-element analysis of concrete structures, considerable work is still required to improve numerical techniques and to create a reliable analytical tool that is accessible to practicing engineers.

Another factor for developing a specific FEA program was the author's professional experience with ANSYS, were numerous attempts were made to model reinforced mass concrete dams on either rock or till foundation. Considerable effort and time was spent to develop a model of the dam that would provide an acceptable answer by the program. The major difficulty was in modeling of the concrete to foundation interface. The outcome of the analysis suggested much higher stresses than expected by hand calculations of verifying examples.

Since FEM-NRC (or FINIT-Y) is a program developed using FORTRAN and not everyone is familiar with this program an introduction and detailed logic of the programing is given in Chapter 6 complete with a few examples that were used to verify the program.

An additional advantage of the FEM-NRC program is that the user has to review the analysis result in detail in order to develop a graphical result output. While this is time consuming, it does facilitate a deeper understanding of the specimen's behaviour during each load step, and during crack initiation and propagation. Since the hypothesis for the behaviour of moment-shaped beams is a modified way of understanding RC beams, it was determined and later proved that this detailed review of the analysis result would lead to a more comprehensive understanding.

2   *Original Contributions*

While this research is not the only engineering research to study the behaviour fabric-formed form-active reinforced concrete beams, it is the first and only research that directly compares the form-active or moment-shaped beams with conventional rectangular reinforced concrete beams by numerical analysis and physical experiments.

This research has made the following original contributions to the reinforced concrete industry and to the analysis of moment-shaped beams:

1- Created innovative reinforced concrete (RC) moment-shaped (form-active beams) beams and studied their stress path, stress distribution and redistribution under loading.

2- Experimental and numerical structural optimization of RC moment-shaped beams, approaching a more structurally optimized form for RC beams with reduced concrete and steel as compared with the conventional beams but with the same serviceability failure load.

3- Innovative design philosophy of RC beams construction without shear reinforcement.

4- Reconstruction of FINIT-Y algorithm, a finite element analysis program that can be used to accurately predict the failure mode of moment-shaped or RC elements.

5- Development of accurate finite element model and modeling system for FEM analysis of moment-shaped RC beams.

6- Establishment of logic and means of studying form and shape of RC beams to create a research and design perspective to reduce material and move toward more sustainable design and construction practices.

END OF SECTION

3 *Background and History*

3.1 General

Over the years fabric formwork has been used for concrete in a variety of different applications such as to cast concrete for preventing soil erosion, for casting footings and for casting wall panels and thin shells. It has also been used for casting columns and beams. Most of the previous work with fabric formwork has been limited to containing concrete or to obtaining a certain texture on the finished surface of the concrete. Fabric formwork can be designed to construct more efficient structural members and systems; however, many designers have not been aware of this property of fabric forming. This section will review some of the previous work in fabric or flexible forming. After the recent work at the Center for Architectural Structures and Technology (CAST) at the University of Manitoba, researchers have begun to explore the possibility with fabric or flexible forming for reinforced concrete members for structural purposes. This work and research will be introduced in this chapter.

3.2 Fabric Formwork Used to Prevent Soil Erosion

Fabriform Products® is one of many companies producing fabric forming for control and prevention of soil erosion. They produce and market products such as FilterPoint, shown in Figure 3.1; Unimat Revetment, shown in Figure 3.2;

Articulated Block Revetment, shown in Figure 3.3; Concrete Bags, shown in Figure 3.4, and Pile Jackets, Figure 3.5.

Figure 3.1 – Filterpoint soil erosion prevention**,** installed in 1967 on the Allegheny Reservoir New York (Fabriform)

Figure 3.2 – Unimat Revetment reservoir lining, both before and after concrete pour (Fabriform)
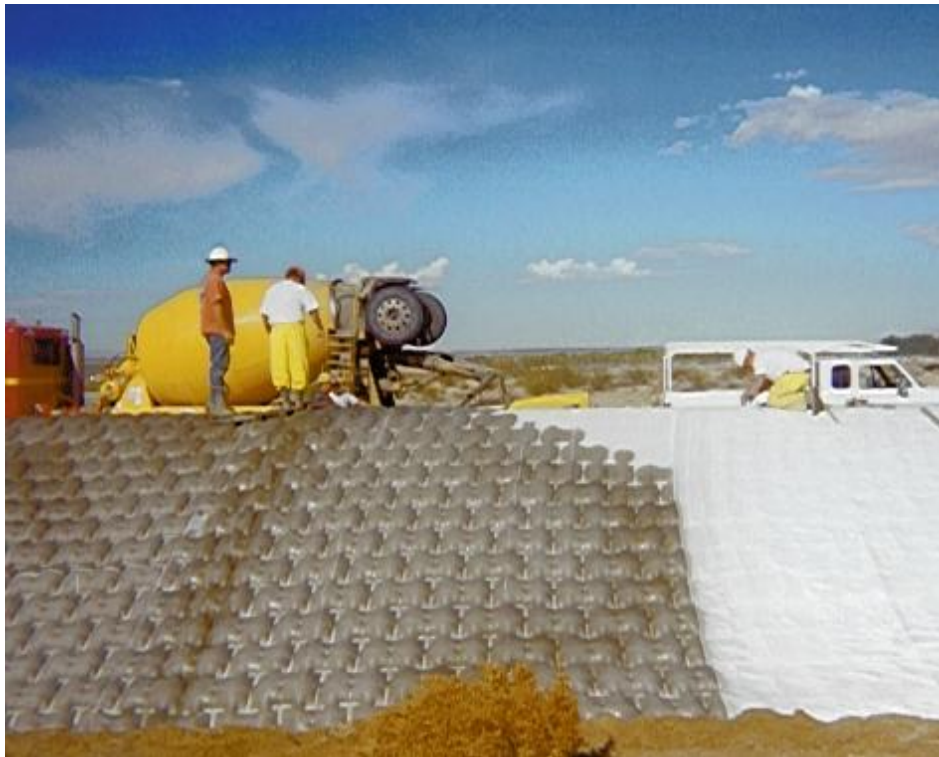
Figure 3.3 – Articulated Block Revetment, California Flood Control (Fabriform)

Figure 3.4 – Concrete Bags, (Fabriform)

Figure 3.5 – Installation of pile jacket, (Fabriform)

The Fabriform products are designed to contain the concrete during pouring and curing. These types of forming provide protection against soil erosion by laying a mattress of concrete over the soil. The thickness of concrete varies according to the slope of the grade and the amount of concrete required for soil protection, as specified by the designers. Soil anchors may be required for stabilization of the concrete layer, depending on the slope of the grade on which the concrete has been placed.

Although these types of erosion control are an effective method of erosion prevention, they crack over the years due to movement of the base material, resulting in unsightly landscaping.

3.3   Architectural Wall Panels

Architects, such as Miguel Fisac (1913-2006) and Kenzo Unno, have been working with precast wall panels cast using flexible forming for years. Fisac, after a decade of making exposed concrete, realized that the concrete surface could take on the texture of the planks used for forming. He decided to give concrete an expression of its own (AV, 2003). In the Mupag Rehabilitation Centre project, he asked the contractor to form the precast wall panels by using plastic sheets and reinforcement tie wire on the exposed side of the wall panels (AV, 2003). Figure 3.6 shows the precast wall panels for the Mupag Rehabilitation Centre project in Madrid (1973).

Fisac perfected his casting and design of the precast wall method over the following years and was able to create different façades using flexible concrete forming. Figure 3.7 shows the drawing of a wall panel for the Hermanas Hospitalarias Social Centre project in Madrid (1985-1986). Figure 3.8 shows the wall panels after casting and construction. Fisac's major intention by using fabric forming was to achieve a certain texture and pattern on his wall panels.

Figure 3.6 – Mupag Rehabilitation Centre, Madrid 1969 – 1973,
Architectural wall panels by M. Fisac (AV 2003)
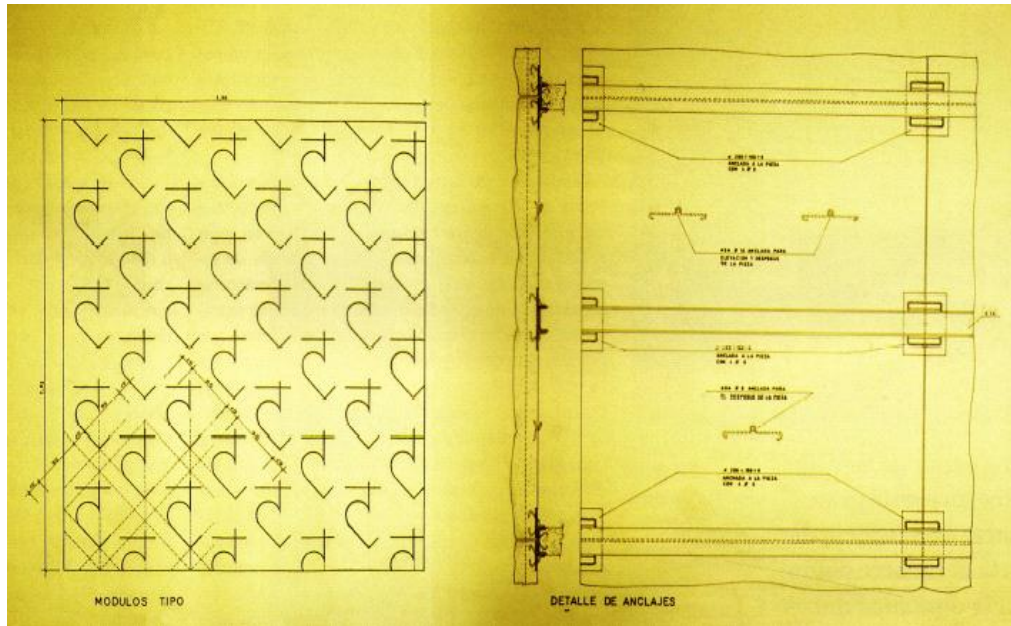
Figure 3.7 – Drawings for the wall panels for the Hermanas Hospitalarias Social Centre project, Madrid 1985 – 1986, by M. Fisac (AV 2003)

Figure 3.8 – Wall panels after construction, Hermanas Hospitalarias Social Centre project, Madrid 1985 – 1986, by M. Fisac (AV 2003)

Kenzo Unno developed construction methods for cast-in-place architectural wall panels using flexible forming, as shown in Figure 3.9.

Figure 3.9 – Fabric formed wall system by K. Unno, (Toto Tsushin Vol.4, 1999)

3.4   Fabric Formed Beams

Over the past twenty years, architecture professor Mark West of the University of Manitoba has been working on flexible forming for casting concrete. His work evolved from fabric formed sculptures to columns to precast panels and compression shells, as shown in Figures 3.10 and 3.11.
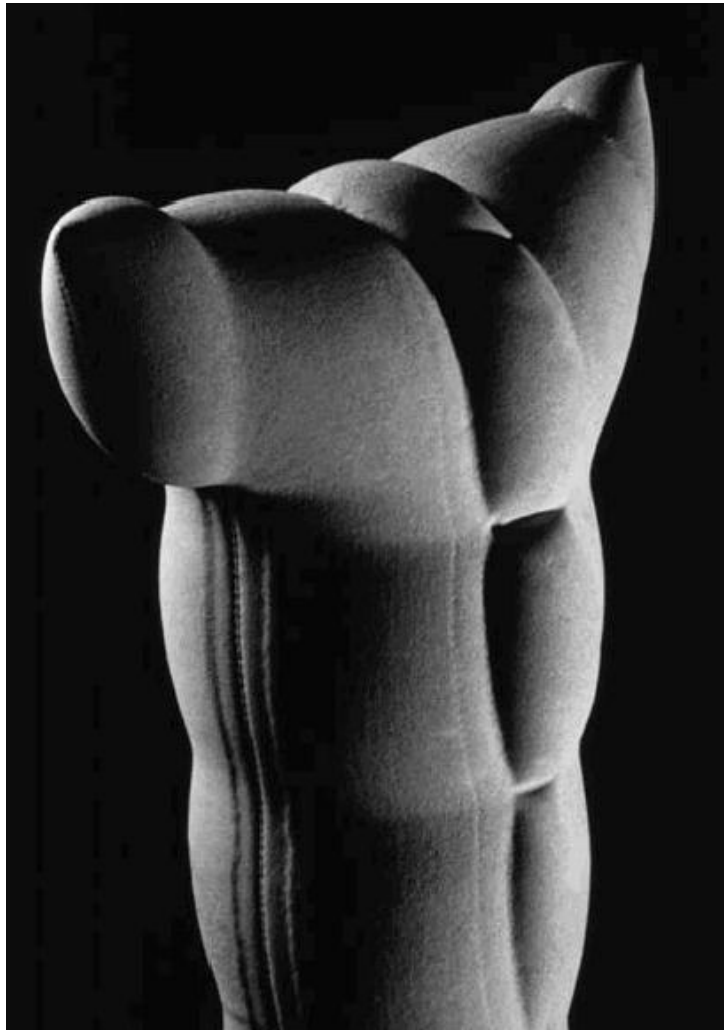
Figure 3.10 – Azbollard, Fabric formed sculpture by Prof. Mark West
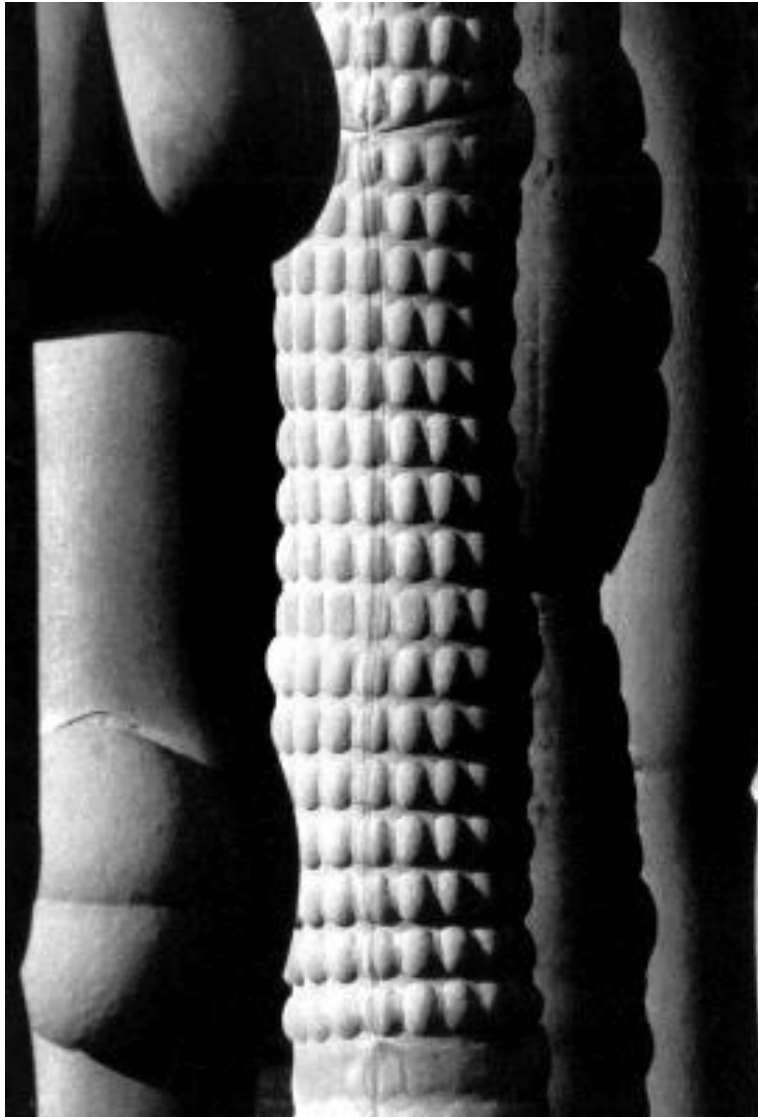
Figure 3.11 – Fabric formed columns by Prof. Mark West

Currently, Prof. West and his students at the University of Manitoba are working on fabric-formed compression shells, beams and trusses. Using properties of fabric forming, the author and Prof. West are able to form concrete beams that closely follow the shape of the bending moment diagram of a continuous beam. Based on the author's design and analysis, this method of forming will result in a

more efficient reinforced concrete beam. In 2002, Mark West and the author designed and fabricated a double cantilever beam spanning 12 m from a single flat sheet of geotextile fabric, Figure 3.14. This beam used 50% less concrete and 30% less reinforcing steel than a conventionally cast prismatic beam. Although no physical tests were performed on this beam theoretical analysis showed that this beam could sustain the same amount of load as a conventional rectangular beam designed as a control model. Figure 3.12 shows the plaster scaled model of the double cantilever beam and Figure 3.13 shows the actual concrete beam during transportation to the University of Manitoba.
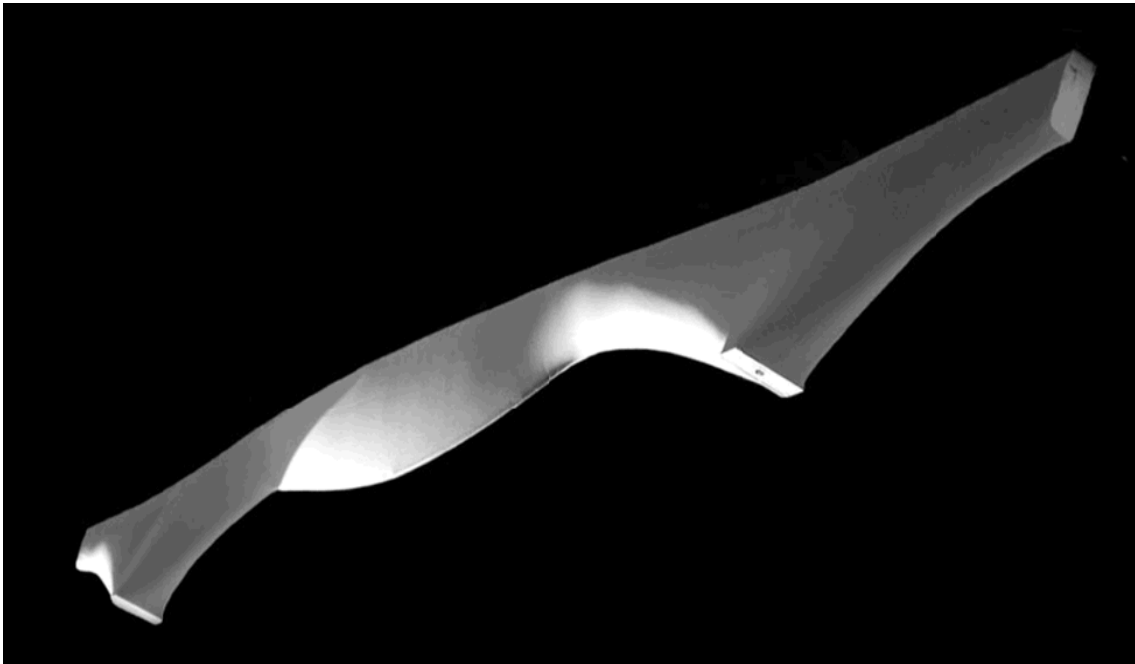
Figure 3.12 – Plaster model of a double cantilever beam

The fabric-formed reinforced concrete beam shown in Figure 3.13 is the first full size beam cast using the properties of the fabric to construct a concrete beam. Figure 3.14 shows the formwork for the beam prior to concrete placement. This

beam was never physically tested and is permanently on display in front of the Centre for Architectural Structures and Technology building at the University of Manitoba in Winnipeg.

Figure 3.13 – Fabric formed concrete beam

Figure 3.14 – Formwork for the fabric formed concrete beam

3.5   Beam Research at the University of Edinburgh

Following the work at CAST, Dr. Remo Pedreschi, professor at the University of Edinburgh, began extensive research on fabric formed concrete members in 2006. Dr. Pedreschi's Ph.D. student Mr. Daniel Lee studied curve beams with slab, essentially a T-beam, as part of his Ph.D. research. In his research entitled "Study of Construction Methodology and Structural Behaviour of Fabric-formed Form-efficient Reinforced Concrete Beams" Mr. Lee constructed 3100mm beams without shear stirrups and with a maximum depth of 163mm, with the slab width of 320mm, as shown in Figure 3.15.

Figure 3.15 – Form-active beam (Lee/Pedreschi)

Mr. Lee used two different curvatures for the bottom of the beams and end anchor details as shown in Figures.3.16 and 3.17.
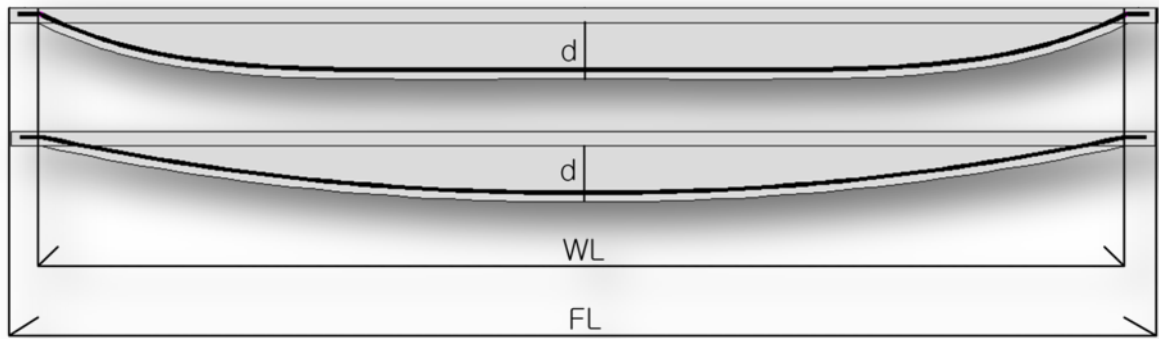
Figure 3.16 – Different curve configuration (Lee/Pedreschi)
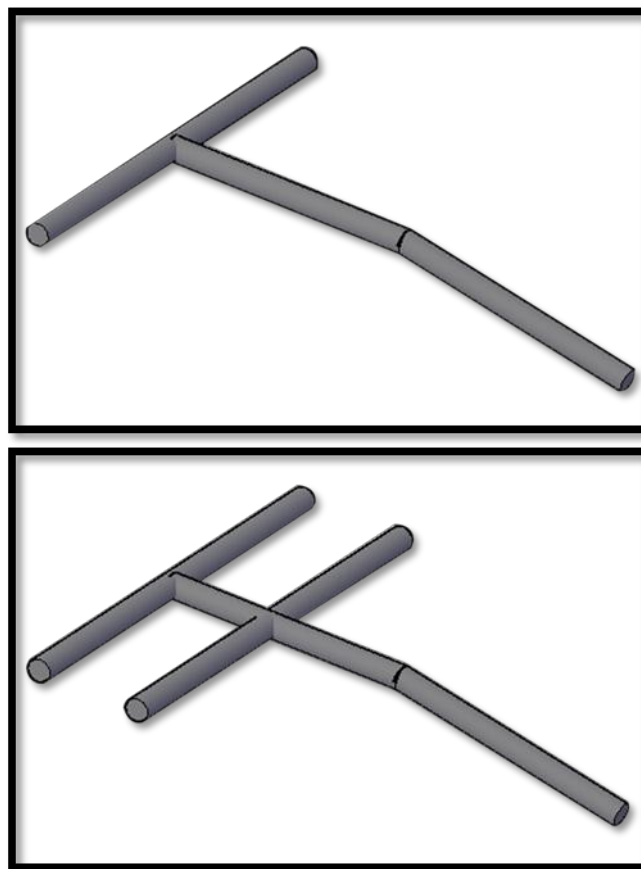
Figure 3.17 – Two variations of the end anchor detail (Lee/Pedreschi)

The beams were loaded under six point loading as shown below:

Figure 3.18 – Six-point loading (Lee/Pedreschi)
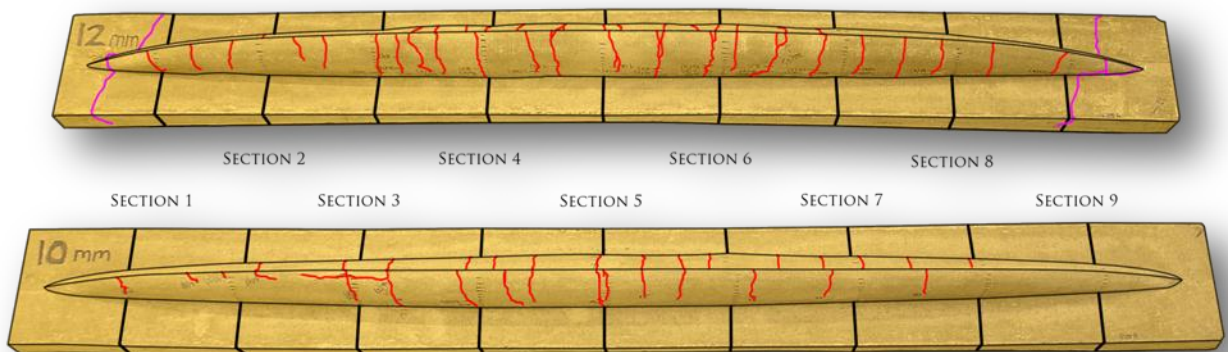
Figure 3.19 – Crack pattern and failure mode (Lee/Pedreschi)

Figure 3.20 – Failure detail (Lee/Pedreschi)

Separation of Web and Flange
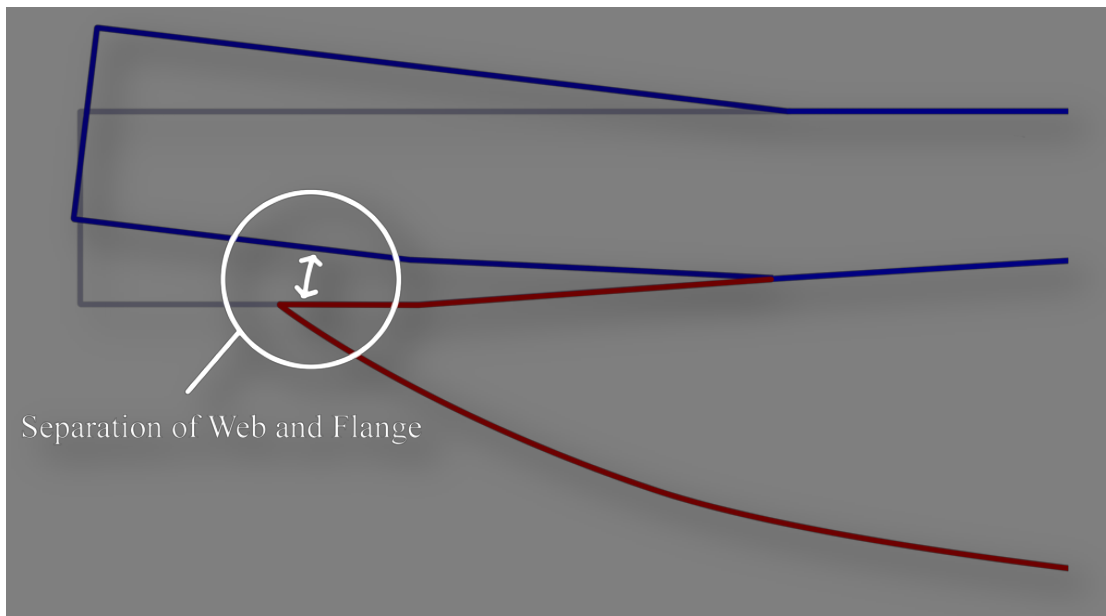
Figure 3.21 – Failure mechanism (Lee/Pedreschi)
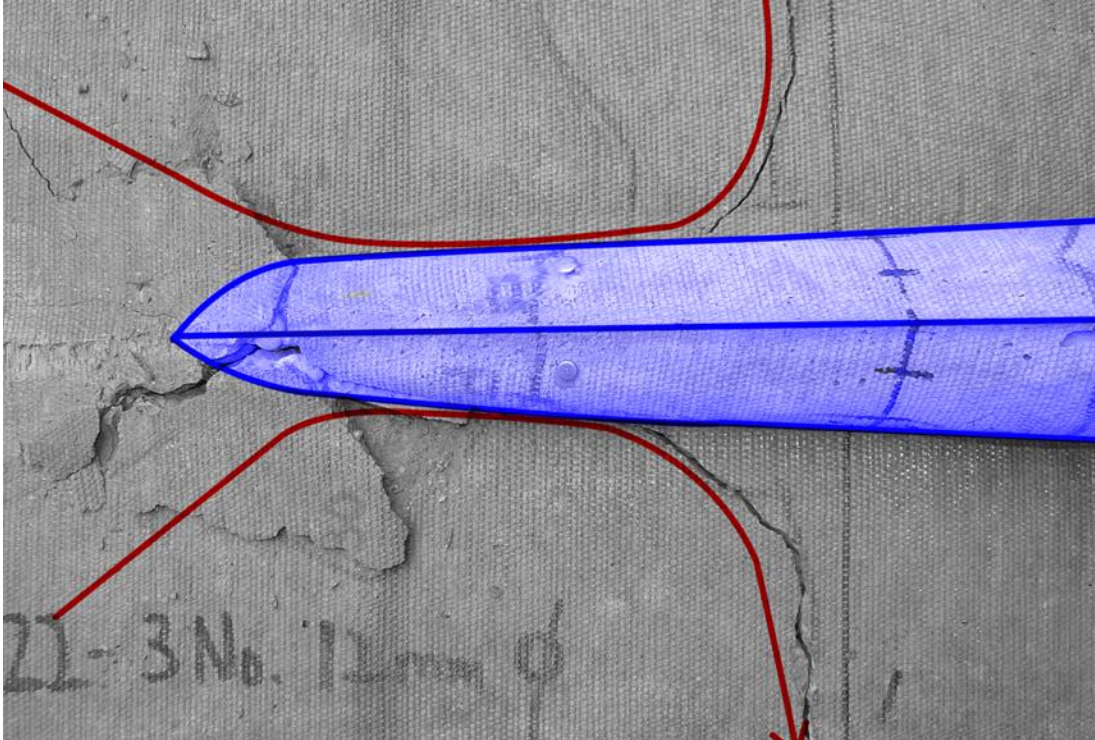
Figure 3.22 – Failure mechanism (Lee/Pedreschi)

Mr. Lee followed the following beam design cycle.
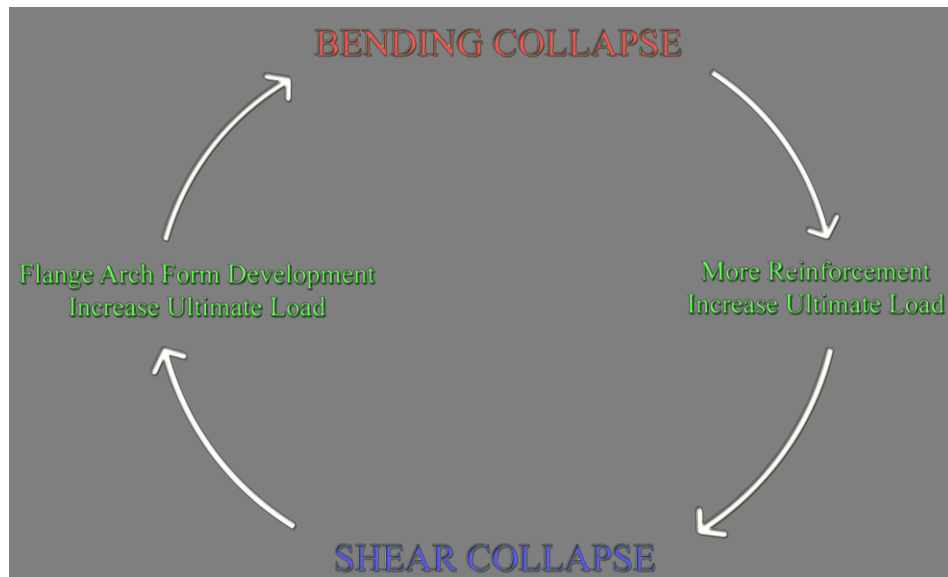
Figure 3.23 – Beam design cycle (Lee/Pedreschi)

In the beginning the failure mode was primarily shear failure which occurred suddenly. Pedreschi and Lee's main focus was to eliminate this type of failure in active-form beams. Through an iterative process Pedreschi and Lee fabricated several beams using the above strategy, designing various concrete and end detail profiles. They successfully managed to fabricate a beam with an effective concrete profile, reinforcing area and end anchor detail that failed in tension mode and demonstrated ductile behaviour. Figure 3.24 compares the applied bending moment and the beam capacity prior to the modification (first iteration of beams), and Figure 3.25 compares the applied moment and the beam's capacity after the modifications (last iteration of beams). As these figures illustrate the capacity of the beams increased considerably and the applied moment is below the moment capacity of the beam along the beam.
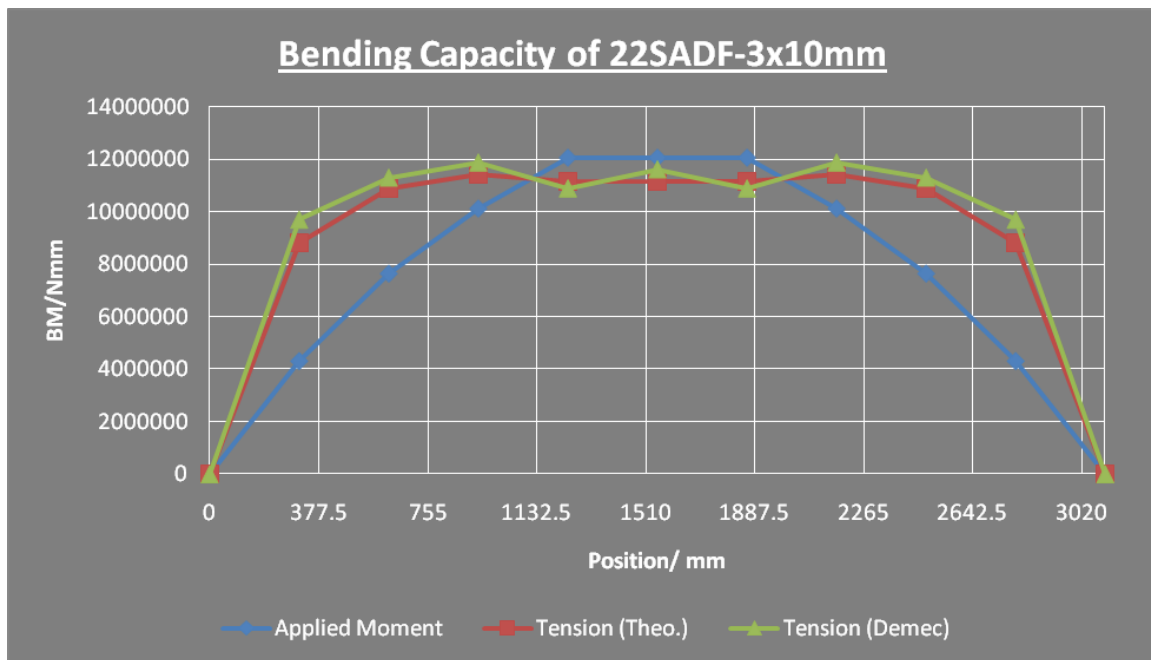
Figure 3.24 – Applied bending moment and beam capacity comparison
for the first generation of beams (Lee/Pedreschi)
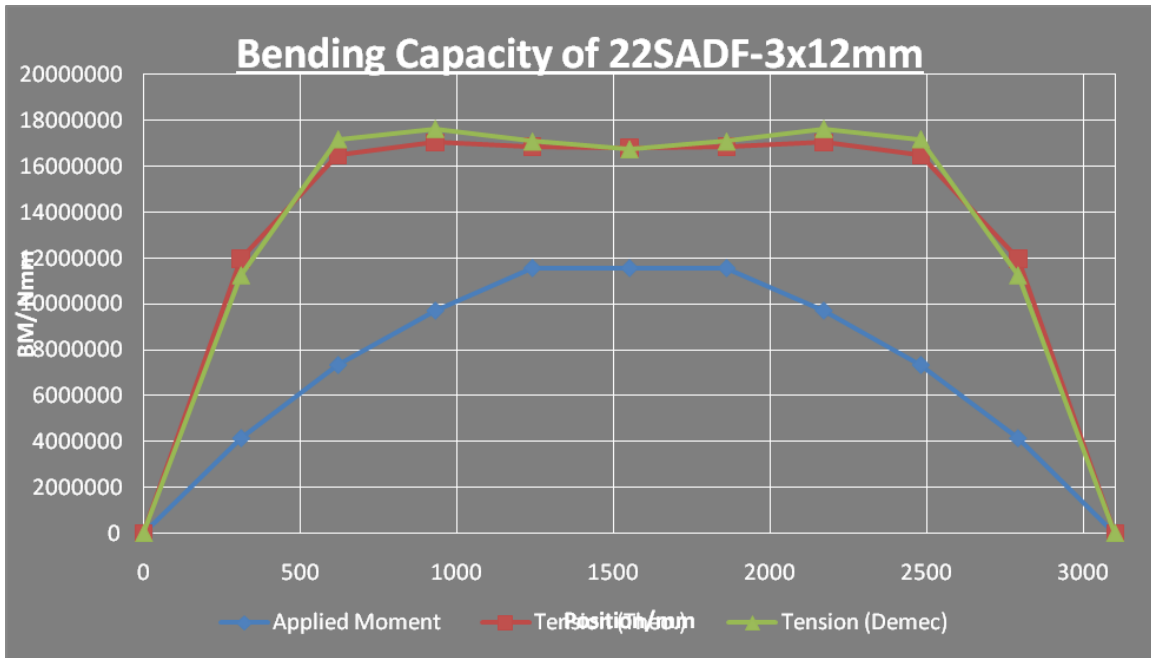
Figure 3.25 – Applied bending moment and beam capacity comparison
for the last generation of beams (Lee/Pedreschi)

More research in this area has been started in 2009 by Mr. John Orr, a Ph.D. student at the University of Bath. Mr. Orr's research will focus on reduction of concrete in the web of fabric-formed T-beams and form of the flange of beams, though Mr. Orr utilizes "shear" stirrups in his designs.

END OF SECTION

4   *Experimental Investigation and Test Setup*

The experimental work in the present thesis was conducted in the following three phases:

Phase I – Full-size rectangular beams and curved beams

Phase II – Quarter-length curved beams

Phase III – Full-size curved beams

Each phase consisted of formwork setup, construction of the beams, and testing. The same formwork was used for all phases of the experimental work with slight modifications. The following sections detail the experimental investigations as well as the formwork and construction of each phase.

Each phase consisted of one or more concrete pours. During each concrete pour at least three concrete cylinders were cast for each beam. The concrete cylinders were cured under the same condition as the beams and they were tested next day after the beam's test. The concrete property test data for individual beams are presented in Appendix B.

4.1   *Formwork Design and Fabrication*

The focus of this study is to investigate the behaviour of curved or active-form beams and compare them directly with conventional rectangular beams.   The reason for using wood formwork was to ensure that the rectangular cross-section was maintained thus providing test specimens with only one altered parameter – beam depth.   Beams constructed using fabric formwork will inherently have a curved cross section, making direct comparisons to conventional beams problematic.   Figure 4.1 shows a cross section of a concrete beam constructed using fabric formwork.   Theoretically, the size or shape of the cross curvature of the beam as it would be constructed by casting in fabric would not affect the beams behaviour after cracking since that would only change the depth of the compression block, though further research for verification is required.
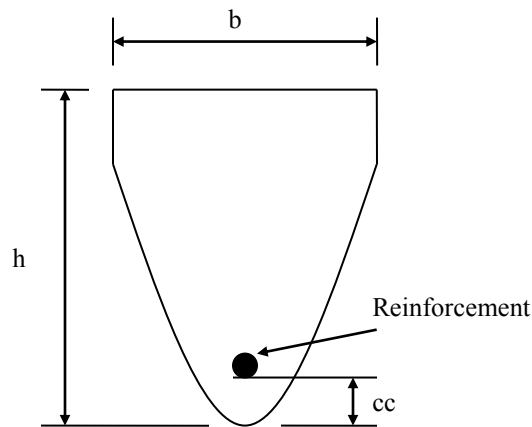
Figure 4.1 – General cross section of fabric-formed
concrete beam

Furthermore, this study is an investigation into the properties and behaviour of reinforced concrete beams with longitudinal curvature.   In order to direct the

research to this single variable, curvature had to be limited to the longitudinal direction. Wood formworks were constructed to produce beams with dimensions shown in Figures 4.2 and 4.3.
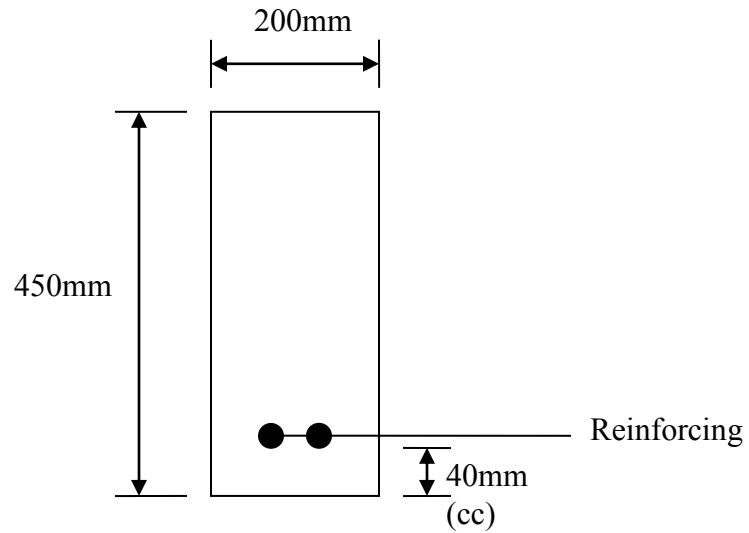
Figure 4.2 – General cross section of wood-formed
concrete curve beam at the centre
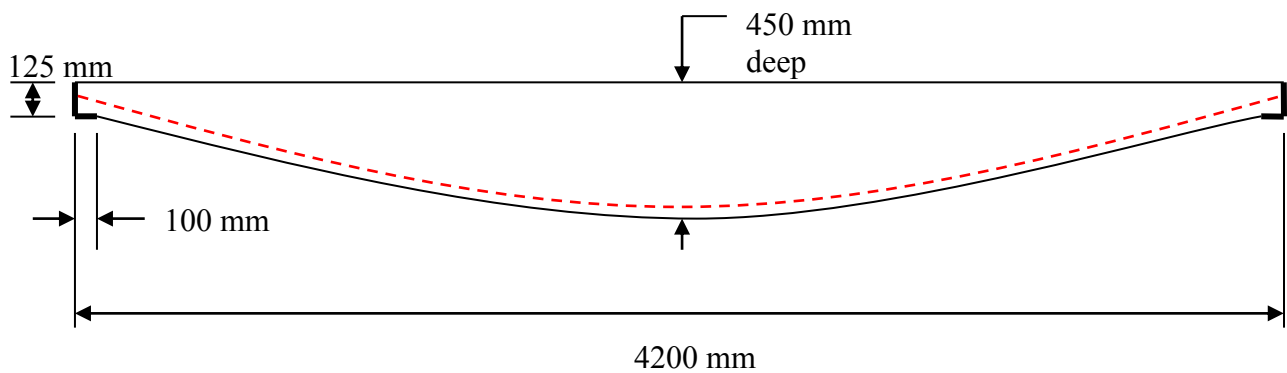
Figure 4.3 – Overall dimensions of concrete curve

Construction of the formwork was very straightforward as illustrated in the following figures. The curvature profile of the beams was a catenary curve which is the curve taken on by a heavy cable or rope of uniform density hanging between two points. The aspect ratio (span to depth ratio) of the beam as a catenary is materially indistinguishable from a parabola for a uniformly distributed load. The catenary provides a simple means of fabricating the beams that can be easily reproduced in a manufacturing shop or at the construction site.

Figures 4.4 through 4.7 demonstrate the curvature construction for the formwork. Figure 4.4 shows the profile of the curve beam with the hanging chain to mark the longitudinal curve.

Figure 4.4 – Catenary curve for the construction of formwork

Figure 4.5 – Drawing the beam profile on the side wall of the formwork
(scale 1:1)
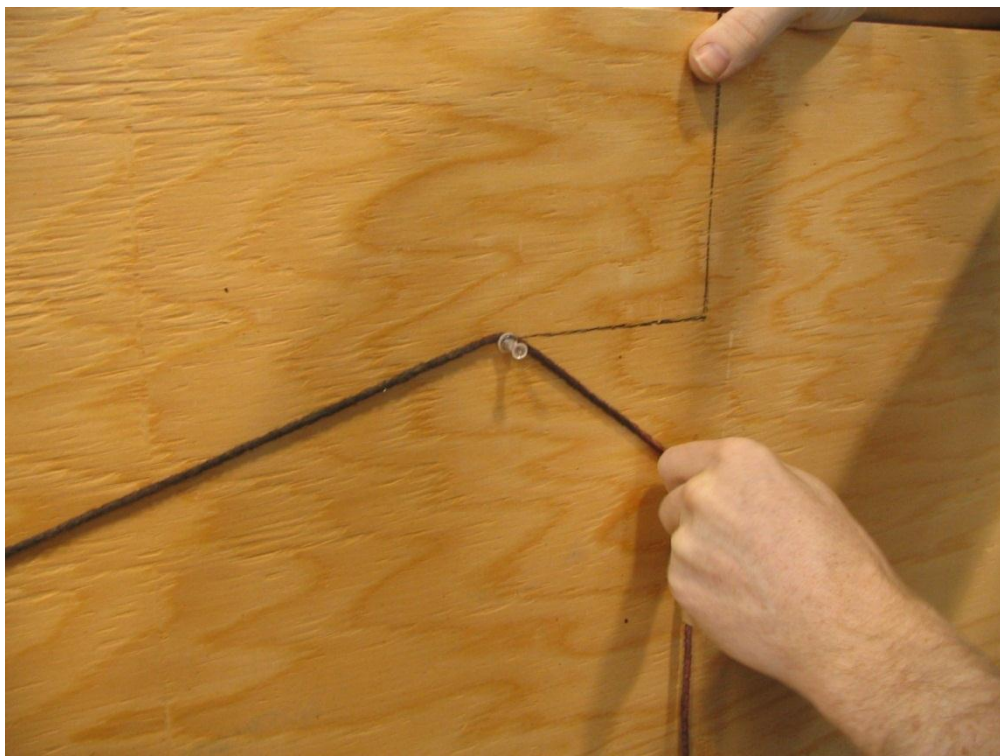
Figure 4.6 – Hanging a uniform density rope
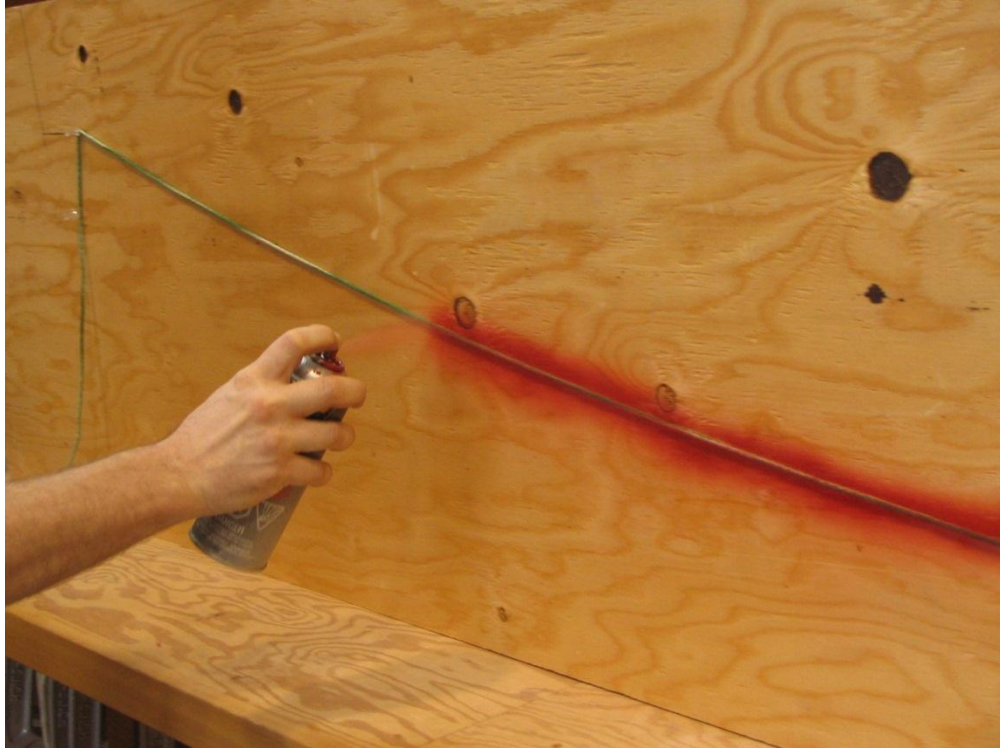
Figure 4.7 – Marking the curve on the plywood
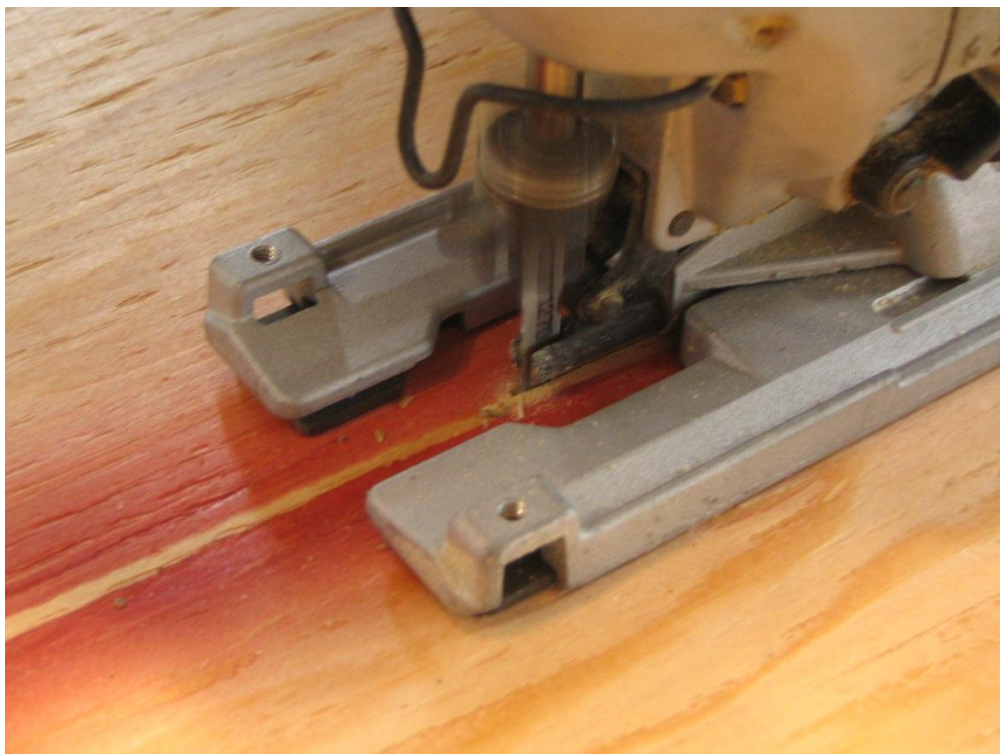
Figure 4.8 – Cutting the curve

Figure 4.9 – Fairing of the curve
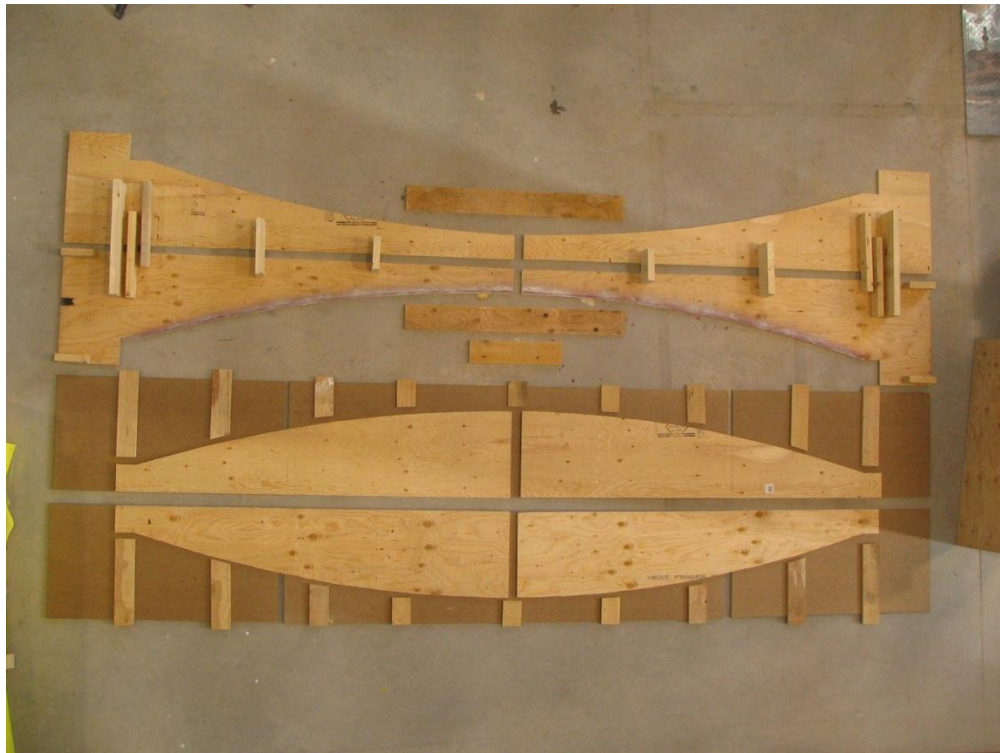
Figure 4.10 – All parts for the formwork of one beam

Figure 4.11 – Levelling the sides and quality control
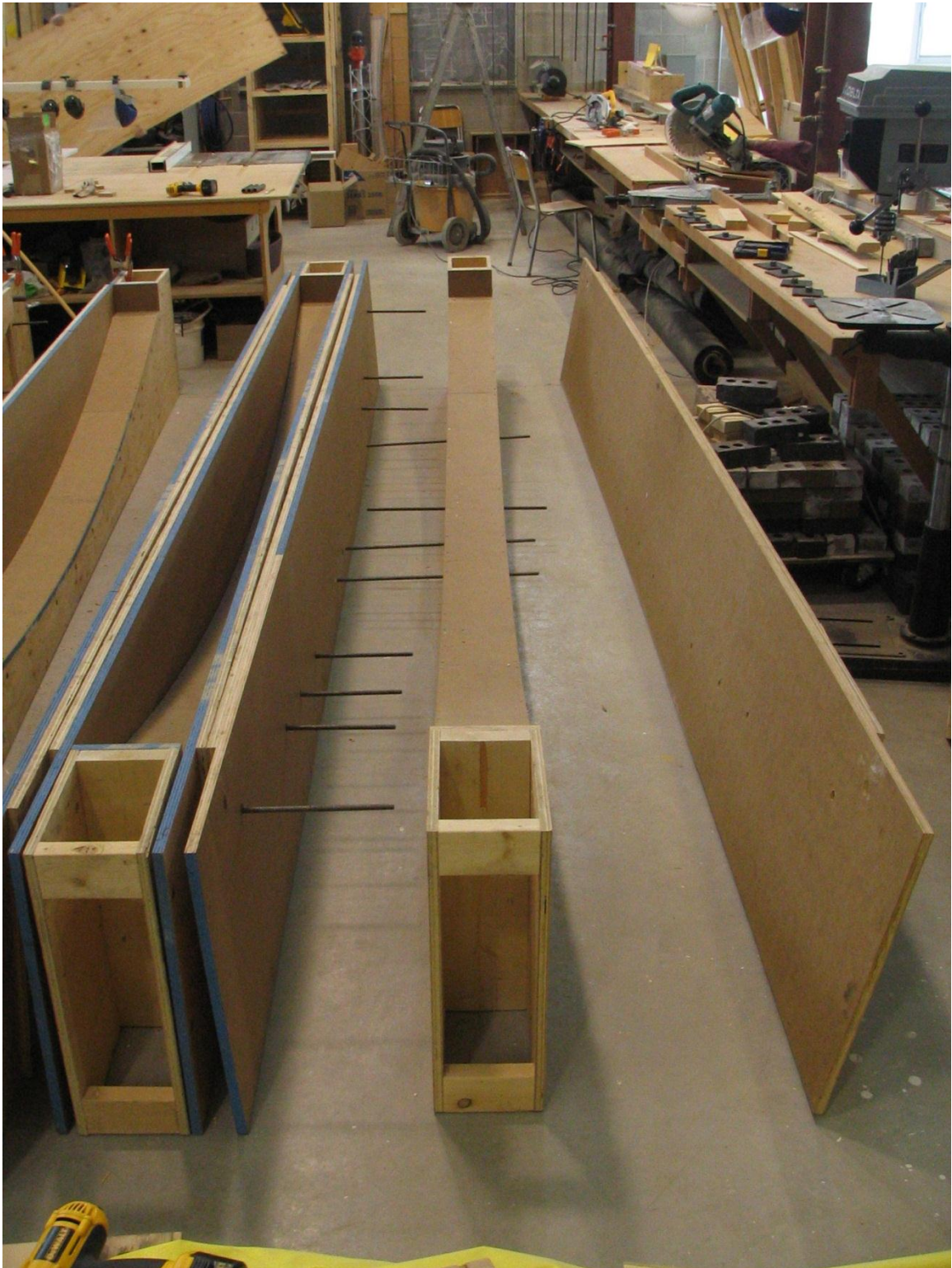
Figure 4.12 – Side wall and centre piece assembly
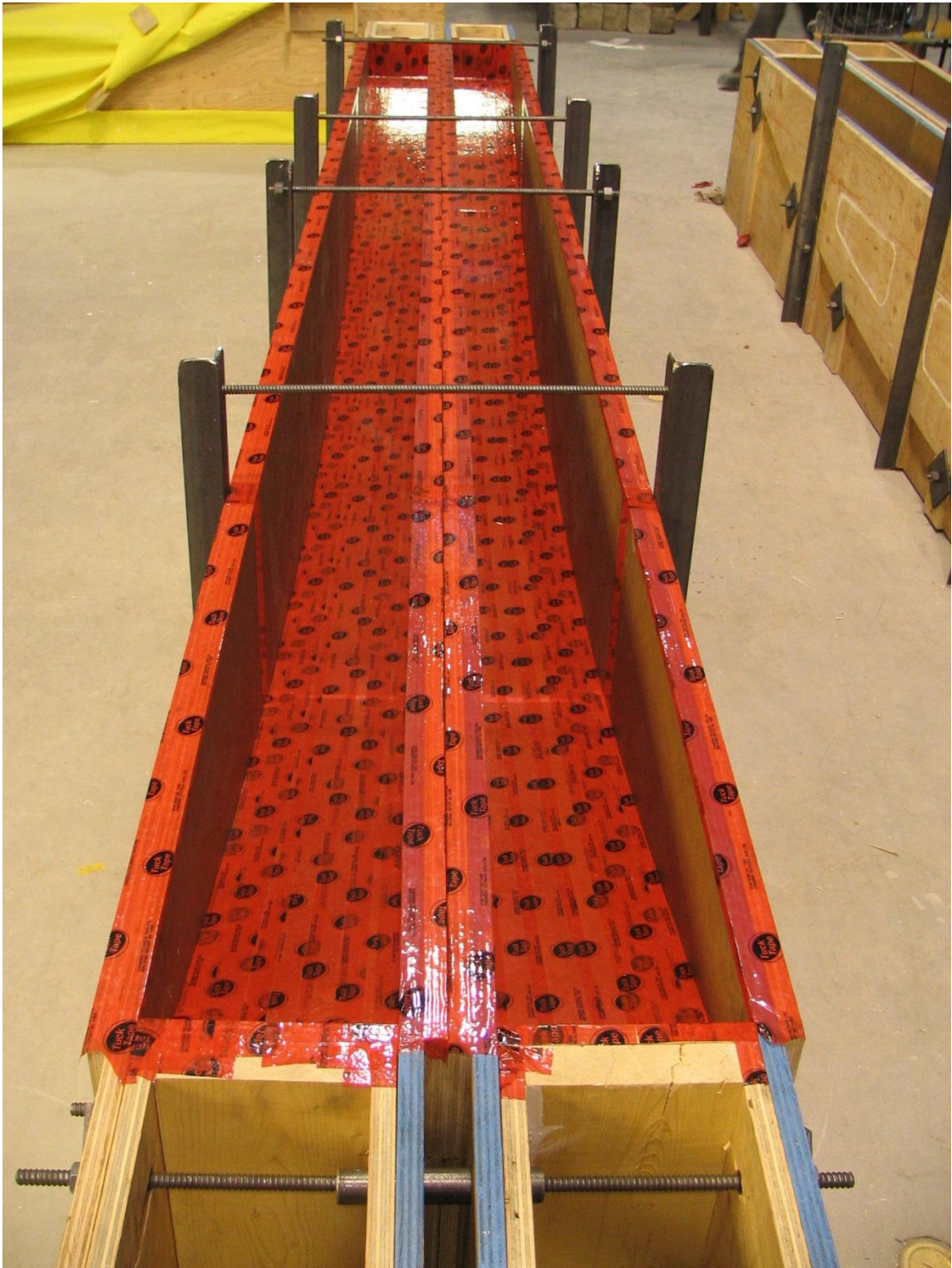
Figure 4.13 – Final formwork assembly for casting two beams side by side

4.2 *Phase I Test Setup – Full Size Beams*

In Phase I all beams were subjected to a six-point loading configuration. The bending moment diagram produced by this loading configuration is the closest to a true uniformly distributed load that can be produced in the laboratory. The six-point loading configurations for Phase I are shown in Figures 4.14 for curved beams and Figure 4.15 for rectangular beams. Figure 4.16 shows the actual test setup.

CB1, CB2, CB3, CCB1, and CCB2

Figure 4.14 – Loading configuration for curve beams

RB1, RB2, RB3, and RB4

Figure 4.15 – Loading configuration for rectangular beams
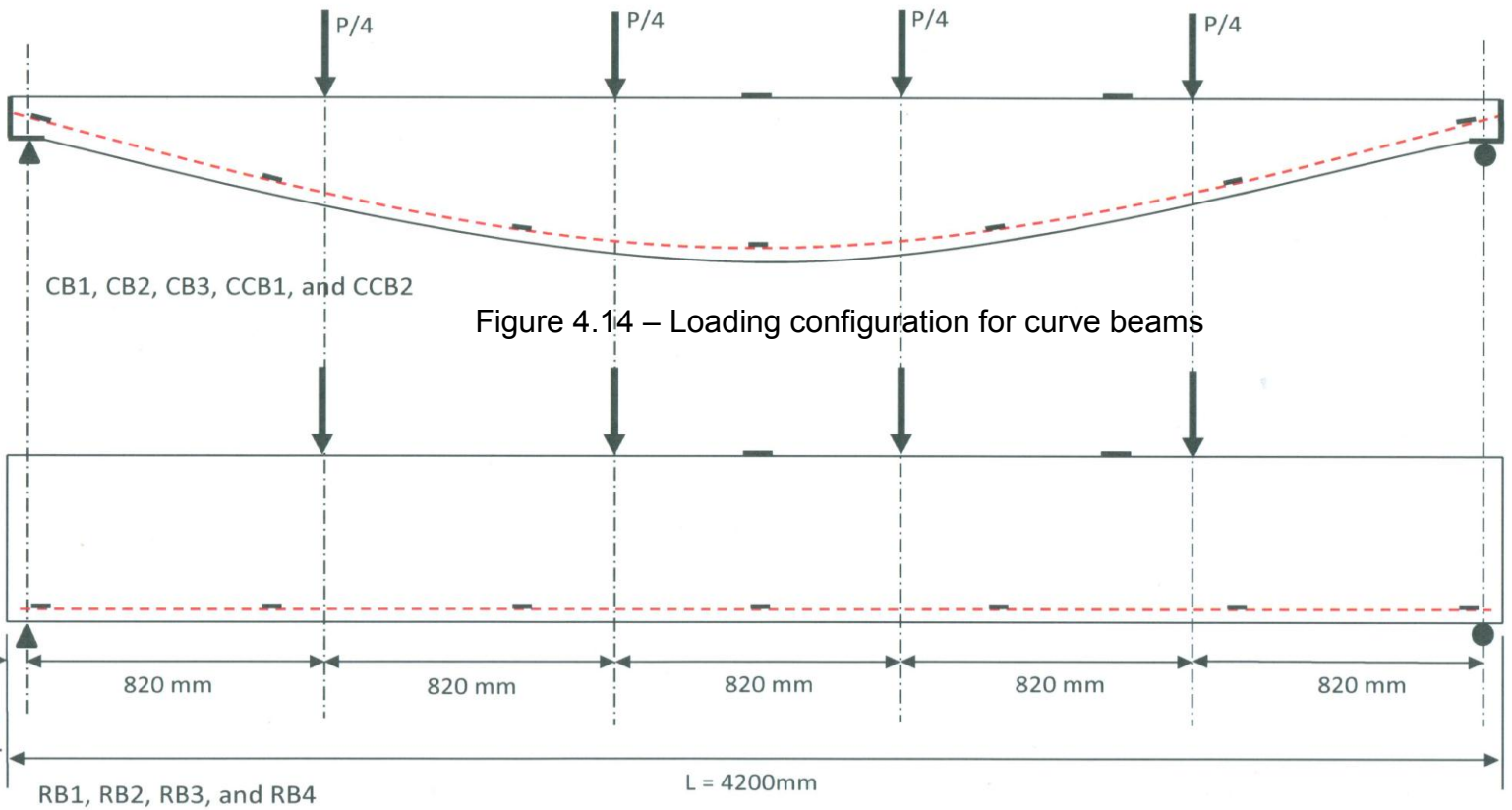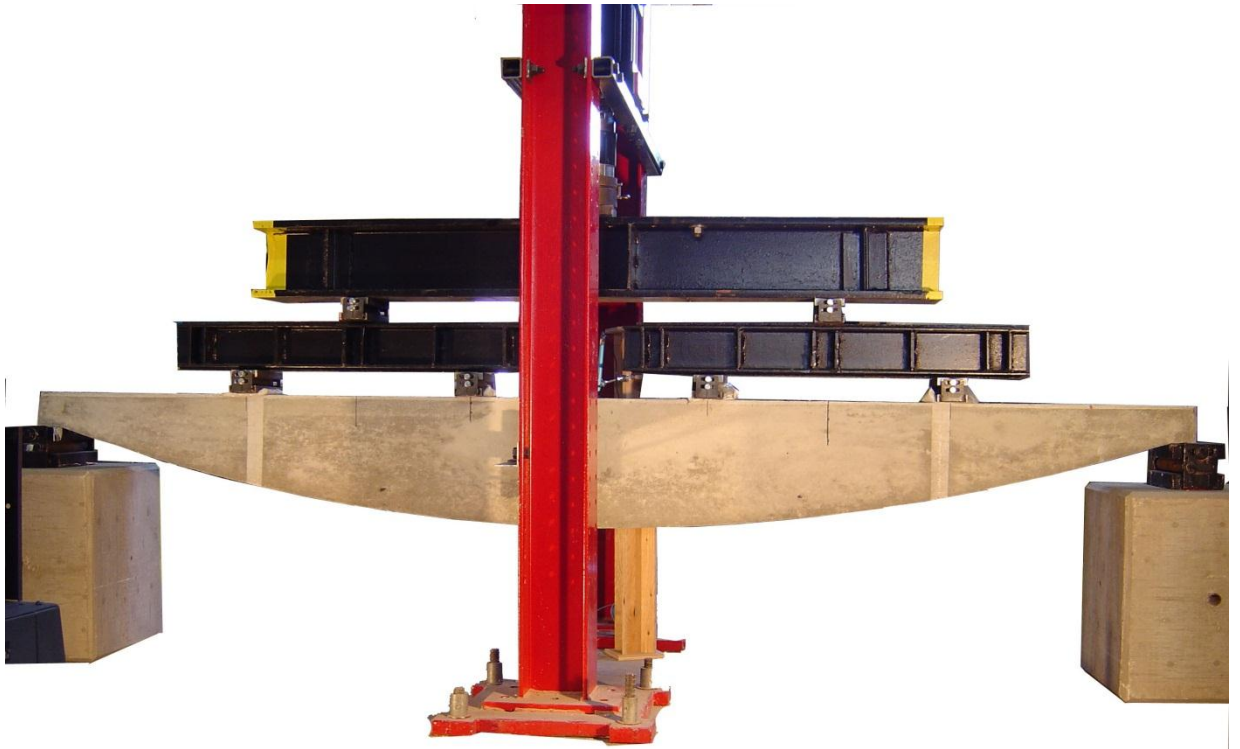
Figure 4.16 – Six-point loading configuration

4.3   Phase I Test Specimens

In Phase I of the project, seven 4200mm long beams were constructed and tested. Three of these were curved beams and four were rectangular beams. All curved beams had the same profile and reinforcing and the four rectangular beams had the same concrete profile but different reinforcing both in terms of quantity and profile. Design methodology will be discussed in the chapter on analysis. All beams in this phase were cast from same batch of concrete.

4.3.1 Curved Beams

The three Curved Beams (CB) in Phase I were fabricated and designated: CB1, CB2, and CB3. These beams had exactly the same dimensions and reinforcing profile. The curved beams were 4200mm long by 200mm wide; they were 450mm deep at the centre and 150mm deep at the support. One line of primary reinforcement was provided, with no other reinforcing in the beam.   The reinforcing and concrete followed the same catenary curve profile.   End-angles were placed at both ends of each beam. The reinforcing was welded to a 10mm weld plate which was a part of the end-angle. Figures 4.17, 4.18, 4.19, 4.20, and 4.21 show the dimensions of the beams, the fabrication process, end-angle detail, and the final fabricated beams.
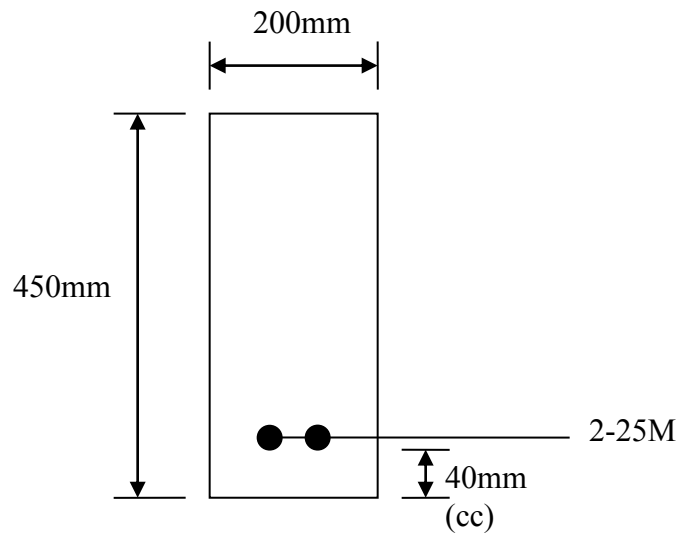
Figure 4.17 – Cross section of curved beam at the centre
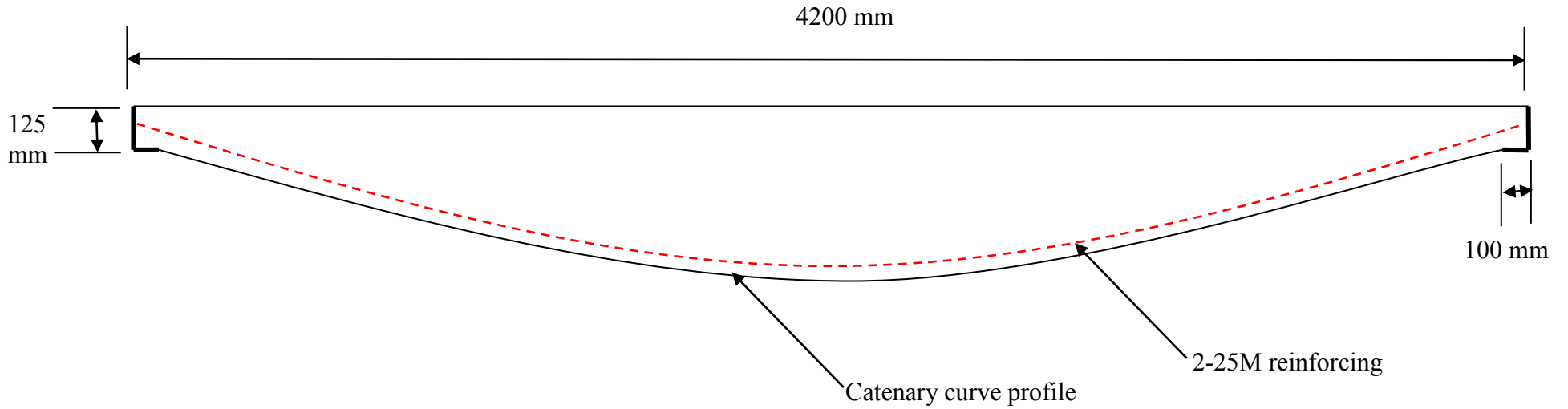
Figure 4.18 – Overall dimension of the Curved Beams. See also Figure 4.3
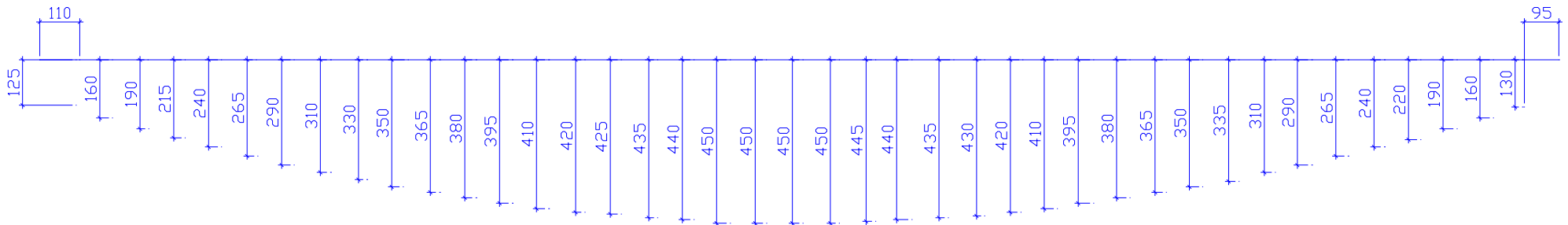
Figure 4.19 – Depth of the beam at 100mm intervals along the beam's length; depth of the catenary curve.

The end-angle consisted of a L125X100X10. Two 100X90X10mm thick plates were welded to the angle to receive the reinforcing. In phase I of the experiments, the weld plates were welded to the inside of the end-angle. Figure 4.20 and 4.21 show the end angle detail, and Figures 4.22 through 4.26 illustrate preparations and final fabrication of the beams.
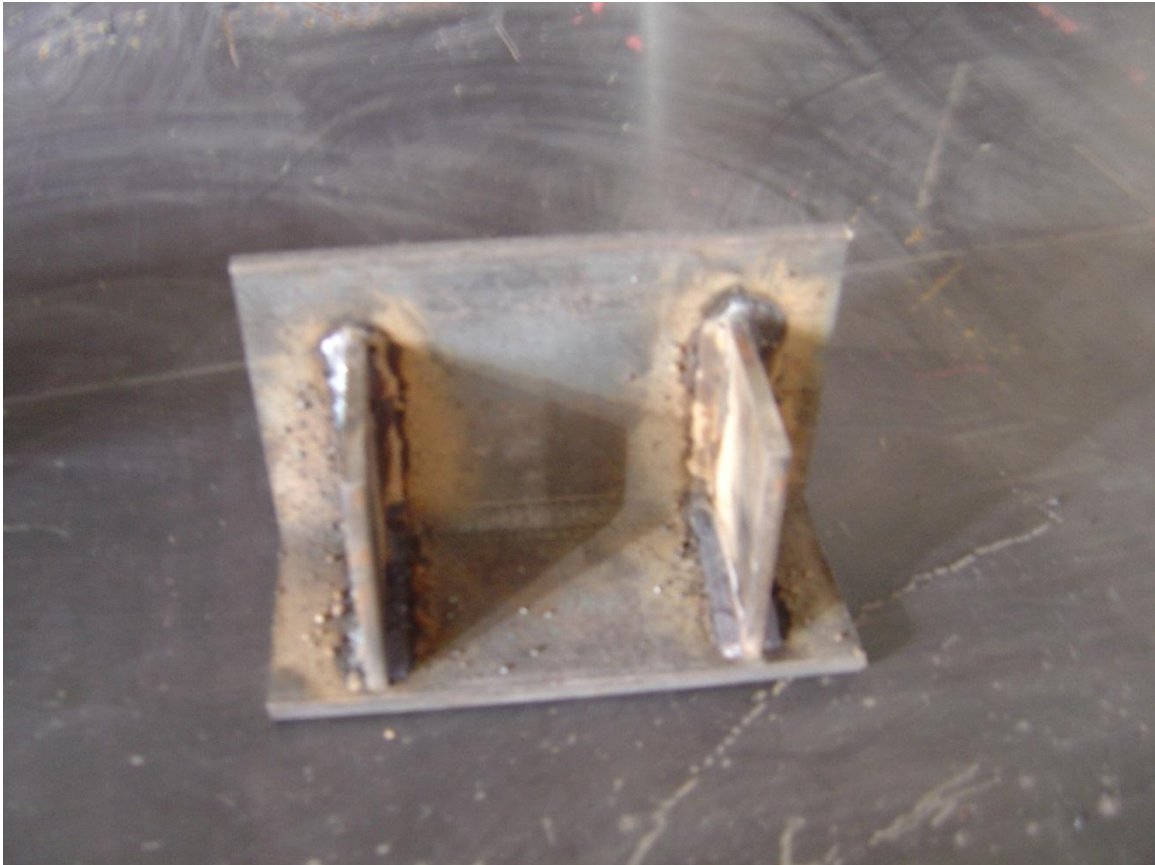
Figure 4.20 – End-angle complete with 10mm weld plates

End-Angle L125x100x10

Weld Plate
100x90x10
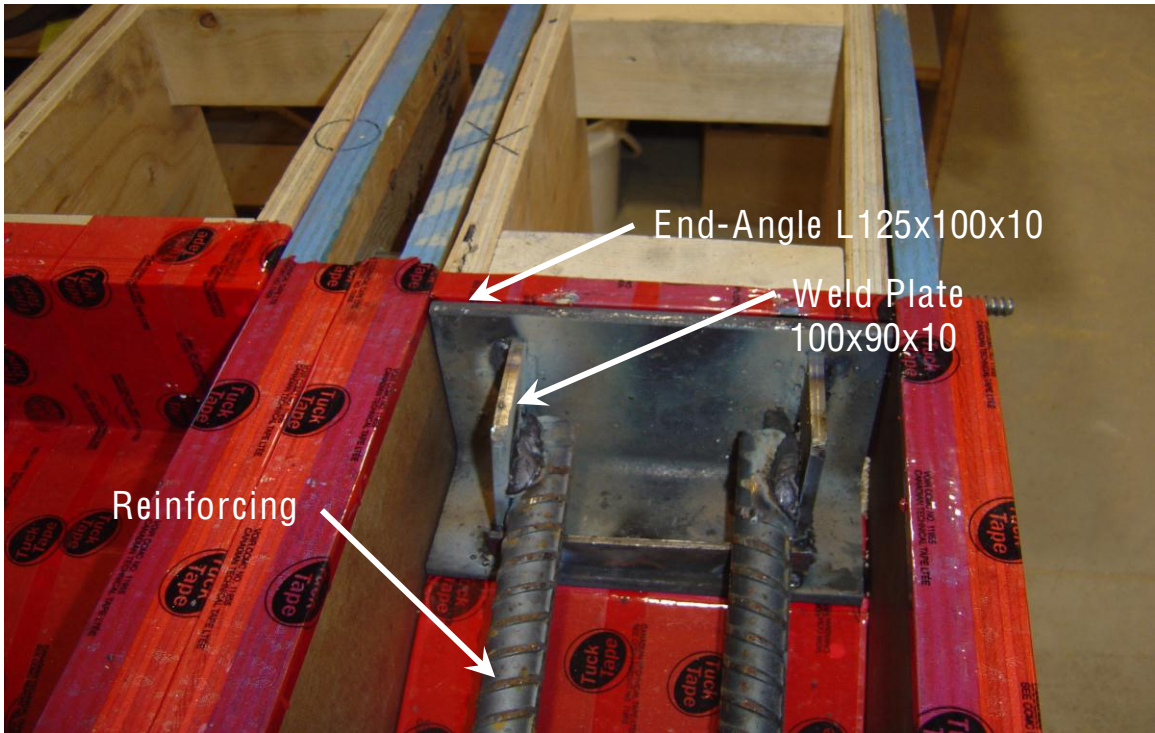
Reinforcing

Figure 4.21 – End-angle in place and welded to the reinforcing

Figure 4.22 – Reinforcement preparation, 2-25M bars

Figure 4.23 – Preparing reinforcement for strain gauge installation

Figure 4.24 – Reinforcement placement in formwork

Figure 4.25 – Showing the three steel rods that were used to spring the reinforcing in place to maintain the catenary curvature prior and during the concrete placement

Figure 4.26 – Shows the beams right after concrete placement. The curing process for these and all other beams consisted of covering the beams with a sheet of poly-plastic for three days and testing after 28 days or more. No testing was conducted before the 28 day curing period was complete. Three concrete cylinders were cast for each beam to determine f'$_c$ of each beam

4.3.2 Rectangular Beams

In Phase I of this project, three Rectangular Beams, RB1, RB2 and RB3, were fabricated along with the curved beams. The three rectangular beams had the same concrete profile and primary dimensions (maximum depth and span) but different reinforcement quantity and profile. Overall concrete dimensions for these beams are shown in Figures 4.27 and 4.28.
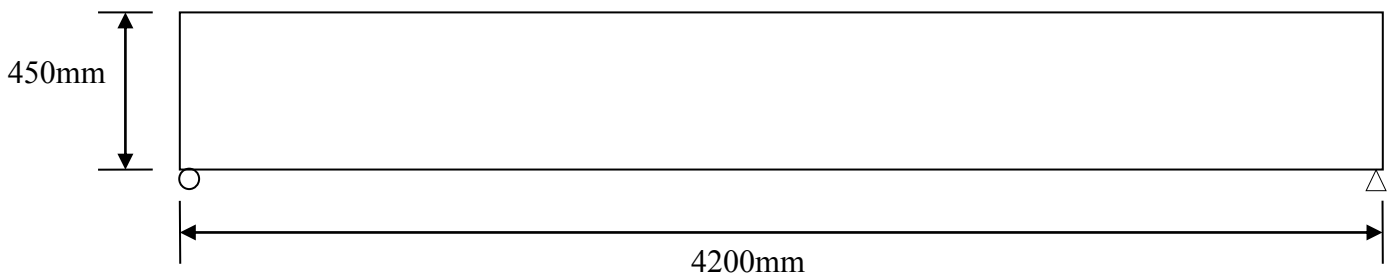
Figure 4.27 – Rectangular beam elevation view
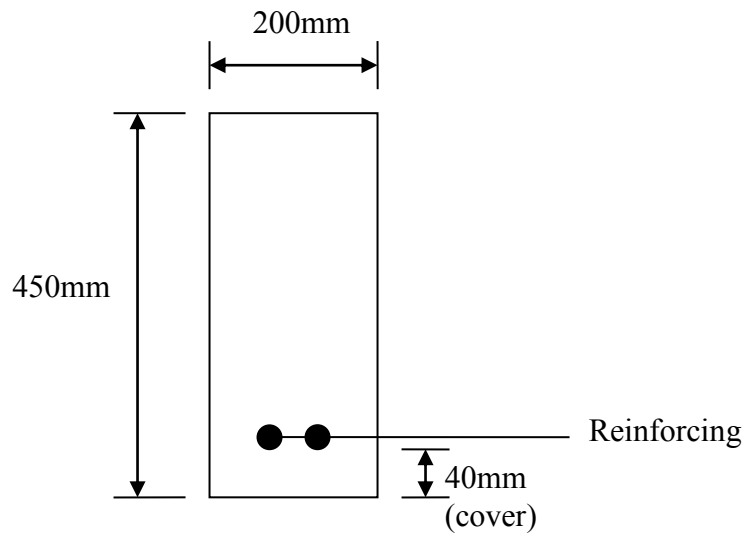
Figure 4.28 – Rectangular beam cross sectional view

RB1 was the first rectangular beam to be tested. This beam had only horizontal reinforcing at the bottom. The horizontal reinforcing consisted of two 25M bars – the same quantity of steel as the curved beams CB1, CB2 and CB3. The purpose of this beam was to study a pure shear failure mode since this beam, like its curved counter parts, had no shear reinforcement. Figure 4.29 shows the reinforcing profile and loading pattern.
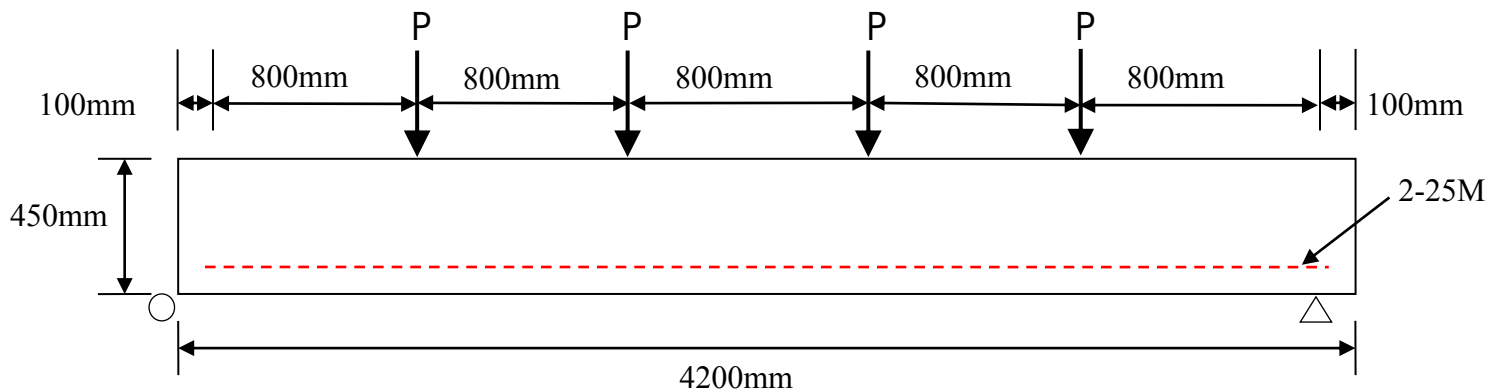
Figure 4.29 – RB1 reinforcing profile and loading pattern

RB2 was a rectangular beam also reinforced with two 25M reinforcing bars. However, the bars follow the same catenary curve profile as the curved beams. Figure 4.30 shows the reinforcing profile for RB2. The purpose of this beam was
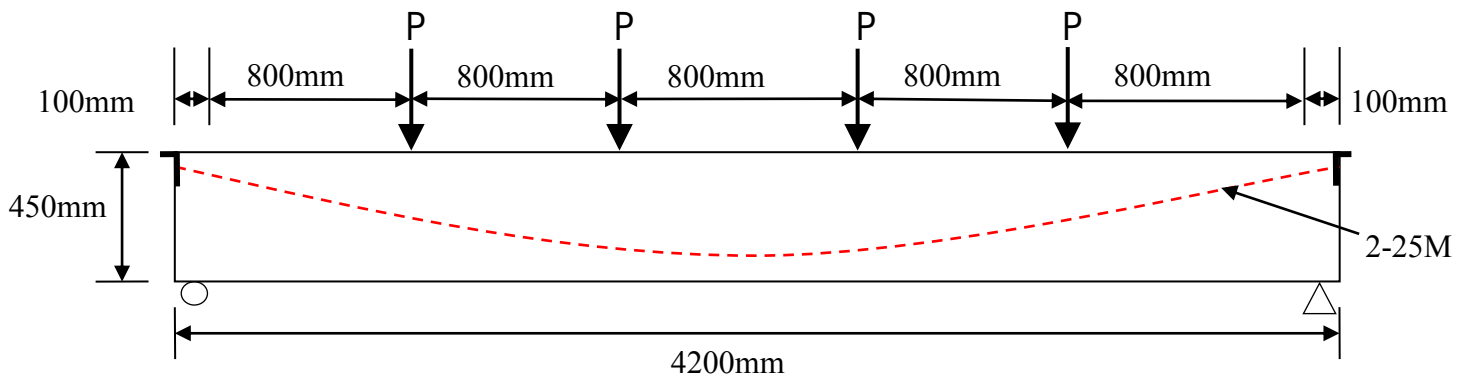
Figure 4.30 – RB2 reinforcing profile and loading pattern

to study the effect of curved reinforcing within a uniform section rectangular concrete beam. As with the curved beams, the reinforcing in this beam was also confined and welded to the end-angle to create a closed system of internal forces. Figure 4.31 shows formwork and reinforcing for both RB1 and RB2. Figure 4.32 shows the end-angle detail for RB2.
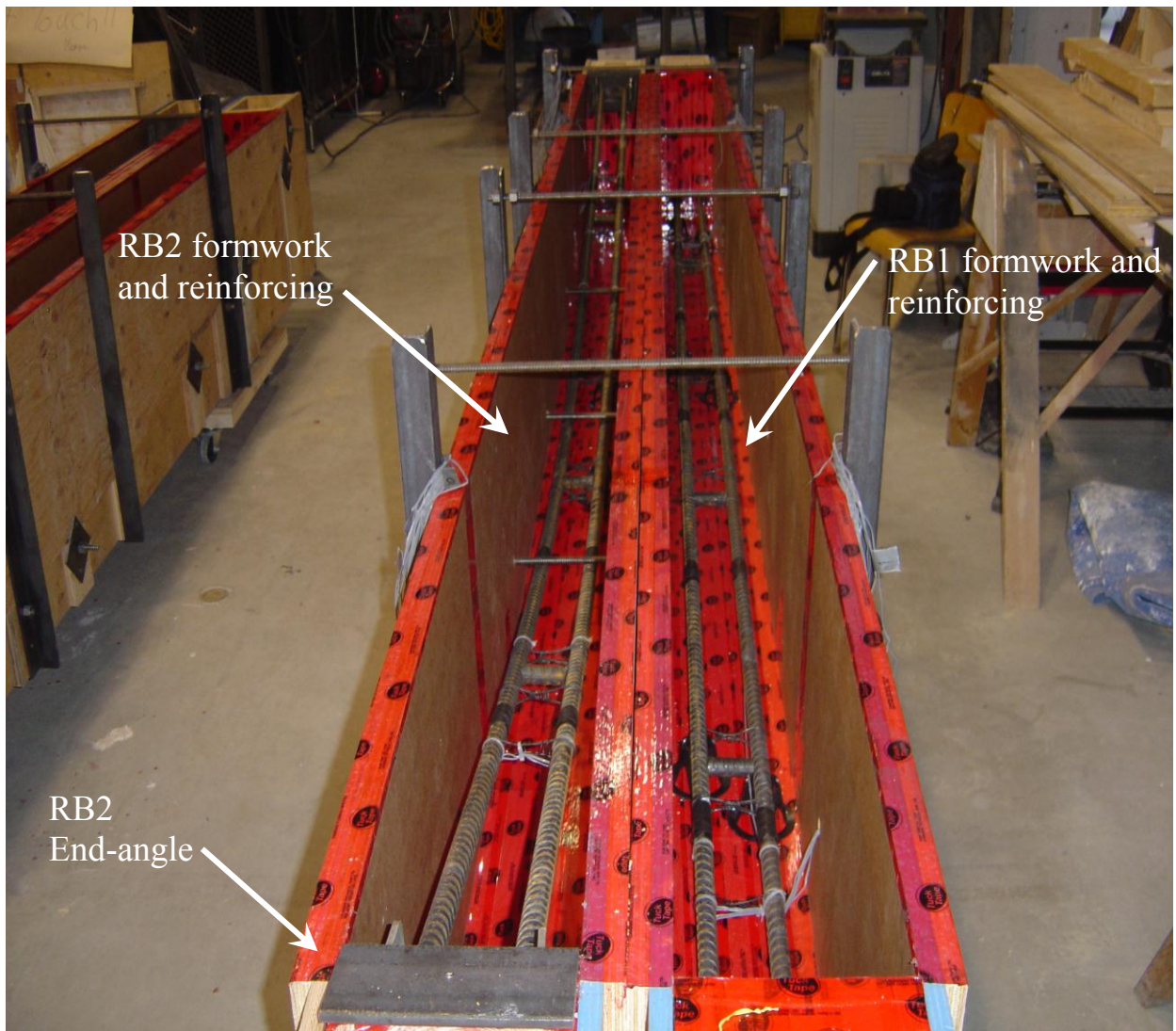
Figure 4.31 – Formwork and reinforcing in RB1 and RB 2
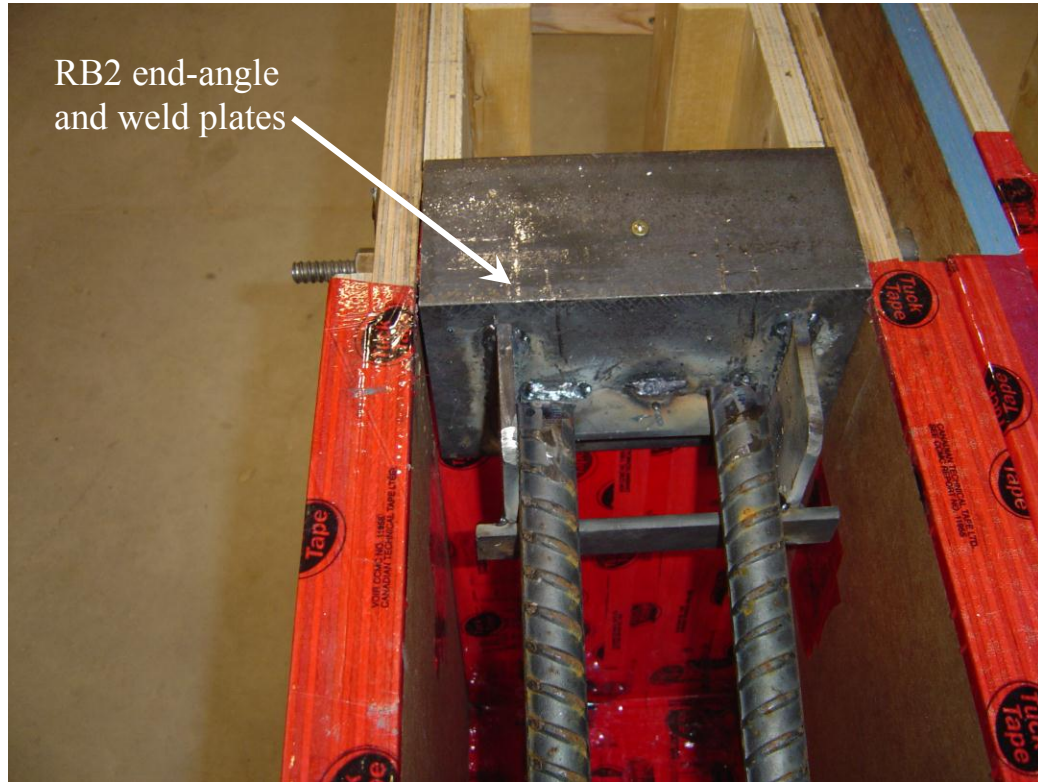
Figure 4.32 – End-angle detail for RB2

RB4 was the last rectangular beam with same amount of flexural reinforcement as the rest of the beams (2-25M) placed at the bottom of the beam the same as RB1 and RB3. The reinforcing bars in RB4 where welded to a weld angle at each end similar to the curved beams. Figure 4.33 shows RB4's reinforcing profile.
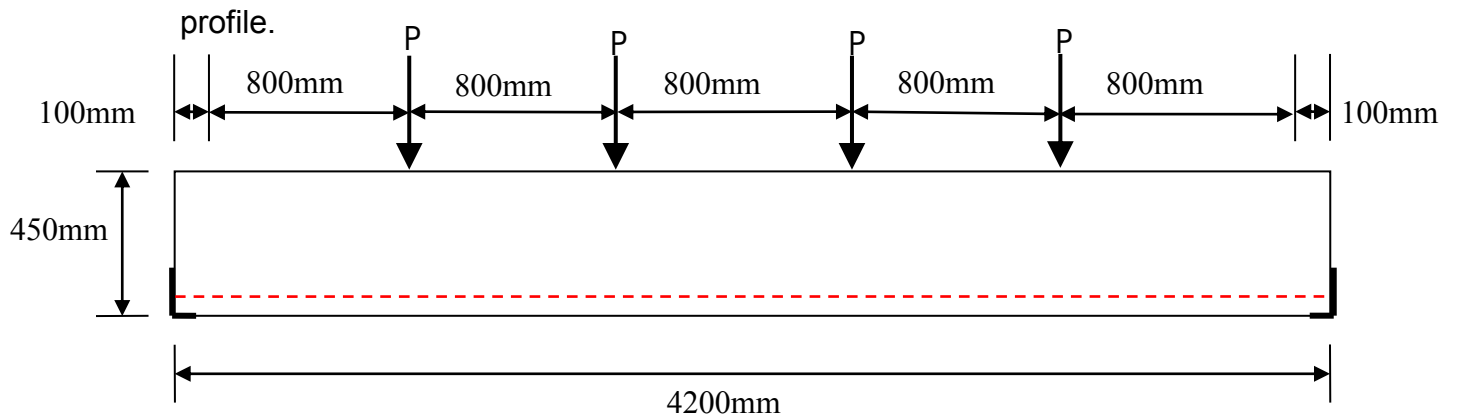
Figure 4.33 – RB4 reinforcing profile and loading pattern

Figure 4.34 shows the end detail of RB4. The flexural reinforcing is welded to an end-angle at each support to create closed path for the internal forces.

Figure 4.34 – End-angle detail for RB4

To monitor the "shear" development in the area close to the support, five strain gauges were installed on one end of the beam, as shown in Figure 4.35.
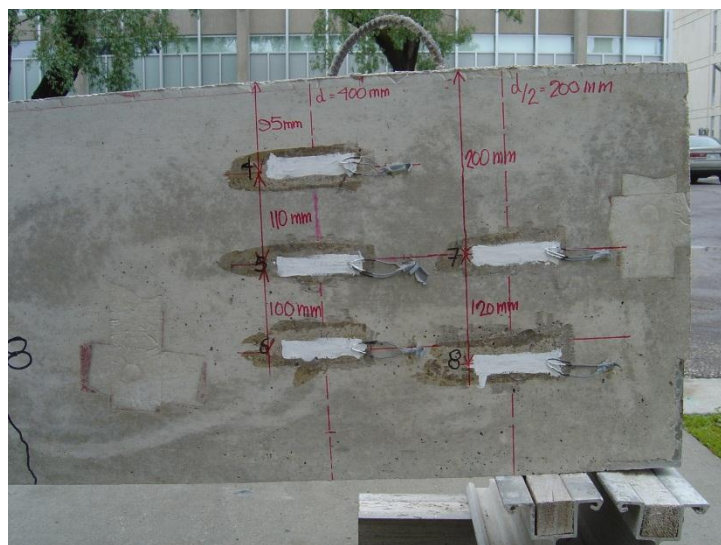
Figure 4.35 – Strain gauges close to the support to monitor "Shear"

4.3.3 Control Beam

RB3 was designed and fabricated in accordance with the CSA Standard A23.3 code for comparing the curved-beams' performance with a conventionally designed rectangular beam. RB3 was designed with the same amount of flexural reinforcements as the curved beams (2-25M reinforcing bars). Shear reinforcing was also placed in RB3 in accordance with Section 11 of CSA standard A23.3. Figures 4.36 and 4.37 show RB3. A 2.5mm diameter rod was used at the top to hold the stirrups prior to and during concrete placement.
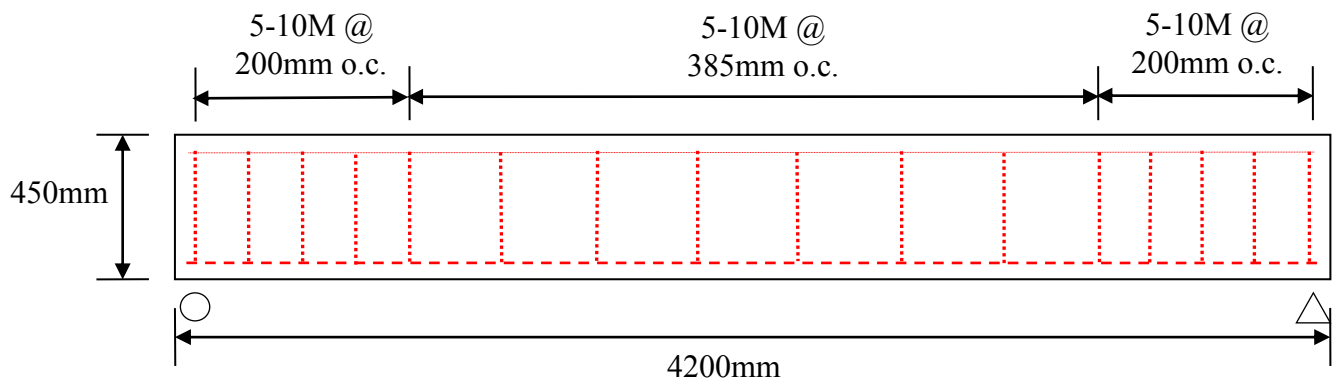
Figure 4.36 – RB3 overall dimensions and stirrup locations, elevation view
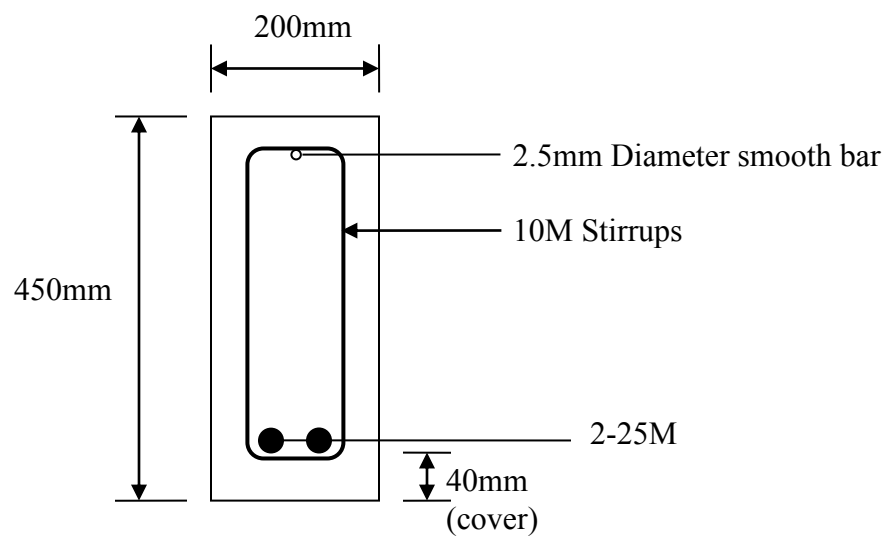
Figure 4.37 – RB3 cross sectional view

Phase II Test Setup – Quarter Length End-beams

FEM analysis in Phase I showed the mode of failure of the curved-beams, and experimental testing clearly confirmed these numerical findings. The failures were always at one end of the beams due to deflection resulting in rotation at the end support, as described in detail in chapter 5 – Experimental Results.

To further investigate the end failure and to experiment with the effects of different end support conditions, Phase II of the project was developed. In Phase II, eight (8) end-beams were fabricated, each with a different end support condition and additional steel to explore the possibilities of resolving or entirely avoiding the end failure without adding shear reinforcing stirrups.   The following sections 4.5 and 4.6 explain the general configuration of the end beams and testing setup while the test results will be presented in Chapter 5. Figure 4.38 shows the overall size and configuration for the end-beams.
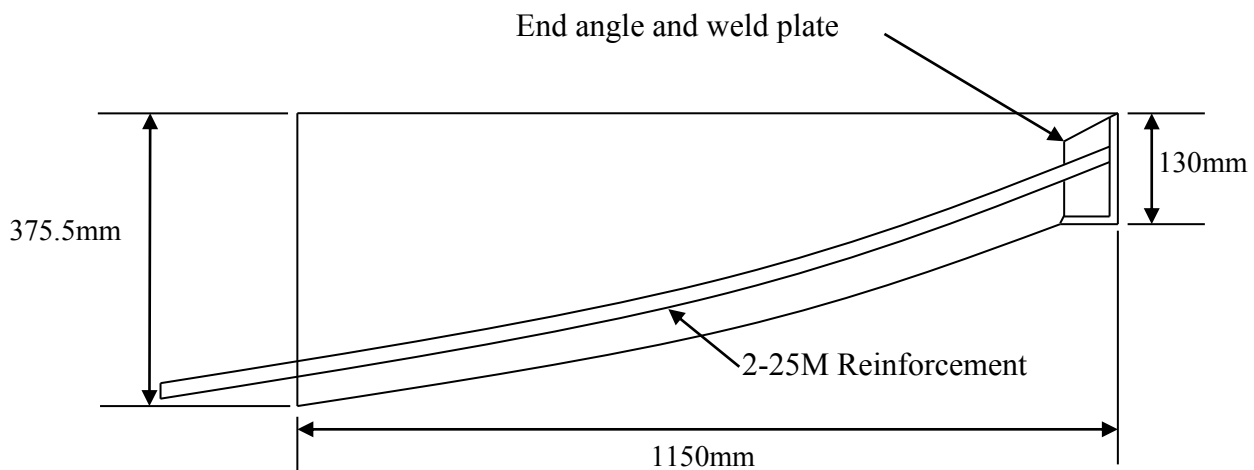
Figure 4.38 – Overall concrete dimensions for the end-beams (NTS), 25mm concrete cover (cc)

4.5   Phase II Test Specimens

In Phase II, eight (8) end-beams were constructed; their numbers and designations are as follows:

1-   Two end-beams exactly similar to the previous curved beams to verify the testing setup and results. These beams were designated as End Curve Beam: ECB1 and ECB2 (Figure 4.39).

2-   Two end-beams with end angles reversed. These beams were designated as End Curve Beams (with) Reverse Angle: ECB-RA1 and ECB-RA2 (Figures 4.40, 4.41 and 4.42).

3-   Two end-beams with top steel for additional reinforcement. These beams were designated as End Curve Beams (with) Top Steel: ECB-TS1 and ECB-TS2 (Figures 4.43 and 4.44).

4-   Two end-beams with end angles reversed and top reinforcement. These beams were designated as End Curve Beam (with) Top Steel (and) Reverse Angle: ECB-TS-RA1 and ECB-TS-RA2 (Figures 4.45 and 4.46).

Figure 4.39 – ECB1 and ECB2

Figure 4.40 – ECB-RA1 and ECB-RA2

Figure 4.41 – End-angle configuration for ECB-RA1 and ECB-RA2.

375.5mm

130mm

1150mm
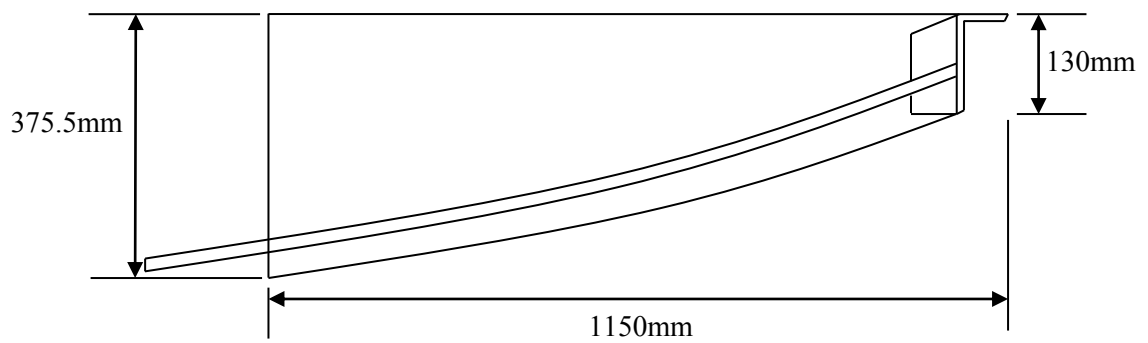
Figure 4.42 – ECB-RA1 and 2 (25mm concrete cover)

2-15M Top reinforcement

375.5mm

130mm

1150mm
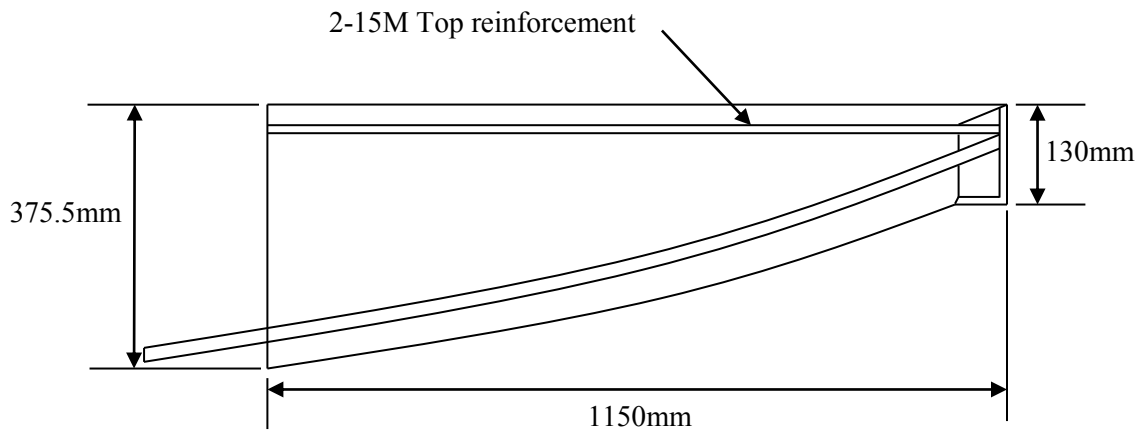
Figure 4.43 – ECB-TS1 and 2 (25mm concrete cover)

Figure 4.44 – ECB-TS1 prior to concrete pour
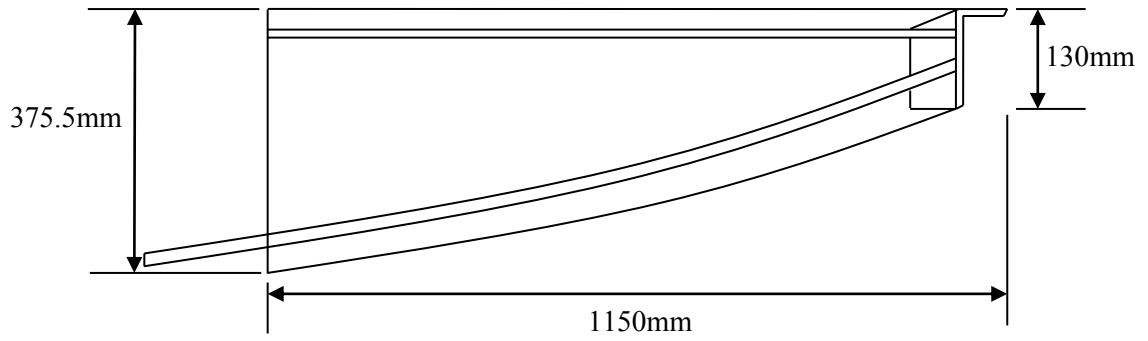
Figure 4.45 – ECB-TS-RA1 and 2 (25mm concrete cover)

375.5mm

130mm

1150mm

Figure 4.46 – ECB-TS-RA1 prior to concrete pour

4.6   Testing Frame and Configuration

The end-beams were tested upside down to replicate the same end condition as the full-size curved beams. Figure 4.47 shows the end-beams test setup.
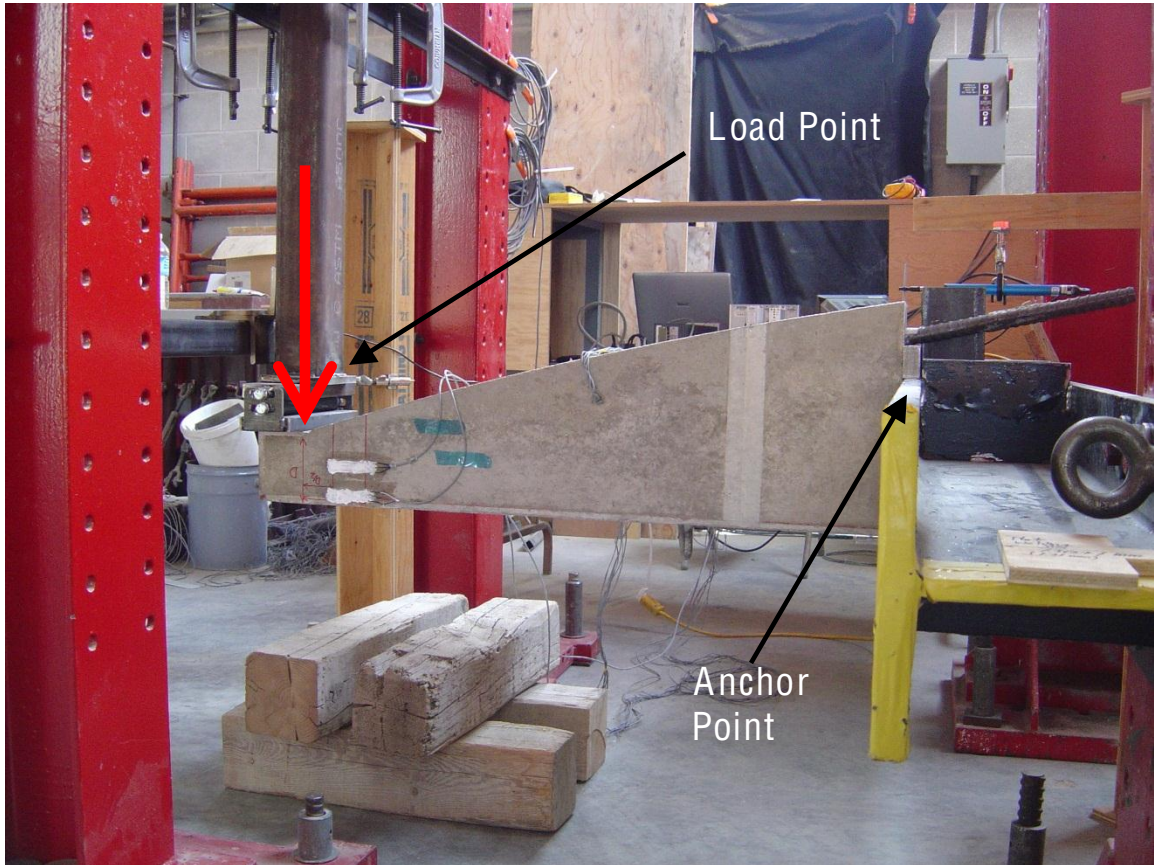
Figure 4.47 – Testing frame and testing configuration for end-beams

Due to the shorter length of the end-beams, only 3 strain gauges were installed exactly at the same locations as strain gauges 1, 2, and 3 for the full-size curved beams.

Two concrete strain gauges were also installed on the side of the end-beams to monitor the compression stress strain.   The location of the concrete strain gauges is illustrated above in Figure 4.47, and in detail in Figure 4.48.
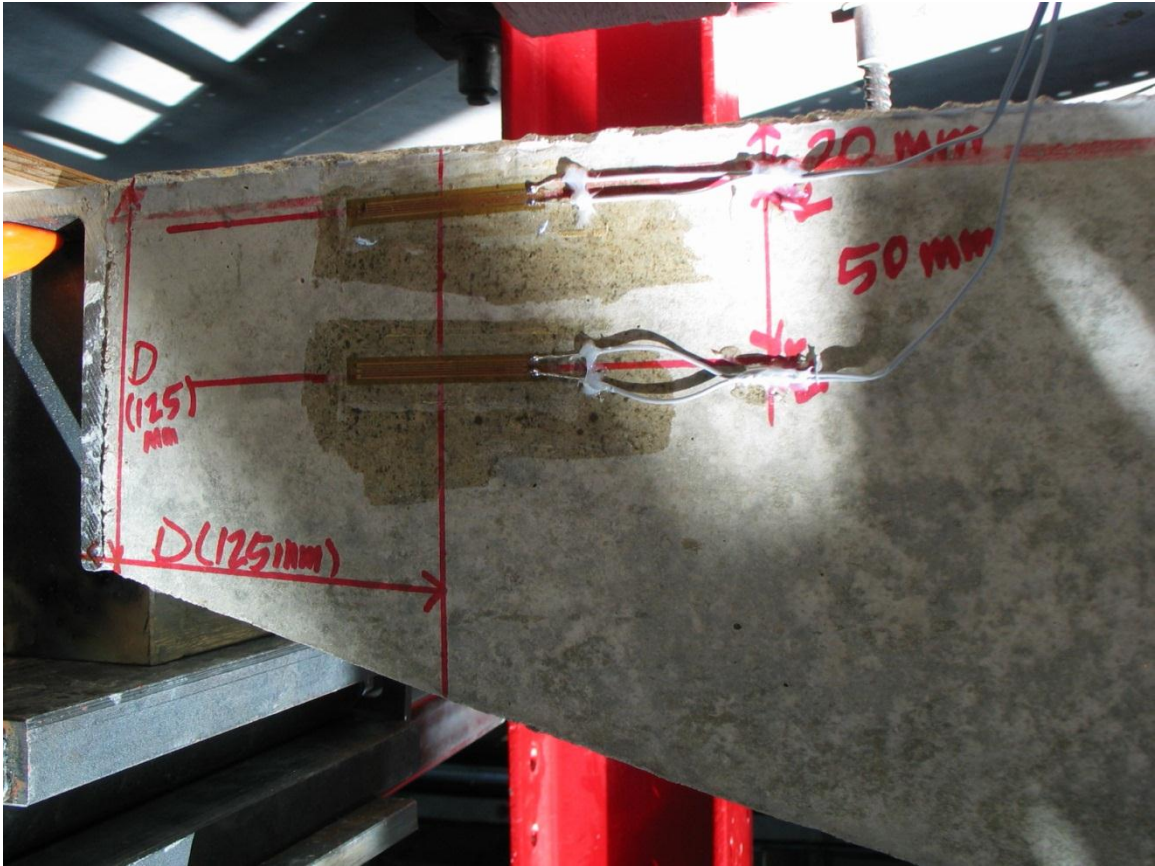
Figure 4.48 – Location of concrete strain gauges (ECB-RA1 shown)

The result of the testing of the end-beams will be presented in Chapter 5 – Experimental Results.

## 4.7	*Phase III Test Setup – Cambered Full-Size Curved Beams*

Phase III of the testing consisted of two full-size (4200mm) beams with a camber on top. The end-beam experiments showed that the additional compression steel and reverse angle were not effective solutions to the flexibility and failure mode of the beams. The Phase II testing was formulated with the anticipation that the end-beam study would provide a solution to this issue. The force/stress path studies together with the FEM analysis suggested that adding camber at the top of the beam would increase the stiffness and reduce the overall deflection by providing and maintaining an effective compression force path in the top of the beam.

The following sections describe the Cambered Curved Beams' (CCB) configuration and testing setup and procedure.

## 4.8	*Phase III Test Specimens*

The curved beams in this phase were cambered at the top by adding a catenary curve (a curve created by a hanging chain) with a 100mm apex. The total length of the curve was 4200mm to match the length of the beams. A camber of 100mm was deemed to be practical since in a conventional reinforced concrete building the depth of the concrete slab above the beam would be more than 100mm (up to 200mm depending on the framing system) allowing this amount of camber to be "absorbed" in the depth of a floor slab. 100mm camber is large enough to provide a path for the primary compression stress during the testing, but it is small enough to not appreciably increase the amount of concrete.

Adding 100mm camber increases the volume of concrete by less than 5%. Further studies are required to determine the optimum camber to provide an efficient primary compression path. This study should also investigate if the camber is necessarily proportional to the span of the beam. It is of the author's opinion that the camber would not be proportional to the span of the beam and could be optimized based on the design load and the load pattern.

The configuration of the CCBs is illustrated in Figure 4.49.
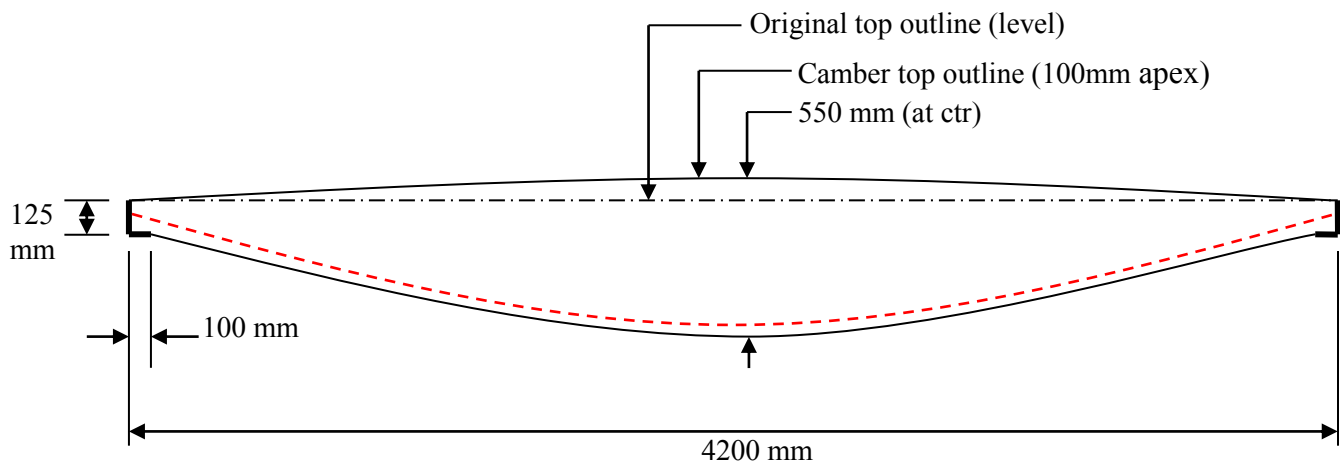
Figure 4.49 – Concrete outline and overall dimension of CCBs

Except for the top camber, all other parameters including reinforcing and strain gauge locations (both on steel reinforcing and on concrete) remained exactly the same as with the CBs from Phase I.

The formwork for the CBs from Phase I were modified to fabricate CCBs. Plywood cut with a catenary curve was installed on the top of the original formwork to shape the camber on the CCBs. Figures 4.50 and 4.51 show the modified formwork.

Figure 4.50 – Modified formwork to fabricate CCB's
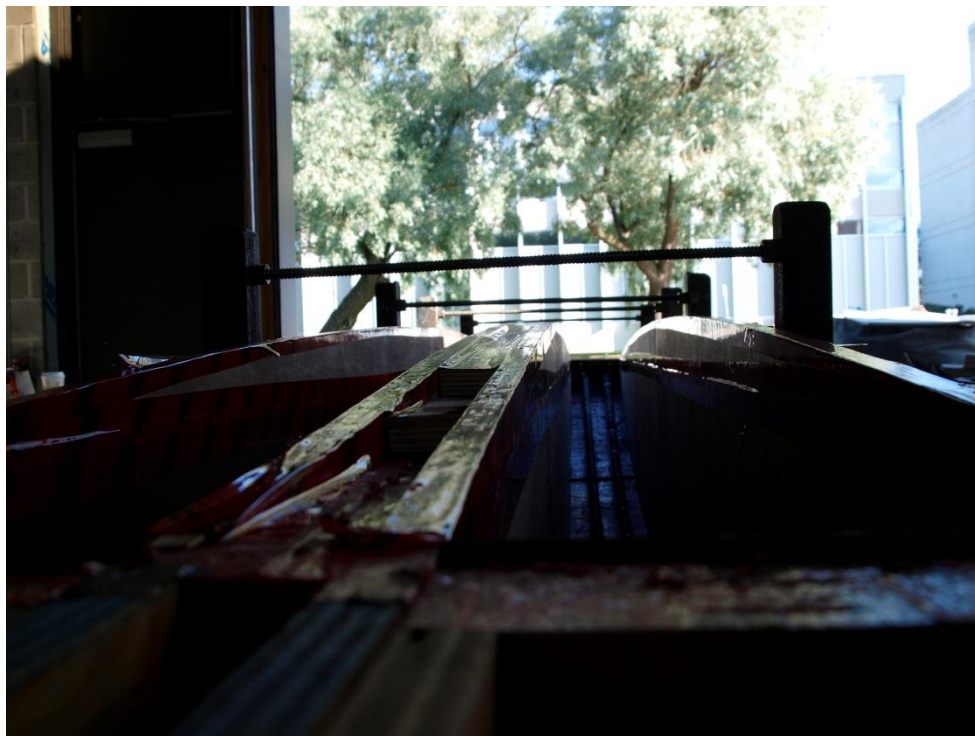
Figure 4.51 – Modified formwork to fabricate CCBs

4.9 Test Setup for Cambered Curved Beams

The test methodology, setup, and configuration for the CCBs was exactly the same as those for the CBs in Phase I (six-point loading), and therefore, will not be detailed further in this section. Figure 4.52 shows the test setup for CCBs prior to testing.
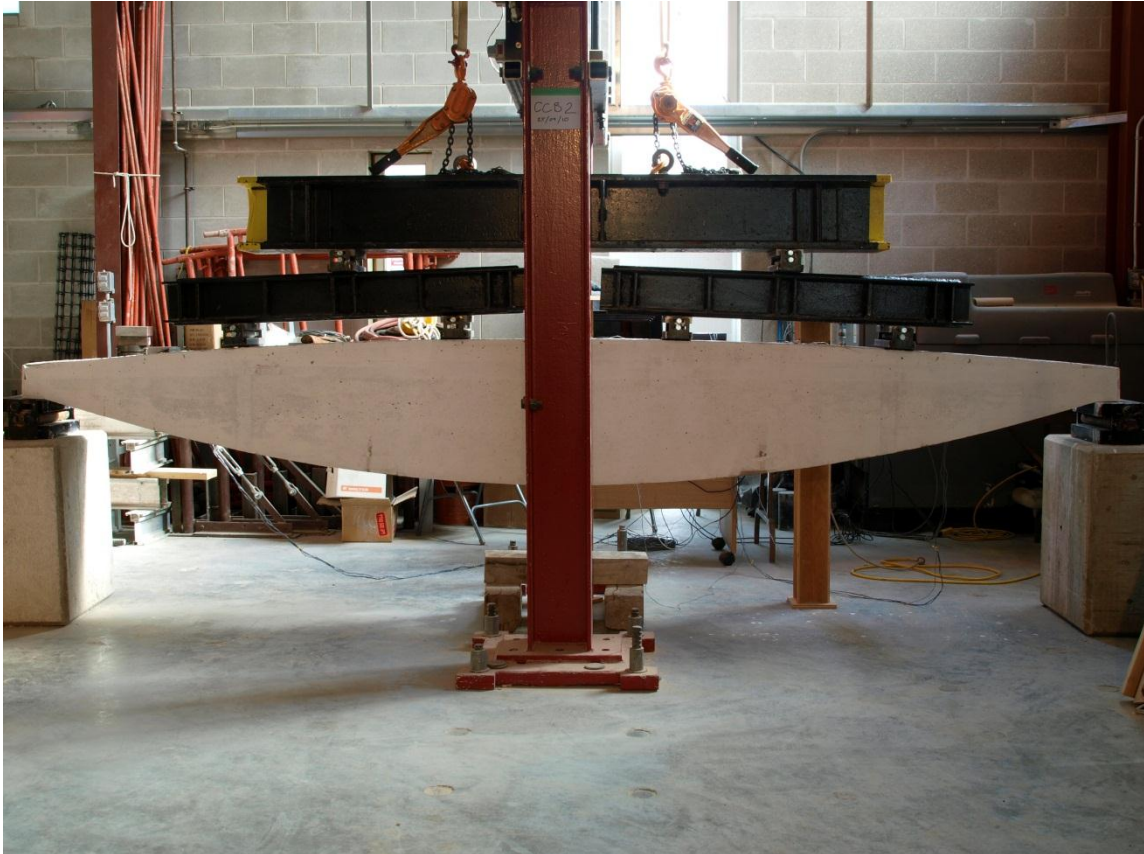
Figure 4.52 – CCB1 test setup

4.10 Instrumentation Strategy

To accurately compare all of the beams in this study, they were instrumented in the same way. The detailed drawings of the instrumentation of each beam and instrument type will be presented in Chapter 5 in the section outlining the test result for each beam as there may be slight changes to instrumentations in each beam. The general instrumentation schematic is presented in this section. The strategy for placing strain gauges on the reinforcement is to have strain readings at 680mm intervals along the length of the beams. Figure 4.53 shows the location and numbering system used for the strain gauges installed on the steel reinforcement. The locations shown are measured horizontally along a straight line at the center line of each gauge.
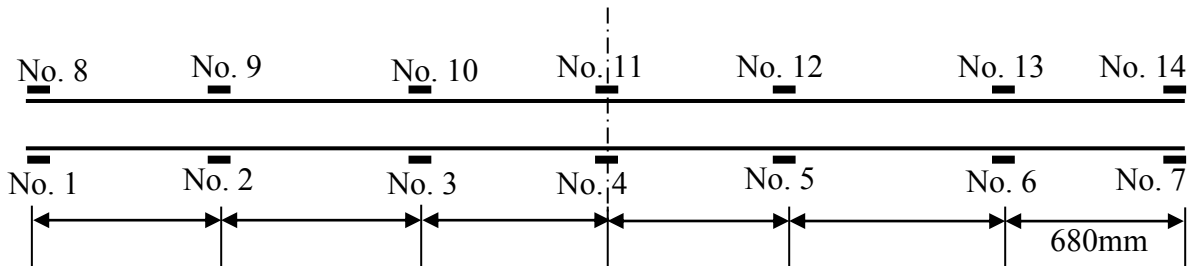
Figure 4.53 – Strain gauge schematic on steel reinforcement (NTS)

Two concrete gauges, registering stain due to compression, were installed on the top of the beam. One was at the mid-span (2100mm) and one at the quarter-span (1100mm). Two Linear Voltage Displacement Transducers (LVDT), recording the deflections of the beams, were also installed at the top of the beam, one at the mid-span and one at the quarter-span of each full-size beam.

END OF SECTION

5   *Experimental Results and Beam Comparison*

This chapter describes the experimental results for all three phases of the project and they will be presented in order of each phase. A detailed comparison of the experimental results, design analysis and numerical analysis will be provided in later chapters.

5.1   *Results for Phase I Tests*

To reiterate the test setup for Phase I as discussed in Chapter 4.3; full-size curved and rectangular beams of 4200mm in length were tested under a six-point loading condition. The loading condition was designed to produce a bending moment diagram close to a uniformly distributed load (UDL). A uniformly distributed loading condition was chosen as the main testing criteria since it is the design criteria for the majority of the buildings defined by the National Building Code of Canada.

Figures 5.1 and 5.2 show the bending moment diagram produced by UDL and six-point loading conditions, while Figure 5.3 shows two bending moment diagrams overlapped. Figure 5.3 shows the condition in which the loads produce the maximum bending moment in the beam. The magnitude of the maximum bending moment is dependent on the amount of load on the beam when all other variables are similar.
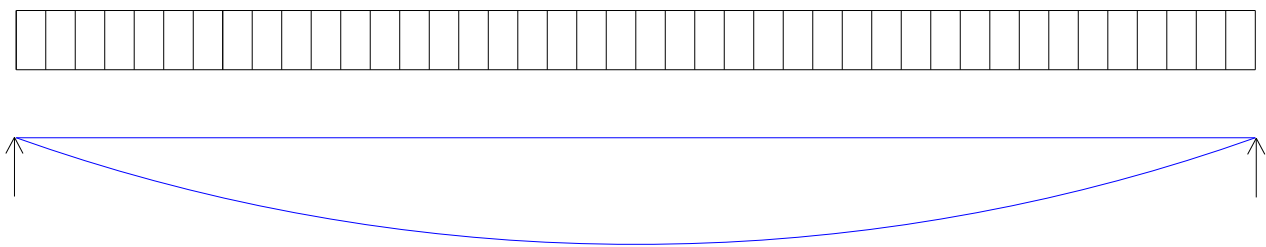
Figure 5.1 – Bending moment diagram produced by UDL
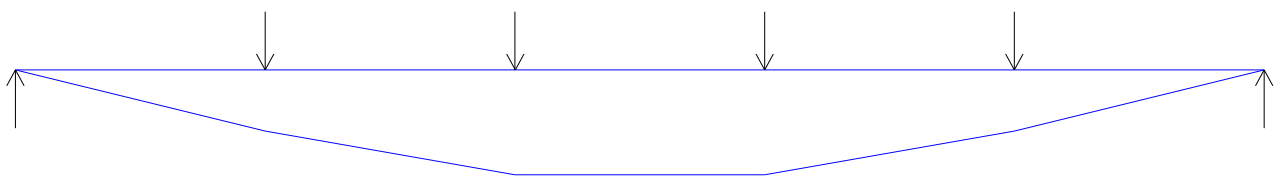
Figure 5.2 – Bending moment diagram produced by six-point loading

Figure 5.3 – Overlapped bending moment diagrams

5.1.1 Beam Instrumentation

Steel Strain Gauges

Reinforcing bars in all of the beams were equipped with 10mm strain gauges to measure tension strain. In Phase I strain gauges were installed on both reinforcing bars. This was to demonstrate that the stresses in both bars are the same, and it proved valuable since some gauges might be damaged during the concrete placement. The locations of the steel strain gauges for both rectangular beams and curved beams are shown in Figures 5.5 and 5.6. It must be noted that the location of gauges in Figure 5.5 is given along the curve; therefore it is shown longer than the straight line.

Compression Strain Gauges (or Concrete Gauges)

Strain gauges 50mm in length were used to measure compression strain. Concrete strain gauges were installed on the surface of the concrete of each beam. The locations of the concrete gauges on the beams varied slightly and will be presented individually.

In the first two experiments a study was conducted to determine the difference between the data collected from a PI gauge and a 50mm strain gauge; the data collected by the strain gauge proved to be more accurate. Therefore, for all other experiments only 50mm strain gauges were used to determine the compression strain in concrete. Figure 5.7 shows the locations of both PI gauges and the compression strain gauges for the first two experiments. PI gauges were not used for the subsequent experiments.

Liner Voltage Displacement Transducers (LVDT)

Two LVDTs were used in each experiment to determine the deflection of the beam. (The restrictions of the Data Acquisition System (DAQ) allowed for only two.) This proved to be sufficient, for the deflection measurements of 4200mm long beams. The placement of the LVDTs was at the top of the beam on the half point and quarter point for each beam and the locations are shown in Figure 5.7.

Figure 5.4 – Steel strain gauges location for rectangular beams, elevation view

680 mm 680 mm 680 mm 680 mm 680 mm 680 mm

4200 mm

700 mm 700 mm 700 mm 700 mm 700 mm 700 mm

4200 mm

Figure 5.5 – Steel strain gauge location for curved beams, elevation view
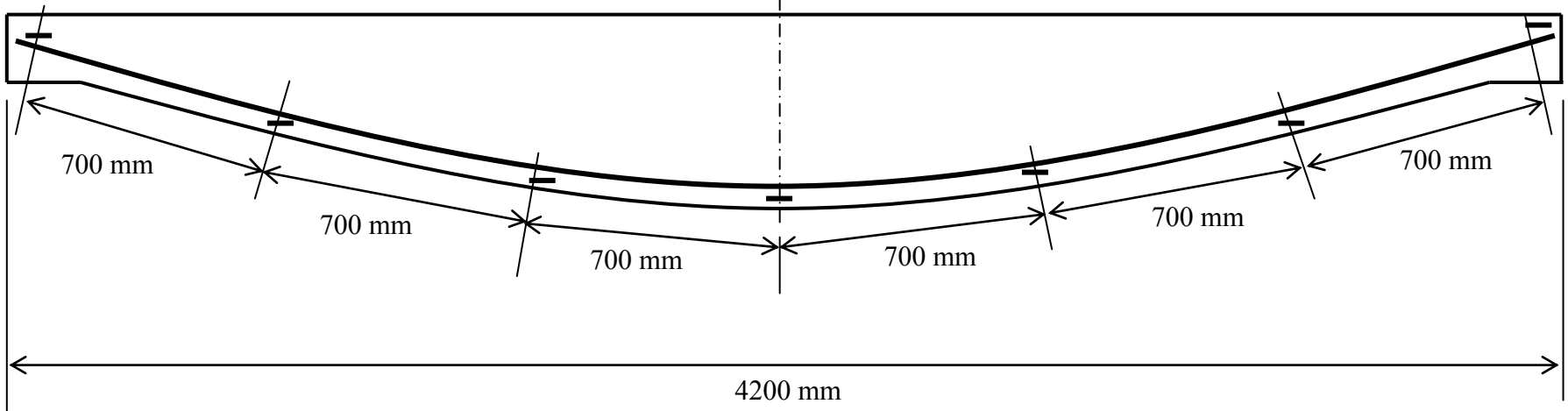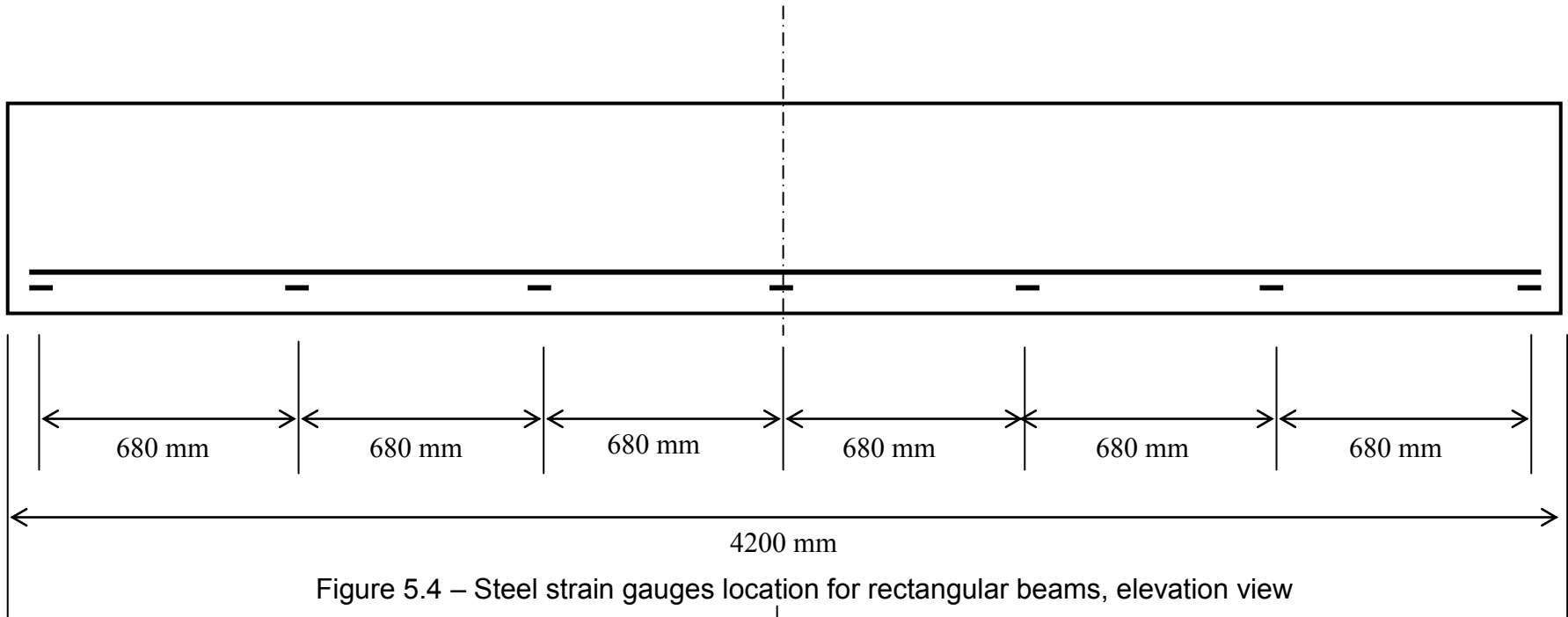
Figure 5.6 explains the strain gauge numbering system. Strain gauges were placed along the bottom of the reinforcing bars with the exception of the four end gauges in the curved reinforcement: Numbers1, 8, 7 and 14. These gauges were placed at the top of the bar after the bars were welded to the end angle.

No. 8　　　　No. 9　　　　No. 10　　　　No. 11　　　　No. 12　　　　No. 13　　　　No. 14

No. 1　　　　No. 2　　　　No. 3　　　　No. 4　　　　No. 5　　　　No. 6　　　　No. 7

Reinforcing bars (2-25M)
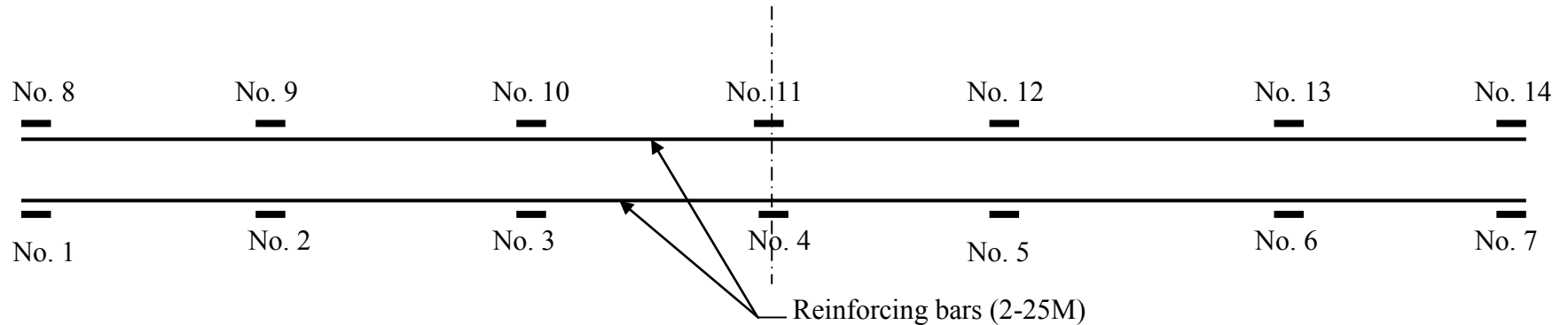
Figure 5.6 – Strain gauge numbering, plan view
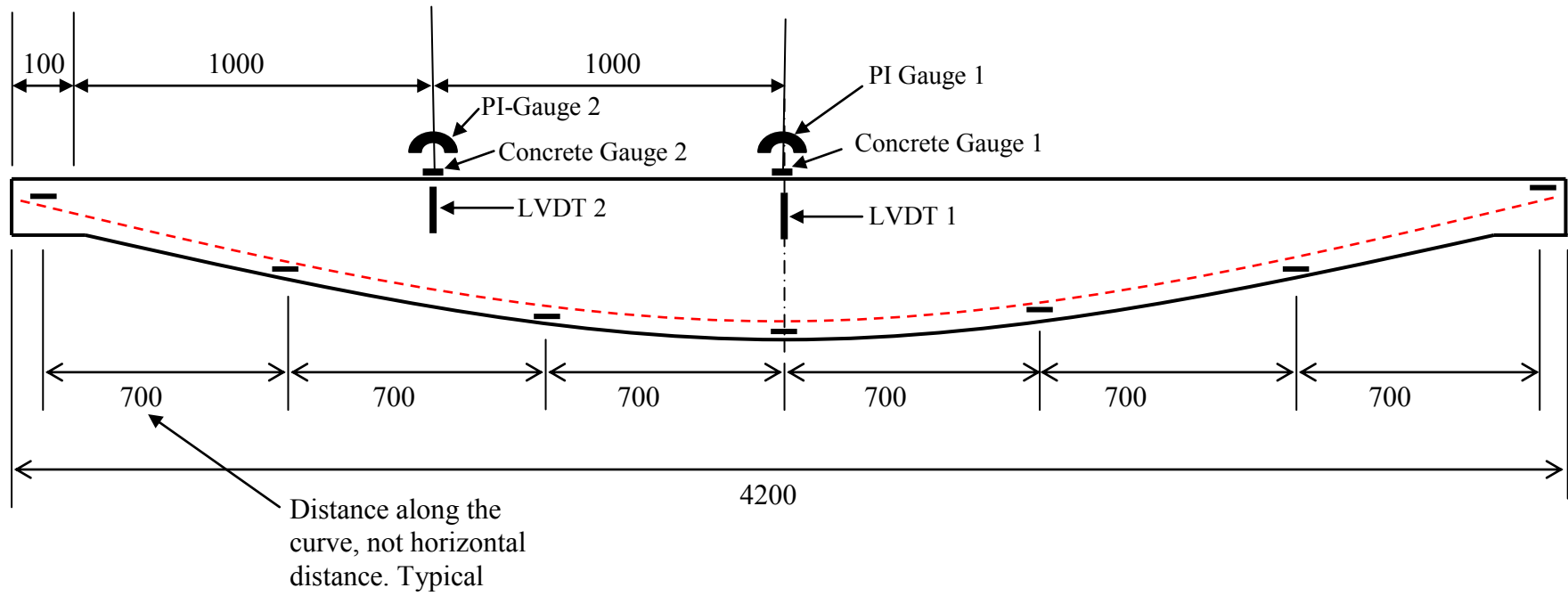
Figure 5.7 – Curved Beam instrumentation,

PI Gauges were only included for CB1 and CB2

5.1.2 Curved Beams

Three curved-beams were constructed and tested in Phase I and all of them behaved the same during the testing. To avoid repetition the curved beams will be presented as a group and not individually. See Appendix B for the individual results of each curve beam.

Each curved beam was named by the acronym CB (Curved Beam) and a number associated with their construction and testing sequence, CB1, CB2 and CB3.

5.1.3 Behaviour of Curved Beams

During the testing, at 20% of maximum load cracks started to appear uniformly along the bottom of the beams. As the load increased, the number of cracks also increased. Generally, by the time 50% of the maximum load was reached no new cracks developed but the existing crack width increased to the range of 10mm to 17mm. Figures 5.8 to 5.11 are presented in sequence of testing and show CB3 during the testing and at failure. The numbers on the cracks correspond to the specific load during the testing where the actuator was programmed to hold the load constant to allow the beam to be inspected for new crack development and to monitor the existing cracks.

Figure 5.8 – Start of the test

Figure 5.9 – Crack propagation at 45kN

Figure 5.10 – Crack propagation at 140kN

Figure 5.11 - CB3 After the failure

Figure 5.12 shows the final crack pattern for the beam CB2. In this investigation, a best fitted line was drawn on each crack in order to measure the angle of each crack with respect to the bottom curve profile. The angle of all cracks was between 80 and 100 degrees with the majority of the cracks at almost at 90-degree angle to the curve profile.
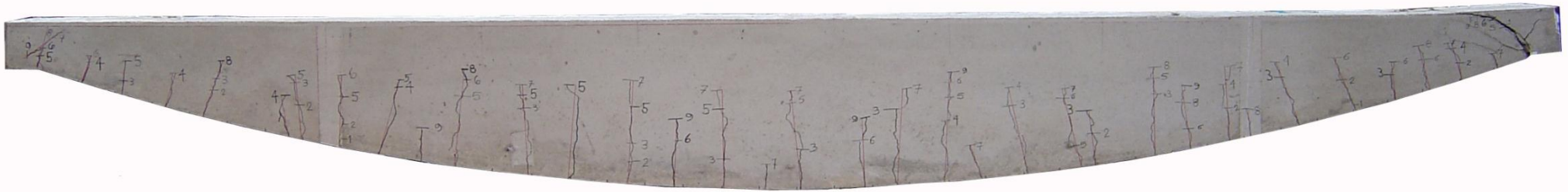
Figure 5.12 – Crack pattern and angle of cracks for CB2

5.1.4 Test Results

The next few sections will discuss the stress in the steel and the mode of failure in general, while the following specific sections for each beam will demonstrate the behaviour and the mode of failure in detail for each beam. To examine entire data set collected during the experiments, see the Appendices.

5.1.5 Testing of Steel Reinforcement and Stress in the Steel

As part of this research three 25M steel reinforcement bars were tested to verify the material properties of the steel reinforcement used in this research with respect to the properties supplied by the steel manufacturer.

The tension testing of the reinforcements were conducted in accordance with ASTM A 615/A 615M – 07, "Standard Specification for Deformed and Plain Carbon-Steel Bars for Concrete Reinforcement". The following figures show the test setup.

Figure 5.13 – Strain gauge on reinforcement for tension test

Figure 5.14 – Reinforcement tension test setup

The following table compares the material properties supplied by the manufacturer with those obtained from testing:

Property	From supplier	Avg. from testing
E	200,000 MPa	186,000 MPa
ε_y	2000 $\mu\varepsilon$	2000 $\mu\varepsilon$
f_y	400 MPa	416 MPa

Table 5.1 – Material property comparison

The following stress-strain curves show the test result of all three tests.

STRESS-STRAIN CURVE
25M Rebar Tension Test 1
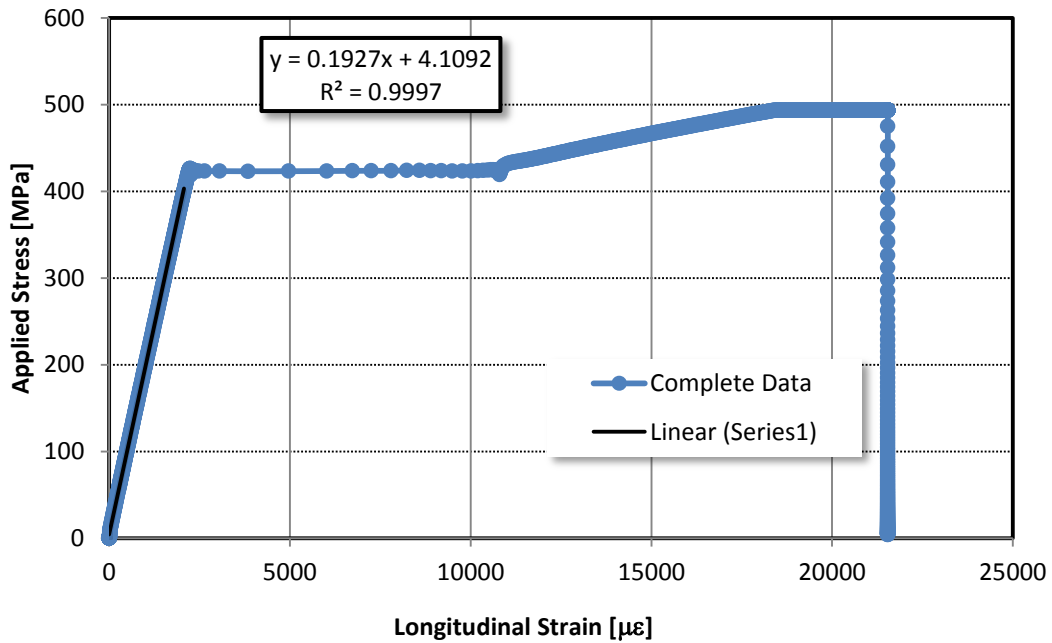
Figure 5.15 – Stress-strain curve for rebar 1

STRESS-STRAIN CURVE
25M Rebar Tension Test 2
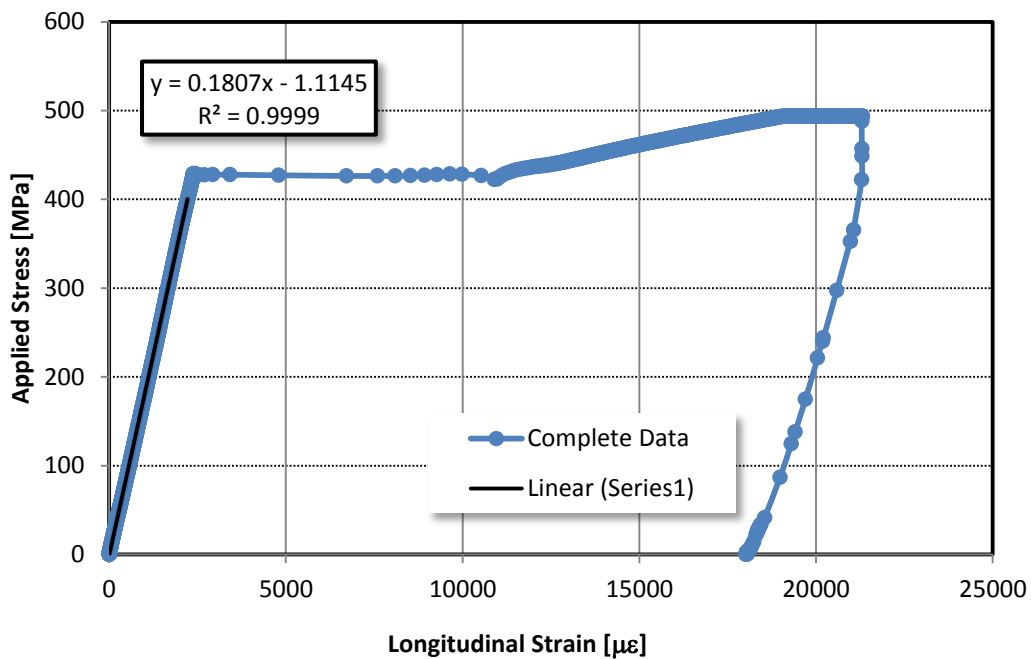
Figure 5.16 – Stress-strain curve for rebar 2

STRESS-STRAIN CURVE
25M Rebar Tension Test 3
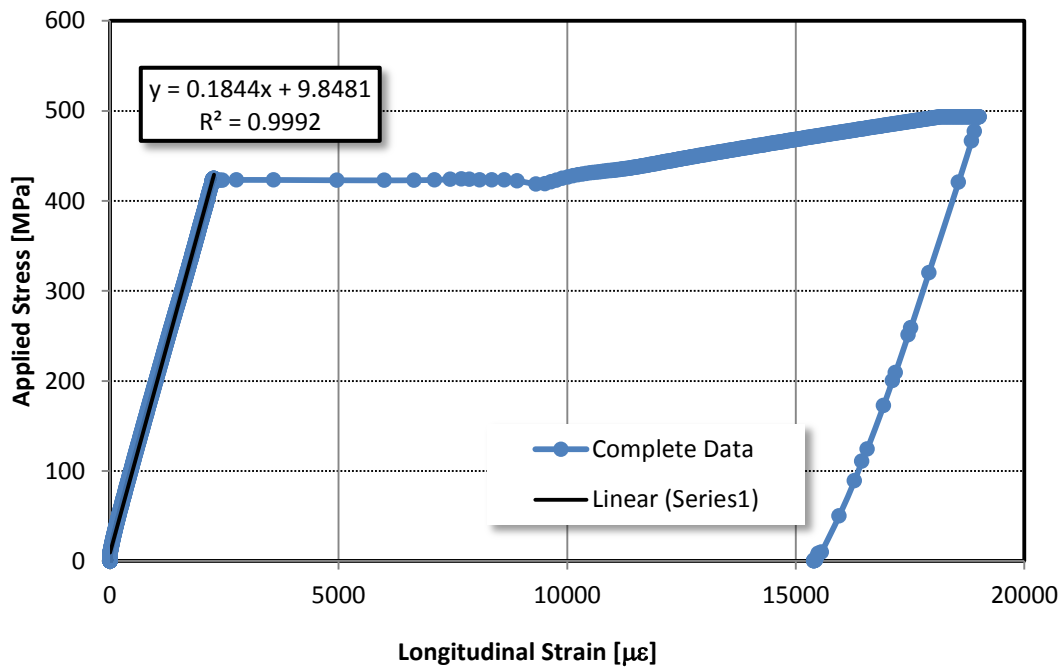
Figure 5.17 – Stress-strain curve for rebar 3

The average modulus of elasticity found from rebar tests is 186,000 MPa, about 14 MPa less than the E provided by the supplier. This study uses the value determined by the experiments (E = 186,000 MPa) for all analyses.

As mentioned previously, in Phase I, a total of 14 strain gauges were installed on the steel reinforcing in each beam – seven strain gauges on each bar. Both rebars were instrumented to investigate the similarity of the strain and stress in both rebars. As expected, this investigation resulted in identical strain and stress in both bars in all beams.

An extensive amount of data was gathered during each experiment. A sample of the results from the strain gauges is presented in Figures 5.18, 5.19 and 5.20. More detailed discussion on the stress in steel will be presented for each beam in

the respective sections. Figures 5.18, 5.19 and 5.20 show the stress distribution along one of the reinforcements in each of the curved beams. The following graphs show that the steel in the three curve beams in Phase I (CB1, CB2 and CB3) did not yield, as the strain in the strain gauge at the centre span remained below 2000 micro-strains which is the yield strain of the steel reinforcing in accordance to CSA – A23.3. Maximum strain in the reinforcement in CB1, CB2 and CB3 reached 930, 1838 and 1755 micro-strains respectively. The stress in the reinforcement in each can be calculated to be 186 MPa for CB1, 367.6 MPa for CB2 and 351 MPa for CB3.

The tensile stresses are 46.5%, 91.9% and 87.8% of the yield stress of 400 MPa for CB1, CB2 and CB3 respectively.

Load vs. Steel Strain (CB1)
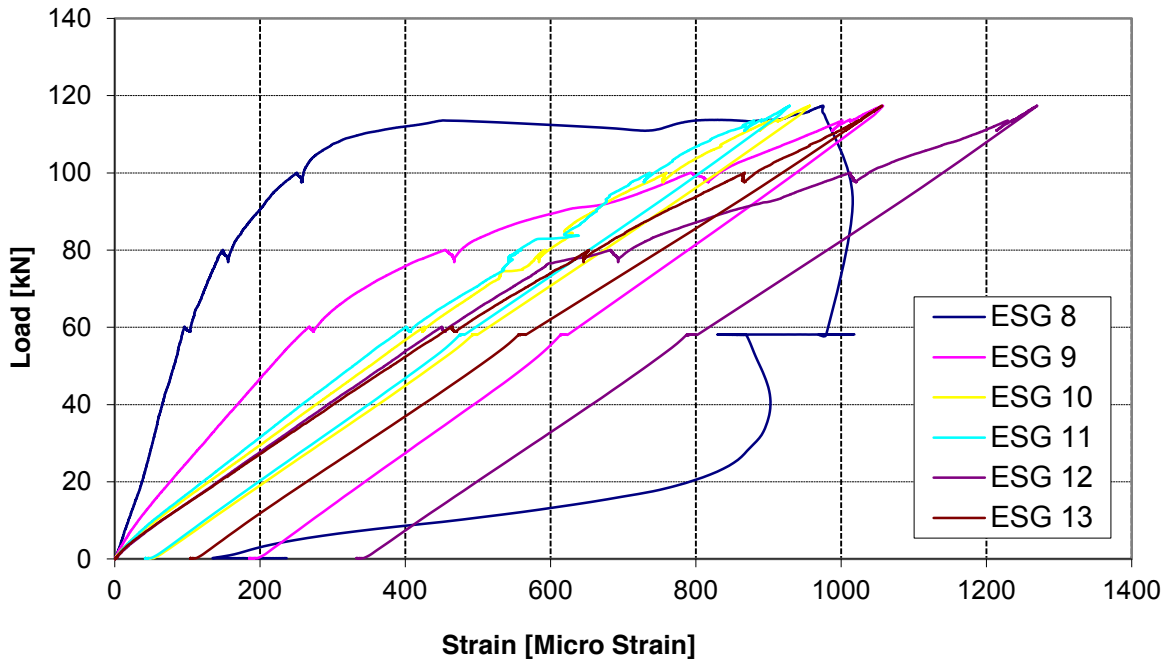
Figure 5.18 – Stress in Steel reinforcement in CB1

Load vs. Steel Strain (CB2)
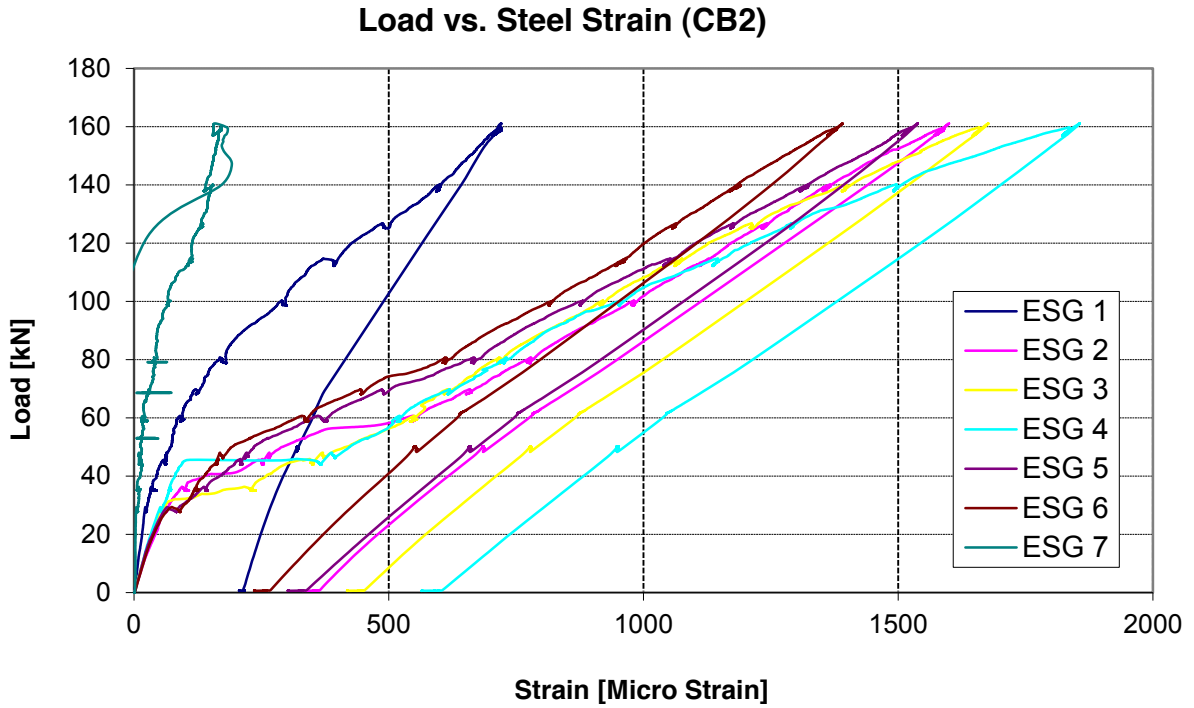
Figure 5.19 – Stress in Steel reinforcement in CB2

Load vs. Steel Strain (CB3)
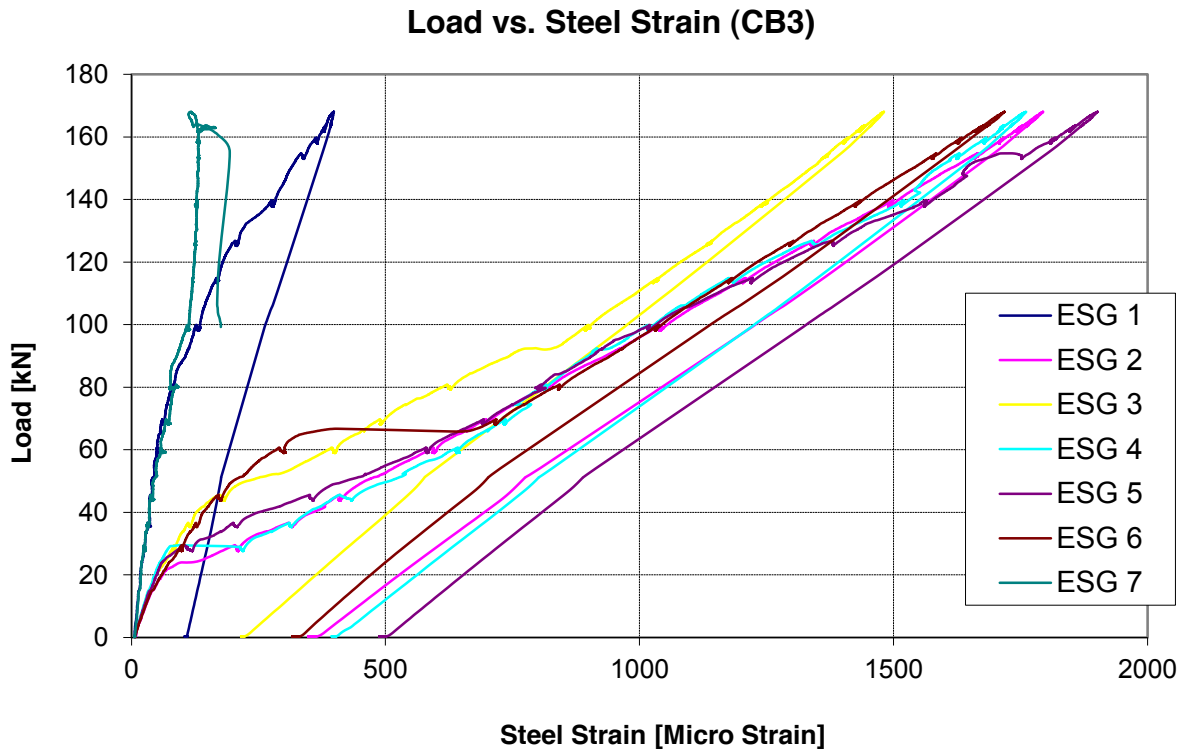
Figure 5.20 – Stress in Steel reinforcement in CB3

5.1.6 Serviceability Criteria

Total failure would be described as a total sectional failure, in which a beam would experience a total material failure where cracks are through the entire cross section of the beam and the beam cannot sustain additional load, as shown in Figures 5.21, 5.22 and 5.23. It is obvious that all curved beams would fail due to serviceability prior to the total failure, as would the rectangular CSA-designed control beam.

The allowable serviceability deflection given in Table 9-2 CSA Standard A23.3, for a 4200mm long beam, would be as follows:

L / 360 $\longrightarrow$ 4200mm / 360 = 11.67mm rounded up to 12mm

The maximum deflection for curve beams in Phase I prior to the total failure was about 20mm, 60% higher than the allowable serviceability deflection. All curved beams reached the allowable deflection (12mm) at approximately 70% of the ultimate load. Although at 12mm deflection these beams are considered to have failed due to serviceability criteria outlined in the Canadian design code, they were able to sustain additional load past that point.

The total failure for all curved beams occurred at one end about 300mm from the support. Figures 5.21, 5.22 and 5.23 show the support area which was the failure area for each curved beam.

Figure 5.21 – CB1's end failure

Figure 5.22 – CB2's end failure
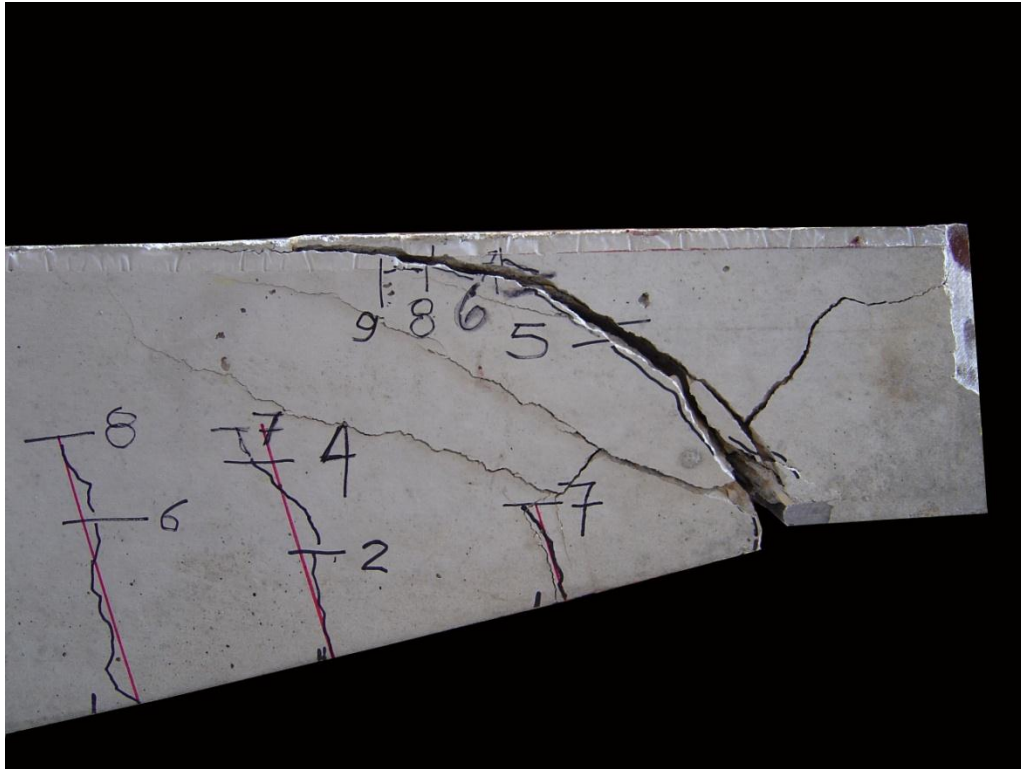
Figure 5.23 – CB2, crack propagation sequence, and angle of cracks

Visual inspection of the weld between the reinforcing and weld plates was conducted for CB1, CB2 and CB3, and none of the welds in any of the beams showed signs of failure. Figure 5.24 shows a close-up of the weld quality between the reinforcing and the weld plate in CB1 as a part of the weld quality investigation. CB1 was the first beam to be constructed with many aspects of the construction still under development at that time. It was considered that CB1 would have the worst weld quality since it was the first beam welded and the weld procedure for the beams had not yet been perfected. The weld quality improved consistently after the construction of the first beam.

Figure 5.24 – Weld quality investigation, CB1

5.1.7 CB1

Figure 5.25 shows the beam (CB1) at failure, and Figure 5.26 shows the end where the failure occurred, while Figure 5.27 shows the close-up of the failure section of the beam.

Figure 5.25 – Beam CB1 at final failure
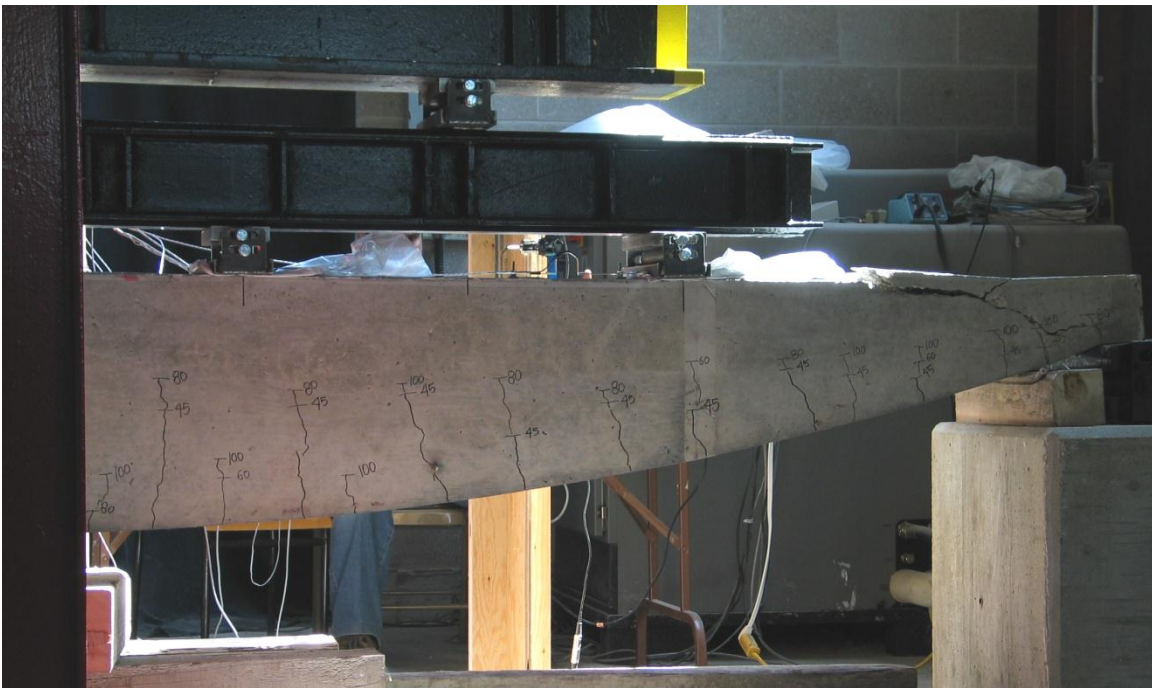
Figure 5.26 – Failure end of CB1

Figure 5.27 – Failure close-up for CB1

The following graphs illustrate the overall deflection and stresses in the steel and concrete.
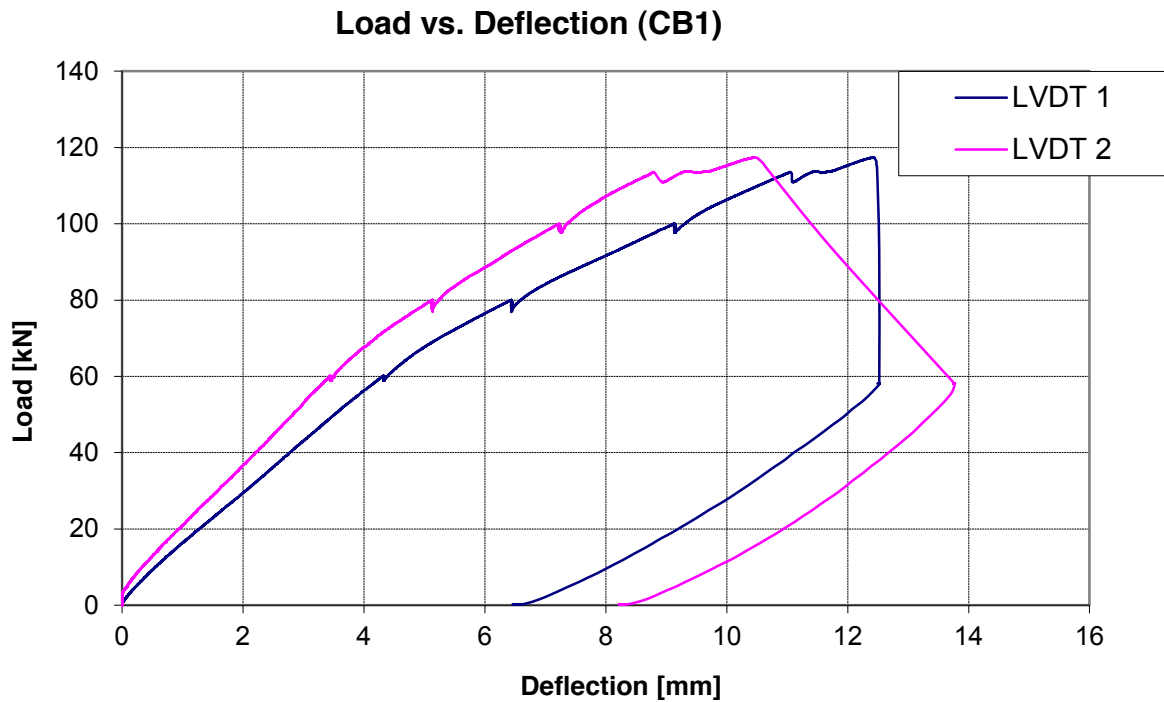
Figure 5.28 – Load-deflection curve for CB1

Load vs. Strain (CB1)
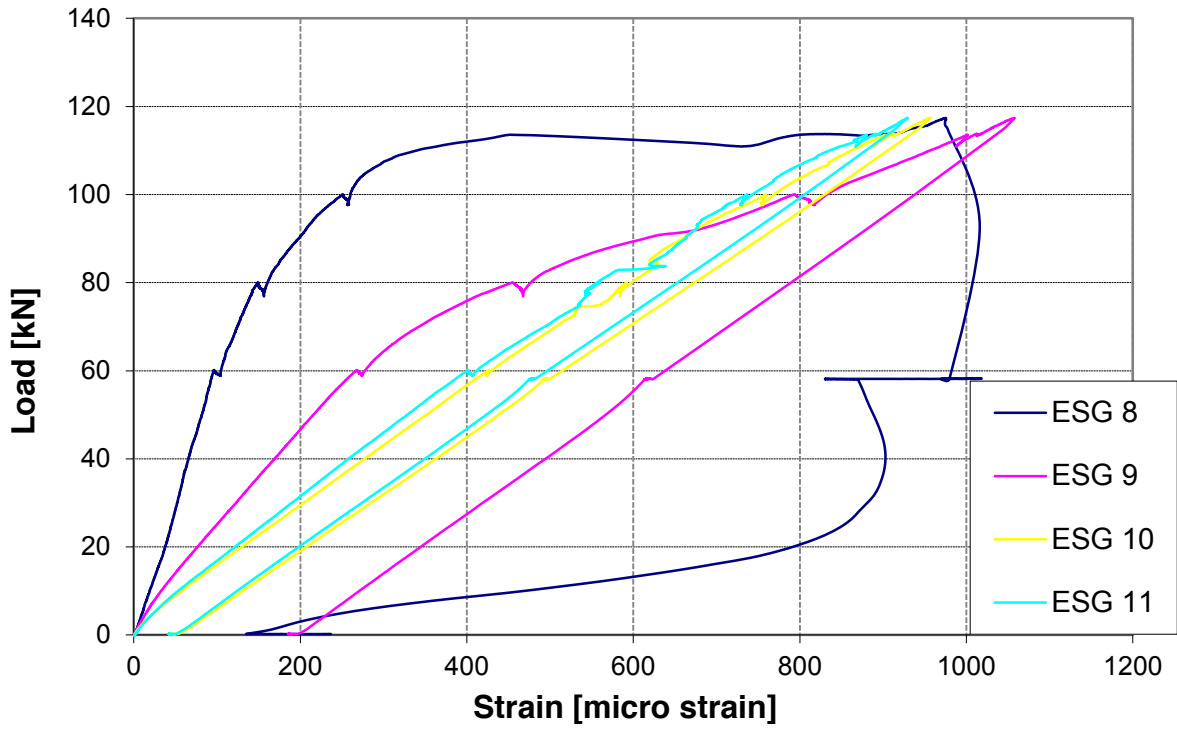
Figure 5.29 – Strain in steel reinforcement

Load vs. Concrete Strain (CB1)
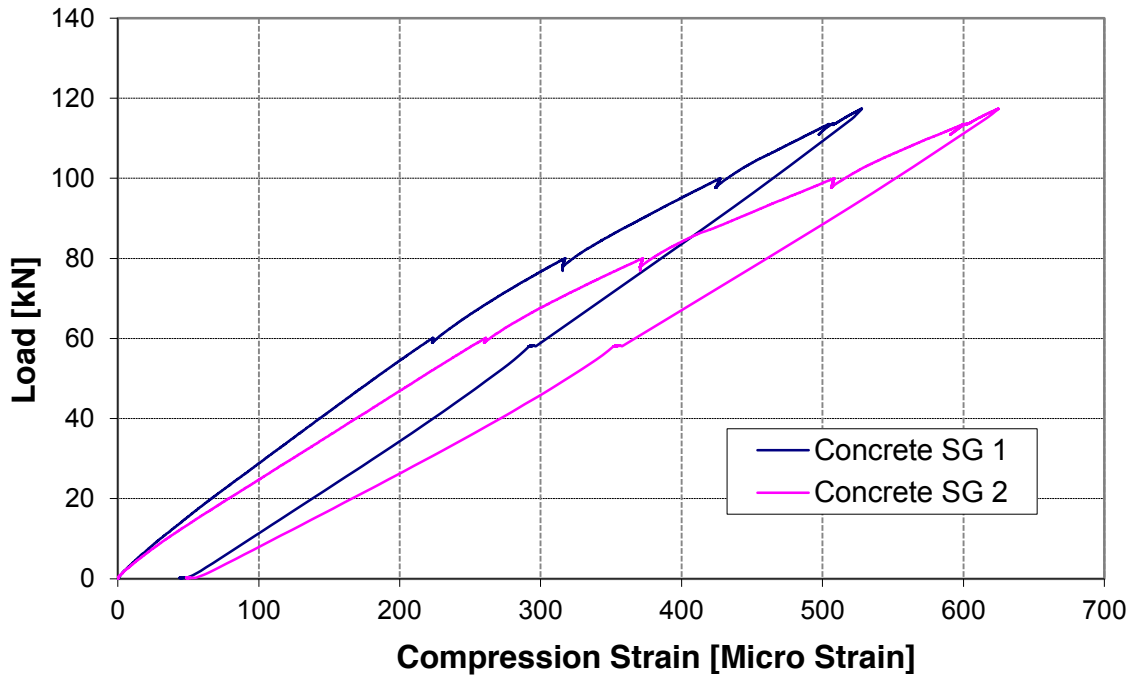
Figure 5.30 – Strain in concrete

5.1.8 CB2

Figures 5.31, 5.32 and 5.33 show the failure and failure detail for the second beam, CB2. As illustrated, the mode of failure is the same as the first beam, CB1.
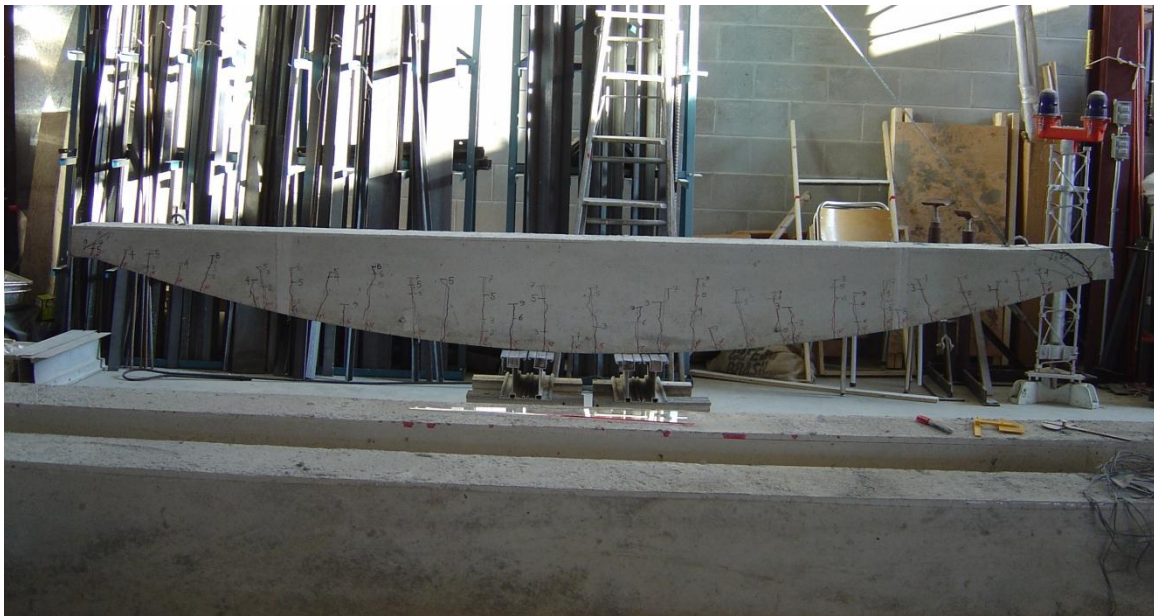
Figure 5.31 – Failure mode and crack pattern for CB2

Figure 5.32 shows the angle of the cracks at the failure end of CB2. The average angle of inclination for CB2, calculated and shown in the Figure 5.32, matches the other curved beams' crack angles and the crack angles predicted by the FEM analysis.

Figure 5.33 shows the failure end in detail without the crack lines marked during the testing.
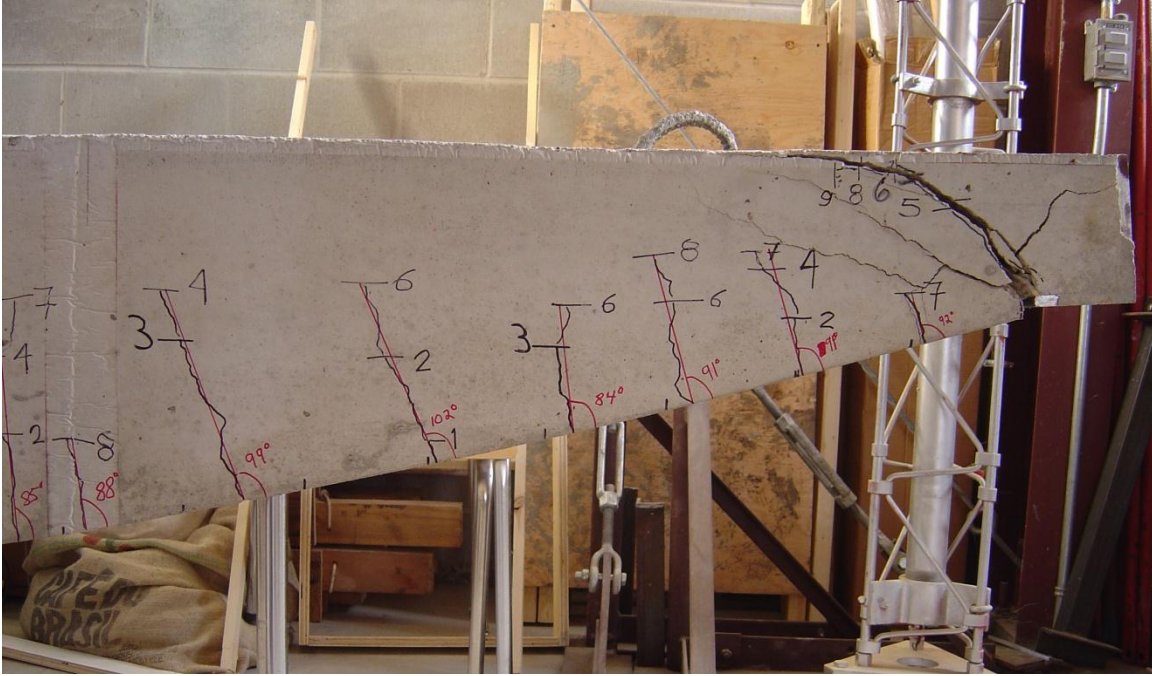
Figure 5.32 – Crack angles at the failure end for CB2

Figure 5.33 – Failure end detail for CB2

Load vs. Steel Strain (CB2)
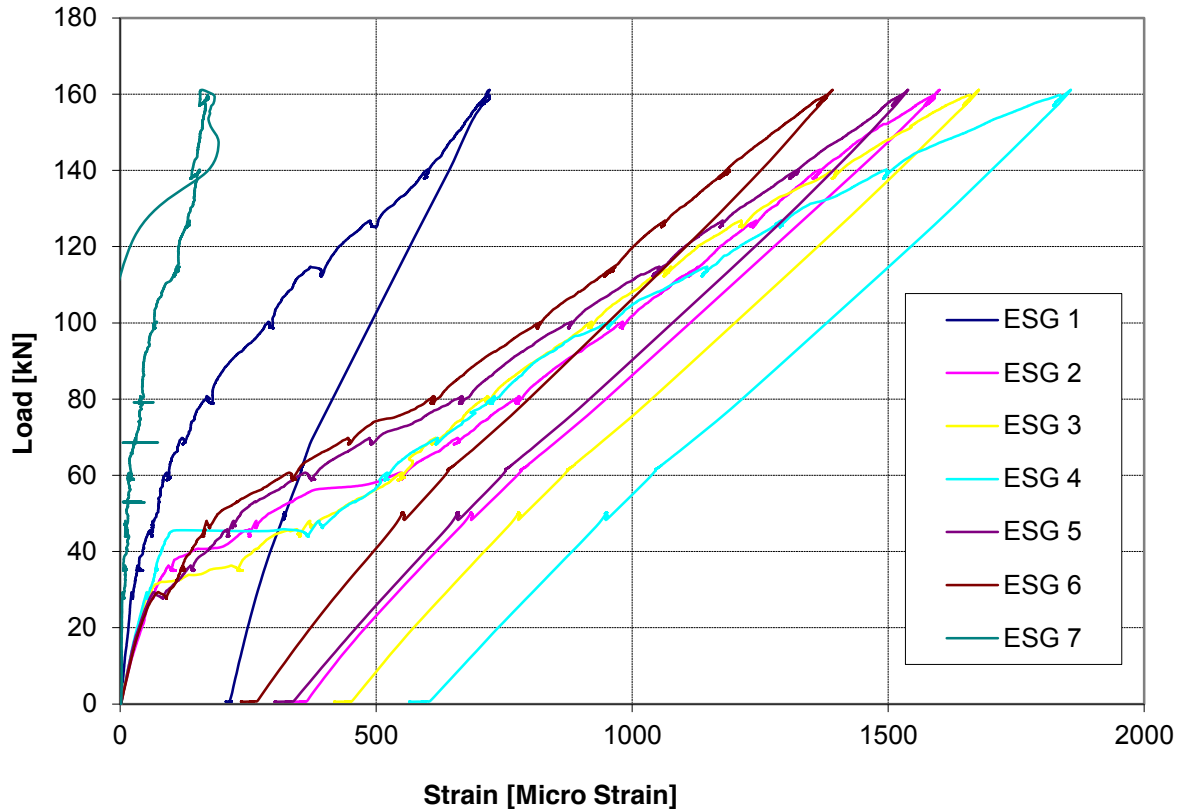
Figure 5.34 – Steel strain along one rebar for CB2

Figure 5.34 (above) shows the strain in the reinforcing rebar along the beam CB2. Except for the sensor located at each end of the rebar; sensors 1 and 7, all other sensors show the strain, and therefore stress, is approximately uniformly distributed along the length of the rebar which is consistent with the original theory. The reason for Sensor 1 and 7 (ESG 1 and ESG 7) showing less strain is due to the stiffness of the end angle assembly.

Load vs. Deflection (CB2)
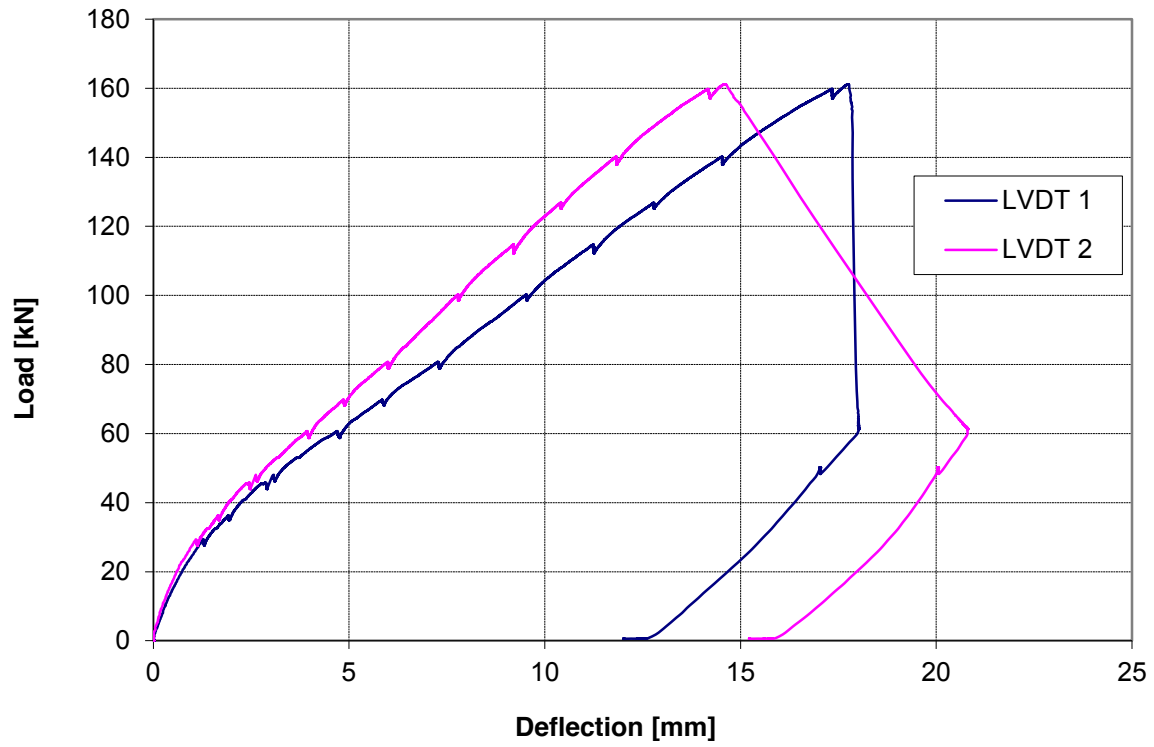
Figure 5.35 – Deflection diagram

Figure 5.35 shows the deflection diagram for the CB2. LVDT 1 is at the centerline of the beam and LVDT 2 is at the quarter point.

5.1.9 CB3

The third and last curved beam tested with no additional modification was CB3. CB3 failed the same way as the two other beams. Figures 5.36, 5.37 and 5.38 show the failure mode for CB3 and the close-up of the failure end.
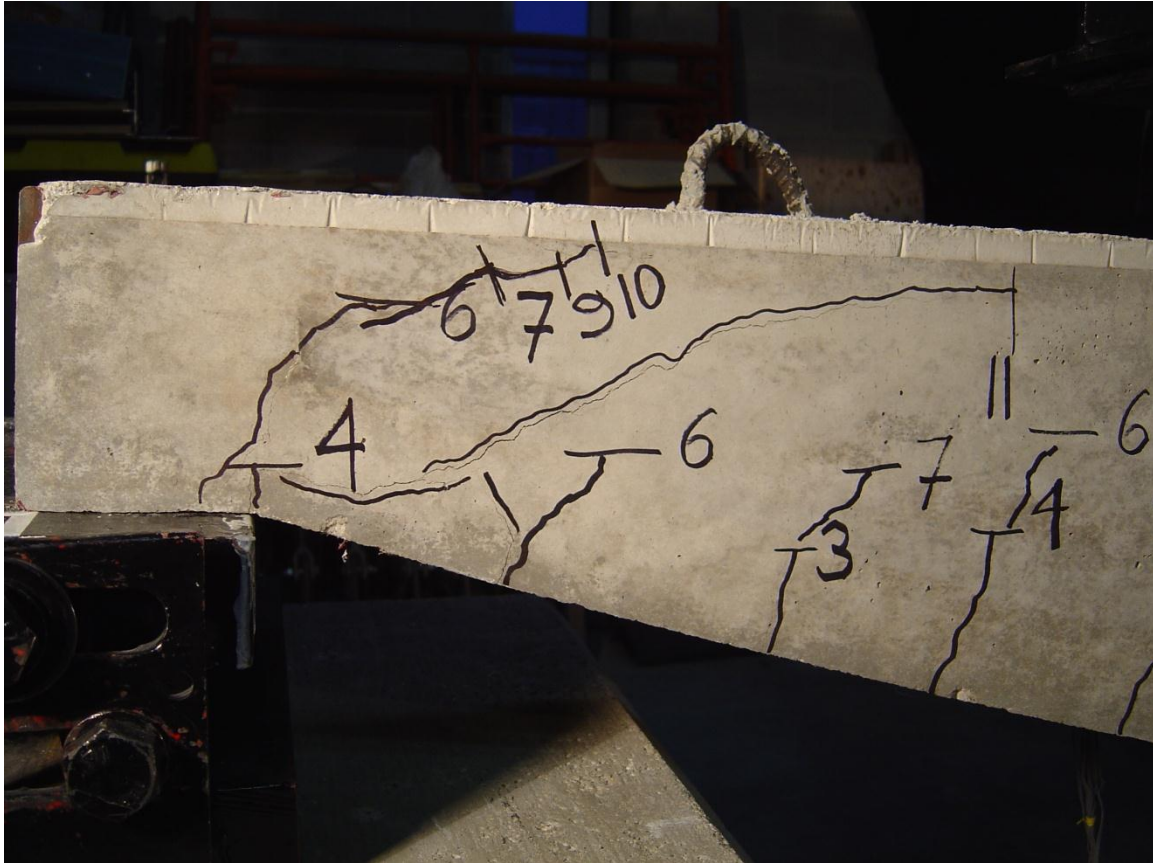
Figure 5.36 - CB3 just before failure
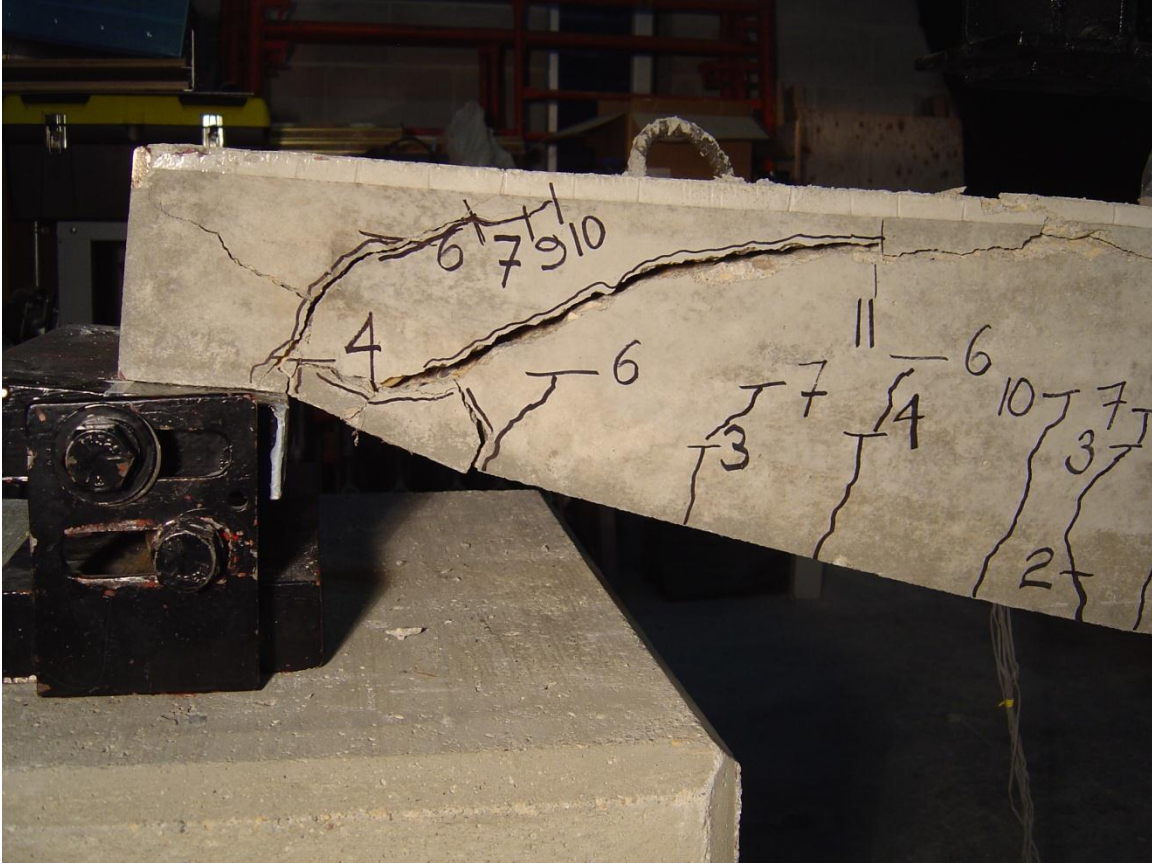
Figure 5.37 – CB3 right after failure
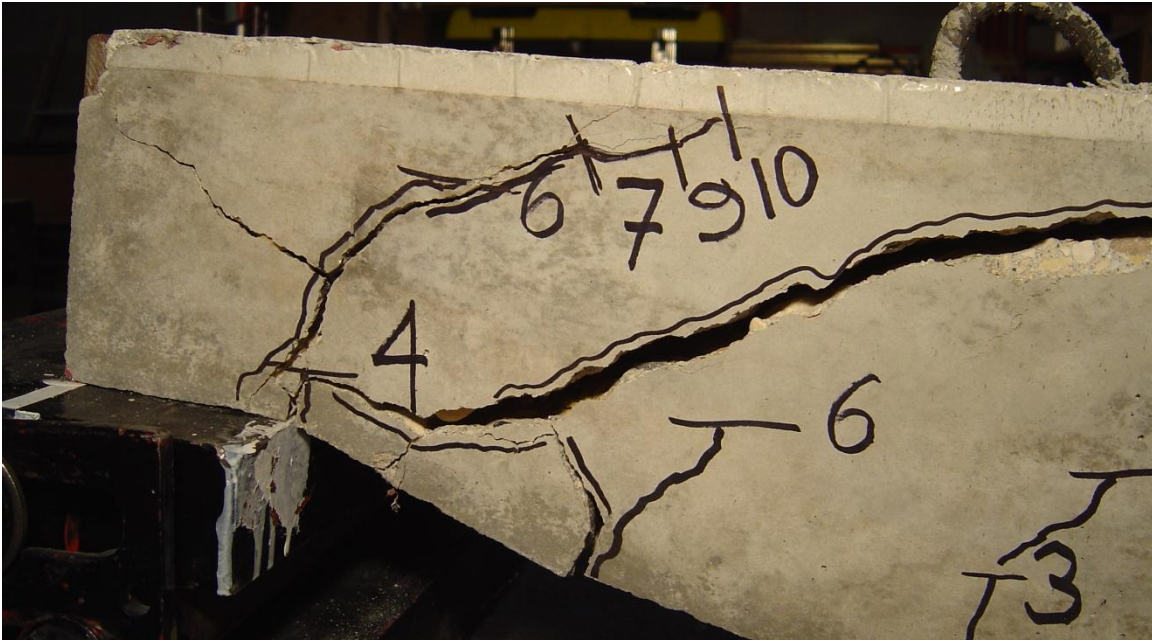
Figure 5.38 – Close-up of the failure end

Figure 5.39 – The failure end at the top of the beam.
Concrete is not crushed but slipped horizontally

Figure 5.40 shows the strain in the sensors along the reinforcing bar. This graph shows once again that the stress in the rebar is approximately uniformly distributed along the length of the rebar and it is very similar to that of CB2 and CB1. The first and last sensor (ESG1 and ESG 7) are very close to the end and they register higher stiffness due to higher stiffness of the end support assembly.

Load vs. Steel Strain (CB3)
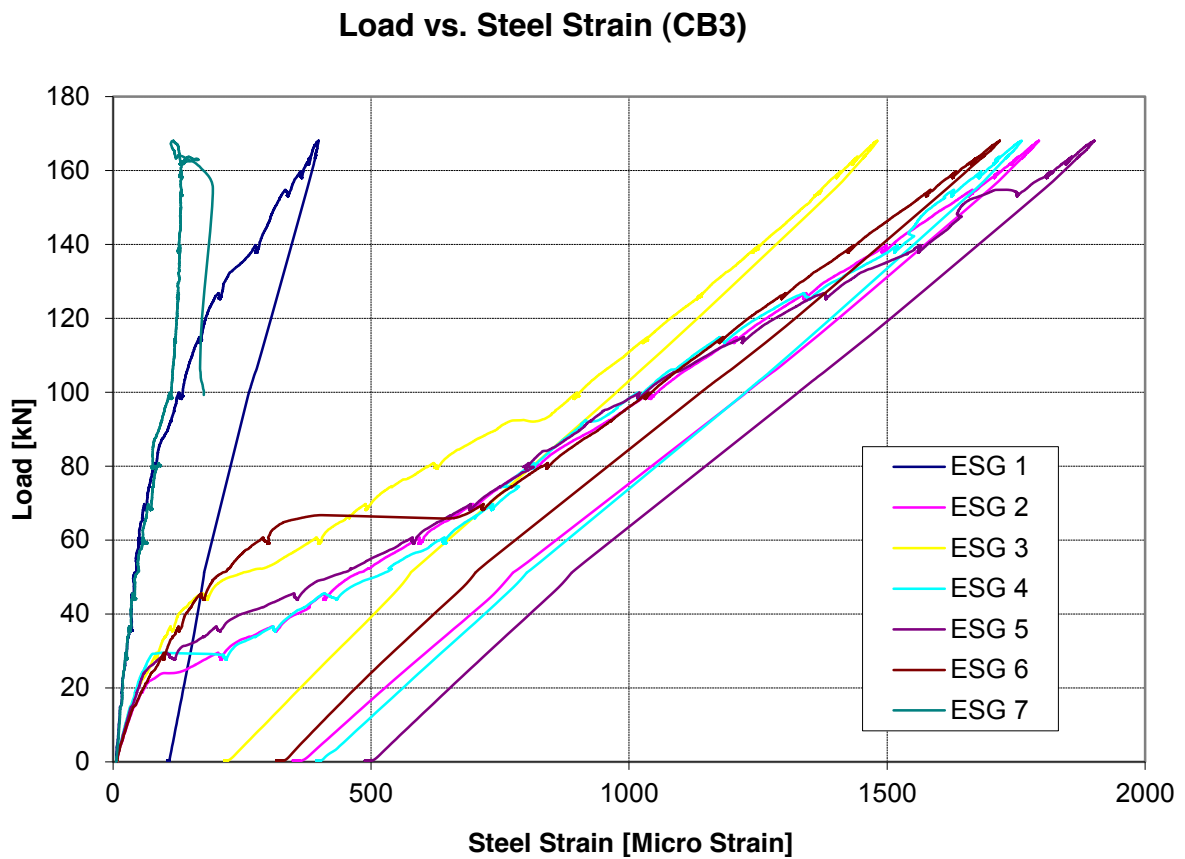
Figure 5.40 – Steel strain along one rebar for CB3

Figure 5.41 shows the overall deflection of the CB3 during the test and at the time of failure.

Load vs. Deflection (CB3)
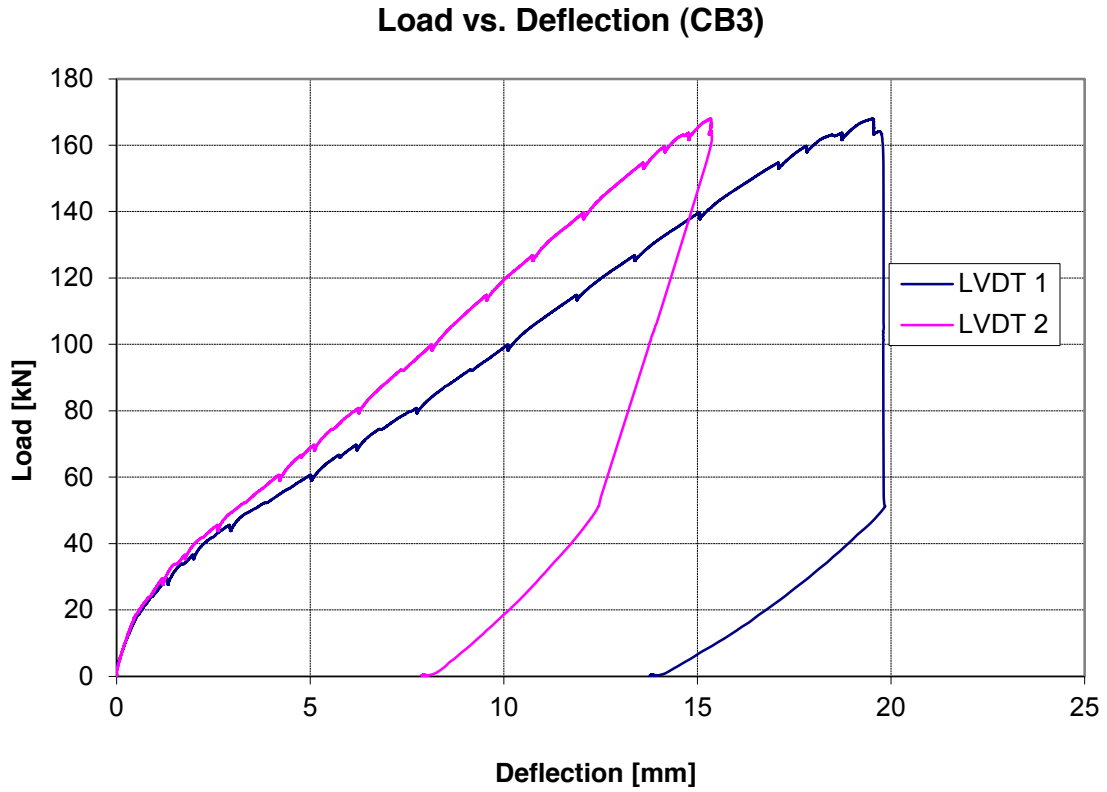
Figure 5.41 – Deflection for CB3

5.1.10 RB1

RB1 is one of the first three beams fabricated as part of the concrete pour in Phase I of the experiments. It is rectangular in cross-section and in profile and was the first rectangular beam to be tested. The beam was reinforced with two 25M steel reinforcing bars longitudinally and with no shear reinforcement. Figures 5.42 and 5.43 show the beam's configuration.
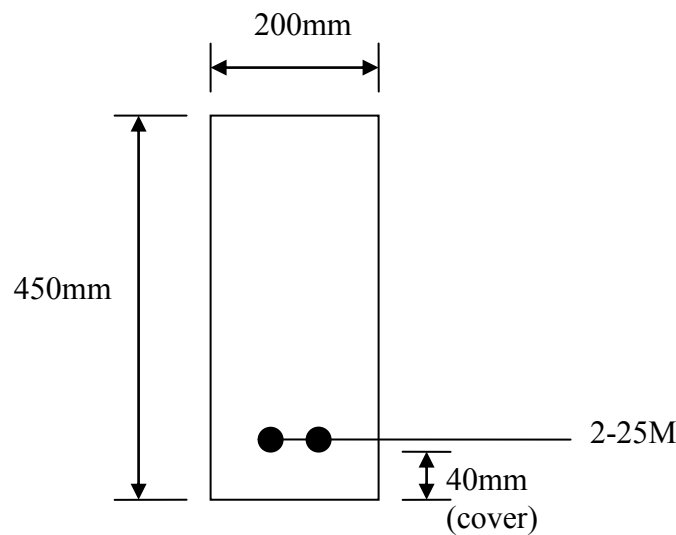
Figure 5.42 - RB1 Cross-section (Constant)
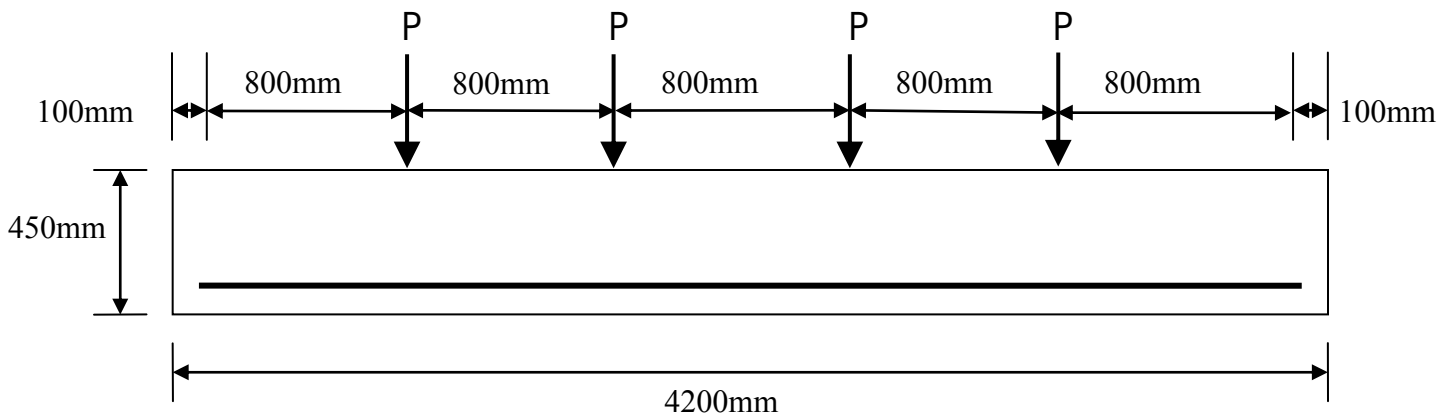
Figure 5.43 - Over-all dimensions of RB1 and loading scheme

Originally only PI gauges were going to be utilized for measuring compression strain in the concrete at the top of the beam. However, it was unclear if PI gauges were suitable for reading compression strain; therefore, it was decided to place two concrete strain gauges directly below the PI gauges 1 and 2. This would eliminate any questions regarding the accuracy of the PI gauges as the data collected from the PI gauges could be compared with the data from the concrete strain gauges.
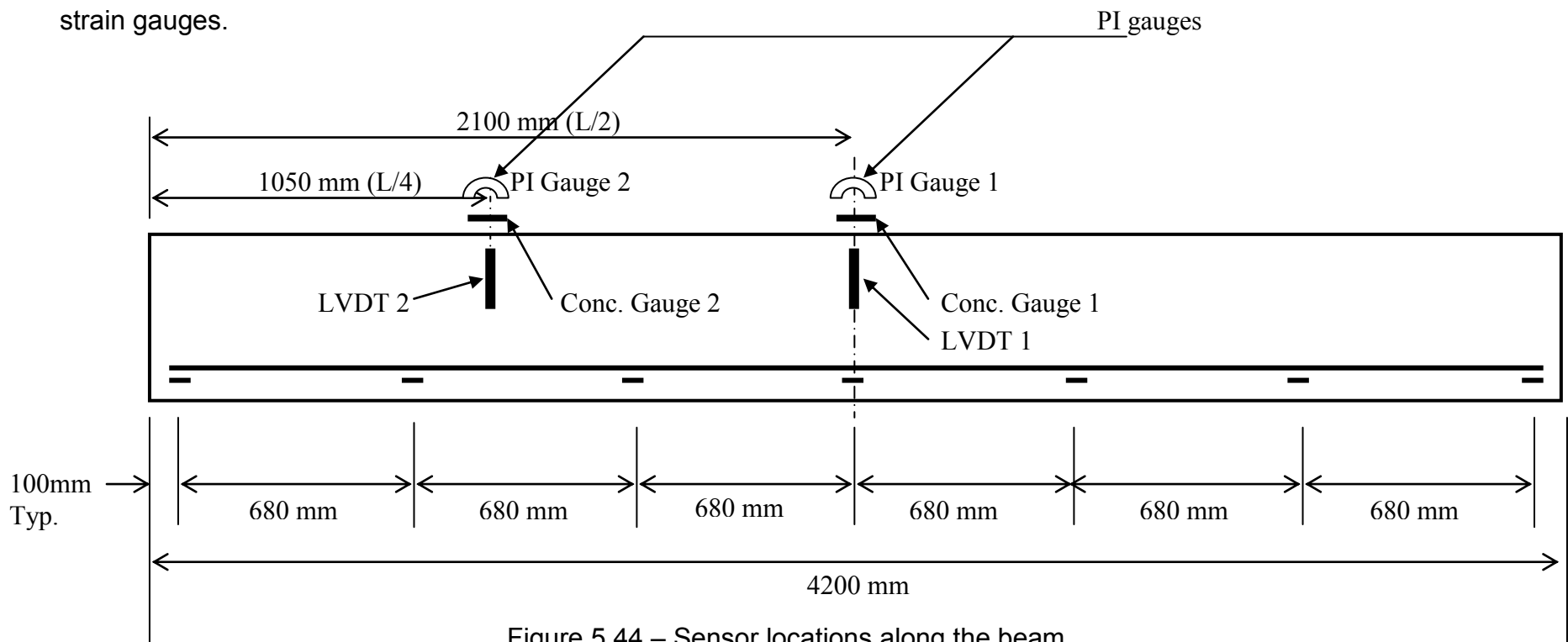
Figure 5.44 – Sensor locations along the beam

Strain gauges were also placed along the bottom of the reinforcement, numbers 1, 8, 7 and 14. These gauges where placed at the top of the bar after the bars were welded to the end angle.

No. 8   No. 9   No. 10   No. 11   No. 12   No. 13   No. 14

No. 1   No. 2   No. 3   No. 4   No. 5   No. 6   No. 7

Two reinforcing bars
in each beam
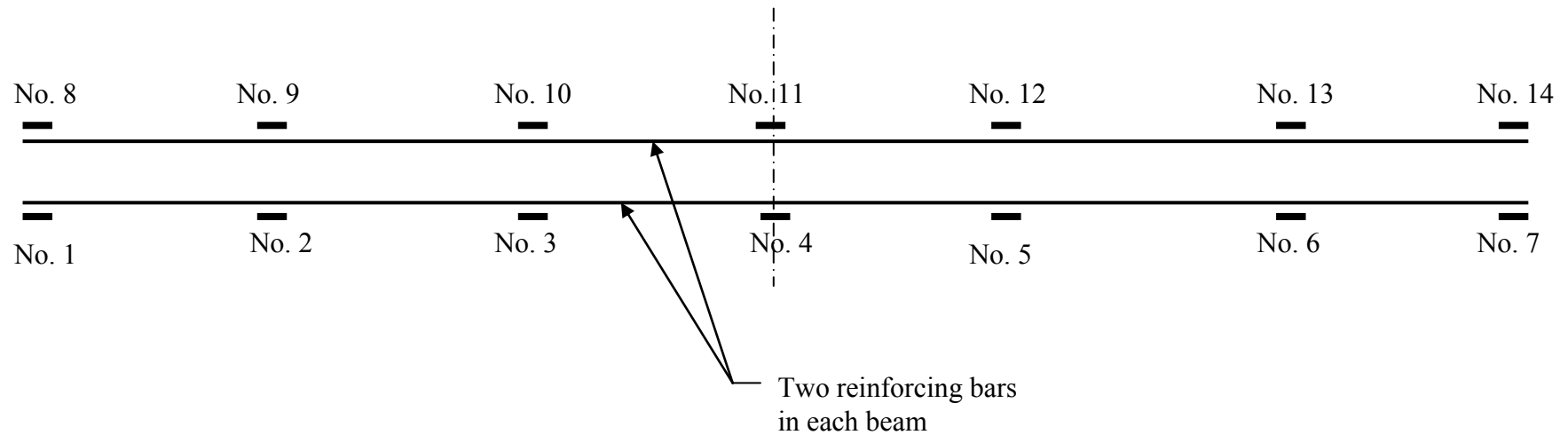
Figure 5.45 - The numbering system for the steel strain gauges

RB1 had the same amount of flexural reinforcement as the curved beams (2-25M steel reinforcing bars) and no shear stirrups. The purpose for the fabrication and testing of this beam was to more fully understand pure shear failure in reinforced concrete beams. As anticipated this beam failure was very sudden well below the flexural design capacity. RB1 failed at the final load of 185 kN at 60% of its flexural capacity. The following photos show RB1's test set up and failure.

Figure 5.46 – RB1 test setup

In CSA code based design this type of failure must be avoided. The final failure for reinforced concrete members must be a ductile failure to provide warning for adequate time for the occupants to leave the structure. The final failure is shown in the Figures 5.47 and 5.48.

Figure 5.47 – RB1 at failure

Figure 5.48 – Close-up of the failure end of RB1

Figure 5.49 shows the deflection of the beam during the test. As illustrated in the deflection curve the beam shows no ductility prior to failure. This is a dangerous mode of failure in reinforced concrete members.
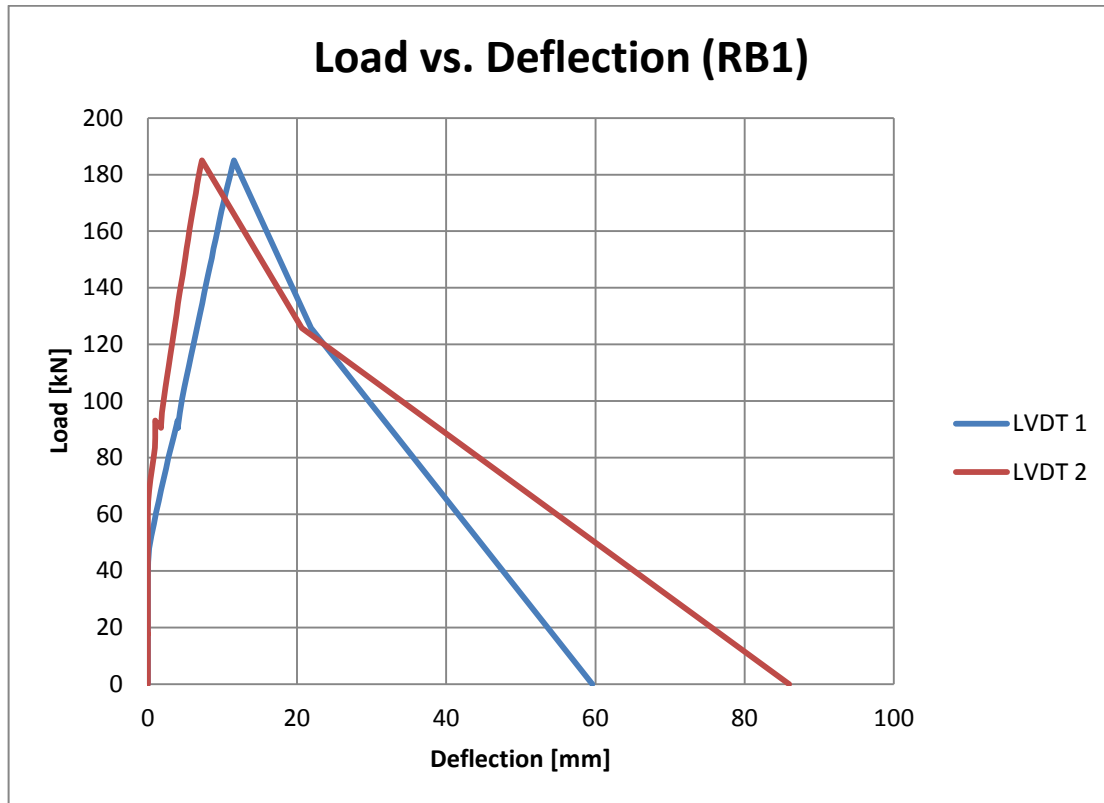
Figure 5.49 – Deflection for RB1

Load vs. steel strain curves for one of the reinforcement is illustrated in Figure 5.50. The shear failure in RB1 occurred prior to the beam reaching its potential flexural capacity as neither of the reinforcement bars reached yield. As shown in the graph, the centre-span strain gauge (ESG 4) did not register the maximum strain but the strain gauges at each side of the centre-span (ESG 3 and ESG 5) did register the highest strain during the experiment. ESG 4 reached 75% of yield strain while both ESG 3 and ESG 5 reached up to 84% of yield strain.
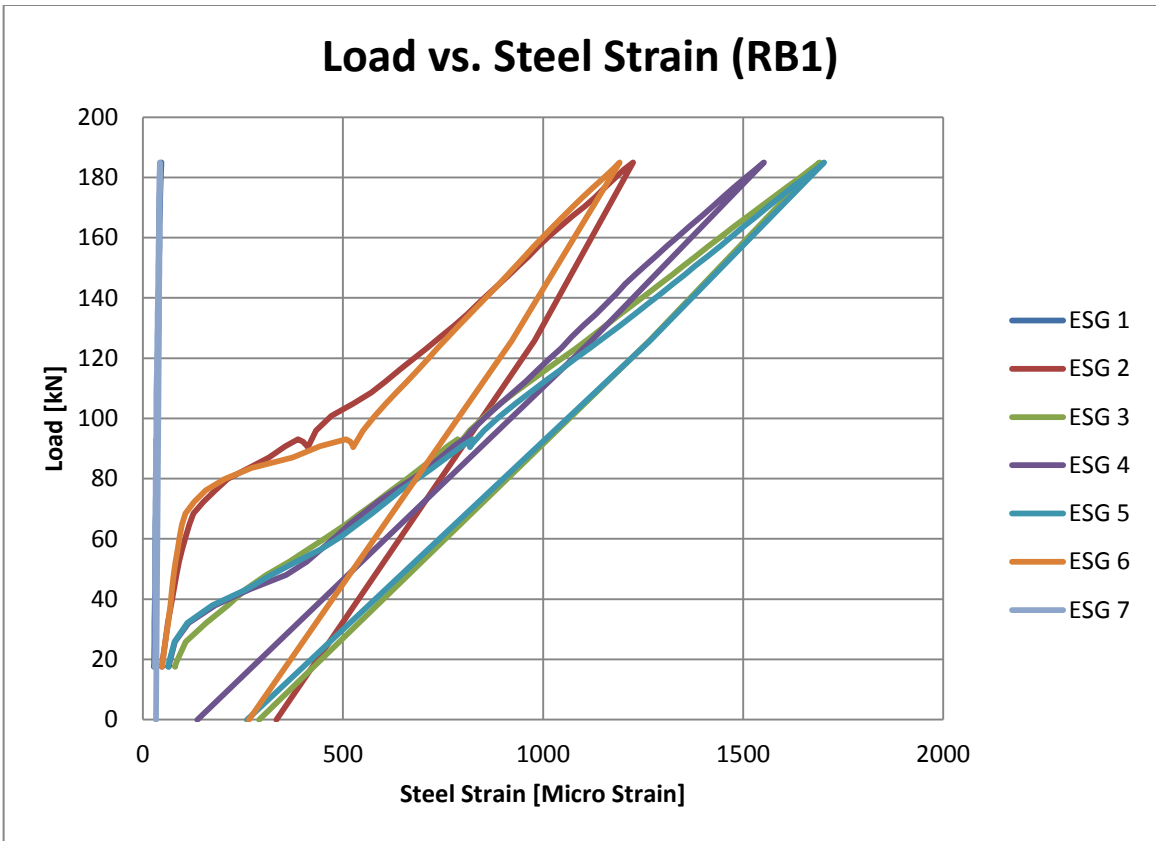
Figure 5.50 – Steel strain along one rebar for RB1

5.1.11 RB2

RB2 was the second rectangular beam to be tested. It is rectangular in cross-section and in profile. The beam is reinforced with two 25M steel reinforcing bars longitudinally and with no shear reinforcement. The reinforcing in this beam follows same parabolic curve as the curved beams. The following figures show the beam's configuration.
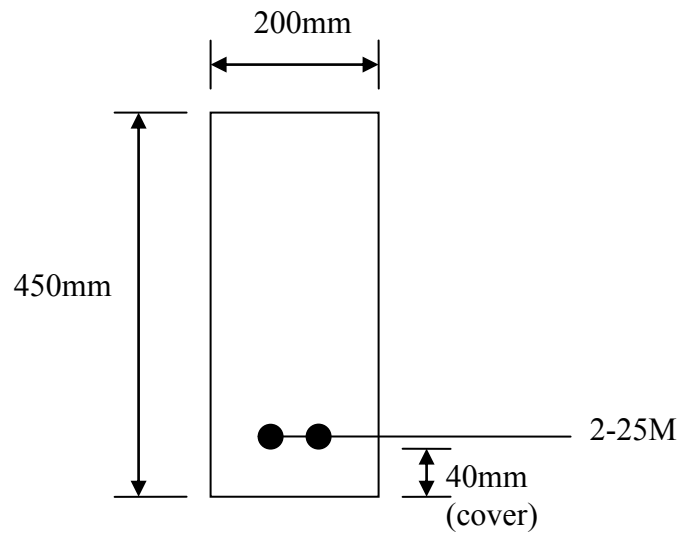
Figure 5.51 - Cross-section at centre line
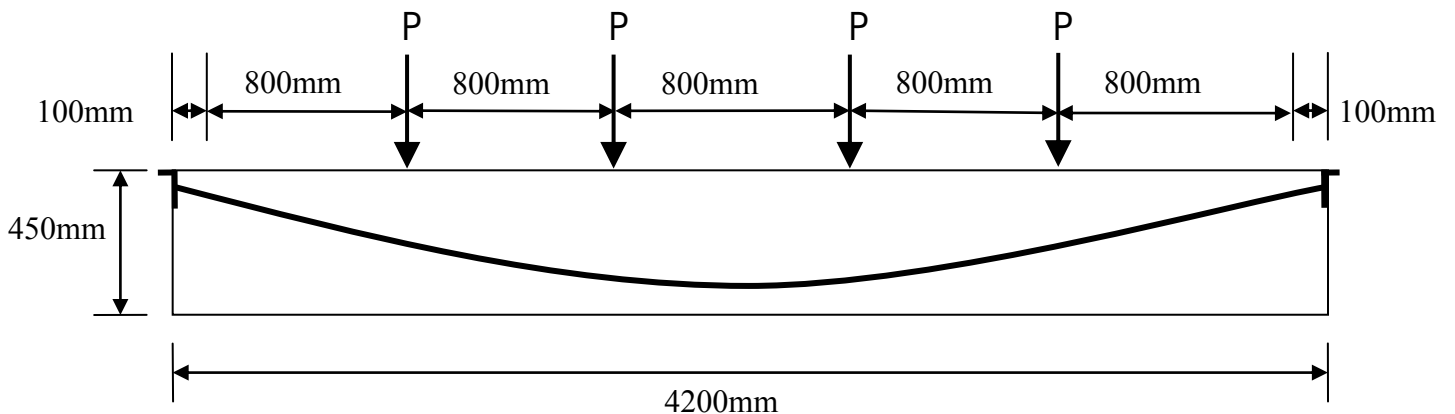
Figure 5.52 - Loading scheme and overall dimensions of RB2

As in RB1 strain gauges were placed directly below the two PI gauges to measure the compression
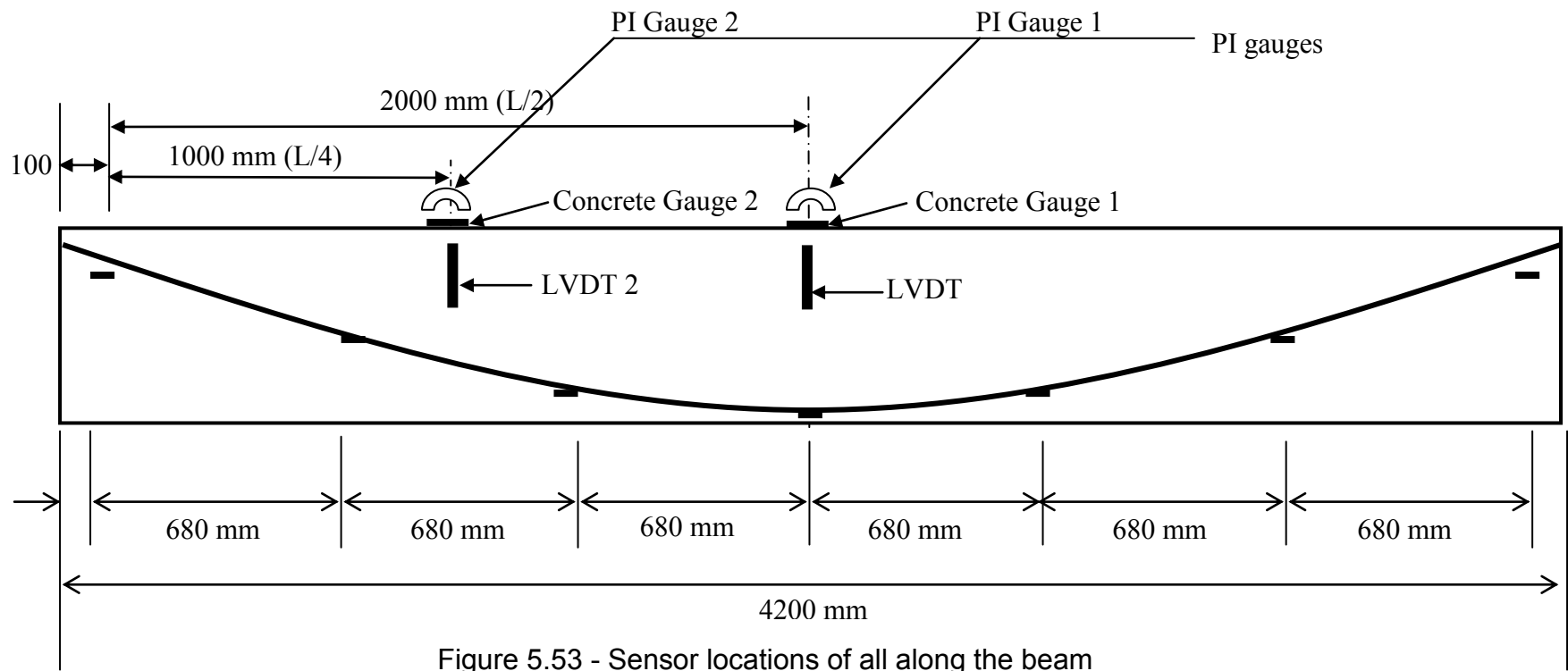
.

Figure 5.53 - Sensor locations of all along the beam

Strain gauges were placed along the bottom of the reinforcement bars, numbers1, 8, 7 and 14. These gauges where place at the top of the bar after the bars were welded to the end angle.

No. 8   No. 9   No. 10   No.11   No. 12   No. 13   No. 14

No. 1   No. 2   No. 3   No. 4   No. 5   No. 6   No. 7

Two reinforcing bars
in each beam
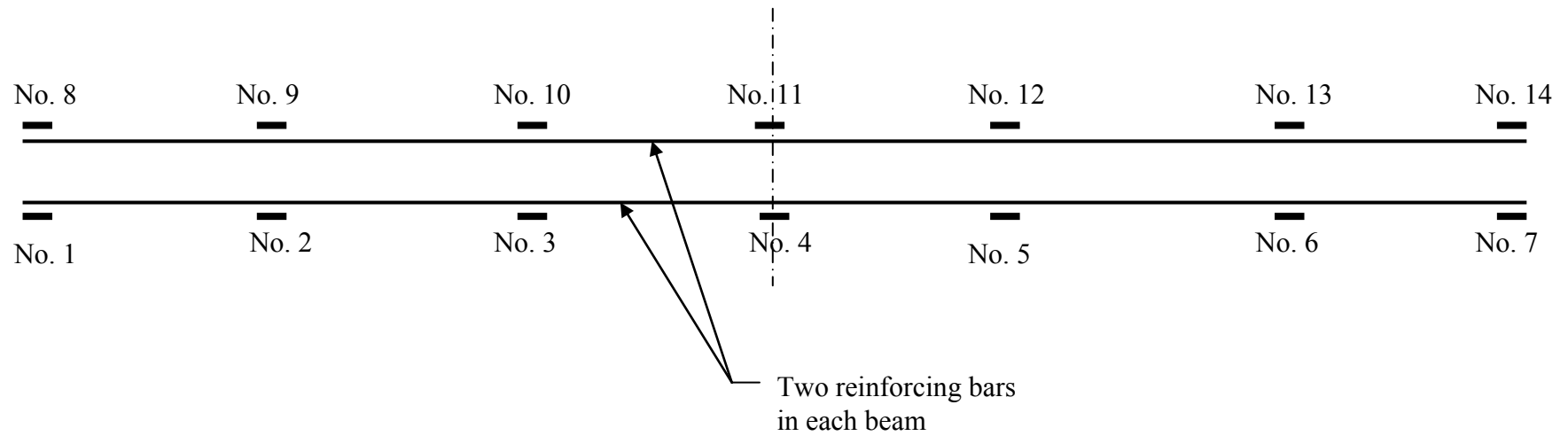
Figure 5.54 - The numbering system for the steel strain gauges

The purpose for constructing and testing RB2 was to determine if simply curving the primary reinforcing steel along the bending moment curve within the rectangular concrete section would make a difference in the final capacity and final mode of failure. As illustrated in Figure 5.55 this beam exhibited very ductile behaviour until total failure. The beam reached the maximum load of 244kN at deflection of 34mm.
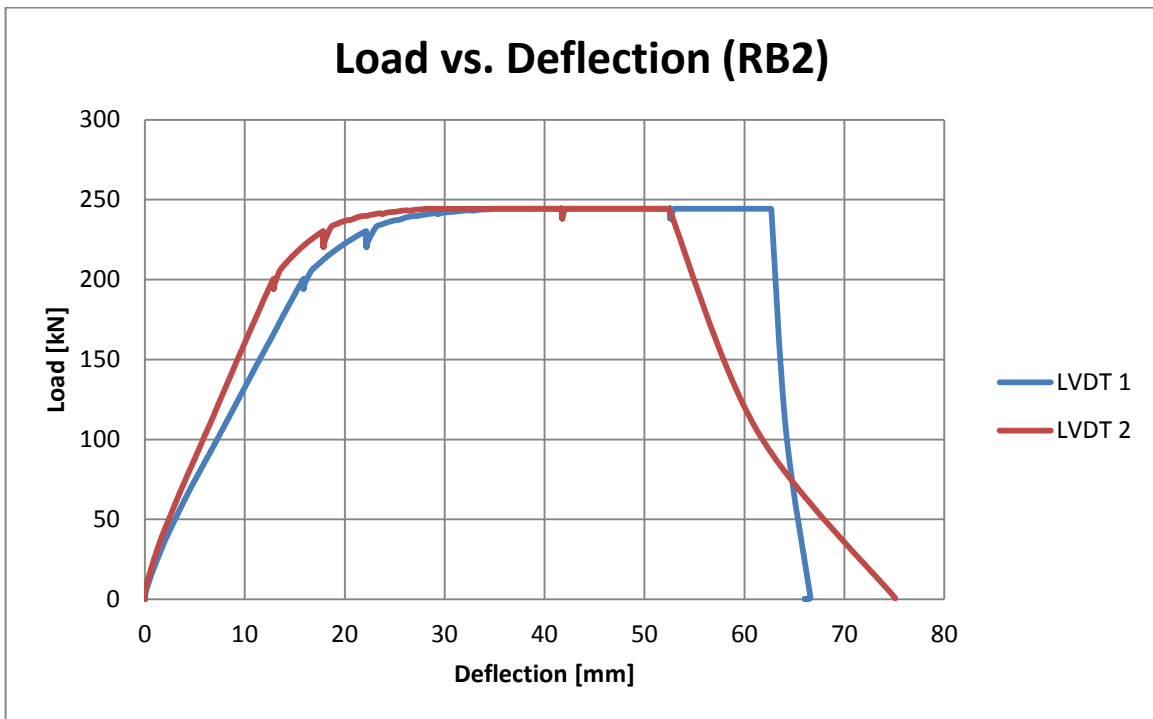
Figure 5.55 – Load-deflection curve for RB2

Demonstrating the behaviour of this beam is best provided by a series of photographs from the beginning to the end of the experiment. The Figures 5.56 through 5.63 show RB2 from the beginning of the test until after the failure. The first cracks appeared not at the centre-span where the moment is highest but where the reinforcements start moving upwards to the support. This indicates

that the maximum flexural tension stress developed at those locations (Figure 5.57).

Figure 5.56 – Initial cracks not at centre-span

Figure 5.57 – Uniformly distributed crack propagation

Figure 5.58 – Crack propagation
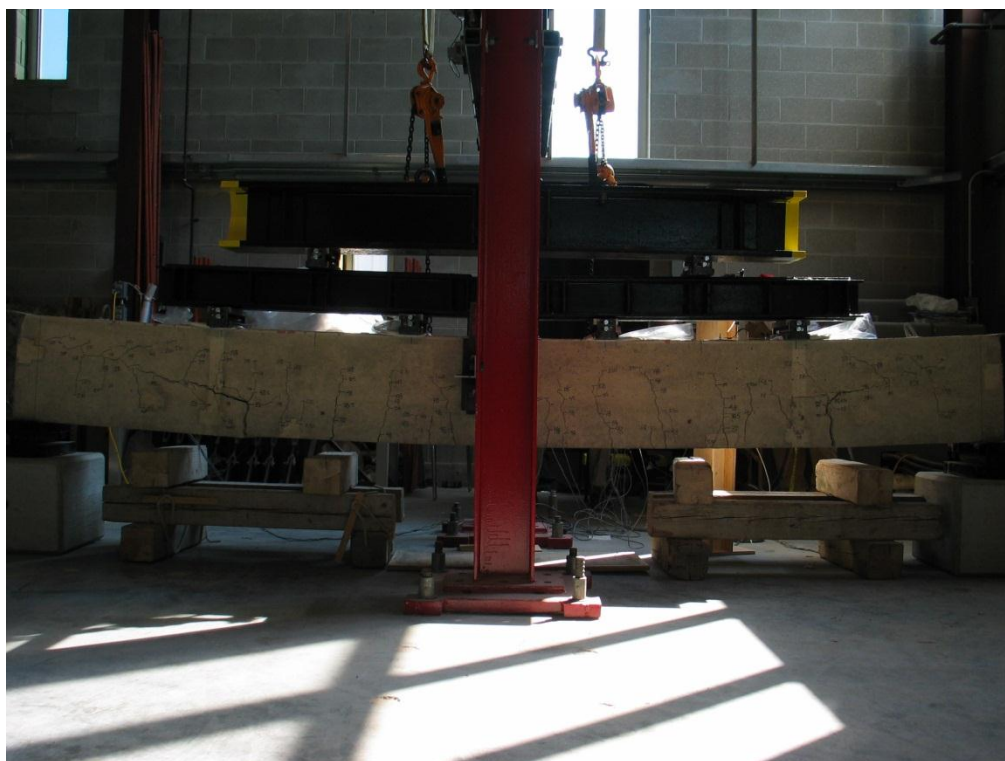
Figure 5.59 – Cracking along the reinforcement

Figure 5.60 – RB2 prior to final failure

Figure 5.61 – RB2 right after final failure

Figure 5.62 – Failure end of RB2

Figure 5.63 – Close-up of failure

As illustrated in Figure 5.65, right after the normal longitudinal tension cracks, a different crack started in the concrete along the entire length of the reinforcement following the same curvature as the reinforcement. This crack (that could be called a curved-crack) shown in Figure 5.65 separated the concrete below the reinforcement from the rest of the beam. In other words, the concrete below the reinforcement was not doing any work except directly over the support where the vertical load was being transferred to the support rollers. Figures 5.64 and 5.65 show the curved-crack and load path at RB2's support end.
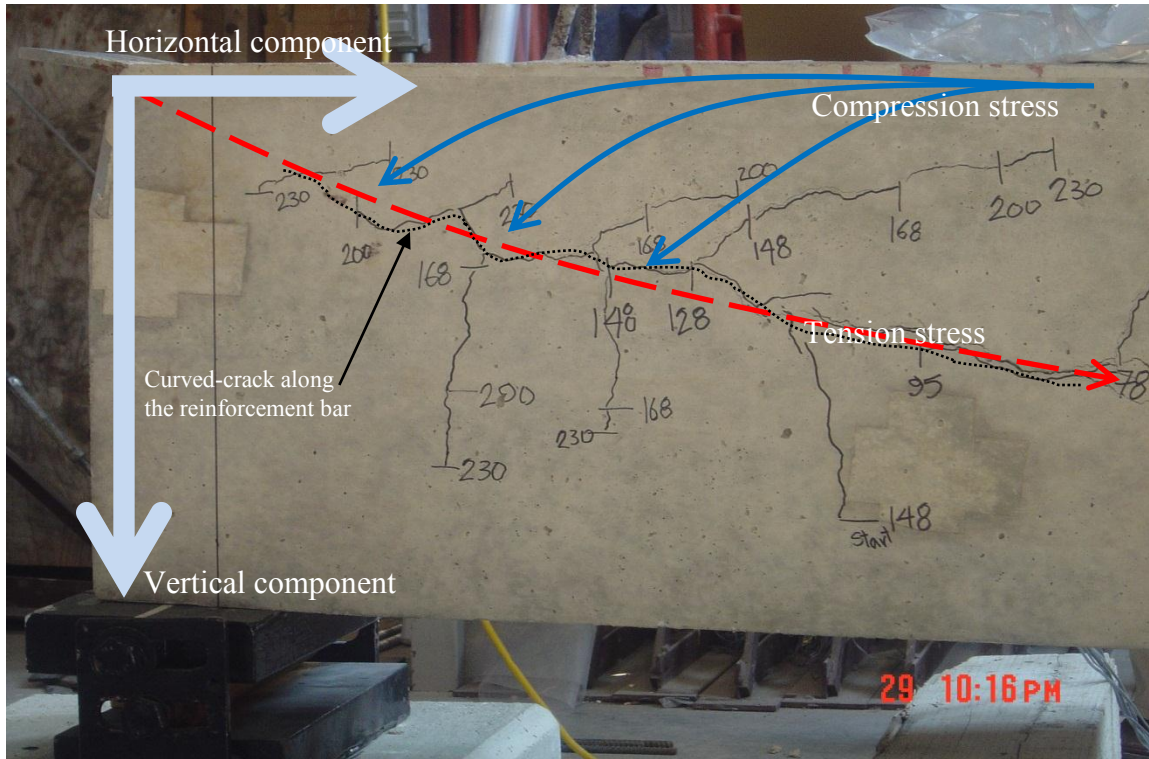
Figure 5.64 – Stress path at the support end
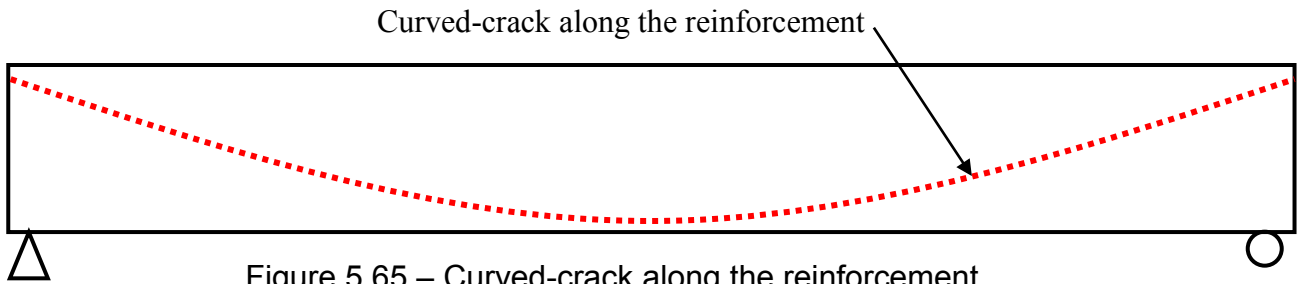
Figure 5.65 – Curved-crack along the reinforcement

Most of the strain gauges attached to the steel reinforcing were damaged during the test due to the horizontal movement of the curved-crack along the reinforcement. However, the data retrieved prior to the gauges being damaged showed that steel did not yield prior to the final failure.

126
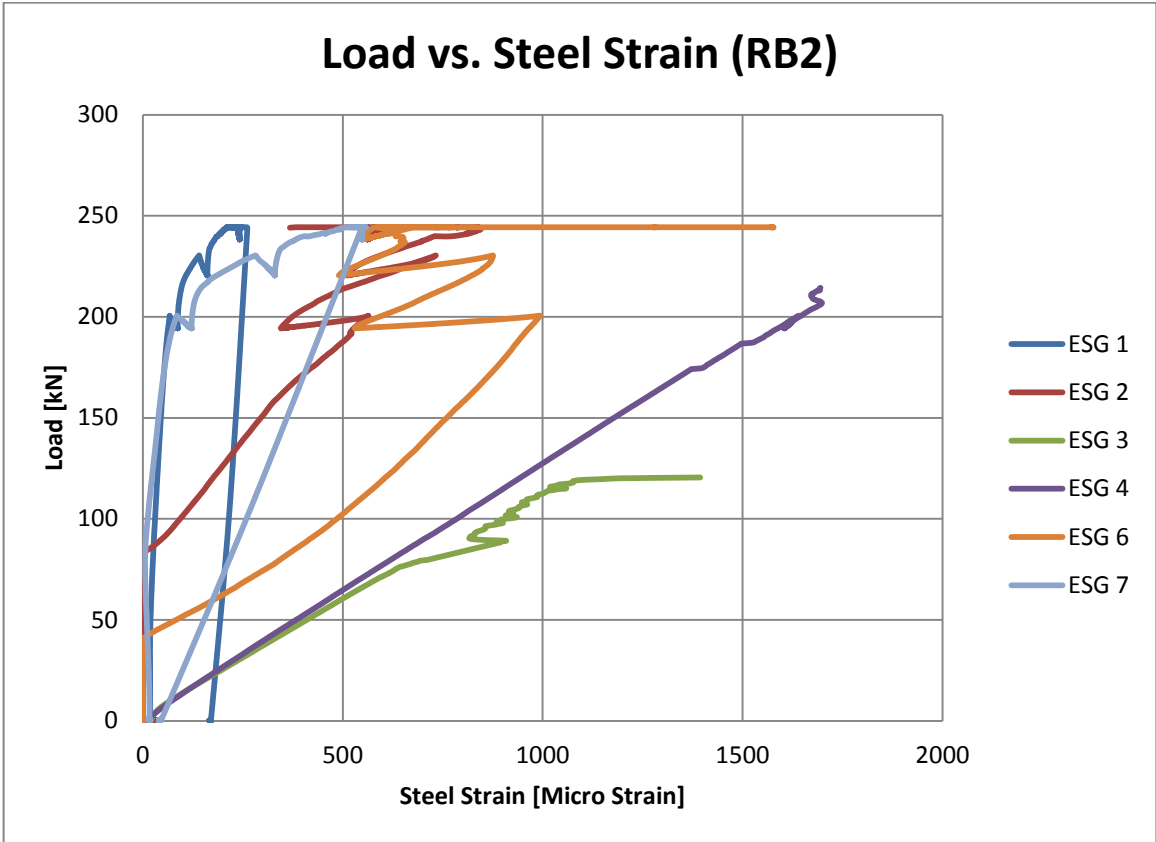
Figure 5.66 – Steel strain along reinforcement in RB2

5.1.12 RB3

This beam is rectangular in cross-section and in profile. It is reinforced with two 25M steel reinforcing bars longitudinally and shear reinforcement designed in accordance with CSA A 23.3 as shown below in Figures 5.67 and 5.68.
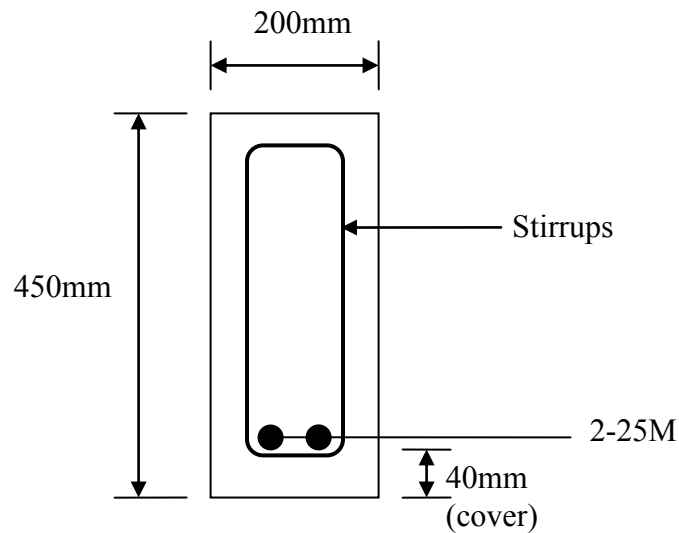
Figure 5.67 – Cross-section at centre line
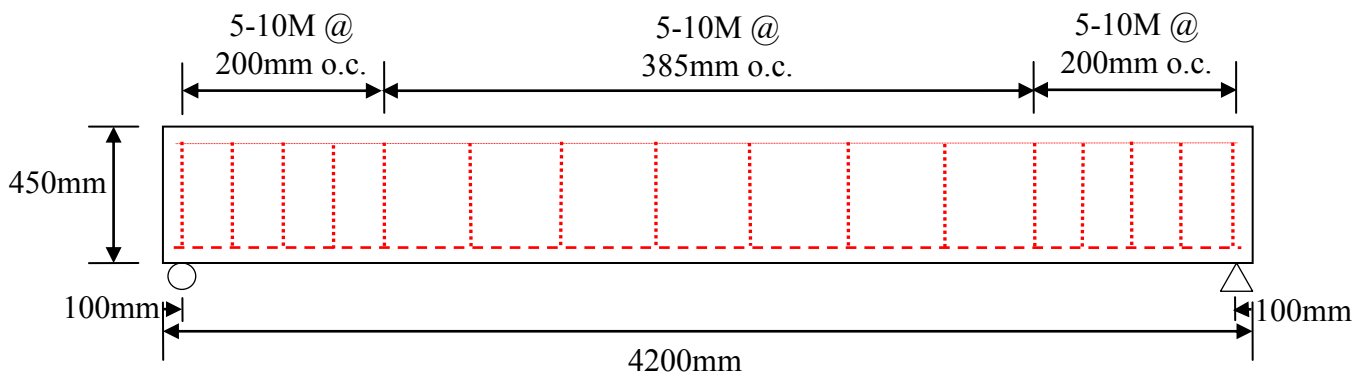
Figure 5.68 – RB3 overall dimensions and stirrup locations, elevation view

The strain gauge locations in RB3 are shown in figure 5.69.
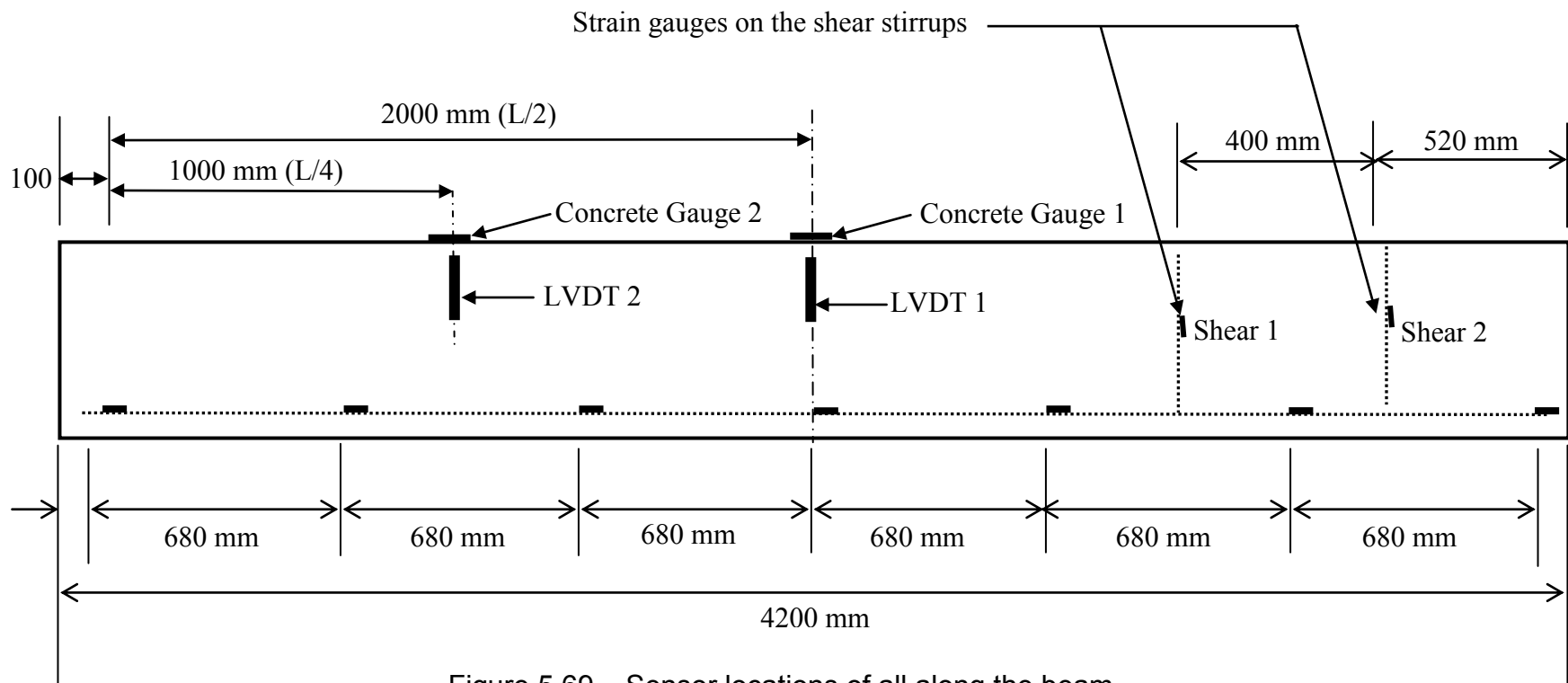
Figure 5.69 – Sensor locations of all along the beam

Reinforcement strain gauges were placed along the bottom of the reinforcement bars, numbers1, 8, 7 and 14. These gauges where place at the top of the bar after the bars were welded to the end angle.

No. 8　　　　　No. 9　　　　　No. 10　　　　　No. 11　　　　　No. 12　　　　　No. 13　　　　No. 14

No. 1　　　　　No. 2　　　　　No. 3　　　　　No. 4　　　　　No. 5　　　　　No. 6　　　　No. 7

Two reinforcing bars
in each beam
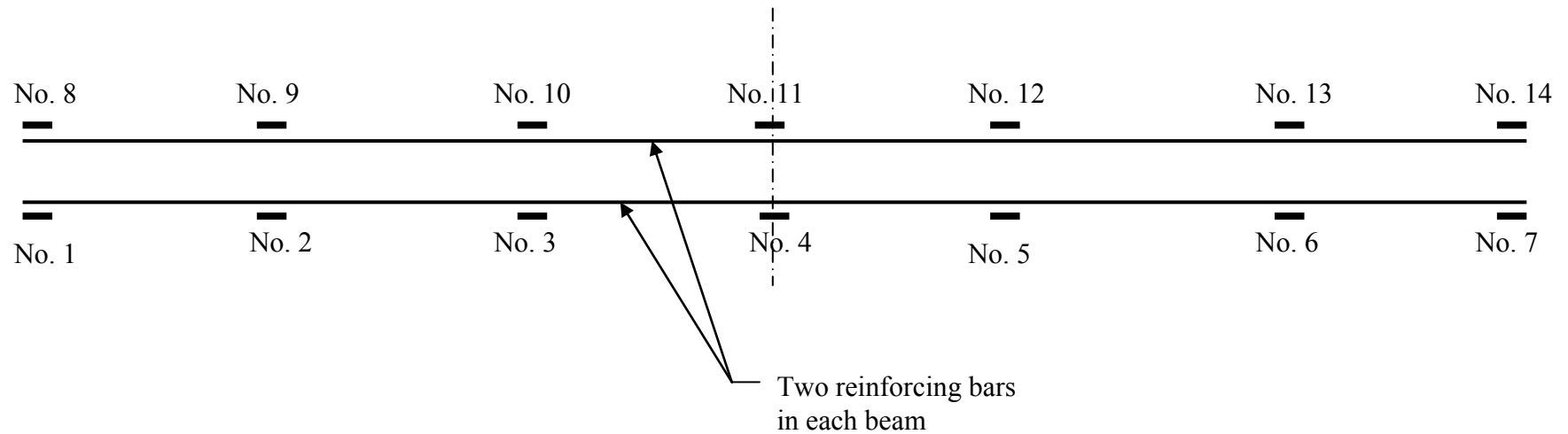
Figure 5.70 – The numbering system for the steel strain gauges

This beam acted as predicted and as outlined in standard concrete design text books. Figure 5.71 illustrates the crack pattern prior to final failure.

Figure 5.71 – RB3 (CSA designed beam) during testing

Cracks initiated at the centre-span where the moment is at maximum and where the flexural tension stress in the steel reinforcement is at the highest. As the load was increased new cracks developed. They were uniformly distributed from the centre-span towards each support and maintain development up to a load of 150kN. Form the load of 150kN to the final load of 244kN no new cracks developed but the existing cracks increased in length and width. The following figure shows RB3 right after failure.

Figure 5.72 – RB3 right after failure

The steel reinforcement in RB3 was yielded at the center-span, as shown in Figure 5.73, while the strain gauges on the reinforcement at the end of the beam close to the supports registered very little strain. The intermediate strain gauges show that the steel did not yield between the mid-span and the supports. This shows that the stress in the steel reinforcement is variable. In other words, steel sustains or carries higher stress at the mid-span than at other locations, which indicates that the steel in CSA designed beam is not used efficiently.

In Figure 5.74 the deflection curve for RB3 also shows a ductile failure as the beam deflected 70mm prior to final failure, almost six (5.83) times the allowable deflection of 12mm.
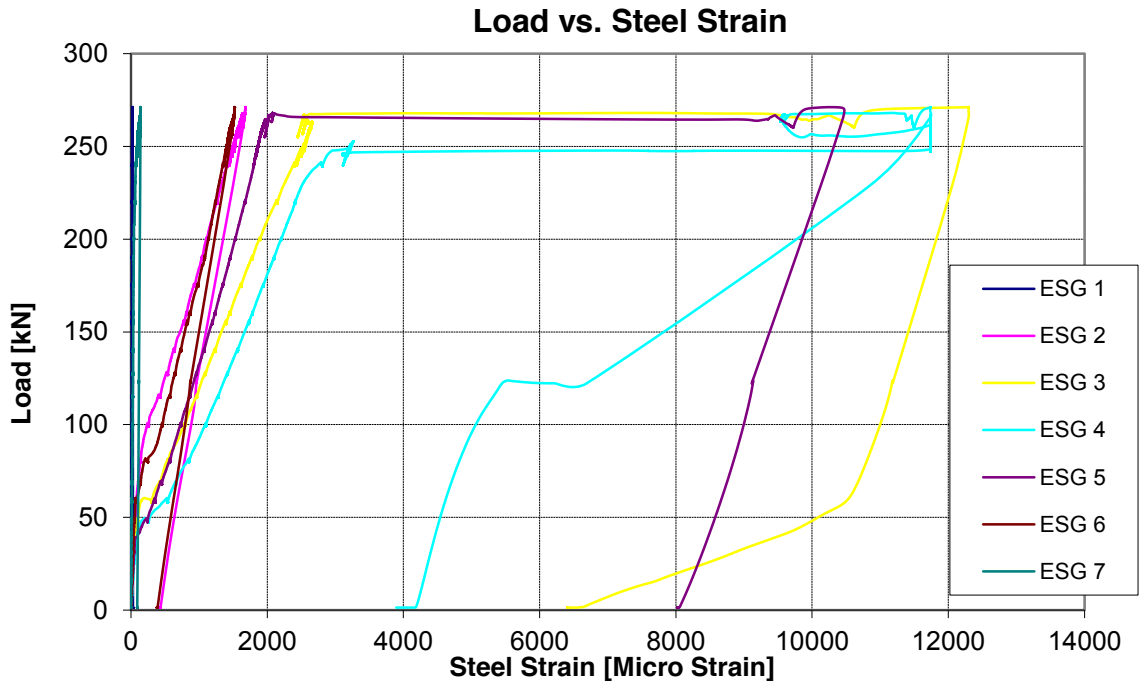
Figure 5.73 – The strain in the reinforcement in RB3
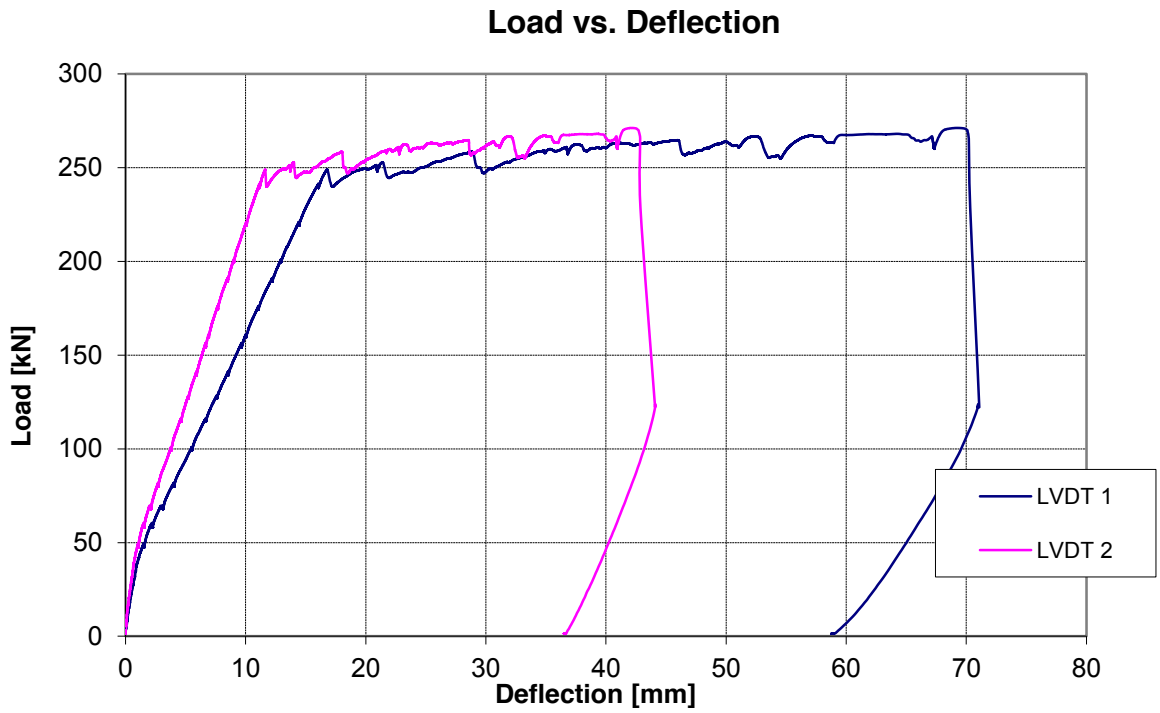
Figure 5.74 – Load-deflection curve for RB3

133

5.1.13 RB4

This beam is rectangular and uniform, in cross-section and in profile.   It is reinforced with flexural reinforcement only (2-25Ms) placed parallel to the bottom of the beam, similar to RB1 and RB3.   There are no shear stirrups in this beam. The flexural reinforcement is welded to an end angle at each end, similar to the curved beams CB.   Figures 5.75 and 5.76 show the cross-section, overall dimension and loading schematic of RB4.
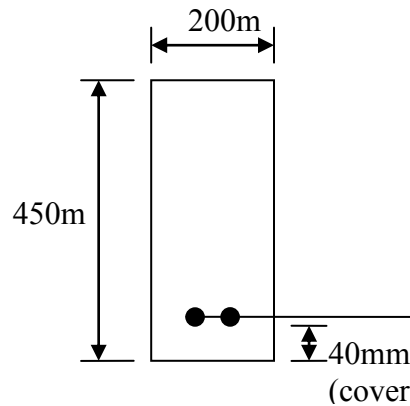
Figure 5.75 – RB4 cross-section (uniform)
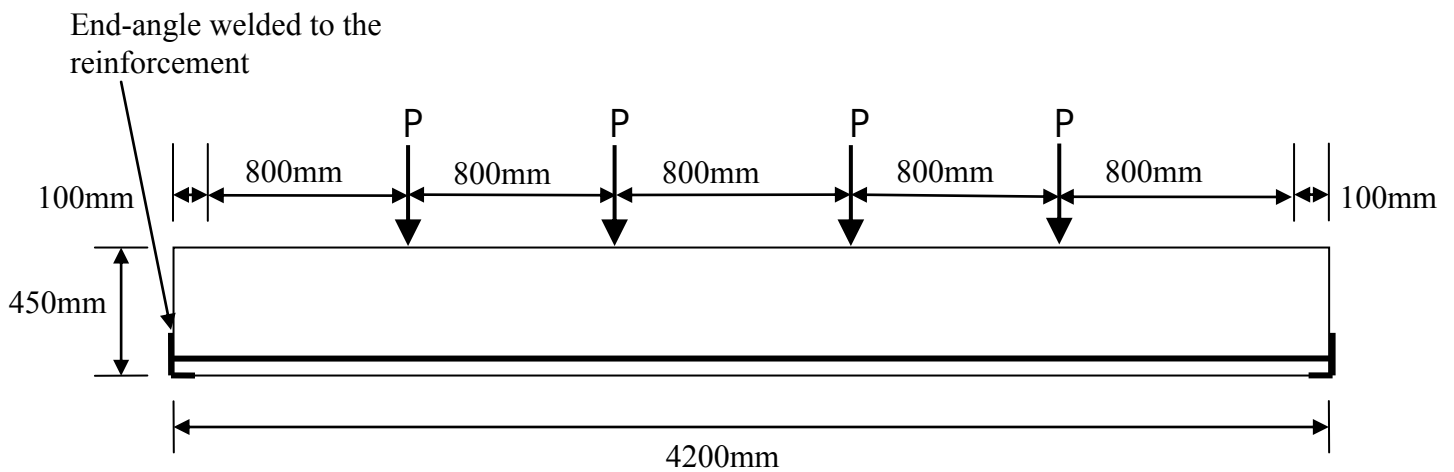
Figure 5.76 – RB4 overall dimension and loading schematic

Figure 5.77 shows the instrumentation schematics and location of the strain gauges.
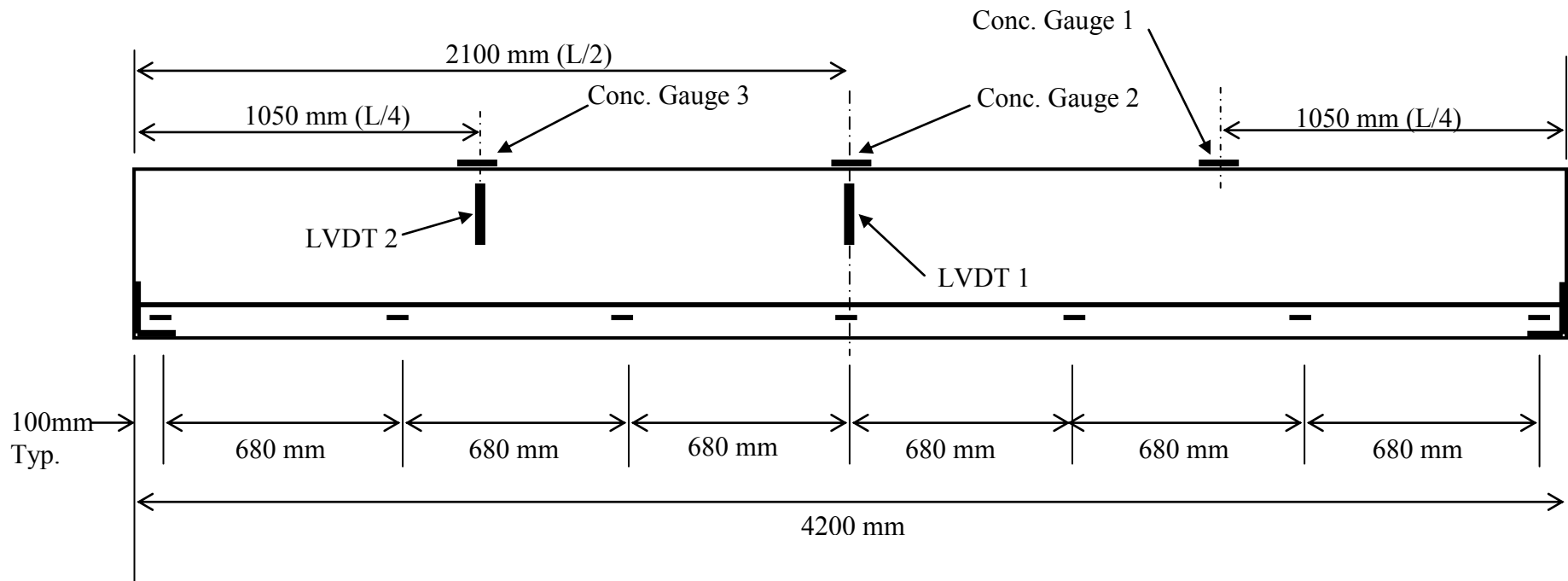
Figure 5.77 – Instrumentation schematic

Figure 5.78 shows the steel strain gauge numbering system. Since all previous tests show the strain gauges on both reinforcements register the same strain only one of the reinforcement bars was instrumented in RB4.

No. 1   No. 2   No. 3   No. 4   No. 5   No. 6   No. 7

Two reinforcing bars
(2-15M)
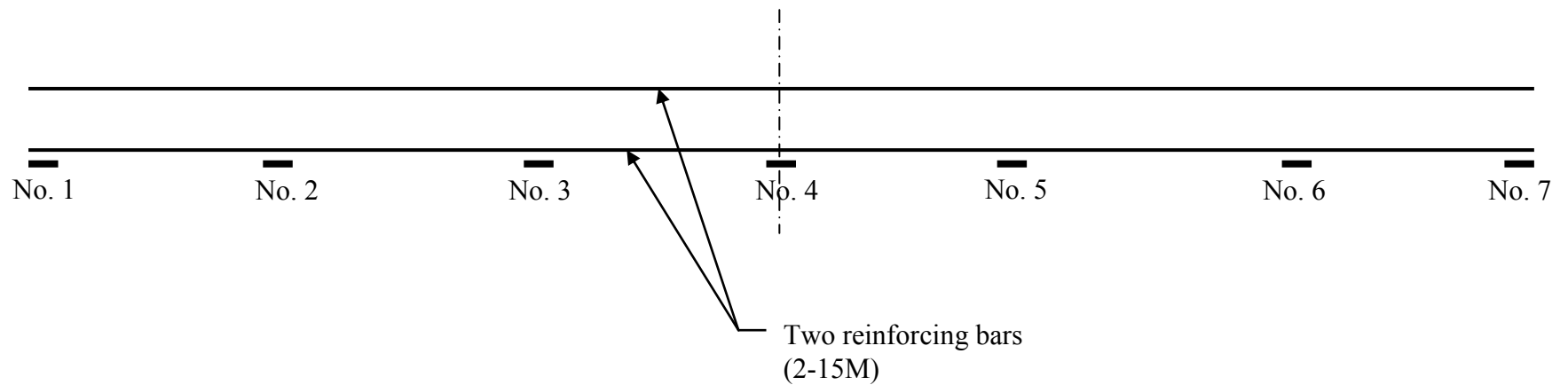
Figure 5.78 – RB4 seven strain gauges on one of the reinforcement rebars

Additional strain gauges were installed on the sides (web portion) at one end of RB4 to monitor the development of "shear" or diagonal tension at locations close to the support. Figure 5.79 shows the location and numbering of the strain gauges.
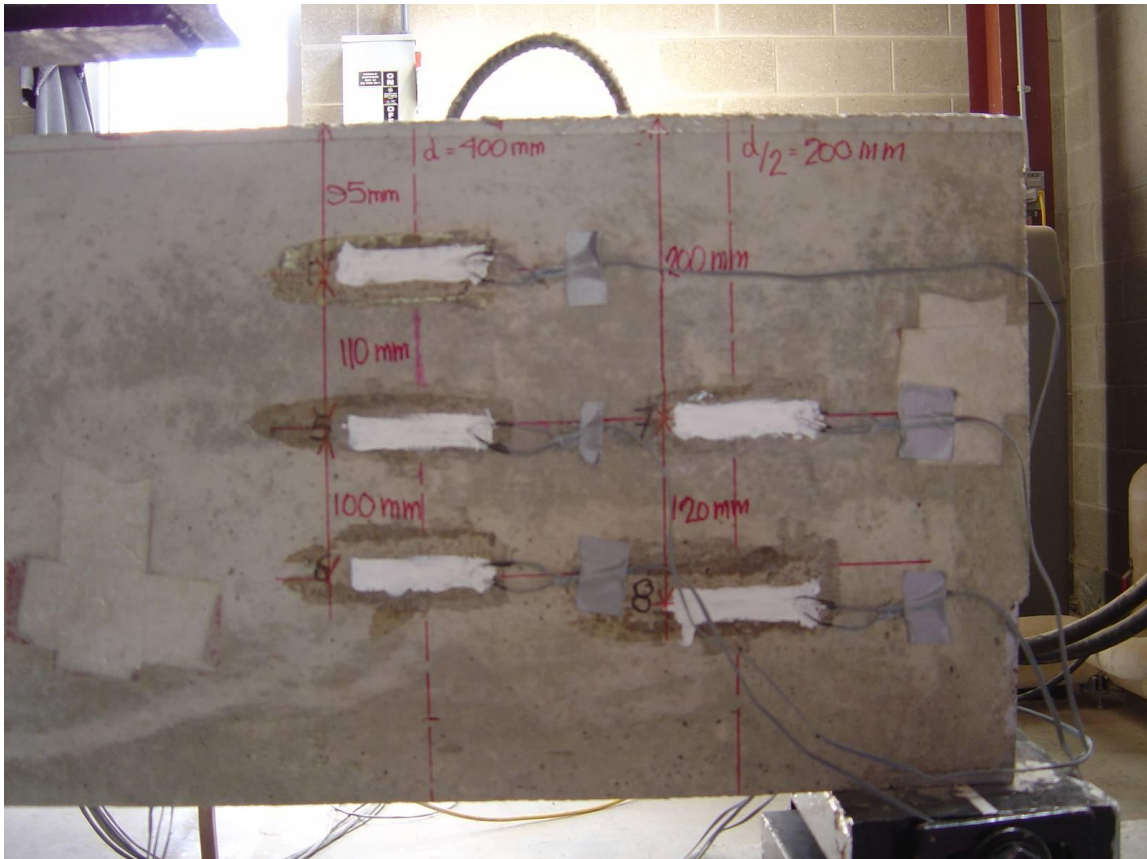
Figure 5.79 – Strain gauges on the web of RB4 to monitor "shear"

RB4 failed at 108 kN, a lower load than the previous beams tested in this phase. The failure was ductile with non-uniform tension stress distribution along the reinforcement. The reinforcement yielded at the mid-span and the strain gauges located closer to the support registered less strain. Figure 5.80 shows RB4 after failure. As illustrated the cracks are due to a concentration of tension forces at the mid-span and no "shear" cracks developed at each end.

Figure 5.80 – RB4 after failure

Figure 5.81 shows that the reinforcement yielded at the middle 1400mm (700mm each side of the center-span). The strain gauges closer to support register much less strain (less than 50%) and the gauges at the supports register near zero strain.
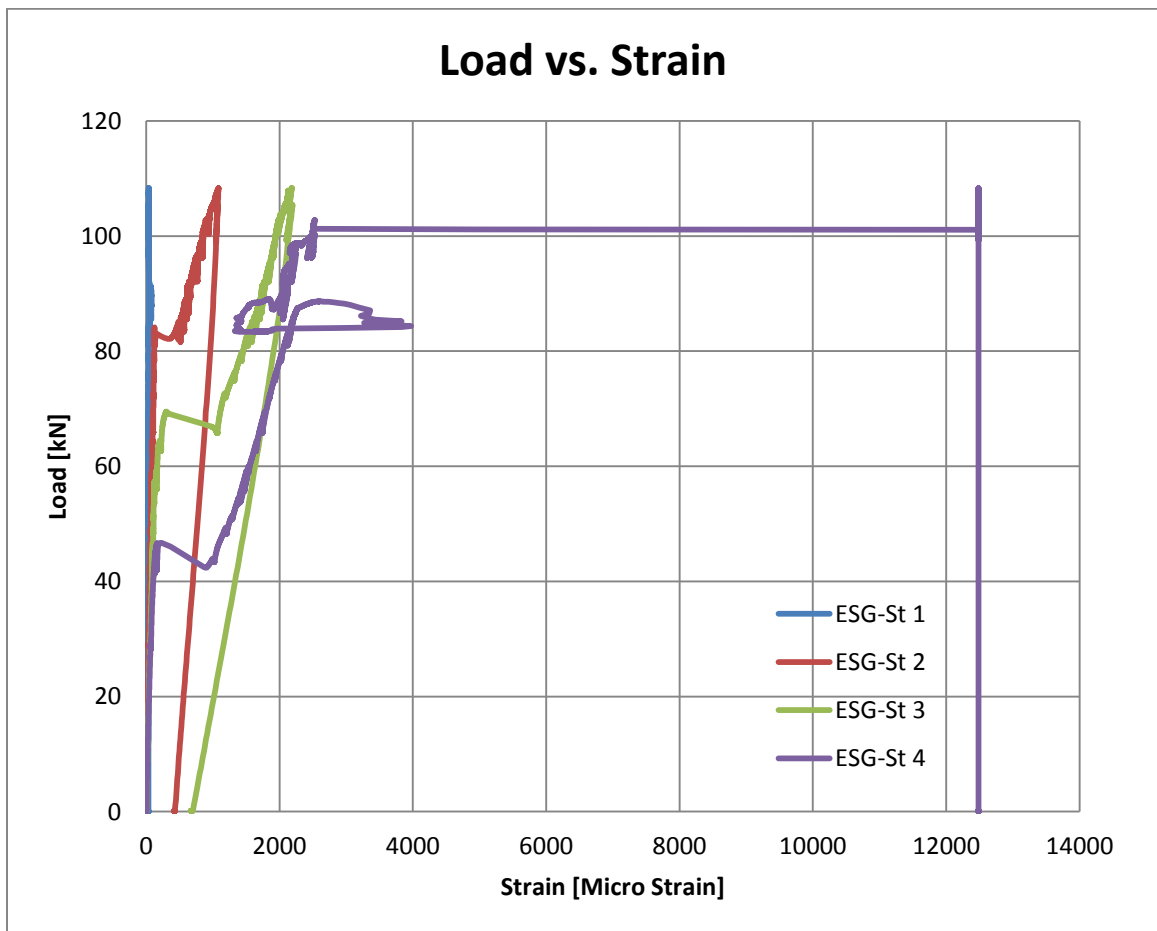
Figure 5.81 – Strain distribution along the reinforcement in RB4

Closer to the support, the strain gauges placed on side of the beam (the web portion) registered practically zero strain at the area that should show highest "shear". Figure 5.82 shows the load vs. strain for the side gauges. The maximum strain registered at this area which should have the highest "shear" was 0.000028 (tension strain); which is virtually zero. Strain gauge 4 located closer to the top of the beam, placed at the effective-depth (400mm) away from the support is the only gauge showing compression strain (0.000023 at maximum). The rest of the strain gauges all show tension strain ranging from 0.000006 to 0.000028.
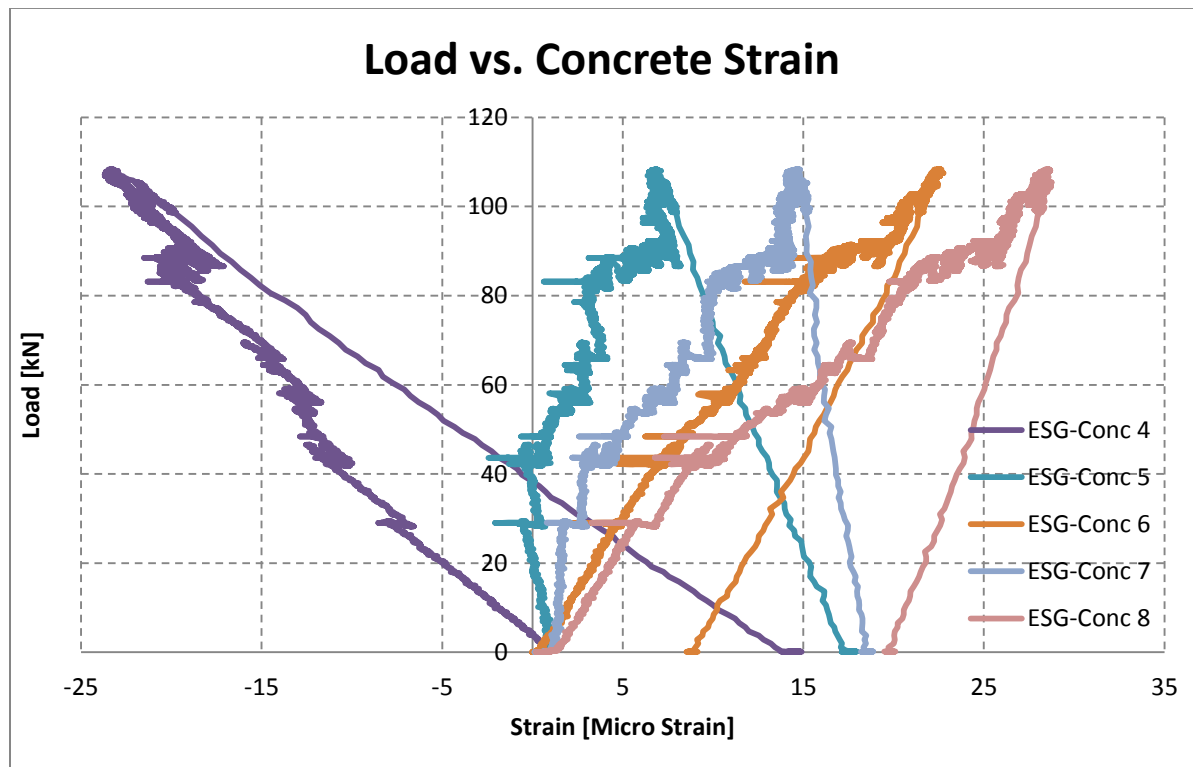
Figure 5.82 – Strain on the side of RB4

The graphs in Figures 5.81 and 5.82, determine that the compression stress does not travel to the support through the concrete but it arches down to the reinforcement at the middle of the beam. This argument is demonstrated in figure 5.83 where the compression stress is approximated by curves travelling between the tension cracks and landing on the reinforcement.
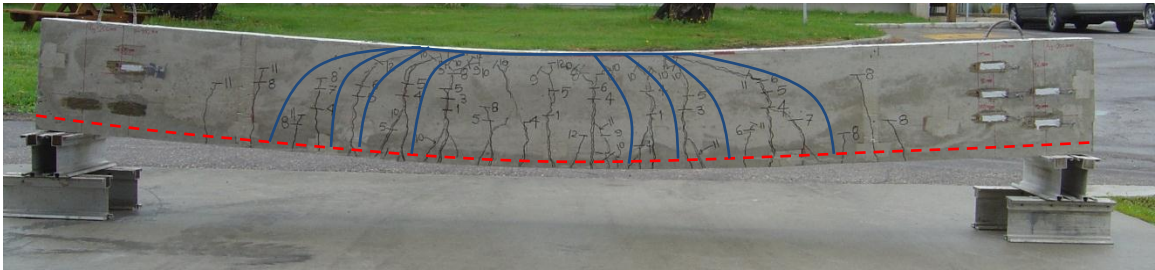
Figure 5.83 – Compression stresses (blue line) and tension stress (red dashed line) in RB4

It was expected that RB4 would fail similar to RB1, the rectangular beam without "shear" reinforcement. It is understood that RB4 did not fail in "shear" because the flexural reinforcements were anchored to the end of the beam by the end-angles.

5.2   Results for Phase II Testing – End-Beams Testing

Phase II consisted of constructing and testing eight end-beams. The detail of the end-beam configuration is outlined in Chapter 4.   The primary purpose for experimenting with the end-beams was to examine a series of solutions to reduce the diagonal tension without adding more concrete.   The end-beams demonstrated a different mode of failure in comparison with the full-size curved beams in Phase I; the initial failure crack and its propagation was not consistent with the full-size beams. This may have been due to the support condition and location of the lifting stirrups, which acted as shear stirrups altering the stress path. Since this behaviour was not anticipated, lifting stirrups and the structural steel support frame were not instrumented to be monitored during the testing. Stress and deflection of the support frame and the stress in the lifting stirrups should have been collected to be considered during the analysis. Therefore, the end-beams tests results cannot be compared to the results of the full-size beams. This document will not cover the testing results for the end-beams, but will discuss the test result in general as a reference for future studies. There are, merits in doing end-beam testing instead of full-size testing to reduce materials for experimental stages of future studies but the researchers should consider monitoring the additional support frame and steel in the specimens. One of the best outcomes of testing the end-beams was to further verify the FEM Analysis Program FINIT-Y. The program accurately predicted the crack pattern and the failure mode of each beam once the mathematical model took the stiffness of the lifting stirrups into account and reduced fixity at the structural steel support frame.

Figure 5.84 shows the crack pattern predicted by the FEM analysis superimposed on top of the photograph of ECB2; as illustrated, the crack pattern is a nearly perfect match.
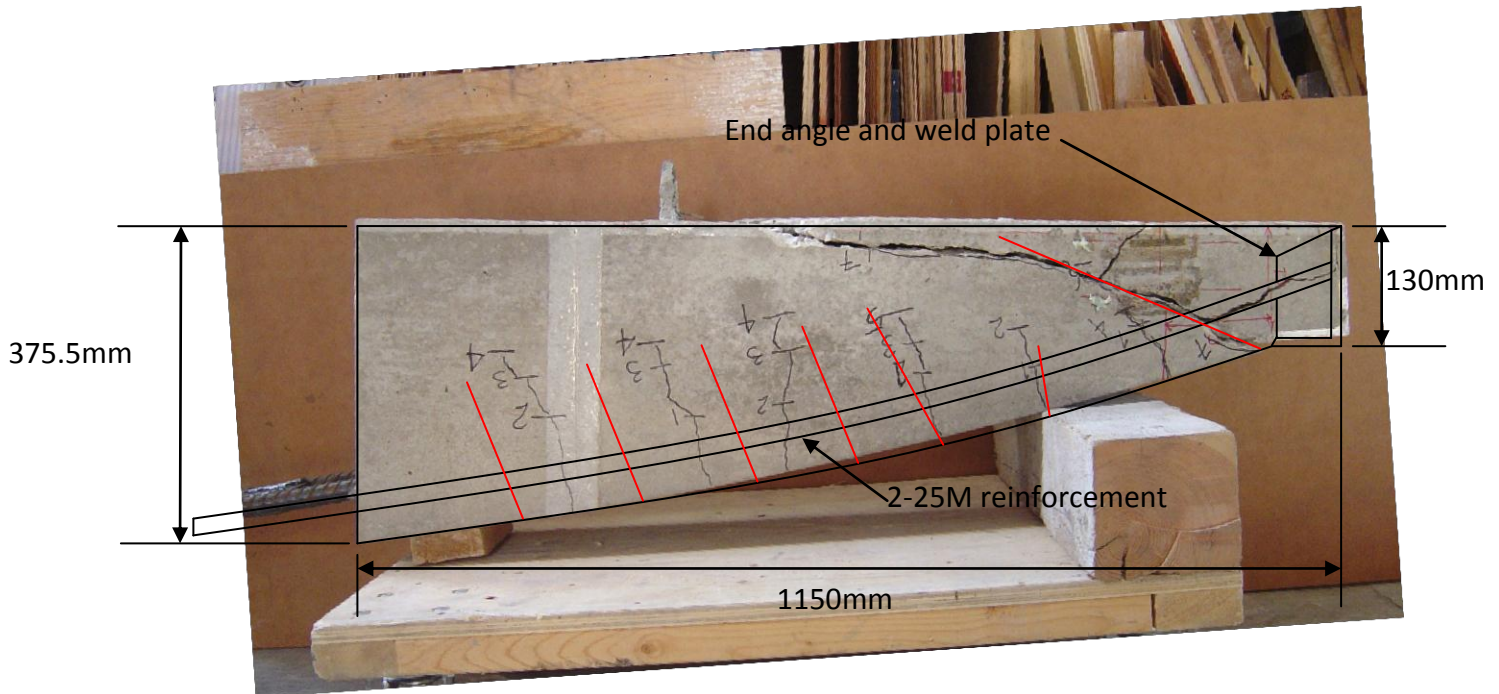
Figure 5.84 – FEM analysis result superimposed on ECB2.
Nearly identical crack pattern compared to the FEM analysis.

5.2.1 ECB1 and ECB2

ECB1 and ECB2 were the control specimens. They were fabricated and tested to prove that the end-beams would react as the full-size beam at the support. As mentioned in the introduction of this section, the failure mode of both ECB1 and ECB2 were not similar to the full-size beams at the final load. This was due to the difference in the support condition (which was discussed in Chapter 4) and to the location and the amount of steel used for the lifting which acted as shear stirrups.   These results were incomparable with the full-size beam results. Figures 5.85 and 5.86 show the failure mode for both ECB1 and ECB2.

Figure 5.85 – ECB1 after testing. Crack pattern

Figure 5.86 – ECB2 after testing. Crack pattern

5.2.2 ECB-RA1 and ECB-RA2

ECB-RA1 and ECB-RA2 were the end-beams with the end support angle reversed as shown in Figures 5. 87 and 5.88.

Figure 5.87 – ECB-RA1 prior to testing, showing the end angle reversed

Figure 5.88 – Close up of the end angle, the arrow indicates the support point

Figure 5.89 shows ECB-RA1 during the testing. As shown, the end angle has been modified by placing a shim between the angle and the roller to allow the load roller to move freely during the test. ECB-RA1 was not tested to total failure since the support system for the rebar snapped first. This was due to quenching of the rebar end during the welding process. The failure of the welded end is shown in Figure 5.90. ECB-RA1 was loaded to 80% capacity.

Figure 5.89 – ECB-RA1 during testing
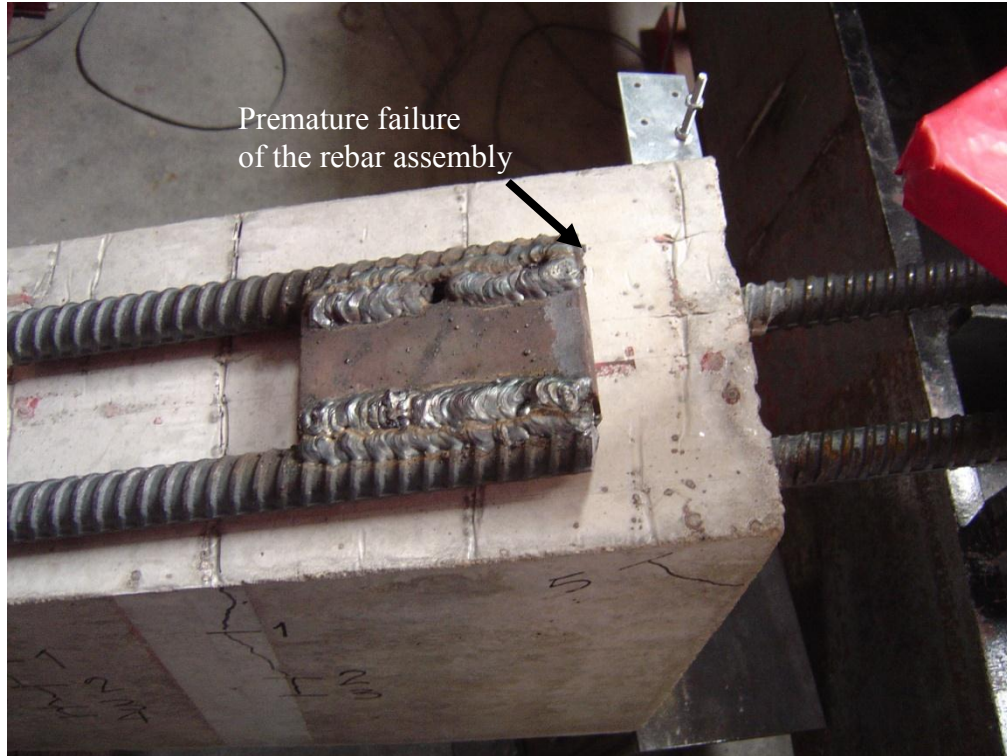
Figure 5.90 – The rebar assembly failure for ECB-RA1

The ECB-RA2 was tested to failure. Figures 5.91 and 5.92 show the failure mode for ECB-RA2.

Figure 5.91 – ECB-RA2 after testing

Figure 5.92 – Close up of the failure section of ECB-RA2
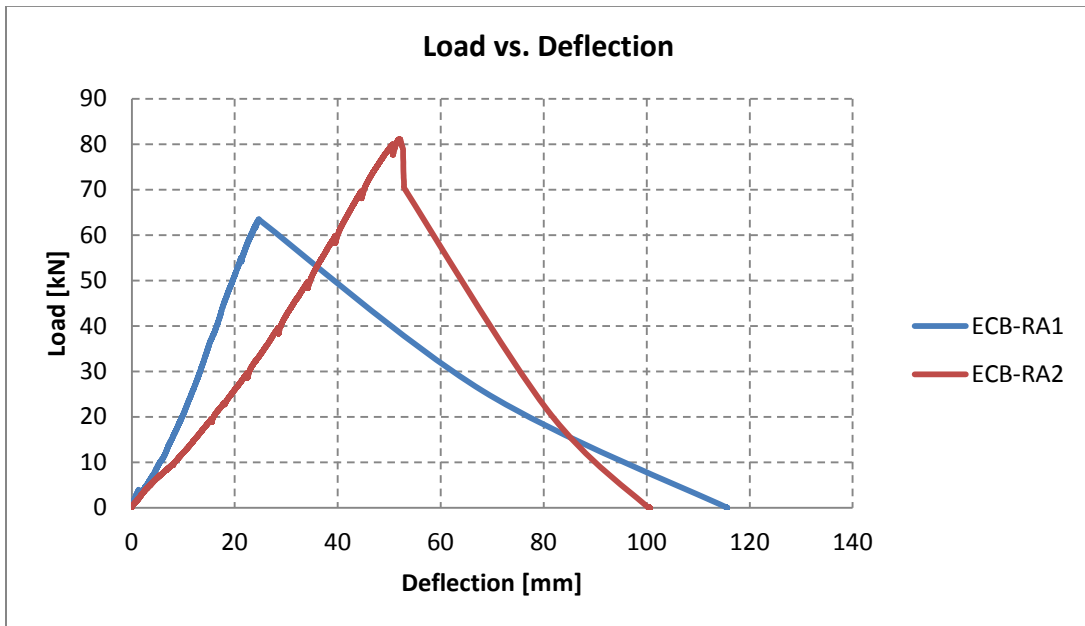
Figure 5.93 – Load-deflection curve comparison for ECB-RA1 and 2

5.2.3 ECB-TS1 and ECB-TS2

ECB-TS1 and 2 were the end-beams with compression steel added at the top of the beam to increase ductile behaviour. All other parameters are similar to those of ECB1 and 2. Figures 5.94 and 5.95 show the crack pattern and failure mode for both ECB-TS1 and ECB-TS2.
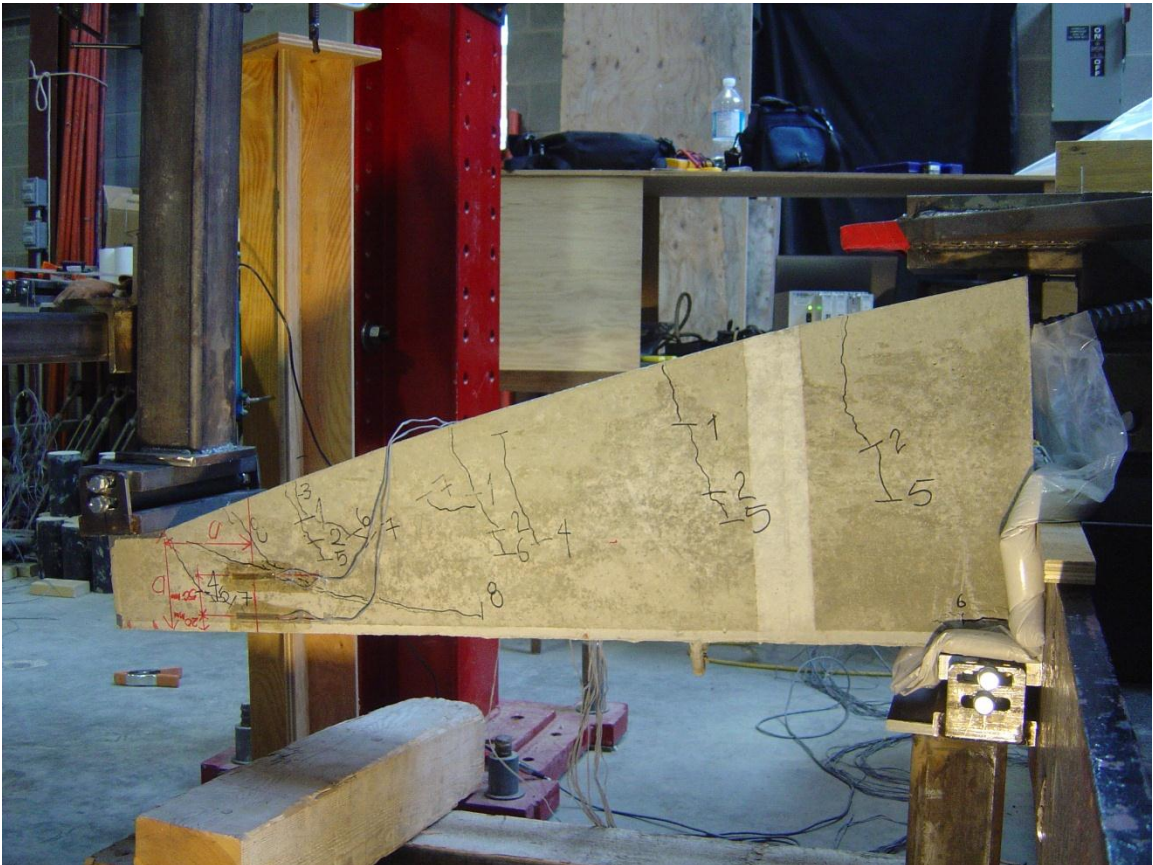
Figure 5.94 – ECB-TS1 during testing and close to failure
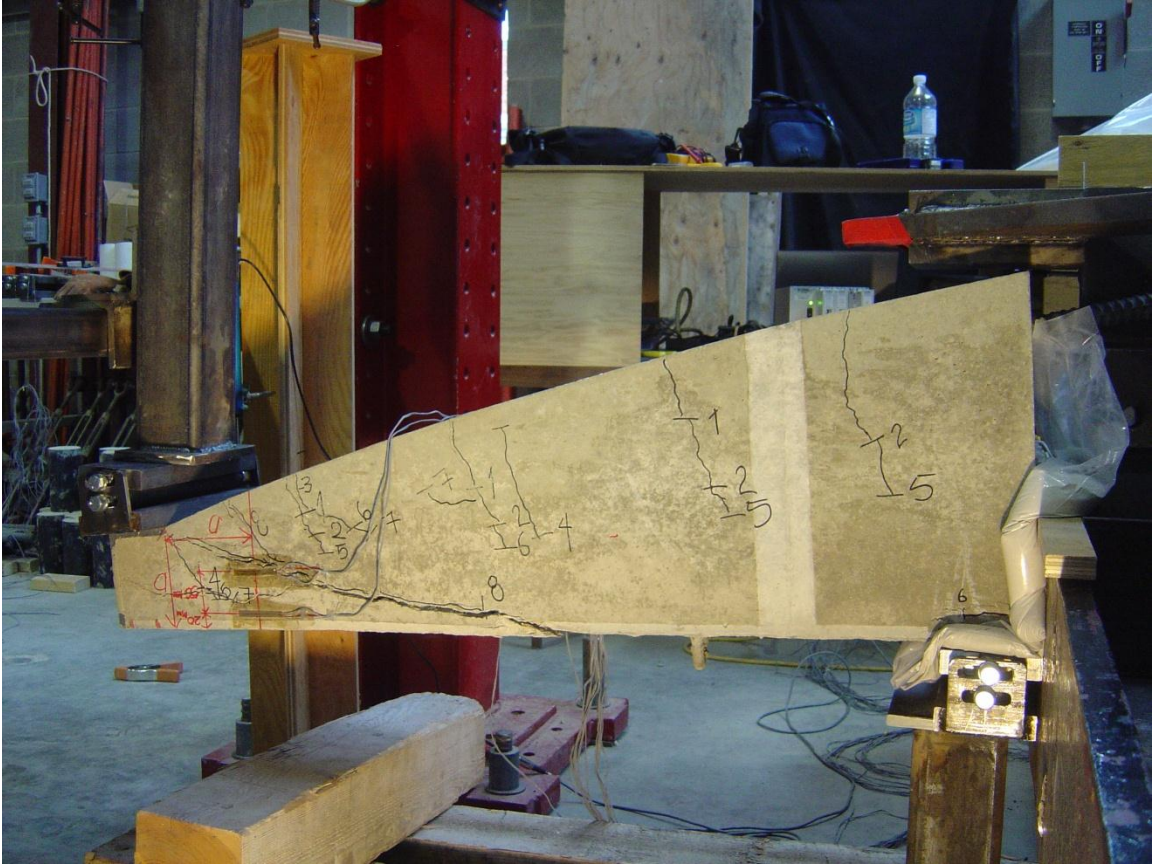
Figure 5.95 – ECB-TS1 after initial failure

As illustrated above, the ECB-TS beams initially failed in the same way as did all other end-beams and full-size beams. After the concrete failure, the top steel kept the concrete together and increased the ductile behaviour of the beam at the final failure.

Figure 5.96 shows the load-deflection diagram for ECB-TS1. The vertical line marks the point of failure.
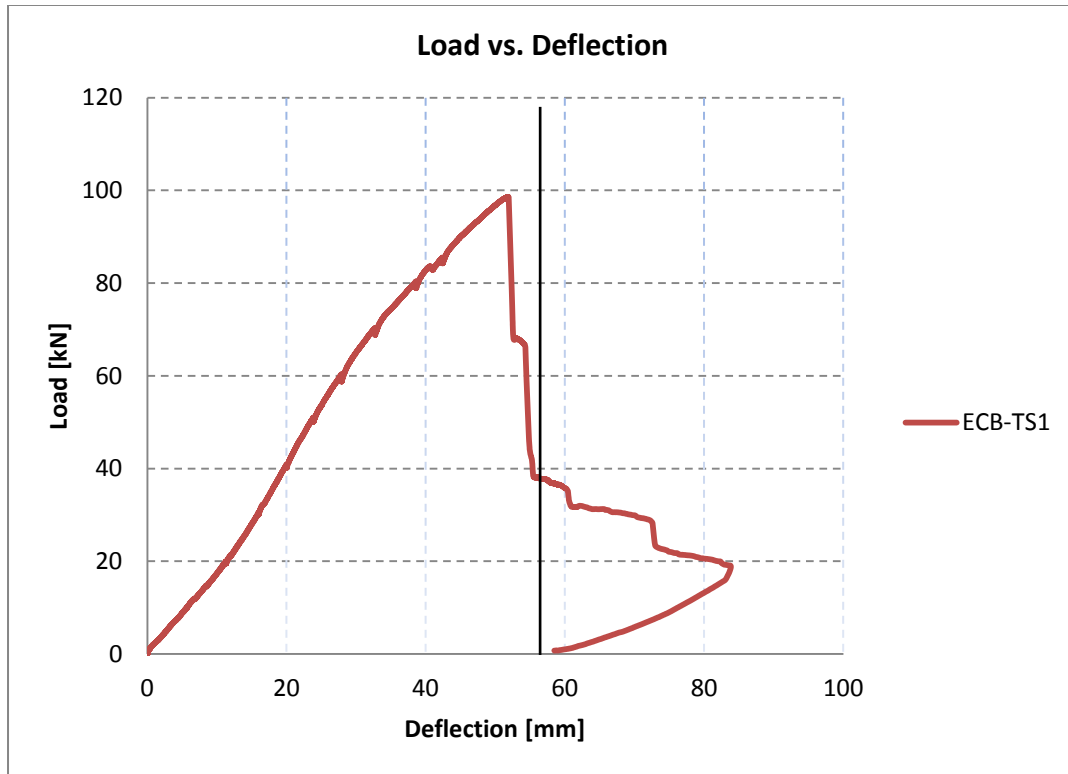
Figure 5.96 – Load-deflection curve for ECB-TS1

The maximum loads sustained by the end-beam shown in Figure 5.87 are much lower than the loads that could be sustained by the full-size CB beams.

The same behaviour was observed in ECB-TS2 illustrated in Figure 5.97.

Figure 5.98 shows a comparison of the load-deflection curves for the end-beams ECB-TS1 and ECB-TS2. The additional strength gain in ECB-TS2 may be due to the additional 10% strength gained by the concrete between the testing of the two end-beams.
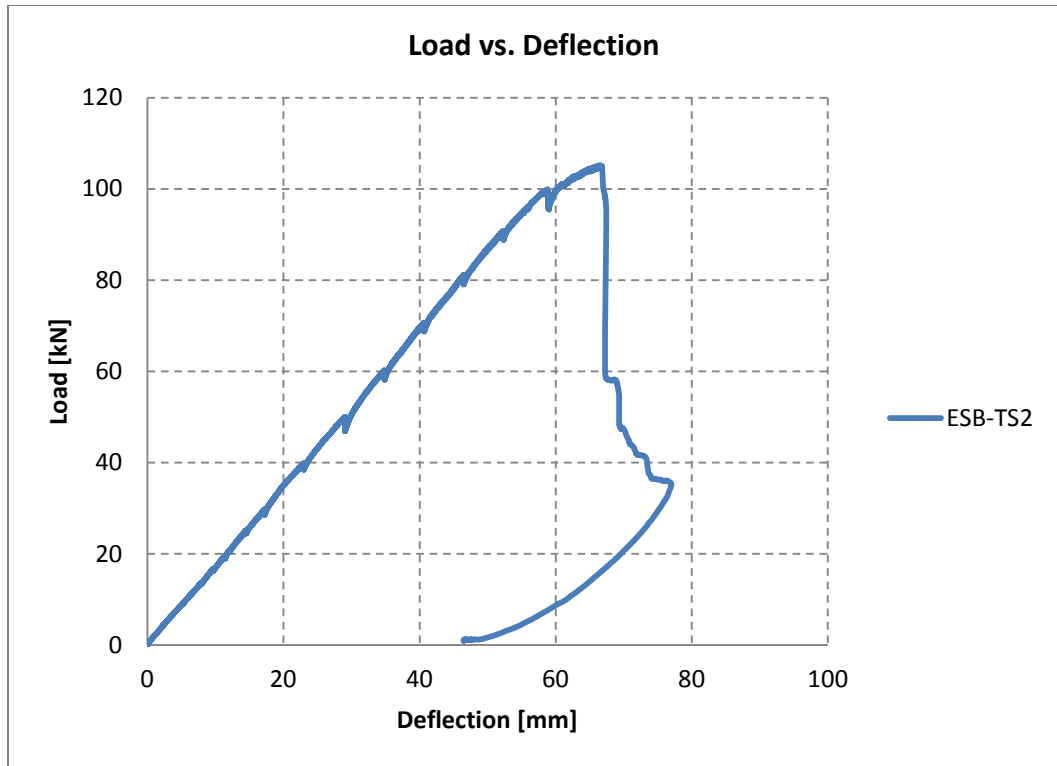
Figure 5.97 – Load-deflection curve for ECB-TS2
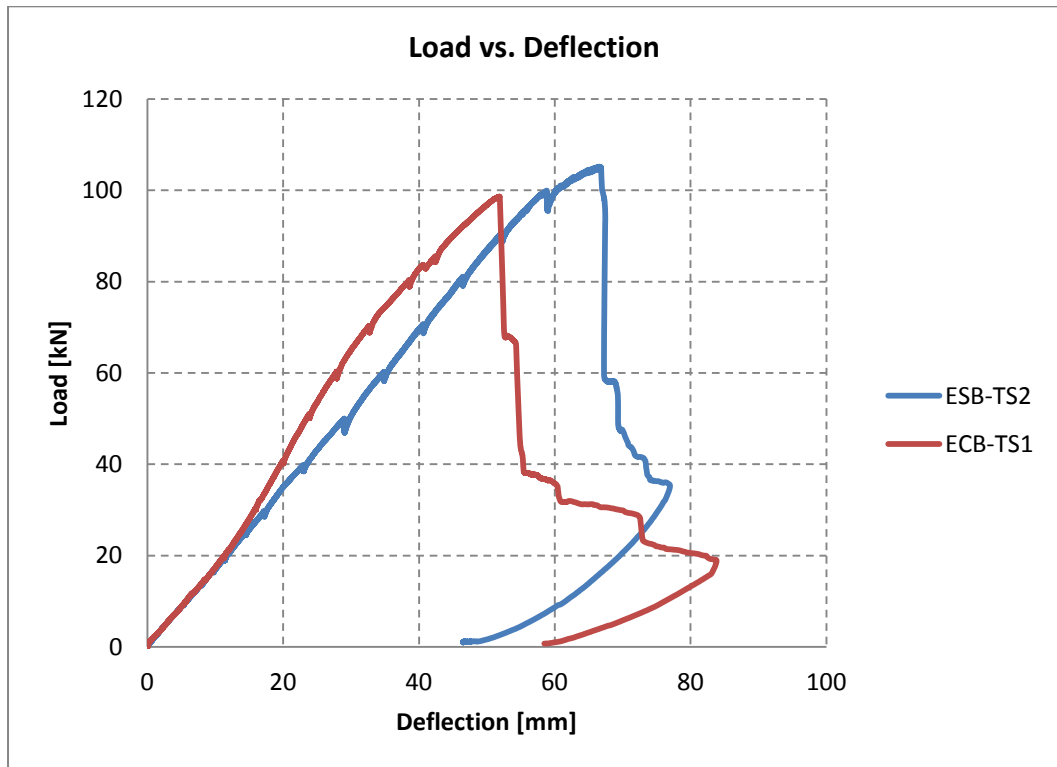
Figure 5.98 – Load-deflection curve comparison for ECB-TS1 and 2

152

5.2.4 ECB-TS-RA1 and ECB-TS-RA2

This end-beam series consisted of both modifications: reversed end angle support (RA) and top compression steel (TS). These end beams demonstrated the same behaviour and failure criteria as the three other end-beam series; the two modifications did not increase the ductile behaviour of the beams. The following Figures 5.99 and 5.100 show both ECB-TS-RA1 and 2 during the testing and after complete failure. The load deflection curve for both end-beams has been illustrated in Figure 5.101.

Figure 5.99 – ECB-TS-RA1 after testing

Figure 5.100 – ECB-TS-RA2 after testing
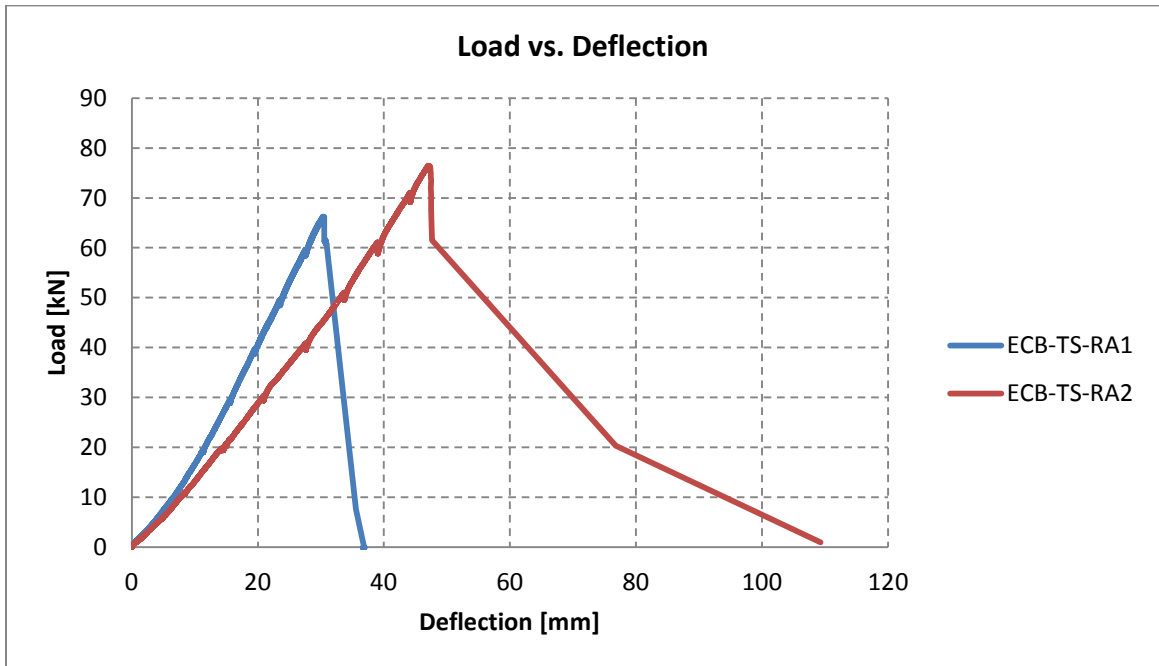
Figure 5.101 – Load-deflection diagram for ECB-TS-RA1 and 2

ECB-TS-RA1 failed at a lower load than ECB-TS-RA2. The reason was discovered during the post-experiment investigation. One of the two top compression steel reinforcement bars was moved during the placing of the concrete to the same level as the tension steel at the bottom and did not contribute to the beam system. Figure 5.102 shows the reinforcement bars from the end where they were welded to the end angle.

The 15M rebar which was moved did not contribute to the tensile capacity since it was not anchored and most likely reduced the bond between the 25M tension reinforcement and the concrete.
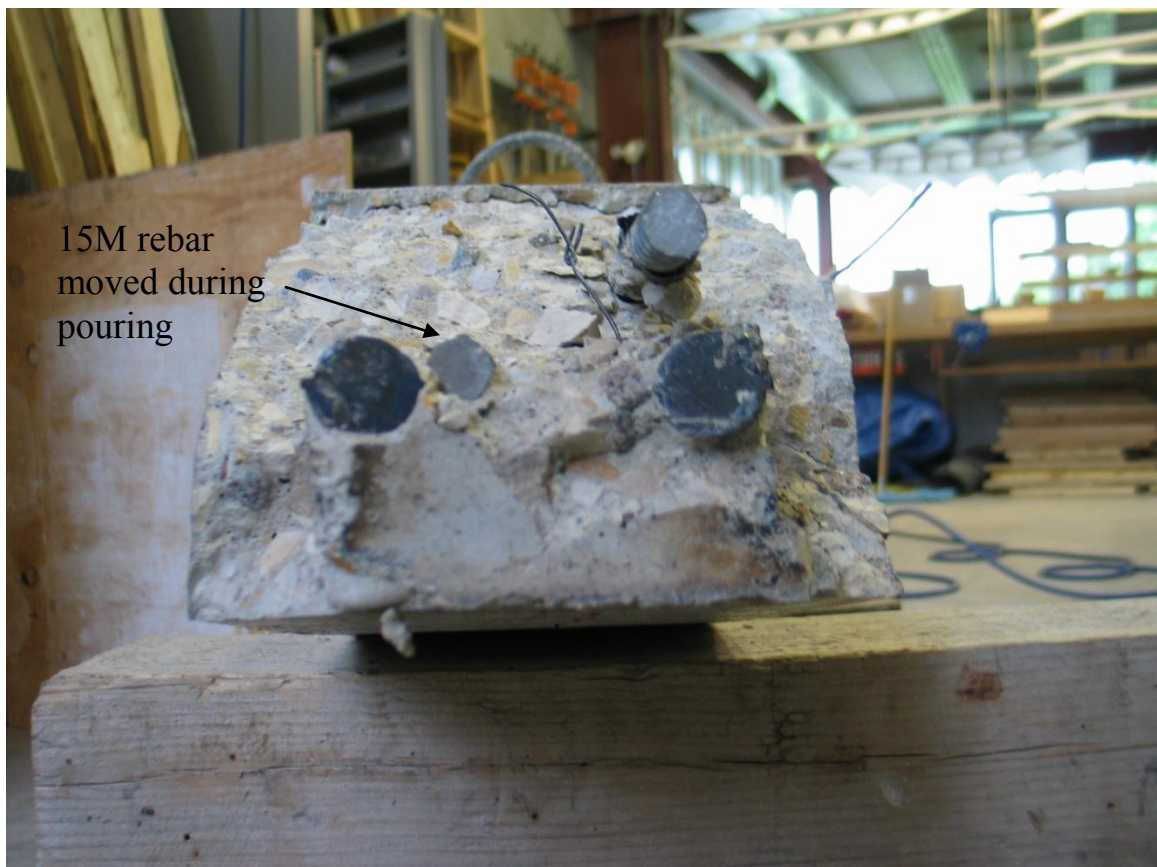
Figure 5.102 – ECB-TS-RA1 – Top rebar has been move to the bottom

5.3   Results for Phase III Testing – Full-size Cambered Curve Beams

In this phase of the research, and after gaining considerable knowledge and understanding through Phases I and II, the final experiment to increase the stiffness, and maximize load carrying capacity was to add more concrete at the top of the beam to introduce a camber, thus creating Cambered Curved Beams (CCB). The camber was hypothesised and later proved to be an effective choice since adding camber does not merely increase the depth of the concrete section at the center, but also provides a better path for the compression stress to the support. As mentioned in Chapter 4, section 4.8, the camber was a catenary curve created by a hanging chain. The apex of the catenary curve at the centre of the beam was an additional 100mm. The discussion on the reason for selecting 100mm height for the apex is also presented in Chapter 4, section 4.8.

The addition of the camber increased the concrete volume by 5%. This means that the total concrete volume reduction from the control rectangular beam is 20%, and since there was no steel added, the total volume reduction for steel in comparison with the CSA-designed control rectangular beam remained at 40%. The cambered curved beam proved to have considerable additional strength. As will be illustrated it has the same load carrying capacity up to and after the serviceability limit as the rectangular beam designed in accordance with CSA-A23.3 design code. The mode of failure remained the same as for the CB beams and at the same location.

The testing results of the CCBs are outlined in the next subsections.

5.3.1 CCB1

CCB1 was the first of the CCBs to be tested and, as mentioned previously, all testing setup and testing methodology was precisely the same as the testing of the CBs. CCB1 showed considerable stiffness at the beginning of the test; in fact, it was as stiff as the CSA control beam. After initial cracking, the stiffness remained and was almost the same as with the CSA control beam. Figure 5.103 shows the load-deflection curve for both CCB1 and CB3, showing the increase of stiffness of the CCB1 over CB3.
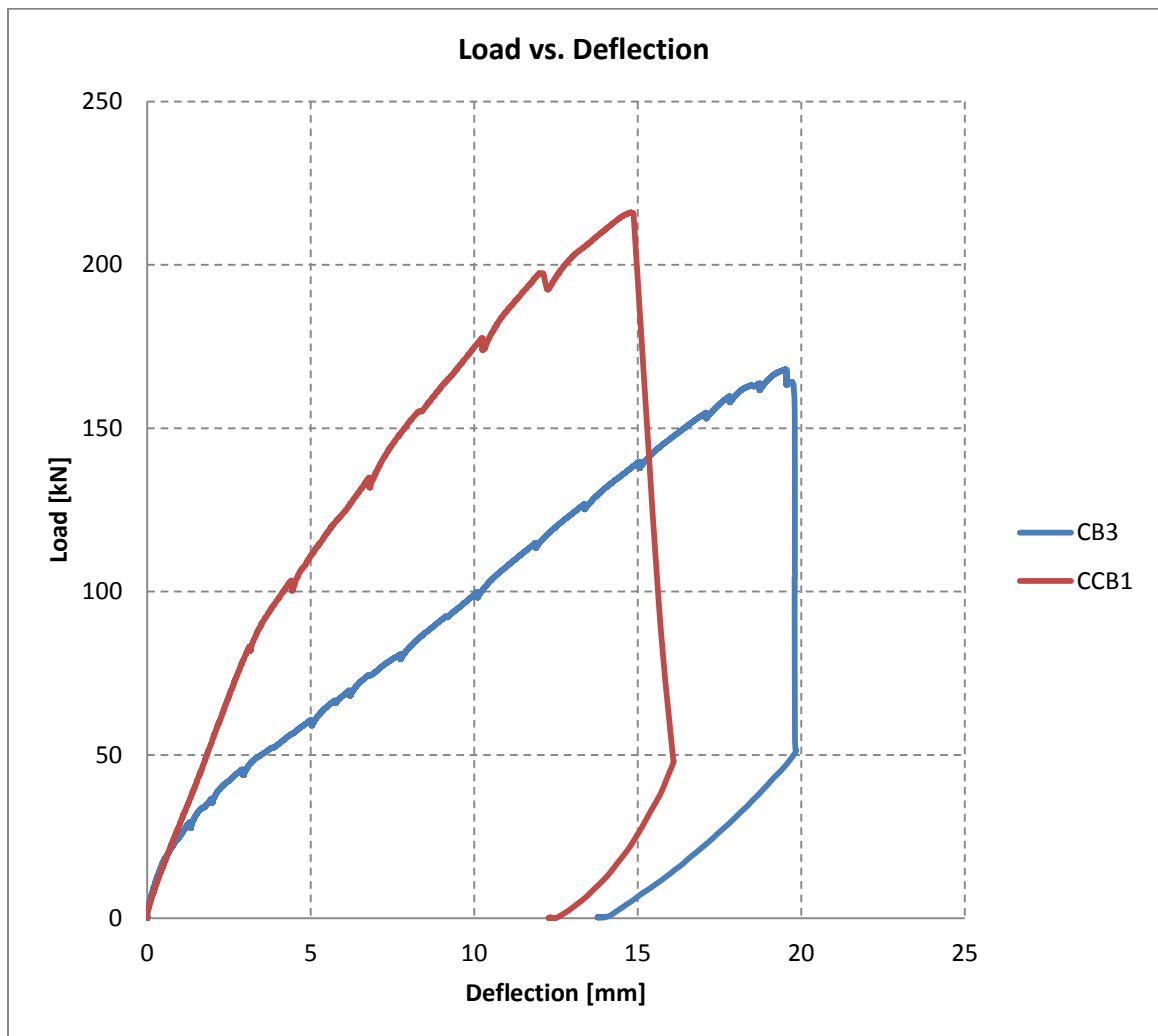
Figure 5.103 – Load-deflection curve for CCB1 and CB3

Figure 5.104 shows the load-deflection curve comparison for the CCB1 and the CSA control beam.
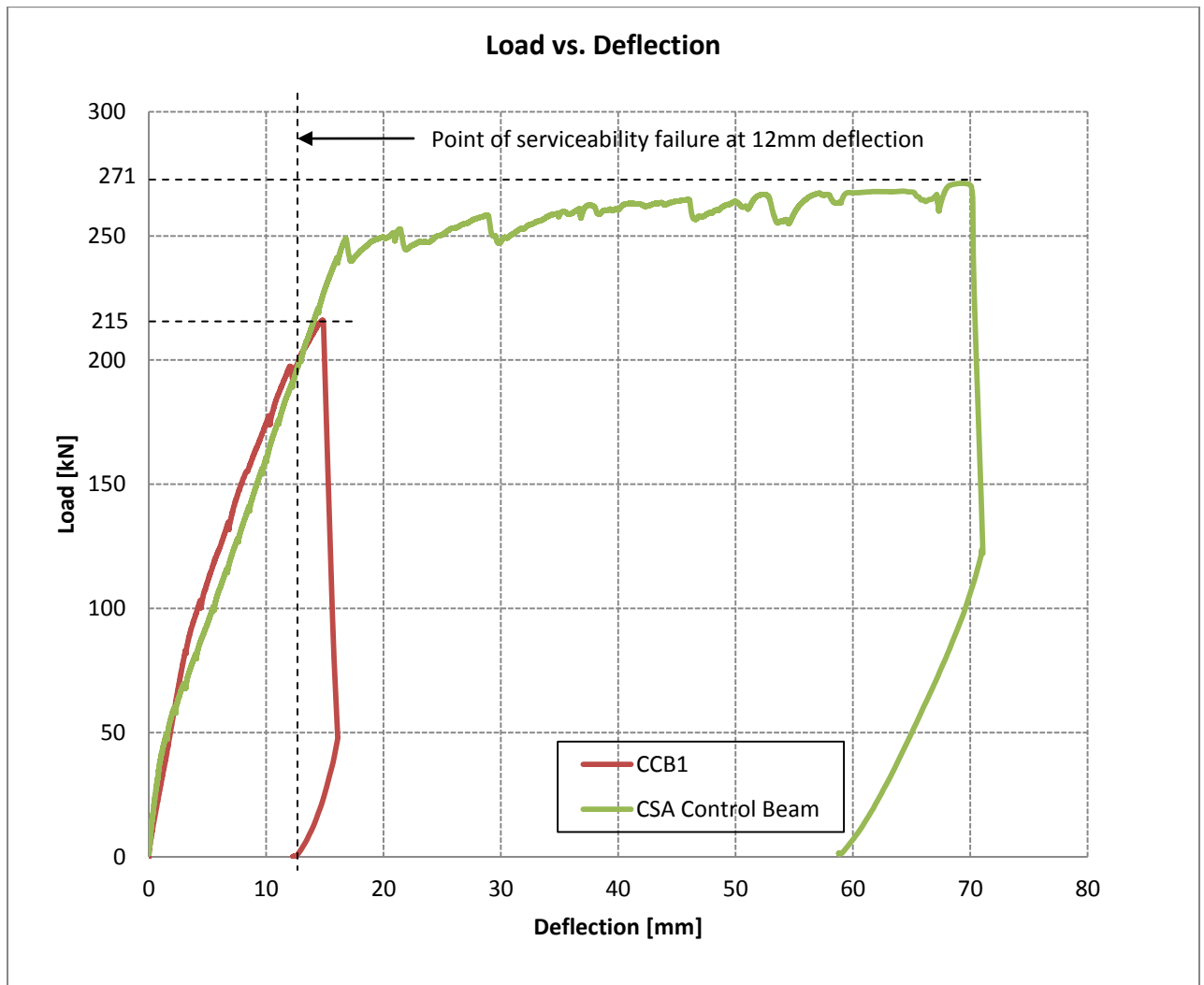
Figure 5.104 – Load-deflection curve for CCB1 and CSA Control Beam

As illustrated in Figure 5.95, up to the serviceability failure (deflection of 12mm) and further up to 215 kN, the CCB1 has the same stiffness and load carrying capacity as the CSA control beam (which has 20% more concrete and 40% more steel). The ultimate load for CCB1 was 215 kN, about 20% less than the CSA control beam which had an ultimate load of 271 kN. It is important to note the control beam demonstrated considerable ductility prior to final failure.

At the ultimate load, CCB1 performed better (by 16%) than RB1, the rectangular beam with no shear reinforcement. An interesting advantage of CCB1 (and CB's) over the RB1 rectangular beam with no shear reinforcement is that it never collapsed completely (see Figure 5. 114) due to the closed force configuration facilitated by the end condition.

Figure 5.105 compares the load-deflection curve of CCB1 and RB1, the rectangular beam with no shear reinforcement but the same amount of flexural reinforcement as CCB1.
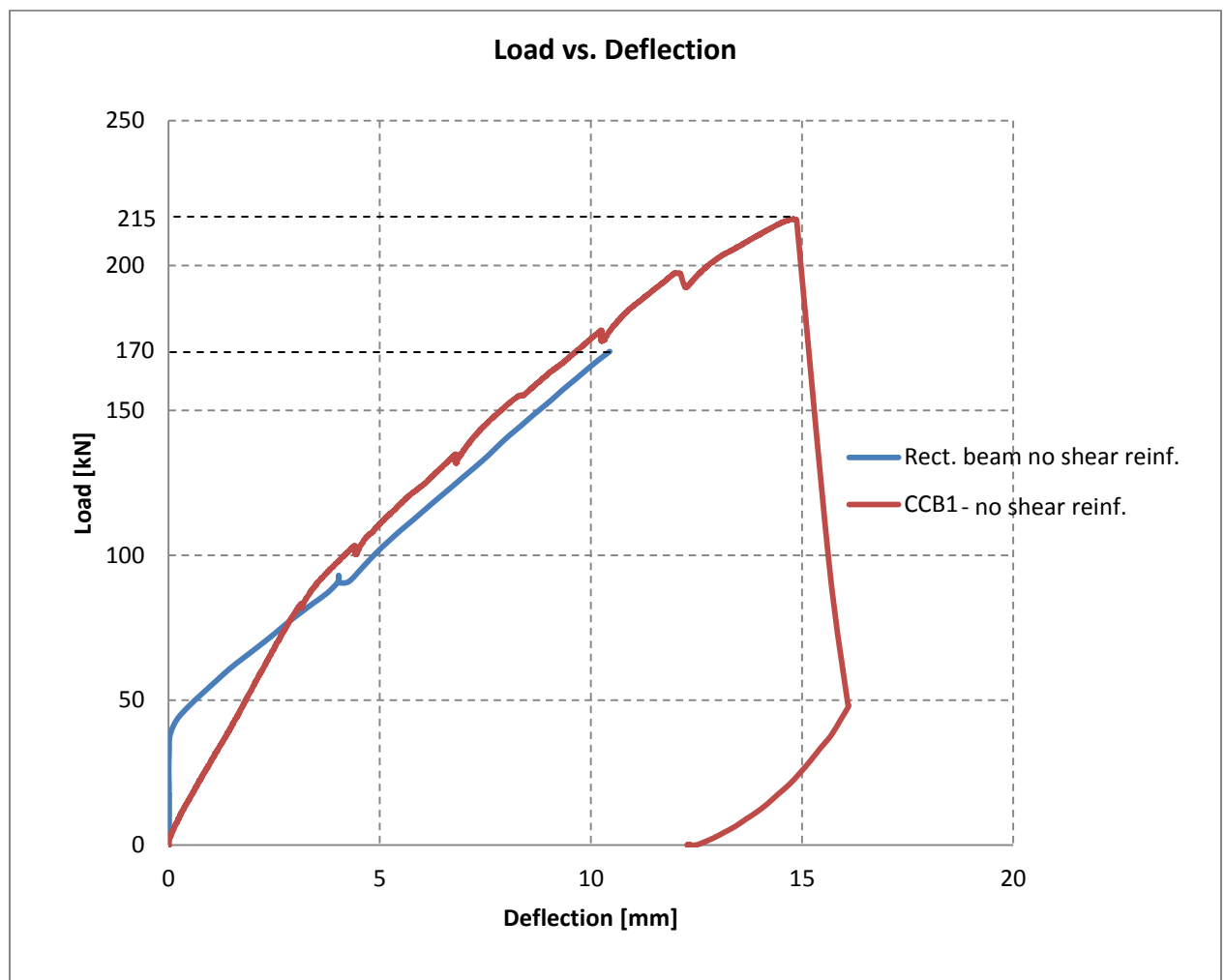
Figure 5.105 – Load-deflection curve for CCB1 and
rectangular beam with no shear reinforcement RB1

The load-deflection curve comparison illustrates that the RB1 failed at an ultimate load (170kN) 26% less than CCB1's ultimate load (215kN). The concrete cross section area of RB1 at the location of failure is over 100% larger than CCB1 as illustrated in Figure 5.106. The failures in both beams are due to diagonal tension, and occur at a distance equal to the effective depth (d) in each beam; 150mm for the CCB1 and 400mm for RB1.
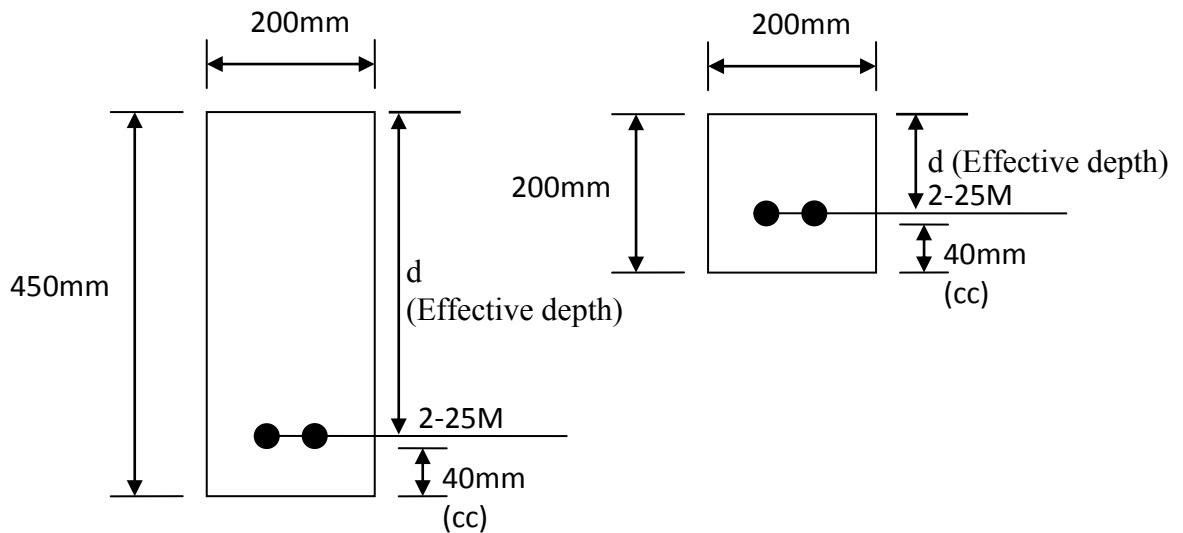
Figure 5.106 – Left: RB1's cross-sectional area at the location of failure
Right: CCB1's cross-sectional area at the location of failure

5.3.2 CCB2

CCB2 demonstrated a 5% lower ultimate load, had the same crack pattern and failure mode than CCB1. Figures 5.107 through 5.115 show the crack development during the entire testing and the final failure for the CCB2.

Figure 5.107 – Test setup for CCB2
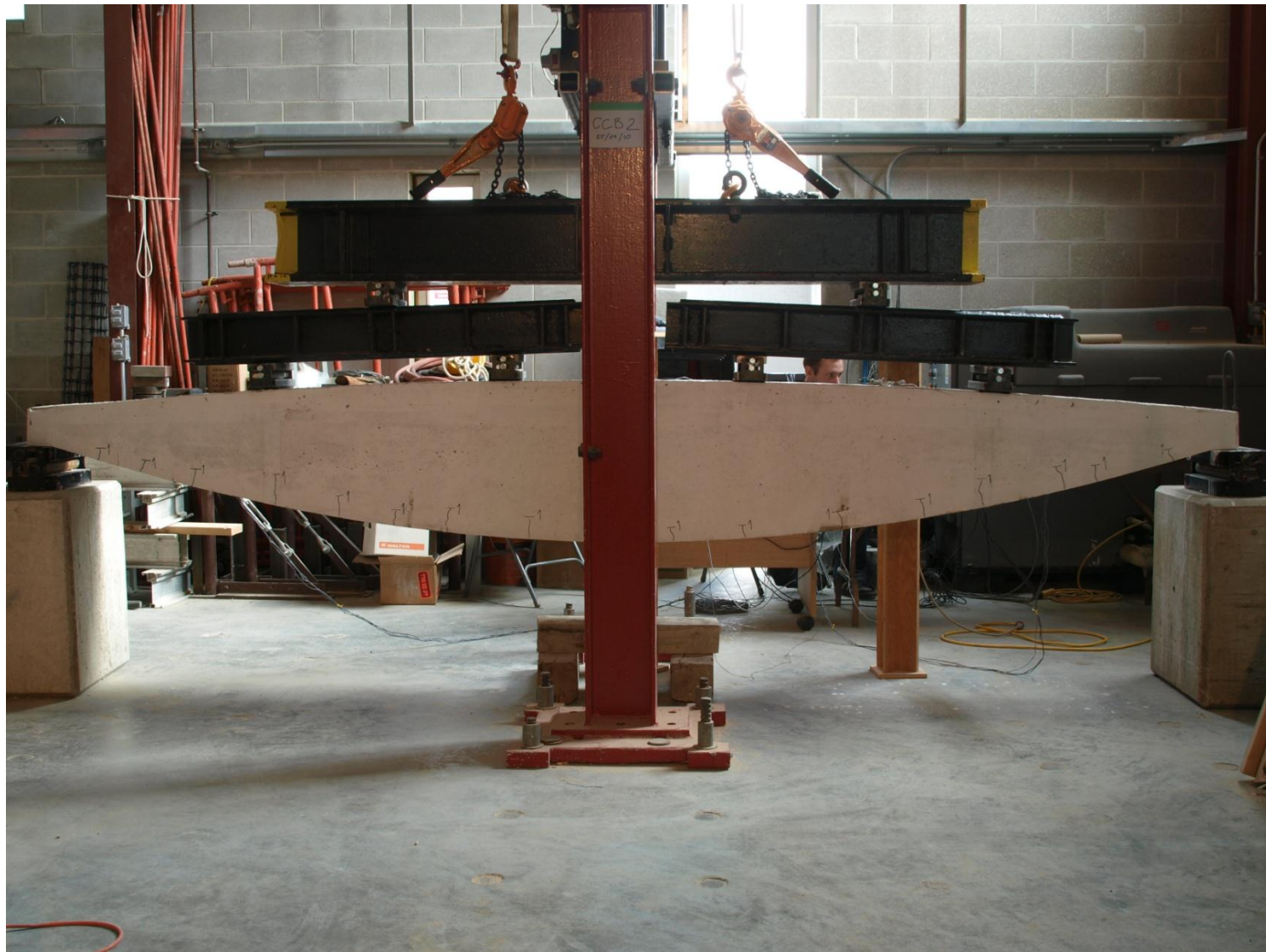
Figure 5.108 – CCB2 at initial cracks. Uniformly distributed cracks appeared at 40 kN

Figure 5.109 – CCB2 – Crack propagation at 60 kN
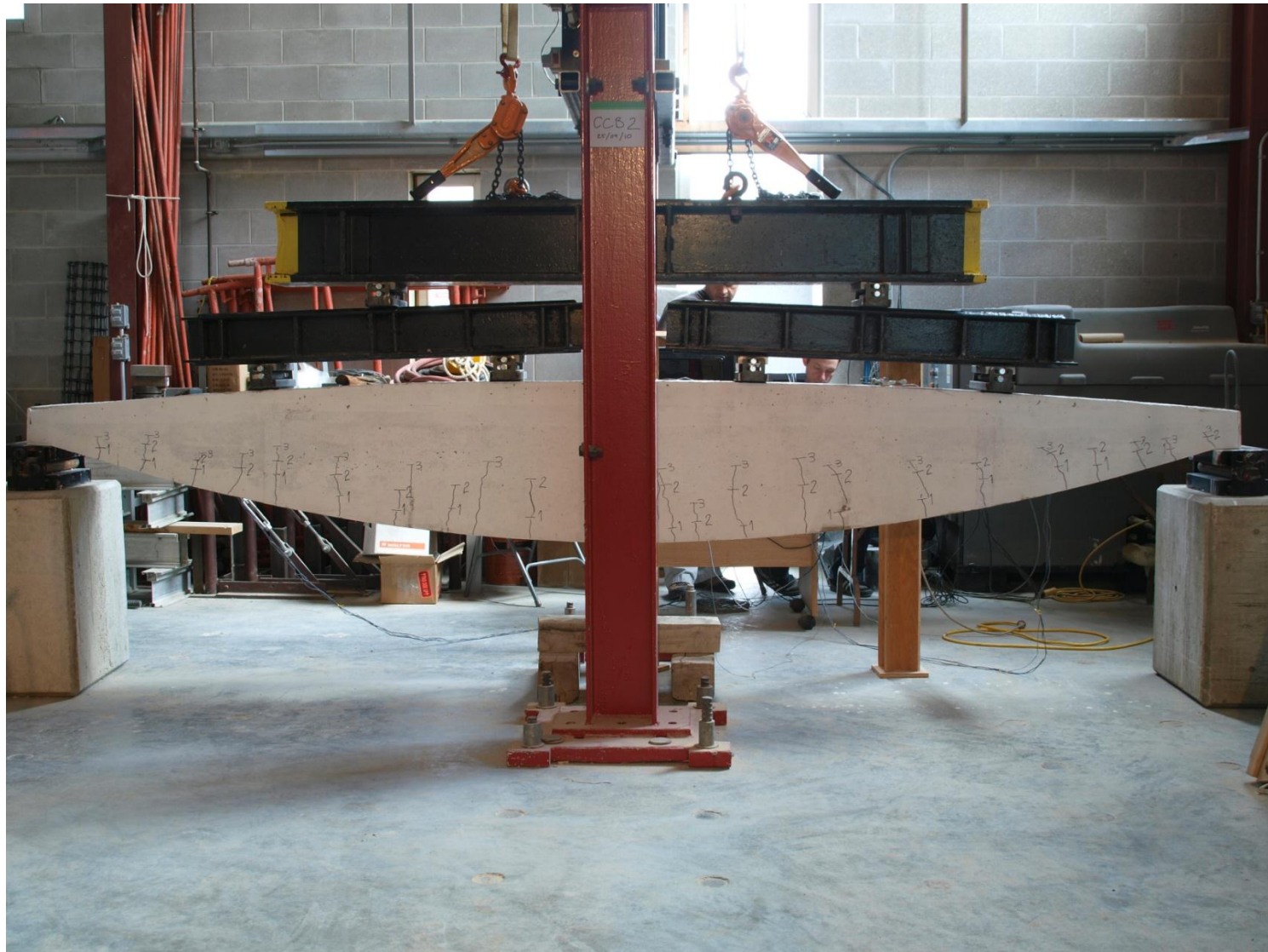
Figure 5.110 – CCB2 – Crack propagation at 82 kN

Figure 5.111 – CCB2 – Crack propagation at 100 kN

Figure 5.112 – CCB2 – Crack propagation at 130 kN
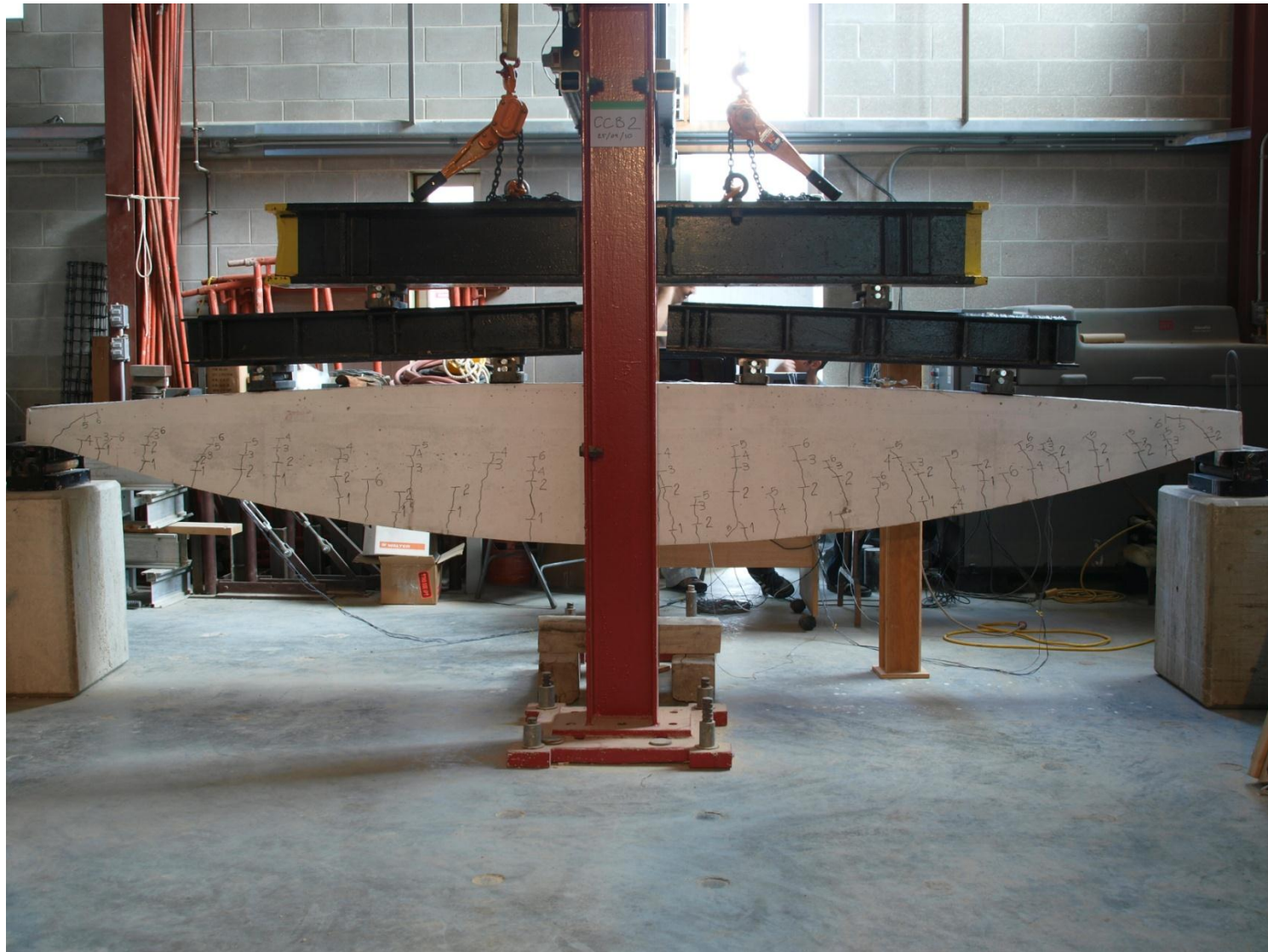
Figure 5.113 – CCB2 – Crack propagation at 150 kN

Figure 5.114 – CCB2 – after failure at 200 kN
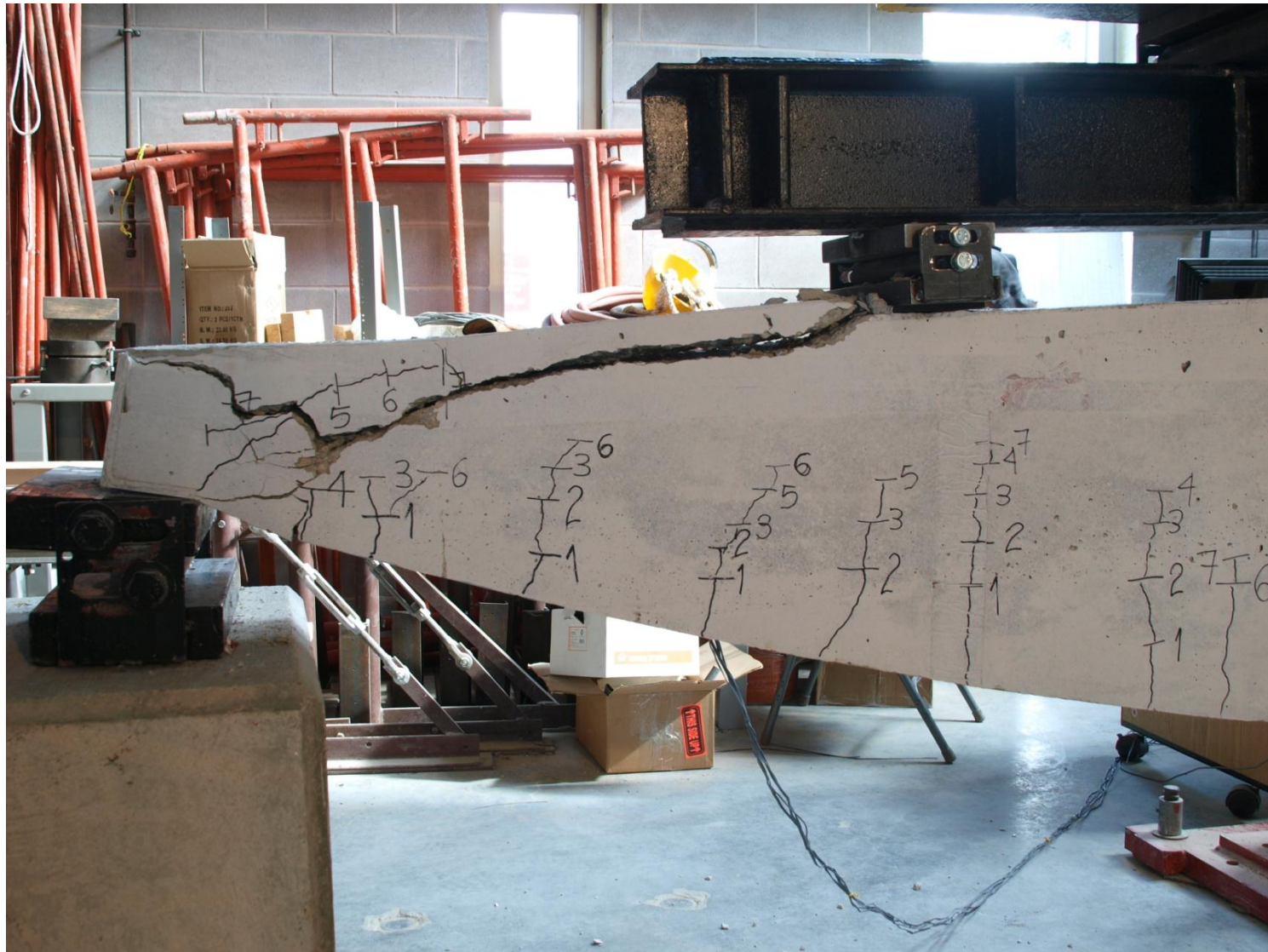
Figure 5.115 – CCB2 – close up of failure end

CCB2 failed at 200 kN – about 5% less than CCB1. The failure mode, as mentioned previously, was the same as for the CCB1, which also matched the failure mode of the CBs from Phase I of this research. Figures 5.116 and 5.117 show both CCB1 and CCB2 after testing.

Figure 5.116 – CCB1 after testing

Figure 5.117 – CCB2 after testing

A compression test from concrete cylinders, taken during the construction of the two CCB beams, shows that the f'$_c$ was 35.7 MPa. The 5% difference in the final failure load, is considered small enough to be negligible, and could be due to a small deviation within the testing setup or the testing frame.

This experimental research has proven that it is possible to achieve greater structural efficiency by forming variable-section beams. The CCBs, up to and beyond the serviceability failure carried the same load with the same stiffness as the rectangular control beam designed using CSA A23.3; as was shown in Figure 5.104. This shows that although more research is required to increase the ductile behaviour after the maximum load, moment-shaped curved beams may be a viable option to traditional rectangular beams. The advantage of the curved beams is the considerable reduction of material in both formwork, through the use of flexible fabric moulds, and in the beam itself and a potentially simplified steel fabrication and assembly due to the possibility of eliminating stirrups.

This point will be discussed in more detail in Chapter 8.

5.3.3 Behaviour and Failure Mode of Curved Beams (CB and CCB comparison)

Both CBs and CCBs demonstrated the same mode of failure but exhibited different behaviour up to the failure point. This section compares the two curve beams to understand the different behaviour. The CCBs were stiffer throughout the testing and after cracking. Figure 5.118 compares the behaviour of CB3 and CCB1.
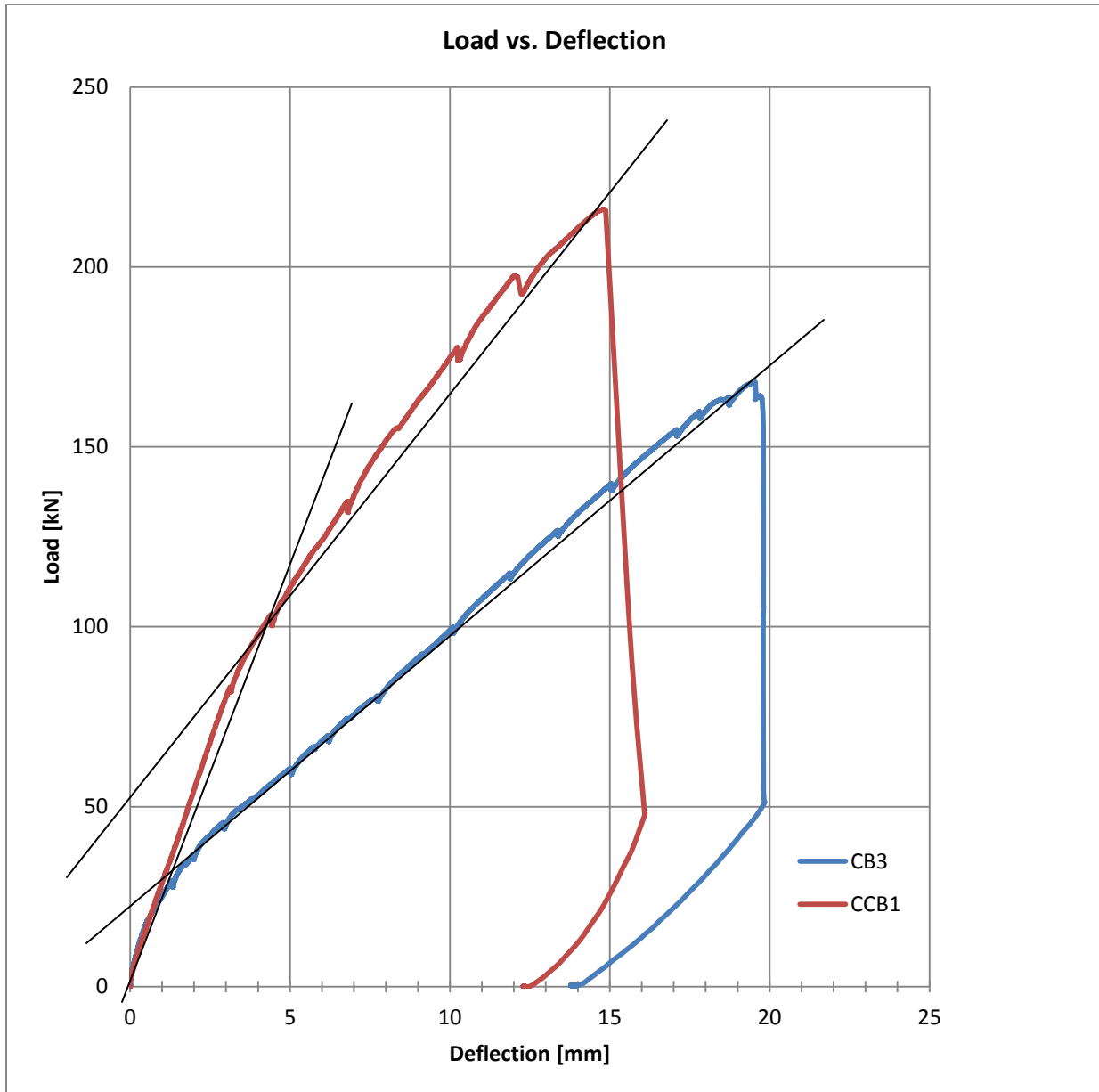
Figure 5.118 – Comparing CB3 and CCB1

The ultimate load for CCB1 was 215kN, 32% higher than CB3 which had an ultimate load of 160kN. As shown above, both beams started with similar initial stiffness; however, tension cracks appeared very early in CB3 and its stiffness was drastically reduced after that point. The initial cracking of the CCB1 commenced at 90kN, about 71% higher than for the CB3. Although CCB1's stiffness was reduced after cracking, it remained higher than that of CB3, and comparable to the stiffness of the CSA control beam after cracking. The mode of failure for both CB3 and CCB1 beams at their ultimate load was the same, as that shown in Figure 5.119.

The cambered curved beam (CCB) type of moment-shaped beam was the final generation created in this study and was proven to have a higher ultimate load carrying capacity; the CCBs' ultimate load carrying capacity was increased by an average of 32% over the first generation curved beams (CBs). This increase is due to additional stiffness of CCBs and "delay" of final failure. The delay in failure could be due to several reasons such as in CCBs the compression and tension stress paths remain separated longer, hence delaying the occurrence of diagonal tension phenomenon, or that CCB fail in an entirely different mode than CBs. This will be explored further later in the section. The final goal of creating different generations of curved beams was to be able to understand enough about their behaviour so a final generation can be created that would behave very similarly to the code-designed rectangular beams. The code-designed beams are the established way of design and construction at this point, so any new way of design and construction should be able to meet the capacity and ductility expectations, while providing improvements in sustainability, economy and constructability.

Figure 5.119 – Same failure mode and pattern for CCB1 (above) and CB3 (below)

This research discovered three modes of failure or three factors contributing to the final failure. These modes are moment failure (rotation at end support); "shear" (diagonal tension) failure; and direct shear failure. The final mode of failure, the

direct shear, was theorized due to the results from the FEM analysis. The first two modes of failure are well known and all three modes will be discussed in Chapter 9. This section will discuss the direct shear failure but it must be noted that this is a possible mode of failure and not the only factor contributing to the final failure.

1.   The compression stresses due to the external load could easily travel to the support point since an uninterrupted path is available. It is hypothesized that the compression and tension meet at the very end of the beam prior to initial cracking and cancel each other out as internal forces, Figure 5.120.
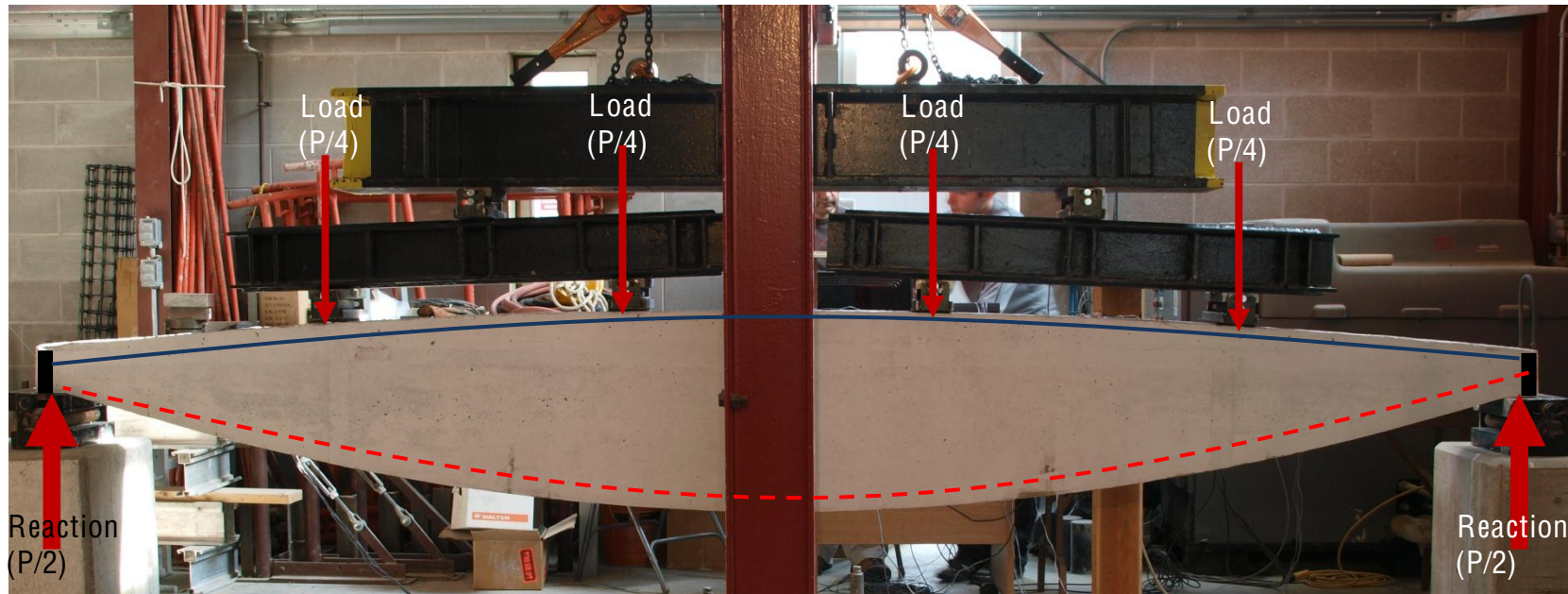
Figure 5.120 – Hypothesized primary compression and tension stress paths within CCB
(Blue lines: Compression Stress Paths, Red dash line: Tension Stress Path)

2. The above behaviour continues until the total load reaches approximately 90% of the maximum load; at this point the compression stress path does not fully reach the support. As a result, the compression stress lands on the steel between 200 to 400mm before the support. This behaviour creates a direct shear stress at the area close to the support resulting in a direct shear failure.
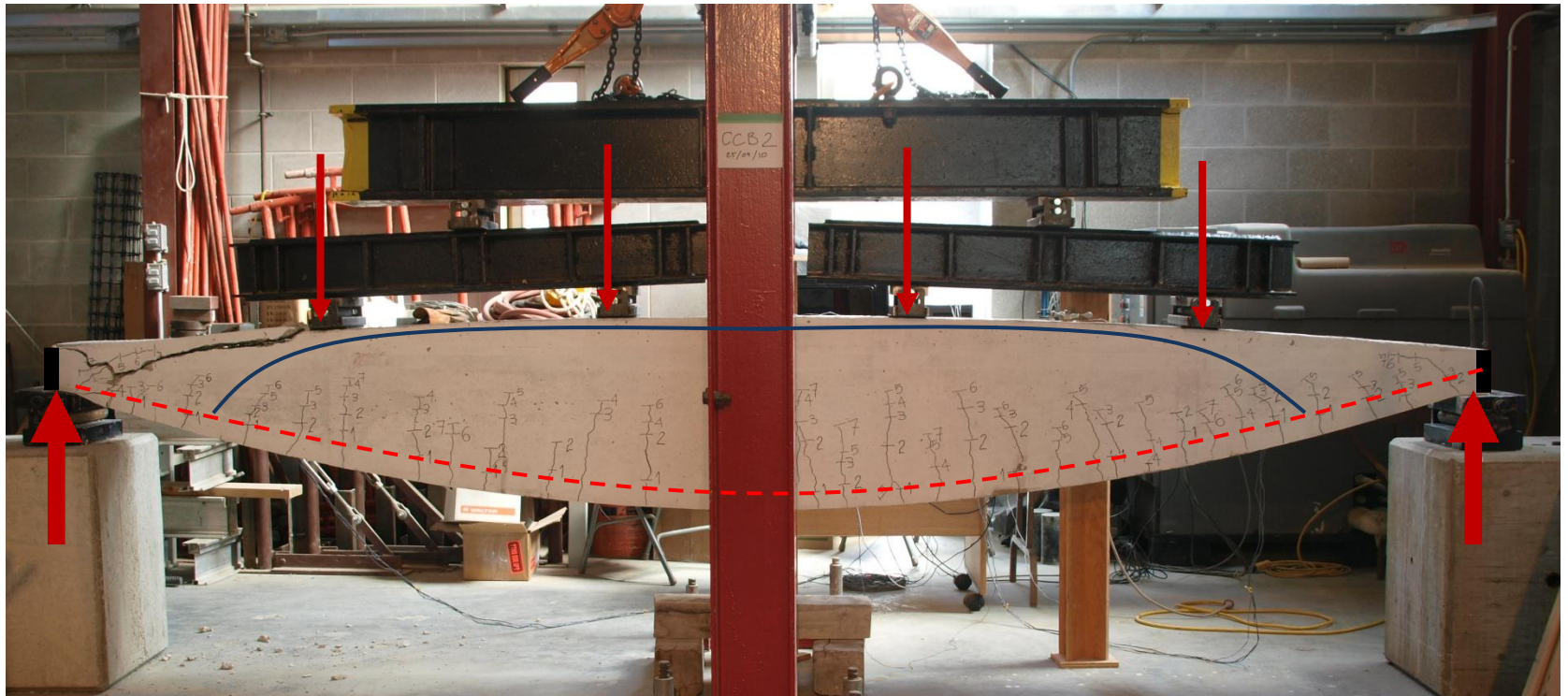
Figure 5.121 – Primary compression stress path

3. The final result is a direct shear failure generated between Compression Force Resultant (CFR) and the Reaction (R) shown in Figure 5.122.
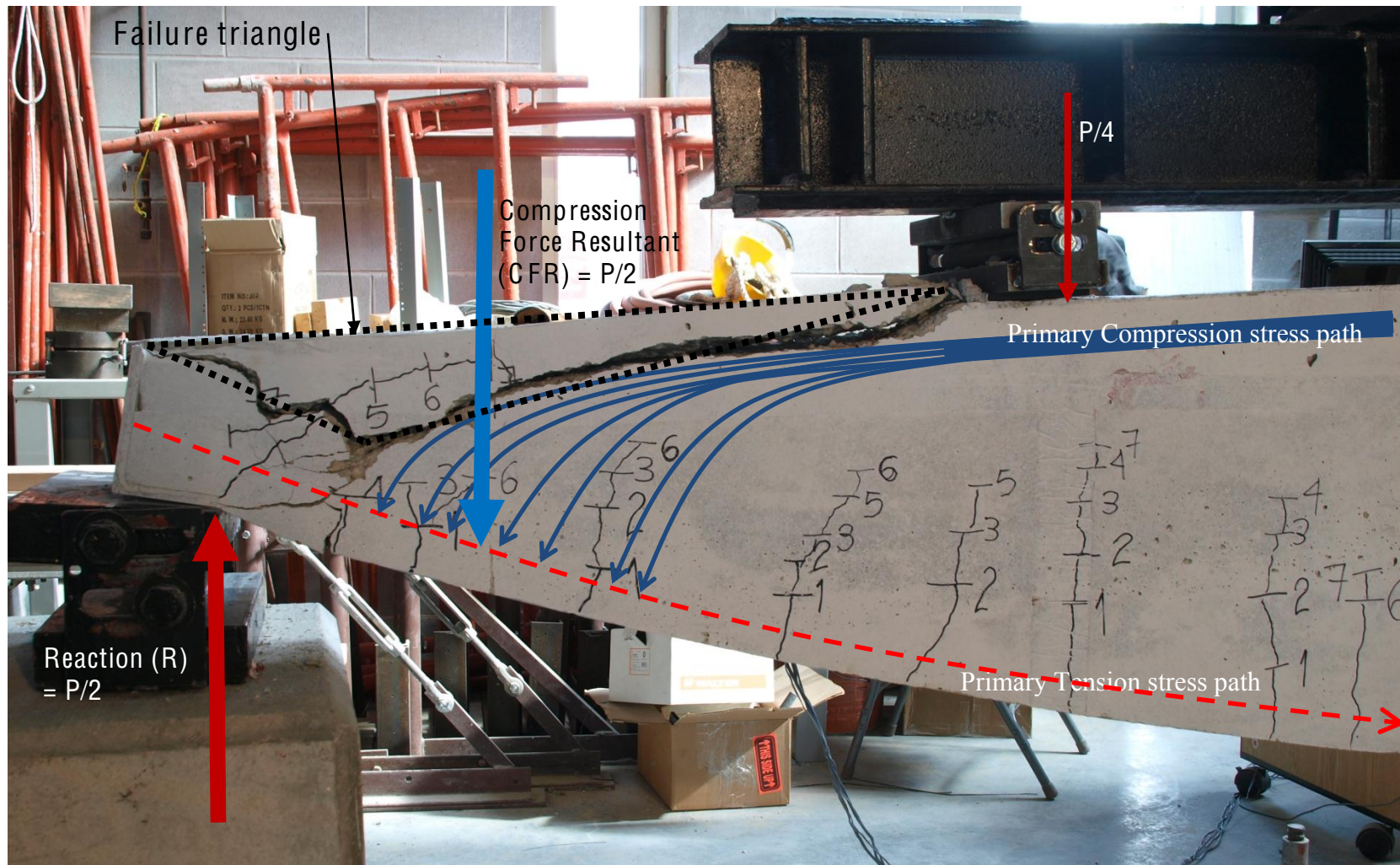
Figure 5.122 – Primary stress paths at the support prior to failure and the resulting forces

177

The direct shear failure of moment-shaped beams, mentioned in point 3, is different from the "shear" failure of conventional rectangular beams. The "shear" failure in conventional rectangular beams is due to diagonal tension that develops as the compression and tension stresses cross paths creating the "disturb zone or region", see Section 1.2 – Behaviour of Concrete Beams.

In moment shaped beams, prior to the failure most of the compression stress lands about 200mm in front of the support due to deflection of the beam and stiffness of the rebar at this location. This phenomenon is conventionally called the dowel action. While CSA 23.3 acknowledges dowel action, it does not, considered the shear resistant calculation due to a very small contribution of the dowel action. This is evident from a crack starting at the edge of the end-angle support, propagating at 45º and then stopping at 18mm from the top of the beam, shown in Figure 5.122 and Figure 5.123a. The resultant force due to compression stress landing in front of the support and the reaction at the support create an area of shear stress as shown in Figure 5.123b and simplified in Figure 5.123c. The final failure of the cambered-beams is failure of the concrete in direct shear within the area confined or bordered by the two opposite forces. The final stage of failure is a triangular section of concrete separating from the top of the beam, Figure 5.122. The beams behaviour and final failure theorized above (shown in Figure 5.123) are also confirmed by the FEM studies that will be presented in detail in Chapter 6, Section 6.3.3. The FEM analysis verifies the experimental findings that the tension remains constant over the entire length of the reinforcement, and the concrete elements at the area of failure are in compression.

Crack (at approx. 45°)

Compression stress
resultant force = P/2

Compression

Tension in steel reinforcement

Support reaction
= P/2

200mm
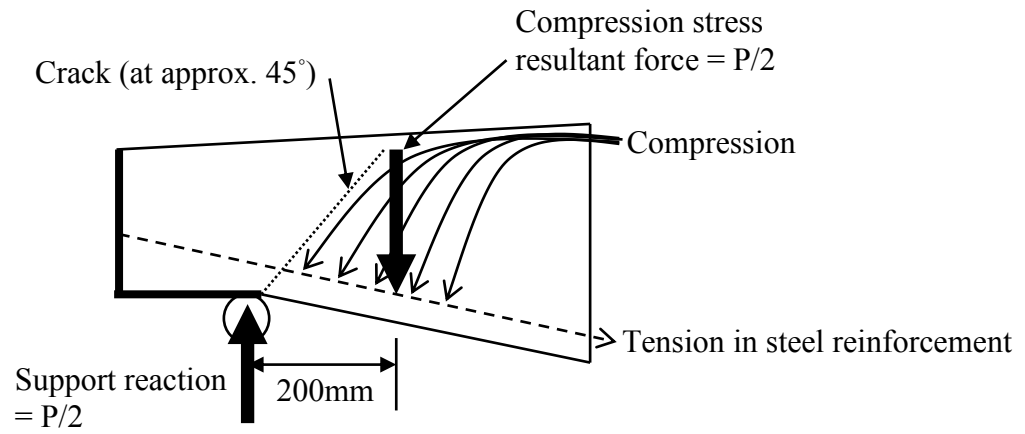
a – Actual stress distribution and resultants

Shear area between forces

Reinforcement
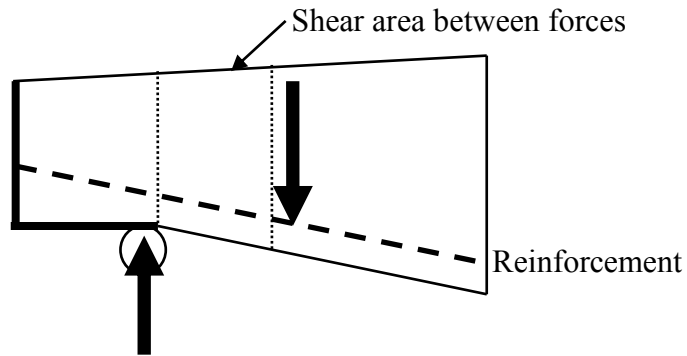
b – Resultant and shear
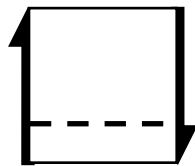
c – Forces acting on the shear area

Figure 5.123 – Theory of failure for cambered curved beams

5.4 Structural Efficiency and Performance Comparison

Structural efficiency can be understood as having all materials in the beam carrying the internal stresses uniformly. In a highly efficient RC beam the tension stress would remain uniformly distributed in the steel along the span of the beam.

In uniform section CSA designed beams it is common knowledge that tension stress varies along the steel reinforcement, with the maximum tension in the steel located at the centre of the beam which is the point of maximum moment for a uniformly distributed loading condition. The tension strain in the steel reinforcement for the CSA designed control beam RB3 is illustrated in Figure 5.124.
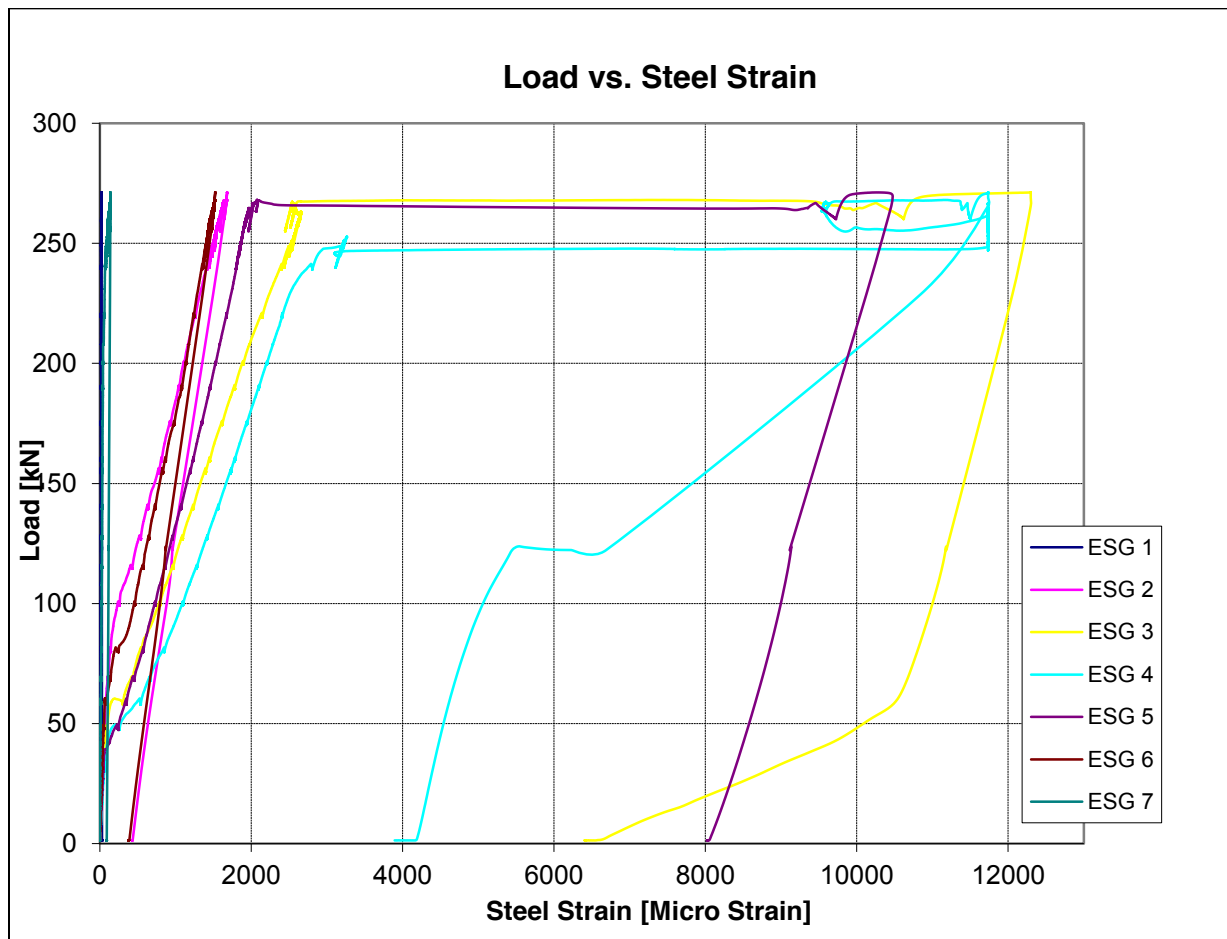
Figure 5.124 – Tension stress in reinforcement in RB3 (CSA-control beam)

ESG 1 to ESG 7 are the strain gauges designation along the reinforcing steel in the CSA designed control beam, RB3. ESG1 is the first strain gauge near the support and ESG4 is the strain gauge at the center the span. As illustrated in Figure 5.73, the three middle strain gauges in RB3, ESG 3 ESG 4 and ESG 5, show that the steel is under the highest stress at the middle of the span as the steel reaches stresses beyond the yield point, while the strain gauges closer to the support register much lower strains.

Tension stress in CCB1 and CCB2 were more uniformly distributed along the reinforcement as shown in Figure 5.125 below.
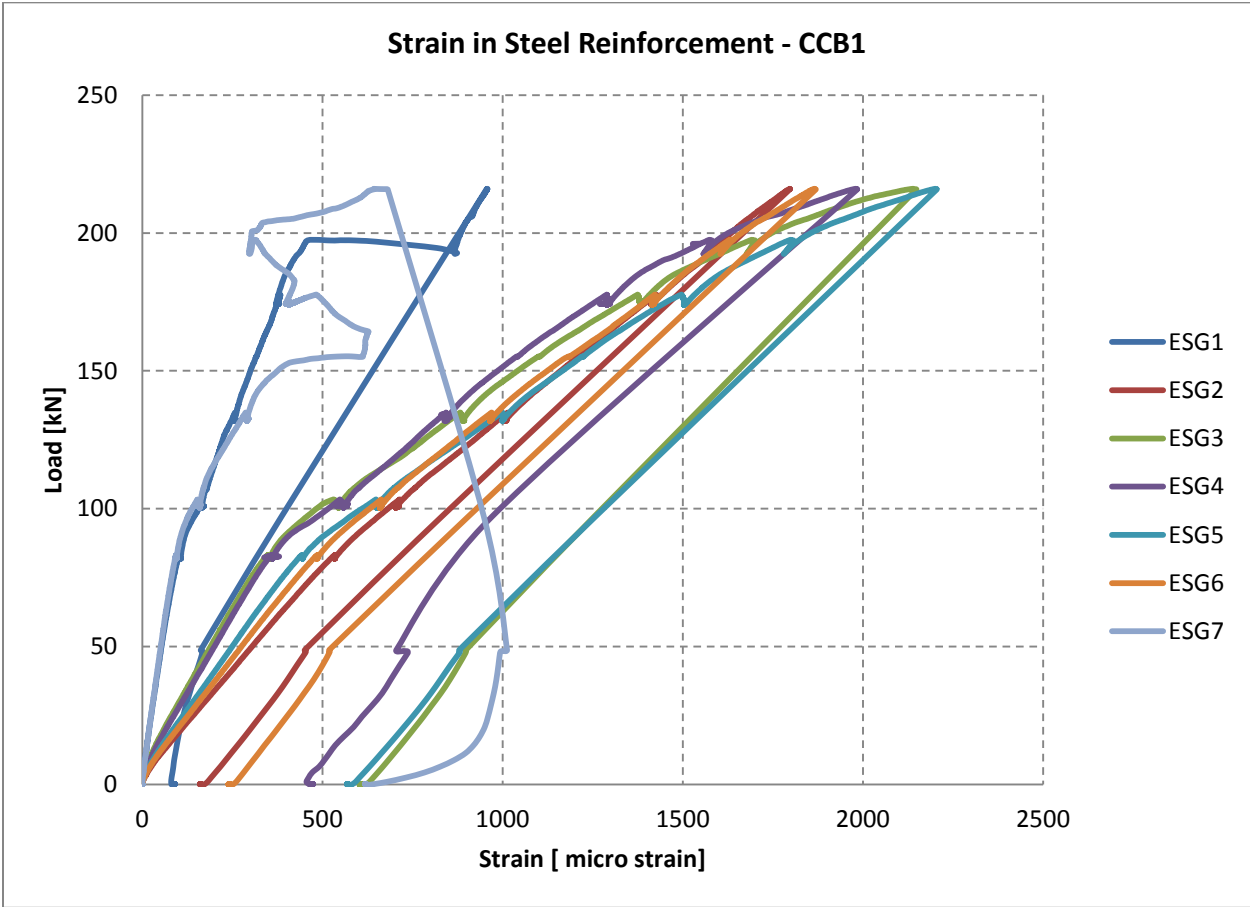
Figure 5.125 – Tension stress in reinforcement in CCB1

ESG 1 and ESG 7 are the strain gauges at the very end of the reinforcement where it is welded to the end angle; therefore, the strain in those gauges can be neglected since the stiffness at the supports is very high due to the large amount of steel at that location due to the weld plates. For clarity Figure 5.126 shows the steel strain without ESG1 and ESG7.
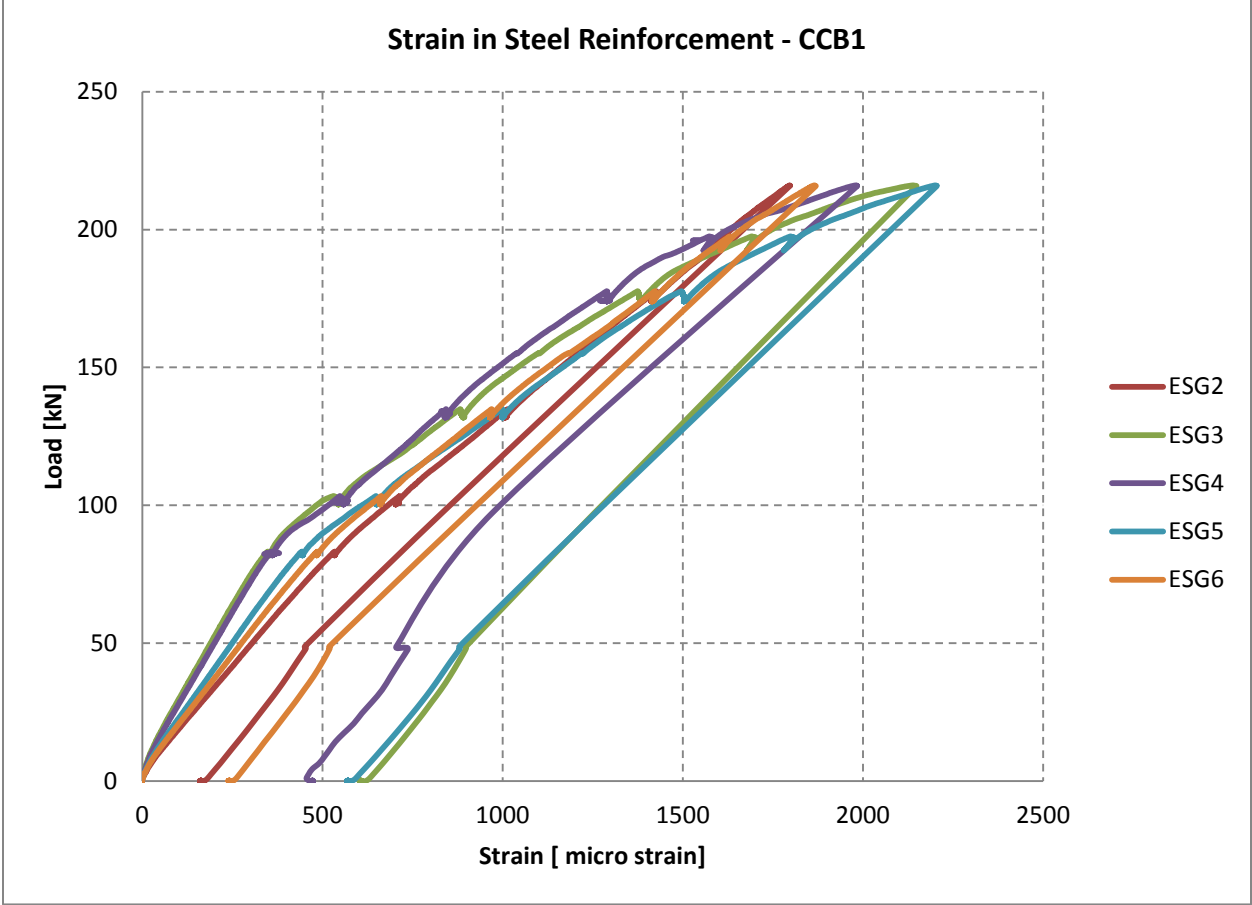
Figure 5.126 – Tension stress in steel in CCB1 (without ESG1 and ESG7)

As seen in Figure 5.126, the stress is uniformly distributed along the reinforcement in the CCBs, which means all of the steel reinforcing works at approximately the same stress level. This indicates that the CCBs use their material more efficiently than the rectangular beams.

Another way to describe structural efficiency is the ratio of maximum load carrying capacity of a beam to the weight (or mass) of the beam. This ratio for the CSA-designed rectangular control beam is 11.22 while the ratio for CCB's is 12.06 demonstrating that cambered curved beams are more efficient structural members than conventional code designed rectangular beams with shear reinforcement, though as previously noted, the CCB beams had a 12% lower ultimate load carrying capacity and lower ductility at ultimate failure load.

5.5 Final Results

This section will compare and discuss the results of Phase I and Phase II of the experiments, where Maximum allowable deflection (Δ_{Allow}) is L/360 = 12 mm.

Table 5.2 – Phase I and Phase III beam information

	Beam	Ultimate Load	Δ at Ult. load	Load at Δ_{Allow}	Failure Mode	f'$_c$ MPa	Concrete batch
Phase I	CB1	117 kN	12.43 mm	115 kN	Flexural/Shear	36	1
	CB2	161 kN	17.78 mm	120 kN	Flexural/Shear	65	2
	CB3	168 kN	19.52 mm	115 kN	Flexural/Shear	65	2
	RB1	182 kN	11.29 mm	182 kN	Shear	38	1
	RB2	244 kN	52.98 mm	155 kN	Flexural	36	1
	RB3 (CSA)	271 kN	69.27 mm	188 kN	Flexural	66	2
	RB4	108 kN	75 mm	87 kN	Flexural	52	2
Phase III	CCB1	216 kN	14.79 mm	197 kN	Flexural/Shear	36	3
	CCB2	197 kN	16.35 mm	147 kN	Flexural/Shear	36	3

As shown in Table 5.2 f'$_c$ for CB2, CB3 and RB3 (CSA) is almost double the f'$_c$ of the other beams as the concrete for these beams were from the same batch. The increase in f'$_c$ reduces the area of the compression stress by reducing the depth of the compression area (a). Reducing "a" will increase the moment arm between the compression force and the tension force within the beam – the resisting moment - therefore, increasing the beam's capacity. The difference in moment arm between beams constructed from 36MPa and 66MPa is 14.45mm. Considering two identical rectangular beams, the difference in f'$_c$ would be a 1% increase in the overall moment capacity of the beam. The difference in f'$_c$ is considered in the design calculations and will be shown in Chapter 7.

The following is the comparison of strain along the reinforcement in the three beams CB3, RB3 and CCB1. Figures 5.127 and 5.128 show the location and numbering system of the strain gauges as a reminder to the reader, see Chapter 4 for details.
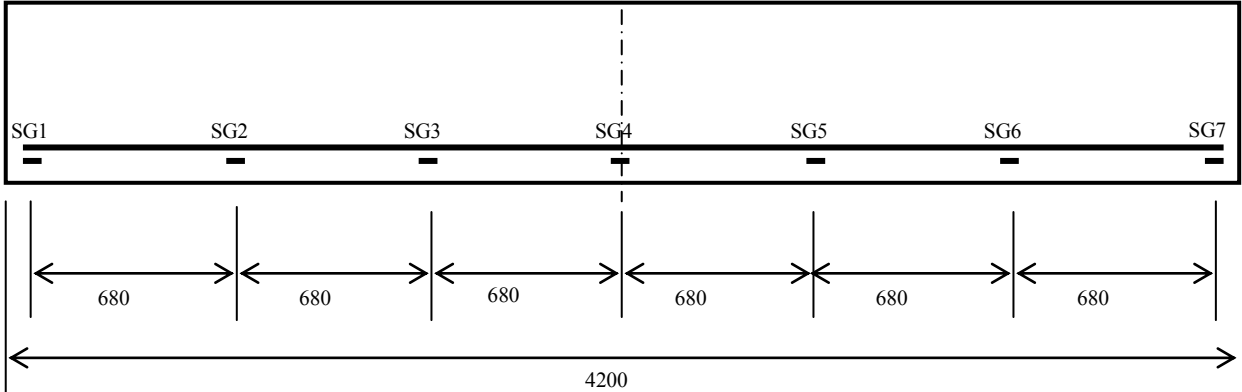
Figure 5.127 – Steel strain gauges no. and location for RB3

184
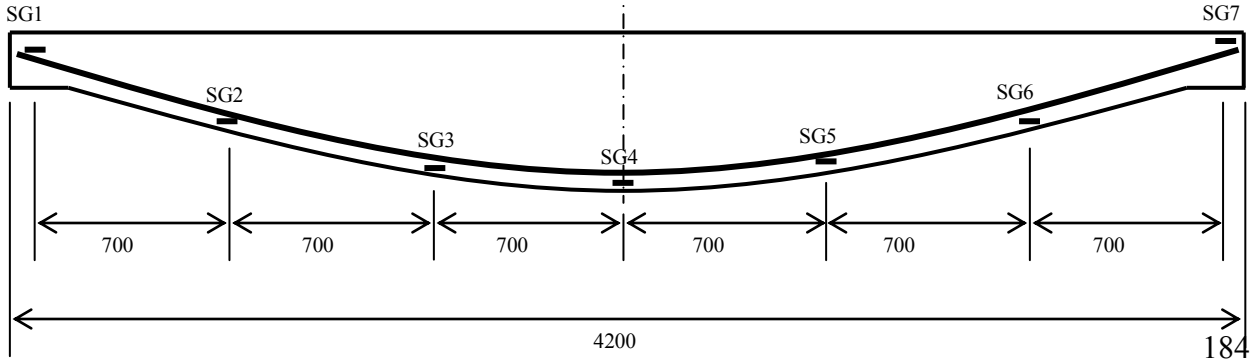
Figure 5.128 – Steel strain gauges location for CB3

As previously explained, the strain gauges SG1 and SG7 are not included in the graphs because the readings from these gauges show an abnormally high stiffness as they are located very close to the end angles and weld plates where the area of steel is much large than the 2-25M bars ($A_{s(2-25M)}$ = 1000mm^2).

Figures 5.129 through 5.133 show and compare the strain in three beams; CB3, RB3 and CCB1. Each graph compares the strain in individual strain gauges along the reinforcement in the beams.
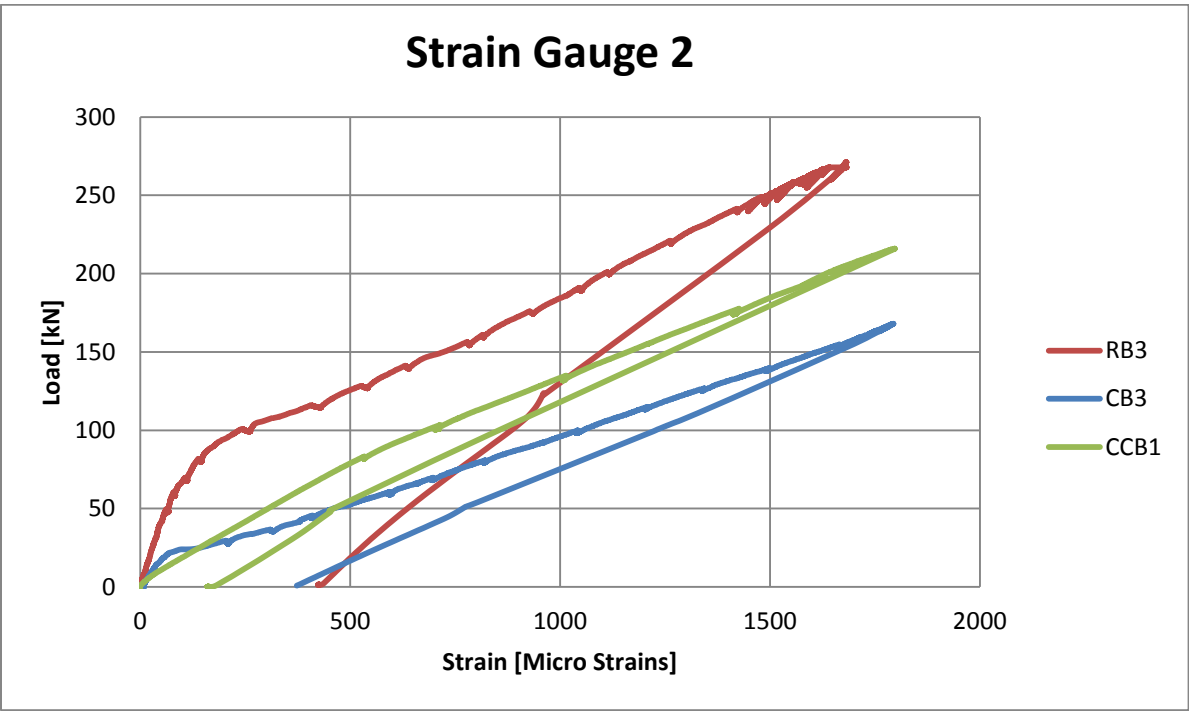
Figure 5.129 – Strain at SG2
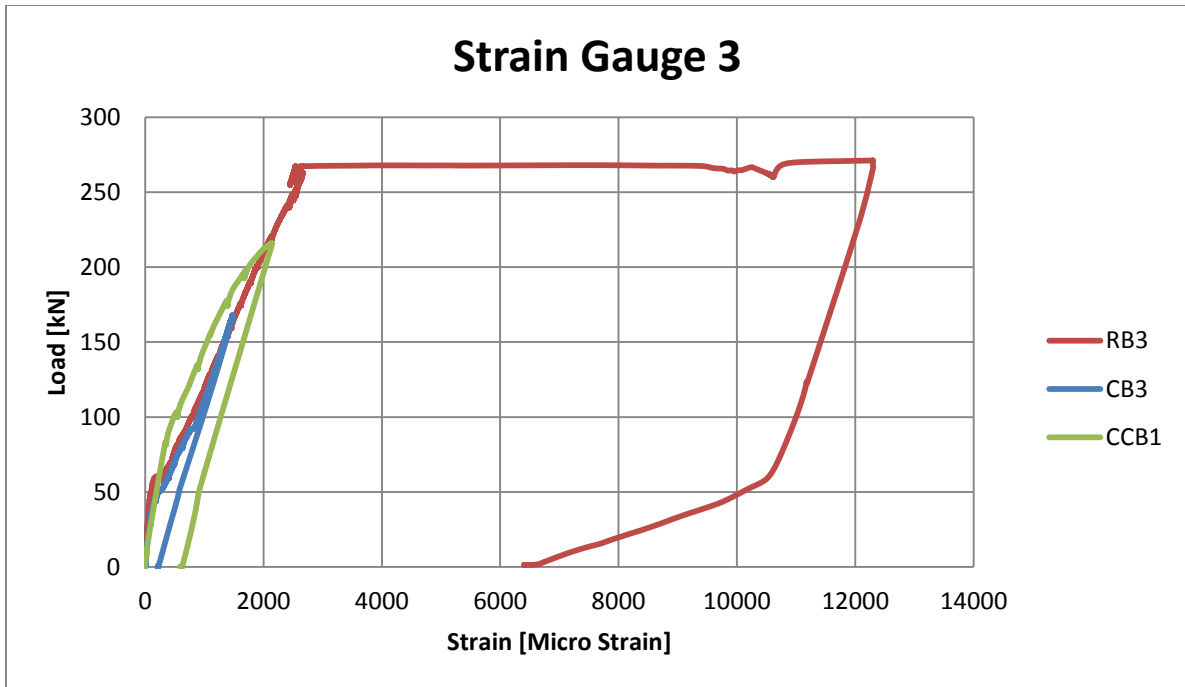
Figure 5.130 – Strain at SG3
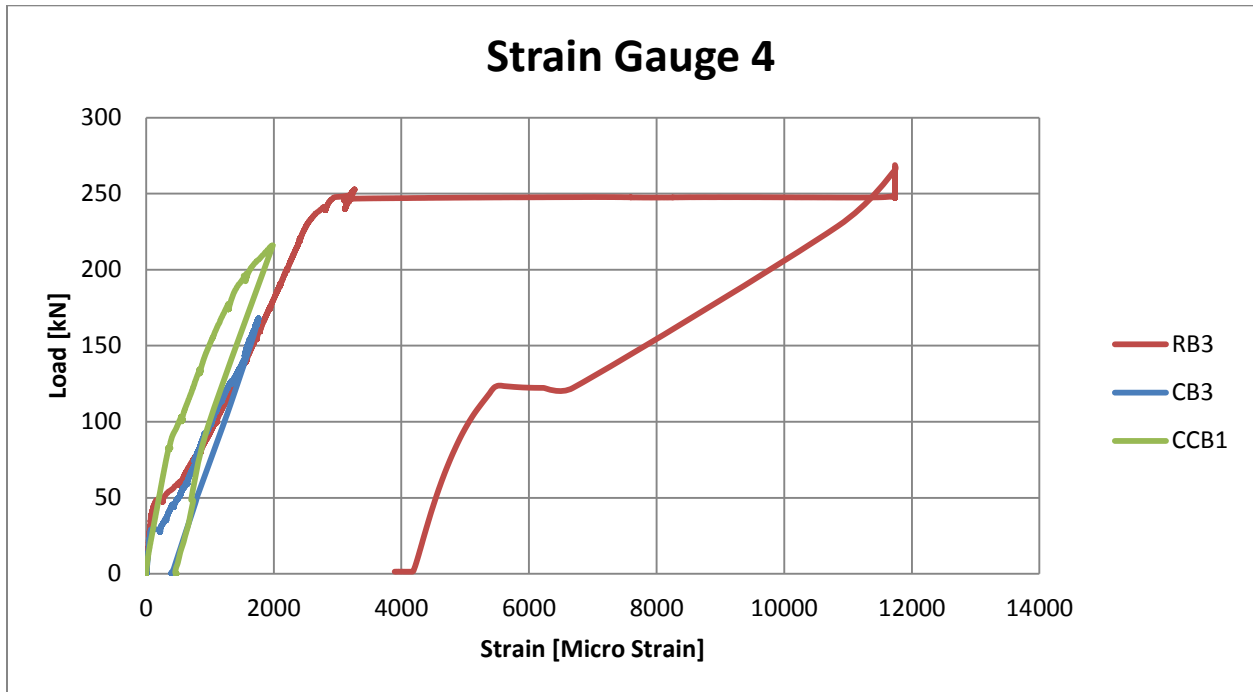
Figure 5.131 – Strain at SG4
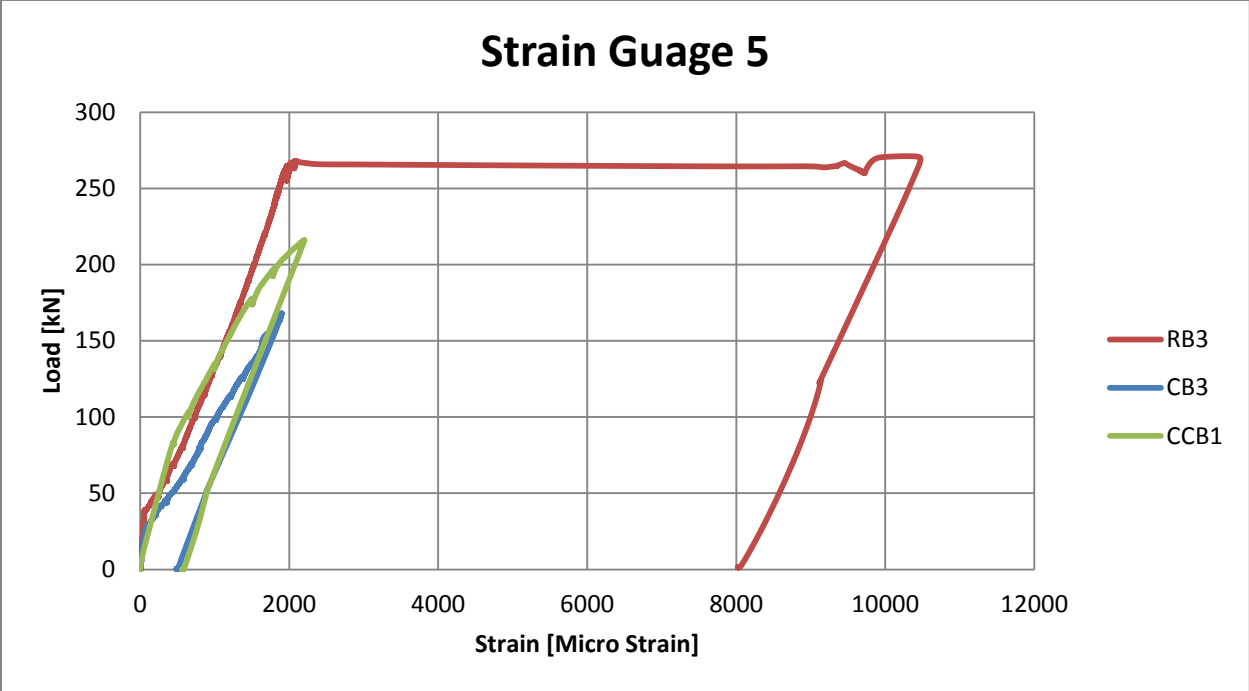
Figure 5.132 – Strain at SG5
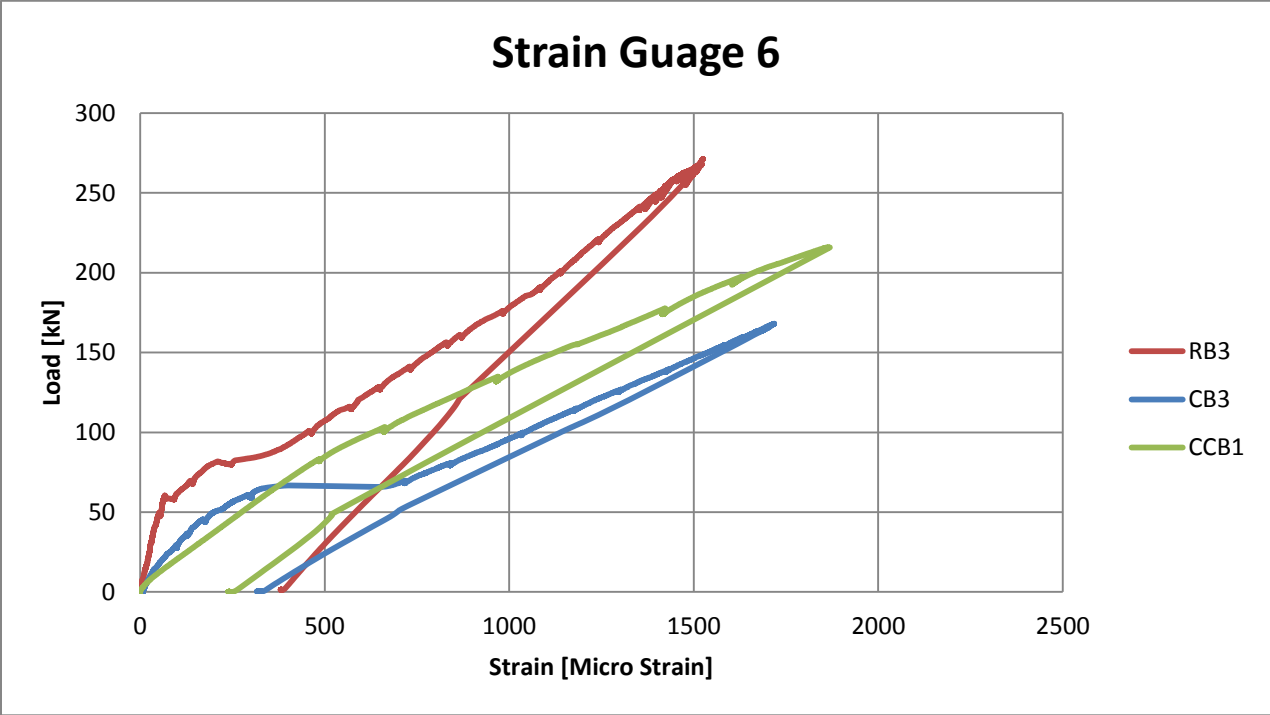
Figure 5.133 – Strain at SG6

As shown in Figures 5.129 through 5.133, the strain, and therefore stress, is more uniformly distributed along both moment-shaped beams CB3 and CCB1. The stress in the reinforcement of the rectangular code-designed control beam RB3 peaked beyond yield stress at the center-span of the beam, but the stresses remained below yield outside of the centre-span area of the beam.

The following discussion illustrates this point in more detail. The graphs in Figures 5.134 through 5.138 compare strain along the length of the beams. These comparison graphs are designed to show the maximum strain at the maximum load right before final failure.
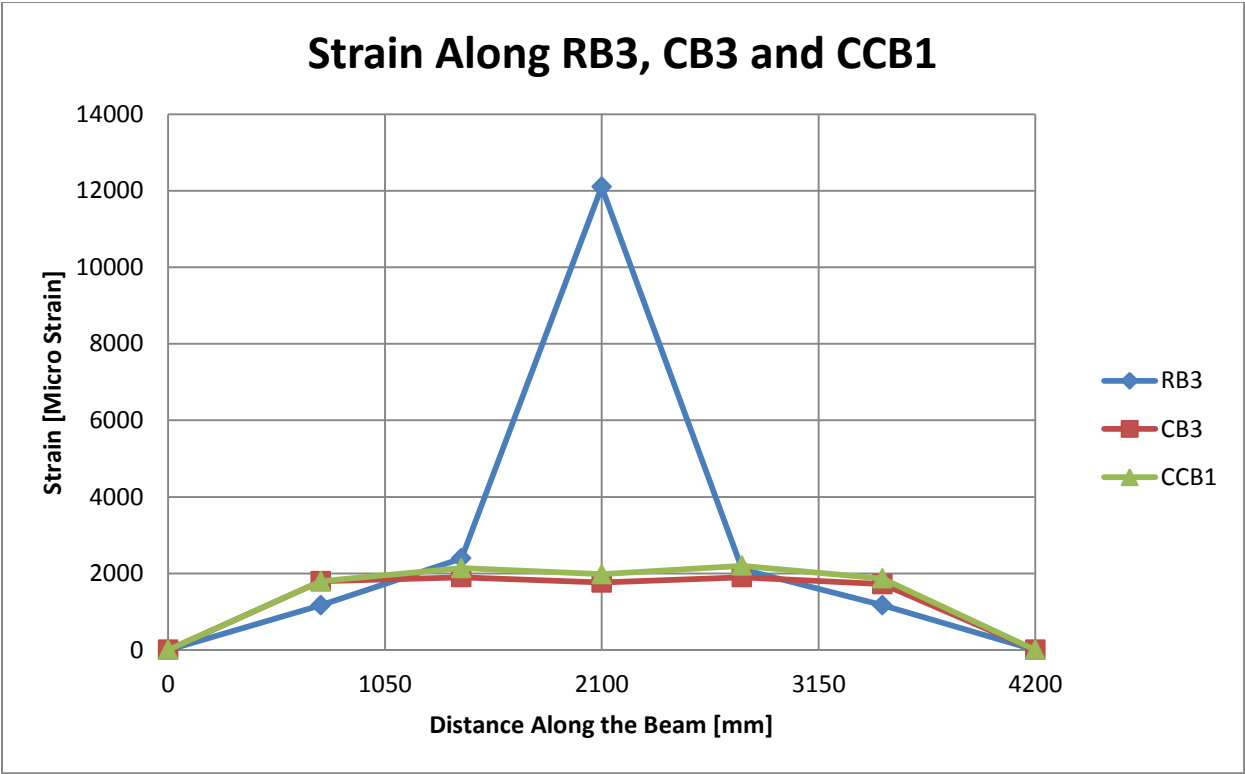
Figure 5.134 – Strain along beams RB3, CB3 and CCB1

Figure 5.126 shows and compares the strain along the beams RB1, RB2 and RB3. These are the three rectangular beams with different reinforcement configurations. All beams in this comparison graph had the same amount of flexural reinforcing (2-25M) but different or no shear reinforcement. RB1 was the rectangular beam with flexural reinforcement but no shear stirrups. The reinforcing in this beam was placed straight at the bottom of the beam similar to that of control beam RB3 which is the CSA-designed beam.

Beam RB2 has a rectangular concrete section similar to RB1 and RB3, the same amount of flexural reinforcement and no shear stirrups. However, the reinforcing in this beam was curved similar to the moment-shaped beams.
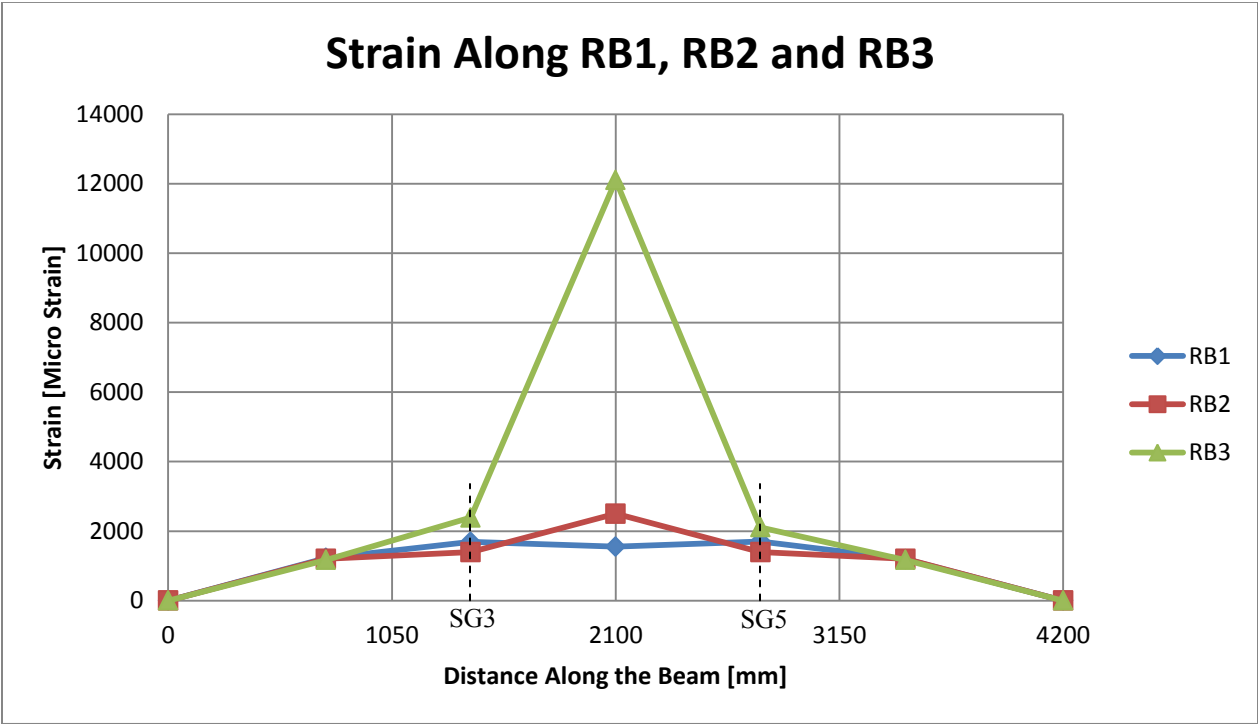
Figure 5.135 – Tension strain along the length of the reinforcement in RB1, RB2 and RB3

This strain comparison shows that the reinforcement in beam RB1 (the rectangular beam with only flexural reinforced and no shear stirrups) did not yield during the testing.

However, the reinforcing in RB2 (the rectangular beam with flexural reinforcing following the same curve as the moment-shaped beams and no shear reinforcement) did yield between SG3 and SG5. The reinforcement yielded about 680mm on each side of the centre-span, for a total length of 1360mm.

Figure 5.136 shows and compares the strains along the beams RB2, CB3 and CCB1. These three beams all have the same curved flexural reinforcement but have different concrete profiles or configurations. RB2 has a rectangular concrete profile. CB3 has a curved profile at the bottom of the beam only while CCB1 has a curved profile at the bottom of the beam with a curved (cambered) top.
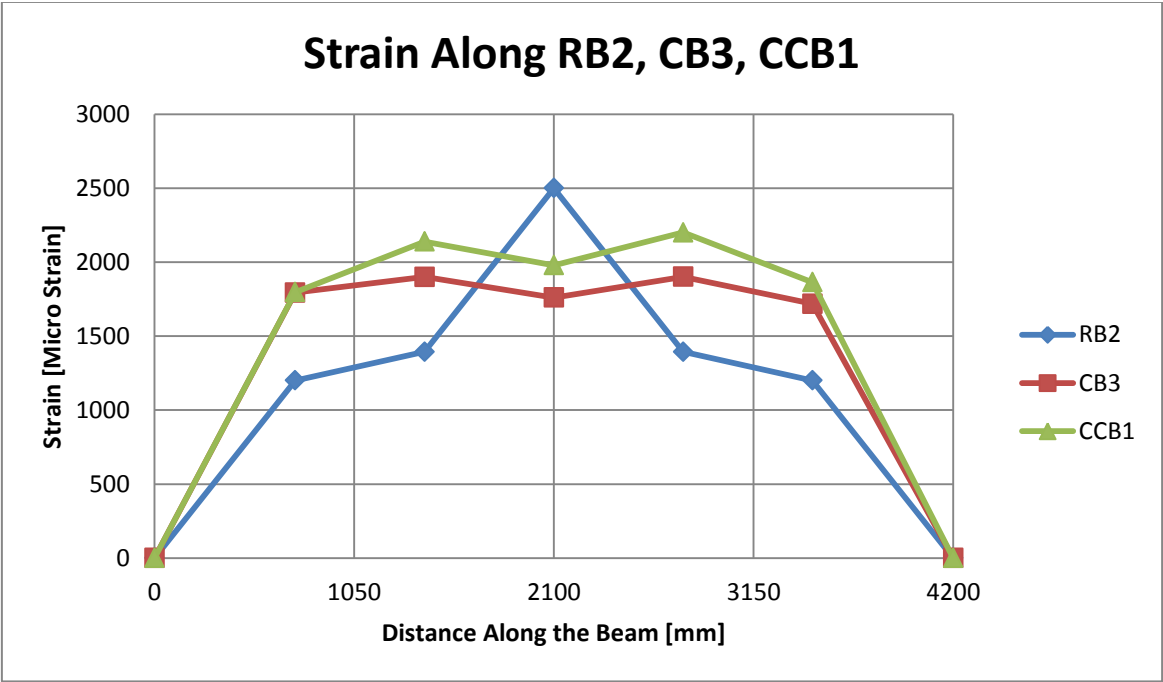
Figure 5.136 – Strain along beams RB2, CB3 and CCB1
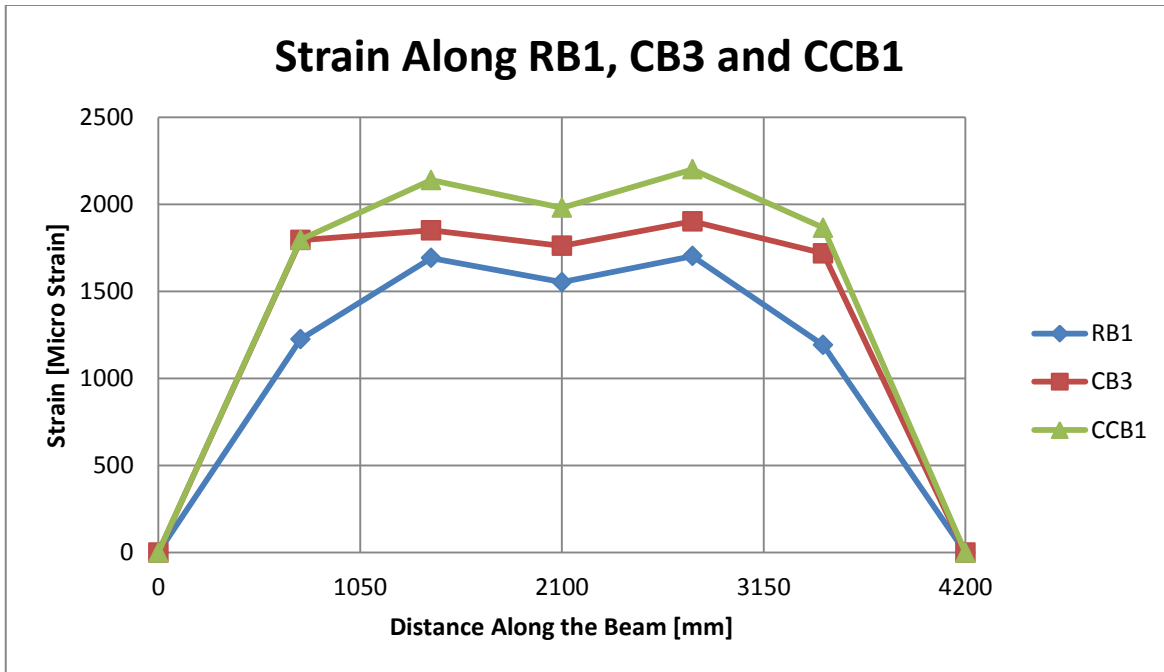
Figure 5.137 – Strain along beams RB1, CB3 and CCB1

The final strain comparison (Figure 5.138) is between CCB1, the best performing moment-shaped beam, and RB3, the CSA-designed conventional control beam. This comparison graph also includes the bending moment (BM) diagram that the six-point loading condition produces in these beams. The bending moment has been multiplied by 10 to increase the scale factor making the bending moment diagram more evident in this graph. The shape of the strain distribution (and, therefore, stress distribution) in CCB1 is comparable to the shape of the bending moment diagram BM (10), as shown in Figure 5.138. Demonstrating that as the tension due to the load increases the resisting, tension in the reinforcement also increases. The strain reading at the center span of the CSA control beam RB3 is 12102 micro-strains, over six times higher than the yield strain of 2000 micro-strains. There is a sudden increase in stress over 1400mm of the midspan of the RB3 beam.
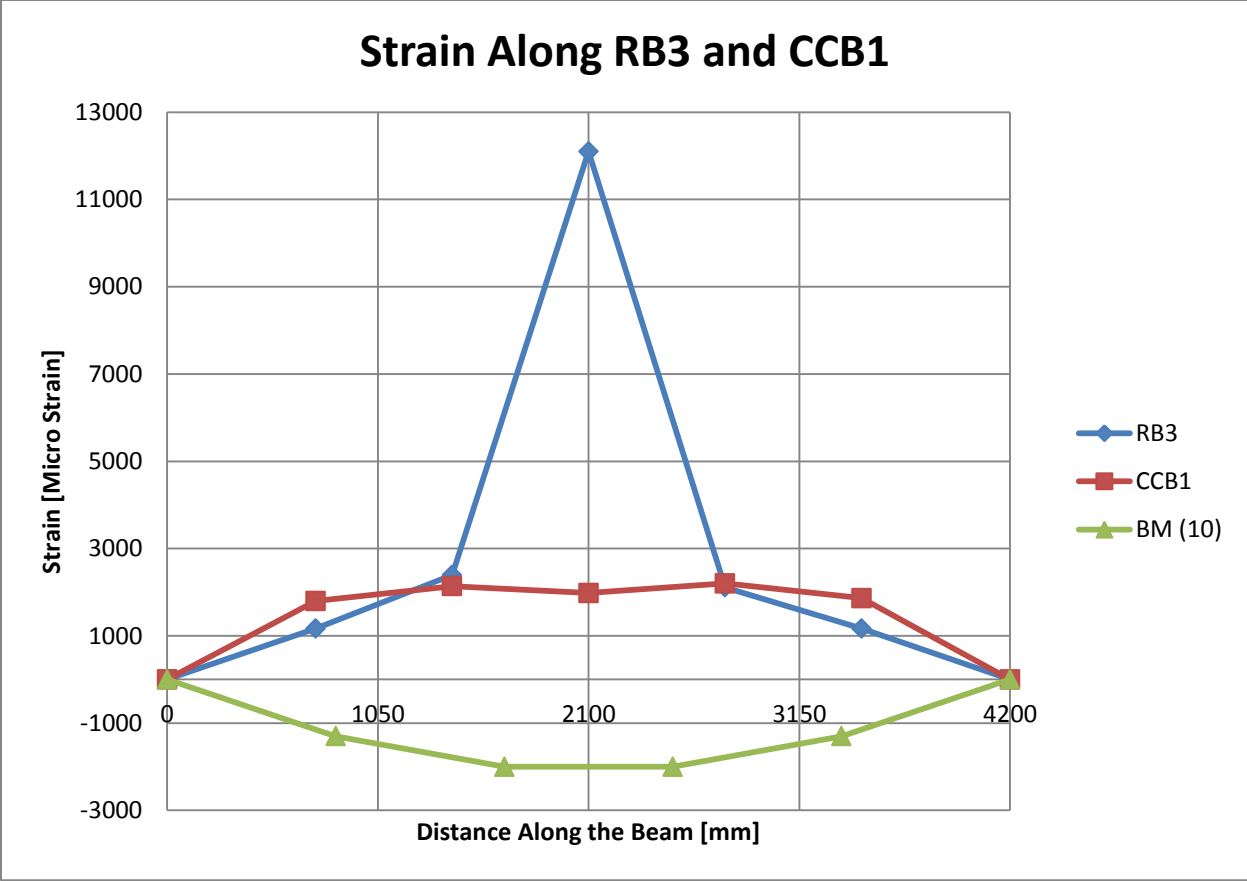
Figure 5.138 – Strain along beams RB3 and CCB1, also showing the bending moment (BM) profile, multiplied by 10 [shown as BM (10)] for clarity

Figure 5.139 illustrates the stress along the reinforcement in both the cambered curved beam CCB1 and the CSA-designed rectangular control beam. The portion of the rebar that yielded is shown in red and the area or the portion of the rebar that the stress is below yield stress is shown in blue.

Note that in Figures 5.134 to 5.139 the strain is shown to be at zero for all beams. While this is correct for rectangular beams it is not the actual representation for curved beams. The numerical analyses that will be discussed in Chapter 6 show that the strain, stress and tension forces remain constant along the reinforcement in the curved beams. The tension force comparison from the FEM analysis is shown in Figure 5.141.

Strain Along RB3 and CCB1
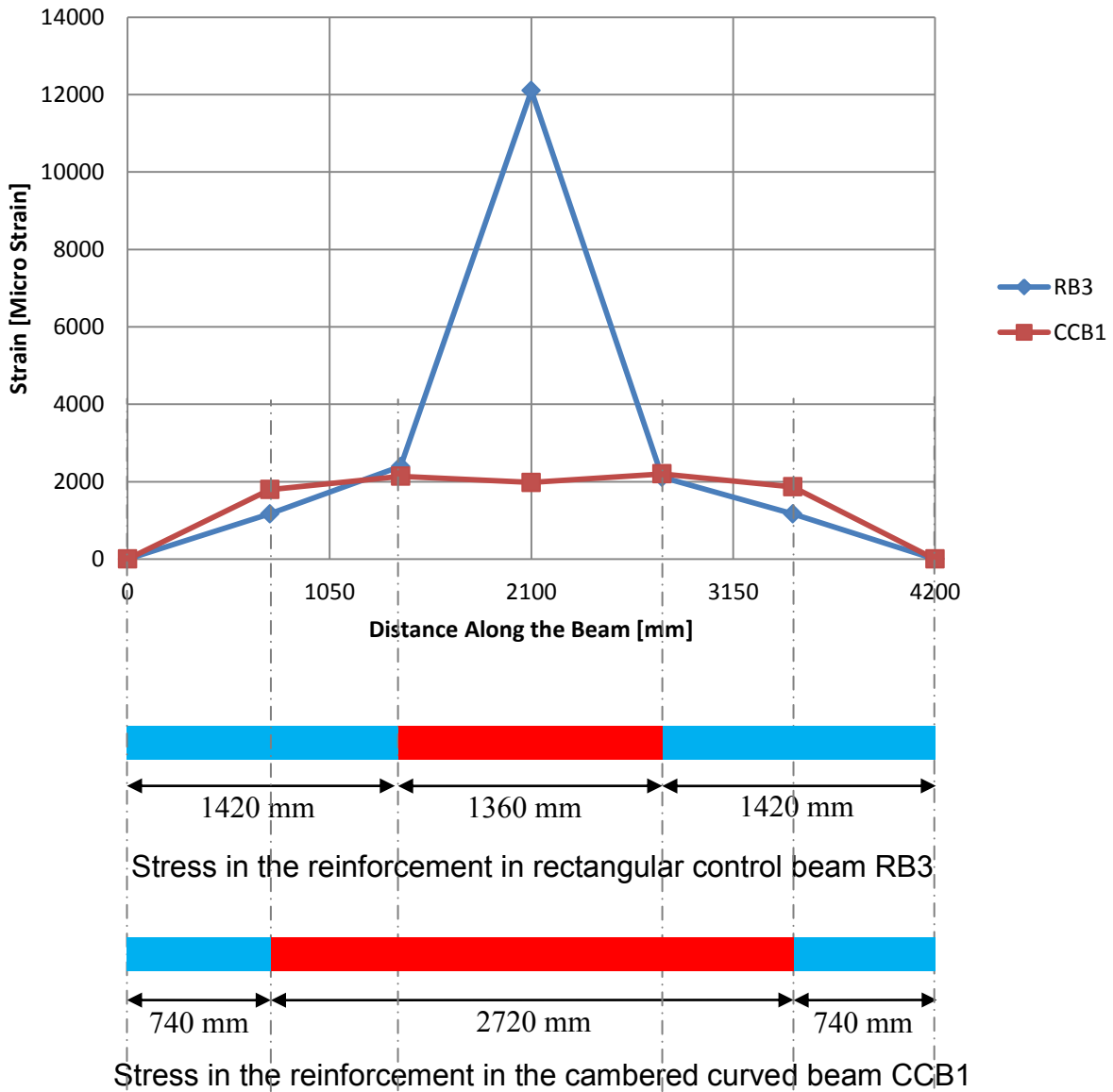
Figure 5.139 – Length of yielded reinforcement in RB3 and CCB1

The above stress comparison shows that the larger length of the steel reinforcement in the CCB1 has been yielded. This indicates that more of the steel is "working" in the moment-shaped curved beam than the rectangular control beam; which is consistent with the proposed efficiency theory. This aspect is shown more clearly in Figure 5.140,

where red indicates the length of steel which has yielded with respect to the strain gauges.

Control Beam RB3

Cambered Curve Beam CCB1
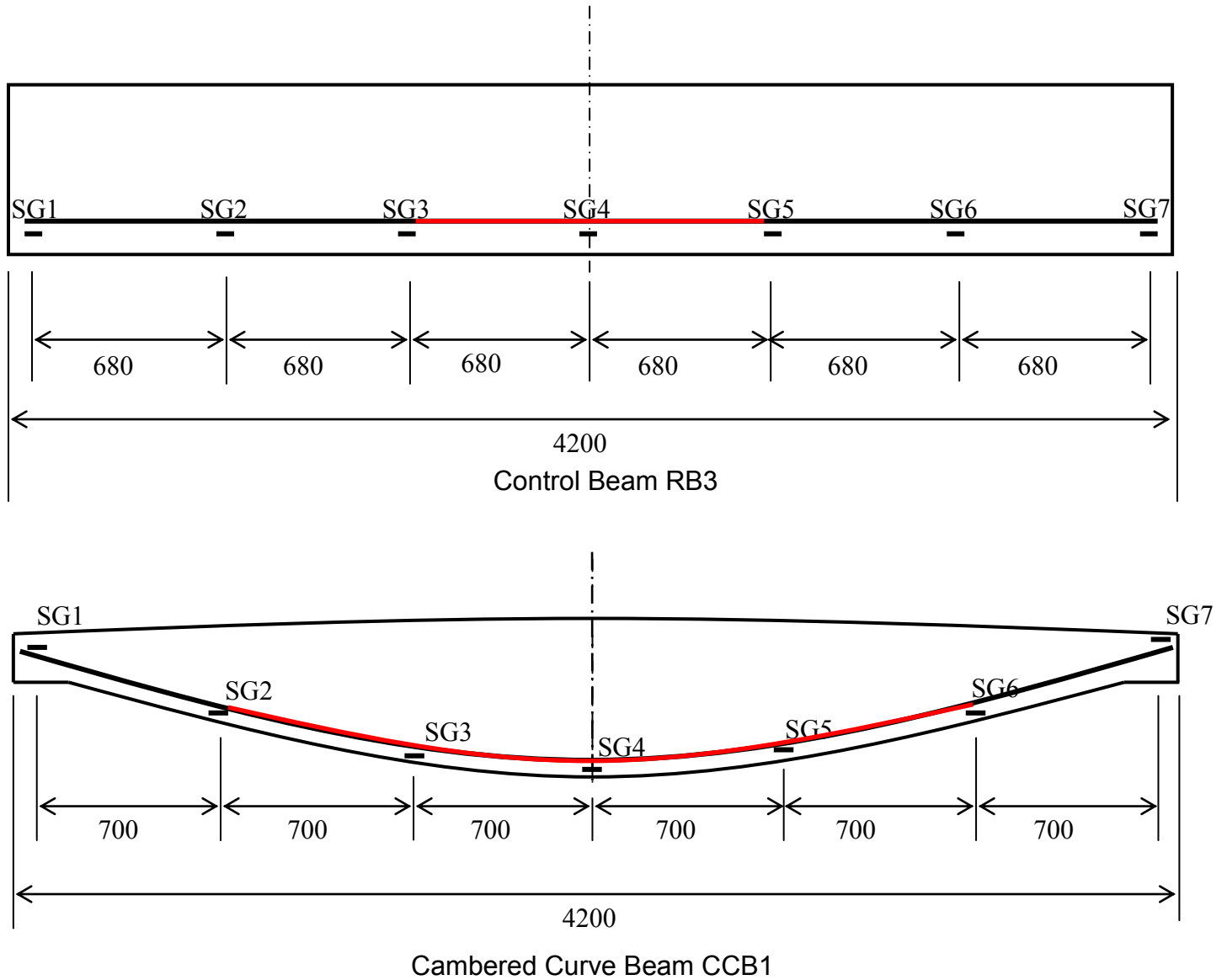
Figure 5.140 – Length of the steel reinforcement yielded in RB3 and CCB1 with respect to strain gauges

A further comparison of RB3, the control beam, and CCB1 can be given by comparing the stresses at each strain gauge. For these calculations 186 MPa will be used for the modulus of elasticity of the steel reinforcement determined by testing the reinforcement shown in Section 5.1.5. The stresses and tension forces are shown in Table 5.3. It should be noted that both the stresses and tension forces are proportional to the strain.

Table 5.3 – Stress comparison

Beam		SG2	SG3	SG4	SG5	SG6
RB3	Stress [MPa]	217	445	2251	393	217
	Tension Force [kN]	109	222	1126	196	109
CCB1	Stress [MPa]	334	398	368	409	347
	Tension Force [kN]	167	199	184	205	173

As the above comparison shows, the cambered curved beam distributed the load more uniformly along the reinforcement. Furthermore, more of the steel reinforcement in the cambered curved beam carried higher stress than the rectangular control beam.

As indicated earlier, numerical analysis shows that the tension force remains constant along the reinforcement in curved beams. Figure 5.141 compares the tension force in the reinforcement in CCB1 from experimental work and from the FEM analysis. The FEM analysis shows that the tension stress (i.e. tension force) remains practically constant along the reinforcement. Results from the FEM analysis will be discussed in detail in chapter 6.
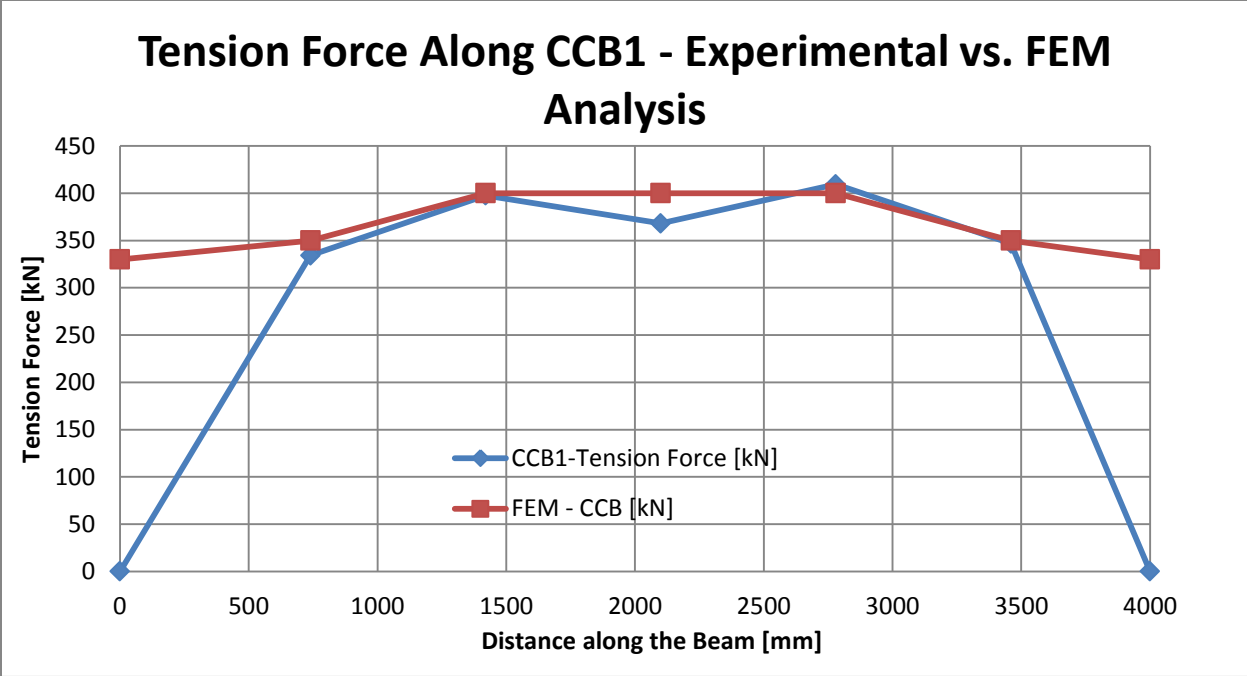
Figure 5.141 – Tension force along the reinforcement in CCB1

END OF SECTION

6 Introduction of FEM-NRC program

Development of suitable analytical models for studies of complete late behaviour (zero load until failure) of reinforced and prestressed concrete structures or their components under any given loading condition is a complex task further complicated due to a lack of sufficient knowledge of the following phenomena:

1. Non-homogeneity of structural concrete (reinforced or prestressed which consists of concrete and intermediate grade or high strength steels).

2. Crack propagation and the absence of suitable criteria for failure of concrete under different stress combinations.

3. Effect of anchorage or pullout, dowel and aggregate interlock forces in the uncracked and cracked sections.

4. Non-linear stress-strain relationships for concrete and lack of suitable constitutive relationships under combined stresses.

5. Creep and shrinkage of concrete.

Incorporating these complexities into a mathematical model based upon the classical theories of continuum mechanics is extremely difficult. A detailed analytical study of stress distribution, deflections, crack propagation, bond, aggregate interlock and dowel action at varying loads up to ultimate load, would be useful to understand the basic behaviour of reinforced concrete members and structures.

It seems possible to take a general approach, based on the finite element

method, which can deal with the above complexities of reinforced concrete.

The versatility of this method and its application to aircraft, nuclear, automobile and ship structures is well established but its application to civil engineering problems such as tall buildings, bridges and in particular to the reinforced concrete structures, is recent. The civil engineering problems pose computing difficulties as it is often necessary to create computer algorithms which are suitable to civil engineering needs and because of the size of the structures involved. Initially progress was restricted due to high computing costs but the advent of a new generation of computers has provided the in-core capacity needed for civil engineering problems and decreased the computing times involved.

The use of finite elements to study the behaviour of reinforced concrete was initiated by Scordelis (Ngo and Scordelis, 1967). He used linear stress-strain relationships for concrete, bond "pullout" and dowel actions, to analyze a singly reinforced beam subjected to a two point symmetrical loading. Symmetrical cracks were arbitrarily introduced on the basis of experimental results and principal stresses were calculated at all element centroids. Scordelis also made some important recommendations for future research.

Nilson (Nilson, 1967) analyzed the pullout specimens tested by Broms (Broms, 1965) using non-linear stress-strain relationships for concrete and bond "pullout" springs and a linear dowel response. An incremental loading technique was used; when a crack appeared the load was removed, the specimen topology was redefined and the specimen reloaded from zero load until the formation of the

next crack. Saenz's non-linear constitutive relationship was adopted for concrete while a non-linear bond "pullout-slip" relationship was derived from the results of the Bresler-Bertero pullout tests (Bresler and Bertero, 1966). Mufti et al, maintained the non-linear material properties and bond-slip characteristics used by Nilson and developed a computer program which examined the behaviour of a specimen through all loading stages (from zero load up to failure) under a monotonically increasing load. This resulted in significant savings in computing time (Mufti et al., 1971). Cracks were introduced when one of the principal stresses equalled or exceeded a predetermined tensile strength of concrete. The stiffness of the cracked element was then automatically deleted from the overall stiffness of the structure, thus modifying it for the next loading increment. The forces in the cracked element were applied at its nodes common with adjacent uncracked elements and redistributed during the next cycle. This eliminated the need for a revision of the specimen topology at the appearance of a crack and made the analysis more efficient.

6.1   Objective and Scope

This part of the research presents and discusses the results of computer analyses of a concentric pullout specimen, previously analysed by Nilson (Nilson, 1967), and a simply supported, singly reinforced concrete beam subjected to a symmetrical two point loading, previously examined by Ngo and Scordelis (1). The following two elements are used for both analyses:

a)   Plane stress triangular element, and

b)   Plane stress rectangular element.

Piecewise linear procedure is used to account for material and bond non-linearities. In the analysis of structures using finite elements, the choice of an element is very important. Plane stress rectangular element has given accurate results when compared to triangular element. But there are some difficulties such as the representation of a crack and its width. The assumptions made by the authors (Mufti et al., 1971) make no distinction between triangular and rectangular elements as far as crack propagation is concerned, because the introduction of a crack in to an element automatically deletes its contribution to overall stiffness. This is a crude but extremely simple technique to modify the stiffness of the structure. The second point which the authors wish to emphasize is the presence of several cracks rather than one or two predefined cracks and the continuous stress redistribution within the structure with the increase of applied loads.

Both of these points, the choice of an element and the continuous modification of the stiffness of the structure as cracks appear and propagate, are examined in detail. Load-deflection curves are obtained using both the triangular and the rectangular elements. Stress distribution for each load increment is shown to illustrate the redistribution of stresses.

Finally, Ref. 10 includes the description of the program using rectangular elements along with a complete FORTRAN listing, a description of the notation used and the input required. Output for one of the problems solved is also included. It is intended to form a user's manual.

6.2 Analysis

6.2.1 The Finite Element Method

The finite element method for the linear elastic analysis is well known and is available in standard texts (Zienkiewicz, 1967). The structure is divided into an assembly of a finite number of discrete elements connected at nodes. The stiffness characteristics of the element are determined using the minimum potential energy theorem and results in the following equation for the plane stress case.

$$\underline{d_e} = \underline{F} \, \underline{\delta_e}$$

(1)

Where
$$\underline{d_e} = \left\{ \frac{u}{v} \right\} \qquad\qquad \underline{\delta_e} = \left\{ \frac{\delta_u}{\delta_v} \right\}$$

and
$$\underline{F} = \begin{bmatrix} f & 0 \\ 0 & f \end{bmatrix}$$

Therefore
$$\left\{ \frac{u}{v} \right\} = \begin{bmatrix} f & 0 \\ 0 & f \end{bmatrix} \left\{ \frac{\delta_u}{\delta_v} \right\}$$

(2)

Where
$$\underline{\delta_u} = \left\{ \begin{array}{c} u_1 \\ u_2 \\ u_3 \\ u_4 \end{array} \right\}$$

and
$$\underline{f} = \left[1 - \frac{x}{a} - \frac{y}{b} + \frac{xy}{b} \quad \frac{x}{a} - \frac{xy}{ab} \quad \frac{y}{b} - \frac{xy}{ab} \right]$$

a = Lenght of an element along x-axis

b = Lenghtod an element along y-axis

$$\underline{\varepsilon} = \left\{ \begin{array}{c} \dfrac{\delta u}{\delta x} \\[2mm] \dfrac{\delta v}{\delta y} \\[2mm] \dfrac{\delta u}{\delta y} + \dfrac{\delta v}{\delta x} \end{array} \right\} = \underset{\sim}{B} \, \underline{\delta_e}$$

(3)

Then
$$\underline{P_e} = \underset{\sim}{K}_e \, \underline{\delta_e}$$
(4)

$$\underset{\sim}{K}_e = t \int \underset{\sim}{B}^T \, \underset{\sim}{E} \, \underset{\sim}{B} \, dA = t \, A \, \underset{\sim}{B}^T \, \underset{\sim}{E} \, \underset{\sim}{B}$$
(5)

Where:
A = area of an element

B = strain matrix

E = elasticity matrix

T = thickness of an element.

The triangular and the rectangular elements are fully described in the text by Zienkiewicz (Zienkiewicz, 1967). The individual element stiffness matrices are added to obtain the global stiffness matrix. The resulting equilibrium equations are solved for the unknown displacements which are used in turn to calculate the stresses and the strains at the element centroids.

The program using the triangular element to analyze the reinforced concrete

structure is described in Ref. 4 and the details are given in Ref. 3. Although the details of the rectangular element follow the same pattern as that of the triangular element they are presented here for completeness.

The program uses rectangular elements and takes into account three types of elements, i.e. the concrete, the steel elements and the connecting springs which were assumed to follow the nonlinear bond-slip characteristics suggested by Nilson (Nilson, 1967), see Figures 6.1.

(a) Actual Cross Section   (b) Unit Cross Section   (c) Steel   (d) Concrete

(e) Finite Element Grid
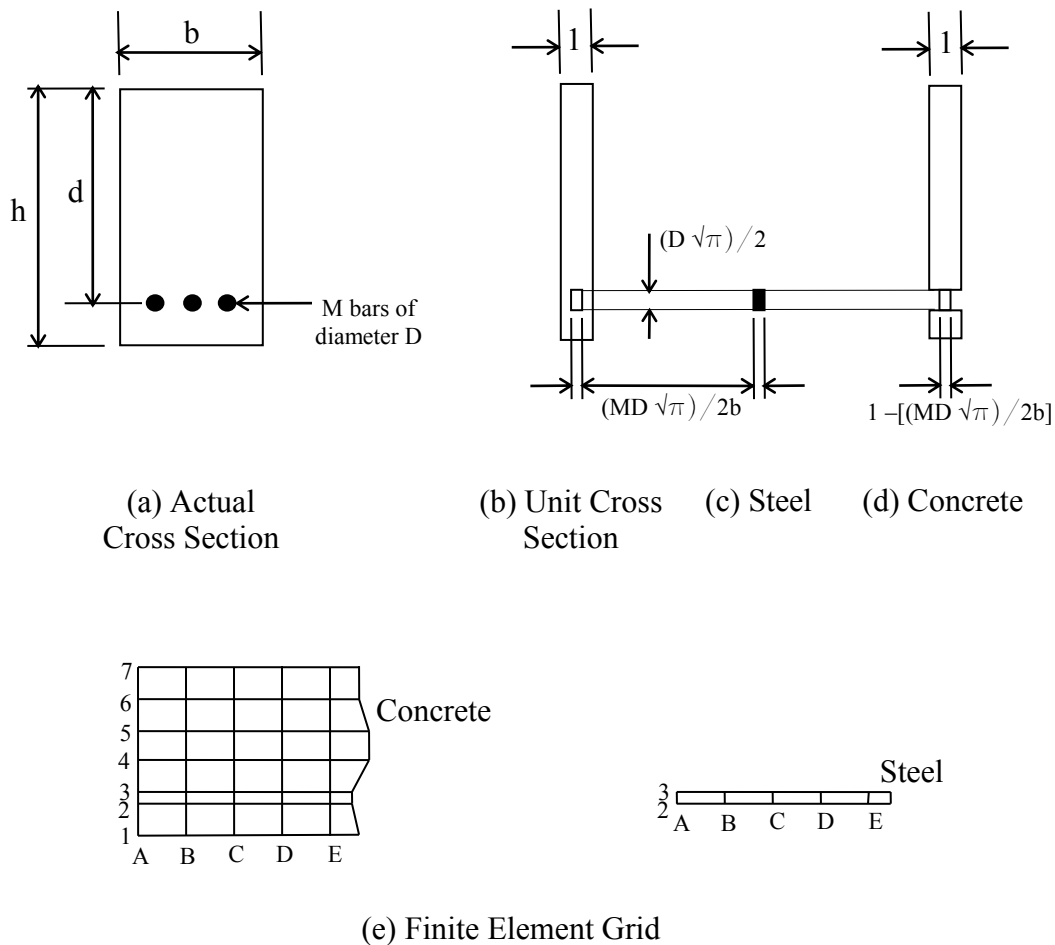
Figure 6.1 - Idealization of a reinforced concrete member
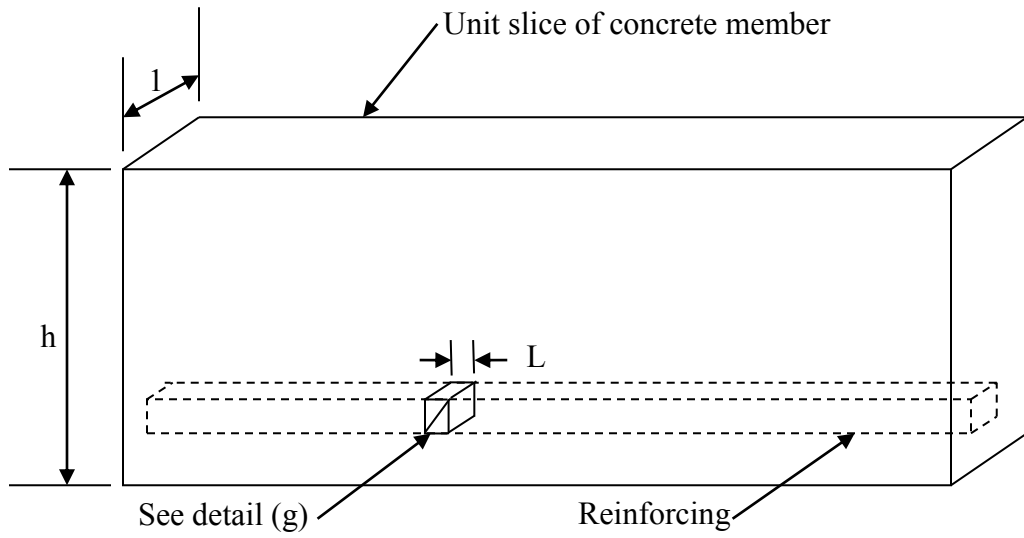
(f) Model of reinforced concrete member
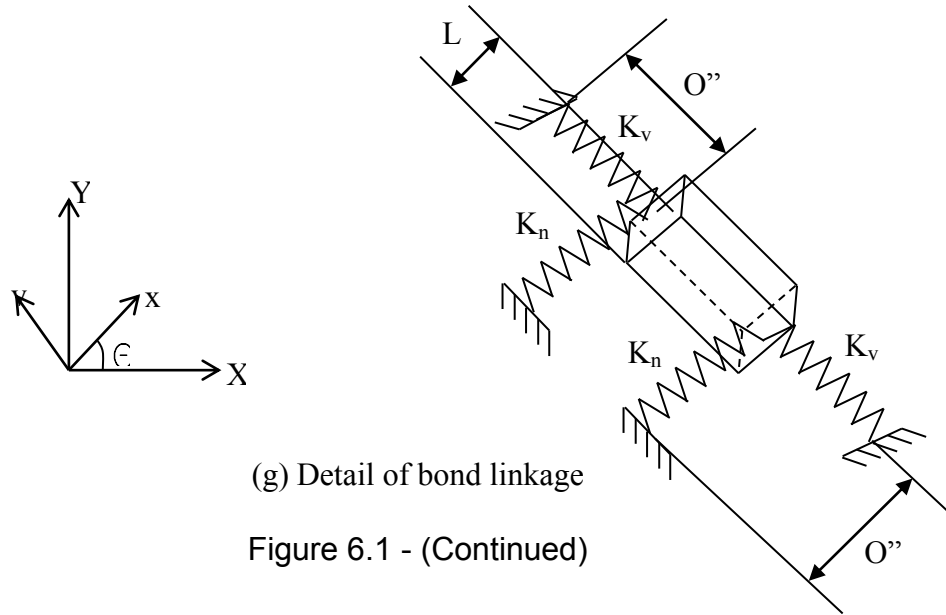
(g) Detail of bond linkage

Figure 6.1 - (Continued)

A typical structural concrete section reinforced with m bars of diameter D, distributed over the width b of the beam, is shown in Figure 6.1(a). For

analysis purposes it is convenient to replace each round bar with an equivalent square bar of the same cross-sectional area. The lateral dimension of the equivalent square bar is given by:

$$t = \frac{D\sqrt{\pi}}{2} \tag{6}$$

This report is limited to the consideration of plane stress problems and it is convenient to use a unit width (instead of b) for the finite element idealization. The width of the idealized steel element (Figure 6.1 (c)) is then:

$$s = \frac{mD\sqrt{\pi}}{2b} \tag{7}$$

where the arrow points to m labelled "No. of bars".

The steel bars occupy a significant fraction of the beam width and the modified width of concrete at the level of steel reinforcement (Figure 6.1 (d)) is:

$$1 - s = 1 - \frac{mD\sqrt{\pi}}{2b} \tag{8}$$

6.2.2 Bond Pullout between Concrete and Steel

The transfer of stress by bond between concrete and steel is extremely difficult to model realistically because several variables affect the bond problem. An experimental investigation was undertaken at McGill University (Houde, 1972) to investigate the bond-slip characteristics, but, for the present investigation the idealized non-linear relationship obtained by Nilson (Nilson, 1967) from the pullout test by Bresler and Bertero (Bresler and Bertero, 1966) is used. The

bond slip d is given by:

$$d = d_s - d_c$$

Where: d_s and d_c are the steel and the concrete displacements respectively.

The bond spring stiffness K_h is the slope of the tangent to the bond stress-slip curve at any point and is given by:

$$K_h = \frac{du}{dd}\, A \qquad (9)$$

Where $$A = \frac{m\pi\, D1}{2b} \qquad (10)$$

Where   1 = the bond linkage spacing.

It is assumed that the steel elements are connected to the concrete elements through bond linkage elements both at the top and at the bottom of the bar segment as shown in Figures 6.1 (f) and (g). For more details, the reader is referred to Ref. 2.

6.2.3 Dowel Action

Studies of the shear strength of reinforced concrete beams have shown the significant effect of dowel action on the behaviour of reinforced concrete beams and slabs. The inclusion of dowel springs in the program increases the order of linkage stiffness matrix to 4 x 4. However, the dowel effects have been taken into account arbitrarily by assuming the dowel spring stiffness K_y to be a very large number. Thus in the local coordinates the linkage stiffness matrix is:

$$\underset{\sim}{K} = \begin{bmatrix} K_h & 0 & -K_h & 0 \\ 0 & K_v & 0 & -K_v \\ -K_h & 0 & K_h & 0 \\ 0 & -K_v & 0 & K_v \end{bmatrix}$$

(11)

To transfer this to the global system of axes the following transformation is required.

$$\underset{\sim}{K}^g = \underset{\sim}{T}^T \ \underset{\sim}{K} \ \underset{\sim}{T}$$

(12)

Where $\underset{\sim}{T} = \begin{bmatrix} \cos\theta & \sin\theta & 0 & 0 \\ -\sin\theta & \cos\theta & 0 & 0 \\ 0 & 0 & \cos\theta & \sin\theta \\ 0 & 0 & -\sin\theta & \cos\theta \end{bmatrix}$

(13)

θ = the angle between linkage element x-axis and the global x-axis

Hence
$$K^g = \begin{bmatrix} \underset{\sim}{K} & -\underset{\sim}{K} \\ -\underset{\sim}{K} & \underset{\sim}{K} \end{bmatrix}$$
(14)

Where
$$\underset{\sim}{K} = \begin{bmatrix} \left(K_h \cos^2\theta + K_v \sin^2\theta \right) & \left(K_h - K_v \right)\cos\theta\sin\theta \\ \left(K_h - K_v \right)\cos\theta\sin\theta & \left(K_h \sin^2\theta - K_v \cos^2\theta \right) \end{bmatrix}$$
(15)

208

6.2.4   *Steel and Concrete Constitutive Relationships*

The stress-strain characteristics for the steel reinforcement are assumed to be linear elastic in tension as well as in compression up to the yield point. Once the steel has yielded, it is assumed to be perfectly plastic and the strain hardening effect is ignored. The response of concrete is assumed to be linear in tension and Saenz's non-linear stress-strain relationship is used for the concrete in compression. It may be noted that separate uniaxial stress-strain relationships are used for the concrete in compression and in tension to examine the generally biaxial plane stress problem. General behaviour of plain concrete under combined stresses (strength, deformations, etc.) is influenced significantly by the nature and magnitude of the stresses acting on the element. Saenz's equation for the concrete stress-strain curve in compression is

$$ f = \frac{E e}{1+\left(R+R_E-2\right)\dfrac{e}{e_0} \;-\; \left(2R-1\right)\left(\dfrac{e}{e_0}\right)^2 + R\left(\dfrac{e}{e_0}\right)^3} \tag{16} $$

where
$$ R = \frac{R_E\left(R_f-1\right)}{\left(R_e-1\right)^2} - \frac{1}{R_e} \tag{17} $$

$$ R_E = \frac{E}{E_s} $$

$$ R_f = \frac{f_0}{f_f} $$

209

$$R_e = \frac{e_f}{e_0}$$

$f =$ Concrete stress

$e =$ Concrete strain

$e_0 =$ Concrete strain corresponding to the maximum stress f_0

$E =$ Initial tangent modulus

$E = \dfrac{2\,f_0}{e_0}$ (Assumed to be equal for tension and compression)

The tangent modulus of elasticity for the concrete at any stress load is given by

$$E_{t=\frac{df}{de}} = \frac{E\left[1+(2R-1)\left(\dfrac{e}{e_0}\right)^2 - 2R\left(\dfrac{e}{e_0}\right)^3\right]}{\left[1+(R+R_E-2)\left(\dfrac{e}{e_0}\right)-(2R-1)\left(\dfrac{e}{e_0}\right)^2+R\left(\dfrac{e}{e_0}\right)^3\right]^2} \tag{18}$$

6.2.5 Analysis - Incremental Loading

An incremental loading procedure is used in this investigation with the loads increasing from zero to the failure load in small increments.

6.2.5.1 First Load Increment:

Initially, the stiffness of all concrete elements is computed using the initial modulus of elasticity E and the stiffness of the bond linkages is calculated as the initial slope of the bond stress-slip curve suggested by Nilson. The global stiffness matrix is compiled from the element stiffnesses of the concrete, the steel, and the bond linkage elements. Equilibrium equations are solved for

the displacements from which the strains and the stresses resulting at the steel and the concrete element centroids and the bond forces at the steel-concrete interface are calculated. The principal tensile stress at the centroid of each concrete element is compared with the modulus of rupture of concrete to check for crack initiation. The calculated bond slip is compared with the permissible slip value to examine the performance of bond linkages in the subsequent load increment.

6.2.5.2   Second and Subsequent Load Increments:

The concrete elements' stiffness is modified by using a value of E obtained for the strain level in each element computed from the previous step. Stiffness of the steel elements does not change until the stress in any element exceeds the¯ yield strength of steel. The stiffness of the elements' bond linkage is modified by using a tangent modulus value corresponding to a slip given by the equation:

$$d_i = \frac{i-1}{\sum\limits_{j=1}^{} \Delta_j + C\Delta_{i-1}}$$

(19)

Where d_i = the average slip assumed for the loading increment i

(The tangent modulus is evaluated at a slip = d_i)

Δ_j = slip corresponding to loading increment j and

C = a coefficient, assumed to be equal to 0.7.

The modified element stiffnesses are added to form the global stiffness matrix which is used to evaluate the displacements. The strains and the stresses at the

concrete and the steel element centroids and the bond stresses are evaluated again and the checks for concrete cracking and bond linkage performance are repeated.

6.2.5.3 Concrete Cracking:

An element is assumed to crack if the principal tensile stress at its centroid equals or exceeds the modulus of rupture. The program modifies the thickness of the cracked element to zero to eliminate its contribution to the global stiffness matrix without making it singular. Also, the forces present in the cracked concrete element are redistributed into the surrounding elements by applying equivalent forces at the nodes of the cracked element.

6.2.5.4 Bond Pullout Failure:

A bond pullout linkage element is assumed to fail if the bond slip at the node equals or exceeds the peak value of 0.00045 in. following Ref. 2. The exterior linkage element (e.g. the bond linkage element at the exterior face of the pull-out specimen) is then considered to have failed, i.e. its strength becomes zero for slip values larger than the peak value. However, stiffness of the interior linkage elements is assumed to be zero for values of slip larger than the peak value, while the bond pullout force is maintained constant and equal to the value at the peak slip.

6.2.5.5 *Further Loading Increment:*

The present program provides for a specified number of loading increments and has the ability to evaluate the response of a structure to applied loads provided the global stiffness matrix does not become singular. Such a situation can arise in a pull out specimen when cracks traverse the entire cross-section and the steel yields thus making the global stiffness matrix singular. Future versions of this program will include suitable failure criteria (e.g. yielding of steel, crushing of concrete, excessive cracking, excessive deformations, etc.). The authors would like to point out that significant advances will have to be made in studying the behaviour of concrete under biaxial and triaxial stresses to provide the load-deformation (or the stress-strain) relationships under different combinations of stress. This will provide the data needed to replace the simplified uniaxial constitutive relationships used at present to formulate the concrete element stiffness matrices.

6.3   Discussion of Results

The following two problems have been analyzed in this part of the research using the computer program listed in Appendix A.

1.   A pullout specimen (Ref. 1)

2.   A singly reinforced beam subjected to a symmetrical two point loading.

6.3.1 Pullout Specimen

The specimen consisted of a concrete prism 33 x 8.1 x 3.5 in. symmetrically reinforced with one No. 8 bar.   Symmetry about the two axes permitted consideration of one-quarter of the specimen as shown in Figure 6.2 along with the bond pullout and dowel springs at the connecting nodes at the steel-concrete interface.   The stiffness of dowel springs was assumed to be an arbitrary value while the stiffness of the bond springs was evaluated using techniques described previously.   The input data required for the computer program is also indicated in Figure 6.2.

The test specimen was subjected to an increment loading in increments of 4 kips each. The details of the cracks and the loads at which they appeared and propagated are shown in Figure 6.3. The crack pattern obtained (Figure 6.3) does not agree with Nilson's results. It may be noted that the cracking criterion was examined at the centroid of each element.   An improvement in the interpretation of the results is obtained in the crack pattern using the rectangular element.

214
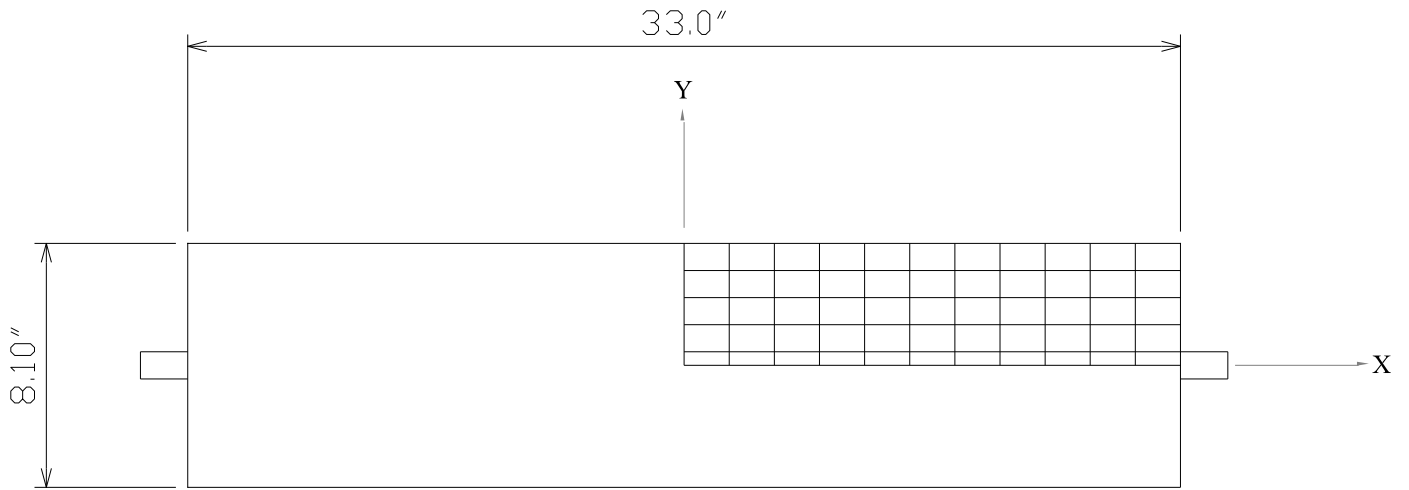
Full specimen
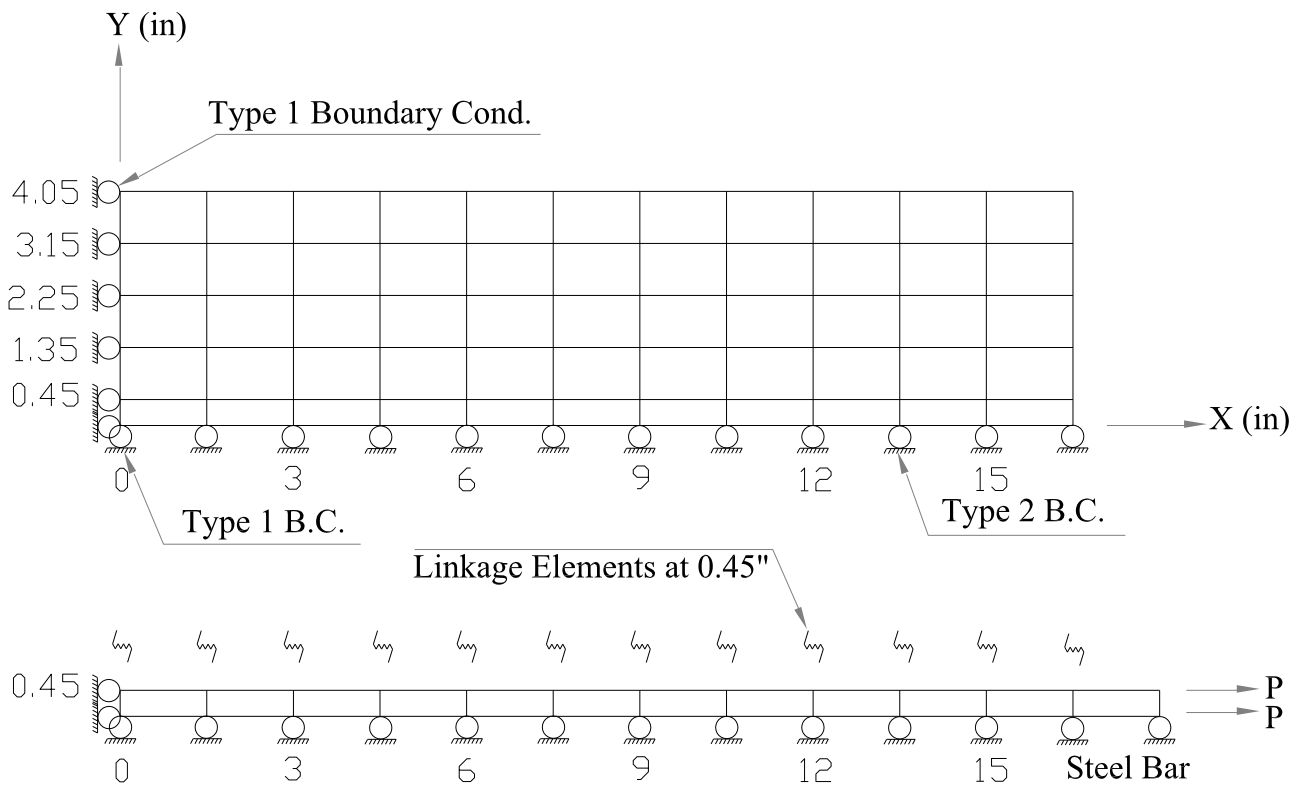
Figure 6.2 - Idealized quarter of the specimen
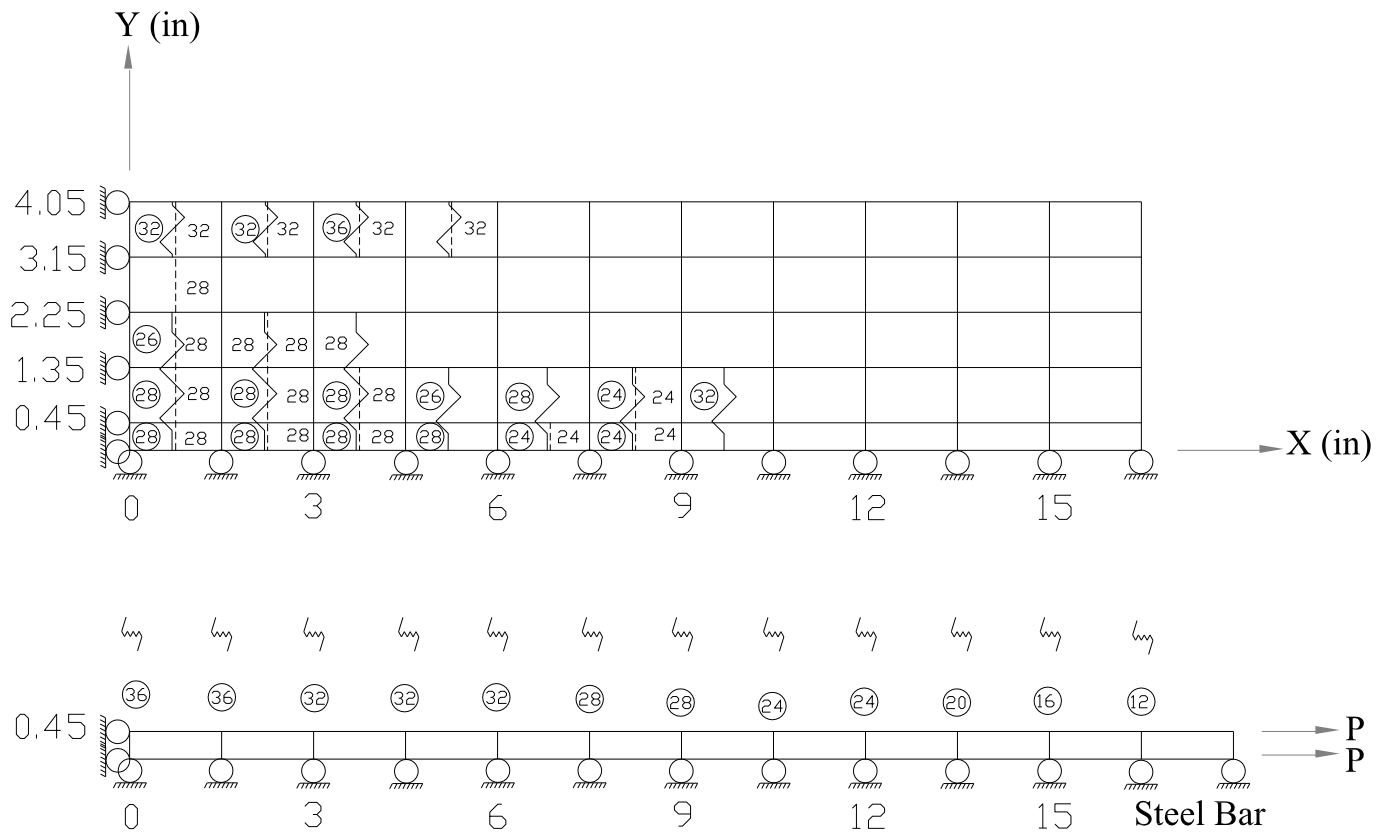
Figure 6.3 - Values of steel bar stress when elements or linkages ruptured

Nilson showed both the distribution of bond stresses at different load levels and the variation of the longitudinal stress in concrete at a load corresponding to a steel stress of 24 ksi (Ref 2). Bond stress distribution appears to be in reasonable agreement with Nilson's results up to a steel stress value of 24 ksi, although there is a slight discrepancy at higher load levels. The higher results can possibly be attributed to a stiff bond spring used by Nilson which was derived from the Bresler-Bertero test (Nilson, 1967).

More experimental work is needed to establish the bond spring characteristics. Also, the assumption of the absence of dowel action in this axi-symmetric test is

216

reasonable but for other specimens the data for the dowel spring characteristics will be required. Suitable tests have been undertaken at McGill University to obtain the dowel force-displacement relationship and will be reported later (Houde, 1972).

There is good agreement with Nilson's results up to a steel stress level of 20ksi and the discrepancies at higher stress levels can be ascribed to insufficient information on the behaviour of bond springs as discussed earlier (the variation of the steel stress with the distance along the bar for different stress levels and the displacement of the free end of the steel bar at different steel stress levels is shown in Ref.2 Figures 5.16a and 5.21 respectively). Two load-displacement curves - one for a stiff spring and the second one for a softer spring, are indicated. The bond spring stiffnesses used are shown in Figure 6.7. The load-deflection curves follow the curve obtained by Nilson very closely up to a steel stress value of 16 ksi and there is reasonable agreement between the computed and the experimental deflection values up to a steel stress of 24 ksi. The curves obtained by the writers deviate from Nilson's curves in the region of progressive cracking and bond failure at a steel stress value of 24ksi. Experiments on specimens examined in this investigation are in progress and suitable experimental data will be available shortly for comparison with the computer results for steel and concrete stresses, bond stress and steel displacements at different load levels. These results will be reported later (Houde, 1972).

It is noted from the results reported in Figure A6.1 to Figure A6.4 that there is very good agreement between the results obtained using the triangular element

and those obtained using the rectangular element. This is because the constant stress pattern in the element is dominant and hence the results obtained using the triangular element (constant stress) are close to the value computed using the rectangular element which assumed a constant stress distribution across the element if it is sufficiently small.

6.3.2   Beam Bending Problem

A single reinforced, simply supported beam 140 × 20 × 12 in. loaded symmetrically under two point loads, as shown in Figure 6.4, was analyzed from zero load to the ultimate load using both the triangular and the rectangular elements. Idealization of the beam using the rectangular elements is shown in Figure 6.8. Similar nodal idealization was used for the triangular element except that the number of elements used was twice the number of the rectangular elements used.

The result of comparing the deflections in the elastic range at various points along the beam span obtained by using the classical beam bending theory and the finite element method indicates that the deflections computed using the rectangular elements are more accurate than the values obtained using the triangular elements. It was not possible to compare the deflections beyond the elastic range due to lack of a suitable classical solution.

Complete load-deflection curves from zero load until the maximum load (failure load) obtained using both the triangular and the rectangular elements, are shown in Figure 6.5.
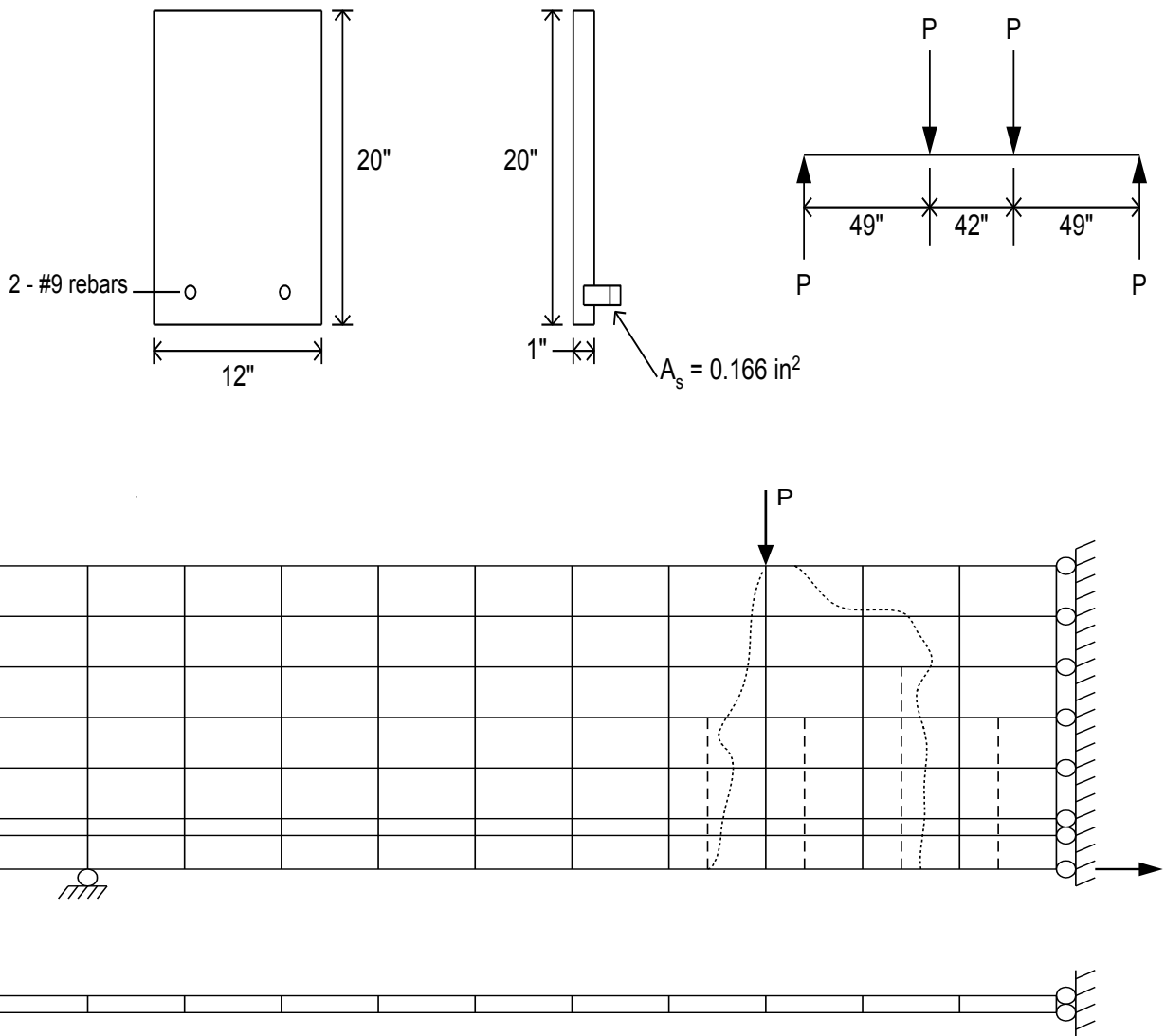
Figure 6.4 - Beam bending – initial idealization
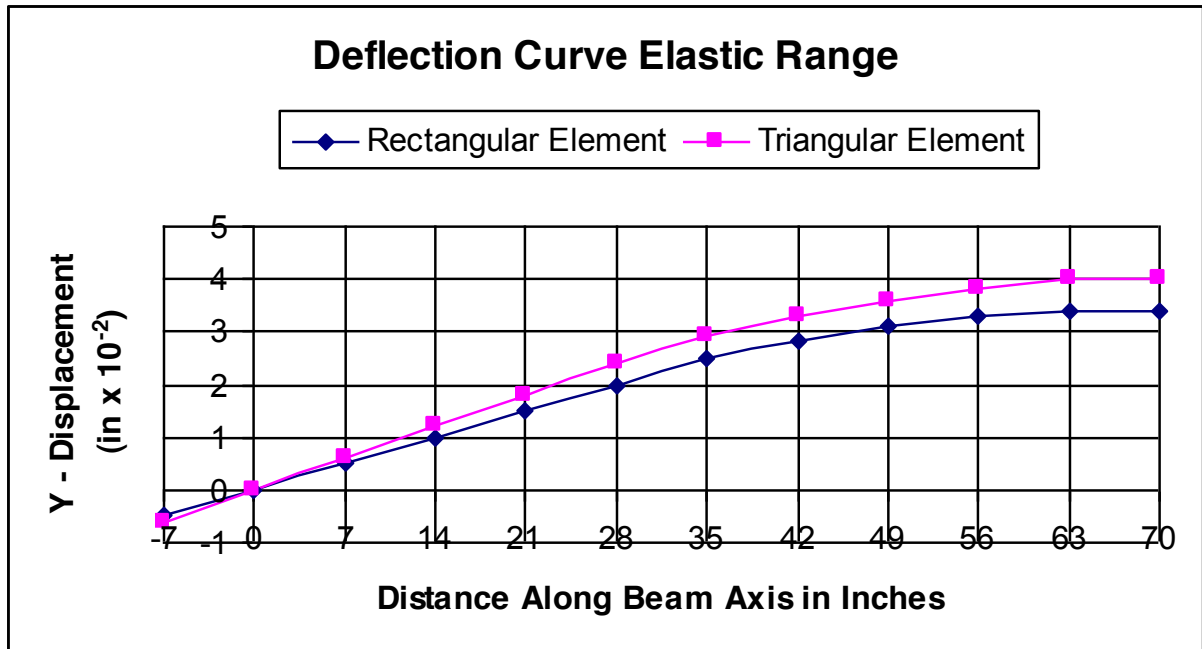
Figure 6.5 - Deflection curve elastic range

The ultimate strength of the beam was calculated using the ACI Code (318-16) and the value of each concentrated load was noted to be 2100 lb. at failure (ACI 318-16). The value of each concentrated load at failure, computed using the rectangular and the triangular elements, was 2090 lb. and 2300 lb. respectively, indicating the improved accuracy obtained using the rectangular elements.

The first load increment for the finite element analysis was taken as 1190 lb. This load level was selected to ensure that the principal tensile stresses at all element centroids were less than or at best equal to the cracking tensile strength of the concrete; this condition must also be satisfied to obtain better accuracy beyond the initial cracking stage. The first element cracks at a load of 1190 lb. Beyond this initial cracking load, the applied loads are increased in increments of 100 lb.

each until failure for computer analysis. The stresses in the concrete and the steel elements, and the bond spring forces are indicated in plots in the reference. These plots give a complete study of the stresses from the initial cracking load to the ultimate load and clearly indicate the redistribution of the stresses and the bond spring forces at the appearance of a crack or the failure of a bond spring.

6.3.3   *Curved-Beam Analysis*

Three reinforced, simply supported concrete curved-beams with the dimensions shown in Figure 6.6 were loaded symmetrically under the six-point loading condition shown in Figure 6.7. The testing results from the experiments were compared with the finite element method using a non-linear analysis program FEM-RC.
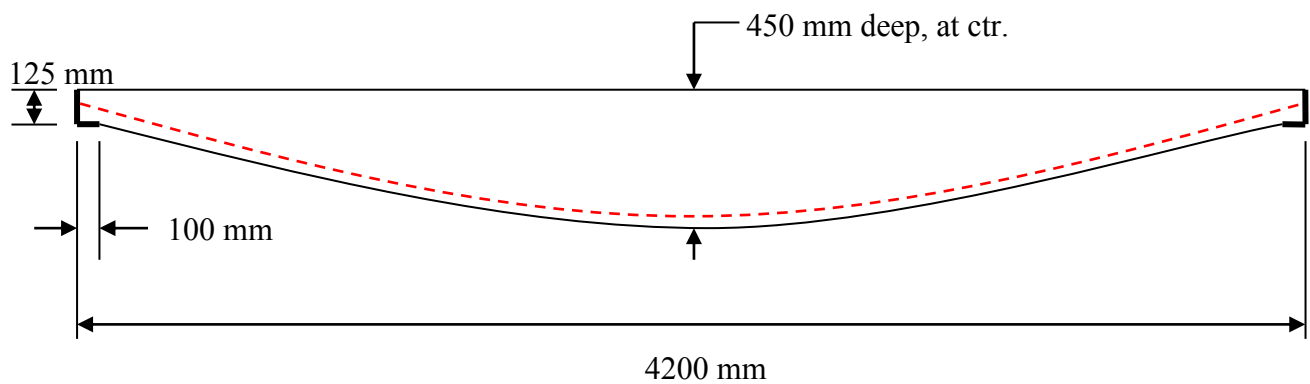
Figure 6.6 –Overall dimensions of concrete curved beam
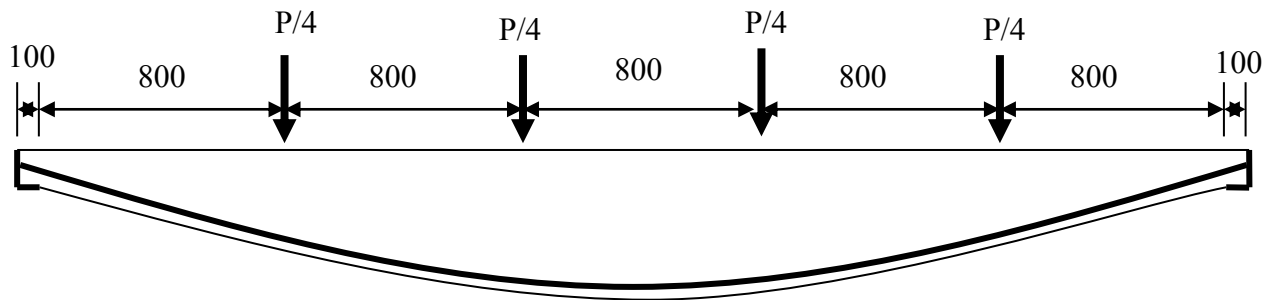
Figure 6.7 - Six point loading configuration

Beams were analyzed using triangular elements. Overall idealization of the beams is shown in Figure 6.8, and Figure 6.9 shows the details of the

idealization at the end of the beam. The idealization of these beams was drawn using AutoCAD to allow greater accuracy in determining the coordinates of the nodes. Rectangular elements provide a more accurate result when analyzing stresses that are uniformly distributed over the length of the element. The beams in this study were analyzed using triangular elements because they provide most accurate geometric representation for modelling beams with a curvature. Quadrilateral elements should be developed and incorporated into the program for idealizing irregular shape members.
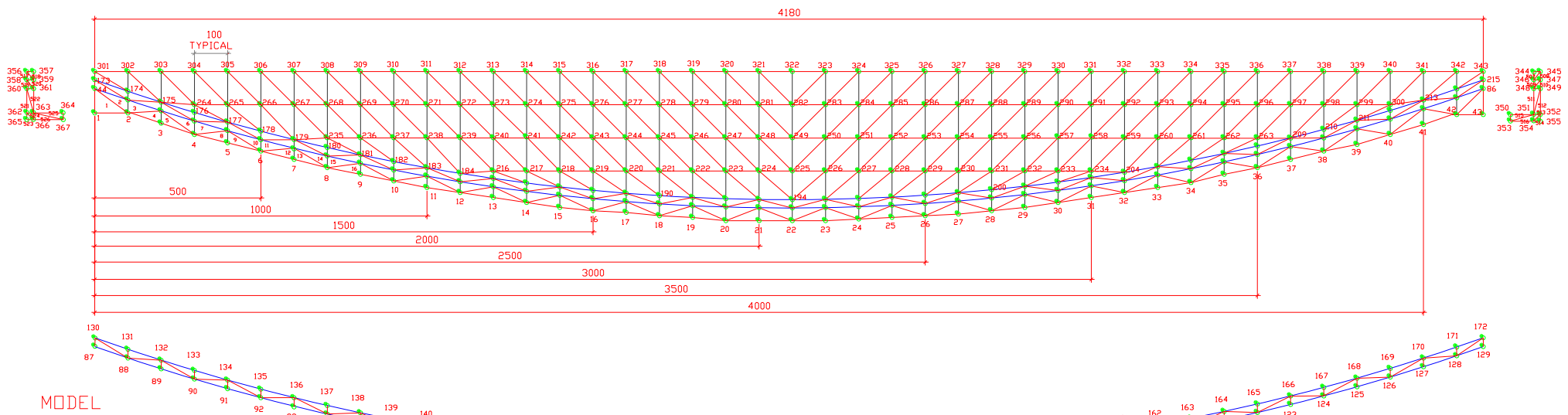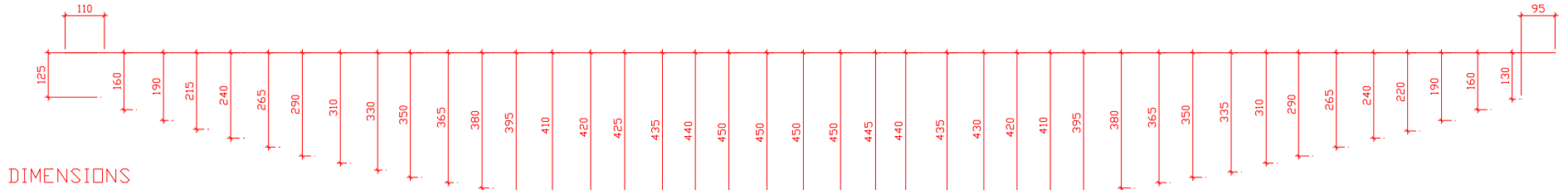
Figure 6.8 - Idealized beam for FEM analysis

224
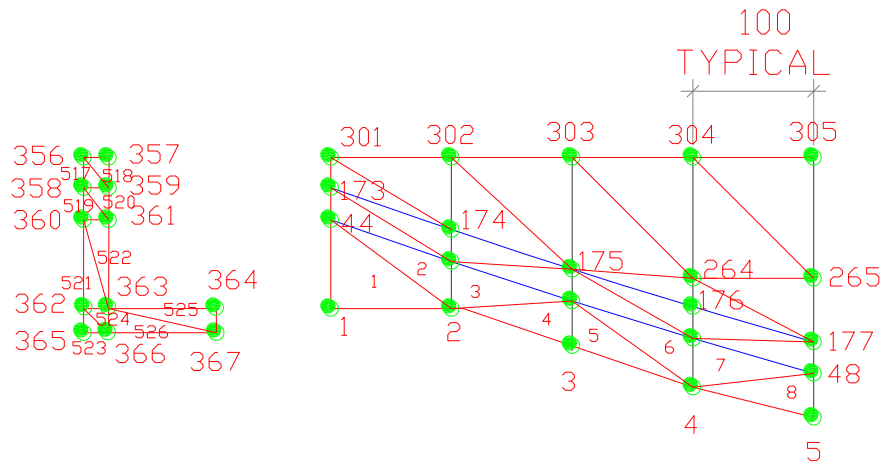
Figure 6.9 - Detail idealization of the support

The idealized beam consisted of 367 nodes, 526 elements and 172 spring elements. An Excel spreadsheet was used to set up the nodal coordinates and nodal connection to determine each element. In case there is a problem with the large number of nodes and elements, it is very beneficial to set up a spreadsheet for the input file. The spreadsheet would allow faster input file setup and facilitates more efficient debugging of the input file.

For FEM analysis one beam was idealized and analyzed then compared with the three experimental beams. The FEM beam was analyzed from 1450 lb (6.4 kN) at each loading point. The total starting load would be 5800 lb (25.8 kN). The starting load was determined by several iterations to identify the exact load at which the principal tensile stress of at least one of the element's centroids was equal to the cracking tensile strength of the concrete. This is the load that would start the first crack and therefore initiate the nonlinear analysis of the beam. The FEM analysis was performed at 100 lb (0.44 kN) loading increments. The analysis continued for 29 iterations up to the final load of 17760 lb (79 kN) where

all elements at the centre of the beams were cracked and the program stops. The failure loads from the experiments were between 13500 lb (60 kN) to 19000 lb (85 kN) where the beams had deflected excessively. However, the beams reached total failure much later in the test at a slightly higher load. The deflection at the point of total failure was in excess of five inches (125mm).

Figure 6.10 shows the load–deflection curve comparison between the experimental result of CB3 and FEM analysis. The FEM-RC program gives a conservative result prior to cracking which is safe and desirable for design purposes. After cracking the result from the program overestimates the strength of the beams which is not desired for design. The overall deflection predicted by the program closely matches those of the experiments.

A comparison of the load-deflection curve obtained from the FEM program and experimental results for CB3 is presented in Figure 6.11. In this case the FEM program gives conservative answers at all points except for the one point where it predicts higher capacity than actual experiments. See Appendix A for the FINIT-Y program algorithm and the program's output for only the first loading iteration of CB3. The stiffness calculated from the FEM is 9.4 which is in reasonably close agreement with the after cracking stiffness of CB3 (7.3, see Figure 9.1).

Although more research is required, at this point the close proximity of the load-deflection curve and stiffness are the evidence or realistic indications that the FEM program predictions and outputs are reliable. They closely approximate the

actual behaviour of the curved beam; therefore, the results of the FEM analysis will be used to develop the failure theory for curved beams.
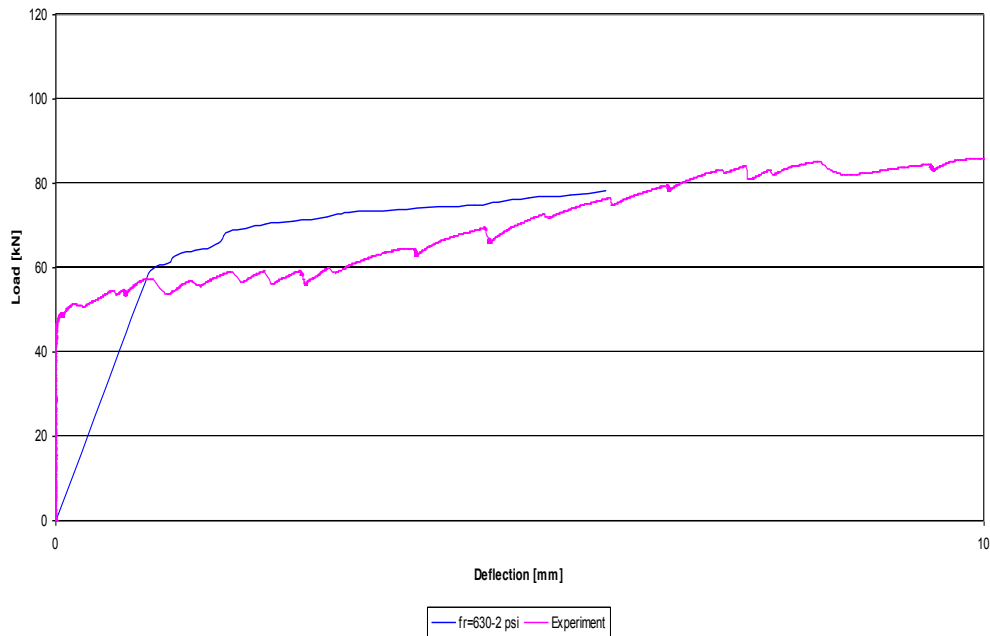
Figure 6.10 - Load-deflection curve comparison for FEM vs. Preliminary beam
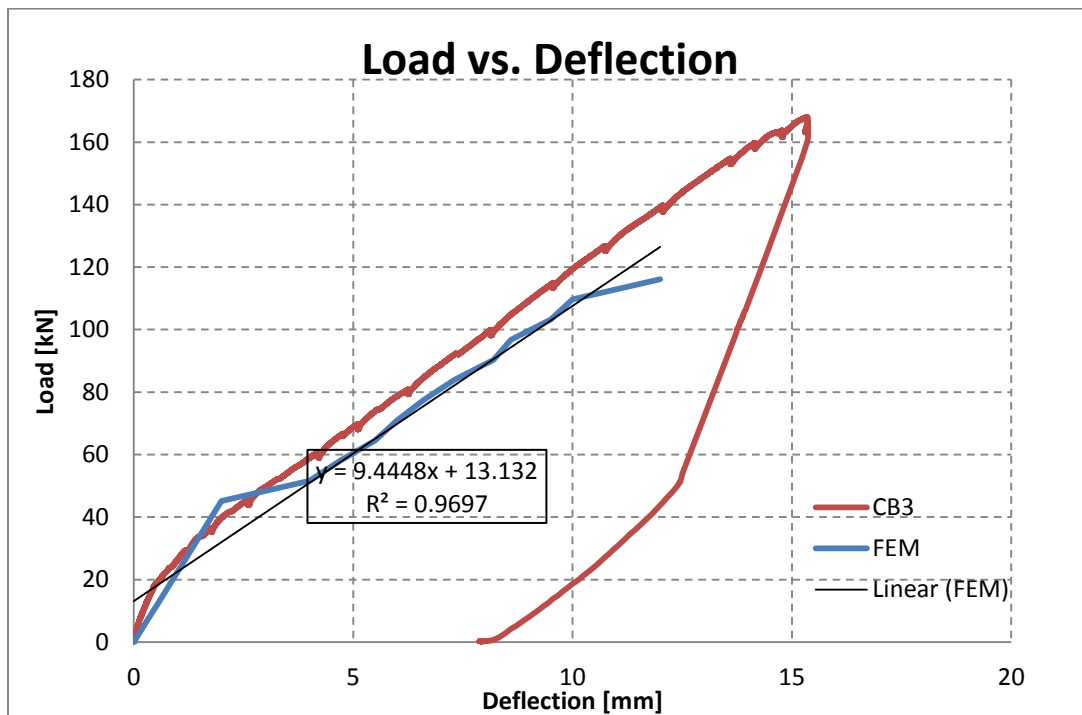
Figure 6.11 - Load-deflection curve comparison for FEM Analysis vs. CB3

227

The reason for the FEM analysis termination at the point shown in Figures 6.10 and 6.11 is that once elements crack in the program they are taken out of the system. When all of the elements along the depth of the beam crack, they create virtual discontinuity in the beam and the program cannot assemble the stiffness matrix after that iteration.

The accuracy of the FEM program has been verified by several examples and it will be used to develop behaviour and failure theories of CCB in this research.

The FEM program final output consists of three items: 1) Nodal displacement in both x and y direction (Table 6.1), 2) principle stresses and the angle of principle stresses for each element (Table 6.2) and the 3) bond stress along the reinforcement (table 6.3). The first iteration of the program output is presented in the Appendix A; herein, are examples of each of the above noted outputs in tabular format given up to the center-span of CCB.

Table 6.1 – Nodal Displacement

Node	X-Disp	Y-Disp	Node	X-Disp	Y-Disp	Node	X-Disp	Y-Disp
1	0.003364	0.000000	2	0.003021	0.000000	3	0.022892	-0.001455
4	0.001761	-0.003038	5	0.001370	-0.004668	6	0.001039	-0.006279
7	0.000783	-0.007801	8	0.000568	-0.009242	9	0.000488	-0.010551
10	0.000433	-0.011749	11	0.000425	-0.012799	12	0.000467	-0.013751
13	0.000532	-0.014574	14	0.000592	-0.015313	15	0.000663	-0.015941
16	0.000763	-0.016496	17	0.000905	-0.016948	18	0.001031	-0.017324
19	0.001179	-0.017593	20	0.001308	-0.017791	21	0.001452	-0.017901
22	0.001600	-0.017950						

Table 6.2 – Element Stresses

Element	CENTROID		CARTESIAN STRESSES			PRINCIPAL STRESSES		PRINCIPAL	CARTESIAN STRAINS			PRINCIPAL STRAINS		YM
NO.	X-CORD	Y-CORD	X	Y	XY	STRESS 1	STRESS 2	ANG	ε_X	ε_Y	ε_{XY}	ε_1	ε_2	
1	1.31	13.45	-252.09	441.18	125.4	463.17	-274.08	80	-8.69E-05	1.26E-04	7.69E-05	1.32E-04	-9.36E-05	3916019
2	2.63	13.98	-77.28	-284.95	235.71	76.45	-438.68	33	-5.18E-06	-6.88E-05	1.44E-04	4.19E-05	-1.16E-04	3916019
3	5.25	13.39	-222.15	-313.93	-200.46	-62.39	-473.68	51	-4.07E-05	-6.88E-05	-1.23E-04	8.26E-06	-1.18E-04	3916019
4	6.56	12.4	-189.97	-8.66	42.39	0.76	-199.39	77	-4.81E-05	7.49E-06	2.60E-05	1.04E-05	-5.10E-05	3916019
5	9.18	11.55	-60.07	17.32	-9.51	18.47	-61.23	7	-1.62E-05	7.49E-06	-5.83E-06	7.84E-06	-1.66E-05	3916019
6	10.5	11.68	-35.1	1	1.15	1.04	-35.14	88	-9.02E-06	2.05E-06	7.04E-07	2.06E-06	-9.03E-06	3916019
7	13.12	10.96	2.81	8.58	-16.66	22.61	-11.21	40	2.80E-07	2.05E-06	-1.02E-05	6.35E-06	-4.02E-06	3916019
8	14.44	10.11	3.46	-2.42	-23.88	24.58	-23.54	49	1.01E-06	-7.95E-07	-1.46E-05	7.48E-06	-7.27E-06	3916019
9	17.06	9.45	62.53	9.39	-16.23	67.1	4.83	74	1.55E-05	-7.95E-07	-9.95E-06	1.69E-05	-2.19E-06	3916019
10	18.38	9.65	29.96	7.65	-35.61	56.12	-18.51	54	7.26E-06	4.23E-07	-2.18E-05	1.53E-05	-7.59E-06	3916019
11	21	8.99	80.46	17.75	-4.88	80.84	17.37	86	1.96E-05	4.23E-07	-2.99E-06	1.98E-05	3.07E-07	3916019
12	22.31	8.14	94.79	-1.82	-54.12	119.03	-26.06	66	2.43E-05	-5.31E-06	-3.32E-05	3.17E-05	-1.27E-05	3916019
13	24.93	7.48	134.13	6.04	-18.98	136.88	3.29	82	3.39E-05	-5.31E-06	-1.16E-05	3.48E-05	-6.15E-06	3916019
14	26.25	7.68	79.75	10.05	-50.33	106.12	-16.32	62	1.99E-05	-1.51E-06	-3.08E-05	2.79E-05	-9.59E-06	3916019
15	28.87	7.09	128.47	19.8	-2.63	128.53	19.73	89	3.18E-05	-1.51E-06	-1.61E-06	3.18E-05	-1.53E-06	3916019
16	30.19	6.3	152.79	-3.76	-60.59	173.5	-24.47	71	3.92E-05	-8.76E-06	-3.71E-05	4.56E-05	-1.51E-05	3916019
17	32.81	5.77	178.62	1.4	-16.26	180.1	-0.08	85	4.55E-05	-8.76E-06	-9.97E-06	4.60E-05	-9.22E-06	3916019
18	34.12	6.04	118.32	9.12	-54.03	140.53	-13.09	68	2.97E-05	-3.71E-06	-3.31E-05	3.66E-05	-1.05E-05	3916019
19	36.74	5.51	151.79	15.81	1.61	151.81	15.79	1	3.80E-05	-3.71E-06	9.84E-07	3.80E-05	-3.72E-06	3916019
20	38.06	4.72	175.05	-2.74	-52.5	189.4	-17.09	75	4.48E-05	-9.64E-06	-3.22E-05	4.92E-05	-1.40E-05	3916019
21	40.68	4.27	179.61	-1.83	-10.87	180.26	-2.48	87	4.60E-05	-9.64E-06	-6.66E-06	4.62E-05	-9.84E-06	3916019
22	42	4.59	134	7.92	-42.7	147.11	-5.18	73	3.38E-05	-4.82E-06	-2.62E-05	3.78E-05	-8.84E-06	3916019
23	44.62	4.2	146.65	10.45	3.52	146.74	10.36	1	3.69E-05	-4.82E-06	2.16E-06	3.69E-05	-4.85E-06	3916019

Element	CENTROID		CARTESIAN STRESSES			PRINCIPAL STRESSES		PRINCIPAL	CARTESIAN STRAIN			PRINCIPAL STRAINS		YM
NO.	X-CORD	Y-CORD	X	Y	XY	STRESS 1	STRESS 2	ANG	ε_X	ε_Y	ε_{XY}	ε_1	ε_2	
24	45.93	3.48	172.5	-2.89	-42.2	182.12	-12.51	77	4.42E-05	-9.55E-06	-2.59E-05	4.71E-05	-1.25E-05	3916019
25	48.55	3.09	167.36	-3.91	-6.76	167.63	-4.18	88	4.29E-05	-9.55E-06	-4.14E-06	4.30E-05	-9.63E-06	3916019
26	49.87	3.41	124.23	7.22	-36.73	134.8	-3.35	74	3.14E-05	-4.50E-06	-2.25E-05	3.46E-05	-7.74E-06	3916019
27	52.49	3.02	132.79	8.93	3.23	132.87	8.85	1	3.35E-05	-4.50E-06	1.98E-06	3.35E-05	-4.53E-06	3916019
28	53.81	2.3	153.87	-3.27	-34.47	161.09	-10.5	78	3.95E-05	-8.69E-06	-2.11E-05	4.17E-05	-1.09E-05	3916019
29	56.43	1.97	152.62	-3.52	-3.57	152.7	-3.6	89	3.92E-05	-8.69E-06	-2.19E-06	3.92E-05	-8.72E-06	3916019
30	57.75	2.36	119.82	5.17	-29.17	126.82	-1.82	77	3.03E-05	-4.80E-06	-1.79E-05	3.25E-05	-6.94E-06	3916019
31	60.37	2.17	129.74	7.15	7.88	130.25	6.65	4	3.28E-05	-4.80E-06	4.83E-06	3.29E-05	-4.95E-06	3916019
32	61.68	1.57	159.76	-5.88	-28.05	164.39	-10.5	81	4.11E-05	-9.66E-06	-1.72E-05	4.25E-05	-1.11E-05	3916019
33	64.3	1.38	162.04	-5.42	2.92	162.09	-5.47	1	4.17E-05	-9.66E-06	1.79E-06	4.17E-05	-9.68E-06	3916019
34	65.62	1.77	122.62	5.86	-27.83	128.91	-0.43	77	3.10E-05	-4.77E-06	-1.71E-05	3.29E-05	-6.69E-06	3916019
35	68.24	1.58	128.22	6.98	11.1	129.23	5.97	5	3.24E-05	-4.77E-06	6.81E-06	3.27E-05	-5.08E-06	3916019
36	69.56	0.98	157.25	-4.4	-23.63	160.63	-7.78	82	4.04E-05	-9.15E-06	-1.45E-05	4.14E-05	-1.02E-05	3916019
37	72.18	0.79	148.13	-6.22	4.66	148.27	-6.36	2	3.81E-05	-9.15E-06	2.85E-06	3.82E-05	-9.20E-06	3916019
38	73.49	1.18	115.84	4.51	-20.39	119.46	0.9	80	2.94E-05	-4.76E-06	-1.25E-05	3.05E-05	-5.87E-06	3916019
39	76.11	1.05	117.51	4.85	11.47	118.67	3.69	6	2.98E-05	-4.76E-06	7.03E-06	3.01E-05	-5.12E-06	3916019
40	77.43	0.52	141.81	-5.51	-13.59	143.06	-6.76	85	3.65E-05	-8.65E-06	-8.33E-06	3.69E-05	-9.03E-06	3916019
41	80.05	0.52	146.61	-4.55	11.68	147.5	-5.45	4	3.77E-05	-8.65E-06	7.16E-06	3.79E-05	-8.93E-06	3916019
42	81.37	1.05	118.47	4.21	-17.19	121	1.68	82	3.00E-05	-4.98E-06	-1.05E-05	3.08E-05	-5.75E-06	3916019

Table 6.3 – Bond stress and forces

ELEMENT	BOND STRESS	STRESS/LTH	BOND FORCE	FORCE/LTH	SLIP
1	58.532	29.7117	362.2515	183.884	0.00001664
2	204.9269	104.0238	1268.2829	643.7984	0.00006250
3	18.0032	4.5693	222.8418	56.5588	0.00000503
4	-115.638	-29.3497	-1431.3557	-363.2883	0.00003374
5	-24.369	-6.185	-301.6368	-76.5576	0.00000683
6	-1.3031	-0.3307	-16.1299	-4.0939	0.00000036
7	-6.9136	-1.7547	-85.5755	-21.7197	0.00000192
8	4.9571	1.2581	61.3579	15.5731	0.00000138
9	-4.5977	-1.1669	-56.9099	-14.4441	0.00000128
10	2.9379	0.7457	36.3656	9.2298	0.00000082
11	-5.813	-1.4754	-71.9531	-18.2622	0.00000162
12	1.7144	0.4351	21.2204	5.3859	0.00000048
13	-0.3451	-0.0876	-4.2714	-1.0841	0.00000010
14	3.3391	0.8475	41.3312	10.4902	0.00000093
15	-4.4741	-1.1356	-55.3805	-14.056	0.00000124
16	2.5397	0.6446	31.4359	7.9786	0.00000071
17	0.7013	0.178	8.6808	2.2033	0.00000019
18	4.2827	1.087	53.0105	13.4544	0.00000119
19	-1.5376	-0.3903	-19.0328	-4.8307	0.00000043
20	2.8848	0.7322	35.7074	9.0628	0.00000080
21	2.4595	0.6242	30.4438	7.7268	0.00000068
22	4.4728	1.1352	55.3637	14.0517	0.00000124
23	-0.5095	-0.1293	-6.306	-1.6005	0.00000014
24	2.9706	0.754	36.7695	9.3324	0.00000082
25	2.5365	0.6438	31.3965	7.9687	0.00000070
26	4.0614	1.0308	50.2712	12.7592	0.00000113
27	0.4551	0.1155	5.6336	1.4299	0.00000013
28	2.8644	0.727	35.4555	8.9989	0.00000080
29	1.5825	0.4016	19.5875	4.9714	0.00000044
30	4.0238	1.0213	49.8062	12.6412	0.00000112
31	-1.2571	-0.3191	-15.56	-3.9492	0.00000035
32	2.8913	0.7338	35.7877	9.0832	0.00000080
33	0.6747	0.1712	8.351	2.1195	0.00000019
34	4.0397	1.0253	50.0024	12.691	0.00000112
35	0.077	0.0195	0.953	0.2419	0.00000002
36	2.5987	0.6596	32.1663	8.164	0.00000072
37	1.9178	0.4867	23.7378	6.0248	0.00000053
38	3.8092	0.9668	47.1496	11.9669	0.00000106
39	0.6776	0.172	8.3874	2.1288	0.00000019
40	2.9551	0.75	36.5778	9.2837	0.00000082
41	-0.5238	-0.133	-6.4841	-1.6457	0.00000015
42	3.7961	0.9635	46.9875	11.9258	0.00000105

The principle stresses in each element and the angle of the principal stresses with the global coordinates system are highlighted in bold in Table 6.3. Chapter 1, Section 1.2). The principal stresses and their direction can be plotted on each element to show the overall direction of stresses in the beam. In the case of curved beams, CB and CCB, the failure occurs at one of the support ends. Figure 6.12 shows the approximate directions of the principal stresses in each element in one end of CCB. For a detailed result of the analysis see Appendix A. In Figure 6.12 the principal stresses in each element are plotted as an arrow and the direction of the stress is approximated from the global coordinate system shown at the bottom of the drawing and at the centre of gravity of each element. The drawing element mesh in Figure 6.12 is to ¼-scale, but the stress arrows are not to scale and are representative only. The FEM shows that near the failure the compression stress in the concrete elements change direction from an average of -200º (actual is from -190º to -210º) to an average of -255º (actual is from -240º to -270º) at 200mm (~effective depth) away from the support. FEM analysis shows that the tension stress is confined within the reinforcement, and it is confirmed to be constant along the reinforcement. One of the principle stresses in the reinforcement elements is parallel to the reinforcement and the other is perpendicular to the reinforcement. All horizontal spring elements broke which means that the concrete cover is only attached to the reinforcement and not contributing to the resistant; this is consistent with after cracking behaviour of RC beams.
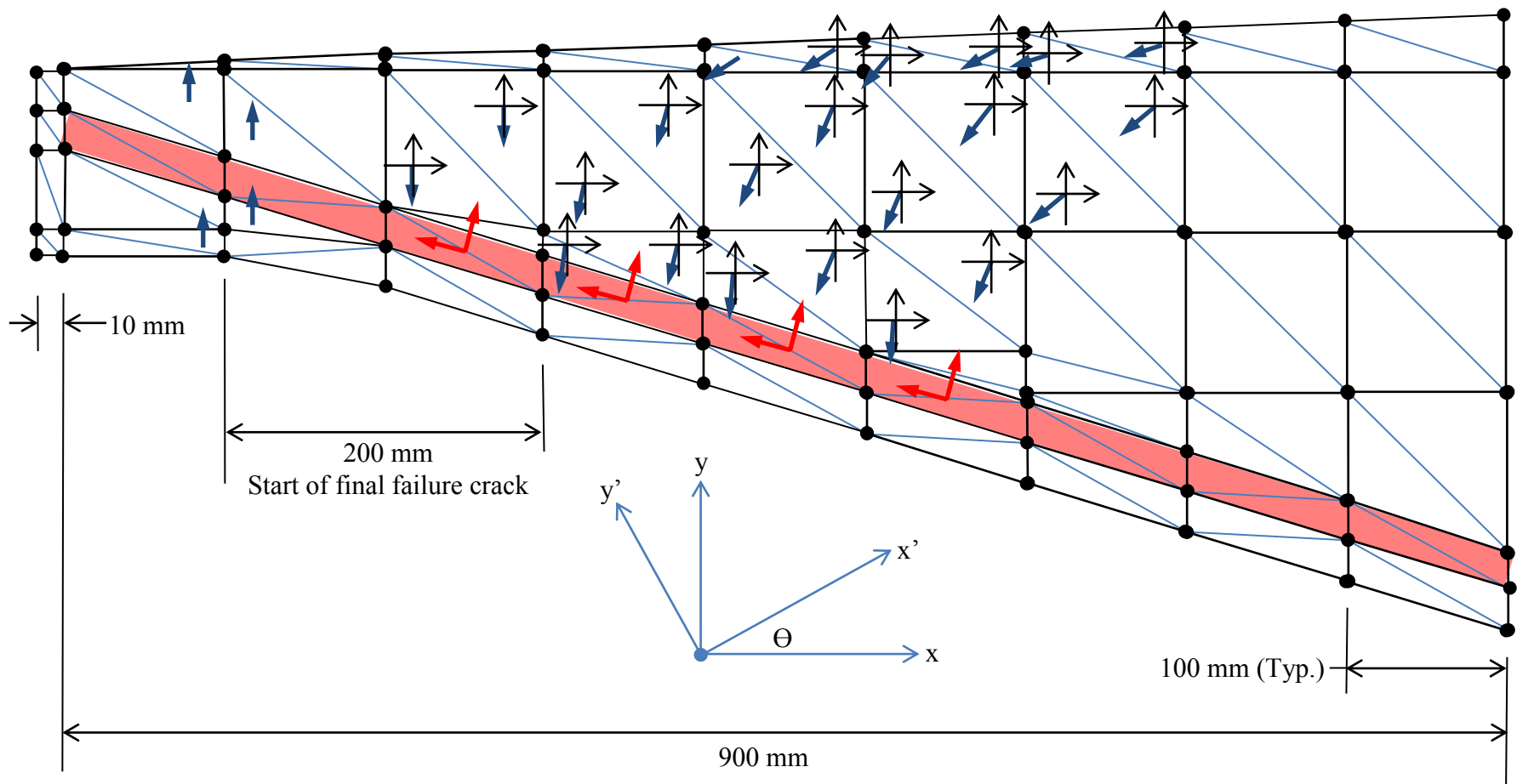
Figure 6.12 – CCB elemental stress distribution prior to cracking (Scale = ¼ for elements, forces not to scale)

233
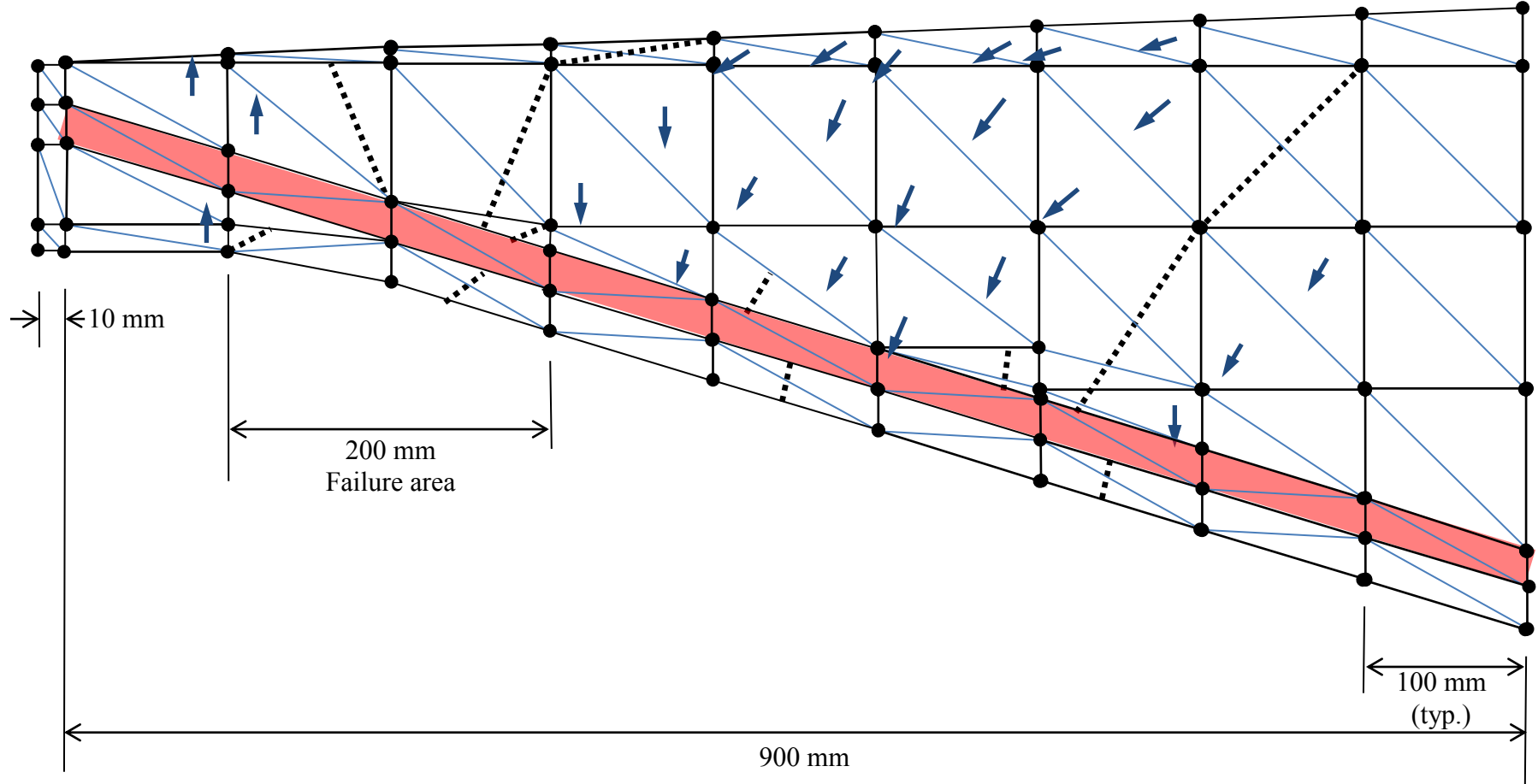
Figure 6.13 – CCB elemental stress distribution after cracking and at failure

234

Based on the above result from the FEM analysis, the direct shear mode of failure has been offered. It was explained in Chapter 5 and will be further discussed in Chapter 9.

The stress result from the FEM analysis closely matched the experimental results of curved beams CB and CCB. Figure 6.14 shows the tension force along the reinforcement in CB3 and CCB1 and compares them to the result from the FEM analysis. FEM analysis shows that the tension force remains approximately constant along the reinforcement. The curves representing the results from the experiments show that the tension force goes to zero after the last strain gauge. This occurred because there was too few strain gauges placed within the end areas of the beam. The FEM analysis shows that the strain and therefore, stress does not approache zero at these locations.
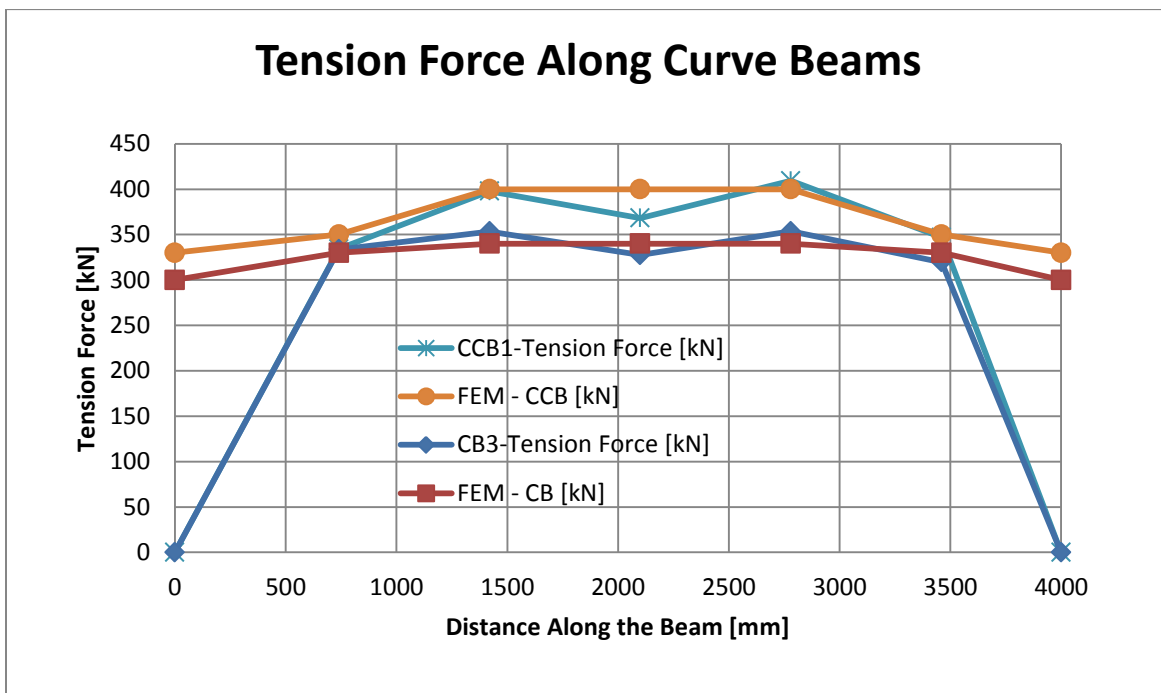
Figure 6.14 – Tension force along the reinforcement, experimental vs. FEM analysis

6.3.4 Corbel Analysis Using Quadrilateral Elements

In 2008 the FEM-RC program was further modified to analyse quadrilateral elements (Isoparametric Type). A quadrilateral element has been shown in Figure 6.15.
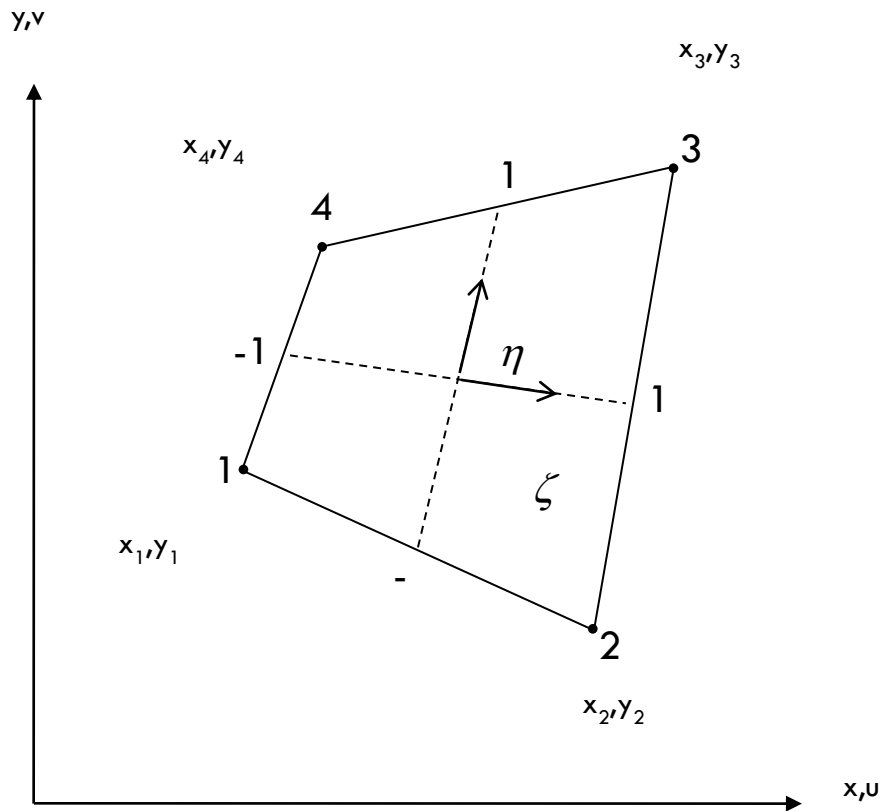
Figure 6.15 – Quadrilateral Element

The stiffness matrix was assembled as given:

$$K = t \int_{-1}^{1} \int_{-1}^{1} [B]^T \bullet [D] \bullet [B] \bullet |J| \partial \zeta \partial \eta$$

Where:
t = Thickness of the element
[B] = Strain matrix
[B]^t = Transposed strain matrix
[D] = Elasticity matrix
J = Jacobian matrix
(Note: see Appendix A for detailed matrix assembly)

In this example, a modified version of the FEM-RC program will be used to analyze an eccentrically loaded precast corbel. The analysis will be conducted for both triangular elements and quadrilateral elements followed by a comparison of the two analyses. Figure 6.16 shows the corbel modeled with triangular elements both in elevation and cross-section. Figure 6.17 shows the same corbel modeled using quadrilateral elements. The reinforcing consists of 4-15M bars at the top face of the corbel and the total area of reinforcing steel in this example is 800 mm^2. The load is applied at the end of the corbel for these analyses. Figure 6.18 and Figure 6.20 show the stress distribution in the corbel analysed using triangular elements while Figure 6.19 and Figure 6.21 show the quadrilateral elements.

The result shows that the modified FEM-RC program was successful in performing a non-linear analysis of reinforced concrete structures using Isoperimetric Elements. The results obtained from the program are compatible with those obtained from the triangular elements programs. Furthermore, similar crack patterns were observed using both types of elements during the analyses.
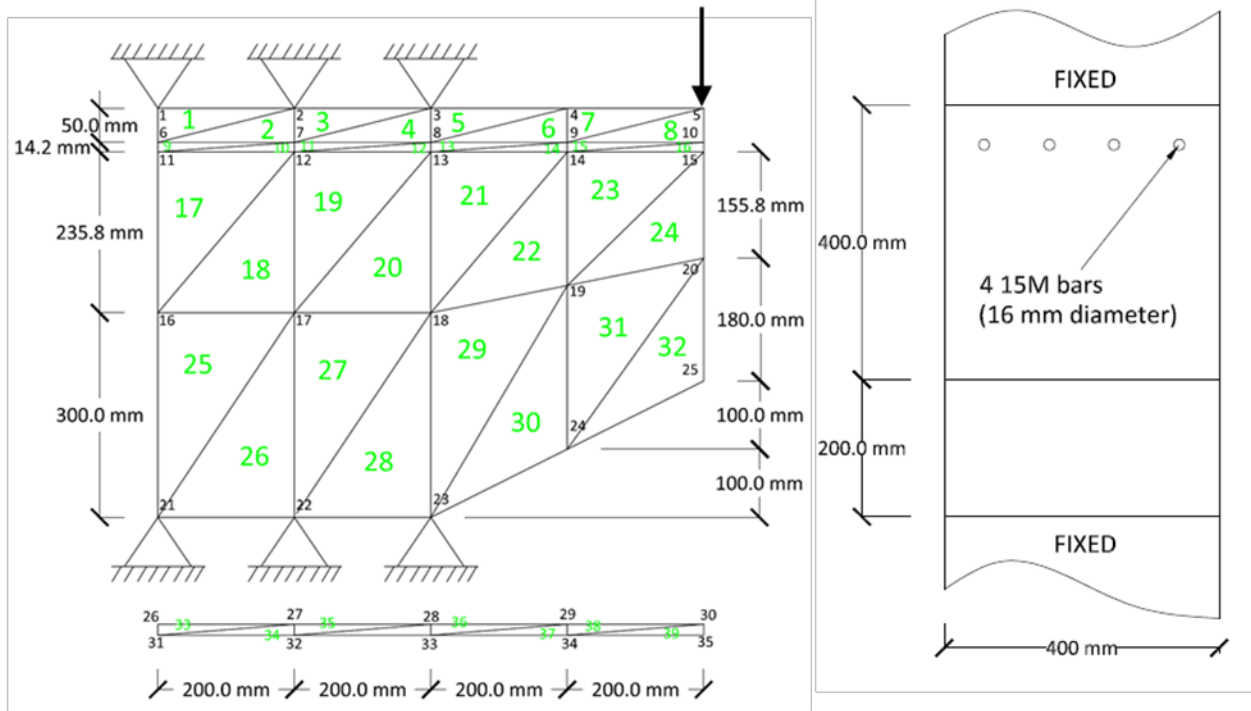
Figure 6.16 – Corbel modeled using triangular elements
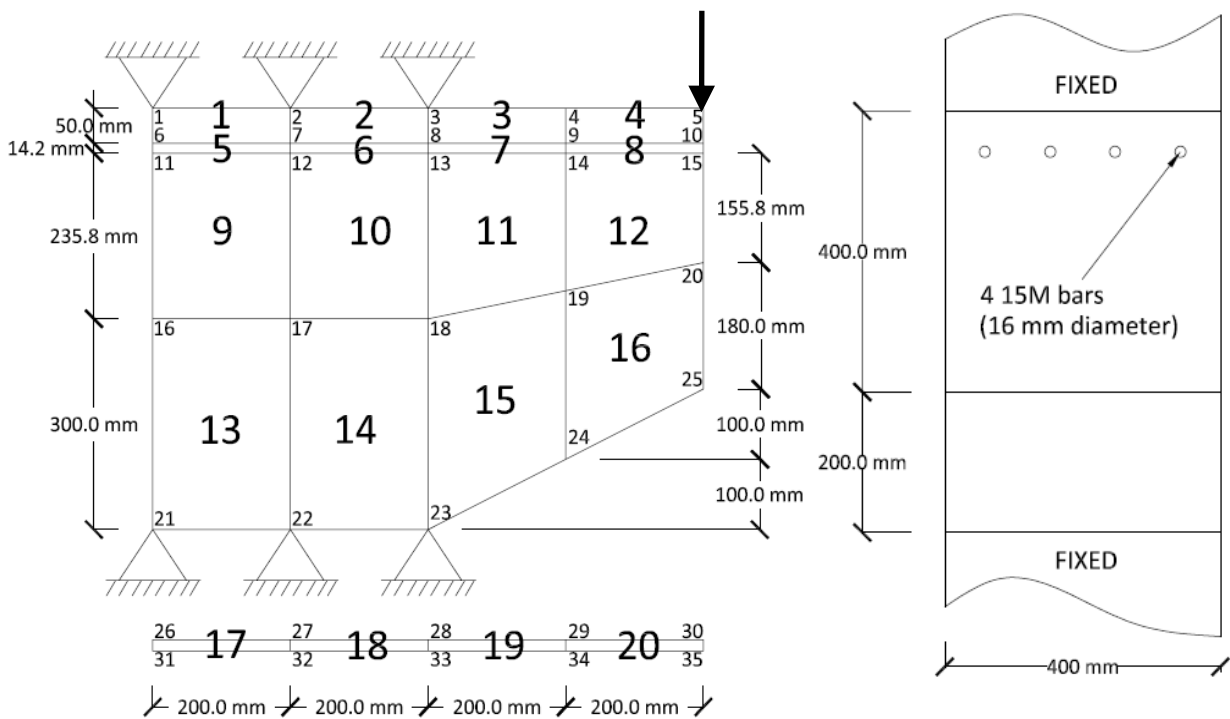
Figure 6.17 – Corbel modeled using quadrilateral elements

238
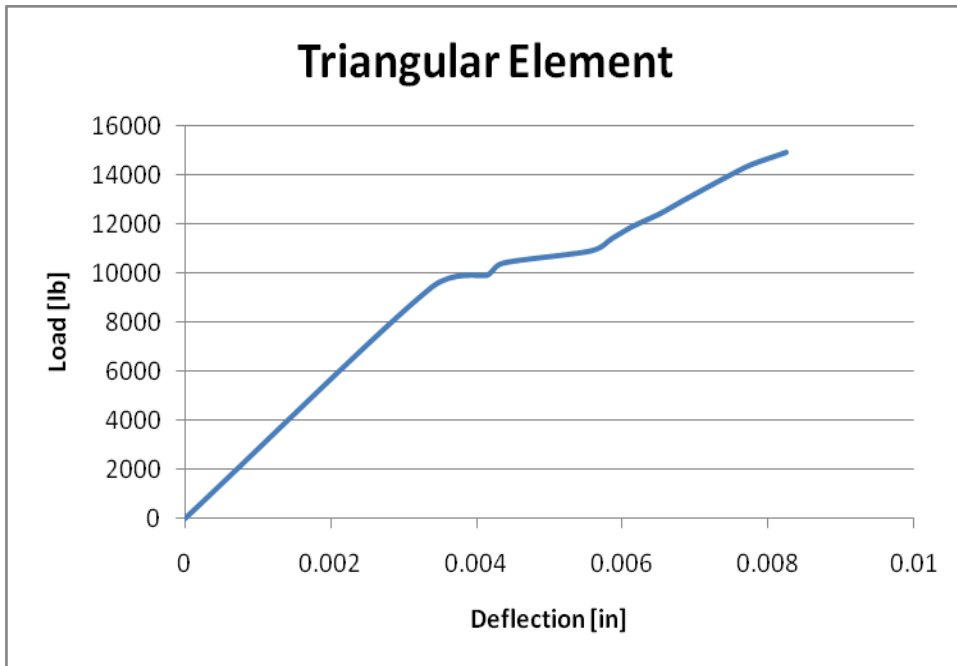
Figure 6.18 – Load-Deflection curve using triangular elements
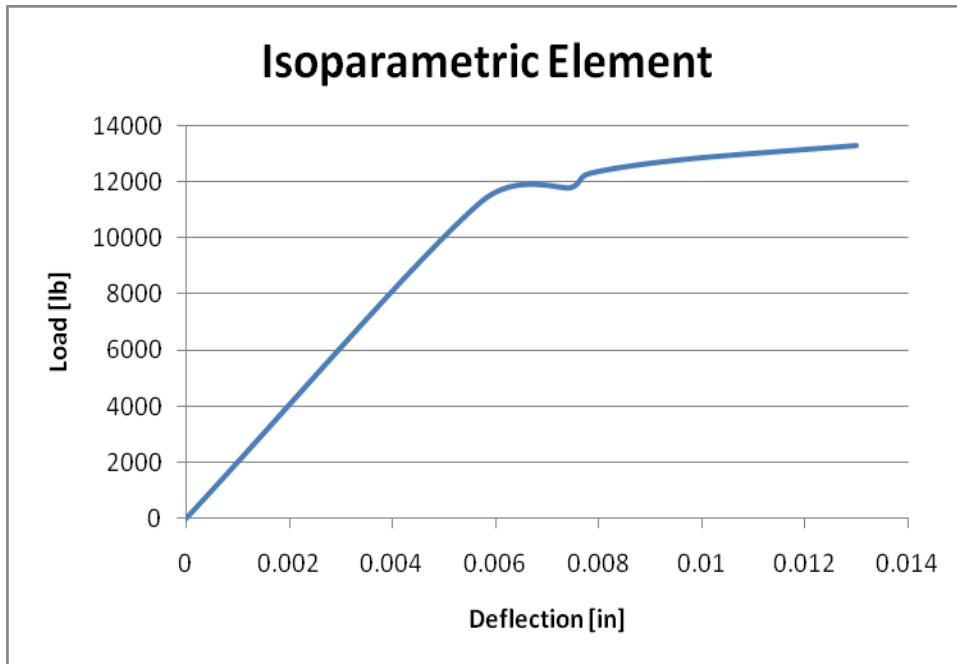
Figure 6.19 – Load-Deflection curve using quadrilateral elements
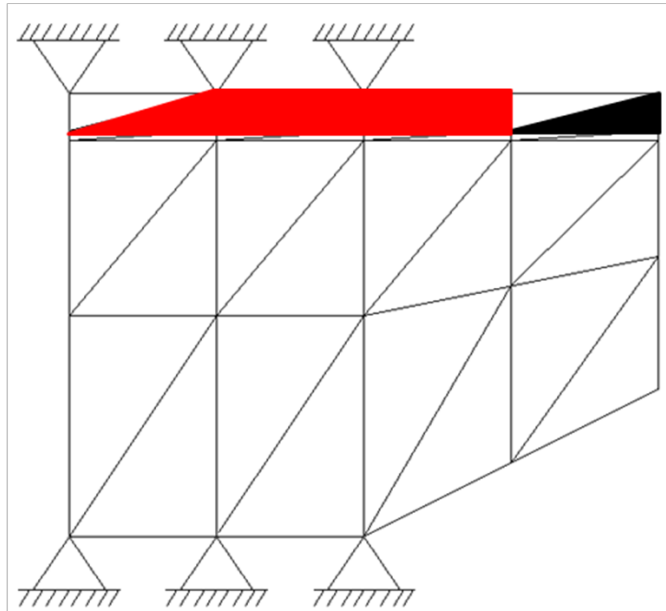
Figure 6.20 – Stress distribution in the corbel using triangular elements
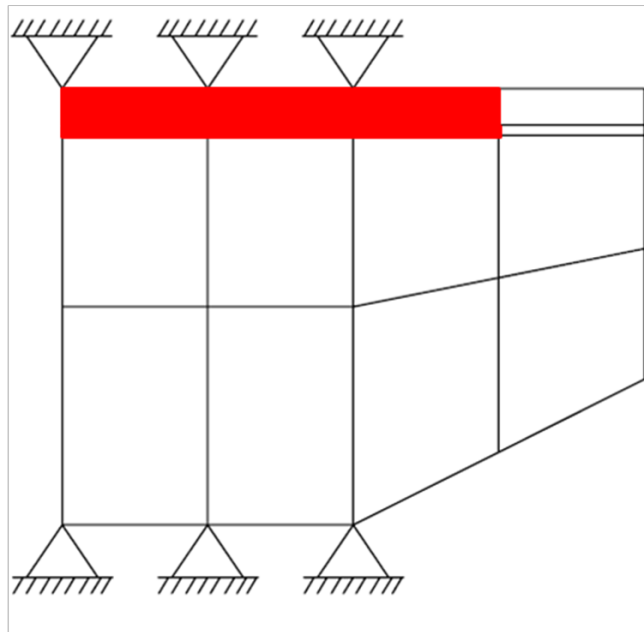
Figure 6.21 – Stress distribution in the corbel using quadrilateral elements

6.3.5 FEM-RC Capacity Increase

Table 6-4 shows the changes in the FEM-RC over the years. The increase in parameters shown in this table allows the program to handle larger problems and/or more defined idealization. More defined idealization means that for a same member, more and therefore smaller elements can be used to idealize the member which will result in more accurate results. Appendix A shows the explanation and the order of the parameter input file.

Table 6.4 – FEM-RC Capacity

No.	Parameter	*Original Program* *(1967)*	*New Version* *(2007)*
1	Nodes	325	1500
2	Triangular Elements	450	2000
3	Spring Elements	120	800
4	Nodal Point Boundary Condition	20	100
5	Partitions	15	15
6	Stirrups	40	200
7	Nodal Loads	5	20
8	Nodes in One Partition	35	500

6.4   Conclusion and Recommendations

The results of this investigation indicate that it is more accurate to use the rectangular elements for the non-linear analysis of a reinforced concrete structure than to use the triangular elements.   Nevertheless, this has the drawback that it cannot reproduce the width of the crack, a characteristic which has not yet been incorporated in the program. The present program does, however, incorporate four nodes to an element and it is therefore convenient to use the general quadrilateral element of Zienkiewicz (Isoparametric type). It has an added advantage that the rectangular element is a special case when all four angles are right angles. The next step shall be to modify the program to produce crack widths accurately.

For this research triangular elements were used to better model the curved beams. The program closely predicted the behaviour and the crack pattern of curved beams.

END OF SECTION

7 *Code Directed Analysis*

The purpose of the numerical analysis shown in this chapter is to suggest a possible simplified design method for future design.

Since CBs and CCBs have never been designed for construction, there are no design criteria or methodology available for their design. The purpose of this research was to understand the behaviour of moment-shaped beams so the majority of numerical analyses were conducted using the FEM analysis discussed in detail in Chapter 6. Traditional code-directed numerical analysis was thus not utilized, except on a very basic level.

For the non-FEM analysis, a series of interactive Excel spreadsheets were developed to design both the rectangular beam and the moment-shaped curved beams. The following sections show sample calculations from each of these spreadsheets (a digital copy of these spreadsheets is attached on a disc).

7.1   Rectangular Beam Design

All rectangular beams were designed using CSA A23.3 Concrete Design Code. As such these calculations were clear cut, using basic accepted design principals. The program is written so that each parameter can be changed. The following are the calculations for this design:

Design of rectangular beams Reinforced with STEEL

Entre data in the yellow cells			
Concrete:			
f_c = 55 MPa			
Φ_c = 1			
α_1 = 0.77	(>= 0.67)		
β_1 = 0.83	(>= 0.67)		
λ = 1			
Analysis: Simply supported			
UDL		**CL**	
w = 70 kN/m		P = 139 kN	
M = 140 kN-m		M = 139 kN-m	
V = 140 kN		V = 70 kN	

Steel:			
		f_y = 400 MPa	
		Φ_s = 1	
	Reinf. Diameter = 30 M		
	No. of bars = 2		
		A_s = 1400 mm^2	
		$A_{s\ min}$ = 334 mm^2	
	Design:		
a = 66 mm			c = 80 mm
M_r = 203 kN-m			c/d = 0.20
	Uniformly Distributed Load w_r = 101 kN/m		
	Concentrated Load P_r = 203 kN		
	(Maximum Shear due to w_r) V = 203 kN		
	(Maximum Shear due to P_r) V = 101 kN		

V at d = **163 kN**

Beam Dimensions:		
Span	L = 4000 mm	
Width	b = 200 mm	
Depth	h = 450 mm	
Conc. Cover	cc = 40 mm	
Eff. Depth	d = 395 mm	
700/(700+f_y) = **0.64**		Tension Failure
Total Load w_r x L = **405 kN**		

Shear Design			
Minimum Shear Reinforcemnt Spacing			
$(V_f - \Phi_p V_p) / (b\,d) =$	2.56		
$0.1 \lambda \quad \Phi_c f'_c =$	5.5		
If "$(V_f - \Phi_p V_p) / (b\,d) < 0.1\lambda \Phi_c f'_c$"			
Lesser of :	**600 mm**	**or**	$0.7\,d =$ **277 mm**
If "$(V_f - \Phi_p V_p) / (b\,d) >= 0.1\lambda \Phi_c f'_c$"			
Lesser of :	**300 mm**	**or**	$0.35\,d =$ **138 mm**

$V_c =$ **109 kN**	(V_c for effective depth greater than 300mm)		
$V_c >$ **59 kN**	(V_c shall not be less than "$0.1\lambda \Phi_c \sqrt{f'_c}\,bd$")		
$0.5\,Vc =$ **55 kN**			
Double leg 10M Stirrups $Av =$ 200 mm^2			
Maximum spacing $S_{max} =$ **899 mm**			

Stirrup spacing to resist the shear force at d from the support:	**163 kN**	
		$s = (\Phi_s A_v f_y d) / (V - Vc)$
		$s =$ **592 mm**

Once the control beam was designed, the other rectangular beams which were made for comparison and as such excluded one of the parameters of the control beam. For example, the comparison beam with no shear reinforcement had exactly the same amount of flexural reinforcement (2-25M Bars) as the control beam but the shear stirrups were omitted to observe and better understand the shear failure.

7.2   Moment-Shaped Curved Beam Design

Since the curved beams have a variable section, the CSA code cannot be used for their design. The design of the curved beams was achieved by using the first principals of concrete design and by running calculations at 100mm intervals along the beam, shown in Table 7.1. The design calculations for the CBs are as follows:

Design of rectangular beams Reinforced with STEEL								
Entre data in the yellow cells								
Concrete:				*Steel:*		*Beam Dimensions:*		
f_c = 70 MPa				fy = 400 MPa		Span L = 4000		
ϕc = 1				ϕs = 1		Width b = 200		
$\alpha 1$ = 0.745	(>= 0.67)			Reinf. Diameter = 30 mm		Depth h = 450		
$\beta 1$ = 0.795	(>= 0.67)			No. of bars = 2		Conc. Cover cc = 38		
λ = 1				A_s = 1400 mm^2		Eff. Depth d = 397		
				$A_{s\ min}$ = 376 mm^2				
	Design:							
a = 54		c = 68						
Mr = 207		c/d = 0.170		700/(700+fy) = 0.636		Tension Failure		

Table 7.1 – Analysis of the beam at 100mm intervals

X [mm]	d [mm]	Eff. Depth	Mr [kN-m]
0	125	72	25
100	125	72	25
200	160	107	45
300	190	137	62
400	215	162	76
500	240	187	90
600	265	212	104
700	290	237	118
800	310	257	129
900	330	277	140
1000	350	297	151
1100	365	312	160
1200	380	327	168
1300	395	342	176
1400	410	357	185
1500	420	367	190
1600	425	372	193
1700	435	382	199
1800	440	387	202
1900	450	397	207
2000	450	397	207
2100	450	397	207
2200	450	397	207
2300	445	392	204
2400	440	387	202
2500	435	382	199
2600	430	377	196
2700	420	367	190
2800	410	357	185
2900	395	342	176
3000	380	327	168
3100	365	312	160
3200	350	297	151
3300	335	282	143
3400	310	257	129
3500	290	237	118
3600	265	212	104
3700	240	187	90
3800	220	167	78
3900	190	137	62
4000	130	77	28
4100	125	72	25
4200	125	72	25

M_1

M_2 (M_{max})
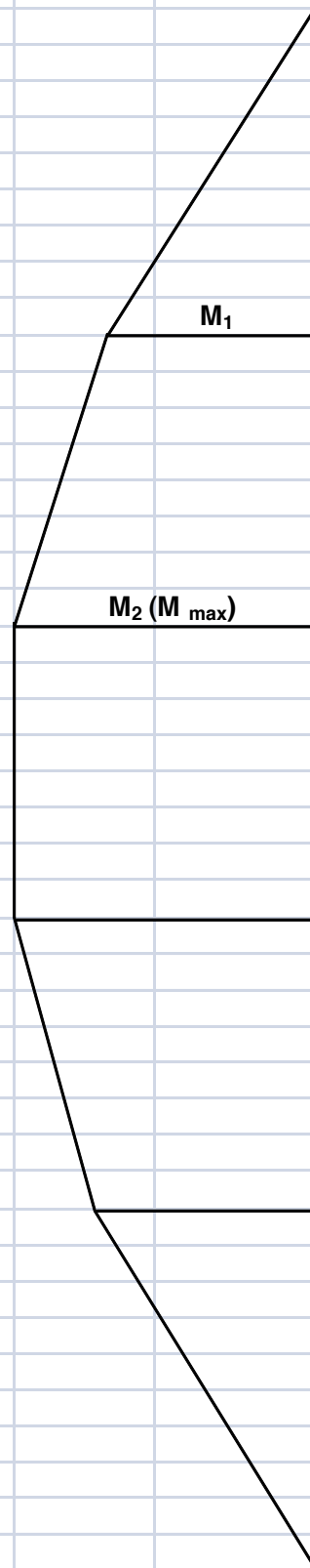
Once the above parameters are given to the program, the spreadsheet will calculate the capacity at 100mm intervals. It is the opinion of the author that at this stage, these calculations are sufficient to be used for preliminary comparison of CBs with the control beam. More studies are required, to properly determine the design criteria and methodology for moment-shaped curved beams.

During the testing a very simple spreadsheet was used to determine the applied moment due to the actuator's point load. These calculations are as follows:
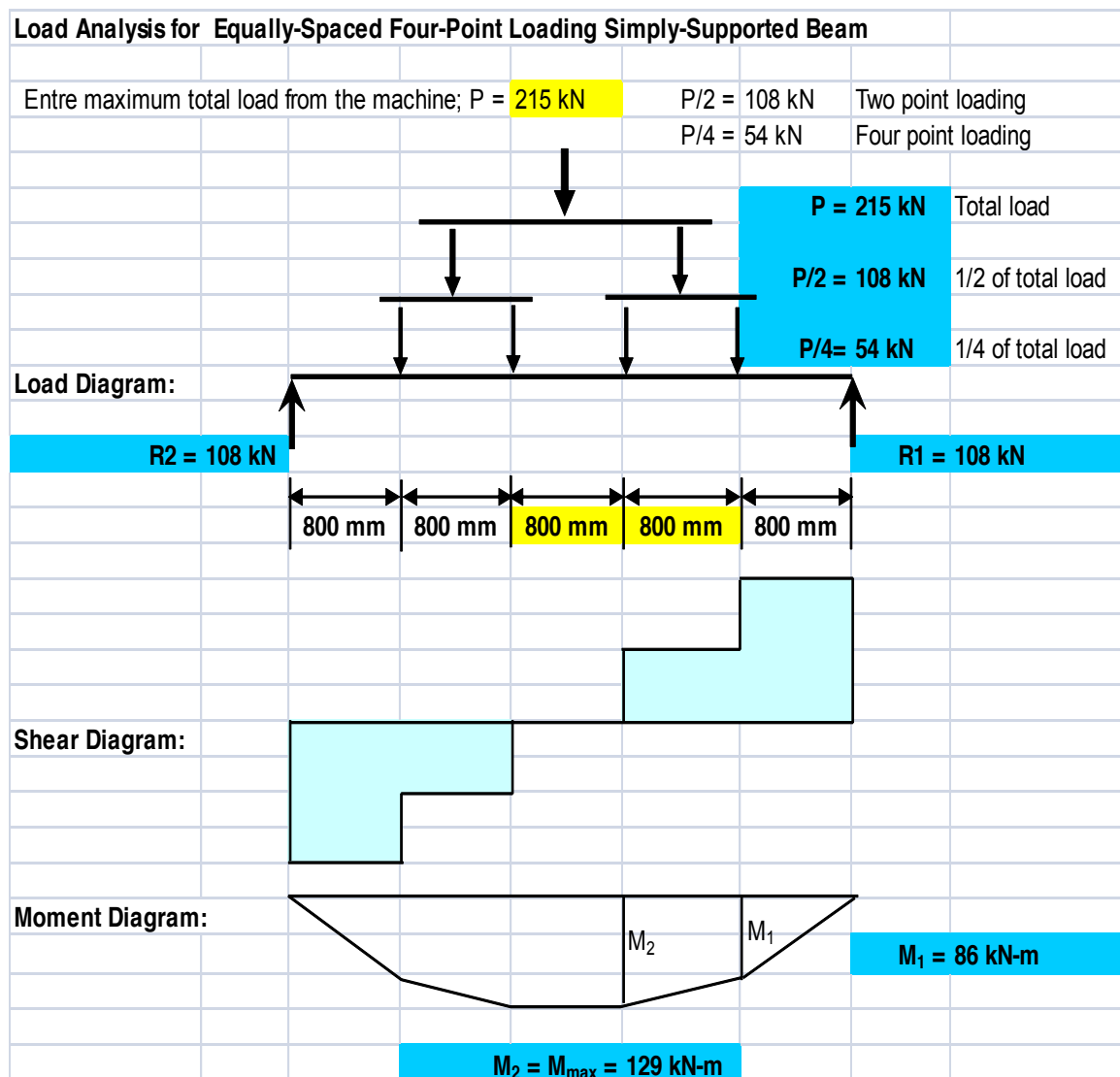
7.3   Conclusion

Code-directed design is presently not an adequate tool for designing Curved Beams and Camber Curved Beams. Analysis and design based on the code outlined in this chapter resulted in overestimating the capacity of moment-shaped beams. Existing design codes are generally based on rectangular beam behaviour and it is logical that it does not fit the design of variable section beams. This point reiterates the need for further research to develop design criteria and methodology for moment-shaped beams.

At this time, it is highly recommended that FEM analysis be used to design camber curved beams or any other moment-shaped beams.

END OF SECTION

8   *Implications for More Sustainable Concrete Construction*

This research has proven, with certain important limitations, that it is possible to change the geometry of a horizontal load-bearing RC member to achieve a more efficient structural member with a much smaller carbon footprint. The efficiency here is to carry the same load with the same stiffness as the conventionally designed and constructed RC beam but with less material. This functionality was achieved by creating a Cambered Curve Beam that has 20% less concrete and 40% less steel than the conventional beam yet carries the same load up to serviceability failure and beyond. At the ultimate capacity, the conventional beam had 12% additional strength compared to the cambered moment-shaped beams and considerable ductility after serviceability failure.

The percentage reduction in materials would translate to 170 kg less concrete and 13 kg less steel in a 4200mm long beam. Table 8.1 shows the material reduction in tabulated format.

Table 8.1 – CSA beam and CCB comparison

Beam	Length	Ultimate Load	Wt. of Steel	Wt. of Concrete	Load/Wt Ratio
RB3-CSA beam	4200 mm	244 kN	46 kg	888 kg	11.22
CCB	4200 mm	215 kN	33 kg	719 kg	12.06
Reduction		29 kN	16 kg	170 kg	
% Reduction		12%	40%	20%	

Such reductions in material would have a significant domino effect on all other structural members in a structure. A reduction of materials in horizontal load-bearing members will result in a material reduction of the vertical load-bearing

members (columns) since they carry less dead load. These reductions cascade through the structure and affect the foundations which would be proportionally smaller as well. Foundations are estimated to be about 40% of the overall building cost for commercial, healthcare and institutional buildings. Reducing the materials in the structural members reduces the dead load which is the load that is there 100% of the time and is a major cause of fatigue and creep.

Such material savings would reduce not only the overall weight of the building but also the cost of transportation since lower material volumes are transported to the construction site.

Although the material reduction in formwork, concrete and steel in moment-shaped beams are apparent, it is not possible to compare overall savings in material and Green House Gas (GHG) emissions since there are no actual buildings designed and fabricated using fabric-formed moment-shaped beams (and structural system) that would provide data for comparison.

It is highly recommended that further study be initiated with regards to the potential overall material CO_2 reductions that these more efficient beams might provide; this study should also include life cycle analysis.

END OF SECTION

9   Discussion and Conclusions

This chapter presents the discussion of the results presented in Chapter 5 – Experimental Results and Comparison, and the conclusions of this research.

9.1   Discussion

The main focus of this study was to gain a comprehensive understanding of two types of curved beams, CB and CCB, and compare the experimental results to the CSA-designed rectangular control beam.   CBs are the curved beams fabricated in Phase I of this study following the bending-moment shape at the bottom of the beam with a flat top.   CCBs are the cambered curved beams fabricated in Phase III of this study having the same bottom curve as the CBs with an additional catenary curve at the top having a maximum additional height of 100mm at the centre-span.

Section 5.3.3 compares the results of the two types of curved beams; CBs and CCBs. Figure 5.109 shows the load vs. deflection diagram for beams CB3 and CCB1. Figure 9.1 shows the same comparison with trendlines plotted on the graphs. One trendline shows the average overall behaviour of CB. Since the first cracks appeared at a very low load for CB (at 5% of total load), rendering the difference between uncracked and cracked behaviour inappreciable.   The formula for the CB's load-deflection curve trendline is:

$Y = 7.330X + 19.649$ $(R^2 = 0.771)$

Because the behaviour of CCB changes considerably after cracking, and the first crack occurs at a higher load of approximately 80kN (37% of total load), two

trendlines are plotted on the load-deflection curve for CCB, one prior to cracking and one after cracking. These are as follows:

Before cracking   Y = 26.401X + 1.9961   (R^2 = 0.999)

After cracking   Y = 12.111X + 49.157   (R^2 = 0.991)
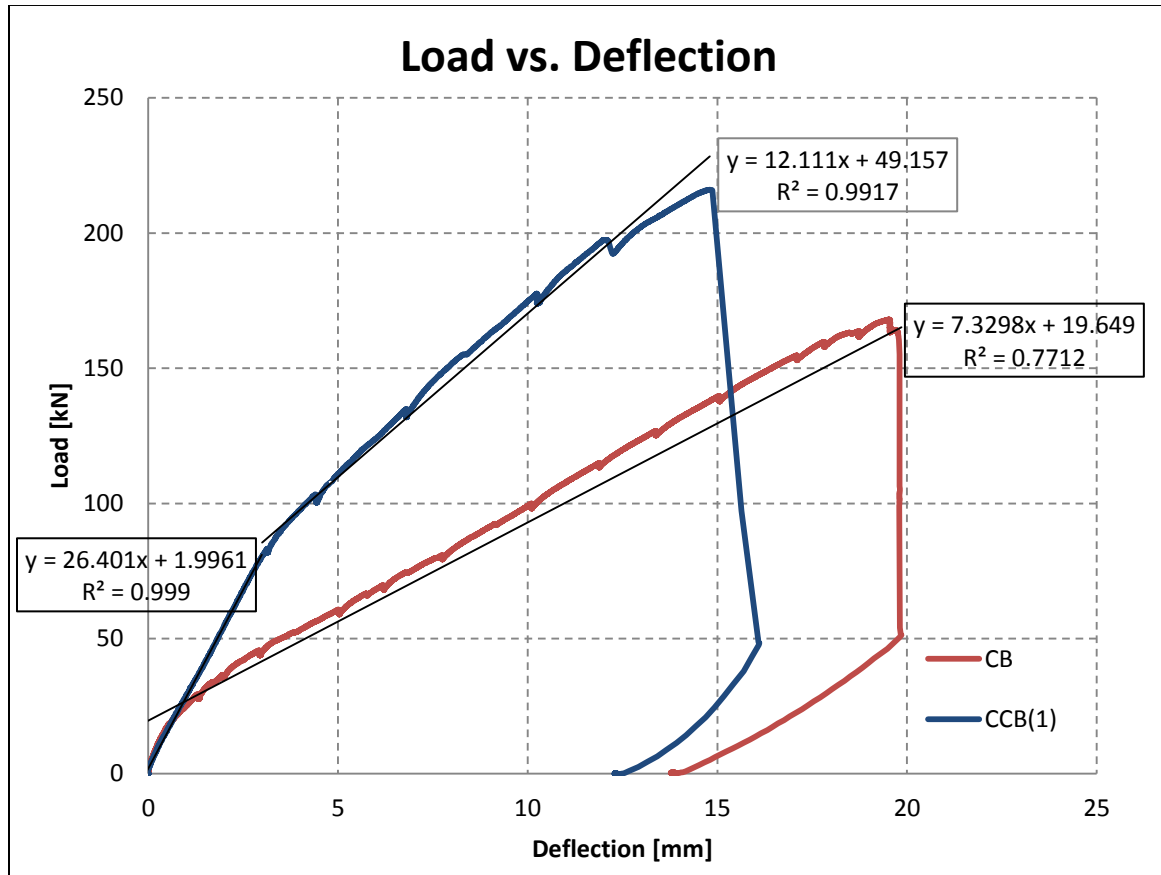
Figure 9.1 – Load vs. deflection comparison for CB3 and CCB1

The slopes of the trendlines of the load-deflection curves represent the stiffness of each beam. The slope of the curve for CCB is 26.40 prior to cracking and 12.11 after cracking, while the slope of the load-deflection curve for CB is 7.32. the addition of the top curve (or camber) increased the concrete volume used to

fabricated CCB by 0.042m^3 over the volume of concrete used to fabricate CB (less than 5% increase in total concrete), yet this small amount of additional concrete increased the stiffness of CCB by 72% prior to cracking and 39% after cracking over CB. The research in Phase I determined that the curved beams CB needed to be stiffer to be comparable to the CSA-designed rectangular control beam. This stiffness comparison and the increase in total load carrying capacity of CCB over CB confirm that adding camber in CCB achieved that objective. Since CCB is established to be the better performing curved beam based on the above evaluation, the rest of this discussion will focus on comparing CCB with the CSA-designed control beam.

Section 5.1.12 describes the configuration of RB3, the rectangular cross-section control beam, designed and fabricated to CSA codes and standards. The purpose of this beam as described in Section 4.3.3 is to have a conventional beam to compare to the behaviour of curved beams. Since the behaviour of code-designed rectangular beams is well established, only one beam was constructed and tested to provide comparison data.

Figure 9.2 shows the load-deflection curve for both the RB3 control beam and CCB1. Before cracking the two curves completely match as they are overlapped. After cracking the trendlines plotted on each curve show that the slopes and the coefficient of variance for both curves are effectively the same, as shown below:

Control beam RB3   Y = 12.993X + 27.94   (R^2 = 0.9887)

CCB1   Y = 12.112X + 49.15   (R^2 = 0.9917)

This evaluation demonstrates that the curved beam with camber CCB had the same stiffness as the CSA control beam.

Section 5.3.1 compares the total capacity of these two beams showing the maximum load for CCB was 20% less than the CSA control beam, and CCB was considerably less ductile than the CSA control beam.

Load vs. Deflection

$y = 12.993x + 27.94$
$R^2 = 0.9887$

$y = 12.112x + 49.149$
$R^2 = 0.9917$

CSA Control Beam
CCB

12mm

Deflection [mm]

Load [kN]
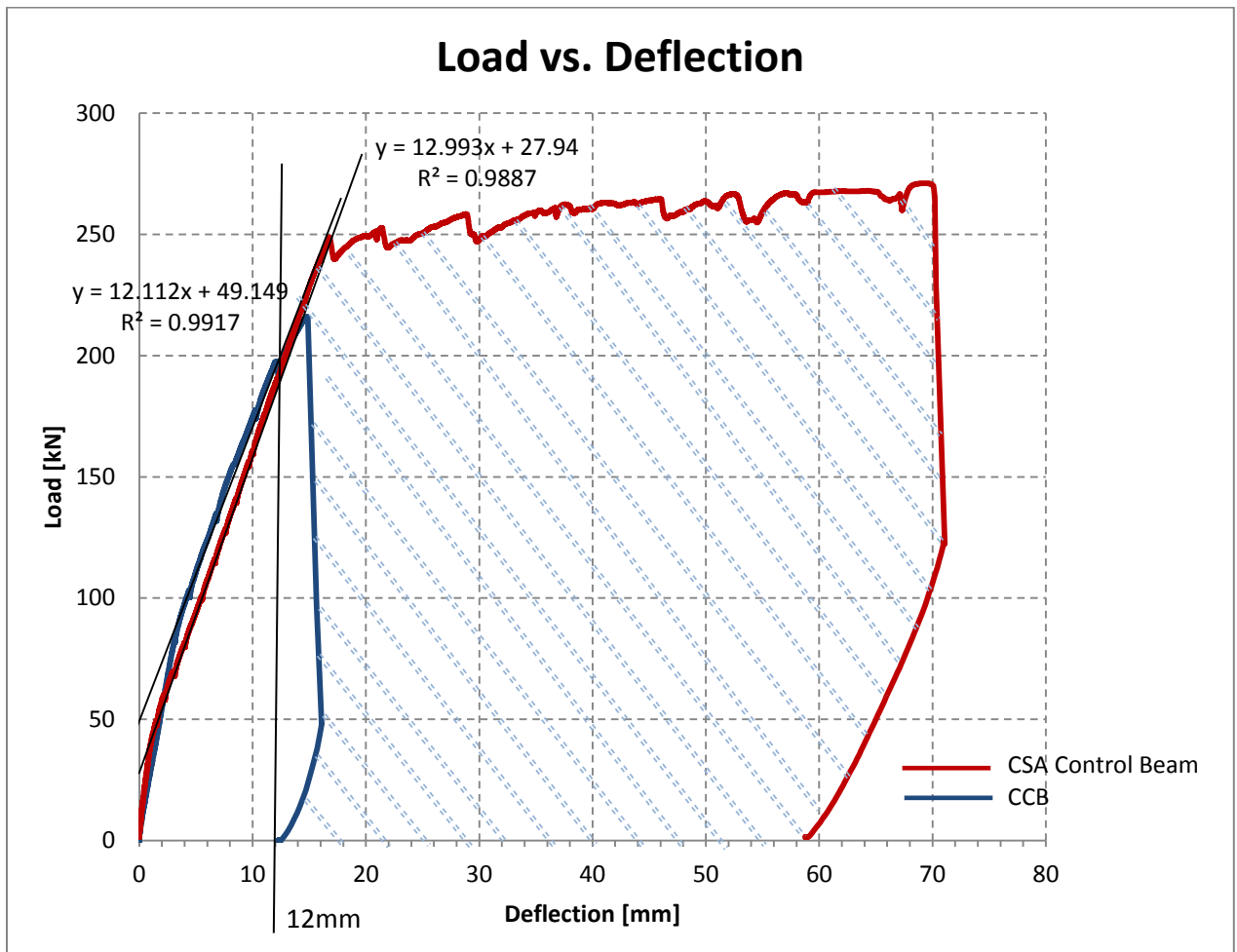
Figure 9.2 – Load vs. deflection comparison for CSA Control Beam and CCB

To summarize the findings in Phase III of this research, CCB curved beams possess virtually the same stiffness as the CSA control beam until failure, and

256

sustained 20% less ultimate load than the CSA control beam. Additionally, CCB curved beams have the same stiffness and carrying capacity as CSA control beam at the point of serviceability failure[1]. However, the ductility until total failure of the CSA control beam is far greater than that of the CCB beam.

The next phase of moment-shape and structural efficiency research should focus on developing solutions to increase the ductility of curved beams. The total energy required to bring in the final failure for the CSA control beam is much larger than CCB. The final failure energy difference of the two beams is the hatched area under the curve shown in Figure 9.2.

9.2 Modes of Failure

In this section three possible modes of failure are described: moment failure (rotation at the end support); "shear" (diagonal tension) failure; and direct shear failure. These are discussed to examine the failure mechanisms and provide an accurate description of curved beam failure, based on the research and numerical analysis performed during this study.

1- *Moment failure at the support – or rotation of the support end:*

It was observed in the curved beams that at the moment of failure the very end of the beam rotated upward as the failure triangular moved up. The failure triangle is shown in Figure 5.122 and Figure 9.3. The rotation of the support end may be seen as the result of a moment arm between the applied load and the reaction at the end. This is shown for CCB1 in Figure 9.3.

---

[1] serviceability failure is at 12mm deflection
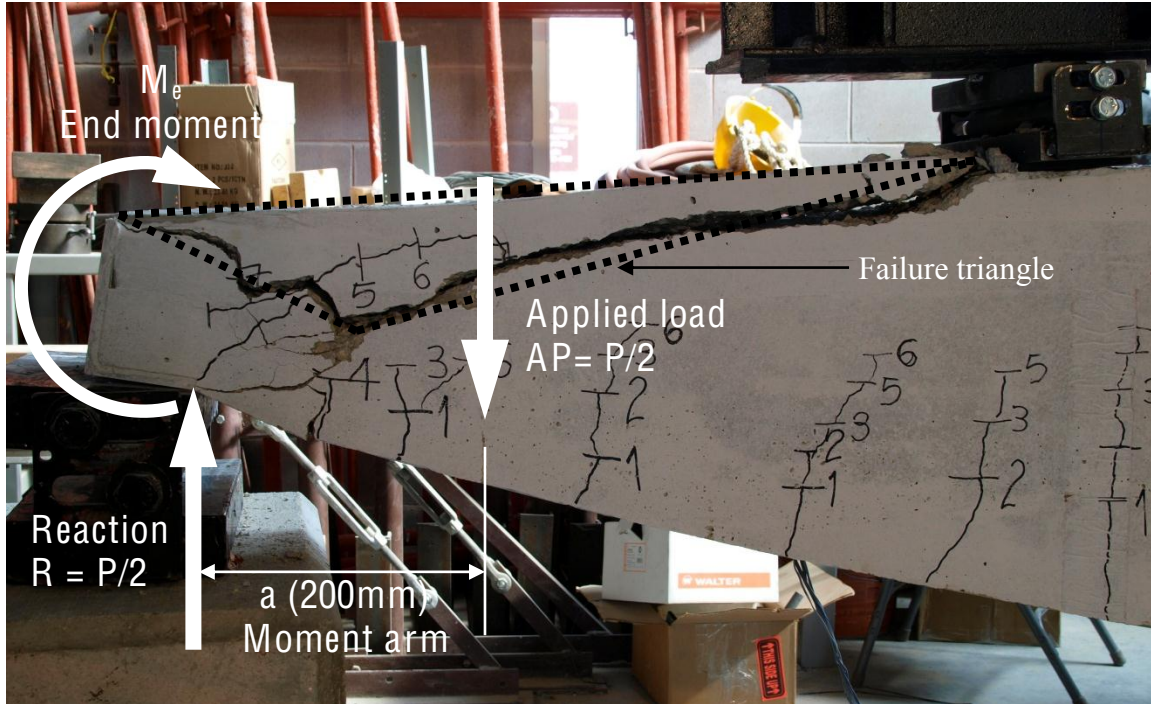
Figure 9.3 – CCB1 possible final failure mode

The moment "M_e" is due to the reaction "R" acting at the moment arm "a" (200mm maximum). The resulting moment at the maximum load for CCB1 can be approximately calculated as follows:

Maximum load   P = 217 kN

Load at support   R = AP = P/2 = 108.5 kN

Maximum moment arm   a = 200mm = 0.2m

End moment M_e = R x a = 108.5 x 0.2 = 21.7 kN-m

The resisting moment or moment capacity (M_r) of the beam 200mm from the support, in accordance with the reinforced concrete design principles is:

$$M_{r\,(200)} = AP \times a = 108.5 \text{ kN} \times 200 \text{ mm} = 52 \text{ kN-m}$$

$$M_{r\,(200)} = 52 \text{ kN-m (58\% higher than } M_e)$$

$$M_{r\,(200)} > M_e$$

The moment applied at 200mm from the support (52 kN-m) is lower than the moment capacity of the CCB section at that point. While a rotation due to this moment certainly occurs, the author understands this to be a consequence after the failure of the beam, not the cause of the failure itself since the beam has more capacity than the end moment (M_e). Further, if the applied end moment was higher than the moment capacity (i.e. $Mr_{(200)} < M_e$) then the final mode of failure should be concrete crushing because at the location of failure the depth of the beam is only 200mm, and the section at this point is considerably over-reinforced. The mode of failure for an over-reinforced section is concrete crushing but this did not occur in the concrete. Instead, a portion of the compression block (the failure triangle Figure 9.3) was displaced upwards. In this case, concrete crushing cannot occur because the failure triangle is not confined and can move upward. If the area of failure was to be confined by, for example, a concrete slab poured with the beam (a t-beam) or a precast slab placed on the beam, then the concrete in this area could not move upward and would certainly crush.

2-   "Shear" or diagonal tension failure:

Prior to the final failure, diagonal cracks at approximately 45º angles, resembling diagonal tension or "shear" cracks, were observed in the curved beams near the supports. This raises the point that "shear' (diagonal tension) could be the failure

mode in the curved beams. Since stress in concrete cannot physically be measured in this area and only the reinforcements were instrumented, data for the internal stresses in this area of the curved beams uses the numerical (FEM) analysis. The FEM analysis as described in Chapter 6 shows that the tension remains constant in the reinforcement all the way to the support end-angles. This is supported by the strain reading from the strain gauges installed on the reinforcement presented in Chapter 5, section 5.5. The strain distribution curve for CCB1 shown in Figure 5.138 illustrates that the strain distribution is uniform along the reinforcement until the last strain gauge. Note that in Figure 5.138 the strain curve at each end of the beam is shown as going to zero right after the last strain gauges; this is because there were no strain gauges placed between the last gauge location (between ESG1 and ESG2; and ESG6 and ESG7) and the support. The FEM analysis shows that the tension strain is constant in the remaining, un-instrumented, length of the reinforcement. This is also consistent with the equilibrium calculations for this portion of the curved beams.

The FEM analysis also shows that the principle stresses in the concrete elements at the failure area have one principle stress (σ_1 - compression forces) directed towards the reinforcement, Figures 6.12 and 9.4. The other principle stress (σ_2 – tension forces) in the concrete elements is nearly zero (σ_2 the tension forces is not shown in Figure 9.4 since they are practically zero); indicating that diagonal tension or "shear" approaches zero near the support as the applied load approaching the maximum capacity of the beam. This means

that diagonal tension or "shear" may not be the final failure mode since all elements in the FEM analysis show near zero diagonal tension.
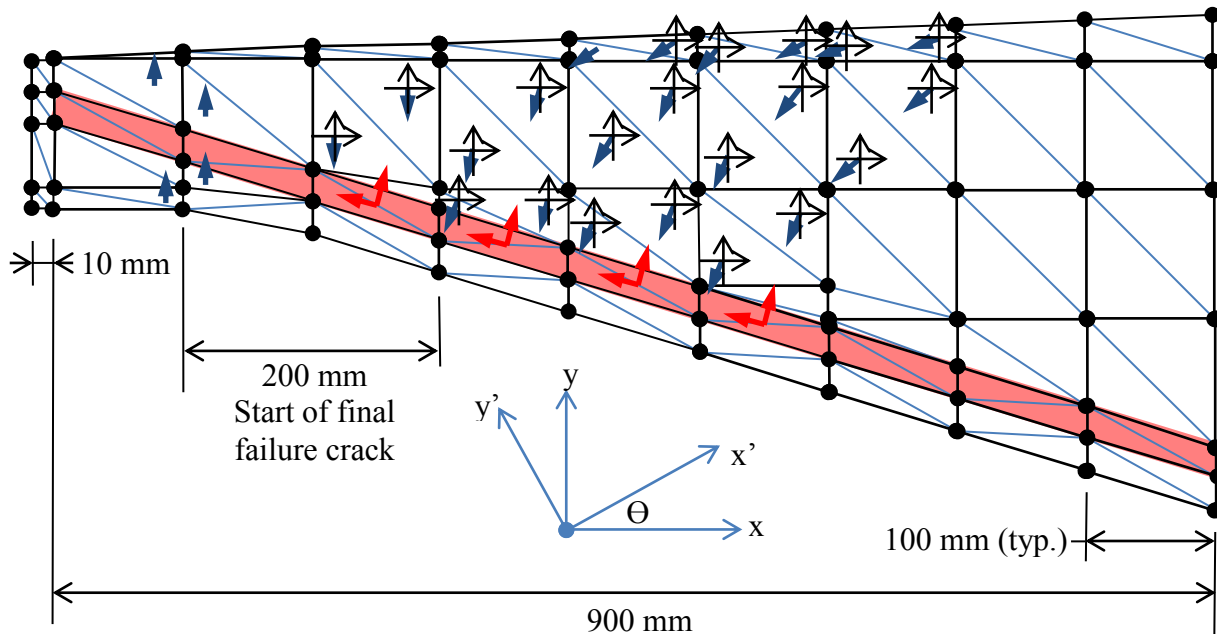
Figure 9.4 – CCB elemental stress distribution near the support

3-   Direct shear failure:

Section 5.3.3 described the evolution of cracks and a possible final mode of failure of CCB that can be confirmed by the FEM analysis (Chapter 6). This possible mode of failure is presented in this thesis to be direct shear. This point is reiterated in this section by presenting additional discussion complementing Section 5.3.3 and chapter 6 through a comparison of CCB with RB1. RB1 is the rectangular beam (same geometric configuration as the CSA control beam) with the same amount of flexural reinforcement as CCB and the CSA control beam but with no shear stirrups. Figure 9.5 shows the load-deflection curve of the

three beams; CCB, CSA control beam and RB1 (no shear stirrups). As illustrated, RB1 completely failed (explosive collapse) at 180kN total load (66% of CSA control beam and 83% of CCB) and at 11.5mm deflection, prior to serviceability failure.
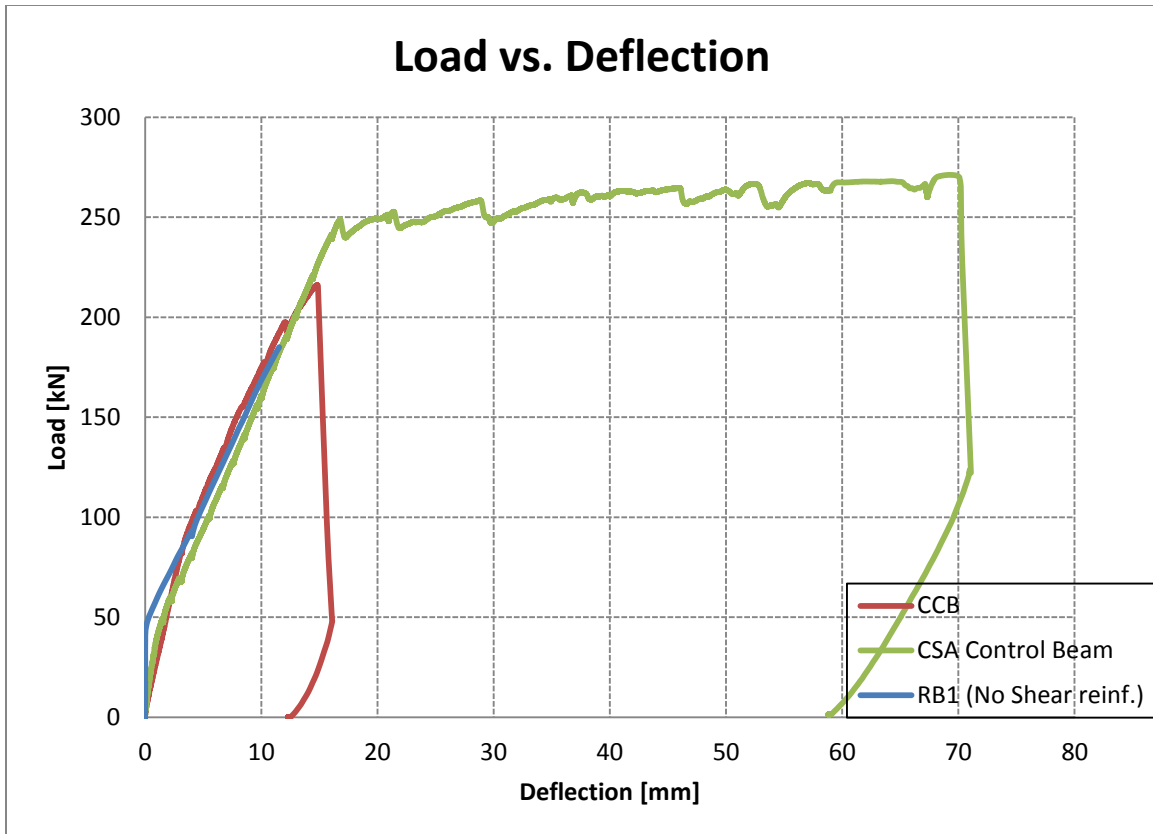
Figure 9.5 – Load-deflection comparison for CSA Control Beam, CCB, and RB1

The third mode of failure is direct shear, as presented in Chapter 5, Section 5.3.3. The results from the numerical analysis in Chapter 6 suggest this mode of failure. In addition to the FEM analysis, we can compare the CCB's and RB1 as all of these beams lacked "shear" reinforcing stirrups. Equation 9.1 from CSA-A 23.3 (EQ 11.6 in CSA-A 23.3) can be used to calculate the "shear" capacity of

the concrete. "Shear" resistance due to "shear" reinforcing stirrups is not included in these calculations since neither of the beams have stirrups.

$$V_c = \Phi_c \, \lambda \, \beta \, (f'_c)^{1/2} \, b_w \, d_v \qquad \qquad \text{Equation 9.1}$$

Where: f'_c is the concrete strength $((f'_c)^{1/2} \le 8 \text{ MPa})$

             b_w is beam width

             d_v is effective shear depth (greater of 0.9 d or 0.72h)

The first three terms of the equation can be omitted as they are reduction factors used in Limit State Design.

According to Equation 9.1 the concrete shear resistance for each beam is as follows:

$V_c = 172.8$ kN   CCB (h = 200mm at the failure plane, Figure 5.114)

$V_c = 440.1$ kN   RB1 (h = 450mm at the failure plane, Figure 5.48)

The concrete section of CCB's resisting the "shear" has only 39% of the "shear" capacity of RB1 at the plane of failure yet the CCB's failed at 17% higher load. According to the shear capacity calculations, if CCB's mode of failure had been the same as rectangular RB1 (diagonal tension or "shear") then it should have failed well before the maximum load at which RB1 failed. There are other factors contributing to the total capacity of RB1 such as aggregate interlock and dowel action of the reinforcement. Although these factors would further increase RB1's vertical shear capacity, they are not considered here due to their small contributions. Furthermore, the capacity of both CCB's and RB1 is higher than the applied vertical shear of 108.5 kN (maximum applied vertical shear for CCB1 at failure).

The additional "shear" capacity of the CCB's is due to the slope of the reinforcement. The reinforcement in curved beams follows the longitudinal (bending moment) curve of the beam hence the tension force, T, in the reinforcement has a vertical and a horizontal component; T_v and T_h respectively. The horizontal component T_h is the force resisting the applied moment (flexure) and the vertical component T_v contributes to the vertical shear resistance of the beam. These components of the tension force in the reinforcement can be confirmed by equilibrium analysis of a section of CCB's. The force diagram in Figure 9.6 shows the components of the tension force in the steel reinforcement.
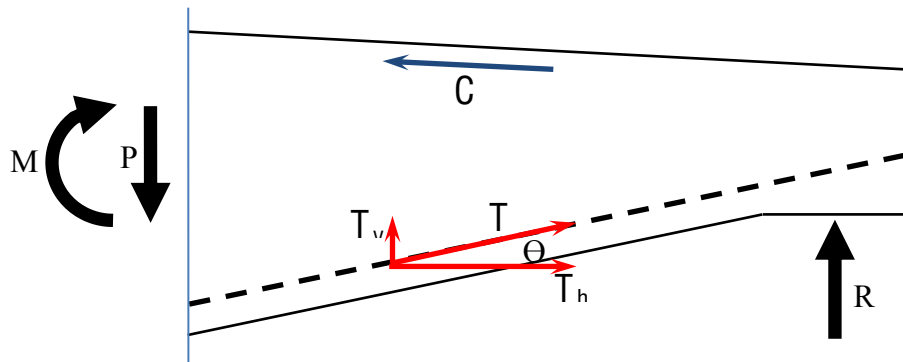
Figure 9.6 – Force diagram for CCB's at support end

The terms in Figure 9.6 are as follows:

C	Internal compression force
T	Internal tension force
Θ	Slope of the reinforcement
T_v = T SinΘ	Vertical component of T
T_h = T CosΘ	Horizontal component of T
R	Reaction at support
P	Applied vertical load
M	Moment due to applied vertical load

The horizontal component of the tension force, T_h, and the compression force, C, in the concrete, resist the external moment M. The vertical component of the tension force contributes to the vertical shear capacity of the beam.

The slope of the reinforcement, Θ, in CB's and CCB's at 200mm away from the support is 20.23°. The following calculations determine the vertical component of the tension force in the reinforcement in CCB1.

Where   Θ = 20.23°

Strain at ESG 2 ε = 1797.38 Micro Strain (at 217 kN Max. load)

Total stress in the reinforcement:

$$\sigma = E\ \varepsilon$$

$$\sigma = (186{,}000 \text{ MPa}) (0.00179738)$$

σ = 334.32 MPa

Tension force in two 25M reinforcement (A_s = 1000mm^2):

$$T = A_s\ \sigma$$

$$T = (1000 \text{ mm}^2) (334.32 \text{ MPa})$$

T = 334 kN   ($T_{one\ bar}$ = 167 kN in one rebar)

Components of tension force:

Vertical component of T   – T_v = T SinΘ

$$T_v = (334 \text{ kN}) \text{Sin}(20.23°)$$

T_v = 115 kN

Horizontal component of T – $T_h = T \cos\Theta$

$T_h = (334 \text{ MPa}) \cos(20.23°)$

$T_h = 313 \text{ kN}$

Hence; the total vertical shear capacity of CCB (average of CCBs) is as follows:

$V_{total} = V_c + T_v$

$V_{total} = (172.8 \text{ kN}) + (137 \text{ kN})$

$V_{total} = 309 \text{ kN}$

The total vertical shear capacity of CCB is still less than RB1's (440 kN), but higher than the applied maximum vertical shear. Figure 9.7 shows these values substituted in the end-beam diagram in Figure 9.6. As established in the above calculations and shown in Figure 9.6 the vertical resistive force generated by the slope of the reinforcement is higher than the applied vertical load by 6.5 kN.
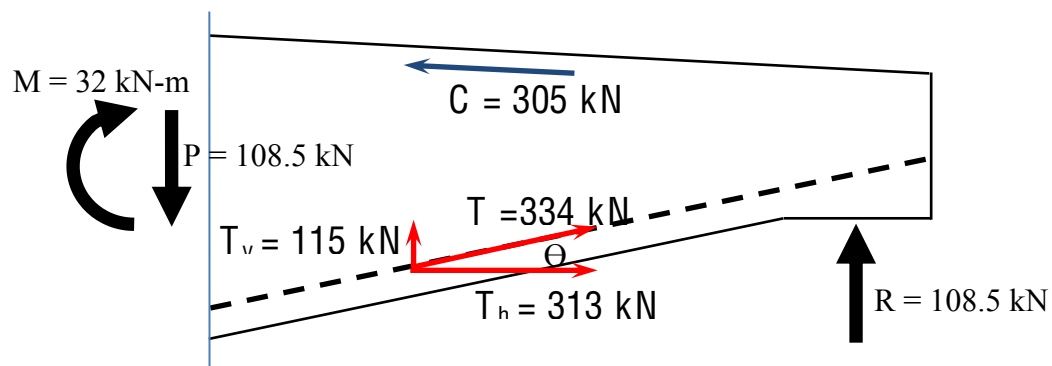
Figure 9.7 – Force diagram for CCB's with values at maximum load

There are two probable explanations for the additional capacity of the vertical force in the reinforcement:

1- The 6.5 kN additional capacity is 5.6% higher than the actual. This could be due to construction errors and errors in measuring the slope of the reinforcement and the depth of the beam. as well as to the discrepancies between the actual beam dimensions and the theoretical design dimensions. These errors were then carried into the calculations.

2- The section is not in equilibrium and the resistive force is higher than the applied.

If the section was not in equilibrium and the resistive force was actually higher than the applied force then the beam should move upward and gain more camber instead of deflecting downwards. This is clearly not occurring, therefore, it is likely that the additional resistive force is due to construction errors resulting in dimensional discrepancies between the actual beam and the theoretical dimensions.

Final mode of failure

Final mode of failure is expected to be the combination of the three modes indicated above since it is not possible to definitively prove any of these modes of failure to be the dominating factor. Although, the FEM analysis suggests that direct shear could contribute more to the final failure. Further research is required to determine the exact percentage, or the amount, that each of the possible failure modes contributes to the final failure.

267

9.3 Conclusions

In Phase I, the first generation of moment-shaped beams designated as CBs were designed and constructed. The CBs in Phase I showed that moment-shaped beams without shear reinforcing are flexible. The stiffness of the CBs was considerably lower than that of the CSA designed control beam.

In Phase III, the second generation of curved beams were designed and constructed. These beams were designed with a camber and were designated as CCBs. This design proved to be the most effective solution as the CCBs demonstrated a substantial increase in stiffness over the first generation CBs and had higher ultimate capacity. The CCBs had the same stiffness as the CSA control beam and exhibited the same behaviour up until ultimate failure. Compared to CCB's the ultimate load for the CSA control beam was higher by 12%, and the CSA control beam demonstrated considerably higher ductility after the ultimate load, which is the desired mode of failure since it is provides a greater opportunity for warning occupants to evacuate a building. Although the CCBs did not exhibit equivalent ductility, crack widths of approximately 12mm were observed before the ultimate failure which may be considered as warning signs of impending failure.

The final mode of failure for both CBs and CCBs determined to be due to three factors: moment failure (rotation at end support); "shear" (diagonal tension) failure; and direct shear failure. Although FEM analysis results show that the direct shear is the factor contributing the most to the final failure, further research is required to determine the exact contribution of each factor.

In conclusion, the moment-shaped beams with camber proved to be a more sustainable solution for constructing reinforced concrete beams. The CCBs had 20% less concrete and 40% less steel yet could sustain a load that was only 12% less than the load of the CSA control beam. Further work remains to be done to increase the ductility of these more efficient beams after ultimate failure.

END OF SECTION

10   Future Work

The material efficiency of moment-shaped beams and the consequent positive effects on both cost and sustainability make this design and construction strategy a valuable option for future construction practice. Further study should focus on developing design criteria to govern the design of moment-shaped beams. This future research would facilitate the inclusion of the moment-shaped beams in applicable codes and standards. The building design industry is required to comply with these codes and it is necessary to develop codes for these beams or other structural members that could be created using flexible-formwork.

The following list presents other aspects and possible solutions of moment-shaped beams that should be the subject of further study and research:

1.   Research to increase the ductility of the moment-shaped beams after achieving maximum load:

    1.1.   Adding additional reinforcement at both ends of the beam to provide containment for the concrete and increase stiffness and tension capacity in those regions. Modifying the shape and configuration of the additional reinforcement at the end can itself be the subject of a separate study. Adding shear reinforcement and studying its geometric configuration of closed stirrups vs. spiral ties vs. diagonal reinforcement.

    1.2.   Increasing the concrete area by increasing the width of the beam at the supports. This can be done easily with fabric formwork by widening the fabric mould at the ends of the beam.

1.3. Increasing the concrete area by adding a slab to the beam and creating a t-beam. The thickness of the slab can be studied to determine the most efficient slab-thickness to overall-depth ratio.

2. End-detail/ condition research – this research should consider various improvements in the anchorage strategy and details of the reinforcing at the supports. The following are possible anchorage strategies:

2.1. Splaying the flexural reinforcement at both ends of the beam to create larger bonding area and to increase the volume of the concrete resisting cone.

2.2. Mechanical stop at the end of the reinforcement to increase the volume of the resisting cone.

3. Investigations of moment-shaped beams loaded to produce bending moments different than the bending moments that they are shaped to follow (i.e. "incorrect" loading).

4. Investigating the bonding effect of the reinforcement. Undertake studies to find the effect of concrete bonded vs. un-bonded reinforcement in the behaviour of curved beams. The reinforcement can be placed in PVC conduits within the concrete section to prevent it from bonding with concrete much like post-tensioned precast sections, or place the reinforcement completely outside of the concrete section with no cover or perhaps with a PVC layer separating the concrete from the reinforcement.

5. Research to determine the effects of pre-stressing or post-tensioning of the reinforcements in moment-shaped beams. Both pre-stressing and

post-tensioning are viable options to increase stiffness and direct shear resistance.

6.   Testing of moment-shapes beams designed for loading conditions other than simply supported, uniformly distributed loading to further understand the behaviour of moment-shaped beams.

7.   Further development of nonlinear FEM program to analyse moment-shaped RC beams.

8.   Optimization of the camber in CCBs.

9.   Investigations of other geometries beside cambers to improve stiffness and final load carrying capacity of moment-shaped RC beams such as integrated slabs (T-beams or bonded slabs).

10.   Externally reinforced CCBs with FRP sheets to increase the overall ductility or as a repair measure after cracking.

11.   Study the use of the flexibility of fabric formwork to reduce the concrete in the tension zone (around the steel) and in the web for greater material savings.

12.   Developing design criteria to aid with design code development.

13.   Developing design modules and design aids for practicing engineers.

END OF SECTION

References and Bibliography

1.   R. W. Spokowski, May 1972. *Finite Element Analysis of Reinforced Concrete Members*, M.Eng. Thesis.

2.   A. H. Nilson, 1971. *Finite Element Analysis of Reinforced Concrete*, Ph.D. Thesis.

3.   W. H. Soong, April, 2001. *Bonding Between the Concrete and Fiber Reinforced Plastic (FRP) Rods*, M.Sc. Thesis.

4.   A. A. Mufti, M.S. Mirza, J.O. McCutcheon, and J. Houde, 1970. *A Study of the Behaviour of Reinforced Concrete Elements Using Finite Elements,* September.

5.   M.D. Kotsovos and M.N. Pavalovic, 1999. *Ultimate Limit-state Design of Concrete Structures – A New Approach*.

6.   S. Brzev and J. Pao, 2009. *Reinforced Concrete Design, A Practical Approach*.

7.   Canadian Concrete Design Handbook, 2006, Third Edition.

8.   CSA A23.3-04, 2004. *Design of Concrete Structures*, Canadian Standard Association.

9.   CSA A23.3-94, 1994. *Design of Concrete Structures*, Canadian Standard Association.

10.   Bartlett, F.M., and MacGregor, J.G., 1999. *Statistical Analysis of the Compressive Strength of Concrete in Structures*, ACI Materials Journal, Vol. 96, No. 2.

11.   Ferguson, P.M., Breen, J.E., and Jirsa, J.O., 1988*. Reinforced Concrete Fundamentals*, Fifth edition.

12.   MacGregor, J.G., and Bartlett, F.M., 2000. *Reinforced Concrete: Mechanics and Design*, First Canadian Edition.

13.   Y.M. Xie, X. Huang, J.W. Tang and P. Felicettim, 2005. *Recent Advances in Evolutionary Structural Optimization*.

14.   Bhatt, P., Kader, M. A. 1998. *Prediction of Shear Strength of Reinforced Concrete Beams by Nonlinear Finite Element Analysis. Computers and Structures.*

15. Fab-Form, Fabric-Formed Concrete, http://www.fab-form.com/.

16. C. Cui, H. Ohmori and M. Sasaki, *Computational Morphogenesis of 3D Structures by Extended ESO Method*, Journal of the International Association for Shell and Spatial Structures, 2003.

17. Allen, E., 2004. *Building a Foam Beam to Demonstrate Web Forces, Form and Forces*; A journal of ideas for teachers of structures.

18. Ashraf H. Elzanaty, Arthur H. Nilson, and Floyd O. Slate, 1986. *Shear Capacity of Reinforced Concrete Beams Using High-Strength Concrete*, ACI Structural Journal, Vol. 83, No. 2, pp. 290-296.

19. K. G. Moody, I . M . Viest, R. C. Elstner, and E. Hognestad, 1954. Shear Strength of Reinforced Concrete Beams Part 1 -Tests of Simple Beams. ACI Structural Journal, Vol. 51, No.12, pp. 317-332.

20. Vecchio, F.J. and Collins, M.P, 1988. *Predicting the Response of Reinforced Concrete Beams Subjected to Shear Using Modified Compression Field Theory*, ACI Structural Journal, Title no. 85-S27. pp. 258-268.

21. L. D. Wegner and A. A. Mufti, 1994. *Finite Element Investigation of Fibre-Reinforced Concrete Deck Slabs Without Internal Steel Reinforcement*, Canadian Journal of Civil Engineering, Vol. 21, No. 2. Pp. 231-236.

Appendix A

FEM-NRC (FINIT-Y)

FINITY FEM Program Algorithm and one iteration of program result


```
C                     *************************
C                      MAIN PROGRAM FINITEY DP
C                     *************************
C
IMPLICIT DOUBLE PRECISION(A-H,O-Z)
DIMENSION X(1500,2),NOD(2000,3),NEP(2000),THICK(2000),
1STRAIN(2000,2),BNUM(800),NODS(800,2),IBREAK(800),ICLKS(800),
2WDT(800),BSTRS(800),NSSS(800),DIA(800),BN(800),E1(2),E2(2),P1(2),
3P2(2),GE(2),ITAG(1),NBRK(1),SKS(4,4),XXE(3,2),XE(3,2),NF(100),
4NB(100,2),BV(100,2),NSTART(15),NEND(15),NFIRST(15),NLAST(15),

5NCHK(15),NSPGST(15),NSPGED(15),NSTR(15),NENDST(15,2),NODSTR(200
,2)
6,STIR(200,3),ILD(40),NYMT(800)
COMMON C(6,6),DBA(3,6),DB(3,6),A(6,6),ST(1000,2000),U(3000,4),
1U1(3000),B(3,6),TSTRES(2000,3,1),TSRN(2000,3,1),U2(800),U3(6),
3U4(3000),T1(2000)
CHARACTER*100 TITLE
C
C
C  READING AND PRINTING OF INPUT DATA
C
C  DATA READ FROM A FILE=FDATA1
OPEN( 5,FILE='FDATA1',STATUS='OLD')
C
C  WRITE RESULTS ON A FILE=FRESULT1
OPEN( 6,FILE='FResult test',STATUS='UNKNOWN')
C
C
OPEN( 1,STATUS='SCRATCH',FORM='UNFORMATTED')
OPEN( 2,STATUS='SCRATCH',FORM='UNFORMATTED')
OPEN( 3,STATUS='SCRATCH',FORM='UNFORMATTED')
OPEN( 4,STATUS='SCRATCH',FORM='UNFORMATTED')
READ (5,111)TITLE
WRITE(6,111)TITLE
 111  FORMAT(A100)
WRITE(6,*) ' '
WRITE(6,*) 'PRINT INPUT DATA'
READ (5,*) NCHECK
READ (5,*) NPART,NPOIN,NELEM,NBOUN,NCOLN,NYM,NP,NFREE,NCONC,
1NS,NELEMS,NUNIT,BTH
WRITE(6,*) ' '
WRITE(6,*) 'Overall Information of FEM Model'
```

```fortran
      WRITE(6,*) ' '
      WRITE(6,*) '      Data Check Yes=1, No=2',NCHECK
      WRITE(6,*) '       Number of Partitions =',NPART
      WRITE(6,*) '      Number of Nodal Points =',NPOIN
      WRITE(6,*) '        Number of Elements =',NELEM
      WRITE(6,*) ' Number of Bondary Conditions =',NBOUN
      WRITE(6,*) '      Number of Load Cases = ',NCOLN
      WRITE(6,*) 'Number of Material Properties =',NYM
      WRITE(6,*) 'Plane Stress =1, Plane Strain=2',NP
      WRITE(6,*) ' Number of Degrees of Freedom =',NFREE
      WRITE(6,*) 'Number of Concentrated Forces =',NCONC
      WRITE(6,*) '        Number of Stirrups =',NS
      WRITE(6,*) '   Number of Spring Elements =',NELEMS
      WRITE(6,*) '        Units FPS=1 and MKS=2',NUNIT
      WRITE(6,*) '              Thickness =',BTH
C    Input X and Y coordinates of Nodes
      WRITE (6,*) ' '
      WRITE (6,*) ' X and Y coordinates of Nodes'
      WRITE (6,*) ' '
      DO 30 II=1,NPOIN
      READ (5,*) I,X(I,1),X(I,2)
      WRITE(6,20) I,X(I,1),X(I,2)
   30 CONTINUE
   20 FORMAT(I4,2F14.5)
      READ (5,*) NCARD
      IF(NCARD-NPOIN) 7000,70,7000
C    Input Element Nodes
   70 CONTINUE
       WRITE (6,*) ' '
      WRITE(6,*) ' Element Nodes'
       WRITE (6,*) ' '
      DO 40 II=1,NELEM
      READ (5,*) I,(NOD(I,J),J=1,3),NEP(I),THICK(I),AN
      WRITE(6,230) I,(NOD(I,J),J=1,3),NEP(I),THICK(I),AN
   40 CONTINUE
      READ (5,*) NCARD
      IF(NCARD-NELEM) 7000,79,7000
   79 IF(NBOUN.EQ.0) GO TO 259
C    Input Node Boundary Conditions
       WRITE (6,*) ' '
      WRITE(6,*) ' Boundary Conditions'
       WRITE(6,*)' '
   80 DO 50 I=1,NBOUN
      READ (5,*) NF(I),NB(I,1),NB(I,2),BV(I,1),BV(I,2)
   50 WRITE(6,240) NF(I),NB(I,1),NB(I,2),BV(I,1),BV(I,2)
  259 CONTINUE
```

```fortran
C     Input Structure Patition Information
      WRITE(6,*)' '
      WRITE(6,*) ' Partition Information'
      WRITE(6,*)' '
      DO 260 I=1,NPART
      READ (5,*) NSTART(I),NEND(I),NFIRST(I),NLAST(I)
  260 WRITE(6,10) NSTART(I),NEND(I),NFIRST(I),NLAST(I)
C     Input Material Properties
      WRITE(6,*)' '
      WRITE(6,*) ' Material Properties'
      WRITE(6,*)' '
      DO 100 I=1,NYM
      READ (5,*) E1(I),E2(I),P1(I),P2(I),GE(I)
      GE(I)=E1(I)/(2.*(1.+P1(I)))
  100 WRITE(6,270) E1(I),E2(I),P1(I),P2(I),GE(I)
      NPOIN2=NPOIN*2
      DO 110 I=1,NPOIN2
      U(I,1)=0.0
      U1(I)=0.
  110 U4(I)=0.
      ICOUNT=0
C     Input Load Data
      WRITE(6,*)' '
      WRITE(6,*) 'Nodal Load Data'
      WRITE(6,*)' '
      DO 140 I=1,NCONC
      READ (5,*) K,U(2*K-1,1),U(2*K,1)
C         NODAL  LOADS  ARE  DIVIDED  BY  BTH  FOR  ELEMENT  OF  UNIT
      THICKNESS -  DSS /APRIL 2007
      U(2*k-1,1) = (U(2*k-1,1))/BTH
      U(2*K,1)   = U(2*K,1)/BTH
      IF(U(2*K-1,1).NE.0.AND.U(2*K,1).NE.0) GO TO 130
      GO TO 120
  130 ICOUNT=ICOUNT+2
      ILD(ICOUNT-1)=2*K-1
      ILD(ICOUNT)=2*K
      GO TO 140
  120 IF(U(2*K-1,1).NE.0.AND.U(2*K,1).EQ.0) GO TO 90
      GO TO 150
   90 ICOUNT=ICOUNT+1
      ILD(ICOUNT)=2*K-1
      GO TO 140
  150 IF(U(2*K-1,1).EQ.0.AND.U(2*K,1).NE.0) GO TO 160
      GO TO 140
  160 ICOUNT=ICOUNT+1
      ILD(ICOUNT)=2*K
```

```
C NODAL LOADS ARE MULTIPLIED BY BTH TO PRINT LOADS FOR
ELEMENT OF THICKNESS BTH - DSS /APRIL 2007
  140 WRITE(6,20) K,U(2*K-1,1)*BTH,U(2*K,1)*BTH
C    Input Nonlinear Analysis Information
      WRITE(6,*)' '
      WRITE (6,*) 'Nonlinear Steps and Increments of Loads'
      WRITE(6,*)' '
      READ (5,*) NSTEPS,DELTAX,DELTAY
      WRITE(6,251) NSTEPS,DELTAX,DELTAY
C     DELTAX AND DELTAY ARE DIVIDED BY BTH FOR ELEMENT OF UNIT
THICKNESS  - DSS /APRIL 2007
      DELTAX = DELTAX/BTH
      DELTAY = DELTAY/BTH
      WRITE(6,*)' '
      WRITE(6,*)' Spring Elements'
      WRITE(6,*)' '
      DO 170 II=1,NELEMS
      ICLKS(II)=0
      U2(II)=0.0
      IBREAK(II)=0
      READ (5,*)I,(NODS(I,J),J=1,2),NSSS(I),WDT(I),BN(I),DIA(I),BNUM(I)
   1 ,NYMT(I)
      WRITE(6,60)I,(NODS(I,J),J=1,2),NSSS(I),WDT(I),BN(I),DIA(I),BNUM(I)
   1 ,NYMT(I)
  170 CONTINUE
      Write(6,*) ' Spring data for Partition'
      DO 180 I=1,NPART
      READ (5,*) NCHK(I)
      WRITE(6,10) NCHK(I)
      IF(NCHK(I))180,180,190
  190 READ (5,*) NSPGST(I),NSPGED(I)
      WRITE(6,10) NSPGST(I),NSPGED(I)
  180 CONTINUE
      WRITE(6,*) ' Stirrup Data'
      DO 200 I=1,NPART
      READ (5,*) NSTR(I)
      WRITE(6,10) NSTR(I)
      IF(NSTR(I)) 200,200,210
  210 READ (5,*) NENDST(I,1),NENDST(I,2)
      WRITE(6,10) NENDST(I,1),NENDST(I,2)
  200 CONTINUE
      IF(NS.EQ.0) GO TO 221
      DO 220 I=1,NS
      READ (5,*) K,(NODSTR(I,J),J=1,2),(STIR(I,J),J=1,3)
  220 WRITE(6,240) K,(NODSTR(I,J),J=1,2),(STIR(I,J),J=1,3)
  221 CONTINUE
```

```
      WRITE(6,*)' '
      WRITE(6,*) '             Concrete Parameters'
      WRITE(6,*)' '
      READ (5,*) FO,FF,SEF,RUPTR
      WRITE(6,*) '          Maximum Concrete Stress=', FO
      WRITE(6,*) '    Concrete Stress at Maximum Strain=',FF
      WRITE(6,*) '           Maximum Concrete Strain=', SEF
      WRITE(6,*) '       Modulus of Rupture of Concrete=',RUPTR
      READ (5,*) EY,ESTHR,E,P
      WRITE(6,*)' '
      WRITE(6,*) '              Steel Parameters'
      WRITE(6,*)' '
      WRITE(6,*) '            Yield Strain of Steel=',EY
      WRITE(6,*) '         Strain at onset of Hardening=',ESTHR
      WRITE(6,*) '      Initial Strain Hardening Modulus=',E
      WRITE(6,*) 'Poisson Ratio in Strain Hardening Range=',P
      IF(NCHECK.EQ.1) STOP
C
C  FORMAT STATEMENTS FOR INPUT DATA
C
   10 FORMAT(12I4,2F16.8)
  230 FORMAT(5I4,3F16.8)
  240 FORMAT(3I4,3F16.8)
  250 FORMAT(2I4,3F10.4)
  251 FORMAT(I4,2F10.4)
   60 FORMAT(4I4,4F10.5)
  270 FORMAT(5F15.5)
C
C   CALCULATION  OF  CONSTANTS  FOR  CONCRETE  STRESS-STRAIN
CURVE
C
      STFO=SQRT(SQRT(FO))
      SEO=0.00001*STFO*(31.5-STFO)
      RSE=SEF/SEO
      RSF=FO/FF
      RE=E1(1)*SEO/FO
      RR=RE*(RSF-1.)/((RSE-1.)**2)
      RR=RR-1./RSE
      C1=2.*RR-1.
      C2=RR
      C3=RR+RE-2.
      DO 280 K=1,NELEM
      DO 280 I=1,3
      TSRN(K,I,1)=0.
      T1(K)=0.
      STRAIN(K,1)=0.0
```

```
      STRAIN(K,2)=0.0
  280 TSTRES(K,I,1)=0.0
C
C  ADDITION OF LOAD INCREMENTS TO LOAD MATRIX
C
      DO 300 LD=1,NSTEPS
      IMAX=1
      WRITE(6,*)
      WRITE(6,290) LD,IMAX
      ITAG(1)=0
      REWIND 1
      REWIND 4
      IF(LD-1) 310,310,320
  320 DO 330 I=1,NPOIN2
      DO 340 II=1,ICOUNT
      IF(ILD(II)-I) 340,350,340
  340 CONTINUE
      GO TO 330
  350 IF(MOD(I,2)) 360,370,360
  360 U(I,1)=U(I,1)+DELTAX
      GO TO 330
  370 U(I,1)=U(I,1)+DELTAY
  330 CONTINUE
  310 INTER=0
C
C  FORMATION OF GLOBAL STIFFNESS MATRIX BY PARTITIONS
C
      DO 5000 II=1,NPART
      DO 1010 J=1,2000
      DO 1010 I=1,1000
 1010 ST(I,J)=0.0
      NST=NSTART(II)
      NEN=NEND(II)
      K=NFIRST(II)
      L=NLAST(II)
      MINUS=K-1
      IF(NCHK(II)) 1020,1020,1030
 1030 NSST=NSPGST(II)
      NSEN=NSPGED(II)
 1020 DO 1040 LK=NST,NEN
      MM=LK-INTER
      DO 1050 I=1,3
      JJ=NOD(LK,I)
      XE(I,1) = X(JJ,1)
 1050 XE(I,2)=X(JJ,2)
      ANG=AN
```

```
      TH=THICK(LK)
      J=NEP(LK)
C
C  CALCULATION OF ELASTIC PROPERTIES FOR FINITE ELEMENTS
C
      IF(J-1) 1060,1060,1090
 1060 AX=ABS(STRAIN(LK,1))
      AY=ABS(STRAIN(LK,2))
      DIFS=AX-AY
      IF(DIFS) 1070,1080,1080
 1080 IF(STRAIN(LK,1)) 1100,1090,1090
 1070 IF(STRAIN(LK,2)) 1110,1090,1090
 1110 COFF=(STRAIN(LK,2))/SEO
      GO TO 1120
 1100 COFF=(STRAIN(LK,1))/SEO
 1120 TNUM=E1(1)*(1.+C1*(COFF**2)-2.*C2*(COFF**3))
      DENAM=1.+C3*COFF-C1*(COFF**2)+C2*(COFF**3)
      YM1=TNUM/(DENAM**2)
      YM2=YM1
      G=(0.5*YM1)/(1.+P1(1))
      PR1=P1(J)
      PR2=P2(J)
      GO TO 1130
 1090 IF(THICK(LK).NE.0.AND.T1(LK).EQ.0) GO TO 1140
      IF(THICK(LK).EQ.0.AND.T1(LK).NE.0) GO TO 1140
      IF(THICK(LK).NE.0.AND.T1(LK).NE.0) GO TO 1150
 1140 YM1=E1(J)
      YM2=E2(J)
      PR1=P1(J)
      PR2=P2(J)
      G=GE(J)
      GO TO 1130
 1150 YM1=E
      YM2=E
      PR1=P
      PR2=P
      G=YM1/(2.*(1.+PR1))
 1130 CONTINUE
C
C  ADDITION OF ELEMENT STIFFNESS MATRIX TO GLOBAL STIFFNESS
MATRIX
C
      CALL FEM(XE,YM1,YM2,PR1,PR2,G,ANG,NP,TH,MM,J,LK)
      DO 1040 LL=1,3
      DO 1040 KK=1,3
      IF(NOD(LK,KK)-K) 1040,1160,1160
```

```
1160 IF(NOD(LK,KK)-L) 1170,1170,1040
1170 M=NFREE*(NOD(LK,KK)-K)
   N = NFREE*(NOD(LK,LL) - K)
   I=NFREE*(KK - 1)
   J=NFREE*(LL - 1)
   IF(N) 1040,1180,1180
1180 DO 1190 NJ=1,NFREE
   DO 1190 MI=1,NFREE
   MMI=M+MI
   NNJ=N+NJ
   IMI=I+MI
   JNJ=J+NJ
1190 ST(MMI,NNJ)=ST(MMI,NNJ)+C(IMI,JNJ)
1040 CONTINUE
   IF(NSTR(II)) 2010,2010,2020
2020 NN1=NENDST(II,1)
   NN2=NENDST(II,2)
C
C   ADDITION OF STIRRUP STIFFNESS MATRIX TO GLOBAL STIFFNESS
MATRIX AND
C  CHECKING OF FAILURE CRITERIA.
C
   DO 2040 NN=NN1,NN2
   IF(STIR(NN,1)) 2040,2040,2030
2030 JJS1=NODSTR(NN,1)
   JJS2=NODSTR(NN,2)
   BNR=STIR(NN,3)*.017453
   XXE(1,1)=ABS(U1(2*JJS2-1)-U1(2*JJS1-1))
   XXE(1,2)=ABS(U1(2*JJS2)-U1(2*JJS1))
   RATIO=XXE(1,2)/XXE(1,1)
   ANGLE=ATAN(RATIO)
   XXE(1,2)=SQRT(XXE(1,1)**2+XXE(1,2)**2)
   XXE(1,1)=XXE(1,2)*COS(ANGLE-BNR)
   ANGLE=XXE(1,1)/STIR(NN,2)
   IF(ANGLE-EY) 2060,2050,2050
2050 STIR(NN,1)=0.0
   WRITE(6,2070) NN
   GO TO 2040
2060 STIFF=E1(2)*STIR(NN,1)/STIR(NN,2)
   CO=COS(BNR)
   S=SIN(BNR)
C
   SKS(1,1)=STIFF*CO*CO
   SKS(1,2)=STIFF*CO*S
   SKS(1,3)=-STIFF*CO*CO
   SKS(1,4)=-SKS(1,2)
```

```
      SKS(2,1)=SKS(1,2)
      SKS(2,2)=STIFF*S*S
      SKS(2,3)=-SKS(1,2)
      SKS(2,4)=-SKS(2,2)
      SKS(3,1)=SKS(1,3)
      SKS(3,2)=-SKS(1,2)
      SKS(3,3)=SKS(1,1)
      SKS(3,4)=SKS(1,2)
      SKS(4,1)=-SKS(1,2)
      SKS(4,2)=-SKS(2,2)
      SKS(4,3)=SKS(1,2)
      SKS(4,4)=SKS(2,2)
C
      DO 2039 LL=1,2
      DO 2038 KK=1,2
      IF(NODSTR(NN,KK)-K) 2038,2080,2080
 2080 IF(NODSTR(NN,KK)-L) 2090,2090,2038
 2090 M=2*(NODSTR(NN,KK)-K)
      N=2*(NODSTR(NN,LL)-K)
      I=2*(KK-1)
      J=2*(LL-1)
      IF(N) 2039,2039,2100
 2100 DO 2110 NJ=1,2
      DO 2110 MI=1,2
      MMI=M+MI
      NNJ=N+NJ
      IMI=I+MI
      JNJ=J+NJ
 2110 ST(MMI,NNJ)=ST(MMI,NNJ)+SKS(IMI,JNJ)
 2038 CONTINUE
 2039 CONTINUE
 2040 CONTINUE
 2010 IF(NCHK(II)) 3010,3010,3020
C
C    ADDITION  OF  SPRING  STIFFNESS  MATRIX  TO  GLOBAL  STIFFNESS
MATRIX AND
C  CHECKING OF FAILURE CRITERIA.
C
 3020 DO 3030 LKS=NSST,NSEN
      ANGE=BN(LKS)*.017453
      JJS1=NODS(LKS,1)
      JJS2=NODS(LKS,2)
      IF(IBREAK(LKS).EQ.1) GO TO 3040
      XE(1,1)=ABS(U1(2*JJS2-1)-U1(2*JJS1-1))
      XE(1,2)=ABS(U1(2*JJS2)-U1(2*JJS1))
      IF(XE(1,1).EQ.0.) GO TO 3021
```

```
      RATIO=XE(1,2)/XE(1,1)
3021 RATIO=0.
   ANGLE=ATAN(RATIO)
   XE(1,2)=SQRT(XE(1,1)**2+XE(1,2)**2)
    XE(1,1)=XE(1,2)*COS(ANGLE-ANGE)
   AAREA=1.5708*BNUM(LKS)*WDT(LKS)*DIA(LKS)/BTH
   IF(NYMT(LKS).EQ.1) SLIP=.000449
   IF(NYMT(LKS).EQ.2) SLIP=.000449
   CHECK=XE(1,1)-SLIP
   IF(CHECK) 3050,3040,3040
3040 SKB=0.0
   SK=0.0
   XXE(1,1)=SLIP
   XE(1,1)=SLIP
   GO TO 3060
3050 XXE(1,1)=ABS(U4(2*JJS2-1)-U4(2*JJS1-1))
   XXE(1,2)=ABS(U4(2*JJS2)-U4(2*JJS1))
   IF(XXE(1,1).EQ.0.) GO TO 3051
   RATIO=XXE(1,2)/XXE(1,1)
3051 RATIO=0.
   ANGLE=ATAN(RATIO)
   XXE(1,2)=SQRT(XXE(1,1)**2+XXE(1,2)**2)
   XXE(1,1)=XXE(1,2)*COS(ANGLE-ANGE)
   IF(XXE(1,1)-SLIP) 3070,3080,3080
3080 CONTINUE
   XXE(1,1)=(SLIP+XE(1,1))*0.5
   IBREAK(LKS)=2
3070 CONTINUE
   IF(NYMT(LKS).EQ.2) GO TO 3059
   IF(NYMT(LKS).EQ.1.AND.BN(LKS).EQ.90.) GO TO 3059
   IF(NUNIT.EQ.2) THEN
     XXE(1,1)=.03937*XXE(1,1)
     SK=0.3606E+07-XXE(1,1)*0.10712E+11+(XXE(1,1)**2)*0.5898E+13
     SKB=SK*AAREA*.00155
     SKB=.175126*SKB
     ELSE
     SK=0.3606E+07-XXE(1,1)*0.10712E+11+(XXE(1,1)**2)*0.5898E+13
     SKB=SK*AAREA
   ENDIF
   GO TO 3060
3059 IF(NUNIT.EQ.1) THEN
   SK=0.3606E+07-XXE(1,1)*0.10712E+11+(XXE(1,1)**2)*0.5898E+13
   SKB=SK*AAREA
   IF(BNUM(LKS).EQ.0.) SKB=SK*BTH*WDT(LKS)
   ELSE
   XXE(1,1)= 25.*XXE(1,1)
```

```fortran
      SK=0.3606E+07-XXE(1,1)*0.10712E+11+(XXE(1,1)**2)*0.5898E+13
      SKB=SK*BTH*WDT(LKS)
      SKB=5.7101744*SKB
      END IF
 3060 CONTINUE
      IF(DIA(LKS).NE.0.) SKD=E1(1)*BNUM(LKS)*DIA(LKS)*WDT(LKS)/BTH
      IF(DIA(LKS).EQ.0.) SKD=E1(1)*BTH*WDT(LKS)
      WRITE(6,3090) LKS,SK,SKB,XXE(1,1),XE(1,1),SKD
      CO=COS(ANG)
      S=SIN(ANG)
C
      SKS(1,1)=SKB*(CO**2)+SKD*(S**2)
      SKS(1,2)=SKB*CO*S-SKD*CO*S
      SKS(1,3)=-SKB*(CO**2)-SKD*(S**2)
      SKS(1,4)=-SKS(1,2)
      SKS(2,1)=SKS(1,2)
      SKS(2,2)=SKB*(S**2)+SKD*(CO**2)
      SKS(2,3)=-SKS(1,2)
      SKS(2,4)=-SKB*(S**2)-SKD*(CO**2)
      SKS(3,1)=SKS(1,3)
      SKS(3,2)=SKS(2,3)
      SKS(3,3)=SKS(1,1)
      SKS(3,4)=SKS(1,2)
      SKS(4,1)=-SKS(1,2)
      SKS(4,2)=SKS(2,4)
      SKS(4,3)=SKS(1,2)
      SKS(4,4)=SKS(2,2)
C
      JJS3=2*(JJS1-K)+1
      IF(ST(JJS3,JJS3)) 3100,3030,3100
 3100 DO 3029 LL=1,2
      DO 3028 KK=1,2
      IF(NODS(LKS,KK)-K) 3028,3110,3110
 3110 IF(NODS(LKS,KK)-L) 3120,3120,3028
 3120 M=2*(NODS(LKS,KK)-K)
      N=2*(NODS(LKS,LL)-K)
      I=2*(KK-1)
      J=2*(LL-1)
      IF(N) 3029,3130,3130
 3130 DO 3140 NJ=1,2
      DO 3140 MI=1,2
      MMI=M+MI
      NNJ=N+NJ
      IMI=I+MI
      JNJ=J+NJ
 3140 ST(MMI,NNJ)=ST(MMI,NNJ)+SKS(IMI,JNJ)
```

```
 3028 CONTINUE
 3029 CONTINUE
 3030 CONTINUE
C
C   ADDITION OF PRESCRIBED BOUNDARY CONDITIONS TO GLOBAL
STIFFNESS MATRIX
C
 3010 DO 4010 I=1,NBOUN
     M=NF(I)-K
     MM=NF(I)-1
     IF(M) 4010,4020,4020
 4020 IF(M-499) 4030,4030,4010
 4030 DO 4040 J=1,NFREE
     IF(NB(I,J)) 4040,4060,4040
 4060 NMI=NFREE*M+J
     ST(NMI,NMI) = ST(NMI,NMI)*.1E+12
     DO 4050 JJ=1,NCOLN
     JNJ=NFREE*MM+J
 4050 U(JNJ,JJ)=ST(NMI,NMI)*BV(I,J)
 4040 CONTINUE
 4010 INTER=NEN
     MI=NFREE*MINUS + 1
     NJ=NFREE*L
     M=NJ-MI+1
     IF(II-NPART) 4070,4080,4070
 4070 NA=NFREE*(NLAST(II+1)-MINUS)
     GO TO 4090
 4080 NA=M+1
 4090 N=NA-M
     MM=M+1
C
C   ADDITION OF ARBITRARY STIFFNESS TO ACCOUNT FOR ISOLATED
JOINTS.
C
     DO 4100 I=1,M
     IF(ST(I,I)-0.) 4100,4110,4100
 4110 ST(I,I)=ST(I,I)+0.1E+18
 4100 CONTINUE
 5000 WRITE(4) M,N,((ST(I,J),I=1,M),J=1,M),((ST(I,J),I=1,M),J=MM,NA),
    1  ((U(I,J),I=MI,NJ),J=1,NCOLN)
     REWIND 1
     REWIND 2
     REWIND 3
     REWIND 4
C
C  SOLUTION OF EQUATIONS OF EQUILIBRIUM
```

```
C
      CALL SOLVE(NPART,NCOLN)
      REWIND 3
C
C  CALCULATION OF ELEMENT STRESSES AND STRAINS, CHECKING OF
FAILURE
C  CRITERIA, AND ADDING ELEMENT NODAL FORCES TO LOAD MATRIX IF
REQUIRED.
C
      CALL                                                    STRESS
(NPART,NFIRST,NLAST,NCOLN,NELEM,NOD,NFREE,NPOIN,
     1 THICK,EY,ESTHR,SEF,NBRK,RUPTR,STRAIN)
      WRITE(6,6440)
C
C   CALCULATION  OF  BOND  SPRING  STRESSES  AND  FORCES,  AND
ADDING OF SPRING
C  NODAL FORCES TO LOAD MATRIX IF FAILURE HAS OCCURRED.
C
      DO 6000 I3=1,NPART
      IF(NCHK(I3)) 6000,6000,6010
 6010 NSST=NSPGST(I3)
      NSEN=NSPGED(I3)
      DO 6001 LKS=NSST,NSEN
      ANG=BN(LKS)*.017453
      JJS1=NODS(LKS,1)
      JJS2=NODS(LKS,2)
      XXE(1,1)=U1(2*JJS2-1)-U1(2*JJS1-1)
      XXE(1,2)=U1(2*JJS2)-U1(2*JJS1)
      IF(IBREAK(LKS).EQ.1) GO TO 6140
      XE(1,1)=ABS(U1(2*JJS2-1)-U1(2*JJS1-1))
      XE(1,2)=ABS(U1(2*JJS2)-U1(2*JJS1))
      RATIO=XE(1,2)/XE(1,1)
      ANGLE=ATAN(RATIO)
      XE(1,2)=SQRT(XE(1,1)**2+XE(1,2)**2)
      XE(1,1)=XE(1,2)*COS(ANGLE-ANG)
      IF(NUNIT.EQ.1.AND.NYMT(LKS).EQ.1) THEN
      BSTRS(LKS)=XE(1,1)*0.3606E+07-(XE(1,1)**2)*0.5356E+10+(XE(1,1)
     $**3)*0.1986E+13
      END IF
      IF(NUNIT.EQ.2.AND.NYMT(LKS).EQ.1) THEN
        XE(1,1)=.039*XE(1,1)
        BSTRS(LKS)=XE(1,1)*0.3606E+07-(XE(1,1)**2)*0.5356E+10+(XE(1,1)
     $**3)*0.1986E+13
      END IF
      IF(NUNIT.EQ.1.AND.NYMT(LKS).EQ.2) THEN
      BSTRS(LKS)=XE(1,1)*0.3606E+07-(XE(1,1)**2)*0.5356E+10+(XE(1,1)
```

```
      $**3)*0.1986E+13
       END IF
      IF(NUNIT.EQ.2.AND.NYMT(LKS).EQ.2) THEN
       XE(1,1)=.039*XE(1,1)
        END IF
      IF(NUNIT.EQ.2.AND.NYMT(LKS).EQ.2)THEN
       BSTRS(LKS)=XE(1,1)*0.3606E+07-(XE(1,1)**2)*0.5356E+10+(XE(1,1)
      $**3)*0.1986E+13
       END IF
       FRICTN=0.
       IF(NYMT(LKS).EQ.1)
      1BFORCE=BSTRS(LKS)*WDT(LKS)*1.5708*DIA(LKS)*BNUM(LKS)
       IF(NYMT(LKS).EQ.2)
      1BFORCE=BSTRS(LKS)*WDT(LKS)*BTH
       CONTINUE
       BFORPC= BFORCE*COS(ANG)
       BFORPS= BFORCE*SIN(ANG)
       CHECK=XE(1,1)-SLIP
       IF(IBREAK(LKS).EQ.2) GO TO 6130
       IF(CHECK) 6020,6130,6130
 6020 IF(NSSS(LKS)) 6040,6030,6040
 6030 IF(ICLKS(LKS)-4) 6050,6100,6050
 6040 IF(ICLKS(LKS)-8) 6050,6100,6050
 6050 DO 6060 LI=1,NELEM
       IF(NEP(LI)-1) 6060,6070,6060
 6070 DO 6059 IK=1,3
       IF(NOD(LI,IK)-NODS(LKS,1)) 6059,6080,6059
 6080 IF(THICK(LI)) 6060,6090,6060
 6090 ICLKS(LKS)=ICLKS(LKS)+1
 6059 CONTINUE
 6060 CONTINUE
       IF(NSSS(LKS)) 6110,6120,6110
 6120 IF(ICLKS(LKS)-4) 6460,6130,6460
 6110 IF(ICLKS(LKS)-8) 6460,6130,6460
 6130 IBREAK(LKS)=1
       ITAG(1)=ITAG(1)+1
 6140 XE(1,1)=SLIP
       IF(NSSS(LKS)) 6150,6150,6160
 6150 IF(U2(LKS)) 6180,6170,6180
 6170 IF(XXE(1,1)) 6200,6190,6190
 6190 U(2*JJS1-1,1)=U(2*JJS1-1,1)-BFORPC
       U(2*JJS2-1,1)=U(2*JJS2-1,1)+BFORPC
       GO TO 6210
 6200 U(2*JJS1-1,1)=U(2*JJS1-1,1)+BFORPC
       U(2*JJS2-1,1)=U(2*JJS2-1,1)-BFORPC
 6210 IF(XXE(1,2)) 6230,6220,6220
```

```
6220 U(2*JJS1,1)=U(2*JJS1,1)-BFORPS
     U(2*JJS2,1)=U(2*JJS2,1)+BFORPS
     GO TO 6180
6230 U(2*JJS1,1)=U(2*JJS1,1)+BFORPS
     U(2*JJS2,1)=U(2*JJS2,1)-BFORPS
6180 U2(LKS)=1.0
     BSTRS(LKS)=0.0
     GO TO 6100
6160 IF(U2(LKS)) 6240,6240,6320
6240 CONTINUE
     IF(NUNIT.EQ.1.AND.NYMT(LKS).EQ.1) THEN
     BSTRS(LKS)=720.
     IF(NUNIT.EQ.1.AND.NYMT(LKS).EQ.2) THEN
     BSTRS(LKS)=400.
     IF(NUNIT.EQ.2.AND.NYMT(LKS).EQ.1) THEN
      BSTRS(LKS)=4.96
      IF(UNIT.EQ.2.AND.NYMT(LKS).EQ.2) THEN
        BSTRS(LKS)=2.76
        END IF
        END IF
        END IF
        END IF
     IF(XXE(1,1)) 6260,6250,6250
6250 U(2*JJS1-1,1)=U(2*JJS1-1,1)-BFORPC+FRICTN*COS(ANG)
     U(2*JJS2-1,1)=U(2*JJS2-1,1)+BFORPC-FRICTN*COS(ANG)
     GO TO 6270
6260 U(2*JJS1-1,1)=U(2*JJS1-1,1)+BFORPC-FRICTN*COS(ANG)
     U(2*JJS2-1,1)=U(2*JJS2-1,1)-BFORPC+FRICTN*COS(ANG)
     IF(NUNIT.EQ.1.AND.NYMT(LKS).EQ.1) THEN
     BSTRS(LKS)=-720.
     END IF
     IF(NUNIT.EQ.1.AND.NYMT(LKS).EQ.2) THEN
     BSTRS(LKS)=-400.
     END IF
     IF(NUNIT.EQ.2.AND.NYMT(LKS).EQ.1) THEN
      BSTRS(LKS)=-4.96
     END IF
      IF(NUNIT.EQ.2.AND.NYMT(LKS).EQ.2) THEN
        BSTRS(LKS)=-2.76
        END IF
6270 IF(XXE(1,2)) 6290,6280,6280
6280 U(2*JJS1,1)=U(2*JJS1,1)-BFORPS+FRICTN*SIN(ANG)
     U(2*JJS2,1)=U(2*JJS2,1)+BFORPS-FRICTN*SIN(ANG)
     GO TO 6300
6290 U(2*JJS1,1)=U(2*JJS1,1)+BFORPS-FRICTN*SIN(ANG)
     U(2*JJS2,1)=U(2*JJS2,1)-BFORPS+FRICTN*SIN(ANG)
```

```
      IF(BFORPC-BFORPS) 6310,6300,6300
6310 CONTINUE
      IF(NUNIT.EQ.1.AND.NYMT(LKS).EQ.1) THEN
      BSTRS(LKS)=-720.
      END IF
      IF(NUNIT.EQ.1.AND.NYMT(LKS).EQ.2) THEN
      BSTRS(LKS)=-400.
      END IF
      IF(NUNIT.EQ.2.AND.NYMT(LKS).EQ.1) THEN
       BSTRS(LKS)=-4.96
       END IF
       IF(NUNIT.EQ.2.AND.NYMT(LKS).EQ.2) THEN
        BSTRS(LKS)=-2.76
        END IF
      GO TO 6300
6320 IF(XXE(1,1)) 6350,6340,6340
6340 U(2*JJS1-1,1)=U(2*JJS1-1,1)+FRICTN*COS(ANG)
      U(2*JJS2-1,1)=U(2*JJS2-1,1)-FRICTN*COS(ANG)
      GO TO 6360
6350 U(2*JJS1-1,1)=U(2*JJS1-1,1)-FRICTN*COS(ANG)
      U(2*JJS2-1,1)=U(2*JJS2-1,1)+FRICTN*COS(ANG)
6360 IF(XXE(1,2)) 6380,6370,6370
6370 U(2*JJS1,1)=U(2*JJS1,1)+FRICTN*SIN(ANG)
      U(2*JJS2,1)=U(2*JJS2,1)-FRICTN*SIN(ANG)
      GO TO 6300
6380 U(2*JJS1,1)=U(2*JJS1,1)-FRICTN*SIN(ANG)
      U(2*JJS2,1)=U(2*JJS2,1)+FRICTN*SIN(ANG)
6300 U2(LKS)=1.0
6100 IF (NYMT(LKS).EQ.1) THEN
      BFORCE=BSTRS(LKS)*WDT(LKS)*1.5708*DIA(LKS)*BNUM(LKS)
      ELSE
      BFORCE=BSTRS(LKS)*WDT(LKS)*BTH
      END IF
      GO TO 6430
6460 IF(BFORPC-BFORPS) 6410,6390,6390
6390 IF(XXE(1,1)) 6400,6430,6430
6400 BSTRS(LKS)=-BSTRS(LKS)
      BFORCE=-BFORCE
      GO TO 6430
6410 IF(XXE(1,2)) 6420,6430,6430
6420 BSTRS(LKS)=-BSTRS(LKS)
      BFORCE=-BFORCE
6430 BSTRS1=BSTRS(LKS)/WDT(LKS)
      BFOR=BFORCE/WDT(LKS)
      WRITE(6,6450) LKS,BSTRS(LKS),BSTRS1,BFORCE,BFOR,XE(1,1)
C
```

```
C  POSITIVE BOND FORCE = POSITIVE FORCE ON CONCRETE.
C
 6001 CONTINUE
 6000 CONTINUE
    WRITE(6,6470) ITAG(1),LD
 290 FORMAT('1','LOADING STEP',I4,5X,'ITERATION NO.',I4//'    LKS',8X,
   1'SK',12X,'SKB',10X,'XXE(1,1)',6X,'XE(1,1)',11X,'SKD'//)
 6440 FORMAT(/'0',' ELEMENT    BOND STRESS    STRESS/LTH    BOND
FORCE
   2    FORCE/LTH         SLIP')
 6450 FORMAT(I8,4(F15.4,10X),10X,E12.5)
 3090 FORMAT(' ',I8,3X,5(E12.5,3X))
 6470  FORMAT('0',I14,'  SPRING  ELEMENTS  BROKEN  DURING  LOADING
STEP',I3)
 2070 FORMAT(1H ,'STIRRUP NUMBER',I4,'  HAS REACHED YIELD')
C
C  USE ARITHMETIC 'IF' STATEMENT HERE TO LIMIT DEFLECTIONS OF
STRUCTURE
C
 300 CONTINUE
 7000 STOP
    END
C
C
    SUBROUTINE
STRESS(NPART,NFIRST,NLAST,NCOLN,NELEM,NOD,NFREE,NPOIN,
   1 THICK,EY,ESTHR,SEF,NBRK,RUPTR,STRAIN)
C
C  SUBROUTINE TO FIND TOTAL STRESSES AND STRAINS IN ELEMENTS
AND TO
C  CHECK FAILURE CRITERIA.
C
    IMPLICIT DOUBLE PRECISION(A-H,O-Z)
    DIMENSION NOD(2000,3),THICK(2000),STRAIN(2000,2),NFIRST(15),
   1NLAST(15),D(3000),NBRK(1),Z(6,1),TZ(6,1),D1(3,3),BB(3,6),XE(3,2)
    COMMON C(6,6),DBA(3,6),DB(3,6),A(6,6),ST(1000,2000),U(3000,4),
   1U1(3000),B(3,6),TSTRES(2000,3,1),TSRN(2000,3,1),U2(800),U3(6),
   2U4(3000),T1(2000)
    NBRK(1)=0
    DO 10 II=1,NPART
    JJ=NPART+1-II
    M=NFREE*(NFIRST(JJ) - 1) + 1
    N= NFREE*NLAST(JJ)
 10 READ(3) ((U(I,J),I=M,N),J=1,NCOLN)
    NPOIN2=2*NPOIN
    DO 20 I=1,NPOIN2
```

```
        U1(I)=U1(I)+U(I,1)
        U4(I)=U1(I)+0.7*U(I,1)
        D(I)=U(I,1)
   20 U(I,1)=0.0
        WRITE(6,600)
        WRITE(6,610) (I,U1(2*I-1),U1(2*I),I=1,NPOIN)
        WRITE(6,620)
C
C   ADDITION OF INCREMENTAL STRESSSES AND STRAINS TO TOTAL
STRESS AND
C  STRAIN MATRICES.
C
        DO 1000 LL=1,NELEM
        READ (1)  ((DBA(I,J),I=1,3),J=1,6),ORX,ORY
       1,YM1,YM2,PR1,PR2,G,JEP,C
        DO 30 I=1,3
        JJ=NOD(LL,I)
        TZ(2*I-1,1)=U1(2*JJ-1)
        TZ(2*I,1)=U1(2*JJ)
        Z(2*I - 1,1) = D(2*JJ - 1)
   30 Z(2*I,1)=D(2*JJ)
        IF((JEP-1).EQ.1.AND.THICK(LL).EQ.0) GO TO 60
        DO 40 J=1,NCOLN
        DO 40 I=1,3
        DB(I,J)=0.
        DO 40 K=1,6
        U3(K)=0.0
   40 DB(I,J)=DB(I,J)+DBA(I,K)*Z(K,J)
        DO 50 I=1,3
        DO 50 J=1,NCOLN
   50 TSTRES(LL,I,J)=TSTRES(LL,I,J)+DB(I,J)
   60 D1(1,1)=1.0/YM1
        D1(1,2)=-PR2/YM2
        D1(1,3)=0.
        D1(2,2)=1.0/YM2
        D1(2,1)=-PR1/YM1
        D1(2,3)=0.
        D1(3,1)=0.
        D1(3,2)=0.
        D1(3,3)=1.0/G
        DO 70 I=1,3
        DO 70 J=1,6
        BB(I,J)=0.
        DO 70 K=1,3
   70 BB(I,J)=BB(I,J)+D1(I,K)*DBA(K,J)
        DO 80 I=1,3
```

```fortran
      DO 80 J=1,6
   80 TSRN(LL,I,1)=TSRN(LL,I,1)+BB(I,J)*Z(J,1)
      DO 90 I=1,3
      DO 90 J=1,NCOLN
   90 DB(I,J)=TSTRES(LL,I,J)
      CALL PRIN(DB,A,NCOLN)
      STRAIN(LL,1)=A(1,1)/YM1-PR2*A(2,1)/YM2
      STRAIN(LL,2)=A(2,1)/YM2-PR1*A(1,1)/YM1
      TA=STRAIN(LL,1)
      TB=STRAIN(LL,2)
      WRITE(6,630)LL,ORX,ORY,((DB(I,J),I=1,3),(A(I,J),I=1,3),J=1,NCOLN),
     1(TSRN(LL,I,1),I=1,3),STRAIN(LL,1),STRAIN(LL,2),YM1
  150 IF(JEP-1) 160,160,420
C
C    CHECK  FAILURE  CRITERIA  FOR  CONCRETE  ELEMENTS,AND  ADD
NODAL FORCES
C  TO LOAD MATRIX IF NECESSARY
C
  160 IF(A(1,1)) 170,170,190
  170 IF(TA) 180,180,210
  180 IF(ABS(TA)-SEF) 210,340,340
  190 CHECK=A(1,1)-RUPTR
      IF(CHECK) 210,200,200
  200 IF(THICK(LL).EQ.0.0) GO TO 330
      WRITE(6,640)
      GO TO 260
  210 IF(A(2,1)) 220,220,240
  220 IF(TB) 230,230,1000
  230 IF(ABS(TB)-SEF) 1000,340,340
  240 CHECK=A(2,1)-RUPTR
      IF(CHECK) 1000,250,250
  250 IF(THICK(LL).EQ.0.0) GO TO 330
      WRITE(6,720)
  260 DO 270 I=1,6
      DO 270 J=1,6
  270 U3(I)=U3(I)+C(I,J)*TZ(J,1)
      DO 280 I=1,3
      JJ=NOD(LL,I)
      U(2*JJ-1,1)=U(2*JJ-1,1)+U3(2*I-1)
  280 U(2*JJ,1)=U(2*JJ,1)+U3(2*I)
      THICK(LL)=0.0
      NBRK(1)=NBRK(1)+1
      GO TO 1000
  330 WRITE(6,650)
      GO TO 1000
  340 IF(THICK(LL).EQ.0.0) GO TO 410
```

```
      WRITE(6,660)
      DO 350 I=1,6
      DO 350 J=1,6
  350 U3(I)=U3(I)+C(I,J)*TZ(J,1)
      DO 360 I=1,3
      JJ=NOD(LL,I)
      U(2*JJ-1,1)=U(2*JJ-1,1)+1.0*U3(2*I-1)
  360 U(2*JJ,1)=U(2*JJ,1)+1.0*U3(2*I)
      THICK(LL)=0.0
      GO TO 1000
  410 WRITE(6,670)
      GO TO 1000
C
C  CHECK FAILURE CRITERIA FOR STEEL ELEMENTS
C
  420 IF(THICK(LL)) 490,490,430
  430 IF(T1(LL)) 440,440,1000
  440 IF(ABS(TA)-EY) 450,460,460
  450 IF(ABS(TB)-EY) 1000,460,460
  460 T1(LL)=THICK(LL)
      THICK(LL)=0.0
      WRITE(6,680)
      GO TO 1000
  490 WRITE(6,690)
      IF(ABS(TA)-ESTHR) 500,510,510
  500 IF(ABS(TB)-ESTHR) 1000,510,510
  510 THICK(LL)=T1(LL)
      WRITE(6,700)
 1000 CONTINUE
      WRITE(6,710) RUPTR,NBRK(1)
C
  600  FORMAT('0',8H        NODE,17H    X-DISPLACEMENTS,17H    Y-
DISPLACEMENTS)
  610 FORMAT(1H ,3(4X,'(',I3,')',1X,2E16.8))
  620  FORMAT('0','ELE    CENTROID     CARTESIAN STRESSES    PRIN
STRESS
    2ES  PRIN',9X,'CARTESIAN STRAINS',12X,'PRINCIPAL STRAINS',8X,'YM',/
    3,' NO. XCORD YCORD    X    Y    XY STRES1 STRES2  ANG
    4   EX',10X,'EY',10X,'EXY',9X,'E1',10X,'E2')
  630 FORMAT(' ',I3,3X,F8.2,3X,F6.2,5F8.2,F5.0,3E12.3,2E12.3,F12.0)
  640 FORMAT('    NEW TENSILE CRACK NORMAL TO 1-1 DIRECTION')
  650 FORMAT('    ELEMENT CRACKED PREVIOUSLY')
  660 FORMAT('     CONCRETE ELEMENT REACHES MAX COMPRESSIVE
STRAIN')
  670 FORMAT('    CONCRETE ELEMENT CRUSHED PREVIOUSLY')
  680 FORMAT('    STEEL ELEMENT HAS REACHED YIELD')
```

```
  690 FORMAT('    STEEL ELEMENT IN YIELD PLATEAU')
  700 FORMAT('    STEEL ELEMENT HAS REACHED STRAIN HARDENING')
  710  FORMAT('0','MOD.   OF   RUPTR=',F9.2,8X,'NO.   OF   ELEMENTS
 BROKEN=',I3)
  720 FORMAT('    NEW TENSILE CRACK NORMAL TO 2-2 DIRECTION')
     RETURN
     END
C
C
C
C
C
     SUBROUTINE PRIN(DB,A,NCOLN)
C
C  SUBROUTINE TO CALCULATE PRINCIPAL STRESSES OF TRIANGULAR
ELEMENTS.
C
     IMPLICIT DOUBLE PRECISION(A-H,O-Z)
     DIMENSION DB(3,6),A(6,6)
     COMP=0.
     DO 3 J=1,NCOLN
     T1=(DB(1,J) + DB(2,J))/2.
     T2=((DB(1,J)-DB(2,J))/2.)**2
     T3=(DB(3,J))**2
     T4=2.*DB(3,J)/(DB(1,J)-DB(2,J))
     A(1,J)=T1 + SQRT(T2+T3)
     A(2,J) = T1 - SQRT(T2+T3)
     THA=0.5*ATAN(T4)
     THB=THA + 0.5*3.14159
     SIG = T1+SQRT(T2)*COS(2.*THA) + SQRT(T3)*SIN(2.*THA)
     COMP= ABS(A(1,J)-SIG)-.0001
     IF(COMP.LE.0.) THEN
     A(3,J)=THA*180./3.14159
     ELSE
     A(3,J)=THB*180./3.14159
     END IF
   3 CONTINUE
     RETURN
     END
C
C
C
     SUBROUTINE FEM(XE,YM1,YM2,PR1,PR2,G,ANG,NP,TH,MM,JEP,LK)
C
C  SUBROUTINE TO FORMULATE ELEMENT STIFFNESS MATRIX.
C
```

```
      IMPLICIT DOUBLE PRECISION(A-H,O-Z)
      DIMENSION D(3,3),BTDBA(6,6),XE(3,2),R(6,6),ZX(3),ZY(3),R1(3,3)
      COMMON C(6,6),DBA(3,6),DB(3,6),A(6,6),ST(1000,2000),U(3000,4),
     1U1(3000),B(3,6),TSTRES(2000,3,1),TSRN(2000,3,1),U2(800),U3(6),
     2U4(3000),T1(2000)
      DO 20 J=1,6
      DO 10 I=1,3
      B(I,J)=0.
      DB(I,J)=0.
   10 DBA(I,J)=0.0
      DO 20 I=1,6
      R(I,J)=0.
      A(I,J)=0.
      BTDBA(I,J)=0.
   20 C(I,J)=0.
      DO 30 J=1,3
      DO 30 I=1,3
   30 D(I,J)=0.0
      ORX=(XE(1,1) + XE(2,1) + XE(3,1))*.333333
      ORY=(XE(1,2) + XE(2,2) + XE(3,2))*.333333
      IF(TH) 40,40,50
   40 IF(JEP-1) 60,60,50
   50 DO 70 I=1,3
      XE(I,1) = XE(I,1)-ORX
   70 XE(I,2)=XE(I,2)-ORY
      IF(TH.EQ.0.AND.JEP.EQ.2) GO TO 80
      GO TO 90
C
C    ELASTIC PROPERTIES OF STEEL ELEMENTS ARE ALTERED IF
ELEMENT IS IN
C  YIELD PLATEAU.
C
   80 TH=T1(LK)
      YM1=10.
      YM2=10.
      PR1=.30
      PR2=.30
      G=YM1/(2.0*(1.+PR1))
   90 ZX(1)=XE(2,2)-XE(3,2)
      ZX(2)= XE(3,2)-XE(1,2)
      ZX(3)= XE(1,2)-XE(2,2)
      ZY(1) = XE(3,1)-XE(2,1)
      ZY(2) = XE(1,1)-XE(3,1)
      ZY(3) = XE(2,1)-XE(1,1)
      ZK=XE(2,1)*XE(3,2) - XE(3,1)*XE(2,2)
      Z=3.*ZK
```

```
C
      A(1,1) = ZK/Z
      A(2,1)=ZX(1)/Z
      A(3,1)=ZY(1)/Z
      A(4,2)=A(1,1)
      A(5,2)=A(2,1)
      A(6,2)=A(3,1)
      A(1,3)=ZK/Z
      A(2,3)=ZX(2)/Z
      A(3,3)=ZY(2)/Z
      A(4,4)=A(1,3)
      A(5,4)=A(2,3)
      A(6,4)=A(3,3)
      A(1,5)=ZK/Z
      A(2,5)=ZX(3)/Z
      A(3,5)=ZY(3)/Z
      A(4,6)=A(1,5)
      A(5,6)=A(2,5)
      A(6,6)=A(3,5)
      B(1,2)=1.
      B(3,3)=1.
      B(3,5)=1.
      B(2,6)=1.
      DEN=(1.-PR1*PR2)
C
C  ELASTICITY MATRIX FOR PLANE STRESS CASE.
C
      D(1,1)=YM1/DEN
      D(2,1)=PR1*YM2/DEN
      D(1,2)=PR2*YM1/DEN
      D(2,2)=YM2/DEN
      D(3,3)=G
      IF(ANG) 100,110,100
  100 CS=COS(ANG*.017453)
      SS=SIN(ANG*.017453)
C
      R(1,1)=CS**2
      R(2,1)=SS**2
      R(3,1)=SS*CS
      R(1,2)=R(2,1)
      R(2,2)=R(1,1)
      R(3,2)=-R(3,1)
      R(1,3)=2.*R(3,2)
      R(2,3)=2.*R(3,1)
      R(3,3)=R(1,1) - R(2,1)
C
```

```
      DO 120 J=1,3
      DO 120 I=1,3
      R1(I,J)=0.
      DO 120 K=1,3
  120 R1(I,J)=R1(I,J)+D(I,K)*R(J,K)
      DO 130 J=1,3
      DO 130 I=1,3
      D(I,J)=0.
      DO 130 K=1,3
  130 D(I,J)=D(I,J)+R(I,K)*R1(K,J)
  110 DO 140 J=1,6
      DO 140 I=1,3
      DO 140 K=1,3
  140 DB(I,J)=DB(I,J)+D(I,K)*B(K,J)
      DO 150 J=1,6
      DO 150 I=1,3
      DO 150 K=1,6
  150 DBA(I,J)=DBA(I,J)+DB(I,K)*A(K,J)
      VOL=.5*TH*Z
C
      DO 160 J=1,6
      DO 160 I=1,6
      DO 160 K=1,3
  160 BTDBA(I,J)=BTDBA(I,J)+B(K,I)*DBA(K,J)*VOL
C
C  STIFFNESS MATRIX C IS FORMED.
C
      DO 170 J=1,6
      DO 170 I=1,6
      DO 170 K=1,6
  170 C(I,J)=C(I,J)+A(K,I)*BTDBA(K,J)
   60 IF(MM) 190,190,180
C
  180 WRITE(1) ((DBA(I,J),I=1,3),J=1,6),ORX,ORY
     1,YM1,YM2,PR1,PR2,G,JEP,C
  190 RETURN
      END
C
C
C
C
C
      SUBROUTINE SOLVE(NPART,NCOLN)
C
C  SUBROUTINE FOR SOLUTION OF EQUATIONS OF EQUILIBRIUM.
C
```

```
      IMPLICIT DOUBLE PRECISION(A-H,O-Z)
      DIMENSION AM(1000,1000),BM(1000,1000),YM(1000,1000),TF(1000,4),
     1RS(1000,4),F(1000,4),  DIS(1000,4)
      COMMON C(6,6),DBA(3,6),DB(3,6),A(6,6),ST(1000,2000),U(3000,4),
     1U1(3000),B(3,6),TSTRES(2000,3,1),TSRN(2000,3,1),U2(800),U3(6),
     2U4(3000),T1(2000)
      EQUIVALENCE(AM(1,1),ST(1,1)),(BM(1,1),ST(1,1001)),(TF(1,1),
     1U(1,1)),  (DIS(1,1),U(1,2)),(RS(1,1),U(1,3)),(F(1,1),U(1,4))
      DO 20 I=1,1000
      DO 10 J=1,NCOLN
      TF(I,J)=0.
 10 RS(I,J)=0.0
      DO 20 J=1,1000
 20 YM(I,J)=0.0
      DO 160 LL=1,NPART
      READ(4) M,N,((AM(I,J),I=1,M),J=1,M),((BM(I,J),I=1,M),J=1,N),
     1  ((F(I,J),I=1,M),J=1,NCOLN)
      DO 110 I=1,M
      DO 100 J=1,NCOLN
      F(I,J)=F(I,J)-TF(I,J)
100 DIS(I,J)=F(I,J)
      DO 110 J=1,M
110 AM(I,J)=AM(I,J)-YM(I,J)
      CALL DCOMP(M,AM,LL)
      CALL INVERT(M,AM)
      CALL MATM(AM,F,DIS,M,M,NCOLN)
      WRITE(2) M,N,((AM(I,J),I=1,M),J=1,M),((BM(I,J),I=1,M),J=1,N),
     1  ((F(I,J),I=1,M),J=1,NCOLN)
      IF(NPART-LL) 170,170,120
120 CALL MATM(AM,F,DIS,M,M,NCOLN)
      CALL MATTM(BM,DIS,TF,N,M,NCOLN)
      DO 130 J=1,N
      DO 130 I=1,M
      YM(I,J)=0.
      DO 130 K=1,M
130 YM(I,J)=YM(I,J)+AM(I,K)*BM(K,J)
      DO 140 J=1,N
      DO 140 I=1,N
      AM(I,J)=0.
      DO 140 K=1,M
140 AM(I,J)=AM(I,J)+BM(K,I)*YM(K,J)
      DO 150 I=1,N
      DO 150 J=1,N
150 YM(I,J)=AM(I,J)
160 CONTINUE
170 REWIND(4)
```

```fortran
      WRITE(3)  ((DIS(I,J),I=1,M),J=1,NCOLN)
      IF(NPART-1) 4000,4000,180
  180 NA=NPART-1
      DO 1010 LL=1,NA
      BACKSPACE 2
      BACKSPACE 2
      READ(2) M,N,((AM(I,J),I=1,M),J=1,M),((BM(I,J),I=1,M),J=1,N),
    1  ((F(I,J),I=1,M),J=1,NCOLN)
      CALL MATM(BM,DIS,TF,M,N,NCOLN)
      DO 1000 J=1,NCOLN
      DO 1000 I=1,M
 1000 F(I,J)=F(I,J)-TF(I,J)
      CALL MATM(AM,F,DIS,M,M,NCOLN)
 1010 WRITE(3) ((DIS(I,J),I=1,M),J=1,NCOLN)
      WRITE(6,3000)
      DO 2020 LL=1,NPART
      READ (4) M,N,((AM(I,J),I=1,M),J=1,M),((BM(I,J),I=1,M),J=1,N),
    1  ((F(I,J),I=1,M),J=1,NCOLN)
      BACKSPACE 3
      READ (3) ((DIS(I,J),I=1,M),J=1,NCOLN)
      BACKSPACE 3
      BACKSPACE 3
      READ (3) ((TF(I,J),I=1,N),J=1,NCOLN)
      DO 2010 J=1,NCOLN
      DO 2010 I=1,M
      F(I,J)=F(I,J) - RS(I,J)
      DO 2000 K=1,M
 2000 F(I,J)=F(I,J)-AM(I,K)*DIS(K,J)
      DO 2010 L=1,N
 2010 F(I,J)=F(I,J)-BM(I,L)*TF(L,J)
      CALL MATTM(BM,DIS,RS,N,M,NCOLN)
 2020 WRITE(6,3010) ((F(I,J),I=1,M),J=1,NCOLN)
 3000 FORMAT(10H RESIDUALS)
 3010 FORMAT(1H ,14E9.2)
 4000 RETURN
      END
C
C
C
C
C
      SUBROUTINE DCOMP(N,A,LL)
C
C  SUBROUTINE TO DECOMPOSE THE SYMMETRIC MATRIX A(N*N).
      IMPLICIT DOUBLE PRECISION(A-H,O-Z)
      DIMENSION A(1000,1000)
```

```fortran
      DO 1 I=1,N
      DO 1 J=1,N
      SUM = A(I,J)
      K1= I-1
      IF(I-1) 3,3,5
5 DO 2 K=1,K1
2 SUM = SUM-A(K,I)*A(K,J)
3 IF(J-I) 4,6,4
6 IF(SUM) 7,7,8
7 WRITE(6,*) 'Sum is less than Zero'
      WRITE(6,*) 'Partition =',LL
      WRITE(6,9) I,J,K1,A(I,J),SUM
      STOP
8 TEMP=1.0/SQRT(SUM)
      A(I,J) = TEMP
      GO TO 1
4 A(I,J)= SUM*TEMP
1 CONTINUE
9 FORMAT('0','I J K1 A(I,J) SUM',3I4,2F12.2)
C      9 FORMAT('0','SUM IS LESS THAN ZERO AND SUBROUTINE
FAILS',3I4,F12.2)
      RETURN
      END
C
C
      SUBROUTINE INVERT(N,U)
C
C  SUBROUTINE TO INVERT THE SYMMETRIC MATRIX U(N*N).
      IMPLICIT DOUBLE PRECISION(A-H,O-Z)
      DIMENSION U(1000,1000)
      I1=N-1
      DO 1 I=1,I1
      J1=I+1
      DO 1 J=J1,N
      SUM=0.0
      K1=J-1
      DO 2 K=I,K1
2 SUM = SUM - U(K,I)*U(K,J)
1 U(J,I) = SUM*U(J,J)
      DO 3 I=1,N
      DO 3 J=I,N
      SUM=0.0
      DO 4 K=J,N
4 SUM = SUM + U(K,I)*U(K,J)
      U(I,J) = SUM
3 U(J,I) = SUM
```

```fortran
      RETURN
      END
C
C
      SUBROUTINE MATM(A,B,C,L,M,N)
C
C  SUBROUTINE USED IN CONJUNCTION WITH SUBROUTINE SOLVE
      IMPLICIT DOUBLE PRECISION(A-H,O-Z)
      DIMENSION A(1000,1000),B(1000,4),C(1000,4)
      DO 100 I=1,L
      DO 100 K=1,N
      C(I,K)=0.0
      DO 100 J=1,M
  100 C(I,K)=C(I,K)+A(I,J)*B(J,K)
      RETURN
      END
C
C
      SUBROUTINE MATTM(A,B,C,L,M,N)

C
C  SUBROUTINE USED IN CONJUNCTION WITH SUBROUTINE SOLVE.
      IMPLICIT DOUBLE PRECISION(A-H,O-Z)
      DIMENSION A(1000,1000),B(1000,4),C(1000,4)
      DO 100 I=1,L
      DO 100 K=1,N
      C(I,K)=0.0
      DO 100 J=1,M
  100 C(I,K)=C(I,K)+A(J,I)*B(J,K)
      RETURN
      END
```

Curve Beam3 – CB3

Overall Information of FEM Model

        Data Check Yes=1, No=2   2
        Number of Partitions =   1
        Number of Nodal Points =   343
        Number of Elements =   506
        Number of Bondary Conditions =   4
        Number of Load Cases =   1
        Number of Material Properties =   2
        Plane Stress =1, Plane Strain=2   1
        Number of Degrees of Freedom =   2
        Number of Concentrated Forces =   4
        Number of Stirrups =   0
        Number of Spring Elements =   172
        Units FPS=1 and MKS=2   1
        Thickness =   7.87400000000

X and Y coordinates of Nodes

1	0.00000	12.80000
2	3.94000	12.80000
3	7.87000	11.42000
4	11.81000	10.24000
5	15.75000	9.25000
6	19.69000	8.27000
7	23.62000	7.28000
8	27.56000	6.30000
9	31.50000	5.51000
10	35.43000	4.72000
11	39.37000	3.94000
12	43.31000	3.35000
13	47.24000	2.76000
14	51.18000	2.17000
15	55.12000	1.57000
16	59.06000	1.18000
17	62.99000	0.98000
18	66.93000	0.59000
19	70.87000	0.39000
20	74.80000	0.00000
21	78.74000	0.00000
22	82.68000	0.00000
23	86.61000	0.00000
24	90.55000	0.20000
25	94.49000	0.39000
26	98.43000	0.59000
27	102.36000	0.79000
28	106.30000	1.18000
29	110.24000	1.57000
30	114.17000	2.17000
31	118.11000	2.76000
32	122.05000	3.35000
33	125.98000	3.94000
34	129.92000	4.53000
35	133.86000	5.51000
36	137.80000	6.30000
37	141.73000	7.28000
38	145.67000	8.27000
39	149.61000	9.06000
40	153.54000	10.24000

41	157.48000	12.60000
42	161.42000	12.80000
43	165.35000	12.80000
44	0.00000	14.76000
45	3.94000	14.37000
46	7.87000	12.99000
47	11.81000	11.81000
48	15.75000	10.83000
49	19.69000	9.84000
50	23.62000	8.86000
51	27.56000	7.87000
52	31.50000	7.09000
53	35.43000	6.30000
54	39.37000	5.51000
55	43.31000	4.92000
56	47.24000	4.33000
57	51.18000	3.74000
58	55.12000	3.15000
59	59.06000	2.76000
60	62.99000	2.56000
61	66.93000	2.17000
62	70.87000	1.97000
63	74.80000	1.57000
64	78.74000	1.57000
65	82.68000	1.57000
66	86.61000	1.57000
67	90.55000	1.77000
68	94.49000	1.97000
69	98.43000	2.17000
70	102.36000	2.36000
71	106.30000	2.76000
72	110.24000	3.15000
73	114.17000	3.74000
74	118.11000	4.33000
75	122.05000	4.92000
76	125.98000	5.51000
77	129.92000	6.10000
78	133.86000	7.09000
79	137.80000	7.87000
80	141.73000	8.86000
81	145.67000	9.84000
82	149.61000	10.63000
83	153.54000	11.81000
84	157.48000	14.17000
85	161.42000	14.37000
86	165.35000	14.76000
87	0.00000	14.76000
88	3.94000	14.37000
89	7.87000	12.99000
90	11.81000	11.81000
91	15.75000	10.83000
92	19.69000	9.84000
93	23.62000	8.86000
94	27.56000	7.87000
95	31.50000	7.09000
96	35.43000	6.30000
97	39.37000	5.51000
98	43.31000	4.92000
99	47.24000	4.33000
100	51.18000	3.74000
101	55.12000	3.15000
102	59.06000	2.76000
103	62.99000	2.56000
104	66.93000	2.17000
105	70.87000	1.97000
106	74.80000	1.57000
107	78.74000	1.57000
108	82.68000	1.57000
109	86.61000	1.57000
110	90.55000	1.77000

111	94.49000	1.97000
112	98.43000	2.17000
113	102.36000	2.36000
114	106.30000	2.76000
115	110.24000	3.15000
116	114.17000	3.74000
117	118.11000	4.33000
118	122.05000	4.92000
119	125.98000	5.51000
120	129.92000	6.10000
121	133.86000	7.09000
122	137.80000	7.87000
123	141.73000	8.86000
124	145.67000	9.84000
125	149.61000	10.63000
126	153.54000	11.81000
127	157.48000	14.17000
128	161.42000	14.37000
129	165.35000	14.76000
130	0.00000	16.73000
131	3.94000	15.24000
132	7.87000	13.86000
133	11.81000	12.68000
134	15.75000	11.70000
135	19.69000	10.71000
136	23.62000	9.73000
137	27.56000	8.75000
138	31.50000	7.96000
139	35.43000	7.17000
140	39.37000	6.38000
141	43.31000	5.79000
142	47.24000	5.20000
143	51.18000	4.61000
144	55.12000	4.02000
145	59.06000	3.63000
146	62.99000	3.43000
147	66.93000	3.04000
148	70.87000	2.84000
149	74.80000	2.45000
150	78.74000	2.45000
151	82.68000	2.45000
152	86.61000	2.45000
153	90.55000	2.64000
154	94.49000	2.84000
155	98.43000	3.04000
156	102.36000	3.23000
157	106.30000	3.63000
158	110.24000	4.02000
159	114.17000	4.61000
160	118.11000	5.20000
161	122.05000	5.79000
162	125.98000	6.38000
163	129.92000	6.97000
164	133.86000	7.96000
165	137.80000	8.75000
166	141.73000	9.73000
167	145.67000	10.71000
168	149.61000	11.50000
169	153.54000	12.68000
170	157.48000	15.05000
171	161.42000	15.24000
172	165.35000	16.73000
173	0.00000	16.73000
174	3.94000	15.24000
175	7.87000	13.86000
176	11.81000	12.68000
177	15.75000	11.70000
178	19.69000	10.71000
179	23.62000	9.73000
180	27.56000	8.75000

181	31.50000	7.96000
182	35.43000	7.17000
183	39.37000	6.38000
184	43.31000	5.79000
185	47.24000	5.20000
186	51.18000	4.61000
187	55.12000	4.02000
188	59.06000	3.63000
189	62.99000	3.43000
190	66.93000	3.04000
191	70.87000	2.84000
192	74.80000	2.45000
193	78.74000	2.45000
194	82.68000	2.45000
195	86.61000	2.45000
196	90.55000	2.64000
197	94.49000	2.84000
198	98.43000	3.04000
199	102.36000	3.23000
200	106.30000	3.63000
201	110.24000	4.02000
202	114.17000	4.61000
203	118.11000	5.20000
204	122.05000	5.79000
205	125.98000	6.38000
206	129.92000	6.97000
207	133.86000	7.96000
208	137.80000	8.75000
209	141.73000	9.73000
210	145.67000	10.71000
211	149.61000	11.50000
212	153.54000	12.68000
213	157.48000	15.05000
214	161.42000	15.24000
215	165.35000	16.73000
216	47.24000	5.91000
217	51.18000	5.91000
218	55.12000	5.91000
219	59.06000	5.91000
220	62.99000	5.91000
221	66.93000	5.91000
222	70.87000	5.91000
223	74.80000	5.91000
224	78.74000	5.91000
225	82.68000	5.91000
226	86.61000	5.91000
227	90.55000	5.91000
228	94.49000	5.91000
229	98.43000	5.91000
230	102.36000	5.91000
231	106.30000	5.91000
232	110.24000	5.91000
233	114.17000	5.91000
234	118.11000	5.91000
235	27.56000	9.84000
236	31.50000	9.84000
237	35.43000	9.84000
238	39.37000	9.84000
239	43.31000	9.84000
240	47.24000	9.84000
241	51.18000	9.84000
242	55.12000	9.84000
243	59.06000	9.84000
244	62.99000	9.84000
245	66.93000	9.84000
246	70.87000	9.84000
247	74.80000	9.84000
248	78.74000	9.84000
249	82.68000	9.84000
250	86.61000	9.84000

251	90.55000	9.84000
252	94.49000	9.84000
253	98.43000	9.84000
254	102.36000	9.84000
255	106.30000	9.84000
256	110.24000	9.84000
257	114.17000	9.84000
258	118.11000	9.84000
259	122.05000	9.84000
260	125.98000	9.84000
261	129.92000	9.84000
262	133.86000	9.84000
263	137.80000	9.84000
264	11.81000	13.78000
265	15.75000	13.78000
266	19.69000	13.78000
267	23.62000	13.78000
268	27.56000	13.78000
269	31.50000	13.78000
270	35.43000	13.78000
271	39.37000	13.78000
272	43.31000	13.78000
273	47.24000	13.78000
274	51.18000	13.78000
275	55.12000	13.78000
276	59.06000	13.78000
277	62.99000	13.78000
278	66.93000	13.78000
279	70.87000	13.78000
280	74.80000	13.78000
281	78.74000	13.78000
282	82.68000	13.78000
283	86.61000	13.78000
284	90.55000	13.78000
285	94.49000	13.78000
286	98.43000	13.78000
287	102.36000	13.78000
288	106.30000	13.78000
289	110.24000	13.78000
290	114.17000	13.78000
291	118.11000	13.78000
292	122.05000	13.78000
293	125.98000	13.78000
294	129.92000	13.78000
295	133.86000	13.78000
296	137.80000	13.78000
297	141.73000	13.78000
298	145.67000	13.78000
299	149.61000	13.78000
300	153.54000	13.78000
301	0.00000	17.72000
302	3.94000	17.72000
303	7.87000	17.72000
304	11.81000	17.72000
305	15.75000	17.72000
306	19.69000	17.72000
307	23.62000	17.72000
308	27.56000	17.72000
309	31.50000	17.72000
310	35.43000	17.72000
311	39.37000	17.72000
312	43.31000	17.72000
313	47.24000	17.72000
314	51.18000	17.72000
315	55.12000	17.72000
316	59.06000	17.72000
317	62.99000	17.72000
318	66.93000	17.72000
319	70.87000	17.72000
320	74.80000	17.72000

```
321    78.74000    17.72000
322    82.68000    17.72000
323    86.61000    17.72000
324    90.55000    17.72000
325    94.49000    17.72000
326    98.43000    17.72000
327   102.36000    17.72000
328   106.30000    17.72000
329   110.24000    17.72000
330   114.17000    17.72000
331   118.11000    17.72000
332   122.05000    17.72000
333   125.98000    17.72000
334   129.92000    17.72000
335   133.86000    17.72000
336   137.80000    17.72000
337   141.73000    17.72000
338   145.67000    17.72000
339   149.61000    17.72000
340   153.54000    17.72000
341   157.48000    17.72000
342   161.42000    17.72000
343   165.35000    17.72000
```

Element Nodes

```
 1  1  2  44  1   1.00000000    0.00000000
 2  2  45  44  1   1.00000000    0.00000000
 3  2  46  45  1   1.00000000    0.00000000
 4  2  3  46  1   1.00000000    0.00000000
 5  3  4  46  1   1.00000000    0.00000000
 6  4  47  46  1   1.00000000    0.00000000
 7  4  48  47  1   1.00000000    0.00000000
 8  4  5  48  1   1.00000000    0.00000000
 9  5  6  48  1   1.00000000    0.00000000
10  6  49  48  1   1.00000000    0.00000000
11  6  50  49  1   1.00000000    0.00000000
12  6  7  50  1   1.00000000    0.00000000
13  7  8  50  1   1.00000000    0.00000000
14  8  51  50  1   1.00000000    0.00000000
15  8  52  51  1   1.00000000    0.00000000
16  8  9  52  1   1.00000000    0.00000000
17  9  10  52  1   1.00000000    0.00000000
18  10  53  52  1   1.00000000    0.00000000
19  10  54  53  1   1.00000000    0.00000000
20  10  11  54  1   1.00000000    0.00000000
21  11  12  54  1   1.00000000    0.00000000
22  12  55  54  1   1.00000000    0.00000000
23  12  56  55  1   1.00000000    0.00000000
24  12  13  56  1   1.00000000    0.00000000
25  13  14  56  1   1.00000000    0.00000000
26  14  57  56  1   1.00000000    0.00000000
27  14  58  57  1   1.00000000    0.00000000
28  14  15  58  1   1.00000000    0.00000000
29  15  16  58  1   1.00000000    0.00000000
30  16  59  58  1   1.00000000    0.00000000
31  16  60  59  1   1.00000000    0.00000000
32  16  17  60  1   1.00000000    0.00000000
33  17  18  60  1   1.00000000    0.00000000
34  18  61  60  1   1.00000000    0.00000000
35  18  62  61  1   1.00000000    0.00000000
36  18  19  62  1   1.00000000    0.00000000
37  19  20  62  1   1.00000000    0.00000000
38  20  63  62  1   1.00000000    0.00000000
39  20  64  63  1   1.00000000    0.00000000
40  20  21  64  1   1.00000000    0.00000000
41  21  22  64  1   1.00000000    0.00000000
42  22  65  64  1   1.00000000    0.00000000
43  22  66  65  1   1.00000000    0.00000000
44  22  23  66  1   1.00000000    0.00000000
```

```
45  23  24  66   1     1.00000000     0.00000000
46  24  67  66   1     1.00000000     0.00000000
47  24  68  67   1     1.00000000     0.00000000
48  24  25  68   1     1.00000000     0.00000000
49  25  26  68   1     1.00000000     0.00000000
50  26  69  68   1     1.00000000     0.00000000
51  26  70  69   1     1.00000000     0.00000000
52  26  27  70   1     1.00000000     0.00000000
53  27  28  70   1     1.00000000     0.00000000
54  28  71  70   1     1.00000000     0.00000000
55  28  72  71   1     1.00000000     0.00000000
56  28  29  72   1     1.00000000     0.00000000
57  29  30  72   1     1.00000000     0.00000000
58  30  73  72   1     1.00000000     0.00000000
59  30  74  73   1     1.00000000     0.00000000
60  30  31  74   1     1.00000000     0.00000000
61  31  32  74   1     1.00000000     0.00000000
62  32  75  74   1     1.00000000     0.00000000
63  32  76  75   1     1.00000000     0.00000000
64  32  33  76   1     1.00000000     0.00000000
65  33  34  76   1     1.00000000     0.00000000
66  34  77  76   1     1.00000000     0.00000000
67  34  78  77   1     1.00000000     0.00000000
68  34  35  78   1     1.00000000     0.00000000
69  35  36  78   1     1.00000000     0.00000000
70  36  79  78   1     1.00000000     0.00000000
71  36  80  79   1     1.00000000     0.00000000
72  36  37  80   1     1.00000000     0.00000000
73  37  38  80   1     1.00000000     0.00000000
74  38  81  80   1     1.00000000     0.00000000
75  38  82  81   1     1.00000000     0.00000000
76  38  39  82   1     1.00000000     0.00000000
77  39  40  82   1     1.00000000     0.00000000
78  40  83  82   1     1.00000000     0.00000000
79  40  84  83   1     1.00000000     0.00000000
80  40  41  84   1     1.00000000     0.00000000
81  41  42  84   1     1.00000000     0.00000000
82  42  85  84   1     1.00000000     0.00000000
83  42  86  85   1     1.00000000     0.00000000
84  42  43  86   1     1.00000000     0.00000000
85  44  45  173  1     0.78000000     0.00000000
86  45  174 173  1     0.78000000     0.00000000
87  45  175 174  1     0.78000000     0.00000000
88  45  46  175  1     0.78000000     0.00000000
89  46  47  175  1     0.78000000     0.00000000
90  47  176 175  1     0.78000000     0.00000000
91  47  177 176  1     0.78000000     0.00000000
92  47  48  177  1     0.78000000     0.00000000
93  48  49  177  1     0.78000000     0.00000000
94  49  178 177  1     0.78000000     0.00000000
95  49  179 178  1     0.78000000     0.00000000
96  49  50  179  1     0.78000000     0.00000000
97  50  51  179  1     0.78000000     0.00000000
98  51  180 179  1     0.78000000     0.00000000
99  51  181 180  1     0.78000000     0.00000000
100 51  52  181  1     0.78000000     0.00000000
101 52  53  181  1     0.78000000     0.00000000
102 53  182 181  1     0.78000000     0.00000000
103 53  183 182  1     0.78000000     0.00000000
104 53  54  183  1     0.78000000     0.00000000
105 54  55  183  1     0.78000000     0.00000000
106 55  184 183  1     0.78000000     0.00000000
107 55  185 184  1     0.78000000     0.00000000
108 55  56  185  1     0.78000000     0.00000000
109 56  57  185  1     0.78000000     0.00000000
110 57  186 185  1     0.78000000     0.00000000
111 57  187 186  1     0.78000000     0.00000000
112 57  58  187  1     0.78000000     0.00000000
113 58  59  187  1     0.78000000     0.00000000
114 59  188 187  1     0.78000000     0.00000000
```

```
115 59 189 188  1    0.78000000    0.00000000
116 59  60 189  1    0.78000000    0.00000000
117 60  61 189  1    0.78000000    0.00000000
118 61 190 189  1    0.78000000    0.00000000
119 61 191 190  1    0.78000000    0.00000000
120 61  62 191  1    0.78000000    0.00000000
121 62  63 191  1    0.78000000    0.00000000
122 63 192 191  1    0.78000000    0.00000000
123 63 193 192  1    0.78000000    0.00000000
124 63  64 193  1    0.78000000    0.00000000
125 64  65 193  1    0.78000000    0.00000000
126 65 194 193  1    0.78000000    0.00000000
127 65 195 194  1    0.78000000    0.00000000
128 65  66 195  1    0.78000000    0.00000000
129 66  67 195  1    0.78000000    0.00000000
130 67 196 195  1    0.78000000    0.00000000
131 67 197 196  1    0.78000000    0.00000000
132 67  68 197  1    0.78000000    0.00000000
133 68  69 197  1    0.78000000    0.00000000
134 69 198 197  1    0.78000000    0.00000000
135 69 199 198  1    0.78000000    0.00000000
136 69  70 199  1    0.78000000    0.00000000
137 70  71 199  1    0.78000000    0.00000000
138 71 200 199  1    0.78000000    0.00000000
139 71 201 200  1    0.78000000    0.00000000
140 71  72 201  1    0.78000000    0.00000000
141 72  73 201  1    0.78000000    0.00000000
142 73 202 201  1    0.78000000    0.00000000
143 73 203 202  1    0.78000000    0.00000000
144 73  74 203  1    0.78000000    0.00000000
145 74  75 203  1    0.78000000    0.00000000
146 75 204 203  1    0.78000000    0.00000000
147 75 205 204  1    0.78000000    0.00000000
148 75  76 205  1    0.78000000    0.00000000
149 76  77 205  1    0.78000000    0.00000000
150 77 206 205  1    0.78000000    0.00000000
151 77 207 206  1    0.78000000    0.00000000
152 77  78 207  1    0.78000000    0.00000000
153 78  79 207  1    0.78000000    0.00000000
154 79 208 207  1    0.78000000    0.00000000
155 79 209 208  1    0.78000000    0.00000000
156 79  80 209  1    0.78000000    0.00000000
157 80  81 209  1    0.78000000    0.00000000
158 81 210 209  1    0.78000000    0.00000000
159 81 211 210  1    0.78000000    0.00000000
160 81  82 211  1    0.78000000    0.00000000
161 82  83 211  1    0.78000000    0.00000000
162 83 212 211  1    0.78000000    0.00000000
163 83 213 212  1    0.78000000    0.00000000
164 83  84 213  1    0.78000000    0.00000000
165 84  85 213  1    0.78000000    0.00000000
166 85 214 213  1    0.78000000    0.00000000
167 85 215 214  1    0.78000000    0.00000000
168 85  86 215  1    0.78000000    0.00000000
169 87  88 130  2    0.22000000    0.00000000
170 88 131 130  2    0.22000000    0.00000000
171 88 132 131  2    0.22000000    0.00000000
172 88  89 132  2    0.22000000    0.00000000
173 89  90 132  2    0.22000000    0.00000000
174 90 133 132  2    0.22000000    0.00000000
175 90 134 133  2    0.22000000    0.00000000
176 90  91 134  2    0.22000000    0.00000000
177 91  92 134  2    0.22000000    0.00000000
178 92 135 134  2    0.22000000    0.00000000
179 92 136 135  2    0.22000000    0.00000000
180 92  93 136  2    0.22000000    0.00000000
181 93  94 136  2    0.22000000    0.00000000
182 94 137 136  2    0.22000000    0.00000000
183 94 138 137  2    0.22000000    0.00000000
184 94  95 138  2    0.22000000    0.00000000
```

```
185  95  96 138   2     0.22000000     0.00000000
186  96 139 138   2     0.22000000     0.00000000
187  96 140 139   2     0.22000000     0.00000000
188  96  97 140   2     0.22000000     0.00000000
189  97  98 140   2     0.22000000     0.00000000
190  98 141 140   2     0.22000000     0.00000000
191  98 142 141   2     0.22000000     0.00000000
192  98  99 142   2     0.22000000     0.00000000
193  99 100 142   2     0.22000000     0.00000000
194 100 143 142   2     0.22000000     0.00000000
195 100 144 143   2     0.22000000     0.00000000
196 100 101 144   2     0.22000000     0.00000000
197 101 102 144   2     0.22000000     0.00000000
198 102 145 144   2     0.22000000     0.00000000
199 102 146 145   2     0.22000000     0.00000000
200 102 103 146   2     0.22000000     0.00000000
201 103 104 146   2     0.22000000     0.00000000
202 104 147 146   2     0.22000000     0.00000000
203 104 148 147   2     0.22000000     0.00000000
204 104 105 148   2     0.22000000     0.00000000
205 105 106 148   2     0.22000000     0.00000000
206 106 149 148   2     0.22000000     0.00000000
207 106 150 149   2     0.22000000     0.00000000
208 106 107 150   2     0.22000000     0.00000000
209 107 108 150   2     0.22000000     0.00000000
210 108 151 150   2     0.22000000     0.00000000
211 108 152 151   2     0.22000000     0.00000000
212 108 109 152   2     0.22000000     0.00000000
213 109 110 152   2     0.22000000     0.00000000
214 110 153 152   2     0.22000000     0.00000000
215 110 154 153   2     0.22000000     0.00000000
216 110 111 154   2     0.22000000     0.00000000
217 111 112 154   2     0.22000000     0.00000000
218 112 155 154   2     0.22000000     0.00000000
219 112 156 155   2     0.22000000     0.00000000
220 112 113 156   2     0.22000000     0.00000000
221 113 114 156   2     0.22000000     0.00000000
222 114 157 156   2     0.22000000     0.00000000
223 114 158 157   2     0.22000000     0.00000000
224 114 115 158   2     0.22000000     0.00000000
225 115 116 158   2     0.22000000     0.00000000
226 116 159 158   2     0.22000000     0.00000000
227 116 160 159   2     0.22000000     0.00000000
228 116 117 160   2     0.22000000     0.00000000
229 117 118 160   2     0.22000000     0.00000000
230 118 161 160   2     0.22000000     0.00000000
231 118 162 161   2     0.22000000     0.00000000
232 118 119 162   2     0.22000000     0.00000000
233 119 120 162   2     0.22000000     0.00000000
234 120 163 162   2     0.22000000     0.00000000
235 120 164 163   2     0.22000000     0.00000000
236 120 121 164   2     0.22000000     0.00000000
237 121 122 164   2     0.22000000     0.00000000
238 122 165 164   2     0.22000000     0.00000000
239 122 166 165   2     0.22000000     0.00000000
240 122 123 166   2     0.22000000     0.00000000
241 123 124 166   2     0.22000000     0.00000000
242 124 167 166   2     0.22000000     0.00000000
243 124 168 167   2     0.22000000     0.00000000
244 124 125 168   2     0.22000000     0.00000000
245 125 126 168   2     0.22000000     0.00000000
246 126 169 168   2     0.22000000     0.00000000
247 126 170 169   2     0.22000000     0.00000000
248 126 127 170   2     0.22000000     0.00000000
249 127 128 170   2     0.22000000     0.00000000
250 128 171 170   2     0.22000000     0.00000000
251 128 172 171   2     0.22000000     0.00000000
252 128 129 172   2     0.22000000     0.00000000
253 184 185 216   1     1.00000000     0.00000000
254 185 186 216   1     1.00000000     0.00000000
```

```
255 186 217 216   1   1.00000000   0.00000000
256 186 187 217   1   1.00000000   0.00000000
257 187 218 217   1   1.00000000   0.00000000
258 187 188 218   1   1.00000000   0.00000000
259 188 219 218   1   1.00000000   0.00000000
260 188 189 219   1   1.00000000   0.00000000
261 189 220 219   1   1.00000000   0.00000000
262 189 190 220   1   1.00000000   0.00000000
263 190 221 220   1   1.00000000   0.00000000
264 190 191 221   1   1.00000000   0.00000000
265 191 222 221   1   1.00000000   0.00000000
266 191 192 222   1   1.00000000   0.00000000
267 192 223 222   1   1.00000000   0.00000000
268 192 193 223   1   1.00000000   0.00000000
269 193 224 223   1   1.00000000   0.00000000
270 193 194 224   1   1.00000000   0.00000000
271 194 225 224   1   1.00000000   0.00000000
272 194 226 225   1   1.00000000   0.00000000
273 194 195 226   1   1.00000000   0.00000000
274 195 227 226   1   1.00000000   0.00000000
275 195 196 227   1   1.00000000   0.00000000
276 196 228 227   1   1.00000000   0.00000000
277 196 197 228   1   1.00000000   0.00000000
278 197 229 228   1   1.00000000   0.00000000
279 197 198 229   1   1.00000000   0.00000000
280 198 230 229   1   1.00000000   0.00000000
281 198 199 230   1   1.00000000   0.00000000
282 199 231 230   1   1.00000000   0.00000000
283 199 200 231   1   1.00000000   0.00000000
284 200 232 231   1   1.00000000   0.00000000
285 200 201 232   1   1.00000000   0.00000000
286 201 233 232   1   1.00000000   0.00000000
287 201 202 233   1   1.00000000   0.00000000
288 202 234 233   1   1.00000000   0.00000000
289 202 203 234   1   1.00000000   0.00000000
290 203 204 234   1   1.00000000   0.00000000
291 179 180 235   1   1.00000000   0.00000000
292 180 181 235   1   1.00000000   0.00000000
293 181 236 235   1   1.00000000   0.00000000
294 181 182 236   1   1.00000000   0.00000000
295 182 237 236   1   1.00000000   0.00000000
296 182 183 237   1   1.00000000   0.00000000
297 183 238 237   1   1.00000000   0.00000000
298 183 184 238   1   1.00000000   0.00000000
299 184 239 238   1   1.00000000   0.00000000
300 184 185 239   1   1.00000000   0.00000000
301 185 240 239   1   1.00000000   0.00000000
302 185 186 240   1   1.00000000   0.00000000
303 186 241 240   1   1.00000000   0.00000000
304 186 187 241   1   1.00000000   0.00000000
305 187 242 241   1   1.00000000   0.00000000
306 187 188 242   1   1.00000000   0.00000000
307 188 243 242   1   1.00000000   0.00000000
308 188 189 243   1   1.00000000   0.00000000
309 189 244 243   1   1.00000000   0.00000000
310 189 190 244   1   1.00000000   0.00000000
311 190 245 244   1   1.00000000   0.00000000
312 190 191 245   1   1.00000000   0.00000000
313 191 246 245   1   1.00000000   0.00000000
314 191 192 246   1   1.00000000   0.00000000
315 192 247 246   1   1.00000000   0.00000000
316 192 193 247   1   1.00000000   0.00000000
317 193 248 247   1   1.00000000   0.00000000
318 193 194 248   1   1.00000000   0.00000000
319 194 249 248   1   1.00000000   0.00000000
320 194 195 249   1   1.00000000   0.00000000
321 195 250 249   1   1.00000000   0.00000000
322 195 196 250   1   1.00000000   0.00000000
323 196 251 250   1   1.00000000   0.00000000
324 196 197 251   1   1.00000000   0.00000000
```

```
325 197 252 251   1   1.00000000   0.00000000
326 197 198 252   1   1.00000000   0.00000000
327 198 253 252   1   1.00000000   0.00000000
328 198 199 253   1   1.00000000   0.00000000
329 199 254 253   1   1.00000000   0.00000000
330 199 200 254   1   1.00000000   0.00000000
331 200 255 254   1   1.00000000   0.00000000
332 200 201 255   1   1.00000000   0.00000000
333 201 256 255   1   1.00000000   0.00000000
334 201 202 256   1   1.00000000   0.00000000
335 202 257 256   1   1.00000000   0.00000000
336 202 203 257   1   1.00000000   0.00000000
337 203 258 257   1   1.00000000   0.00000000
338 203 204 258   1   1.00000000   0.00000000
339 204 259 258   1   1.00000000   0.00000000
340 204 205 259   1   1.00000000   0.00000000
341 205 260 259   1   1.00000000   0.00000000
342 205 206 260   1   1.00000000   0.00000000
343 206 261 260   1   1.00000000   0.00000000
344 206 207 261   1   1.00000000   0.00000000
345 207 262 261   1   1.00000000   0.00000000
346 207 208 262   1   1.00000000   0.00000000
347 208 263 262   1   1.00000000   0.00000000
348 208 209 263   1   1.00000000   0.00000000
349 175 176 264   1   1.00000000   0.00000000
350 176 177 264   1   1.00000000   0.00000000
351 177 265 264   1   1.00000000   0.00000000
352 177 178 265   1   1.00000000   0.00000000
353 178 266 265   1   1.00000000   0.00000000
354 178 179 266   1   1.00000000   0.00000000
355 179 267 266   1   1.00000000   0.00000000
356 179 235 267   1   1.00000000   0.00000000
357 235 268 267   1   1.00000000   0.00000000
358 235 236 268   1   1.00000000   0.00000000
359 236 269 268   1   1.00000000   0.00000000
360 236 237 269   1   1.00000000   0.00000000
361 237 270 269   1   1.00000000   0.00000000
362 237 238 270   1   1.00000000   0.00000000
363 238 271 270   1   1.00000000   0.00000000
364 238 239 271   1   1.00000000   0.00000000
365 239 272 271   1   1.00000000   0.00000000
366 239 240 272   1   1.00000000   0.00000000
367 240 273 272   1   1.00000000   0.00000000
368 240 241 273   1   1.00000000   0.00000000
369 241 274 273   1   1.00000000   0.00000000
370 241 242 274   1   1.00000000   0.00000000
371 242 275 274   1   1.00000000   0.00000000
372 242 243 275   1   1.00000000   0.00000000
373 243 276 275   1   1.00000000   0.00000000
374 243 244 276   1   1.00000000   0.00000000
375 244 277 276   1   1.00000000   0.00000000
376 244 245 277   1   1.00000000   0.00000000
377 245 278 277   1   1.00000000   0.00000000
378 245 246 278   1   1.00000000   0.00000000
379 246 279 278   1   1.00000000   0.00000000
380 246 247 279   1   1.00000000   0.00000000
381 247 280 279   1   1.00000000   0.00000000
382 247 248 280   1   1.00000000   0.00000000
383 248 281 280   1   1.00000000   0.00000000
384 248 249 281   1   1.00000000   0.00000000
385 249 282 281   1   1.00000000   0.00000000
386 249 283 282   1   1.00000000   0.00000000
387 249 250 283   1   1.00000000   0.00000000
388 250 284 283   1   1.00000000   0.00000000
389 250 251 284   1   1.00000000   0.00000000
390 251 285 284   1   1.00000000   0.00000000
391 251 252 285   1   1.00000000   0.00000000
392 252 286 285   1   1.00000000   0.00000000
393 252 253 286   1   1.00000000   0.00000000
394 253 287 286   1   1.00000000   0.00000000
```

```
395 253 254 287  1    1.00000000    0.00000000
396 254 288 287  1    1.00000000    0.00000000
397 254 255 288  1    1.00000000    0.00000000
398 255 289 288  1    1.00000000    0.00000000
399 255 256 289  1    1.00000000    0.00000000
400 256 290 289  1    1.00000000    0.00000000
401 256 257 290  1    1.00000000    0.00000000
402 257 291 290  1    1.00000000    0.00000000
403 257 258 291  1    1.00000000    0.00000000
404 258 292 291  1    1.00000000    0.00000000
405 258 259 292  1    1.00000000    0.00000000
406 259 293 292  1    1.00000000    0.00000000
407 259 260 293  1    1.00000000    0.00000000
408 260 294 293  1    1.00000000    0.00000000
409 260 261 294  1    1.00000000    0.00000000
410 261 295 294  1    1.00000000    0.00000000
411 261 262 295  1    1.00000000    0.00000000
412 262 296 295  1    1.00000000    0.00000000
413 262 263 296  1    1.00000000    0.00000000
414 263 297 296  1    1.00000000    0.00000000
415 263 209 297  1    1.00000000    0.00000000
416 209 298 297  1    1.00000000    0.00000000
417 209 210 298  1    1.00000000    0.00000000
418 210 299 298  1    1.00000000    0.00000000
419 210 211 299  1    1.00000000    0.00000000
420 211 300 299  1    1.00000000    0.00000000
421 211 212 300  1    1.00000000    0.00000000
422 212 213 300  1    1.00000000    0.00000000
423 173 174 301  1    1.00000000    0.00000000
424 174 302 301  1    1.00000000    0.00000000
425 174 175 302  1    1.00000000    0.00000000
426 175 303 302  1    1.00000000    0.00000000
427 175 264 303  1    1.00000000    0.00000000
428 264 304 303  1    1.00000000    0.00000000
429 264 265 304  1    1.00000000    0.00000000
430 265 305 304  1    1.00000000    0.00000000
431 265 266 305  1    1.00000000    0.00000000
432 266 306 305  1    1.00000000    0.00000000
433 266 267 306  1    1.00000000    0.00000000
434 267 307 306  1    1.00000000    0.00000000
435 267 268 307  1    1.00000000    0.00000000
436 268 308 307  1    1.00000000    0.00000000
437 268 269 308  1    1.00000000    0.00000000
438 269 309 308  1    1.00000000    0.00000000
439 269 270 309  1    1.00000000    0.00000000
440 270 310 309  1    1.00000000    0.00000000
441 270 271 310  1    1.00000000    0.00000000
442 271 311 310  1    1.00000000    0.00000000
443 271 272 311  1    1.00000000    0.00000000
444 272 312 311  1    1.00000000    0.00000000
445 272 273 312  1    1.00000000    0.00000000
446 273 313 312  1    1.00000000    0.00000000
447 273 274 313  1    1.00000000    0.00000000
448 274 314 313  1    1.00000000    0.00000000
449 274 275 314  1    1.00000000    0.00000000
450 275 315 314  1    1.00000000    0.00000000
451 275 276 315  1    1.00000000    0.00000000
452 276 316 315  1    1.00000000    0.00000000
453 276 277 316  1    1.00000000    0.00000000
454 277 317 316  1    1.00000000    0.00000000
455 277 278 317  1    1.00000000    0.00000000
456 278 318 317  1    1.00000000    0.00000000
457 278 279 318  1    1.00000000    0.00000000
458 279 319 318  1    1.00000000    0.00000000
459 279 280 319  1    1.00000000    0.00000000
460 280 320 319  1    1.00000000    0.00000000
461 280 281 320  1    1.00000000    0.00000000
462 281 321 320  1    1.00000000    0.00000000
463 281 282 321  1    1.00000000    0.00000000
464 282 322 321  1    1.00000000    0.00000000
```

```
465 282 323 322  1   1.00000000    0.00000000
466 282 283 323  1   1.00000000    0.00000000
467 283 324 323  1   1.00000000    0.00000000
468 283 284 324  1   1.00000000    0.00000000
469 284 325 324  1   1.00000000    0.00000000
470 284 285 325  1   1.00000000    0.00000000
471 285 326 325  1   1.00000000    0.00000000
472 285 286 326  1   1.00000000    0.00000000
473 286 327 326  1   1.00000000    0.00000000
474 286 287 327  1   1.00000000    0.00000000
475 287 328 327  1   1.00000000    0.00000000
476 287 288 328  1   1.00000000    0.00000000
477 288 329 328  1   1.00000000    0.00000000
478 288 289 329  1   1.00000000    0.00000000
479 289 330 329  1   1.00000000    0.00000000
480 289 290 330  1   1.00000000    0.00000000
481 290 331 330  1   1.00000000    0.00000000
482 290 291 331  1   1.00000000    0.00000000
483 291 332 331  1   1.00000000    0.00000000
484 291 292 332  1   1.00000000    0.00000000
485 292 333 332  1   1.00000000    0.00000000
486 292 293 333  1   1.00000000    0.00000000
487 293 334 333  1   1.00000000    0.00000000
488 293 294 334  1   1.00000000    0.00000000
489 294 335 334  1   1.00000000    0.00000000
490 294 295 335  1   1.00000000    0.00000000
491 295 336 335  1   1.00000000    0.00000000
492 295 296 336  1   1.00000000    0.00000000
493 296 337 336  1   1.00000000    0.00000000
494 296 297 337  1   1.00000000    0.00000000
495 297 338 337  1   1.00000000    0.00000000
496 297 298 338  1   1.00000000    0.00000000
497 298 339 338  1   1.00000000    0.00000000
498 298 299 339  1   1.00000000    0.00000000
499 299 340 339  1   1.00000000    0.00000000
500 299 300 340  1   1.00000000    0.00000000
501 300 341 340  1   1.00000000    0.00000000
502 300 213 341  1   1.00000000    0.00000000
503 213 342 341  1   1.00000000    0.00000000
504 213 214 342  1   1.00000000    0.00000000
505 214 343 342  1   1.00000000    0.00000000
506 214 215 343  1   1.00000000    0.00000000
```

Boundary Conditions

```
 1  1  0    0.00000000    0.00000000
 2  1  0    0.00000000    0.00000000
42  0  0    0.00000000    0.00000000
43  0  0    0.00000000    0.00000000
```

Partition Information

```
 1 506   1 343
```

Material Properties

```
 3916019.00000  3916019.00000    0.20000    0.20000  1631674.58333
29000000.00000 29000000.00000    0.30000    0.30000 11153846.15385
```

Nodal Load Data

```
310    0.00000  -1450.00000
318    0.00000  -1450.00000
326    0.00000  -1450.00000
334    0.00000  -1450.00000
```

Nonlinear Steps and Increments of Loads

```
100   0.0000 -100.0000
```

Spring Elements

```
1 44 87  0  1.97000  0.00000  1.00000  2.00000
1
2 44 87  0  1.97000 90.00000  1.00000  2.00000
1
3 45 88  1  3.94000  0.00000  1.00000  2.00000
1
4 45 88  1  3.94000 90.00000  1.00000  2.00000
1
5 46 89  1  3.94000  0.00000  1.00000  2.00000
1
6 46 89  1  3.94000 90.00000  1.00000  2.00000
1
7 47 90  1  3.94000  0.00000  1.00000  2.00000
1
8 47 90  1  3.94000 90.00000  1.00000  2.00000
1
9 48 91  1  3.94000  0.00000  1.00000  2.00000
1
10 48 91  1  3.94000 90.00000  1.00000  2.00000
1
11 49 92  1  3.94000  0.00000  1.00000  2.00000
1
12 49 92  1  3.94000 90.00000  1.00000  2.00000
1
13 50 93  1  3.94000  0.00000  1.00000  2.00000
1
14 50 93  1  3.94000 90.00000  1.00000  2.00000
1
15 51 94  1  3.94000  0.00000  1.00000  2.00000
1
16 51 94  1  3.94000 90.00000  1.00000  2.00000
1
17 52 95  1  3.94000  0.00000  1.00000  2.00000
1
18 52 95  1  3.94000 90.00000  1.00000  2.00000
1
19 53 96  1  3.94000  0.00000  1.00000  2.00000
1
20 53 96  1  3.94000 90.00000  1.00000  2.00000
1
21 54 97  1  3.94000  0.00000  1.00000  2.00000
1
22 54 97  1  3.94000 90.00000  1.00000  2.00000
1
23 55 98  1  3.94000  0.00000  1.00000  2.00000
1
24 55 98  1  3.94000 90.00000  1.00000  2.00000
1
25 56 99  1  3.94000  0.00000  1.00000  2.00000
1
26 56 99  1  3.94000 90.00000  1.00000  2.00000
1
27 57 100  1  3.94000  0.00000  1.00000  2.00000
1
28 57 100  1  3.94000 90.00000  1.00000  2.00000
1
29 58 101  1  3.94000  0.00000  1.00000  2.00000
1
30 58 101  1  3.94000 90.00000  1.00000  2.00000
1
31 59 102  1  3.94000  0.00000  1.00000  2.00000
1
32 59 102  1  3.94000 90.00000  1.00000  2.00000
1
33 60 103  1  3.94000  0.00000  1.00000  2.00000
1
34 60 103  1  3.94000 90.00000  1.00000  2.00000
1
```

35 61 104 1 3.94000 0.00000 1.00000 2.00000
 1
36 61 104 1 3.94000 90.00000 1.00000 2.00000
 1
37 62 105 1 3.94000 0.00000 1.00000 2.00000
 1
38 62 105 1 3.94000 90.00000 1.00000 2.00000
 1
39 63 106 1 3.94000 0.00000 1.00000 2.00000
 1
40 63 106 1 3.94000 90.00000 1.00000 2.00000
 1
41 64 107 1 3.94000 0.00000 1.00000 2.00000
 1
42 64 107 1 3.94000 90.00000 1.00000 2.00000
 1
43 65 108 1 3.94000 0.00000 1.00000 2.00000
 1
44 65 108 1 3.94000 90.00000 1.00000 2.00000
 1
45 66 109 1 3.94000 0.00000 1.00000 2.00000
 1
46 66 109 1 3.94000 90.00000 1.00000 2.00000
 1
47 67 110 1 3.94000 0.00000 1.00000 2.00000
 1
48 67 110 1 3.94000 90.00000 1.00000 2.00000
 1
49 68 111 1 3.94000 0.00000 1.00000 2.00000
 1
50 68 111 1 3.94000 90.00000 1.00000 2.00000
 1
51 69 112 1 3.94000 0.00000 1.00000 2.00000
 1
52 69 112 1 3.94000 90.00000 1.00000 2.00000
 1
53 70 113 1 3.94000 0.00000 1.00000 2.00000
 1
54 70 113 1 3.94000 90.00000 1.00000 2.00000
 1
55 71 114 1 3.94000 0.00000 1.00000 2.00000
 1
56 71 114 1 3.94000 90.00000 1.00000 2.00000
 1
57 72 115 1 3.94000 0.00000 1.00000 2.00000
 1
58 72 115 1 3.94000 90.00000 1.00000 2.00000
 1
59 73 116 1 3.94000 0.00000 1.00000 2.00000
 1
60 73 116 1 3.94000 90.00000 1.00000 2.00000
 1
61 74 117 1 3.94000 0.00000 1.00000 2.00000
 1
62 74 117 1 3.94000 90.00000 1.00000 2.00000
 1
63 75 118 1 3.94000 0.00000 1.00000 2.00000
 1
64 75 118 1 3.94000 90.00000 1.00000 2.00000
 1
65 76 119 1 3.94000 0.00000 1.00000 2.00000
 1
66 76 119 1 3.94000 90.00000 1.00000 2.00000
 1
67 77 120 1 3.94000 0.00000 1.00000 2.00000
 1
68 77 120 1 3.94000 90.00000 1.00000 2.00000
 1
69 78 121 1 3.94000 0.00000 1.00000 2.00000
 1

70 78 121 1 3.94000 90.00000 1.00000 2.00000
 1
71 79 122 1 3.94000 0.00000 1.00000 2.00000
 1
72 79 122 1 3.94000 90.00000 1.00000 2.00000
 1
73 80 123 1 3.94000 0.00000 1.00000 2.00000
 1
74 80 123 1 3.94000 90.00000 1.00000 2.00000
 1
75 81 124 1 3.94000 0.00000 1.00000 2.00000
 1
76 81 124 1 3.94000 90.00000 1.00000 2.00000
 1
77 82 125 1 3.94000 0.00000 1.00000 2.00000
 1
78 82 125 1 3.94000 90.00000 1.00000 2.00000
 1
79 83 126 1 3.94000 0.00000 1.00000 2.00000
 1
80 83 126 1 3.94000 90.00000 1.00000 2.00000
 1
81 84 127 1 3.94000 0.00000 1.00000 2.00000
 1
82 84 127 1 3.94000 90.00000 1.00000 2.00000
 1
83 85 128 1 3.94000 0.00000 1.00000 2.00000
 1
84 85 128 1 3.94000 90.00000 1.00000 2.00000
 1
85 86 129 0 1.97000 0.00000 1.00000 2.00000
 1
86 86 129 0 1.97000 90.00000 1.00000 2.00000
 1
87 173 130 0 1.97000 0.00000 1.00000 2.00000
 1
88 173 130 0 1.97000 90.00000 1.00000 2.00000
 1
89 174 131 1 3.94000 0.00000 1.00000 2.00000
 1
90 174 131 1 3.94000 90.00000 1.00000 2.00000
 1
91 175 132 1 3.94000 0.00000 1.00000 2.00000
 1
92 175 132 1 3.94000 90.00000 1.00000 2.00000
 1
93 176 133 1 3.94000 0.00000 1.00000 2.00000
 1
94 176 133 1 3.94000 90.00000 1.00000 2.00000
 1
95 177 134 1 3.94000 0.00000 1.00000 2.00000
 1
96 177 134 1 3.94000 90.00000 1.00000 2.00000
 1
97 178 135 1 3.94000 0.00000 1.00000 2.00000
 1
98 178 135 1 3.94000 90.00000 1.00000 2.00000
 1
99 179 136 1 3.94000 0.00000 1.00000 2.00000
 1
100 179 136 1 3.94000 90.00000 1.00000 2.00000
 1
101 180 137 1 3.94000 0.00000 1.00000 2.00000
 1
102 180 137 1 3.94000 90.00000 1.00000 2.00000
 1
103 181 138 1 3.94000 0.00000 1.00000 2.00000
 1
104 181 138 1 3.94000 90.00000 1.00000 2.00000
 1

105 182 139 1 3.94000 0.00000 1.00000 2.00000
  1
106 182 139 1 3.94000 90.00000 1.00000 2.00000
  1
107 183 140 1 3.94000 0.00000 1.00000 2.00000
  1
108 183 140 1 3.94000 90.00000 1.00000 2.00000
  1
109 184 141 1 3.94000 0.00000 1.00000 2.00000
  1
110 184 141 1 3.94000 90.00000 1.00000 2.00000
  1
111 185 142 1 3.94000 0.00000 1.00000 2.00000
  1
112 185 142 1 3.94000 90.00000 1.00000 2.00000
  1
113 186 143 1 3.94000 0.00000 1.00000 2.00000
  1
114 186 143 1 3.94000 90.00000 1.00000 2.00000
  1
115 187 144 1 3.94000 0.00000 1.00000 2.00000
  1
116 187 144 1 3.94000 90.00000 1.00000 2.00000
  1
117 188 145 1 3.94000 0.00000 1.00000 2.00000
  1
118 188 145 1 3.94000 90.00000 1.00000 2.00000
  1
119 189 146 1 3.94000 0.00000 1.00000 2.00000
  1
120 189 146 1 3.94000 90.00000 1.00000 2.00000
  1
121 190 147 1 3.94000 0.00000 1.00000 2.00000
  1
122 190 147 1 3.94000 90.00000 1.00000 2.00000
  1
123 191 148 1 3.94000 0.00000 1.00000 2.00000
  1
124 191 148 1 3.94000 90.00000 1.00000 2.00000
  1
125 192 149 1 3.94000 0.00000 1.00000 2.00000
  1
126 192 149 1 3.94000 90.00000 1.00000 2.00000
  1
127 193 150 1 3.94000 0.00000 1.00000 2.00000
  1
128 193 150 1 3.94000 90.00000 1.00000 2.00000
  1
129 194 151 1 3.94000 0.00000 1.00000 2.00000
  1
130 194 151 1 3.94000 90.00000 1.00000 2.00000
  1
131 195 152 1 3.94000 0.00000 1.00000 2.00000
  1
132 195 152 1 3.94000 90.00000 1.00000 2.00000
  1
133 196 153 1 3.94000 0.00000 1.00000 2.00000
  1
134 196 153 1 3.94000 90.00000 1.00000 2.00000
  1
135 197 154 1 3.94000 0.00000 1.00000 2.00000
  1
136 197 154 1 3.94000 90.00000 1.00000 2.00000
  1
137 198 155 1 3.94000 0.00000 1.00000 2.00000
  1
138 198 155 1 3.94000 90.00000 1.00000 2.00000
  1
139 199 156 1 3.94000 0.00000 1.00000 2.00000
  1

140 199 156 1 3.94000 90.00000 1.00000 2.00000
 1
141 200 157 1 3.94000 0.00000 1.00000 2.00000
 1
142 200 157 1 3.94000 90.00000 1.00000 2.00000
 1
143 201 158 1 3.94000 0.00000 1.00000 2.00000
 1
144 201 158 1 3.94000 90.00000 1.00000 2.00000
 1
145 202 159 1 3.94000 0.00000 1.00000 2.00000
 1
146 202 159 1 3.94000 90.00000 1.00000 2.00000
 1
147 203 160 1 3.94000 0.00000 1.00000 2.00000
 1
148 203 160 1 3.94000 90.00000 1.00000 2.00000
 1
149 204 161 1 3.94000 0.00000 1.00000 2.00000
 1
150 204 161 1 3.94000 90.00000 1.00000 2.00000
 1
151 205 162 1 3.94000 0.00000 1.00000 2.00000
 1
152 205 162 1 3.94000 90.00000 1.00000 2.00000
 1
153 206 163 1 3.94000 0.00000 1.00000 2.00000
 1
154 206 163 1 3.94000 90.00000 1.00000 2.00000
 1
155 207 164 1 3.94000 0.00000 1.00000 2.00000
 1
156 207 164 1 3.94000 90.00000 1.00000 2.00000
 1
157 208 165 1 3.94000 0.00000 1.00000 2.00000
 1
158 208 165 1 3.94000 90.00000 1.00000 2.00000
 1
159 209 166 1 3.94000 0.00000 1.00000 2.00000
 1
160 209 166 1 3.94000 90.00000 1.00000 2.00000
 1
161 210 167 1 3.94000 0.00000 1.00000 2.00000
 1
162 210 167 1 3.94000 90.00000 1.00000 2.00000
 1
163 211 168 1 3.94000 0.00000 1.00000 2.00000
 1
164 211 168 1 3.94000 90.00000 1.00000 2.00000
 1
165 212 169 1 3.94000 0.00000 1.00000 2.00000
 1
166 212 169 1 3.94000 90.00000 1.00000 2.00000
 1
167 213 170 1 3.94000 0.00000 1.00000 2.00000
 1
168 213 170 1 3.94000 90.00000 1.00000 2.00000
 1
169 214 171 1 3.94000 0.00000 1.00000 2.00000
 1
170 214 171 1 3.94000 90.00000 1.00000 2.00000
 1
171 215 172 0 1.97000 0.00000 1.00000 2.00000
 1
172 215 172 0 1.97000 90.00000 1.00000 2.00000
 1
 Spring data for Partition
172
 1 172
 Stirrup Data

0

Concrete Parameters

Maximum Concrete Stress=   5221.00000000
Concrete Stress at Maximum Strain=   4367.00000000
Maximum Concrete Strain=   3.000000000000E-03
Modulus of Rupture of Concrete=   522.000000000

Steel Parameters

Yield Strain of Steel=   1.320000000000E-03
Strain at onset of Hardening=   1.800000000000E-02
Initial Strain Hardening Modulus=   550000.000000
Poisson Ratio in Strain Hardening Range=   0.100000000000

1LOADING STEP   1   ITERATION NO.   1

LKS	SK	SKB	XXE(1,1)	XE(1,1)	SKD
1	0.36060E+07	0.28343E+07	0.00000E+00	0.00000E+00	0.19595E+07
2	0.36060E+07	0.28343E+07	0.00000E+00	0.00000E+00	0.19595E+07
3	0.36060E+07	0.56686E+07	0.00000E+00	0.00000E+00	0.39190E+07
4	0.36060E+07	0.56686E+07	0.00000E+00	0.00000E+00	0.39190E+07
5	0.36060E+07	0.56686E+07	0.00000E+00	0.00000E+00	0.39190E+07
6	0.36060E+07	0.56686E+07	0.00000E+00	0.00000E+00	0.39190E+07
7	0.36060E+07	0.56686E+07	0.00000E+00	0.00000E+00	0.39190E+07
8	0.36060E+07	0.56686E+07	0.00000E+00	0.00000E+00	0.39190E+07
9	0.36060E+07	0.56686E+07	0.00000E+00	0.00000E+00	0.39190E+07
10	0.36060E+07	0.56686E+07	0.00000E+00	0.00000E+00	0.39190E+07
11	0.36060E+07	0.56686E+07	0.00000E+00	0.00000E+00	0.39190E+07
12	0.36060E+07	0.56686E+07	0.00000E+00	0.00000E+00	0.39190E+07
13	0.36060E+07	0.56686E+07	0.00000E+00	0.00000E+00	0.39190E+07
14	0.36060E+07	0.56686E+07	0.00000E+00	0.00000E+00	0.39190E+07
15	0.36060E+07	0.56686E+07	0.00000E+00	0.00000E+00	0.39190E+07
16	0.36060E+07	0.56686E+07	0.00000E+00	0.00000E+00	0.39190E+07
17	0.36060E+07	0.56686E+07	0.00000E+00	0.00000E+00	0.39190E+07
18	0.36060E+07	0.56686E+07	0.00000E+00	0.00000E+00	0.39190E+07
19	0.36060E+07	0.56686E+07	0.00000E+00	0.00000E+00	0.39190E+07
20	0.36060E+07	0.56686E+07	0.00000E+00	0.00000E+00	0.39190E+07
21	0.36060E+07	0.56686E+07	0.00000E+00	0.00000E+00	0.39190E+07
22	0.36060E+07	0.56686E+07	0.00000E+00	0.00000E+00	0.39190E+07
23	0.36060E+07	0.56686E+07	0.00000E+00	0.00000E+00	0.39190E+07
24	0.36060E+07	0.56686E+07	0.00000E+00	0.00000E+00	0.39190E+07
25	0.36060E+07	0.56686E+07	0.00000E+00	0.00000E+00	0.39190E+07
26	0.36060E+07	0.56686E+07	0.00000E+00	0.00000E+00	0.39190E+07
27	0.36060E+07	0.56686E+07	0.00000E+00	0.00000E+00	0.39190E+07
28	0.36060E+07	0.56686E+07	0.00000E+00	0.00000E+00	0.39190E+07
29	0.36060E+07	0.56686E+07	0.00000E+00	0.00000E+00	0.39190E+07
30	0.36060E+07	0.56686E+07	0.00000E+00	0.00000E+00	0.39190E+07
31	0.36060E+07	0.56686E+07	0.00000E+00	0.00000E+00	0.39190E+07
32	0.36060E+07	0.56686E+07	0.00000E+00	0.00000E+00	0.39190E+07
33	0.36060E+07	0.56686E+07	0.00000E+00	0.00000E+00	0.39190E+07
34	0.36060E+07	0.56686E+07	0.00000E+00	0.00000E+00	0.39190E+07
35	0.36060E+07	0.56686E+07	0.00000E+00	0.00000E+00	0.39190E+07
36	0.36060E+07	0.56686E+07	0.00000E+00	0.00000E+00	0.39190E+07
37	0.36060E+07	0.56686E+07	0.00000E+00	0.00000E+00	0.39190E+07
38	0.36060E+07	0.56686E+07	0.00000E+00	0.00000E+00	0.39190E+07
39	0.36060E+07	0.56686E+07	0.00000E+00	0.00000E+00	0.39190E+07
40	0.36060E+07	0.56686E+07	0.00000E+00	0.00000E+00	0.39190E+07
41	0.36060E+07	0.56686E+07	0.00000E+00	0.00000E+00	0.39190E+07
42	0.36060E+07	0.56686E+07	0.00000E+00	0.00000E+00	0.39190E+07
43	0.36060E+07	0.56686E+07	0.00000E+00	0.00000E+00	0.39190E+07
44	0.36060E+07	0.56686E+07	0.00000E+00	0.00000E+00	0.39190E+07

45	0.36060E+07	0.56686E+07	0.00000E+00	0.00000E+00	0.39190E+07
46	0.36060E+07	0.56686E+07	0.00000E+00	0.00000E+00	0.39190E+07
47	0.36060E+07	0.56686E+07	0.00000E+00	0.00000E+00	0.39190E+07
48	0.36060E+07	0.56686E+07	0.00000E+00	0.00000E+00	0.39190E+07
49	0.36060E+07	0.56686E+07	0.00000E+00	0.00000E+00	0.39190E+07
50	0.36060E+07	0.56686E+07	0.00000E+00	0.00000E+00	0.39190E+07
51	0.36060E+07	0.56686E+07	0.00000E+00	0.00000E+00	0.39190E+07
52	0.36060E+07	0.56686E+07	0.00000E+00	0.00000E+00	0.39190E+07
53	0.36060E+07	0.56686E+07	0.00000E+00	0.00000E+00	0.39190E+07
54	0.36060E+07	0.56686E+07	0.00000E+00	0.00000E+00	0.39190E+07
55	0.36060E+07	0.56686E+07	0.00000E+00	0.00000E+00	0.39190E+07
56	0.36060E+07	0.56686E+07	0.00000E+00	0.00000E+00	0.39190E+07
57	0.36060E+07	0.56686E+07	0.00000E+00	0.00000E+00	0.39190E+07
58	0.36060E+07	0.56686E+07	0.00000E+00	0.00000E+00	0.39190E+07
59	0.36060E+07	0.56686E+07	0.00000E+00	0.00000E+00	0.39190E+07
60	0.36060E+07	0.56686E+07	0.00000E+00	0.00000E+00	0.39190E+07
61	0.36060E+07	0.56686E+07	0.00000E+00	0.00000E+00	0.39190E+07
62	0.36060E+07	0.56686E+07	0.00000E+00	0.00000E+00	0.39190E+07
63	0.36060E+07	0.56686E+07	0.00000E+00	0.00000E+00	0.39190E+07
64	0.36060E+07	0.56686E+07	0.00000E+00	0.00000E+00	0.39190E+07
65	0.36060E+07	0.56686E+07	0.00000E+00	0.00000E+00	0.39190E+07
66	0.36060E+07	0.56686E+07	0.00000E+00	0.00000E+00	0.39190E+07
67	0.36060E+07	0.56686E+07	0.00000E+00	0.00000E+00	0.39190E+07
68	0.36060E+07	0.56686E+07	0.00000E+00	0.00000E+00	0.39190E+07
69	0.36060E+07	0.56686E+07	0.00000E+00	0.00000E+00	0.39190E+07
70	0.36060E+07	0.56686E+07	0.00000E+00	0.00000E+00	0.39190E+07
71	0.36060E+07	0.56686E+07	0.00000E+00	0.00000E+00	0.39190E+07
72	0.36060E+07	0.56686E+07	0.00000E+00	0.00000E+00	0.39190E+07
73	0.36060E+07	0.56686E+07	0.00000E+00	0.00000E+00	0.39190E+07
74	0.36060E+07	0.56686E+07	0.00000E+00	0.00000E+00	0.39190E+07
75	0.36060E+07	0.56686E+07	0.00000E+00	0.00000E+00	0.39190E+07
76	0.36060E+07	0.56686E+07	0.00000E+00	0.00000E+00	0.39190E+07
77	0.36060E+07	0.56686E+07	0.00000E+00	0.00000E+00	0.39190E+07
78	0.36060E+07	0.56686E+07	0.00000E+00	0.00000E+00	0.39190E+07
79	0.36060E+07	0.56686E+07	0.00000E+00	0.00000E+00	0.39190E+07
80	0.36060E+07	0.56686E+07	0.00000E+00	0.00000E+00	0.39190E+07
81	0.36060E+07	0.56686E+07	0.00000E+00	0.00000E+00	0.39190E+07
82	0.36060E+07	0.56686E+07	0.00000E+00	0.00000E+00	0.39190E+07
83	0.36060E+07	0.56686E+07	0.00000E+00	0.00000E+00	0.39190E+07
84	0.36060E+07	0.56686E+07	0.00000E+00	0.00000E+00	0.39190E+07
85	0.36060E+07	0.28343E+07	0.00000E+00	0.00000E+00	0.19595E+07
86	0.36060E+07	0.28343E+07	0.00000E+00	0.00000E+00	0.19595E+07
87	0.36060E+07	0.28343E+07	0.00000E+00	0.00000E+00	0.19595E+07
88	0.36060E+07	0.28343E+07	0.00000E+00	0.00000E+00	0.19595E+07
89	0.36060E+07	0.56686E+07	0.00000E+00	0.00000E+00	0.39190E+07
90	0.36060E+07	0.56686E+07	0.00000E+00	0.00000E+00	0.39190E+07
91	0.36060E+07	0.56686E+07	0.00000E+00	0.00000E+00	0.39190E+07
92	0.36060E+07	0.56686E+07	0.00000E+00	0.00000E+00	0.39190E+07
93	0.36060E+07	0.56686E+07	0.00000E+00	0.00000E+00	0.39190E+07
94	0.36060E+07	0.56686E+07	0.00000E+00	0.00000E+00	0.39190E+07
95	0.36060E+07	0.56686E+07	0.00000E+00	0.00000E+00	0.39190E+07
96	0.36060E+07	0.56686E+07	0.00000E+00	0.00000E+00	0.39190E+07
97	0.36060E+07	0.56686E+07	0.00000E+00	0.00000E+00	0.39190E+07
98	0.36060E+07	0.56686E+07	0.00000E+00	0.00000E+00	0.39190E+07
99	0.36060E+07	0.56686E+07	0.00000E+00	0.00000E+00	0.39190E+07
100	0.36060E+07	0.56686E+07	0.00000E+00	0.00000E+00	0.39190E+07
101	0.36060E+07	0.56686E+07	0.00000E+00	0.00000E+00	0.39190E+07
102	0.36060E+07	0.56686E+07	0.00000E+00	0.00000E+00	0.39190E+07
103	0.36060E+07	0.56686E+07	0.00000E+00	0.00000E+00	0.39190E+07
104	0.36060E+07	0.56686E+07	0.00000E+00	0.00000E+00	0.39190E+07
105	0.36060E+07	0.56686E+07	0.00000E+00	0.00000E+00	0.39190E+07
106	0.36060E+07	0.56686E+07	0.00000E+00	0.00000E+00	0.39190E+07
107	0.36060E+07	0.56686E+07	0.00000E+00	0.00000E+00	0.39190E+07
108	0.36060E+07	0.56686E+07	0.00000E+00	0.00000E+00	0.39190E+07
109	0.36060E+07	0.56686E+07	0.00000E+00	0.00000E+00	0.39190E+07
110	0.36060E+07	0.56686E+07	0.00000E+00	0.00000E+00	0.39190E+07
111	0.36060E+07	0.56686E+07	0.00000E+00	0.00000E+00	0.39190E+07
112	0.36060E+07	0.56686E+07	0.00000E+00	0.00000E+00	0.39190E+07
113	0.36060E+07	0.56686E+07	0.00000E+00	0.00000E+00	0.39190E+07
114	0.36060E+07	0.56686E+07	0.00000E+00	0.00000E+00	0.39190E+07

```
115   0.36060E+07   0.56686E+07   0.00000E+00   0.00000E+00   0.39190E+07
116   0.36060E+07   0.56686E+07   0.00000E+00   0.00000E+00   0.39190E+07
117   0.36060E+07   0.56686E+07   0.00000E+00   0.00000E+00   0.39190E+07
118   0.36060E+07   0.56686E+07   0.00000E+00   0.00000E+00   0.39190E+07
119   0.36060E+07   0.56686E+07   0.00000E+00   0.00000E+00   0.39190E+07
120   0.36060E+07   0.56686E+07   0.00000E+00   0.00000E+00   0.39190E+07
121   0.36060E+07   0.56686E+07   0.00000E+00   0.00000E+00   0.39190E+07
122   0.36060E+07   0.56686E+07   0.00000E+00   0.00000E+00   0.39190E+07
123   0.36060E+07   0.56686E+07   0.00000E+00   0.00000E+00   0.39190E+07
124   0.36060E+07   0.56686E+07   0.00000E+00   0.00000E+00   0.39190E+07
125   0.36060E+07   0.56686E+07   0.00000E+00   0.00000E+00   0.39190E+07
126   0.36060E+07   0.56686E+07   0.00000E+00   0.00000E+00   0.39190E+07
127   0.36060E+07   0.56686E+07   0.00000E+00   0.00000E+00   0.39190E+07
128   0.36060E+07   0.56686E+07   0.00000E+00   0.00000E+00   0.39190E+07
129   0.36060E+07   0.56686E+07   0.00000E+00   0.00000E+00   0.39190E+07
130   0.36060E+07   0.56686E+07   0.00000E+00   0.00000E+00   0.39190E+07
131   0.36060E+07   0.56686E+07   0.00000E+00   0.00000E+00   0.39190E+07
132   0.36060E+07   0.56686E+07   0.00000E+00   0.00000E+00   0.39190E+07
133   0.36060E+07   0.56686E+07   0.00000E+00   0.00000E+00   0.39190E+07
134   0.36060E+07   0.56686E+07   0.00000E+00   0.00000E+00   0.39190E+07
135   0.36060E+07   0.56686E+07   0.00000E+00   0.00000E+00   0.39190E+07
136   0.36060E+07   0.56686E+07   0.00000E+00   0.00000E+00   0.39190E+07
137   0.36060E+07   0.56686E+07   0.00000E+00   0.00000E+00   0.39190E+07
138   0.36060E+07   0.56686E+07   0.00000E+00   0.00000E+00   0.39190E+07
139   0.36060E+07   0.56686E+07   0.00000E+00   0.00000E+00   0.39190E+07
140   0.36060E+07   0.56686E+07   0.00000E+00   0.00000E+00   0.39190E+07
141   0.36060E+07   0.56686E+07   0.00000E+00   0.00000E+00   0.39190E+07
142   0.36060E+07   0.56686E+07   0.00000E+00   0.00000E+00   0.39190E+07
143   0.36060E+07   0.56686E+07   0.00000E+00   0.00000E+00   0.39190E+07
144   0.36060E+07   0.56686E+07   0.00000E+00   0.00000E+00   0.39190E+07
145   0.36060E+07   0.56686E+07   0.00000E+00   0.00000E+00   0.39190E+07
146   0.36060E+07   0.56686E+07   0.00000E+00   0.00000E+00   0.39190E+07
147   0.36060E+07   0.56686E+07   0.00000E+00   0.00000E+00   0.39190E+07
148   0.36060E+07   0.56686E+07   0.00000E+00   0.00000E+00   0.39190E+07
149   0.36060E+07   0.56686E+07   0.00000E+00   0.00000E+00   0.39190E+07
150   0.36060E+07   0.56686E+07   0.00000E+00   0.00000E+00   0.39190E+07
151   0.36060E+07   0.56686E+07   0.00000E+00   0.00000E+00   0.39190E+07
152   0.36060E+07   0.56686E+07   0.00000E+00   0.00000E+00   0.39190E+07
153   0.36060E+07   0.56686E+07   0.00000E+00   0.00000E+00   0.39190E+07
154   0.36060E+07   0.56686E+07   0.00000E+00   0.00000E+00   0.39190E+07
155   0.36060E+07   0.56686E+07   0.00000E+00   0.00000E+00   0.39190E+07
156   0.36060E+07   0.56686E+07   0.00000E+00   0.00000E+00   0.39190E+07
157   0.36060E+07   0.56686E+07   0.00000E+00   0.00000E+00   0.39190E+07
158   0.36060E+07   0.56686E+07   0.00000E+00   0.00000E+00   0.39190E+07
159   0.36060E+07   0.56686E+07   0.00000E+00   0.00000E+00   0.39190E+07
160   0.36060E+07   0.56686E+07   0.00000E+00   0.00000E+00   0.39190E+07
161   0.36060E+07   0.56686E+07   0.00000E+00   0.00000E+00   0.39190E+07
162   0.36060E+07   0.56686E+07   0.00000E+00   0.00000E+00   0.39190E+07
163   0.36060E+07   0.56686E+07   0.00000E+00   0.00000E+00   0.39190E+07
164   0.36060E+07   0.56686E+07   0.00000E+00   0.00000E+00   0.39190E+07
165   0.36060E+07   0.56686E+07   0.00000E+00   0.00000E+00   0.39190E+07
166   0.36060E+07   0.56686E+07   0.00000E+00   0.00000E+00   0.39190E+07
167   0.36060E+07   0.56686E+07   0.00000E+00   0.00000E+00   0.39190E+07
168   0.36060E+07   0.56686E+07   0.00000E+00   0.00000E+00   0.39190E+07
169   0.36060E+07   0.56686E+07   0.00000E+00   0.00000E+00   0.39190E+07
170   0.36060E+07   0.56686E+07   0.00000E+00   0.00000E+00   0.39190E+07
171   0.36060E+07   0.28343E+07   0.00000E+00   0.00000E+00   0.19595E+07
172   0.36060E+07   0.28343E+07   0.00000E+00   0.00000E+00   0.19595E+07
0   NODE  X-DISPLACEMENTS Y-DISPLACEMENTS
 ( 1)  0.33637957E-02  0.22016970E-14   ( 2)  0.30213783E-02 -0.12115166E-14   ( 3)  0.22891933E-02 -0.14553904E-02
 ( 4)  0.17607273E-02 -0.30382684E-02   ( 5)  0.13695289E-02 -0.46678097E-02   ( 6)  0.10393869E-02 -0.62789018E-02
 ( 7)  0.78298612E-03 -0.78009296E-02   ( 8)  0.56838025E-03 -0.92420468E-02   ( 9)  0.48840625E-03 -0.10550775E-01
 (10)  0.43292585E-03 -0.11749408E-01   (11)  0.42532845E-03 -0.12799494E-01   (12)  0.46702765E-03 -0.13750876E-01
 (13)  0.53163566E-03 -0.14573531E-01   (14)  0.59173342E-03 -0.15312709E-01   (15)  0.66343678E-03 -0.15940820E-01
 (16)  0.76325840E-03 -0.16496123E-01   (17)  0.90513124E-03 -0.16947856E-01   (18)  0.10309551E-02 -0.17324112E-01
 (19)  0.11792370E-02 -0.17592595E-01   (20)  0.13080527E-02 -0.17790509E-01   (21)  0.14518530E-02 -0.17900812E-01
 (22)  0.16002829E-02 -0.17950100E-01   (23)  0.17470136E-02 -0.17903485E-01   (24)  0.18913118E-02 -0.17795582E-01
 (25)  0.20369007E-02 -0.17592762E-01   (26)  0.21848890E-02 -0.17318315E-01   (27)  0.23235133E-02 -0.16939487E-01
 (28)  0.24409499E-02 -0.16486000E-01   (29)  0.25440745E-02 -0.15929356E-01   (30)  0.26182331E-02 -0.15298925E-01
 (31)  0.26802267E-02 -0.14554196E-01   (32)  0.27467980E-02 -0.13722754E-01   (33)  0.27909180E-02 -0.12764124E-01
```

```
(  34)  0.28261170E-02 -0.11703854E-01    (  35)  0.27111293E-02 -0.10498361E-01    (  36)  0.26328103E-02 -0.91821657E-02
(  37)  0.24151584E-02 -0.77353164E-02    (  38)  0.21561250E-02 -0.62030488E-02    (  39)  0.18979924E-02 -0.45883098E-02
(  40)  0.14192643E-02 -0.29626543E-02    (  41)  0.43353696E-03 -0.13959902E-02    (  42)  0.94526677E-15 -0.12462758E-14
(  43) -0.21318975E-14  0.22245429E-14    (  44)  0.35144376E-02  0.24605619E-03    (  45)  0.33999798E-02 -0.10804923E-03
(  46)  0.29072624E-02 -0.14436296E-02    (  47)  0.23950147E-02 -0.30350519E-02    (  48)  0.20001924E-02 -0.46690655E-02
(  49)  0.16461748E-02 -0.62782377E-02    (  50)  0.13446052E-02 -0.78093145E-02    (  51)  0.10923962E-02 -0.92444108E-02
(  52)  0.95733468E-03 -0.10564623E-01    (  53)  0.86047390E-03 -0.11755276E-01    (  54)  0.79624241E-03 -0.12814629E-01
(  55)  0.80315896E-03 -0.13758444E-01    (  56)  0.82192415E-03 -0.14588520E-01    (  57)  0.84884247E-03 -0.15319777E-01
(  58)  0.88402820E-03 -0.15954556E-01    (  59)  0.95597716E-03 -0.16503706E-01    (  60)  0.10603534E-02 -0.16963121E-01
(  61)  0.11525366E-02 -0.17331643E-01    (  62)  0.12647498E-02 -0.17607060E-01    (  63)  0.13654725E-02 -0.17797988E-01
(  64)  0.14827309E-02 -0.17914394E-01    (  65)  0.16010824E-02 -0.17957913E-01    (  66)  0.17192680E-02 -0.17917076E-01
(  67)  0.18334339E-02 -0.17803304E-01    (  68)  0.19473418E-02 -0.17607584E-01    (  69)  0.20595943E-02 -0.17326332E-01
(  70)  0.21681255E-02 -0.16953936E-01    (  71)  0.22491956E-02 -0.16493723E-01    (  72)  0.23228882E-02 -0.15943410E-01
(  73)  0.23595875E-02 -0.15306068E-01    (  74)  0.23878489E-02 -0.14569395E-01    (  75)  0.24072772E-02 -0.13730200E-01
(  76)  0.24135783E-02 -0.12780091E-01    (  77)  0.23975431E-02 -0.11709401E-01    (  78)  0.22425236E-02 -0.10511784E-01
(  79)  0.21059239E-02 -0.91842025E-02    (  80)  0.18502318E-02 -0.77435583E-02    (  81)  0.15467734E-02 -0.62027401E-02
(  82)  0.12690099E-02 -0.45890575E-02    (  83)  0.79697206E-03 -0.29604189E-02    (  84) -0.14142994E-03 -0.13688083E-02
(  85) -0.27176424E-03 -0.10975614E-03    (  86) -0.29967251E-03  0.18480466E-03    (  87)  0.35310781E-02  0.30855202E-03
(  88)  0.34050099E-02 -0.14178677E-03    (  89)  0.29004354E-02 -0.14439910E-02    (  90)  0.23930920E-02 -0.30336745E-02
(  91)  0.19989150E-02 -0.46682498E-02    (  92)  0.16445589E-02 -0.62777620E-02    (  93)  0.13445095E-02 -0.78083873E-02
(  94)  0.10911532E-02 -0.92437058E-02    (  95)  0.95752922E-03 -0.10563434E-01    (  96)  0.86004721E-03 -0.11754475E-01
(  97)  0.79692517E-03 -0.12813387E-01    (  98)  0.80301765E-03 -0.13757619E-01    (  99)  0.82262829E-03 -0.14587392E-01
( 100)  0.84896871E-03 -0.15318981E-01    ( 101)  0.88446732E-03 -0.15953438E-01    ( 102)  0.95562837E-03 -0.16502903E-01
( 103)  0.10605406E-02 -0.16961998E-01    ( 104)  0.11525580E-02 -0.17330922E-01    ( 105)  0.12652820E-02 -0.17606002E-01
( 106)  0.13656604E-02 -0.17797167E-01    ( 107)  0.14825856E-02 -0.17913340E-01    ( 108)  0.16011204E-02 -0.17957144E-01
( 109)  0.17191519E-02 -0.17916012E-01    ( 110)  0.18332129E-02 -0.17802553E-01    ( 111)  0.19470628E-02 -0.17606505E-01
( 112)  0.20597315E-02 -0.17325568E-01    ( 113)  0.21679574E-02 -0.16952788E-01    ( 114)  0.22492665E-02 -0.16492915E-01
( 115)  0.23224484E-02 -0.15942294E-01    ( 116)  0.23594840E-02 -0.15305267E-01    ( 117)  0.23871389E-02 -0.14568245E-01
( 118)  0.24073700E-02 -0.13729422E-01    ( 119)  0.24131815E-02 -0.12778800E-01    ( 120)  0.23980448E-02 -0.11708543E-01
( 121)  0.22419935E-02 -0.10510593E-01    ( 122)  0.21072737E-02 -0.91835410E-02    ( 123)  0.18503579E-02 -0.77426485E-02
( 124)  0.15484139E-02 -0.62022623E-02    ( 125)  0.12707649E-02 -0.45881468E-02    ( 126)  0.79898640E-03 -0.29589989E-02
( 127) -0.13348677E-03 -0.13706940E-02    ( 128) -0.27063867E-03 -0.13929989E-03    ( 129) -0.33472898E-03  0.24197416E-03
( 130)  0.38341190E-02  0.33649298E-03    ( 131)  0.35989795E-02 -0.14905711E-03    ( 132)  0.32222384E-02 -0.14401566E-02
( 133)  0.27432383E-02 -0.30333412E-02    ( 134)  0.23495179E-02 -0.46690857E-02    ( 135)  0.19844200E-02 -0.62787364E-02
( 136)  0.16584284E-02 -0.78129078E-02    ( 137)  0.13884984E-02 -0.92468554E-02    ( 138)  0.12200646E-02 -0.10571112E-01
( 139)  0.10978006E-02 -0.11759665E-01    ( 140)  0.10052100E-02 -0.12822132E-01    ( 141)  0.99082088E-03 -0.13763915E-01
( 142)  0.98533729E-03 -0.14596223E-01    ( 143)  0.99240354E-03 -0.15324829E-01    ( 144)  0.10074291E-02 -0.15961558E-01
( 145)  0.10628564E-02 -0.16508904E-01    ( 146)  0.11470149E-02 -0.16970893E-01    ( 147)  0.12199779E-02 -0.17336867E-01
( 148)  0.13127451E-02 -0.17614544E-01    ( 149)  0.13978511E-02 -0.17803051E-01    ( 150)  0.15001864E-02 -0.17921597E-01
( 151)  0.16014610E-02 -0.17963200E-01    ( 152)  0.17033150E-02 -0.17924212E-01    ( 153)  0.18011703E-02 -0.17808612E-01
( 154)  0.18973753E-02 -0.17615162E-01    ( 155)  0.19901138E-02 -0.17331794E-01    ( 156)  0.20808262E-02 -0.16961266E-01
( 157)  0.21429002E-02 -0.16499002E-01    ( 158)  0.21990562E-02 -0.15950573E-01    ( 159)  0.22151410E-02 -0.15311201E-01
( 160)  0.22232264E-02 -0.14577181E-01    ( 161)  0.22178240E-02 -0.13735678E-01    ( 162)  0.22014560E-02 -0.12788013E-01
( 163)  0.21581312E-02 -0.11713530E-01    ( 164)  0.19799868E-02 -0.10518090E-01    ( 165)  0.18080702E-02 -0.91865245E-02
( 166)  0.15346169E-02 -0.77471148E-02    ( 167)  0.12072759E-02 -0.62034159E-02    ( 168)  0.91929614E-03 -0.45889542E-02
( 169)  0.45521916E-03 -0.29586975E-02    ( 170) -0.45143943E-03 -0.13605826E-02    ( 171) -0.44200053E-03 -0.15506026E-03
( 172) -0.60590841E-03  0.25841186E-03    ( 173)  0.38541019E-02  0.34744653E-03    ( 174)  0.36069824E-02 -0.14770673E-03
( 175)  0.32154987E-02 -0.14451988E-02    ( 176)  0.27365317E-02 -0.30332340E-02    ( 177)  0.23439382E-02 -0.46683767E-02
( 178)  0.19801120E-02 -0.62774410E-02    ( 179)  0.16547737E-02 -0.78116979E-02    ( 180)  0.13851163E-02 -0.92459010E-02
( 181)  0.12181446E-02 -0.10569981E-01    ( 182)  0.10965048E-02 -0.11759474E-01    ( 183)  0.10052444E-02 -0.12821290E-01
( 184)  0.99122269E-03 -0.13763547E-01    ( 185)  0.98678197E-03 -0.14595286E-01    ( 186)  0.99313502E-03 -0.15324361E-01
( 187)  0.10079788E-02 -0.15960908E-01    ( 188)  0.10622777E-02 -0.16508483E-01    ( 189)  0.11472127E-02 -0.16969945E-01
( 190)  0.12201072E-02 -0.17336450E-01    ( 191)  0.13138604E-02 -0.17613733E-01    ( 192)  0.13981148E-02 -0.17802809E-01
( 193)  0.15000193E-02 -0.17920777E-01    ( 194)  0.16014497E-02 -0.17962991E-01    ( 195)  0.17031385E-02 -0.17923344E-01
( 196)  0.18006519E-02 -0.17808069E-01    ( 197)  0.18968392E-02 -0.17614244E-01    ( 198)  0.19901710E-02 -0.17331414E-01
( 199)  0.20807416E-02 -0.16960602E-01    ( 200)  0.21429538E-02 -0.16498625E-01    ( 201)  0.21984001E-02 -0.15949865E-01
( 202)  0.22144502E-02 -0.15310688E-01    ( 203)  0.22218806E-02 -0.14576196E-01    ( 204)  0.22174168E-02 -0.13735124E-01
( 205)  0.22019250E-02 -0.12787158E-01    ( 206)  0.21592161E-02 -0.11713555E-01    ( 207)  0.19819313E-02 -0.10517148E-01
( 208)  0.18115122E-02 -0.91853790E-02    ( 209)  0.15381624E-02 -0.77457838E-02    ( 210)  0.12118109E-02 -0.62021826E-02
( 211)  0.92475043E-03 -0.45889467E-02    ( 212)  0.46018049E-03 -0.29593448E-02    ( 213) -0.44419838E-03 -0.13644234E-02
( 214) -0.45000080E-03 -0.15209054E-03    ( 215) -0.62632371E-03  0.26688495E-03    ( 216)  0.11269435E-02 -0.14600154E-01
( 217)  0.12147709E-02 -0.15331870E-01    ( 218)  0.12870896E-02 -0.15970400E-01    ( 219)  0.13491490E-02 -0.16519395E-01
( 220)  0.14012438E-02 -0.16981023E-01    ( 221)  0.14483835E-02 -0.17348219E-01    ( 222)  0.14897457E-02 -0.17625016E-01
( 223)  0.15308188E-02 -0.17815146E-01    ( 224)  0.15687558E-02 -0.17931395E-01    ( 225)  0.16028146E-02 -0.17960423E-01
( 226)  0.16369975E-02 -0.17934036E-01    ( 227)  0.16757776E-02 -0.17819972E-01    ( 228)  0.17156331E-02 -0.17625785E-01
( 229)  0.17573579E-02 -0.17343158E-01    ( 230)  0.18034683E-02 -0.16972101E-01    ( 231)  0.18570022E-02 -0.16509611E-01
( 232)  0.19184918E-02 -0.15959494E-01    ( 233)  0.19913421E-02 -0.15318372E-01    ( 234)  0.20805509E-02 -0.14581126E-01
( 235)  0.17382212E-02 -0.92488042E-02    ( 236)  0.17753713E-02 -0.10576305E-01    ( 237)  0.18076688E-02 -0.11773620E-01
( 238)  0.18328600E-02 -0.12837004E-01    ( 239)  0.18448588E-02 -0.13778553E-01    ( 240)  0.18448482E-02 -0.14609011E-01
( 241)  0.18360087E-02 -0.15339937E-01    ( 242)  0.18203712E-02 -0.15978113E-01    ( 243)  0.17987045E-02 -0.16528030E-01
```

325

```
(244)  0.17711337E-02 -0.16990515E-01   (245)  0.17428959E-02 -0.17363754E-01   (246)  0.17124575E-02 -0.17636992E-01
(247)  0.16795905E-02 -0.17824768E-01   (248)  0.16422482E-02 -0.17938171E-01   (249)  0.16036782E-02 -0.17982792E-01
(250)  0.15649021E-02 -0.17938730E-01   (251)  0.15270570E-02 -0.17825096E-01   (252)  0.14918497E-02 -0.17633560E-01
(253)  0.14621685E-02 -0.17355900E-01   (254)  0.14330934E-02 -0.16978750E-01   (255)  0.14055962E-02 -0.16512495E-01
(256)  0.13825968E-02 -0.15959454E-01   (257)  0.13649171E-02 -0.15319086E-01   (258)  0.13543874E-02 -0.14582201E-01
(259)  0.13535257E-02 -0.13742165E-01   (260)  0.13640041E-02 -0.12793160E-01   (261)  0.13884314E-02 -0.11721366E-01
(262)  0.14175358E-02 -0.10516069E-01   (263)  0.14540011E-02 -0.91839123E-02   (264)  0.31588626E-02 -0.30281518E-02
(265)  0.31424930E-02 -0.46633563E-02   (266)  0.31216129E-02 -0.62725013E-02   (267)  0.30908320E-02 -0.78045403E-02
(268)  0.30423438E-02 -0.92428265E-02   (269)  0.29774751E-02 -0.10572218E-01   (270)  0.29015943E-02 -0.11779896E-01
(271)  0.28180056E-02 -0.12833600E-01   (272)  0.27208862E-02 -0.13768712E-01   (273)  0.26194020E-02 -0.14597171E-01
(274)  0.25143276E-02 -0.15328307E-01   (275)  0.24060984E-02 -0.15966566E-01   (276)  0.22945723E-02 -0.16517015E-01
(277)  0.21804543E-02 -0.16982839E-01   (278)  0.20663490E-02 -0.17366511E-01   (279)  0.19543568E-02 -0.17631040E-01
(280)  0.18372585E-02 -0.17812452E-01   (281)  0.17208733E-02 -0.17921291E-01   (282)  0.16022750E-02 -0.17954266E-01
(283)  0.14836466E-02 -0.17921355E-01   (284)  0.13663349E-02 -0.17811727E-01   (285)  0.12475684E-02 -0.17626949E-01
(286)  0.11345732E-02 -0.17358758E-01   (287)  0.10198168E-02 -0.16971663E-01   (288)  0.90448285E-03 -0.16501508E-01
(289)  0.79145222E-03 -0.15947388E-01   (290)  0.68153461E-03 -0.15306398E-01   (291)  0.57441458E-03 -0.14569494E-01
(292)  0.47097389E-03 -0.13731581E-01   (293)  0.37270921E-03 -0.12789909E-01   (294)  0.28830508E-03 -0.11728328E-01
(295)  0.21157153E-03 -0.10511650E-01   (296)  0.14631285E-03 -0.91777321E-02   (297)  0.98009813E-04 -0.77387110E-02
(298)  0.67545369E-04 -0.61981200E-02   (299)  0.48087878E-04 -0.45856860E-02   (300)  0.36117061E-04 -0.29564007E-02
(301)  0.40443436E-02  0.36647236E-03   (302)  0.42741495E-02 -0.18700161E-03   (303)  0.45091339E-02 -0.14839491E-02
(304)  0.46370473E-02 -0.30426276E-02   (305)  0.46672957E-02 -0.46645303E-02   (306)  0.46230913E-02 -0.62642947E-02
(307)  0.45246054E-02 -0.77889866E-02   (308)  0.43852973E-02 -0.92225552E-02   (309)  0.42150801E-02 -0.10551507E-01
(310)  0.40240481E-02 -0.11781807E-01   (311)  0.38097882E-02 -0.12805696E-01   (312)  0.36047613E-02 -0.13737847E-01
(313)  0.34021191E-02 -0.14565860E-01   (314)  0.32007105E-02 -0.15297150E-01   (315)  0.30006316E-02 -0.15935628E-01
(316)  0.28007694E-02 -0.16486888E-01   (317)  0.25998190E-02 -0.16956663E-01   (318)  0.23971546E-02 -0.17365892E-01
(319)  0.21840495E-02 -0.17602518E-01   (320)  0.19873079E-02 -0.17781719E-01   (321)  0.17941681E-02 -0.17887721E-01
(322)  0.16014598E-02 -0.17907633E-01   (323)  0.14086951E-02 -0.17887460E-01   (324)  0.12140634E-02 -0.17780472E-01
(325)  0.10149407E-02 -0.17598106E-01   (326)  0.80017976E-03 -0.17357933E-01   (327)  0.59662688E-03 -0.16945475E-01
(328)  0.39394514E-03 -0.16471111E-01   (329)  0.19209763E-03 -0.15916004E-01   (330) -0.10099229E-04 -0.15274605E-01
(331) -0.21429472E-03 -0.14537593E-01   (332) -0.41980492E-03 -0.13700315E-01   (333) -0.62588356E-03 -0.12761985E-01
(334) -0.84036895E-03 -0.11730388E-01   (335) -0.10314081E-02 -0.10491003E-01   (336) -0.12012437E-02 -0.91573616E-02
(337) -0.13400835E-02 -0.77231204E-02   (338) -0.14385739E-02 -0.61902373E-02   (339) -0.14830404E-02 -0.45873808E-02
(340) -0.14565082E-02 -0.29685590E-02   (341) -0.13378678E-02 -0.13914968E-02   (342) -0.10303353E-02 -0.19282153E-03
(343) -0.79424357E-03  0.28110298E-03   (
```

```
0ELE   CENTROID   CARTESIAN STRESSES   PRIN STRESSES PRIN      CARTESIAN STRAINS           PRINCIPAL
STRAINS       YM
 NO. XCORD YCORD   X     Y     XY   STRES1 STRES2 ANG  EX       EY       EXY       E1         E2
  1   1.31   13.45 -252.09 441.18 125.40 463.17 -274.08 80. -0.869E-04  0.126E-03  0.769E-04  0.132E-03 -0.936E-04
3916019.
  2   2.63   13.98  -77.28 -284.95 235.71  76.45 -438.68 33. -0.518E-05 -0.688E-04  0.144E-03  0.419E-04 -0.116E-03
3916019.
  3   5.25   13.39 -222.15 -313.93 -200.46 -62.39 -473.68 51. -0.407E-04 -0.688E-04 -0.123E-03  0.826E-05 -0.118E-03
3916019.
  4   6.56   12.40 -189.97  -8.66  42.39   0.76 -199.39 77. -0.481E-04  0.749E-05  0.260E-04  0.104E-04 -0.510E-04
3916019.
  5   9.18   11.55  -60.07  17.32  -9.51  18.47 -61.23  7. -0.162E-04  0.749E-05 -0.583E-05  0.784E-05 -0.166E-04
3916019.
  6  10.50   11.68  -35.10   1.00   1.15   1.04 -35.14 88. -0.902E-05  0.205E-05  0.704E-06  0.206E-05 -0.903E-05
3916019.
  7  13.12   10.96    2.81   8.58 -16.66  22.61 -11.21 40.  0.280E-06  0.205E-05 -0.102E-04  0.635E-05 -0.402E-05
3916019.
  8  14.44   10.11    3.46  -2.42 -23.88  24.58 -23.54 49.  0.101E-05 -0.795E-06 -0.146E-04  0.748E-05 -0.727E-05
3916019.
  9  17.06    9.45   62.53   9.39 -16.23  67.10   4.83 74.  0.155E-04 -0.795E-06 -0.995E-05  0.169E-04 -0.219E-05
3916019.
 10  18.38    9.65   29.96   7.65 -35.61  56.12 -18.51 54.  0.726E-05  0.423E-06 -0.218E-04  0.153E-04 -0.759E-05
3916019.
 11  21.00    8.99   80.46  17.75  -4.88  80.84  17.37 86.  0.196E-04  0.423E-06 -0.299E-05  0.198E-04  0.307E-06
3916019.
 12  22.31    8.14   94.79  -1.82 -54.12 119.03 -26.06 66.  0.243E-04 -0.531E-05 -0.332E-04  0.317E-04 -0.127E-04
3916019.
 13  24.93    7.48  134.13   6.04 -18.98 136.88   3.29 82.  0.339E-04 -0.531E-05 -0.116E-04  0.348E-04 -0.615E-05
3916019.
 14  26.25    7.68   79.75  10.05 -50.33 106.12 -16.32 62.  0.199E-04 -0.151E-05 -0.308E-04  0.279E-04 -0.959E-05
3916019.
 15  28.87    7.09  128.47  19.80  -2.63 128.53  19.73 89.  0.318E-04 -0.151E-05 -0.161E-05  0.318E-04 -0.153E-05
3916019.
 16  30.19    6.30  152.79  -3.76 -60.59 173.50 -24.47 71.  0.392E-04 -0.876E-05 -0.371E-04  0.456E-04 -0.151E-04
3916019.
```

17   32.81   5.77 178.62   1.40 -16.26 180.10 -0.08 85. 0.455E-04 -0.876E-05 -0.997E-05 0.460E-04 -0.922E-05
3916019.
18   34.12   6.04 118.32   9.12 -54.03 140.53 -13.09 68. 0.297E-04 -0.371E-05 -0.331E-04 0.366E-04 -0.105E-04
3916019.
19   36.74   5.51 151.79 15.81   1.61 151.81 15.79 1. 0.380E-04 -0.371E-05 0.984E-06 0.380E-04 -0.372E-05
3916019.
20   38.06   4.72 175.05 -2.74 -52.50 189.40 -17.09 75. 0.448E-04 -0.964E-05 -0.322E-04 0.492E-04 -0.140E-04
3916019.
21   40.68   4.27 179.61 -1.83 -10.87 180.26 -2.48 87. 0.460E-04 -0.964E-05 -0.666E-05 0.462E-04 -0.984E-05
3916019.
22   42.00   4.59 134.00   7.92 -42.70 147.11 -5.18 73. 0.338E-04 -0.482E-05 -0.262E-04 0.378E-04 -0.884E-05
3916019.
23   44.62   4.20 146.65 10.45   3.52 146.74 10.36 1. 0.369E-04 -0.482E-05 0.216E-05 0.369E-04 -0.485E-05
3916019.
24   45.93   3.48 172.50 -2.89 -42.20 182.12 -12.51 77. 0.442E-04 -0.955E-05 -0.259E-04 0.471E-04 -0.125E-04
3916019.
25   48.55   3.09 167.36 -3.91 -6.76 167.63 -4.18 88. 0.429E-04 -0.955E-05 -0.414E-05 0.430E-04 -0.963E-05
3916019.
26   49.87   3.41 124.23   7.22 -36.73 134.80 -3.35 74. 0.314E-04 -0.450E-05 -0.225E-04 0.346E-04 -0.774E-05
3916019.
27   52.49   3.02 132.79   8.93   3.23 132.87   8.85 1. 0.335E-04 -0.450E-05 0.198E-05 0.335E-04 -0.453E-05
3916019.
28   53.81   2.30 153.87 -3.27 -34.47 161.09 -10.50 78. 0.395E-04 -0.869E-05 -0.211E-04 0.417E-04 -0.109E-04
3916019.
29   56.43   1.97 152.62 -3.52 -3.57 152.70 -3.60 89. 0.392E-04 -0.869E-05 -0.219E-05 0.392E-04 -0.872E-05
3916019.
30   57.75   2.36 119.82   5.17 -29.17 126.82 -1.82 77. 0.303E-04 -0.480E-05 -0.179E-04 0.325E-04 -0.694E-05
3916019.
31   60.37   2.17 129.74   7.15   7.88 130.25   6.65 4. 0.328E-04 -0.480E-05 0.483E-05 0.329E-04 -0.495E-05
3916019.
32   61.68   1.57 159.76 -5.88 -28.05 164.39 -10.50 81. 0.411E-04 -0.966E-05 -0.172E-04 0.425E-04 -0.111E-04
3916019.
33   64.30   1.38 162.04 -5.42   2.92 162.09 -5.47 1. 0.417E-04 -0.966E-05 0.179E-05 0.417E-04 -0.968E-05
3916019.
34   65.62   1.77 122.62   5.86 -27.83 128.91 -0.43 77. 0.310E-04 -0.477E-05 -0.171E-04 0.329E-04 -0.669E-05
3916019.
35   68.24   1.58 128.22   6.98 11.10 129.23   5.97 5. 0.324E-04 -0.477E-05 0.681E-05 0.327E-04 -0.508E-05
3916019.
36   69.56   0.98 157.25 -4.40 -23.63 160.63 -7.78 82. 0.404E-04 -0.915E-05 -0.145E-04 0.414E-04 -0.102E-04
3916019.
37   72.18   0.79 148.13 -6.22   4.66 148.27 -6.36 2. 0.381E-04 -0.915E-05 0.285E-05 0.382E-04 -0.920E-05
3916019.
38   73.49   1.18 115.84   4.51 -20.39 119.46   0.90 80. 0.294E-04 -0.476E-05 -0.125E-04 0.305E-04 -0.587E-05
3916019.
39   76.11   1.05 117.51   4.85 11.47 118.67   3.69 6. 0.298E-04 -0.476E-05 0.703E-05 0.301E-04 -0.512E-05
3916019.
40   77.43   0.52 141.81 -5.51 -13.59 143.06 -6.76 85. 0.365E-04 -0.865E-05 -0.833E-05 0.369E-04 -0.903E-05
3916019.
41   80.05   0.52 146.61 -4.55 11.68 147.50 -5.45 4. 0.377E-04 -0.865E-05 0.716E-05 0.379E-04 -0.893E-05
3916019.
42   81.37   1.05 118.47   4.21 -17.19 121.00   1.68 82. 0.300E-04 -0.498E-05 -0.105E-04 0.308E-04 -0.575E-05
3916019.
43   83.99   1.05 118.61   4.24 17.79 121.31   1.53 9. 0.301E-04 -0.498E-05 0.109E-04 0.309E-04 -0.580E-05
3916019.
44   85.30   0.52 145.23 -4.85 -9.48 145.83 -5.45 86. 0.373E-04 -0.866E-05 -0.581E-05 0.375E-04 -0.884E-05
3916019.
45   87.92   0.59 145.98 -4.70 16.57 147.78 -6.50 6. 0.375E-04 -0.866E-05 0.102E-04 0.381E-04 -0.921E-05
3916019.
46   89.24   1.18 121.82   5.10 -12.63 123.17   3.75 84. 0.308E-04 -0.492E-05 -0.774E-05 0.313E-04 -0.533E-05
3916019.
47   91.86   1.31 121.55   5.05 21.31 125.33   1.27 10. 0.308E-04 -0.492E-05 0.131E-04 0.319E-04 -0.608E-05
3916019.
48   93.18   0.85 154.22 -5.89 -7.76 154.59 -6.27 87. 0.397E-04 -0.938E-05 -0.475E-05 0.398E-04 -0.950E-05
3916019.
49   95.80   0.98 157.29 -5.28 21.94 160.20 -8.19 8. 0.404E-04 -0.938E-05 0.134E-04 0.413E-04 -0.103E-04
3916019.
50   97.12   1.58 128.50   5.83 -12.50 129.76   4.57 84. 0.325E-04 -0.507E-05 -0.766E-05 0.329E-04 -0.546E-05
3916019.
51   99.74   1.71 124.15   4.96 25.62 129.43 -0.32 12. 0.315E-04 -0.507E-05 0.157E-04 0.331E-04 -0.669E-05
3916019.

327

```
 52   101.05    1.25 156.91  -4.65  -3.44 156.99  -4.73 89.  0.403E-04 -0.920E-05 -0.211E-05  0.403E-04 -0.922E-05
3916019.
 53   103.67    1.44 154.03  -5.23  27.80 158.74  -9.94 10.  0.396E-04 -0.920E-05  0.170E-04  0.410E-04 -0.106E-04
3916019.
 54   104.99    2.10 130.21   6.90  -6.63 130.56   6.54 87.  0.329E-04 -0.489E-05 -0.406E-05  0.330E-04 -0.500E-05
3916019.
 55   107.61    2.36 121.31   5.12  30.67 128.91  -2.48 14.  0.307E-04 -0.489E-05  0.188E-04  0.330E-04 -0.722E-05
3916019.
 56   108.93    1.97 156.02  -3.63   3.54 156.10  -3.70  1.  0.400E-04 -0.889E-05  0.217E-05  0.401E-04 -0.892E-05
3916019.
 57   111.55    2.30 156.89  -3.45  35.54 164.41 -10.98 12.  0.402E-04 -0.889E-05  0.218E-04  0.425E-04 -0.112E-04
3916019.
 58   112.86    3.02 135.27   9.24  -3.08 135.35   9.16 89.  0.341E-04 -0.455E-05 -0.189E-05  0.341E-04 -0.457E-05
3916019.
 59   115.48    3.41 126.18   7.42  37.39 136.97  -3.37 16.  0.318E-04 -0.455E-05  0.229E-04  0.351E-04 -0.786E-05
3916019.
 60   116.80    3.09 170.03  -3.90   6.92 170.30  -4.18  2.  0.436E-04 -0.968E-05  0.424E-05  0.437E-04 -0.976E-05
3916019.
 61   119.42    3.48 174.77  -2.96  42.82 184.55 -12.74 13.  0.448E-04 -0.968E-05  0.262E-04  0.478E-04 -0.127E-04
3916019.
 62   120.74    4.20 148.35  11.10  -4.16 148.47  10.97 88.  0.373E-04 -0.474E-05 -0.255E-05  0.374E-04 -0.478E-05
3916019.
 63   123.36    4.59 135.11   8.45  42.77 148.20  -4.64 17.  0.341E-04 -0.474E-05  0.262E-04  0.381E-04 -0.875E-05
3916019.
 64   124.67    4.27 184.66  -2.89   8.34 185.03  -3.26  3.  0.473E-04 -0.102E-04  0.511E-05  0.474E-04 -0.103E-04
3916019.
 65   127.29    4.66 174.94  -4.84  49.41 187.63 -17.52 14.  0.449E-04 -0.102E-04  0.303E-04  0.488E-04 -0.141E-04
3916019.
 66   128.61    5.38 147.27  15.62  -1.14 147.28  15.61 90.  0.368E-04 -0.353E-05 -0.699E-06  0.368E-04 -0.354E-05
3916019.
 67   131.23    5.91 116.42   9.45  52.01 137.54 -11.67 22.  0.292E-04 -0.353E-05  0.319E-04  0.357E-04 -0.100E-04
3916019.
 68   132.55    5.71 174.92   1.72  18.75 176.93  -0.29  6.  0.446E-04 -0.849E-05  0.115E-04  0.452E-04 -0.911E-05
3916019.
 69   135.17    6.30 154.55  -2.36  63.92 177.30 -25.10 20.  0.396E-04 -0.849E-05  0.392E-04  0.466E-04 -0.155E-04
3916019.
 70   136.49    7.09 128.53  20.63   2.63 128.60  20.56  1.  0.318E-04 -0.130E-05  0.161E-05  0.318E-04 -0.132E-05
3916019.
 71   139.11    7.68  78.40  10.60  51.08 105.81 -16.81 28.  0.195E-04 -0.130E-05  0.313E-04  0.279E-04 -0.970E-05
3916019.
 72   140.42    7.48 133.51   6.28  19.43 136.41   3.38  8.  0.338E-04 -0.522E-05  0.119E-04  0.347E-04 -0.610E-05
3916019.
 73   143.04    8.14  94.03  -1.62  53.29 117.81 -25.40 24.  0.241E-04 -0.522E-05  0.327E-04  0.314E-04 -0.125E-04
3916019.
 74   144.36    8.99  79.78  16.73   4.73  80.14  16.37  4.  0.195E-04  0.197E-06  0.290E-05  0.196E-04  0.884E-07
3916019.
 75   146.98    9.58  30.03   6.78  34.92  55.21 -18.40 36.  0.732E-05  0.197E-06  0.214E-04  0.150E-04 -0.752E-05
3916019.
 76   148.30    9.32  60.03  10.14  15.18  64.28   5.89 16.  0.148E-04 -0.476E-06  0.930E-05  0.161E-04 -0.178E-05
3916019.
 77   150.92    9.98  -6.61  -3.19  21.49  16.66 -26.45 47. -0.152E-05 -0.476E-06  0.132E-04  0.561E-05 -0.761E-05
3916019.
 78   152.23   10.89  -3.33   4.91  28.75  29.84 -28.26 49. -0.110E-05  0.142E-05  0.176E-04  0.906E-05 -0.874E-05
3916019.
 79   154.85   12.07  -1.93   5.19  11.01  13.20  -9.94 54. -0.757E-06  0.142E-05  0.675E-05  0.388E-05 -0.321E-05
3916019.
 80   156.17   12.34 -111.60  45.47  34.32  52.64 -118.77 78. -0.308E-04  0.173E-04  0.210E-04  0.195E-04 -0.330E-04
3916019.
 81   158.79   13.19 -358.85  -3.98 -20.86  -2.76 -360.07  3. -0.914E-04  0.173E-04 -0.128E-04  0.177E-04 -0.918E-04
3916019.
 82   160.11   13.78 -156.13 -304.99 244.76  25.27 -486.38 37. -0.243E-04 -0.699E-04  0.150E-03  0.313E-04 -0.125E-03
3916019.
 83   162.73   13.98  -15.93 -276.95 -148.82  51.50 -344.38 66.  0.101E-04 -0.699E-04 -0.912E-04  0.307E-04 -0.906E-04
3916019.
 84   164.04   13.45   76.91 384.57 -249.44 523.80 -62.32 29. -0.783E-15  0.943E-04 -0.153E-03  0.137E-03 -0.427E-04
3916019.
     NEW TENSILE CRACK NORMAL TO 1-1 DIRECTION
 85     1.31   15.29  -6.89 200.16 142.99 273.17 -79.90 63. -0.120E-04  0.515E-04  0.876E-04  0.738E-04 -0.344E-04
3916019.
```

328

86   2.63   15.45 74.00 -163.69 155.04 150.50 -240.19 26. 0.273E-04 -0.456E-04 0.950E-04 0.507E-04 -0.690E-04
3916019.
87   5.25   14.49 -102.71 -199.04 -176.57 32.15 -333.90 53. -0.161E-04 -0.456E-04 -0.108E-03 0.253E-04 -0.869E-04
3916019.
88   6.56   13.74 -5.41 -8.14 22.55 15.81 -29.36 43. -0.965E-06 -0.180E-05 0.138E-04 0.554E-05 -0.831E-05
3916019.
89   9.18   12.89 -98.97 -26.86 -81.84 26.52 -152.35 33. -0.239E-04 -0.180E-05 -0.502E-04 0.146E-04 -0.403E-04
3916019.
90   10.50   12.78 -14.61   5.26 -16.12 14.26 -23.61 29. -0.400E-05 0.209E-05 -0.988E-05 0.485E-05 -0.676E-05
3916019.
91   13.12   12.06 -6.47   6.89 -35.80 36.63 -36.21 40. -0.200E-05 0.209E-05 -0.219E-04 0.112E-04 -0.111E-04
3916019.
92   14.44   11.45 -7.24   1.65 -31.68 29.20 -34.78 41. -0.193E-05 0.792E-06 -0.194E-04 0.923E-05 -0.104E-04
3916019.
93   17.06   10.79 39.10 10.92 -21.39 50.62 -0.60 62. 0.943E-05 0.792E-06 -0.131E-04 0.130E-04 -0.274E-05
3916019.
94   18.38   10.75 17.49   7.08 -39.69 52.32 -27.74 49. 0.410E-05 0.916E-06 -0.243E-04 0.148E-04 -0.976E-05
3916019.
95   21.00   10.09 53.49 14.28 -10.33 56.05 11.73 76. 0.129E-04 0.916E-06 -0.633E-05 0.137E-04 0.133E-06
3916019.
96   22.31   9.48 47.39 -1.25 -55.08 83.28 -37.13 57. 0.122E-04 -0.274E-05 -0.338E-04 0.232E-04 -0.137E-04
3916019.
97   24.93   8.82 102.06   9.68 -13.72 104.05   7.69 82. 0.256E-04 -0.274E-05 -0.841E-05 0.262E-04 -0.335E-05
3916019.
98   26.25   8.78 56.93   4.76 -51.88 88.91 -27.22 58. 0.143E-04 -0.169E-05 -0.318E-04 0.241E-04 -0.115E-04
3916019.
99   28.87   8.19 97.81 12.93 -6.14 98.25 12.49 86. 0.243E-04 -0.169E-05 -0.376E-05 0.245E-04 -0.183E-05
3916019.
100   30.19   7.64 97.23 -4.67 -59.58 124.68 -32.11 65. 0.251E-04 -0.616E-05 -0.365E-04 0.335E-04 -0.146E-04
3916019.
101   32.81   7.12 140.25   3.94 -7.21 140.63   3.55 87. 0.356E-04 -0.616E-05 -0.442E-05 0.357E-04 -0.627E-05
3916019.
102   34.12   7.14 92.26 -0.44 -52.77 116.15 -24.32 66. 0.236E-04 -0.483E-05 -0.323E-04 0.309E-04 -0.121E-04
3916019.
103   36.74   6.62 123.47   5.80   1.36 123.49   5.78 1. 0.312E-04 -0.483E-05 0.836E-06 0.312E-04 -0.483E-05
3916019.
104   38.06   6.06 123.74 -5.24 -49.23 140.38 -21.88 71. 0.319E-04 -0.766E-05 -0.302E-04 0.370E-04 -0.128E-04
3916019.
105   40.68   5.60 147.65 -0.45 -0.75 147.65 -0.46 90. 0.377E-04 -0.766E-05 -0.461E-06 0.377E-04 -0.766E-05
3916019.
106   42.00   5.70 112.74 -0.42 -38.94 124.84 -12.52 73. 0.288E-04 -0.586E-05 -0.239E-04 0.325E-04 -0.957E-05
3916019.
107   44.62   5.30 122.98   1.63   5.95 123.27   1.34 3. 0.313E-04 -0.586E-05 0.365E-05 0.314E-04 -0.595E-05
3916019.
108   45.93   4.82 129.17 -4.62 -37.35 138.89 -14.34 75. 0.332E-04 -0.778E-05 -0.229E-04 0.362E-04 -0.108E-04
3916019.
109   48.55   4.42 137.26 -3.00   4.45 137.40 -3.14 2. 0.352E-04 -0.778E-05 0.273E-05 0.352E-04 -0.782E-05
3916019.
110   49.87   4.52 103.58   0.08 -32.60 113.00 -9.33 74. 0.264E-04 -0.527E-05 -0.200E-04 0.293E-04 -0.815E-05
3916019.
111   52.49   4.12 112.37   1.84   5.72 112.67   1.54 3. 0.286E-04 -0.527E-05 0.350E-05 0.287E-04 -0.536E-05
3916019.
112   53.81   3.64 117.50 -5.09 -32.20 125.44 -13.03 76. 0.303E-04 -0.730E-05 -0.197E-04 0.327E-04 -0.973E-05
3916019.
113   56.43   3.31 126.05 -3.38   3.87 126.17 -3.49 2. 0.324E-04 -0.730E-05 0.237E-05 0.324E-04 -0.734E-05
3916019.
114   57.75   3.47 101.07 -1.29 -28.29 108.37 -8.58 76. 0.259E-04 -0.549E-05 -0.173E-04 0.281E-04 -0.773E-05
3916019.
115   60.37   3.27 109.04   0.31   7.32 109.53 -0.18 4. 0.278E-04 -0.549E-05 0.448E-05 0.280E-04 -0.564E-05
3916019.
116   61.68   2.92 122.66 -6.19 -28.49 128.68 -12.20 78. 0.316E-04 -0.784E-05 -0.175E-04 0.335E-04 -0.969E-05
3916019.
117   64.30   2.72 129.34 -4.85   9.02 129.95 -5.45 4. 0.333E-04 -0.784E-05 0.553E-05 0.335E-04 -0.803E-05
3916019.
118   65.62   2.88 102.32 -1.17 -25.94 108.46 -7.31 77. 0.262E-04 -0.552E-05 -0.159E-04 0.281E-04 -0.741E-05
3916019.
119   68.24   2.68 108.64   0.09 11.44 109.83 -1.10 6. 0.277E-04 -0.552E-05 0.701E-05 0.281E-04 -0.589E-05
3916019.
120   69.56   2.33 121.60 -5.71 -22.59 125.49 -9.60 80. 0.313E-04 -0.767E-05 -0.138E-04 0.325E-04 -0.886E-05
3916019.

329

121   72.18   2.13 121.71 -5.69 11.56 122.76 -6.73 5.   0.314E-04 -0.767E-05 0.709E-05 0.317E-04 -0.799E-05
3916019.
122   73.49   2.29 98.00 -1.85 -18.86 101.44 -5.30 80.   0.251E-04 -0.548E-05 -0.116E-04 0.262E-04 -0.653E-05
3916019.
123   76.11   2.16 101.03 -1.25 11.67 102.35 -2.56 6.   0.259E-04 -0.548E-05 0.715E-05 0.263E-04 -0.588E-05
3916019.
124   77.43   1.86 115.48 -5.31 -16.15 117.60 -7.43 83.   0.298E-04 -0.725E-05 -0.990E-05 0.304E-04 -0.790E-05
3916019.
125   80.05   1.86 116.61 -5.08 14.03 118.20 -6.68 6.   0.300E-04 -0.725E-05 0.860E-05 0.305E-04 -0.774E-05
3916019.
126   81.37   2.16 100.31 -2.54 -16.80 102.98 -5.21 81.   0.257E-04 -0.577E-05 -0.103E-04 0.266E-04 -0.659E-05
3916019.
127   83.99   2.16 100.84 -2.43 17.14 103.61 -5.20 9.   0.259E-04 -0.577E-05 0.105E-04 0.267E-04 -0.662E-05
3916019.
128   85.30   1.86 116.85 -4.52 -12.95 118.22 -5.89 84.   0.301E-04 -0.712E-05 -0.794E-05 0.305E-04 -0.754E-05
3916019.
129   87.92   1.93 116.18 -4.65 17.80 118.74 -7.22 8.   0.299E-04 -0.712E-05 0.109E-04 0.307E-04 -0.791E-05
3916019.
130   89.24   2.29 103.90 -0.67 -13.31 105.57 -2.34 83.   0.266E-04 -0.548E-05 -0.816E-05 0.271E-04 -0.599E-05
3916019.
131   91.86   2.42 102.92 -0.86 19.24 106.37 -4.32 10.   0.263E-04 -0.548E-05 0.118E-04 0.274E-04 -0.653E-05
3916019.
132   93.18   2.19 123.70 -5.23 -13.03 125.00 -6.54 84.   0.319E-04 -0.765E-05 -0.798E-05 0.323E-04 -0.805E-05
3916019.
133   95.80   2.33 121.98 -5.58 22.39 125.80 -9.39 10.   0.314E-04 -0.765E-05 0.137E-04 0.326E-04 -0.882E-05
3916019.
134   97.12   2.68 108.39 -1.20 -12.59 109.82 -2.62 84.   0.277E-04 -0.584E-05 -0.772E-05 0.282E-04 -0.628E-05
3916019.
135   99.74   2.81 104.98 -1.88 24.21 110.21 -7.11 12.   0.269E-04 -0.584E-05 0.148E-04 0.285E-04 -0.744E-05
3916019.
136   101.05   2.59 126.20 -4.76 -8.67 126.77 -5.34 86.   0.325E-04 -0.766E-05 -0.531E-05 0.326E-04 -0.784E-05
3916019.
137   103.67   2.78 119.27 -6.15 27.97 125.23 -12.10 12.   0.308E-04 -0.766E-05 0.171E-04 0.326E-04 -0.949E-05
3916019.
138   104.99   3.21 110.39   0.02 -7.00 110.83 -0.43 86.   0.282E-04 -0.563E-05 -0.429E-05 0.283E-04 -0.577E-05
3916019.
139   107.61   3.47 102.12 -1.64 28.91 109.63 -9.15 15.   0.262E-04 -0.563E-05 0.177E-04 0.285E-04 -0.794E-05
3916019.
140   108.93   3.31 128.01 -3.45 -4.38 128.15 -3.59 88.   0.329E-04 -0.742E-05 -0.268E-05 0.329E-04 -0.746E-05
3916019.
141   111.55   3.64 119.66 -5.12 32.95 127.83 -13.29 14.   0.308E-04 -0.742E-05 0.202E-04 0.333E-04 -0.992E-05
3916019.
142   112.86   4.12 114.50   2.10 -5.53 114.77   1.83 87.   0.291E-04 -0.531E-05 -0.339E-05 0.292E-04 -0.539E-05
3916019.
143   115.48   4.52 105.27   0.26 33.27 114.92 -9.39 16.   0.269E-04 -0.531E-05 0.204E-04 0.298E-04 -0.827E-05
3916019.
144   116.80   4.42 139.40 -2.73 -4.28 139.53 -2.86 88.   0.357E-04 -0.782E-05 -0.262E-05 0.358E-04 -0.786E-05
3916019.
145   119.42   4.82 130.26 -4.56 38.17 140.32 -14.62 15.   0.335E-04 -0.782E-05 0.234E-04 0.366E-04 -0.109E-04
3916019.
146   120.74   5.30 124.07   2.65 -6.38 124.41   2.31 87.   0.315E-04 -0.566E-05 -0.391E-05 0.317E-04 -0.576E-05
3916019.
147   123.36   5.70 112.95   0.43 38.89 125.08 -11.71 17.   0.288E-04 -0.566E-05 0.238E-04 0.325E-04 -0.938E-05
3916019.
148   124.67   5.60 148.88 -2.03 -0.49 148.88 -2.03 90.   0.381E-04 -0.812E-05 -0.302E-06 0.381E-04 -0.812E-05
3916019.
149   127.29   6.00 125.37 -6.73 48.43 141.23 -22.59 18.   0.324E-04 -0.812E-05 0.297E-04 0.372E-04 -0.130E-04
3916019.
150   128.61   6.48 119.23   5.14 -1.20 119.24   5.13 89.   0.302E-04 -0.478E-05 -0.736E-06 0.302E-04 -0.478E-05
3916019.
151   131.23   7.01 93.35 -0.03 50.45 115.40 -22.08 24.   0.238E-04 -0.478E-05 0.309E-04 0.306E-04 -0.115E-04
3916019.
152   132.55   7.05 141.47   4.15   9.76 142.16   3.46 4.   0.359E-04 -0.617E-05 0.598E-05 0.361E-04 -0.638E-05
3916019.
153   135.17   7.64 95.43 -5.06 63.04 125.80 -35.43 26.   0.246E-04 -0.617E-05 0.386E-04 0.339E-04 -0.155E-04
3916019.
154   136.49   8.19 96.11 13.99   6.07 96.56 13.54 4.   0.238E-04 -0.134E-05 0.372E-05 0.240E-04 -0.147E-05
3916019.
155   139.11   8.78 55.50   5.86 52.36 88.62 -27.26 32.   0.139E-04 -0.134E-05 0.321E-04 0.240E-04 -0.115E-04
3916019.

156 140.42   8.82 101.10 10.20 13.90 103.18   8.12 9. 0.253E-04 -0.256E-05 0.852E-05 0.259E-04 -0.319E-05
3916019.
157 143.04   9.48 47.68 -0.48 53.85 82.59 -35.39 33. 0.122E-04 -0.256E-05 0.330E-04 0.229E-04 -0.133E-04
3916019.
158 144.36 10.09 53.29 13.17 10.78 56.00 10.46 14. 0.129E-04 0.641E-06 0.660E-05 0.138E-04 -0.190E-06
3916019.
159 146.98 10.68 18.23   6.16 39.67 52.31 -27.93 41. 0.434E-05 0.641E-06 0.243E-04 0.148E-04 -0.980E-05
3916019.
160 148.30 10.66 36.17   7.73 22.58 48.63 -4.73 29. 0.884E-05 0.127E-06 0.138E-04 0.127E-04 -0.369E-05
3916019.
161 150.92 11.31 -5.20 -0.54 30.47 27.69 -33.43 47. -0.130E-05 0.127E-06 0.187E-04 0.878E-05 -0.995E-05
3916019.
162 152.23 12.00 -7.06   3.42 44.34 42.83 -46.46 48. -0.198E-05 0.123E-05 0.272E-04 0.133E-04 -0.141E-04
3916019.
163 154.85 13.18 14.56   7.75 27.65 39.02 -16.71 41. 0.332E-05 0.123E-05 0.169E-04 0.108E-04 -0.626E-05
3916019.
164 156.17 13.68 -126.82 -5.85 92.87 44.49 -177.16 62. -0.321E-04 0.498E-05 0.569E-04 0.204E-04 -0.475E-04
3916019.
165 158.79 14.53 -59.62   7.59 -40.38 26.52 -78.55 25. -0.156E-04 0.498E-05 -0.247E-04 0.108E-04 -0.214E-04
3916019.
166 160.11 14.89 -5.41 -191.63 171.61 96.72 -293.76 31. 0.841E-05 -0.487E-04 0.105E-03 0.397E-04 -0.800E-04
3916019.
167 162.73 15.45 94.14 -171.76 -130.25 147.31 -224.93 68. 0.328E-04 -0.487E-04 -0.798E-04 0.491E-04 -0.650E-04
3916019.
168 164.04 15.29 72.14 177.57 -154.98 288.55 -38.85 36. 0.935E-05 0.417E-04 -0.950E-04 0.757E-04 -0.247E-04
3916019.
169   1.31 15.29 -398.83 291.65 456.54 518.80 -625.98 64. -0.168E-04 0.142E-04 0.409E-04 0.244E-04 -0.270E-04
29000000.
170   2.63 15.45 705.13 -30.79 1076.92 1475.22 -800.88 36. 0.246E-04 -0.836E-05 0.966E-04 0.592E-04 -0.429E-04
29000000.
171   5.25 14.49 -639.90 -434.30 -1210.18 677.43 -1751.64 43. -0.176E-04 -0.836E-05 -0.108E-03 0.415E-04 -0.674E-04
29000000.
172   6.56 13.74 89.75 154.74 447.11 570.54 -326.05 47. 0.149E-05 0.441E-05 0.401E-04 0.230E-04 -0.171E-04
29000000.
173   9.18 12.89 -531.09 -31.52 -359.85 156.74 -719.36 28. -0.180E-04 0.441E-05 -0.323E-04 0.128E-04 -0.264E-04
29000000.
174   10.50 12.78 -29.41   2.29 -19.85 11.84 -38.96 26. -0.104E-05 0.383E-06 -0.178E-05 0.811E-06 -0.147E-05
29000000.
175   13.12 12.06   9.30 13.90 -140.54 152.17 -128.96 45. 0.177E-06 0.383E-06 -0.126E-04 0.658E-05 -0.602E-05
29000000.
176   14.44 11.45 -3.08 -28.79 -135.12 119.79 -151.66 48. 0.192E-06 -0.961E-06 -0.121E-04 0.570E-05 -0.647E-05
29000000.
177   17.06 10.79 351.58 77.61 -64.19 365.87 63.32 77. 0.113E-04 -0.961E-06 -0.575E-05 0.120E-04 -0.160E-05
29000000.
178   18.38 10.75 164.32 16.82 -202.74 306.30 -125.16 55. 0.549E-05 -0.112E-05 -0.182E-04 0.119E-04 -0.748E-05
29000000.
179   21.00 10.09 450.18 102.58 -0.10 450.18 102.58 90. 0.145E-04 -0.112E-05 -0.877E-08 0.145E-04 -0.112E-05
29000000.
180   22.31   9.48 384.63 -35.29 -333.96 569.15 -219.80 61. 0.136E-04 -0.520E-05 -0.299E-04 0.219E-04 -0.135E-04
29000000.
181   24.93   8.82 790.34 86.43 -53.24 794.34 82.42 86. 0.264E-04 -0.520E-05 -0.477E-05 0.265E-04 -0.538E-05
29000000.
182   26.25   8.78 460.80 34.45 -300.51 616.07 -120.82 63. 0.155E-04 -0.358E-05 -0.269E-04 0.225E-04 -0.105E-04
29000000.
183   28.87   8.19 762.46 124.95 11.92 762.68 124.73 1. 0.250E-04 -0.358E-05 0.107E-05 0.250E-04 -0.359E-05
29000000.
184   30.19   7.64 738.62 -34.34 -389.69 900.98 -196.70 67. 0.258E-04 -0.882E-05 -0.349E-04 0.331E-04 -0.161E-04
29000000.
185   32.81   7.12 1058.20 61.55 -34.27 1059.37 60.37 88. 0.359E-04 -0.882E-05 -0.307E-05 0.359E-04 -0.888E-05
29000000.
186   34.12   7.14 702.15 37.65 -338.51 844.21 -104.42 67. 0.238E-04 -0.597E-05 -0.303E-04 0.302E-04 -0.123E-04
29000000.
187   36.74   6.62 940.22 109.07 27.01 941.09 108.19 2. 0.313E-04 -0.597E-05 0.242E-05 0.313E-04 -0.600E-05
29000000.
188   38.06   6.06 923.08 -14.58 -349.85 1039.23 -130.72 72. 0.320E-04 -0.101E-04 -0.314E-04 0.372E-04 -0.153E-04
29000000.
189   40.68   5.60 1095.58 37.18 -19.52 1095.94 36.82 89. 0.374E-04 -0.101E-04 -0.175E-05 0.374E-04 -0.101E-04
29000000.
190   42.00   5.70 844.54 43.53 -270.46 927.31 -39.24 73. 0.287E-04 -0.724E-05 -0.242E-04 0.324E-04 -0.109E-04
29000000.

191   44.62   5.30 919.08 65.89 33.42 920.38 64.58 2. 0.310E-04 -0.724E-05 0.300E-05 0.311E-04 -0.729E-05
29000000.
192   45.93   4.82 956.70 -7.36 -285.98 1035.15 -85.81 75. 0.331E-04 -0.102E-04 -0.256E-04 0.366E-04 -0.137E-04
29000000.
193   48.55   4.42 1008.41   8.17 -2.02 1008.42   8.16 90. 0.347E-04 -0.102E-04 -0.181E-06 0.347E-04 -0.102E-04
29000000.
194   49.87   4.52 779.64 38.99 -234.93 847.87 -29.24 74. 0.265E-04 -0.672E-05 -0.211E-04 0.295E-04 -0.978E-05
29000000.
195   52.49   4.12 844.01 58.30 25.15 844.81 57.50 2. 0.285E-04 -0.672E-05 0.225E-05 0.285E-04 -0.676E-05
29000000.
196   53.81   3.64 872.34 -8.92 -235.24 931.20 -67.79 76. 0.302E-04 -0.933E-05 -0.211E-04 0.328E-04 -0.120E-04
29000000.
197   56.43   3.31 932.12   9.02 10.64 932.24   8.90 1. 0.320E-04 -0.933E-05 0.954E-06 0.321E-04 -0.934E-05
29000000.
198   57.75   3.47 771.14 31.32 -182.39 813.66 -11.20 77. 0.263E-04 -0.690E-05 -0.164E-04 0.282E-04 -0.880E-05
29000000.
199   60.37   3.27 816.36 44.88 59.62 820.94 40.30 4. 0.277E-04 -0.690E-05 0.534E-05 0.279E-04 -0.710E-05
29000000.
200   61.68   2.92 914.13 -22.25 -200.12 955.11 -63.22 78. 0.318E-04 -0.102E-04 -0.179E-04 0.336E-04 -0.121E-04
29000000.
201   64.30   2.72 959.98 -8.48 52.96 962.87 -11.37 3. 0.332E-04 -0.102E-04 0.475E-05 0.333E-04 -0.104E-04
29000000.
202   65.62   2.88 769.24 32.60 -179.23 810.53 -8.69 77. 0.262E-04 -0.683E-05 -0.161E-04 0.280E-04 -0.868E-05
29000000.
203   68.24   2.68 810.34 44.92 74.41 817.51 37.76 6. 0.275E-04 -0.683E-05 0.667E-05 0.278E-04 -0.715E-05
29000000.
204   69.56   2.33 906.09 -12.87 -175.78 938.57 -45.34 80. 0.314E-04 -0.982E-05 -0.158E-04 0.328E-04 -0.113E-04
29000000.
205   72.18   2.13 896.97 -15.59 54.80 900.25 -18.87 3. 0.311E-04 -0.982E-05 0.491E-05 0.312E-04 -0.996E-05
29000000.
206   73.49   2.29 741.86 28.68 -134.39 766.35   4.20 80. 0.253E-04 -0.669E-05 -0.120E-04 0.264E-04 -0.778E-05
29000000.
207   76.11   2.16 763.80 35.26 72.42 770.93 28.13 6. 0.260E-04 -0.669E-05 0.649E-05 0.263E-04 -0.701E-05
29000000.
208   77.43   1.86 855.97 -15.30 -105.78 868.63 -27.96 83. 0.297E-04 -0.938E-05 -0.948E-05 0.302E-04 -0.995E-05
29000000.
209   80.05   1.86 868.99 -11.39 99.07 880.00 -22.40 6. 0.301E-04 -0.938E-05 0.888E-05 0.306E-04 -0.988E-05
29000000.
210   81.37   2.16 753.34 26.42 -113.46 770.64   9.12 81. 0.257E-04 -0.688E-05 -0.102E-04 0.265E-04 -0.766E-05
29000000.
211   83.99   2.16 760.13 28.45 114.97 777.77 10.81 9. 0.259E-04 -0.688E-05 0.103E-04 0.267E-04 -0.767E-05
29000000.
212   85.30   1.86 867.97 -9.81 -83.99 875.93 -17.77 85. 0.300E-04 -0.932E-05 -0.753E-05 0.304E-04 -0.967E-05
29000000.
213   87.92   1.93 862.54 -11.44 125.73 880.27 -29.16 8. 0.299E-04 -0.932E-05 0.113E-04 0.307E-04 -0.101E-04
29000000.
214   89.24   2.29 781.51 32.47 -79.80 789.92 24.06 84. 0.266E-04 -0.696E-05 -0.715E-05 0.270E-04 -0.734E-05
29000000.
215   91.86   2.42 771.14 29.36 140.79 796.96   3.54 10. 0.263E-04 -0.696E-05 0.126E-04 0.274E-04 -0.812E-05
29000000.
216   93.18   2.19 918.05 -13.12 -76.38 924.28 -19.34 85. 0.318E-04 -0.995E-05 -0.685E-05 0.321E-04 -0.102E-04
29000000.
217   95.80   2.33 908.50 -15.98 163.91 936.71 -44.18 10. 0.315E-04 -0.995E-05 0.147E-04 0.328E-04 -0.112E-04
29000000.
218   97.12   2.68 811.14 35.83 -86.29 820.63 26.34 84. 0.276E-04 -0.716E-05 -0.774E-05 0.280E-04 -0.758E-05
29000000.
219   99.74   2.81 790.46 29.62 162.93 823.88 -3.80 12. 0.270E-04 -0.716E-05 0.146E-04 0.284E-04 -0.865E-05
29000000.
220   101.05   2.59 938.65 -1.01 -53.81 941.72 -4.08 87. 0.324E-04 -0.974E-05 -0.482E-05 0.325E-04 -0.988E-05
29000000.
221   103.67   2.78 888.46 -16.07 195.82 929.03 -56.65 12. 0.308E-04 -0.975E-05 0.176E-04 0.326E-04 -0.116E-04
29000000.
222   104.99   3.21 830.76 46.33 -47.11 833.58 43.51 87. 0.282E-04 -0.700E-05 -0.422E-05 0.283E-04 -0.712E-05
29000000.
223   107.61   3.47 773.01 29.00 196.62 821.77 -19.76 14. 0.264E-04 -0.700E-05 0.176E-04 0.285E-04 -0.918E-05
29000000.
224   108.93   3.31 948.26   8.53 -12.67 948.43   8.36 89. 0.326E-04 -0.952E-05 -0.114E-05 0.326E-04 -0.952E-05
29000000.
225   111.55   3.64 887.86 -9.60 241.94 948.92 -70.67 14. 0.307E-04 -0.952E-05 0.217E-04 0.335E-04 -0.123E-04
29000000.

332

```
226    112.86    4.12  859.03  59.89  -24.51  859.78  59.14  88.  0.290E-04  -0.682E-05  -0.220E-05  0.290E-04  -0.685E-05
29000000.
227    115.48    4.52  791.98  39.78  238.81  861.39  -29.63  16.  0.269E-04  -0.682E-05  0.214E-04  0.300E-04  -0.993E-05
29000000.
228    116.80    4.42 1024.48   9.49   2.17 1024.48   9.49   0.  0.352E-04  -0.103E-04  0.194E-06  0.352E-04  -0.103E-04
29000000.
229    119.42    4.82  964.48  -8.52  290.35 1044.54  -88.57  15.  0.333E-04  -0.103E-04  0.260E-04  0.369E-04  -0.139E-04
29000000.
230    120.74    5.30  927.29  69.62  -35.83  928.78  68.12  88.  0.313E-04  -0.719E-05  -0.321E-05  0.313E-04  -0.726E-05
29000000.
231    123.36    5.70  840.90  43.70  271.58  924.62  -40.02  17.  0.285E-04  -0.719E-05  0.243E-04  0.323E-04  -0.109E-04
29000000.
232    124.67    5.60 1110.10  25.98   1.29 1110.10  25.98   0.  0.380E-04  -0.106E-04  0.115E-06  0.380E-04  -0.106E-04
29000000.
233    127.29    6.00  937.64  -25.77  333.06 1041.57 -129.69  17.  0.326E-04  -0.106E-04  0.299E-04  0.373E-04  -0.152E-04
29000000.
234    128.61    6.48  910.78 106.98  -24.46  911.53 106.24  88.  0.303E-04  -0.573E-05  -0.219E-05  0.303E-04  -0.577E-05
29000000.
235    131.23    7.01  712.53  47.49  324.49  844.62  -84.59  22.  0.241E-04  -0.573E-05  0.291E-04  0.300E-04  -0.117E-04
29000000.
236    132.55    7.05 1066.81  70.17  56.39 1069.99  66.99   3.  0.361E-04  -0.862E-05  0.506E-05  0.362E-04  -0.876E-05
29000000.
237    135.17    7.64  727.90  -31.52  416.74  911.97 -215.59  24.  0.254E-04  -0.862E-05  0.374E-04  0.337E-04  -0.169E-04
29000000.
238    136.49    8.19  749.67 126.57  -15.21  750.04 126.20  89.  0.245E-04  -0.339E-05  -0.136E-05  0.246E-04  -0.341E-05
29000000.
239    139.11    8.78  452.14  37.31  302.34  611.37 -121.92  28.  0.152E-04  -0.339E-05  0.271E-04  0.223E-04  -0.105E-04
29000000.
240    140.42    8.82  780.99  85.44  55.90  785.45  80.97   5.  0.260E-04  -0.513E-05  0.501E-05  0.262E-04  -0.533E-05
29000000.
241    143.04    9.48  385.40  -33.25  326.99  564.33 -212.18  29.  0.136E-04  -0.513E-05  0.293E-04  0.217E-04  -0.132E-04
29000000.
242    144.36   10.09  447.83  95.89   0.21  447.83  95.89   0.  0.145E-04  -0.133E-05  0.190E-07  0.145E-04  -0.133E-05
29000000.
243    146.98   10.68  163.57  10.61  199.84  301.06 -126.88  35.  0.553E-05  -0.133E-05  0.179E-04  0.117E-04  -0.749E-05
29000000.
244    148.30   10.66  326.76  71.12  65.50  342.57  55.31  14.  0.105E-04  -0.928E-06  0.587E-05  0.112E-04  -0.164E-05
29000000.
245    150.92   11.31   31.07  -17.59  120.83  130.00 -116.51  39.  0.125E-05  -0.928E-06  0.108E-04  0.569E-05  -0.536E-05
29000000.
246    152.23   12.00   21.01  16.35  218.47  237.16 -199.81  45.  0.555E-06  0.346E-06  0.196E-04  0.102E-04  -0.934E-05
29000000.
247    154.85   13.18  244.50  83.40  114.58  304.01  23.89  27.  0.757E-05  0.346E-06  0.103E-04  0.102E-04  -0.232E-05
29000000.
248    156.17   13.68  -535.39 172.56  389.56  344.95 -707.78  66.  -0.202E-04  0.115E-04  0.349E-04  0.192E-04  -0.280E-04
29000000.
249    158.79   14.53  -414.94 208.69  -550.43  529.49 -735.74  30.  -0.165E-04  0.115E-04  -0.493E-04  0.259E-04  -0.308E-04
29000000.
250    160.11   14.89  205.85 -463.58 1225.51 1141.53 -1399.26  37.  0.119E-04  -0.181E-04  0.110E-03  0.538E-04  -0.601E-04
29000000.
251    162.73   15.45  877.66 -262.13 -947.01 1413.03 -797.50  61.  0.330E-04  -0.181E-04  -0.849E-04  0.570E-04  -0.421E-04
29000000.
252    164.04   15.29   -4.60  240.56 -462.45  596.40 -360.44  38.  -0.265E-05  0.834E-05  -0.415E-04  0.243E-04  -0.186E-04
29000000.
253     45.93    5.63  110.69  -4.71  -24.89  115.83  -9.85  78.  0.285E-04  -0.686E-05  -0.153E-04  0.301E-04  -0.843E-05
3916019.
254     48.55    5.24  121.56  -2.54  18.50  124.26  -5.24   8.  0.312E-04  -0.686E-05  0.113E-04  0.320E-04  -0.768E-05
3916019.
255     49.87    5.48   86.22  -5.37  -24.84   92.52  -11.68  76.  0.223E-04  -0.578E-05  -0.152E-04  0.242E-04  -0.771E-05
3916019.
256     52.49    4.85  114.79   0.34  13.16  116.28  -1.15   6.  0.293E-04  -0.578E-05  0.806E-05  0.298E-04  -0.623E-05
3916019.
257     53.81    5.28   70.78  -5.51  -23.47   77.42  -12.16  74.  0.184E-04  -0.502E-05  -0.144E-04  0.204E-04  -0.706E-05
3916019.
258     56.43    4.52  111.74   2.68  13.38  113.36   1.06   7.  0.284E-04  -0.502E-05  0.820E-05  0.289E-04  -0.552E-05
3916019.
259     57.75    5.15   60.35  -6.67  -22.06   66.95  -13.28  73.  0.158E-04  -0.479E-05  -0.135E-04  0.178E-04  -0.681E-05
3916019.
260     60.37    4.32  110.37   3.33  13.31  112.00   1.70   7.  0.280E-04  -0.479E-05  0.816E-05  0.285E-04  -0.529E-05
3916019.
```

333

```
261    61.68   5.08  50.43  -7.41 -24.53  59.43 -16.41 70.  0.133E-04 -0.447E-05 -0.150E-04  0.160E-04 -0.722E-05
3916019.
262    64.30   4.13 113.18   5.14  14.63 115.12   3.20  8.  0.286E-04 -0.447E-05  0.897E-05  0.292E-04 -0.506E-05
3916019.
263    65.62   4.95  45.46  -6.97 -22.29  53.65 -15.16 70.  0.120E-04 -0.410E-05 -0.137E-04  0.145E-04 -0.661E-05
3916019.
264    68.24   3.93 110.18   5.98  14.61 112.19   3.97  8.  0.278E-04 -0.410E-05  0.895E-05  0.284E-04 -0.472E-05
3916019.
265    69.56   4.89  39.82  -6.43 -21.15  48.04 -14.64 69.  0.105E-04 -0.368E-05 -0.130E-04  0.130E-04 -0.619E-05
3916019.
266    72.18   3.73 107.64   7.14  14.38 109.66   5.12  8.  0.271E-04 -0.368E-05  0.882E-05  0.277E-04 -0.429E-05
3916019.
267    73.49   4.76  39.72  -6.02 -16.36  44.97 -11.27 72.  0.105E-04 -0.357E-05 -0.100E-04  0.121E-04 -0.517E-05
3916019.
268    76.11   3.60 102.59   6.56  13.73 104.51   4.63  8.  0.259E-04 -0.357E-05  0.841E-05  0.265E-04 -0.415E-05
3916019.
269    77.43   4.76  36.77  -4.66 -15.73  42.07  -9.96 71.  0.963E-05 -0.307E-05 -0.964E-05  0.113E-04 -0.469E-05
3916019.
270    80.05   3.60 102.50   8.48  14.93 104.82   6.17  9.  0.257E-04 -0.307E-05  0.915E-05  0.265E-04 -0.378E-05
3916019.
271    81.37   4.76  35.87  10.08 -11.38  40.17   5.78 69.  0.864E-05  0.742E-06 -0.697E-05  0.996E-05 -0.576E-06
3916019.
272    83.99   4.76  36.09  10.12  11.60  40.51   5.70 21.  0.870E-05  0.742E-06  0.711E-05  0.101E-04 -0.614E-06
3916019.
273    85.30   3.60 103.02   8.50 -14.73 105.26   6.26 81.  0.259E-04 -0.309E-05 -0.903E-05  0.266E-04 -0.378E-05
3916019.
274    87.92   4.76  37.63  -4.58  16.05  43.04  -9.98 19.  0.984E-05 -0.309E-05  0.983E-05  0.115E-04 -0.475E-05
3916019.
275    89.24   3.67 105.49   6.84 -14.28 107.52   4.82 82.  0.266E-04 -0.364E-05 -0.875E-05  0.272E-04 -0.426E-05
3916019.
276    91.86   4.82  38.29  -6.60  18.11  44.69 -12.99 19.  0.101E-04 -0.364E-05  0.111E-04  0.121E-04 -0.560E-05
3916019.
277    93.18   3.80 108.73   7.03 -15.73 111.11   4.65 81.  0.274E-04 -0.376E-05 -0.964E-05  0.281E-04 -0.449E-05
3916019.
278    95.80   4.89  40.13  -6.70  20.74  47.99 -14.56 21.  0.106E-04 -0.376E-05  0.127E-04  0.130E-04 -0.617E-05
3916019.
279    97.12   3.93 110.08   5.99 -14.89 112.17   3.90 82.  0.278E-04 -0.409E-05 -0.913E-05  0.284E-04 -0.473E-05
3916019.
280    99.74   4.95  44.52  -7.12  21.70  52.43 -15.02 20.  0.117E-04 -0.409E-05  0.133E-04  0.142E-04 -0.651E-05
3916019.
281   101.05   4.06 110.90   5.38 -14.52 112.86   3.42 82.  0.280E-04 -0.429E-05 -0.890E-05  0.286E-04 -0.489E-05
3916019.
282   103.67   5.02  51.92  -6.42  22.72  59.73 -14.22 19.  0.136E-04 -0.429E-05  0.139E-04  0.160E-04 -0.668E-05
3916019.
283   104.99   4.26 112.41   3.61 -12.52 113.83   2.19 84.  0.285E-04 -0.482E-05 -0.767E-05  0.290E-04 -0.525E-05
3916019.
284   107.61   5.15  59.73  -6.92  23.18  67.00 -14.19 17.  0.156E-04 -0.482E-05  0.142E-04  0.178E-04 -0.705E-05
3916019.
285   108.93   4.52 113.04   2.66 -13.57 114.68   1.01 83.  0.287E-04 -0.509E-05 -0.832E-05  0.292E-04 -0.560E-05
3916019.
286   111.55   5.28  71.46  -5.66  24.53  78.60 -12.80 16.  0.185E-04 -0.509E-05  0.150E-04  0.207E-04 -0.728E-05
3916019.
287   112.86   4.85 116.93   0.24 -13.21 118.40  -1.24 84.  0.298E-04 -0.591E-05 -0.809E-05  0.303E-04 -0.636E-05
3916019.
288   115.48   5.48  87.54  -5.64  25.29  93.96 -12.06 14.  0.226E-04 -0.591E-05  0.155E-04  0.246E-04 -0.788E-05
3916019.
289   116.80   5.24 123.61  -2.47 -18.92 126.39  -5.25 82.  0.317E-04 -0.694E-05 -0.116E-04  0.325E-04 -0.779E-05
3916019.
290   119.42   5.63 111.30  -4.93  25.21 116.53 -10.17 12.  0.287E-04 -0.694E-05  0.155E-04  0.303E-04 -0.855E-05
3916019.
291    26.25   9.44  47.33  -0.96 -66.45  93.88 -47.52 55.  0.121E-04 -0.266E-05 -0.407E-04  0.264E-04 -0.169E-04
3916019.
292    28.87   8.85  89.91   7.55 -20.63  94.79   2.67 77.  0.226E-04 -0.266E-05 -0.126E-04  0.241E-04 -0.416E-05
3916019.
293    30.19   9.21  35.72  -6.03 -66.13  84.19 -54.50 54.  0.943E-05 -0.336E-05 -0.405E-04  0.243E-04 -0.182E-04
3916019.
294    32.81   8.32 114.04   9.64 -11.34 115.25   8.42 84.  0.286E-04 -0.336E-05 -0.695E-05  0.290E-04 -0.374E-05
3916019.
295    34.12   8.95  29.20 -14.91 -62.50  73.43 -59.13 55.  0.822E-05 -0.530E-05 -0.383E-04  0.218E-04 -0.189E-04
3916019.
```

334

296   36.74   7.80 119.04   3.06 -6.86 119.44   2.66 87. 0.302E-04 -0.530E-05 -0.421E-05 0.304E-04 -0.542E-05
3916019.
297   38.06   8.69 22.38 -13.31 -50.09 57.71 -48.64 55. 0.639E-05 -0.454E-05 -0.307E-04 0.172E-04 -0.154E-04
3916019.
298   40.68   7.34 127.88   7.79 -1.04 127.89   7.78 90. 0.323E-04 -0.454E-05 -0.636E-06 0.323E-04 -0.454E-05
3916019.
299   42.00   8.49   9.40 -12.63 -46.01 45.69 -48.92 52. 0.305E-05 -0.371E-05 -0.282E-04 0.142E-04 -0.148E-04
3916019.
300   44.62   6.94 121.44   9.78 -2.32 121.49   9.73 89. 0.305E-04 -0.371E-05 -0.142E-05 0.305E-04 -0.372E-05
3916019.
301   45.93   8.29 -2.42 -12.07 -43.05 36.07 -50.57 48. -0.269E-08 -0.296E-05 -0.264E-04 0.118E-04 -0.148E-04
3916019.
302   48.55   6.55 117.12 11.84 -0.91 117.13 11.83 90. 0.293E-04 -0.296E-05 -0.559E-06 0.293E-04 -0.296E-05
3916019.
303   49.87   8.10 -11.58 -13.98 -39.74 26.97 -52.53 46. -0.224E-05 -0.298E-05 -0.244E-04 0.957E-05 -0.148E-04
3916019.
304   52.49   6.16 111.38 10.61 -1.38 111.40 10.59 89. 0.279E-04 -0.298E-05 -0.845E-06 0.279E-04 -0.298E-05
3916019.
305   53.81   7.90 -18.60 -15.30 -36.53 19.62 -53.52 44. -0.397E-05 -0.296E-05 -0.224E-04 0.774E-05 -0.147E-04
3916019.
306   56.43   5.83 110.16 10.46   0.51 110.16 10.45 0. 0.276E-04 -0.296E-05 0.315E-06 0.276E-04 -0.296E-05
3916019.
307   57.75   7.77 -25.00 -17.33 -34.24 13.29 -55.62 42. -0.550E-05 -0.315E-05 -0.210E-04 0.623E-05 -0.149E-04
3916019.
308   60.37   5.63 110.20   9.71   1.64 110.23   9.69 1. 0.276E-04 -0.315E-05 0.101E-05 0.277E-04 -0.316E-05
3916019.
309   61.68   7.70 -31.24 -18.81 -33.20   8.75 -58.80 40. -0.702E-05 -0.321E-05 -0.203E-04 0.524E-05 -0.155E-04
3916019.
310   64.30   5.44 112.15   9.86   6.52 112.56   9.45 4. 0.281E-04 -0.321E-05 0.400E-05 0.283E-04 -0.334E-05
3916019.
311   65.62   7.57 -32.51 -22.23 -29.13   2.21 -56.94 40. -0.717E-05 -0.402E-05 -0.178E-04 0.347E-05 -0.147E-04
3916019.
312   68.24   5.24 109.70   6.22 10.28 110.71   5.21 6. 0.277E-04 -0.402E-05 0.630E-05 0.280E-04 -0.432E-05
3916019.
313   69.56   7.51 -34.22 -19.86 -20.24 -5.56 -48.52 35. -0.773E-05 -0.332E-05 -0.124E-04 0.106E-05 -0.121E-04
3916019.
314   72.18   5.04 107.79   8.55 13.87 109.69   6.64 8. 0.271E-04 -0.332E-05 0.850E-05 0.277E-04 -0.391E-05
3916019.
315   73.49   7.38 -36.54 -18.94 -15.81 -9.65 -45.84 30. -0.836E-05 -0.297E-05 -0.969E-05 -0.122E-06 -0.112E-04
3916019.
316   76.11   4.91 103.07   8.98 13.29 104.92   7.14 8. 0.259E-04 -0.297E-05 0.815E-05 0.264E-04 -0.354E-05
3916019.
317   77.43   7.38 -40.58 -17.33 -15.56 -9.54 -48.38 27. -0.948E-05 -0.235E-05 -0.954E-05 0.360E-07 -0.119E-04
3916019.
318   80.05   4.91 103.09 11.40 13.92 105.15   9.33 8. 0.257E-04 -0.235E-05 0.853E-05 0.264E-04 -0.299E-05
3916019.
319   81.37   7.38 -42.12 -18.92 -17.99 -9.11 -51.92 29. -0.979E-05 -0.268E-05 -0.110E-04 0.324E-06 -0.128E-04
3916019.
320   83.99   4.91 103.36 10.18 16.95 106.34   7.19 10. 0.259E-04 -0.268E-05 0.104E-04 0.268E-04 -0.359E-05
3916019.
321   85.30   7.38 -41.95 -16.54 -12.23 -11.61 -46.88 22. -0.987E-05 -0.208E-05 -0.749E-05 -0.572E-06 -0.114E-04
3916019.
322   87.92   4.98 102.93 12.43 17.38 106.15   9.21 11. 0.256E-04 -0.208E-05 0.107E-04 0.266E-04 -0.307E-05
3916019.
323   89.24   7.44 -41.11 -17.48 -14.94 -10.25 -48.35 26. -0.961E-05 -0.236E-05 -0.916E-05 -0.148E-06 -0.118E-04
3916019.
324   91.86   5.11 105.52 11.84 18.46 109.02   8.34 11. 0.263E-04 -0.236E-05 0.113E-04 0.274E-04 -0.344E-05
3916019.
325   93.18   7.51 -38.70 -18.55 -15.08 -10.49 -46.76 28. -0.894E-05 -0.276E-05 -0.924E-05 -0.290E-06 -0.114E-04
3916019.
326   95.80   5.24 106.35 10.46 22.95 111.56   5.25 13. 0.266E-04 -0.276E-05 0.141E-04 0.282E-04 -0.436E-05
3916019.
327   97.12   7.57 -33.67 -20.83 -11.71 -13.90 -40.60 31. -0.753E-05 -0.360E-05 -0.718E-05 -0.148E-05 -0.966E-05
3916019.
328   99.74   5.37 106.38   7.18 27.54 113.51   0.04 15. 0.268E-04 -0.360E-05 0.169E-04 0.290E-04 -0.579E-05
3916019.
329   101.05   7.64 -32.42 -17.24 -3.28 -16.56 -33.10 12. -0.740E-05 -0.275E-05 -0.201E-05 -0.254E-05 -0.761E-05
3916019.
330   103.67   5.57 102.74   9.80 31.90 112.63 -0.10 17. 0.257E-04 -0.275E-05 0.196E-04 0.288E-04 -0.578E-05
3916019.

```
331   104.99    7.77 -30.29 -14.81  -0.65 -14.78 -30.32   2. -0.698E-05 -0.223E-05 -0.398E-06 -0.223E-05 -0.699E-05
3916019.
332   107.61    5.83 103.52  11.96  33.88 114.69   0.79  18.  0.258E-04 -0.223E-05  0.208E-04  0.292E-04 -0.566E-05
3916019.
333   108.93    7.90 -25.16 -11.48   0.32 -11.48 -25.16  89. -0.584E-05 -0.165E-05  0.193E-06 -0.165E-05 -0.584E-05
3916019.
334   111.55    6.16 101.15  13.78  37.06 114.75   0.17  20.  0.251E-04 -0.165E-05  0.227E-04  0.293E-04 -0.582E-05
3916019.
335   112.86    8.10 -19.66 -10.22   0.83 -10.15 -19.73  85. -0.450E-05 -0.161E-05  0.509E-06 -0.158E-05 -0.452E-05
3916019.
336   115.48    6.55 105.60  14.83  39.52 120.39   0.03  21.  0.262E-04 -0.161E-05  0.242E-04  0.307E-04 -0.614E-05
3916019.
337   116.80    8.29 -11.96  -7.46   0.11  -7.46 -11.96  89. -0.267E-05 -0.129E-05  0.670E-07 -0.129E-05 -0.267E-05
3916019.
338   119.42    6.94 108.52  16.64  43.57 125.89  -0.74  22.  0.269E-04 -0.129E-05  0.267E-04  0.322E-04 -0.662E-05
3916019.
339   120.74    8.49  -2.31  -7.27  -0.16  -2.31  -7.28  88. -0.219E-06 -0.174E-05 -0.994E-07 -0.217E-06 -0.174E-05
3916019.
340   123.36    7.34 113.12  15.82  45.96 131.39  -2.46  22.  0.281E-04 -0.174E-05  0.282E-04  0.337E-04 -0.734E-05
3916019.
341   124.67    8.69   9.46  -4.90  -1.14   9.55  -4.99  86.  0.267E-05 -0.173E-05 -0.696E-06  0.269E-05 -0.176E-05
3916019.
342   127.29    7.73 102.29  13.67  49.88 124.70  -8.74  24.  0.254E-04 -0.173E-05  0.306E-04  0.323E-04 -0.860E-05
3916019.
343   128.61    8.88  23.07  -6.04   5.65  24.13  -7.10  11.  0.620E-05 -0.272E-05  0.346E-05  0.652E-05 -0.305E-05
3916019.
344   131.23    8.26  89.50   7.24  58.37 119.77 -23.03  27.  0.225E-04 -0.272E-05  0.358E-04  0.318E-04 -0.120E-04
3916019.
345   132.55    9.21  30.60   8.37   9.30  33.98   4.99  20.  0.739E-05  0.574E-06  0.570E-05  0.842E-05 -0.462E-06
3916019.
346   135.17    8.85  69.57  16.16  61.49 109.90 -24.17  33.  0.169E-04  0.574E-06  0.377E-04  0.293E-04 -0.118E-04
3916019.
347   136.49    9.48  38.85  13.04  16.51  46.90   4.99  26.  0.925E-05  0.135E-05  0.101E-04  0.117E-04 -0.112E-05
3916019.
348   139.11    9.44  51.00  15.47  61.97  97.70 -31.23  37.  0.122E-04  0.135E-05  0.380E-04  0.265E-04 -0.130E-04
3916019.
349    10.50   13.44 -23.07  13.48 -28.94  29.43 -39.02  29. -0.658E-05  0.462E-05 -0.177E-04  0.951E-05 -0.115E-04
3916019.
350    13.12   12.72 -13.14  15.46 -48.82  52.04 -49.72  37. -0.415E-05  0.462E-05 -0.299E-04  0.158E-04 -0.154E-04
3916019.
351    14.44   13.09 -14.98   6.46 -50.75  47.61 -56.13  39. -0.415E-05  0.241E-05 -0.311E-04  0.150E-04 -0.168E-04
3916019.
352    17.06   12.06  18.80  13.21 -38.94  55.04 -23.03  47.  0.413E-05  0.241E-05 -0.239E-04  0.152E-04 -0.869E-05
3916019.
353    18.38   12.76 -20.30   2.24 -59.70  51.72 -69.79  40. -0.530E-05  0.161E-05 -0.366E-04  0.168E-04 -0.205E-04
3916019.
354    21.00   11.41  41.84  14.67 -29.65  60.87  -4.36  57.  0.994E-05  0.161E-05 -0.182E-04  0.158E-04 -0.422E-05
3916019.
355    22.31   12.43 -30.51   0.82 -57.52  44.77 -74.45  37. -0.783E-05  0.177E-05 -0.352E-04  0.152E-04 -0.213E-04
3916019.
356    24.93   11.12  47.45  16.41 -16.67  54.71   9.16  66.  0.113E-04  0.177E-05 -0.102E-04  0.135E-04 -0.455E-06
3916019.
357    26.25   12.47 -48.96  -3.85 -55.56  33.56 -86.37  34. -0.123E-04  0.152E-05 -0.341E-04  0.130E-04 -0.238E-04
3916019.
358    28.87   11.15  39.70  13.88  -9.68  42.93  10.65  72.  0.943E-05  0.152E-05 -0.593E-05  0.104E-04  0.528E-06
3916019.
359    30.19   12.47 -66.31  -9.20 -52.71  22.19 -97.71  31. -0.165E-04  0.104E-05 -0.323E-04  0.107E-04 -0.261E-04
3916019.
360    32.81   11.15  34.37  10.94   0.72  34.39  10.91   2.  0.822E-05  0.104E-05  0.442E-06  0.822E-05  0.103E-05
3916019.
361    34.12   12.47 -80.06 -22.25 -48.38   5.20 -107.51 30. -0.193E-04 -0.159E-05 -0.297E-04  0.682E-05 -0.277E-04
3916019.
362    36.74   11.15  24.78  -1.28  12.65  29.91  -6.41  22.  0.639E-05 -0.159E-05  0.775E-05  0.796E-05 -0.316E-05
3916019.
363    38.06   12.47 -85.84 -13.78 -28.39  -3.94 -95.68  19. -0.212E-04  0.864E-06 -0.174E-04  0.388E-05 -0.242E-04
3916019.
364    40.68   11.15  13.13   6.01  18.05  27.97  -8.83  39.  0.305E-05  0.864E-06  0.111E-04  0.759E-05 -0.368E-05
3916019.
365    42.00   12.47 -98.51  -9.92 -24.47  -3.61 -104.82 14. -0.246E-04  0.250E-05 -0.150E-04  0.443E-05 -0.266E-04
3916019.
```

336

366   44.62   11.15   2.03   10.19   18.00   24.56 -12.35 51. -0.269E-08   0.250E-05   0.110E-04   0.690E-05 -0.441E-05
3916019.
367   45.93   12.47 -102.88   -8.81 -23.20   -3.40 -108.29 13. -0.258E-04   0.301E-05 -0.142E-04   0.466E-05 -0.275E-04
3916019.
368   48.55   11.15   -6.70   10.43   18.07   21.86 -18.13 58. -0.224E-05   0.301E-05   0.111E-04   0.651E-05 -0.575E-05
3916019.
369   49.87   12.47 -106.38   -9.72 -21.87   -5.00 -111.10 12. -0.267E-04   0.295E-05 -0.134E-04   0.440E-05 -0.281E-04
3916019.
370   52.49   11.15 -13.78   8.80   16.62   17.61 -22.59 62. -0.397E-05   0.295E-05   0.102E-04   0.565E-05 -0.667E-05
3916019.
371   53.81   12.47 -109.66 -10.45 -21.75   -5.89 -114.22 12. -0.275E-04   0.293E-05 -0.133E-04   0.433E-05 -0.289E-04
3916019.
372   56.43   11.15 -20.04   7.47   14.83   13.94 -26.51 66. -0.550E-05   0.293E-05   0.909E-05   0.491E-05 -0.748E-05
3916019.
373   57.75   12.47 -113.18 -11.69 -22.60   -6.88 -117.99 12. -0.283E-04   0.280E-05 -0.139E-04   0.427E-05 -0.298E-04
3916019.
374   60.37   11.15 -26.34   5.68   13.34   10.51 -31.16 70. -0.702E-05   0.280E-05   0.817E-05   0.427E-05 -0.849E-05
3916019.
375   61.68   12.47 -116.86 -15.74 -23.89 -10.38 -122.22 13. -0.290E-04   0.195E-05 -0.146E-04   0.359E-05 -0.307E-04
3916019.
376   64.30   11.15 -27.64   2.10   14.94   8.31 -33.85 67. -0.717E-05   0.195E-05   0.916E-05   0.385E-05 -0.907E-05
3916019.
377   65.62   12.47 -118.71 -26.48 -24.94 -20.17 -125.02 14. -0.290E-04 -0.700E-06 -0.153E-04   0.123E-05 -0.309E-04
3916019.
378   68.24   11.15 -32.08   -9.16   20.79   3.12 -44.36 59. -0.772E-05 -0.700E-06   0.127E-04   0.306E-05 -0.115E-04
3916019.
379   69.56   12.47 -114.71 -17.03   -9.37 -16.14 -115.61   5. -0.284E-04   0.151E-05 -0.574E-05   0.178E-05 -0.287E-04
3916019.
380   72.18   11.15 -32.88   -0.66   22.21   10.67 -44.21 63. -0.836E-05   0.151E-05   0.136E-04   0.498E-05 -0.118E-04
3916019.
381   73.49   12.47 -118.99 -11.56 -10.02 -10.63 -119.92   5. -0.298E-04   0.313E-05 -0.614E-05   0.341E-05 -0.301E-04
3916019.
382   76.11   11.15 -36.11   5.02   18.33   12.00 -43.09 69. -0.948E-05   0.313E-05   0.112E-04   0.527E-05 -0.116E-04
3916019.
383   77.43   12.47 -117.00   -6.62 -12.51   -5.22 -118.40   6. -0.295E-04   0.428E-05 -0.767E-05   0.471E-05 -0.300E-04
3916019.
384   80.05   11.15 -36.43   9.49   14.08   13.46 -40.41 74. -0.979E-05   0.428E-05   0.863E-05   0.550E-05 -0.110E-04
3916019.
385   81.37   12.47 -116.88   4.98 -14.24   6.62 -118.52   7. -0.301E-04   0.724E-05 -0.873E-05   0.774E-05 -0.306E-04
3916019.
386   83.99   12.47 -117.22   4.91   13.08   6.29 -118.61 84. -0.302E-04   0.724E-05   0.802E-05   0.766E-05 -0.306E-04
3916019.
387   85.30   11.15 -36.65   9.94 -15.36   14.54 -41.25 17. -0.987E-05   0.441E-05 -0.941E-05   0.582E-05 -0.113E-04
3916019.
388   87.92   12.47 -117.86   -6.30   11.75   -5.08 -119.08 84. -0.298E-04   0.441E-05   0.720E-05   0.478E-05 -0.301E-04
3916019.
389   89.24   11.15 -36.41   6.00 -19.50   13.61 -44.01 21. -0.960E-05   0.339E-05 -0.120E-04   0.572E-05 -0.119E-04
3916019.
390   91.86   12.47 -120.19 -10.75   9.96   -9.85 -121.09 85. -0.301E-04   0.339E-05   0.611E-05   0.367E-05 -0.304E-04
3916019.
391   93.18   11.15 -35.08   -0.45 -21.84   10.11 -45.64 26. -0.894E-05   0.168E-05 -0.134E-04   0.491E-05 -0.122E-04
3916019.
392   95.80   12.47 -115.62 -16.55   9.90 -15.57 -116.60 84. -0.287E-04   0.168E-05   0.607E-05   0.198E-05 -0.290E-04
3916019.
393   97.12   11.15 -31.32   -9.10 -20.68   3.26 -43.68 31. -0.753E-05 -0.725E-06 -0.127E-04   0.306E-05 -0.113E-04
3916019.
394   99.74   12.47 -119.70 -26.78   25.05 -20.46 -126.03 76. -0.292E-04 -0.725E-06   0.154E-04   0.121E-05 -0.311E-04
3916019.
395   101.05   11.15 -28.71   1.30 -14.56   7.21 -34.61 22. -0.740E-05   0.180E-05 -0.892E-05   0.361E-05 -0.921E-05
3916019.
396   103.67   12.47 -117.94 -16.54   23.56 -11.34 -123.14 78. -0.293E-04   0.180E-05   0.144E-04   0.339E-05 -0.309E-04
3916019.
397   104.99   11.15 -26.19   5.68 -14.43   11.25 -31.76 21. -0.698E-05   0.279E-05 -0.885E-05   0.449E-05 -0.868E-05
3916019.
398   107.61   12.47 -114.75 -12.03   21.95   -7.53 -119.24 78. -0.287E-04   0.279E-05   0.135E-04   0.417E-05 -0.301E-04
3916019.
399   108.93   11.15 -21.31   7.73 -15.78   14.65 -28.23 24. -0.584E-05   0.306E-05 -0.967E-05   0.518E-05 -0.796E-05
3916019.
400   111.55   12.47 -111.59 -10.32   21.32   -6.02 -115.90 79. -0.280E-04   0.306E-05   0.131E-04   0.438E-05 -0.293E-04
3916019.

337

```
 401   112.86   11.15 -15.72   9.47 -17.14  18.14  -24.40 27. -0.450E-05  0.322E-05 -0.105E-04  0.588E-05 -0.716E-05
3916019.
 402   115.48   12.47 -108.28  -9.04  22.16  -4.32 -113.00 78. -0.272E-04  0.322E-05  0.136E-04  0.467E-05 -0.286E-04
3916019.
 403   116.80   11.15  -8.27  10.97 -17.84  21.62  -18.92 31. -0.267E-05  0.322E-05 -0.109E-04  0.649E-05 -0.594E-05
3916019.
 404   119.42   12.47 -104.46  -8.26  23.99  -2.61 -110.12 77. -0.263E-04  0.323E-05  0.147E-04  0.496E-05 -0.280E-04
3916019.
 405   120.74   11.15   1.30  10.78 -17.61  24.27  -12.19 37. -0.219E-06  0.269E-05 -0.108E-04  0.682E-05 -0.435E-05
3916019.
 406   123.36   12.47 -99.80  -9.44  25.48  -2.75 -106.49 75. -0.250E-04  0.269E-05  0.156E-04  0.474E-05 -0.271E-04
3916019.
 407   124.67   11.15  11.55   5.54 -16.51  25.33   -8.24 50.  0.267E-05  0.825E-06 -0.101E-04  0.689E-05 -0.340E-05
3916019.
 408   127.29   12.47 -86.71 -14.11  29.11  -3.88  -96.94 71. -0.214E-04  0.825E-06  0.178E-04  0.396E-05 -0.246E-04
3916019.
 409   128.61   11.15  23.85  -2.15 -11.73  28.36   -6.66 69.  0.620E-05 -0.177E-05 -0.719E-05  0.758E-05 -0.315E-05
3916019.
 410   131.23   12.47 -80.89 -23.10  48.27   4.26 -108.25 60. -0.195E-04 -0.177E-05  0.296E-04  0.662E-05 -0.279E-04
3916019.
 411   132.55   11.15  31.04  10.60  -0.28  31.05   10.60 89.  0.739E-05  0.112E-05 -0.169E-06  0.739E-05  0.112E-05
3916019.
 412   135.17   12.47 -66.65  -8.94  52.99  22.54  -98.13 59. -0.166E-04  0.112E-05  0.325E-04  0.108E-04 -0.262E-04
3916019.
 413   136.49   11.15  39.03  13.95  10.13  42.61   10.37 19.  0.925E-05  0.157E-05  0.621E-05  0.104E-04  0.471E-06
3916019.
 414   139.11   12.47 -48.86  -3.63  55.90  34.06  -86.55 56. -0.123E-04  0.157E-05  0.343E-04  0.131E-04 -0.238E-04
3916019.
 415   140.42   11.12  48.18  16.47  16.95  55.53    9.11 23.  0.115E-04  0.175E-05  0.104E-04  0.137E-04 -0.509E-06
3916019.
 416   143.04   12.43 -30.12   0.82  57.79  45.18  -74.48 52. -0.773E-05  0.175E-05  0.354E-04  0.153E-04 -0.213E-04
3916019.
 417   144.36   11.41  41.37  13.46  30.55  61.00   -6.17 33.  0.988E-05  0.132E-05  0.187E-04  0.159E-04 -0.469E-05
3916019.
 418   146.98   12.76 -19.07   1.37  59.59  51.61  -69.31 50. -0.494E-05  0.132E-05  0.365E-04  0.167E-04 -0.203E-04
3916019.
 419   148.30   12.00  18.45   9.29  40.24  54.37  -26.63 42.  0.424E-05  0.143E-05  0.247E-04  0.152E-04 -0.958E-05
3916019.
 420   150.92   13.02 -11.26   3.35  49.07  45.66  -53.57 49. -0.305E-05  0.143E-05  0.301E-04  0.144E-04 -0.160E-04
3916019.
 421   152.23   12.65  -7.85   8.91  46.24  47.52  -46.46 50. -0.246E-05  0.268E-05  0.283E-04  0.145E-04 -0.143E-04
3916019.
 422   154.85   13.84  11.80  12.84  28.85  41.18  -16.54 46.  0.236E-05  0.268E-05  0.177E-04  0.114E-04 -0.633E-05
3916019.
 423     1.31   16.56  56.26  86.51 120.34 192.67  -49.90 49.  0.995E-05  0.192E-04  0.738E-04  0.518E-04 -0.226E-04
3916019.
 424     2.63   16.89 224.99 -17.05 209.74 346.12 -138.18 30.  0.583E-04 -0.158E-04  0.129E-03  0.954E-04 -0.530E-04
3916019.
 425     5.25   15.61 -33.93 -68.83 -108.82  58.83 -161.59 50. -0.515E-05 -0.158E-04 -0.667E-04  0.233E-04 -0.443E-04
3916019.
 426     6.56   16.43 235.71   7.83   8.36 236.02    7.52  2.  0.598E-04 -0.100E-04  0.513E-05  0.599E-04 -0.101E-04
3916019.
 427     9.18   15.12 -39.07 -47.13 -109.04  66.02 -152.21 46. -0.757E-05 -0.100E-04 -0.668E-04  0.246E-04 -0.422E-04
3916019.
 428    10.50   16.41 129.43  11.50 -33.33 138.20    2.73 75.  0.325E-04 -0.367E-05 -0.204E-04  0.352E-04 -0.636E-05
3916019.
 429    13.12   15.09 -19.94 -18.38 -65.03  45.87  -84.19 45. -0.415E-05 -0.367E-05 -0.399E-04  0.160E-04 -0.238E-04
3916019.
 430    14.44   16.41  31.07   5.05 -40.21  60.33  -24.20 54.  0.768E-05 -0.298E-06 -0.246E-04  0.166E-04 -0.926E-05
3916019.
 431    17.06   15.09 -21.86  -5.54 -34.93  22.17  -49.57 38. -0.530E-05 -0.298E-06 -0.214E-04  0.819E-05 -0.138E-04
3916019.
 432    18.38   16.41 -44.07  -0.66 -40.70  23.77  -68.49 31. -0.112E-04  0.208E-05 -0.249E-04  0.957E-05 -0.187E-04
3916019.
 433    21.00   15.09 -30.25   2.11 -14.27   7.50  -35.64 21. -0.783E-05  0.208E-05 -0.875E-05  0.374E-05 -0.949E-05
3916019.
 434    22.31   16.41 -99.00  -4.34 -39.26   9.82 -113.17 20. -0.251E-04  0.395E-05 -0.241E-04  0.829E-05 -0.294E-04
3916019.
 435    24.93   15.09 -46.98   6.06  -1.87   6.13  -47.04  2. -0.123E-04  0.395E-05 -0.115E-05  0.397E-05 -0.123E-04
3916019.
```

338

```
436    26.25   16.41 -140.03   -7.86 -37.53    2.05 -149.94  15.  -0.354E-04  0.514E-05 -0.230E-04  0.818E-05 -0.384E-04
3916019.
437    28.87   15.09  -62.96    7.56   5.62    8.00  -63.41  85.  -0.165E-04  0.514E-05  0.344E-05  0.528E-05 -0.166E-04
3916019.
438    30.19   16.41 -171.94  -13.80 -37.83   -5.22 -180.52  13.  -0.432E-04  0.526E-05 -0.232E-04  0.789E-05 -0.458E-04
3916019.
439    32.81   15.09  -74.47    5.69  11.12    7.20  -75.98  82.  -0.193E-04  0.526E-05  0.682E-05  0.572E-05 -0.198E-04
3916019.
440    34.12   16.41 -198.68  -41.63 -45.96  -29.17 -211.14  15.  -0.486E-04 -0.485E-06 -0.282E-04  0.333E-05 -0.524E-04
3916019.
441    36.74   15.09  -86.93  -19.29  28.47   -8.90  -97.32  70.  -0.212E-04 -0.485E-06  0.174E-04  0.270E-05 -0.244E-04
3916019.
442    38.06   16.41 -216.05  -15.48 -13.30  -14.60 -216.93   4.  -0.544E-04  0.708E-05 -0.815E-05  0.735E-05 -0.546E-04
3916019.
443    40.68   15.09  -94.77    8.78  23.47   13.85  -99.84  78.  -0.246E-04  0.708E-05  0.144E-04  0.864E-05 -0.262E-04
3916019.
444    42.00   16.41 -205.88  -10.50 -19.99   -8.47 -207.90   6.  -0.520E-04  0.783E-05 -0.123E-04  0.845E-05 -0.527E-04
3916019.
445    44.62   15.09  -98.94   10.89  22.08   15.16 -103.21  79.  -0.258E-04  0.783E-05  0.135E-04  0.914E-05 -0.271E-04
3916019.
446    45.93   16.41 -203.85   -9.65 -19.63   -7.69 -205.81   6.  -0.516E-04  0.795E-05 -0.120E-04  0.855E-05 -0.522E-04
3916019.
447    48.55   15.09 -102.30   10.66  21.36   14.56 -106.20  80.  -0.267E-04  0.795E-05  0.131E-04  0.914E-05 -0.279E-04
3916019.
448    49.87   16.41 -202.07   -9.45 -18.60   -7.67 -203.85   5.  -0.511E-04  0.791E-05 -0.114E-04  0.845E-05 -0.517E-04
3916019.
449    52.49   15.09 -105.60    9.85  19.93   13.19 -108.94  80.  -0.275E-04  0.791E-05  0.122E-04  0.893E-05 -0.285E-04
3916019.
450    53.81   16.41 -200.74   -9.40 -18.20   -7.68 -202.45   5.  -0.508E-04  0.785E-05 -0.112E-04  0.838E-05 -0.513E-04
3916019.
451    56.43   15.09 -109.05    8.94  18.26   11.70 -111.81  81.  -0.283E-04  0.785E-05  0.112E-04  0.870E-05 -0.292E-04
3916019.
452    57.75   16.41 -200.68  -10.19 -18.66   -8.38 -202.49   6.  -0.507E-04  0.765E-05 -0.114E-04  0.820E-05 -0.513E-04
3916019.
453    60.37   15.09 -112.20    7.50  16.23    9.66 -114.37  82.  -0.290E-04  0.765E-05  0.995E-05  0.831E-05 -0.297E-04
3916019.
454    61.68   16.41 -203.16  -14.62 -21.37  -12.22 -205.55   6.  -0.511E-04  0.664E-05 -0.131E-04  0.738E-05 -0.519E-04
3916019.
455    64.30   15.09 -112.71    3.47  14.78    5.32 -114.56  83.  -0.290E-04  0.664E-05  0.906E-05  0.721E-05 -0.295E-04
3916019.
456    65.62   16.41 -209.69  -41.32 -32.48  -35.28 -215.74  11.  -0.514E-04  0.157E-06 -0.199E-04  0.201E-05 -0.533E-04
3916019.
457    68.24   15.09 -115.81  -22.55  27.45  -15.07 -123.29  75.  -0.284E-04  0.157E-06  0.168E-04  0.245E-05 -0.307E-04
3916019.
458    69.56   16.41 -214.72  -14.60  -2.87  -14.56 -214.77   1.  -0.541E-04  0.724E-05 -0.176E-05  0.725E-05 -0.541E-04
3916019.
459    72.18   15.09 -115.63    5.22  19.80    8.38 -118.79  81.  -0.298E-04  0.724E-05  0.121E-04  0.821E-05 -0.308E-04
3916019.
460    73.49   16.41 -197.84   -9.02 -12.26   -8.23 -198.64   4.  -0.501E-04  0.780E-05 -0.751E-05  0.804E-05 -0.503E-04
3916019.
461    76.11   15.09 -114.12    7.72  17.07   10.06 -116.47  82.  -0.295E-04  0.780E-05  0.105E-04  0.852E-05 -0.303E-04
3916019.
462    77.43   16.41 -193.01   -5.24 -13.54   -4.26 -193.98   4.  -0.490E-04  0.852E-05 -0.830E-05  0.882E-05 -0.493E-04
3916019.
463    80.05   15.09 -115.83   10.20  16.70   12.37 -118.00  83.  -0.301E-04  0.852E-05  0.102E-04  0.919E-05 -0.308E-04
3916019.
464    81.37   16.41 -189.86    8.38  -8.58    8.75 -190.23   2.  -0.489E-04  0.118E-04 -0.526E-05  0.119E-04 -0.490E-04
3916019.
465    83.99   16.41 -190.42    8.26   8.04    8.59 -190.75  88.  -0.490E-04  0.118E-04  0.493E-05  0.119E-04 -0.491E-04
3916019.
466    85.30   15.09 -116.11   10.47 -17.37   12.81 -118.45   8.  -0.302E-04  0.860E-05 -0.106E-04  0.932E-05 -0.309E-04
3916019.
467    87.92   16.41 -194.49   -5.21  13.27   -4.28 -195.41  86.  -0.494E-04  0.860E-05  0.813E-05  0.889E-05 -0.497E-04
3916019.
468    89.24   15.09 -114.98    8.07 -17.66   10.55 -117.46   8.  -0.298E-04  0.793E-05 -0.108E-04  0.869E-05 -0.305E-04
3916019.
469    91.86   16.41 -199.68   -8.87  12.46   -8.06 -200.49  86.  -0.505E-04  0.793E-05  0.764E-05  0.818E-05 -0.508E-04
3916019.
470    93.18   15.09 -116.98    5.27 -19.81    8.40 -120.11   9.  -0.301E-04  0.732E-05 -0.121E-04  0.828E-05 -0.311E-04
3916019.
```

339

471   95.80   16.41 -216.37 -14.61   3.12 -14.56 -216.42 89. -0.545E-04 0.732E-05 0.191E-05 0.734E-05 -0.545E-04
3916019.
472   97.12   15.09 -116.81 -22.54 -27.41 -15.15 -124.20 15. -0.287E-04 0.209E-06 -0.168E-04 0.247E-05 -0.309E-04
3916019.
473   99.74   16.41 -211.11 -41.40 32.76 -35.30 -217.21 79. -0.518E-04 0.209E-06 0.201E-04 0.208E-05 -0.537E-04
3916019.
474   101.05   15.09 -113.68   3.29 -14.54   5.07 -115.46 7. -0.292E-04 0.665E-05 -0.891E-05 0.719E-05 -0.297E-04
3916019.
475   103.67   16.41 -204.42 -14.85 21.19 -12.51 -206.76 84. -0.514E-04 0.665E-05 0.130E-04 0.736E-05 -0.522E-04
3916019.
476   104.99   15.09 -113.10   7.59 -16.72   9.86 -115.38 8. -0.293E-04 0.771E-05 -0.102E-04 0.841E-05 -0.300E-04
3916019.
477   107.61   16.41 -202.68 -10.32 18.46 -8.57 -204.44 85. -0.512E-04 0.771E-05 0.113E-04 0.825E-05 -0.518E-04
3916019.
478   108.93   15.09 -110.52   9.09 -18.73 11.95 -113.38 9. -0.287E-04 0.796E-05 -0.115E-04 0.884E-05 -0.296E-04
3916019.
479   111.55   16.41 -203.37 -9.48 18.09 -7.81 -205.04 85. -0.514E-04 0.797E-05 0.111E-04 0.848E-05 -0.520E-04
3916019.
480   112.86   15.09 -107.50 10.10 -20.30 13.50 -110.90 10. -0.280E-04 0.807E-05 -0.124E-04 0.911E-05 -0.290E-04
3916019.
481   115.48   16.41 -204.82 -9.37 18.79 -7.58 -206.61 85. -0.518E-04 0.807E-05 0.115E-04 0.862E-05 -0.524E-04
3916019.
482   116.80   15.09 -104.29 10.85 -21.45 14.71 -108.16 10. -0.272E-04 0.810E-05 -0.131E-04 0.928E-05 -0.284E-04
3916019.
483   119.42   16.41 -206.16 -9.53 20.11 -7.49 -208.20 84. -0.522E-04 0.810E-05 0.123E-04 0.872E-05 -0.528E-04
3916019.
484   120.74   15.09 -100.61 10.95 -21.89 15.09 -104.75 11. -0.263E-04 0.793E-05 -0.134E-04 0.920E-05 -0.275E-04
3916019.
485   123.36   16.41 -207.42 -10.41 20.68 -8.26 -209.57 84. -0.524E-04 0.794E-05 0.127E-04 0.859E-05 -0.531E-04
3916019.
486   124.67   15.09 -96.20   8.51 -22.58 13.17 -100.86 12. -0.250E-04 0.709E-05 -0.138E-04 0.851E-05 -0.264E-04
3916019.
487   127.29   16.41 -216.28 -15.50 13.67 -14.58 -217.20 86. -0.544E-04 0.709E-05 0.838E-05 0.737E-05 -0.547E-04
3916019.
488   128.61   15.09 -87.80 -19.61 -27.78 -9.72 -97.69 20. -0.214E-04 -0.523E-06 -0.170E-04 0.251E-05 -0.244E-04
3916019.
489   131.23   16.41 -198.21 -41.69 45.85 -29.25 -210.65 75. -0.485E-04 -0.523E-06 0.281E-04 0.329E-05 -0.523E-04
3916019.
490   132.55   15.09 -75.16   5.49 -10.89   6.93 -76.61 8. -0.195E-04 0.524E-05 -0.667E-05 0.568E-05 -0.199E-04
3916019.
491   135.17   16.41 -171.56 -13.79 37.55 -5.31 -180.04 77. -0.431E-04 0.524E-05 0.230E-04 0.784E-05 -0.457E-04
3916019.
492   136.49   15.09 -63.34   7.58 -5.65   8.02 -63.79 5. -0.166E-04 0.517E-05 -0.346E-05 0.531E-05 -0.167E-04
3916019.
493   139.11   16.41 -139.89 -7.73 37.41   2.12 -149.75 75. -0.353E-04 0.517E-05 0.229E-04 0.819E-05 -0.383E-04
3916019.
494   140.42   15.09 -46.90   6.11   1.90   6.18 -46.97 88. -0.123E-04 0.396E-05 0.116E-05 0.398E-05 -0.123E-04
3916019.
495   143.04   16.41 -98.74 -4.25 39.25   9.93 -112.92 70. -0.250E-04 0.396E-05 0.241E-04 0.830E-05 -0.293E-04
3916019.
496   144.36   15.09 -29.90   1.85 14.27   7.33 -35.38 69. -0.773E-05 0.200E-05 0.875E-05 0.368E-05 -0.941E-05
3916019.
497   146.98   16.41 -44.40 -1.05 40.06 22.83 -68.28 59. -0.113E-04 0.200E-05 0.246E-04 0.932E-05 -0.186E-04
3916019.
498   148.30   15.09 -20.49 -5.78 33.67 21.32 -47.60 51. -0.494E-05 -0.430E-06 0.206E-04 0.788E-05 -0.132E-04
3916019.
499   150.92   16.41   27.19   3.75 38.02 55.26 -24.32 36. 0.675E-05 -0.430E-06 0.233E-04 0.154E-04 -0.903E-05
3916019.
500   152.23   15.09 -14.94 -15.07 58.30 43.30 -73.31 45. -0.305E-05 -0.309E-05 0.357E-04 0.148E-04 -0.209E-04
3916019.
501   154.85   16.41 120.31 11.98 34.97 130.62   1.67 16. 0.301E-04 -0.309E-05 0.214E-04 0.333E-04 -0.624E-05
3916019.
502   156.17   15.52 -65.45 -52.79 118.47 59.52 -177.76 47. -0.140E-04 -0.101E-04 0.726E-04 0.243E-04 -0.484E-04
3916019.
503   158.79   16.83 310.12 22.32 -49.72 318.47 13.97 80. 0.781E-04 -0.101E-04 -0.305E-04 0.806E-04 -0.127E-04
3916019.
504   160.11   16.00   26.62 -58.98 121.52 112.66 -145.02 35. 0.981E-05 -0.164E-04 0.745E-04 0.362E-04 -0.428E-04
3916019.
505   162.73   16.89 231.65 -17.98 -185.05 330.04 -116.38 62. 0.601E-04 -0.164E-04 -0.113E-03 0.902E-04 -0.466E-04
3916019.

340

```
 506   164.04   16.56   91.01   74.44 -111.68  194.71  -29.26  47.   0.194E-04   0.144E-04  -0.684E-04   0.512E-04  -0.174E-04
3916019.
0MOD. OF RUPTR=,  522.00      NO. OF ELEMENTS BROKEN=  1
```

0 ELEMENT	BOND STRESS	STRESS/LTH	BOND FORCE	FORCE/LTH	SLIP
1	58.5320	29.7117	362.2515	183.8840	0.16641E-04
2	204.9269	104.0238	1268.2829	643.7984	0.62496E-04
3	18.0032	4.5693	222.8418	56.5588	0.50301E-05
4	-115.6380	-29.3497	-1431.3557	-363.2883	0.33738E-04
5	-24.3690	-6.1850	-301.6368	-76.5576	0.68269E-05
6	-1.3031	-0.3307	-16.1299	-4.0939	0.36157E-06
7	-6.9136	-1.7547	-85.5755	-21.7197	0.19227E-05
8	4.9571	1.2581	61.3579	15.5731	0.13775E-05
9	-4.5977	-1.1669	-56.9099	-14.4441	0.12774E-05
10	2.9379	0.7457	36.3656	9.2298	0.81573E-06
11	-5.8130	-1.4754	-71.9531	-18.2622	0.16159E-05
12	1.7144	0.4351	21.2204	5.3859	0.47576E-06
13	-0.3451	-0.0876	-4.2714	-1.0841	0.95712E-07
14	3.3391	0.8475	41.3312	10.4902	0.92726E-06
15	-4.4741	-1.1356	-55.3805	-14.0560	0.12430E-05
16	2.5397	0.6446	31.4359	7.9786	0.70503E-06
17	0.7013	0.1780	8.6808	2.2033	0.19454E-06
18	4.2827	1.0870	53.0105	13.4544	0.11898E-05
19	-1.5376	-0.3903	-19.0328	-4.8307	0.42668E-06
20	2.8848	0.7322	35.7074	9.0628	0.80094E-06
21	2.4595	0.6242	30.4438	7.7268	0.68276E-06
22	4.4728	1.1352	55.3637	14.0517	0.12427E-05
23	-0.5095	-0.1293	-6.3060	-1.6005	0.14131E-06
24	2.9706	0.7540	36.7695	9.3324	0.82480E-06
25	2.5365	0.6438	31.3965	7.9687	0.70415E-06
26	4.0614	1.0308	50.2712	12.7592	0.11282E-05
27	0.4551	0.1155	5.6336	1.4299	0.12624E-06
28	2.8644	0.7270	35.4555	8.9989	0.79529E-06
29	1.5825	0.4016	19.5875	4.9714	0.43913E-06
30	4.0238	1.0213	49.8062	12.6412	0.11177E-05
31	-1.2571	-0.3191	-15.5600	-3.9492	0.34879E-06
32	2.8913	0.7338	35.7877	9.0832	0.80275E-06
33	0.6747	0.1712	8.3510	2.1195	0.18715E-06
34	4.0397	1.0253	50.0024	12.6910	0.11221E-05
35	0.0770	0.0195	0.9530	0.2419	0.21352E-07
36	2.5987	0.6596	32.1663	8.1640	0.72143E-06
37	1.9178	0.4867	23.7378	6.0248	0.53224E-06
38	3.8092	0.9668	47.1496	11.9669	0.10580E-05
39	0.6776	0.1720	8.3874	2.1288	0.18796E-06
40	2.9551	0.7500	36.5778	9.2837	0.82049E-06
41	-0.5238	-0.1330	-6.4841	-1.6457	0.14530E-06
42	3.7961	0.9635	46.9875	11.9258	0.10544E-05
43	0.1369	0.0347	1.6944	0.4300	0.37963E-07
44	2.7713	0.7034	34.3033	8.7064	0.76941E-06
45	-0.4186	-0.1062	-5.1810	-1.3150	0.11610E-06

46	3.8304	0.9722	47.4127	12.0337	0.10639E-05
47	-0.7967	-0.2022	-9.8609	-2.5028	0.22100E-06
48	2.7057	0.6867	33.4903	8.5001	0.75116E-06
49	-1.0055	-0.2552	-12.4464	-3.1590	0.27897E-06
50	3.8859	0.9863	48.0989	12.2078	0.10793E-05
51	0.4945	0.1255	6.1213	1.5536	0.13717E-06
52	2.7528	0.6987	34.0733	8.6481	0.76425E-06
53	-0.6059	-0.1538	-7.4995	-1.9034	0.16806E-06
54	4.1322	1.0488	51.1477	12.9816	0.11479E-05
55	0.2556	0.0649	3.1644	0.8031	0.70902E-07
56	2.9100	0.7386	36.0199	9.1421	0.80796E-06
57	-1.5849	-0.4022	-19.6172	-4.9790	0.43979E-06
58	4.0207	1.0205	49.7676	12.6314	0.11168E-05
59	-0.3732	-0.0947	-4.6190	-1.1723	0.10350E-06
60	2.8850	0.7322	35.7108	9.0637	0.80102E-06
61	-2.5577	-0.6492	-31.6584	-8.0351	0.71003E-06
62	4.1415	1.0511	51.2628	13.0109	0.11505E-05
63	0.3344	0.0849	4.1391	1.0505	0.92745E-07
64	2.8039	0.7116	34.7058	8.8086	0.77845E-06
65	-1.4300	-0.3629	-17.7005	-4.4925	0.39680E-06
66	4.6460	1.1792	57.5082	14.5960	0.12909E-05
67	1.8077	0.4588	22.3756	5.6791	0.50168E-06
68	3.0892	0.7841	38.2381	9.7051	0.85778E-06
69	-1.9100	-0.4848	-23.6421	-6.0005	0.53010E-06
70	4.2887	1.0885	53.0847	13.4733	0.11914E-05
71	4.8573	1.2328	60.1232	15.2597	0.13497E-05
72	2.3831	0.6049	29.4982	7.4869	0.66153E-06
73	0.4543	0.1153	5.6233	1.4272	0.12601E-06
74	3.2760	0.8315	40.5505	10.2920	0.90972E-06
75	5.9011	1.4977	73.0435	18.5390	0.16405E-05
76	1.7222	0.4371	21.3171	5.4104	0.47793E-06
77	6.3118	1.6020	78.1265	19.8291	0.17549E-05
78	3.2795	0.8324	40.5936	10.3030	0.91069E-06
79	7.2420	1.8381	89.6407	22.7514	0.20143E-05
80	5.1100	1.2970	63.2515	16.0537	0.14201E-05
81	28.3061	7.1843	350.3703	88.9265	0.79432E-05
82	-6.7816	-1.7212	-83.9417	-21.3050	0.18859E-05
83	4.0520	1.0284	50.1556	12.7298	0.11256E-05
84	-101.9112	-25.8658	-1261.4466	-320.1641	0.29544E-04
85	-119.9169	-60.8715	-742.1600	-376.7309	0.35056E-04
86	189.0218	95.9502	1169.8469	593.8309	0.57170E-04
87	-69.9354	-35.5002	-432.8266	-219.7089	0.19983E-04
88	-38.8603	-19.7261	-240.5048	-122.0837	0.10954E-04
89	-28.5164	-7.2377	-352.9739	-89.5873	0.80029E-05
90	-4.8605	-1.2336	-60.1623	-15.2696	0.13506E-05
91	24.0603	6.1067	297.8166	75.5880	0.67396E-05
92	18.0466	4.5804	223.3794	56.6953	0.50423E-05
93	23.9436	6.0771	296.3716	75.2212	0.67066E-05
94	-0.3869	-0.0982	-4.7885	-1.2154	0.10730E-06
95	19.9540	5.0645	246.9893	62.6876	0.55797E-05
96	-2.5545	-0.6484	-31.6199	-8.0254	0.70916E-06
97	15.4353	3.9176	191.0569	48.4916	0.43080E-05
98	-4.6625	-1.1834	-57.7121	-14.6477	0.12955E-05
99	13.1072	3.3267	162.2401	41.1777	0.36547E-05
100	-4.3555	-1.1055	-53.9118	-13.6832	0.12100E-05
101	12.1347	3.0799	150.2026	38.1225	0.33821E-05

102	-3.4370	-0.8723	-42.5427	-10.7976	0.95448E-06
103	6.9037	1.7522	85.4538	21.6888	0.19200E-05
104	-4.0700	-1.0330	-50.3786	-12.7864	0.11306E-05
105	4.6636	1.1837	57.7254	14.6511	0.12958E-05
106	-0.6892	-0.1749	-8.5306	-2.1651	0.19118E-06
107	-0.1238	-0.0314	-1.5319	-0.3888	0.34322E-07
108	-3.0305	-0.7692	-37.5113	-9.5206	0.84146E-06
109	-1.4481	-0.3675	-17.9239	-4.5492	0.40181E-06
110	-1.3260	-0.3365	-16.4126	-4.1656	0.36791E-06
111	-5.1983	-1.3194	-64.3446	-16.3311	0.14447E-05
112	-3.3764	-0.8570	-41.7928	-10.6073	0.93764E-06
113	-2.6348	-0.6687	-32.6139	-8.2776	0.73148E-06
114	-1.6842	-0.4275	-20.8467	-5.2911	0.46738E-06
115	-1.9804	-0.5026	-24.5134	-6.2217	0.54965E-06
116	-2.3401	-0.5939	-28.9651	-7.3516	0.64956E-06
117	2.0850	0.5292	25.8077	6.5502	0.57869E-06
118	-1.5180	-0.3853	-18.7898	-4.7690	0.42123E-06
119	-0.7132	-0.1810	-8.8283	-2.2407	0.19785E-06
120	-3.4147	-0.8667	-42.2671	-10.7277	0.94829E-06
121	-0.4662	-0.1183	-5.7705	-1.4646	0.12931E-06
122	-1.5046	-0.3819	-18.6243	-4.7270	0.41752E-06
123	-4.0151	-1.0191	-49.6988	-12.6139	0.11153E-05
124	-2.9207	-0.7413	-36.1519	-9.1756	0.81093E-06
125	-0.9504	-0.2412	-11.7641	-2.9858	0.26367E-06
126	-0.8719	-0.2213	-10.7925	-2.7392	0.24188E-06
127	0.6024	0.1529	7.4564	1.8925	0.16710E-06
128	-2.9531	-0.7495	-36.5530	-9.2774	0.81993E-06
129	0.0406	0.0103	0.5031	0.1277	0.11272E-07
130	-0.7539	-0.1914	-9.3321	-2.3686	0.20914E-06
131	0.6364	0.1615	7.8769	1.9992	0.17652E-06
132	-3.1264	-0.7935	-38.6981	-9.8219	0.86811E-06
133	1.8677	0.4740	23.1183	5.8676	0.51834E-06
134	-1.9575	-0.4968	-24.2296	-6.1497	0.54328E-06
135	1.9315	0.4902	23.9076	6.0679	0.53606E-06
136	-3.3054	-0.8389	-40.9144	-10.3844	0.91790E-06
137	-0.2065	-0.0524	-2.5559	-0.6487	0.57268E-07
138	-1.3684	-0.3473	-16.9376	-4.2989	0.37969E-06
139	0.3049	0.0774	3.7736	0.9578	0.84555E-07
140	-2.3938	-0.6076	-29.6308	-7.5205	0.66451E-06
141	-0.1935	-0.0491	-2.3955	-0.6080	0.53673E-07
142	-1.3612	-0.3455	-16.8493	-4.2765	0.37771E-06
143	2.3635	0.5999	29.2548	7.4251	0.65607E-06
144	-2.5508	-0.6474	-31.5731	-8.0135	0.70811E-06
145	2.4884	0.6316	30.8006	7.8174	0.69077E-06
146	-1.8502	-0.4696	-22.9021	-5.8127	0.51349E-06
147	4.8432	1.2292	59.9490	15.2155	0.13458E-05
148	-3.5474	-0.9004	-43.9092	-11.1445	0.98519E-06
149	1.4674	0.3724	18.1628	4.6099	0.40717E-06
150	-1.9975	-0.5070	-24.7255	-6.2755	0.55441E-06
151	-1.6900	-0.4289	-20.9188	-5.3093	0.46899E-06
152	-3.0778	-0.7812	-38.0964	-9.6691	0.85460E-06
153	-3.9057	-0.9913	-48.3450	-12.2703	0.10849E-05
154	0.0895	0.0227	1.1075	0.2811	0.24812E-07
155	-6.9914	-1.7745	-86.5388	-21.9642	0.19444E-05
156	-3.3902	-0.8605	-41.9641	-10.6508	0.94148E-06
157	-12.3483	-3.1341	-152.8464	-38.7935	0.34420E-05

343

158	-4.1241	-1.0467	-51.0482	-12.9564	0.11456E-05
159	-12.7178	-3.2279	-157.4201	-39.9543	0.35455E-05
160	-4.7904	-1.2158	-59.2946	-15.0494	0.13311E-05
161	-16.2431	-4.1226	-201.0555	-51.0293	0.45350E-05
162	-4.4396	-1.1268	-54.9528	-13.9474	0.12334E-05
163	-19.5092	-4.9516	-241.4826	-61.2900	0.54543E-05
164	-0.0276	-0.0070	-0.3421	-0.0868	0.76648E-08
165	-17.7590	-4.5074	-219.8190	-55.7916	0.49613E-05
166	2.3324	0.5920	28.8705	7.3275	0.64744E-06
167	-25.8312	-6.5561	-319.7357	-81.1512	0.72411E-05
168	13.7718	3.4954	170.4656	43.2654	0.38410E-05
169	28.5072	7.2353	352.8591	89.5581	0.80003E-05
170	-10.6624	-2.7062	-131.9777	-33.4969	0.29699E-05
171	71.4022	36.2448	441.9046	224.3170	0.20415E-04
172	-30.1725	-15.3160	-186.7364	-94.7900	0.84736E-05

0   0 SPRING ELEMENTS BROKEN DURING LOADING STEP 1

APPENDIX B

Individual Beam Fabrication Data

Curved Beam 1 (CB1)

Beam Configuration

This beam is one of the first three beams fabricated as a part of a concrete pour on Wednesday April 19, 2006. This beam is rectangular in cross-section and was the first beam to be tested. It is reinforced with two 25M steel reinforcing bars longitudinally and no shear reinforcement. The following figures show the beams configuration.
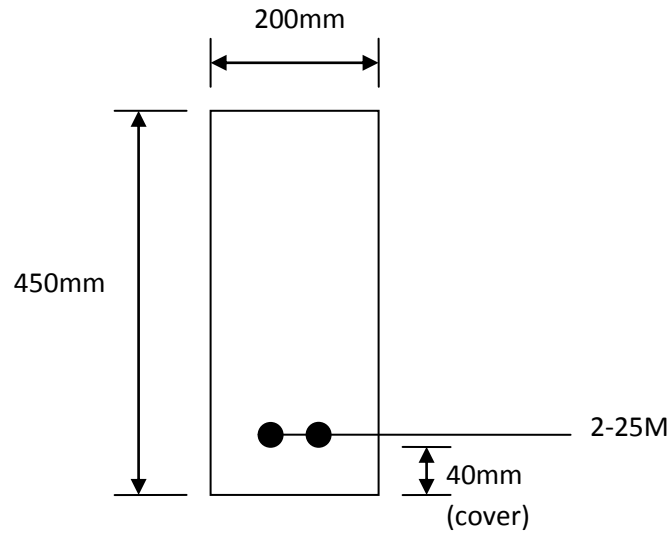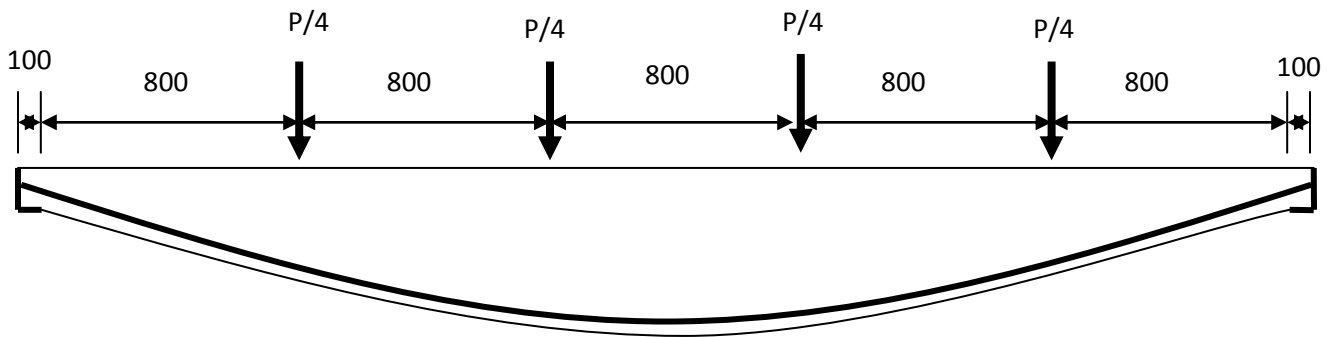

Figure B1 - CB1 Cross-section (at centre, variable-section)

Figure B2 – Overall dimensions of the beam and loading system

Strain Gauge Locations:

Rectangular beams:

Originally only PI gauges were going to be utilized for measuring compression strain in the concrete at the top of the beam. However, due to information discrepancies regarding the suitability of PI gauges for reading compression strain, it was decided to place two concrete strain gauges directly below the PI gauges 1 and 2. This would eliminate any questions regarding the accuracy of the PI gauges because the data from the PI gauges could be compared with the data from concrete strain gauges.
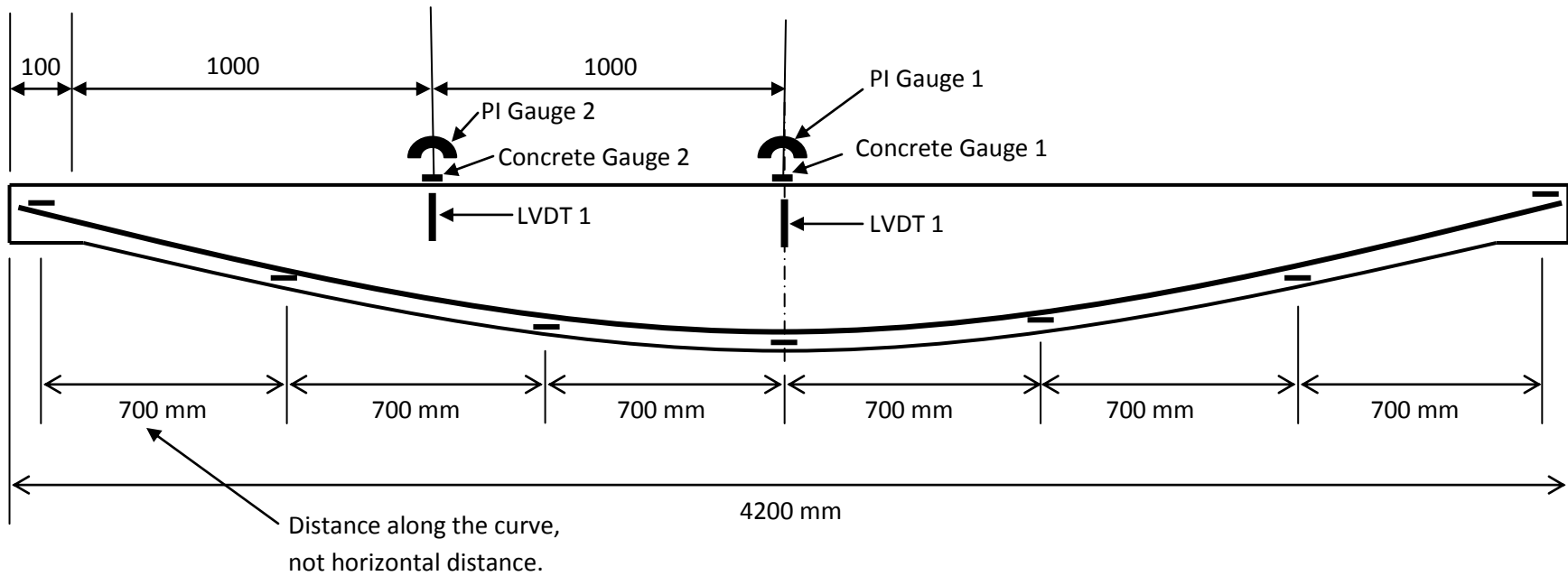
Figure B3 – Sensor location of all along the beam

347

Strain Gauge Numbering System:

Strain gauges were placed along the bottom of the bar with the exception of the four end gauges in the curved reinforcement, gauge Numbers 1, 8, 7 and 14. These gauges where place at the top of the bar after the bars were welded to the end angle.

No. 8   No. 9   No. 10   No. 11   No. 12   No. 13   No. 14

No. 1   No. 2   No. 3   No. 4   No. 5   No. 6   No. 7

Two reinforcing bars in each beam
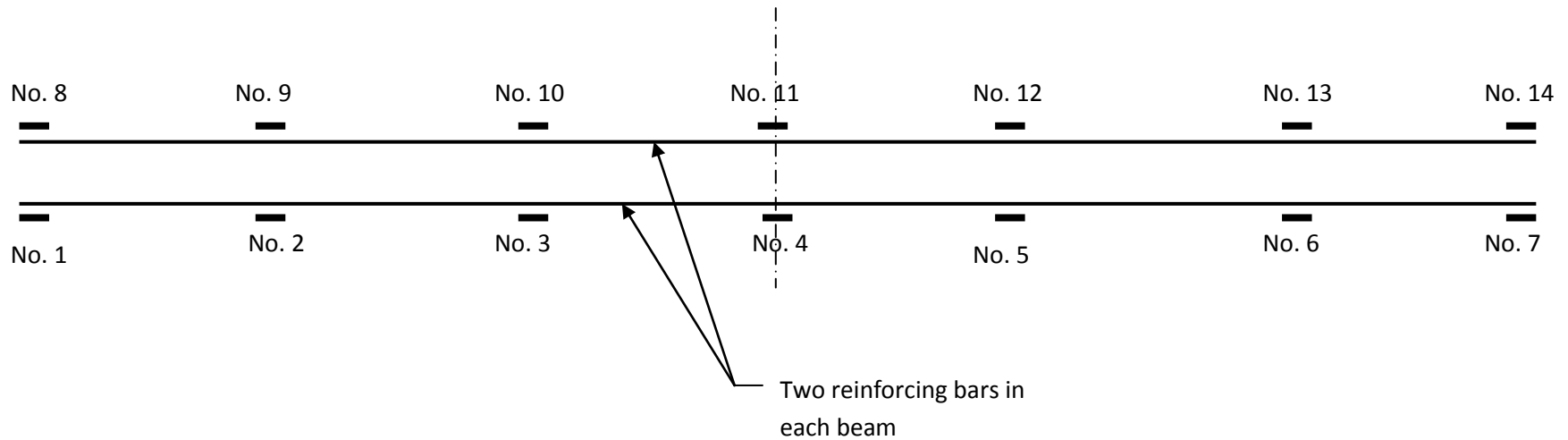
Figure B4- The numbering system for the steel strain gauges

Testing

This beam was tested at 10:30 A.M. on Thursday July 6, 2006, 78 days after casting the beam. This delay was due to the availability of the Data Acquisition System (DAQ).

Three cylinders were tested for compression strength prior to the testing of the beam. The cylinders were tested on July 5, 2006. The results of the tests are as follows:

Total Cylinder compression load: 260 kN, 300 kN and 290 kN.

Cylinder diameter = 100mm (small cylinders)   Area = 7850 mm^2

f'$_c$ for each cylinder respectively: 33.12 MPa, 38.22 MPa and 36.94 MPa

Average f'$_c$ = 36 MPa

Failure

This beam failed suddenly at 117kN way below the design load. The failure occurred at the left hand side of the beam. The failure consisted of a portion of the concrete at the top of the beam separating from the beam completely and jumping up at the exact time of failure, see photographs of the testing in the photo file. Several factors may have contributed to this failure as follows:

1. The concrete in this region was of pour quality due to improper vibration
2. welding of the reinforcing was visually inspected and there were no cracks on the welded connection.

Curved Beam 2 (CB2)

Beam Configuration

This beam is one of the second set of beams fabricated as a part of a concrete pour on *Friday August 25, 2006*. This beam is rectangular in cross-section, reinforced with two 25M steel reinforcing bars longitudinally and no shear reinforcement. The following figures show the beams configuration. This beam is the same as CB1 (Curve Beam 1).

Strain Gauge Locations:

PI gauges were not use in this test as in the previous test they were proven inaccurate for this application. Two concrete gauges were used for measuring the concrete stress as indicated for CB1. Two LVDTs were used to measure deflection at L/2 and L/4.

Testing

This beam was tested at 10:00 A.M. on November 21, 2006, 89 days after casting the beam. This delay was due to the availability of the Data Acquisition System (DAQ).

On November 22, 2006 four cylinders were tested for compression strength prior to testing of the beam. The results of the tests are as follows:

Area of concrete cylinder = πr^2 = (3.14) (50)^2 = 7850 mm^2

Cylinders	Total Load [kN]	f'$_c$ [MPa]
1	520	66.24
2	510	64.97
3	530	67.52
4	360 (too low; disregard this cylinder)	

Average f'$_c$ = 66 MPa

Curved Beam 3 (CB3)

Beam Configuration

This beam is one of the first three beams fabricated as a part of a concrete pour on *Friday August 25, 2006*. This beam is rectangular in cross-section, and is reinforced with two 25M steel reinforcing bars longitudinally and has no shear reinforcement. The following figures show the beams configuration.

Testing

This beam was tested at 10:30 A.M. on Thursday December 7, 2006, 105 days after casting the beam. This delay was due to the availability of the Data Acquisition System (DAQ).

On December 8, 2006 four cylinders were tested for compression strength prior to the testing of the beam. The cylinders were tested. The results of the tests are as follows:

Cylinder diameter = 100mm (small cylinders)

Area of concrete cylinder = π r^2 = (3.14) (50)^2 = 7850 mm^2

Cylinders	Total Load [kN]	f'$_c$ [MPa]
1	540	68.8
2	460	58.6
3	520	66.2
4	240 (too low; disregard this cylinder)	

Average f'$_c$ = 65 MPa

Rectangular Beam 1 (RB1)

Beam Configuration

This beam is one of the first three beams fabricated as part of the concrete pour on Wednesday April 19, 2006. This is the first beam to be tested and is rectangular in cross-section and in profile. The beam is reinforced with two 25M steel reinforcing bars longitudinally and no shear reinforcement. The following figures show the beams configuration.
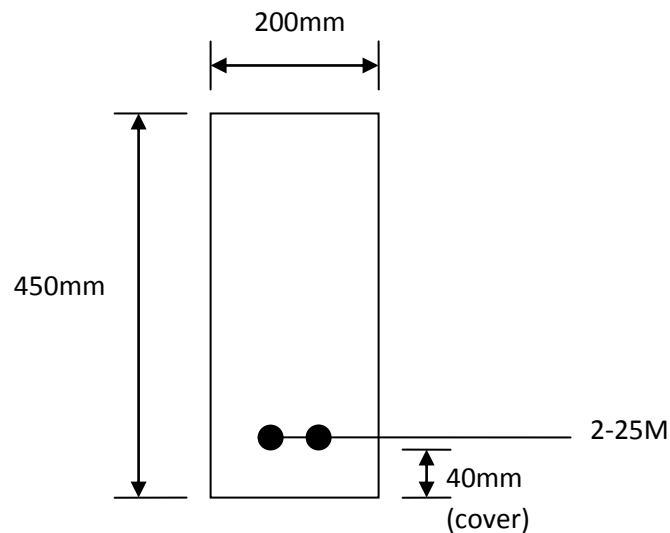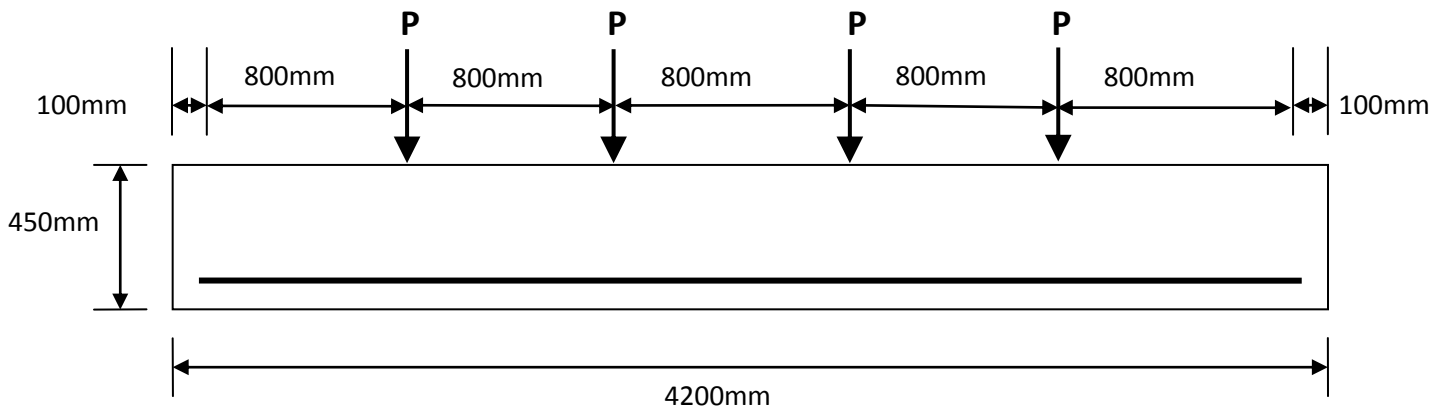
Figure B5- RB1 Cross-section (Constant)

Figure B6 – Overall dimensions of the beam and loading scheme

Strain Gauge Locations:

Rectangular beams:

Originally only PI gauges were going to be utilized for measuring compression strain in the concrete at the top of the beam. However, due to information discrepancies regarding the suitability of PI gauges for reading compression strain, it was decided to place two concrete strain gauges directly below the PI gauges 1 and 2.
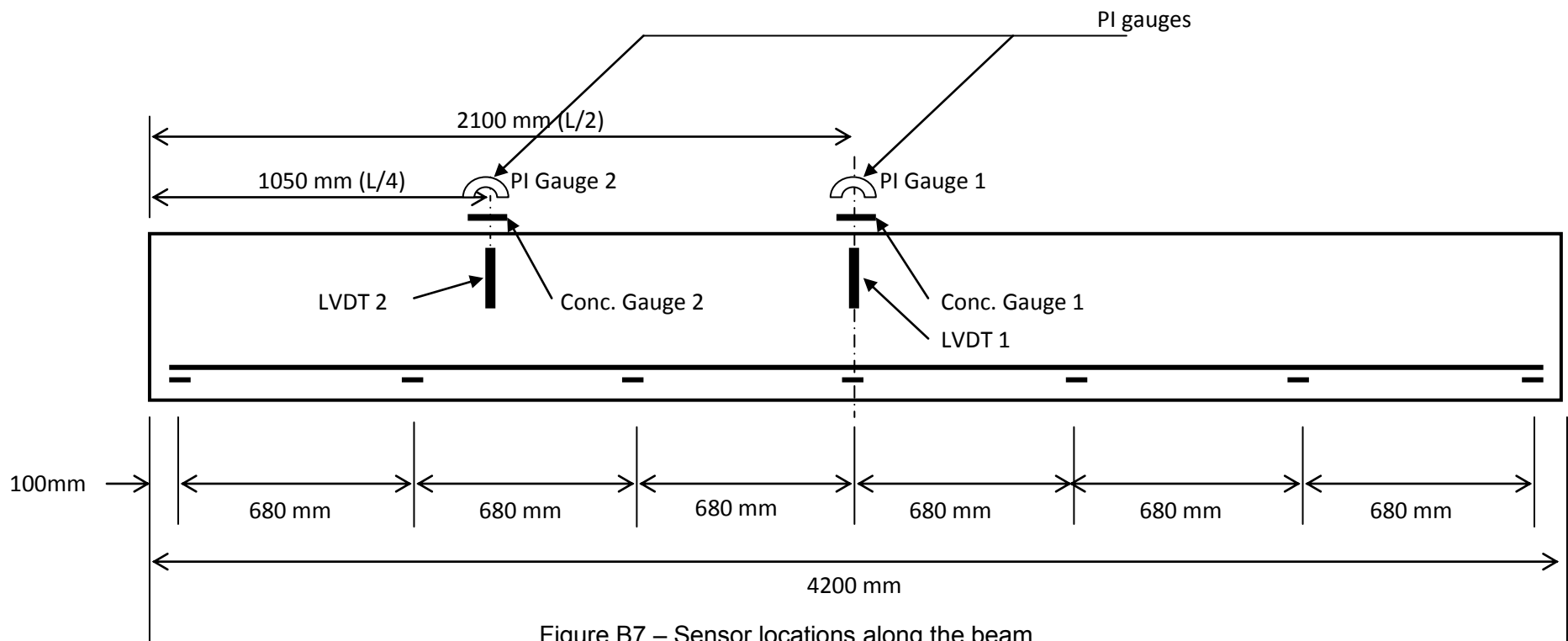
Figure B7 – Sensor locations along the beam

Strain Gauge Numbering System:

Strain gauges were placed along the bottom of the bar with the exception of the four end gauges in the curved reinforcement, gauge Numbers 1, 8, 7 and 14. These gauges where place at the top of the bar after the bars were welded to the end angle.

No. 8 No. 9 No. 10 No. 11 No. 12 No. 13 No. 14

No. 1 No. 2 No. 3 No. 4 No. 5 No. 6 No. 7

Two reinforcing bars in each beam
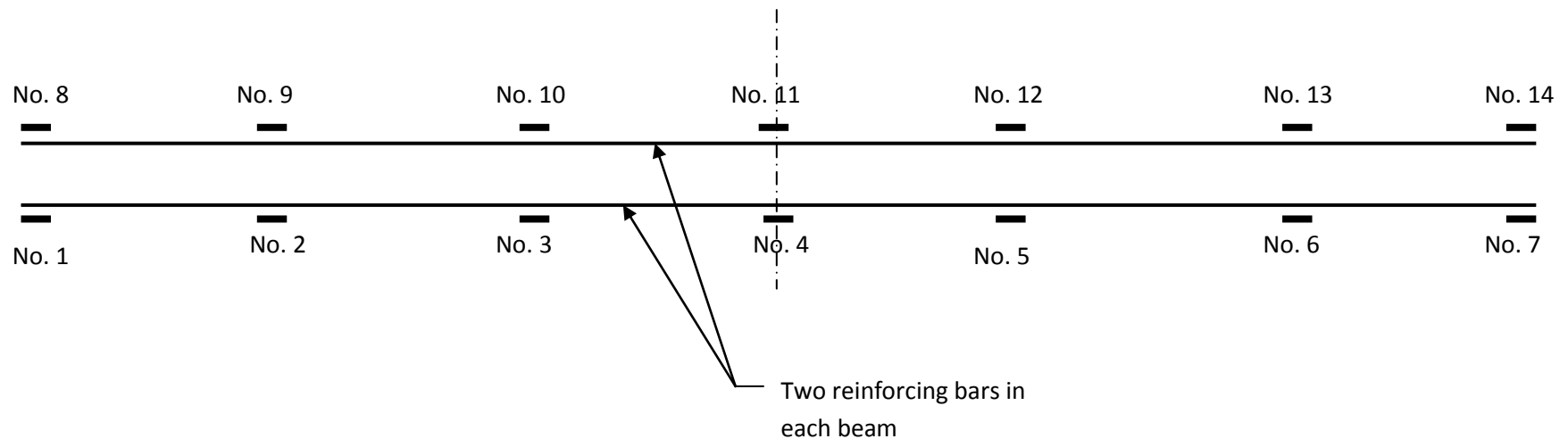
Figure B8 – The numbering system for the steel strain gauges

Testing

This beam was tested at 2:30 P.M. on June 12, 2006, 54 days after casting the beam. This delay was due to the availability of the Data Acquisition System (DAQ).

On June 8, 2006 three cylinders were tested for compression strength prior to the testing of the beam. The cylinders were tested. The results of the tests are as follows:

Cylinder diameter = 100mm (small cylinders)

Area of concrete cylinder = $\pi \, r^2$ = (3.14) (50)^2 = 7850 mm^2

Cylinders	Total Load [kN]	f'$_c$ [MPa]
1	310	39.49
2	300	38.22
3	290	36.94

Average f'$_c$ = 38 MPa

Failure

This beam failed completely in shear on one side. The failure was very sudden with a complete shear crack on one side only.

Rectangular Beam 2 (RB2)

Beam Configuration

This beam is one of the first three beams fabricated as part of the concrete pour on Wednesday April 19, 2006. This is the first beam to be tested. This beam is rectangular in cross-section and in profile. The beam is reinforced with two 25M steel reinforcing bars longitudinally and no shear reinforcement. The reinforcing in this beam follows a parabolic curve, the same curve as the curved beams. The following figures show the beams configuration.
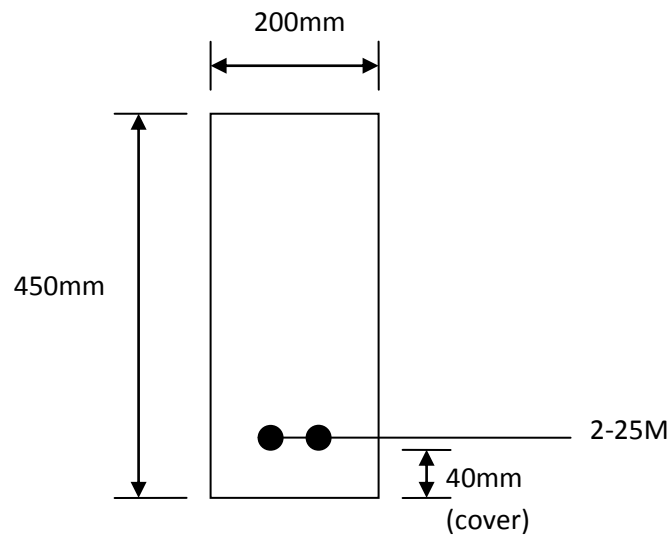

Figure B9 – Cross-section at centre line
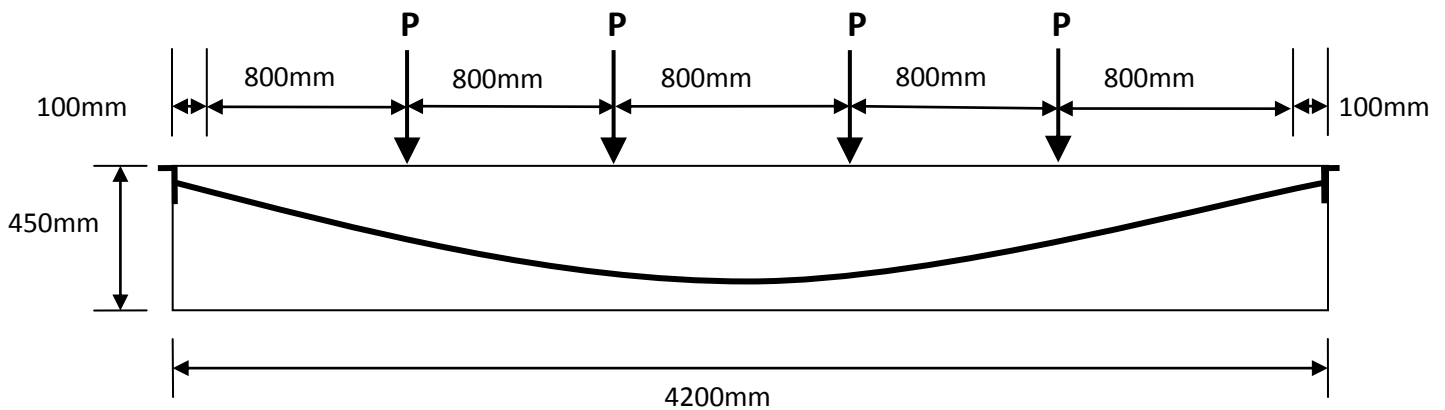
Figure B10 – Overall dimensions of the beam and loading scheme

Strain Gauge Locations:

Rectangular beams:

Originally only PI gauges were going to be utilized for measuring compression strain in the concrete at the top of the beam. However, due to information discrepancies regarding the suitability of PI gauges for reading compression strain, it was decided to place two concrete strain gauges directly below the PI gauges 1 and 2.
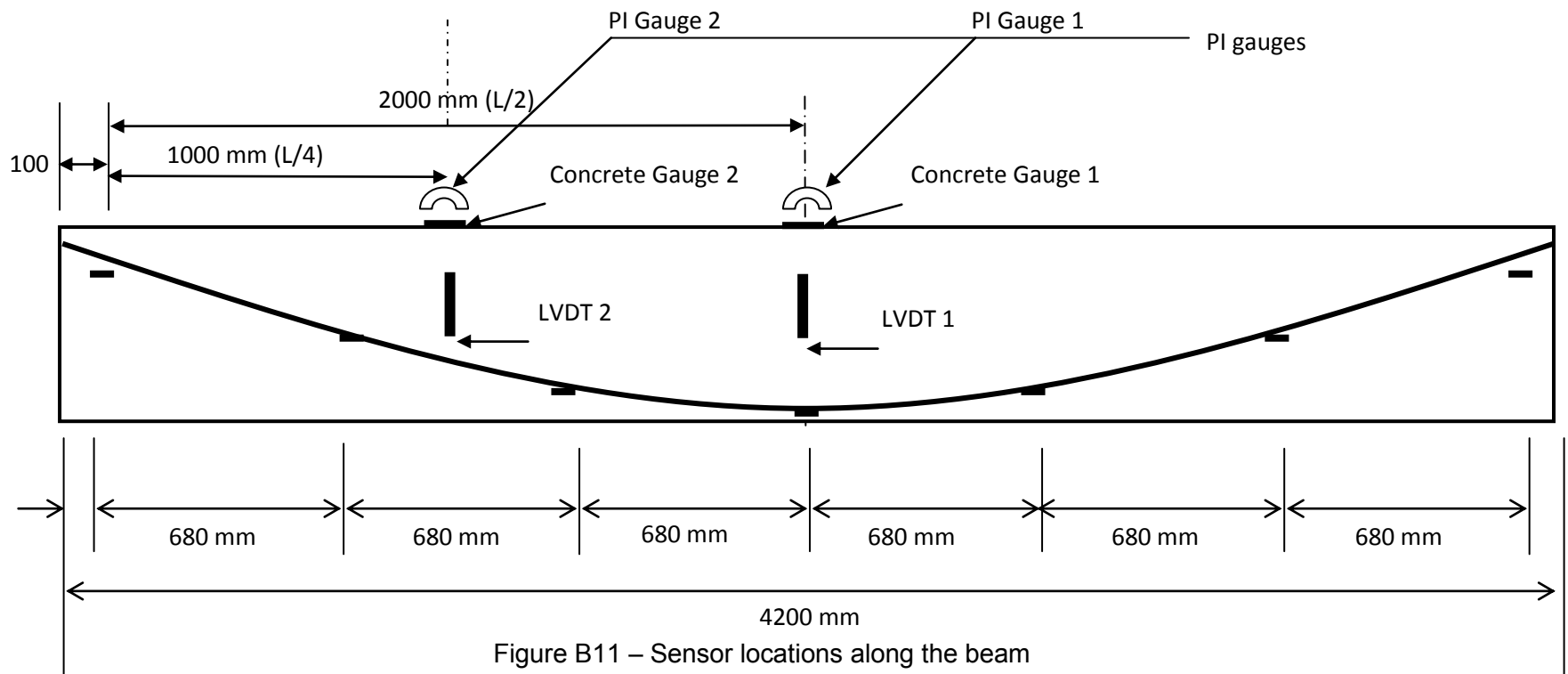

Figure B11 – Sensor locations along the beam

Strain Gauge Numbering System:

Strain gauges were placed along the bottom of the bar with the exception of the four end gauges in the curved reinforcement, gauge numbers 1, 8, 7 and 14. These gauges where place at the top of the bar after the bars were welded to the end angle.
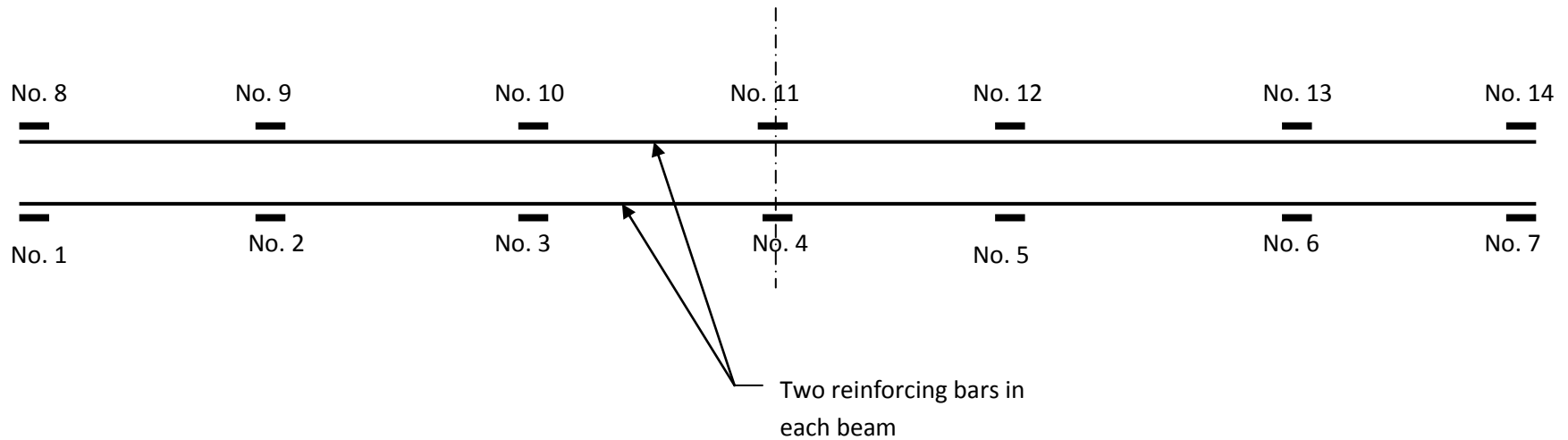

No. 8   No. 9   No. 10   No. 11   No. 12   No. 13   No. 14

No. 1   No. 2   No. 3   No. 4   No. 5   No. 6   No. 7

Two reinforcing bars in each beam

Figure B12 – The numbering system for the steel strain gauges

Testing

This beam was tested at 10:30 A.M. on Wednesday June 28, 2006, 70 days after casting the beam. The beam was tested first on the 28th up to 200 kN, but due to the limit put on the actuator the pump stopped at that load. On Thursday June 29th the limit was removed and the beam was tested to failure, 260 kN.

On June 29, 2006 three cylinders were tested for compression strength after the testing of the beam. The cylinders were tested. The results of the tests are as follows:

Total cylinder compression load: 300 kN, 260 kN and 290 kN.

Cylinder diameter = 100mm (small cylinders)

Area of concrete cylinder = $\pi\ r^2$ = (3.14) (50)^2 = 7850 mm^2

Cylinders	Total Load [kN]	f'$_c$ [MPa]
1	300	38.22
2	260	33.12
3	290	36.94

Average f'$_c$ = 36 MPa

Rectangular Beam 3 (RB3)

Beam Configuration

This beam was fabricated as a part of a concrete pour on *Friday August 25, 2006*. This beam is rectangular in cross-section and in profile. It is reinforced with two 25M steel reinforcing bars longitudinally and shear reinforcement designed in accordance with CSA A 23.3.
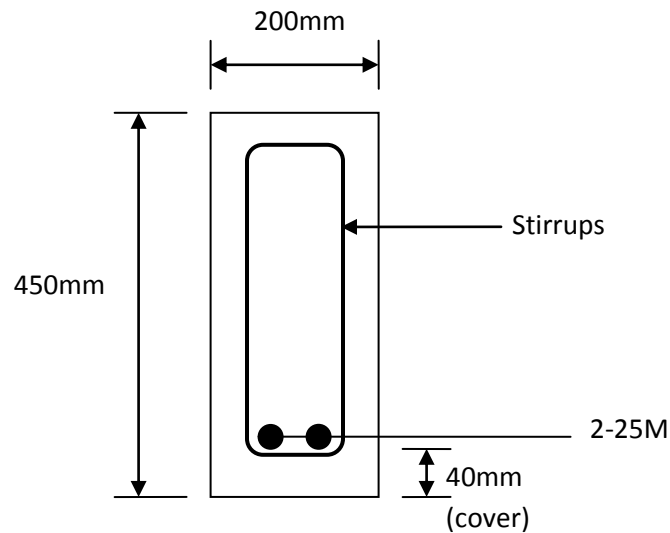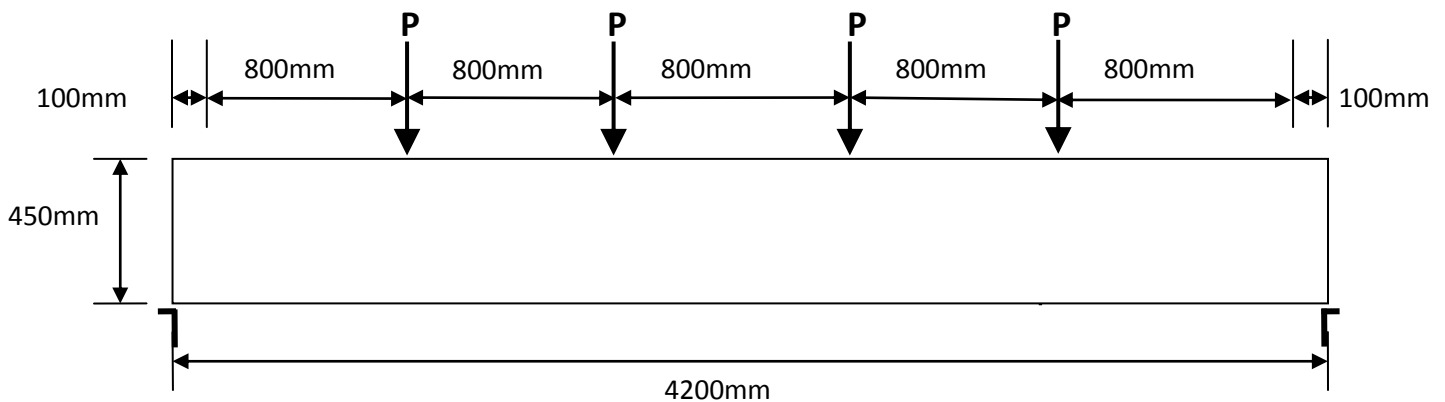

Figure B13 – Cross-section at Centre Line

Figure B14 – Overall dimensions of the beam and loading scheme
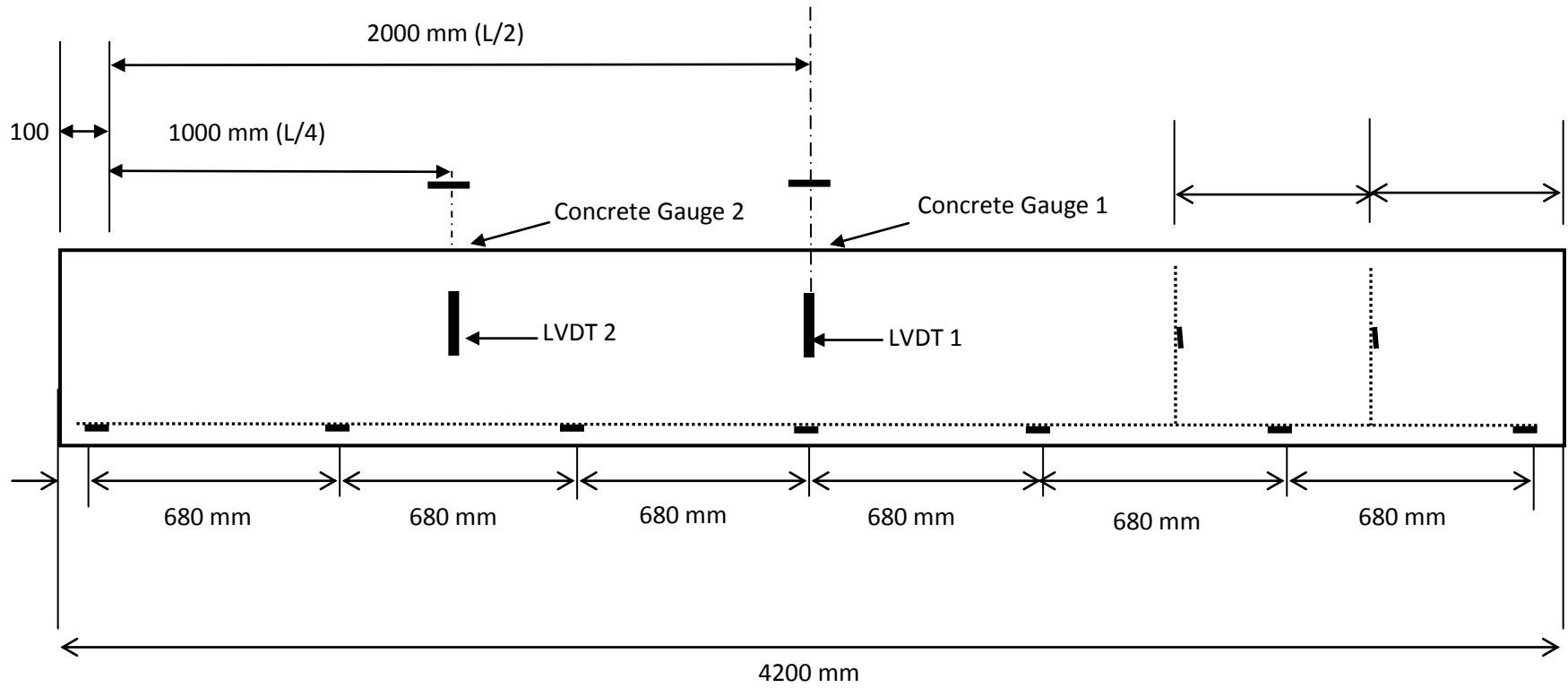
Strain Gauge Locations:

Figure B15 – Sensor locations along the beam

Strain Gauge Numbering System:

Strain gauges were placed along the bottom of the bar with the exception of the four end gauges in the curved reinforcement, gauge numbers 1, 8, 7 and 14. These gauges where place at the top of the bar after the bars were welded to the end angle.
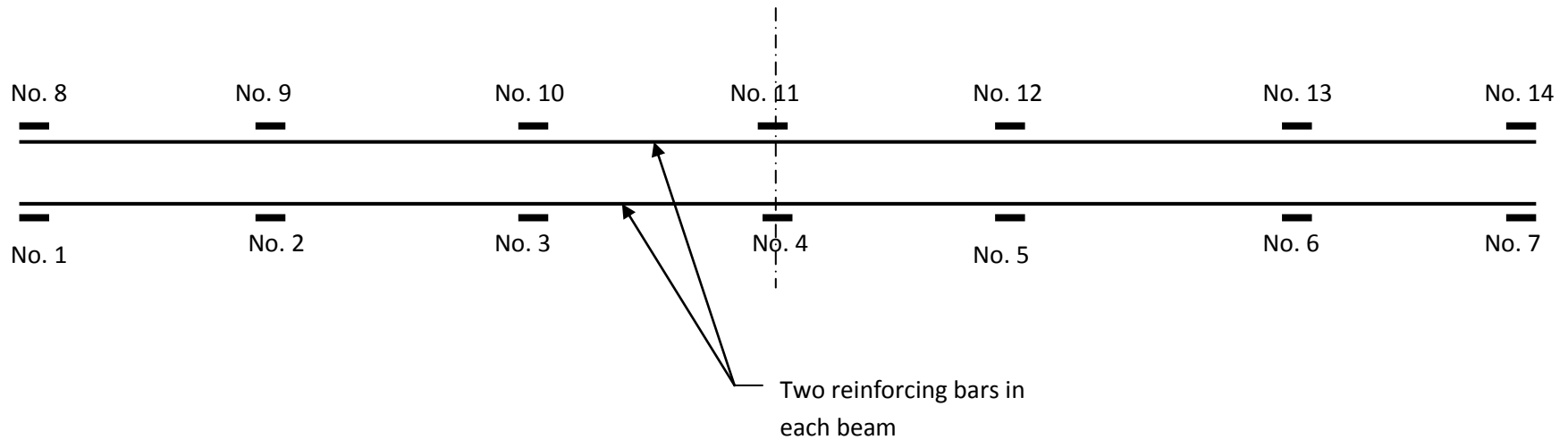
No. 8   No. 9   No. 10   No. 11   No. 12   No. 13   No. 14

No. 1   No. 2   No. 3   No. 4   No. 5   No. 6   No. 7

Two reinforcing bars in each beam

Figure B16 – The numbering system for the steel strain gauges

Testing

This beam was tested at 11:00 A.M. on Monday January 15, 2007, 143 days after casting the beam.

On January 16, 2007 four cylinders were tested for compression strength after the testing of the beam. The results of the tests are as follows:

Cylinder diameter = 100mm (small cylinders)   Area = 7850 mm^2

Area of concrete cylinder = π r^2 = (3.14) (50)^2 = 7850 mm^2

Cylinders	Total Load [kN]	f'$_c$ [MPa]
1	320	40.76
2	310	39.49
3	300	38.22
4	310	39.49

Average f'$_c$ = 39 MPa

Rectangular Beam 4 (RB4)

Beam Configuration

This beam was fabricated as a part of a concrete pour on *Friday August 25, 2006*. This beam is rectangular in cross-section and in profile. It is reinforced with two 15M steel reinforcing bars longitudinally and no shear reinforcement. Designed in accordance with CSA A 23.3.
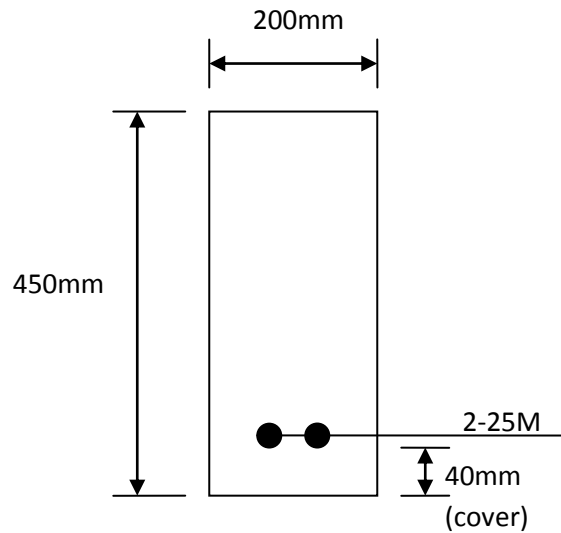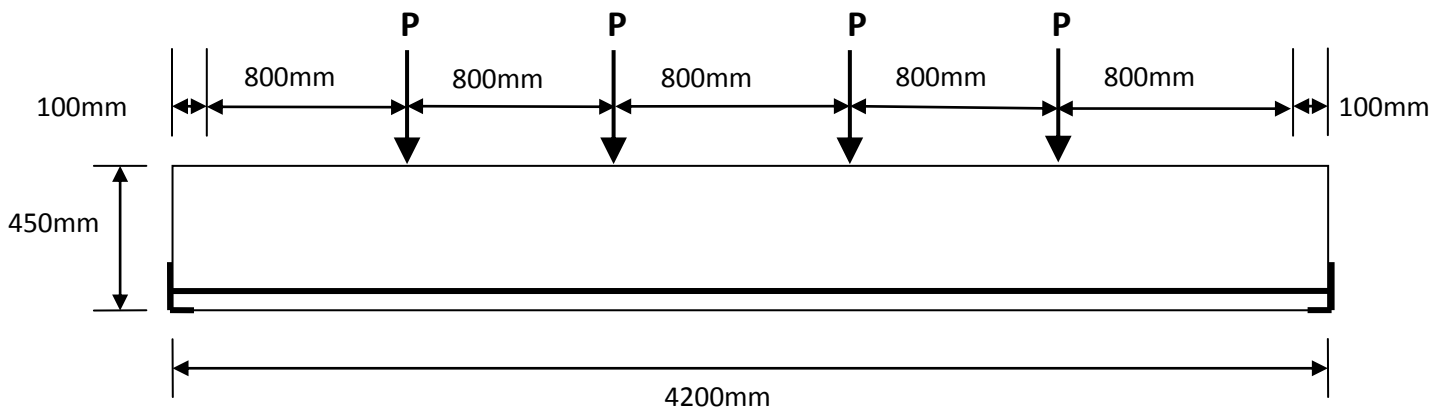

Figure B17 – Cross-section (Constant)

Figure B18 – Overall dimensions of the beam and loading scheme

Strain Gauge Locations:

Only one rebar was instrumented with seven strain gauges. An additional 9 concrete gauges could be installed on this beam because there are 16 strain gauge channels available on the DAQ. The additional concrete gauges were installed on the side of the beam, Figure 4 and 5. All other strain gauges and LVDTs are shown in Figure B19.
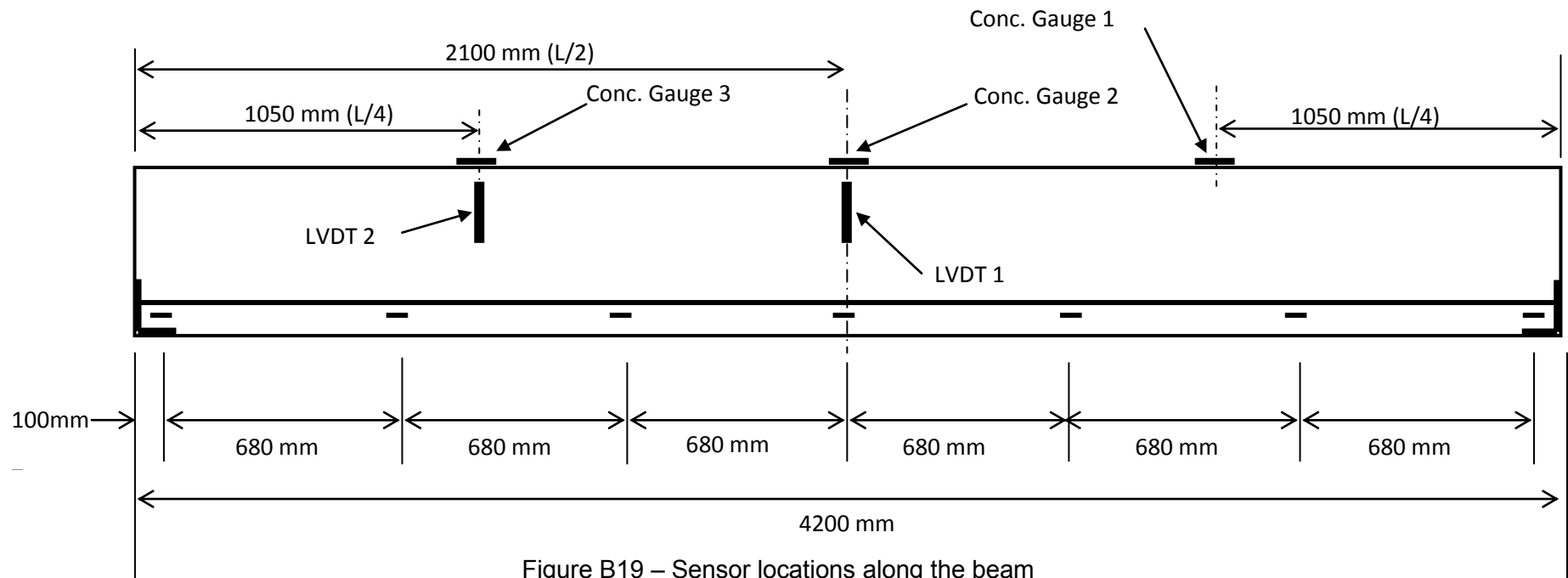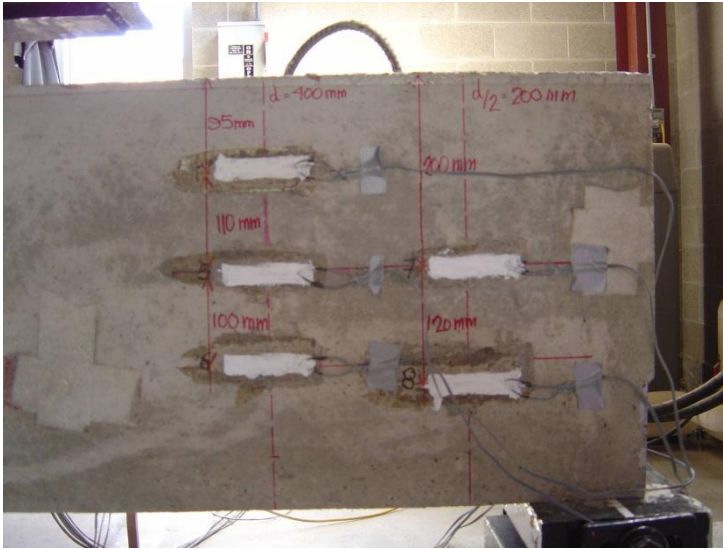

Figure B19 – Sensor locations along the beam

Figure B20 – Location of strain gauges on the side of the beam

Figure B21 – Location of strain gauges on the side of the beam

Steel Strain Gauge Numbering System:

The strain in both reinforcing bars is the same as the strain gauges gave similar data for both rebars for this reason steel strain gauges were placed only along one rebar. .   Strain gauges were installed at the bottom of the bar with the exception of the four end gauges, gauge numbers 1, 7. These gauges where placed at the top of the bar after the bars were welded to the end angle.
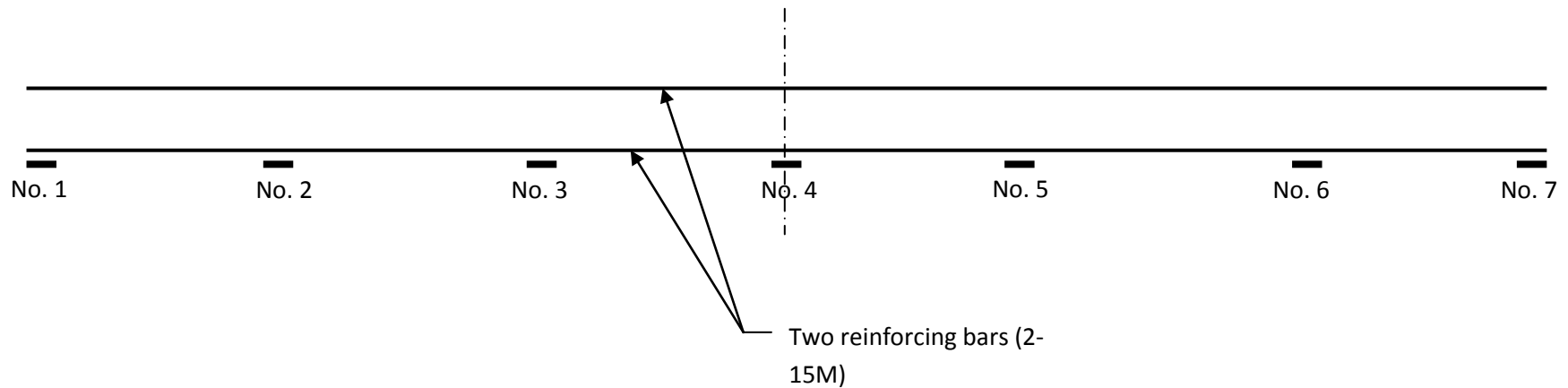
No. 1   No. 2   No. 3   No. 4   No. 5   No. 6   No. 7

Two reinforcing bars (2-
15M)

Figure B22 – The numbering system for the steel strain gauges

Testing

This beam was tested at 10:00 A.M. on Thursday May 17, 2007, 257 days after casting. This delay was due to the availability of the Data Acquisition System (DAQ).

On May 18, 2007 three cylinders were tested for compression strength prior to the testing of the beam. The cylinders were tested. The results of the tests are as follows:

Cylinder diameter = 100mm (small cylinders)

Area of concrete cylinder = π r^2 = (3.14) (50)^2 = 7850 mm^2

Cylinders	Total Load [kN]	f'$_c$ [MPa]
1	396	50.4
2	413	52.6
3	410	52.2
4	520 (too high; disregard this cylinder)	

Average f'$_c$ = 52 MPa